

Westinghouse Non-Proprietary Class

WCAP-14740

Revision 3 of AP600
Level 2 IRA
(Chapters 35 through 43)

Westinghouse Energy Systems



9610020176 960930
PDR ADOCK 05200003
A PDR

Westinghouse Non-Proprietary Class 3

WCAP-14745

◆ ◆ ◆ ◆ ◆ ◆ ◆ ◆

**Revision 3 of AP600
Level 2 PRA
(Chapters 35 through 43)**

Westinghouse Energy Systems



9610020176 960930
PDR ADOCK 05200003
A PDR

AP600 DOCUMENT COVER SHEET

Form 58202G(5/94) [t:\xxxx.wpf:1x]

AP600 CENTRAL FILE USE ONLY:

TDC: _____

IDS: I _____ S _____

0058.FRM

RFS#:

RFS ITEM #:

AP600 DOCUMENT NO. GWGL028	REVISION NO. 0	Page 1 of 1	ASSIGNED TO
-------------------------------	-------------------	-------------	-------------

ALTERNATE DOCUMENT NUMBER:

WORK BREAKDOWN #: 3.1.2

DESIGN AGENT ORGANIZATION: Westinghouse

TITLE: WCAP-14745, Revision 3 of the AP600 Level 2 PRA (Chapters 35 - 43)

ATTACHMENTS:	DCP #/REV. INCORPORATED IN THIS DOCUMENT REVISION:
CALCULATION/ANALYSIS REFERENCE:	

ELECTRONIC FILENAME	ELECTRONIC FILE FORMAT	ELECTRONIC FILE DESCRIPTION

(C) WESTINGHOUSE ELECTRIC CORPORATION 1995

☐ WESTINGHOUSE PROPRIETARY CLASS 2

This document contains information proprietary to Westinghouse Electric Corporation; it is submitted in confidence and is to be used solely for the purpose for which it is furnished and returned upon request. This document and such information is not to be reproduced, transmitted, disclosed or used otherwise in whole or in part without prior written authorization of Westinghouse Electric Corporation, Energy Systems Business Unit, subject to the legends contained hereof.

☐ WESTINGHOUSE PROPRIETARY CLASS 2C

This document is the property of and contains Proprietary Information owned by Westinghouse Electric Corporation and/or its subcontractors and suppliers. It is transmitted to you in confidence and trust, and you agree to treat this document in strict accordance with the terms and conditions of the agreement under which it was provided to you.

☒ WESTINGHOUSE CLASS 3 (NON PROPRIETARY)

COMPLETE 1 IF WORK PERFORMED UNDER DESIGN CERTIFICATION OR COMPLETE 2 IF WORK PERFORMED UNDER FOAKE.

1 ☒ DOE DESIGN CERTIFICATION PROGRAM - GOVERNMENT LIMITED RIGHTS STATEMENT [See page 2]

Copyright statement: A license is reserved to the U.S. Government under contract DE-AC03-90SF18495.

☐ DOE CONTRACT DELIVERABLES (DELIVERED DATA)

Subject to specified exceptions, disclosure of this data is restricted until September 30, 1995 or Design Certification under DOE contract DE-AC03-90SF18495, whichever is later.

EPRI CONFIDENTIAL: NOTICE: 1 ☒ 2 ☐ 3 ☐ 4 ☐ 5 ☐ CATEGORY: A ☒ B ☐ C ☐ D ☐ E ☐ F ☐

2 ☐ ARC FOAKE PROGRAM - ARC LIMITED RIGHTS STATEMENT [See page 2]

Copyright statement: A license is reserved to the U.S. Government under contract DE-FC02-NE34267 and subcontract ARC-93-3-SC-001.

☐ ARC CONTRACT DELIVERABLES (CONTRACT DATA)

Subject to specified exceptions, disclosure of this data is restricted under ARC Subcontract ARC-93-3-SC-001.

ORIGINATOR C. L. Haag	SIGNATURE/DATE <i>Cynthia L. Haag</i> 9-26-96
AP600 RESPONSIBLE MANAGER B. A. McIntyre	SIGNATURE* <i>B. A. McIntyre</i> APPROVAL DATE 9-28-96

*Approval of the responsible manager signifies that document is complete, all required reviews are complete, electronic file is attached and document is released for use.

Form 58202G(5/94)

LIMITED RIGHTS STATEMENTS

DOE GOVERNMENT LIMITED RIGHTS STATEMENT

- (A) These data are submitted with limited rights under government contract No. DE-AC03-90SF18495. These data may be reproduced and used by the government with the express limitation that they will not, without written permission of the contractor, be used for purposes of manufacture nor disclosed outside the government; except that the government may disclose these data outside the government for the following purposes, if any, provided that the government makes such disclosure subject to prohibition against further use and disclosure:
- (i) This "Proprietary Data" may be disclosed for evaluation purposes under the restrictions above.
 - (ii) The "Proprietary Data" may be disclosed to the Electric Power Research Institute (EPRI), electric utility representatives and their direct consultants, excluding direct commercial competitors, and the DOE National Laboratories under the prohibitions and restrictions above.
- (B) This notice shall be marked on any reproduction of these data, in whole or in part.

ARC LIMITED RIGHTS STATEMENT:

This proprietary data, furnished under Subcontract Number ARC-93-3-SC-001 with ARC may be duplicated and used by the government and ARC, subject to the limitations of Article H-17.F. of that subcontract, with the express limitations that the proprietary data may not be disclosed outside the government or ARC, or ARC's Class 1 & 3 members or EPRI or be used for purposes of manufacture without prior permission of the Subcontractor, except that further disclosure or use may be made solely for the following purposes:

This proprietary data may be disclosed to other than commercial competitors of Subcontractor for evaluation purposes of this subcontract under the restriction that the proprietary data be retained in confidence and not be further disclosed, and subject to the terms of a non-disclosure agreement between the Subcontractor and that organization, excluding DOE and its contractors.

DEFINITIONS

CONTRACT/DELIVERED DATA — Consists of documents (e.g. specifications, drawings, reports) which are generated under the DOE or ARC contracts which contain no background proprietary data.

EPRI CONFIDENTIALITY / OBLIGATION NOTICES

NOTICE 1: The data in this document is subject to no confidentiality obligations.

NOTICE 2: The data in this document is proprietary and confidential to Westinghouse Electric Corporation and/or its Contractors. It is forwarded to recipient under an obligation of Confidence and Trust for limited purposes only. Any use, disclosure to unauthorized persons, or copying of this document or parts thereof is prohibited except as agreed to in advance by the Electric Power Research Institute (EPRI) and Westinghouse Electric Corporation. Recipient of this data has a duty to inquire of EPRI and/or Westinghouse as to the uses of the information contained herein that are permitted.

NOTICE 3: The data in this document is proprietary and confidential to Westinghouse Electric Corporation and/or its Contractors. It is forwarded to recipient under an obligation of Confidence and Trust for use only in evaluation tasks specifically authorized by the Electric Power Research Institute (EPRI). Any use, disclosure to unauthorized persons, or copying this document or parts thereof is prohibited except as agreed to in advance by EPRI and Westinghouse Electric Corporation. Recipient of this data has a duty to inquire of EPRI and/or Westinghouse as to the uses of the information contained herein that are permitted. This document and any copies or excerpts thereof that may have been generated are to be returned to Westinghouse, directly or through EPRI, when requested to do so.

NOTICE 4: The data in this document is proprietary and confidential to Westinghouse Electric Corporation and/or its Contractors. It is being revealed in confidence and trust only to Employees of EPRI and to certain contractors of EPRI for limited evaluation tasks authorized by EPRI. Any use, disclosure to unauthorized persons, or copying of this document or parts thereof is prohibited. This Document and any copies or excerpts thereof that may have been generated are to be returned to Westinghouse, directly or through EPRI, when requested to do so.

NOTICE 5: The data in this document is proprietary and confidential to Westinghouse Electric Corporation and/or its Contractors. Access to this data is given in Confidence and Trust only at Westinghouse facilities for limited evaluation tasks assigned by EPRI. Any use, disclosure to unauthorized persons, or copying of this document or parts thereof is prohibited. Neither this document nor any excerpts therefrom are to be removed from Westinghouse facilities.

EPRI CONFIDENTIALITY / OBLIGATION CATEGORIES

CATEGORY "A" — (See Delivered Data) Consists of CONTRACTOR Foreground Data that is contained in an issued report.

CATEGORY "B" — (See Delivered Data) Consists of CONTRACTOR Foreground Data that is not contained in an issued report, except for computer programs.

CATEGORY "C" — Consists of CONTRACTOR Background Data except for computer programs.

CATEGORY "D" — Consists of computer programs developed in the course of performing the Work.

CATEGORY "E" — Consists of computer programs developed prior to the Effective Date or after the Effective Date but outside the scope of the Work.

CATEGORY "F" — Consists of administrative plans and administrative reports.

WESTINGHOUSE NON-PROPRIETARY CLASS 3

WCAP-14745

**Revision 3 of AP600 Level 2 PRA
(Chapters 35 through 43)**

September 1996

Westinghouse Electric Corporation
Energy System Business Unit
P.O. Box 355
Pittsburgh, PA 15230-0355

© 1996 Westinghouse Electric Corporation
All Rights Reserved

TABLE OF CONTENTS

LIST OF TABLES	viii
LIST OF FIGURES	x
1 INTRODUCTION	1-1
CHAPTER 35 CONTAINMENT EVENT TREE ANALYSIS	
35.1 Introduction	35-1
35.2 Containment Event Tree - General Discussion	35-1
35.3 Event Tree Construction	35-2
35.4 Fission-Product Release Considerations	35-3
35.4.1 Fission-Product Release Timing	35-3
35.4.2 Containment Failure Considerations	35-4
35.5 AP600 Release Categories	35-6
35.5.1 Release Category IC	35-7
35.5.2 Release Category ICP	35-7
35.5.3 Release Category XL	35-7
35.5.4 Release Category BP	35-7
35.5.5 Release Category CI	35-8
35.5.6 Release Category CI-C	35-8
35.5.7 Release Category CFE	35-8
35.5.8 Release Category CFE-C	35-8
35.5.9 Release Category CFI	35-8
35.5.10 Release Category CFL	35-9
35.5.11 Release Category CFV	35-9
35.6 Containment Event Tree Nodes	35-9
35.6.1 Node DP	35-9
35.6.2 Node SG	35-10
35.6.3 Node CR	35-10
35.6.4 Node IS	35-11
35.6.5 Node PC	35-11
35.6.6 Node IG	35-11
35.6.7 Node IK	35-12
35.6.8 Node SE	35-12
35.6.9 Node VF	35-12
35.6.10 Node HCI	35-13
35.6.11 Node DQ	35-13
35.6.12 Node SCC	35-13
35.6.13 Node CFI	35-14
35.6.14 Node RW	35-14
35.6.15 Node HC2	35-14
35.6.16 Node CF2	35-15
35.6.17 Node HC3	35-15
35.6.18 Node CF3	35-15
35.6.19 Node CF4	35-16
35.6.20 Node EX	35-16

TABLE OF CONTENTS (continued)

35.7	AP600 Containment Event Tree Structure	35-17
35.8	Core Damage Sequence Grouping	35-17
35.9	References	35-18
 CHAPTER 36 DECOMPOSITION EVENT TREE - ANALYSIS OF IN-VESSEL RETENTION OF MOLTEN CORE DEBRIS		
36.1	Discussion of the Issue	36-1
36.2	Analysis Methodology	36-2
36.3	Discussion of Uncertainties	36-6
36.3.1	Behavior of the Reactor Vessel Insulation	36-6
36.3.2	Cavity Flooding Rate	36-7
36.3.3	Debris Pool Characteristics	36-8
36.3.4	Decay Power in the Debris Pool	36-8
36.3.5	Radiation Heat Transfer to the Upper Vessel	36-9
36.4	In-Vessel Retention Decomposition Event Tree	36-9
36.4.1	Analysis of the Combined Uncertainties	36-10
36.5	Quantification of the Decomposition Event Tree	36-10
36.5.1	Node FL	36-10
36.5.2	Node MD	36-10
36.5.3	Node DK	36-11
36.5.4	Node QUP	36-11
36.5.5	Node IVR	36-12
36.6	Results	36-12
36.7	References	36-13
 CHAPTER 37 DECOMPOSITION EVENT TREE - ANALYSIS OF THERMALLY INDUCED FAILURES OF THE REACTOR COOLANT SYSTEM PRESSURE BOUNDARY		
37.1	Background	37-1
37.1.1	Vessel Failure Induced by Molten Core Debris	37-2
37.1.2	Primary System Piping Failures into Containment	37-3
37.1.3	Steam Generator Tube Failures into the Secondary System	37-3
37.2	Controlling Phenomena and Uncertainties	37-3
37.2.1	Natural Circulation of High Temperature Gases in the Reactor Coolant System	37-3
37.2.2	Creep Rupture Failure of Hot Leg Nozzle, Surge Line, and Steam Generator Tubes	37-5
37.2.3	Degradation of Steam Generator Tubes	37-7
37.3	MAAP4 Analyses	37-7
37.3.1	Base Cases	37-8
37.3.2	Sensitivity Cases	37-9
37.4	Reactor Coolant System Piping and Steam Generator Tube Failure	37-10
37.4.1	Creep Rupture Timing	37-10
37.4.2	Results of the Component Failure Analysis	37-11
37.4.3	Conclusions from the Component Failure Analysis	37-12

TABLE OF CONTENTS (continued)

37.5	Development of the Decomposition Event Tree	37-12
37.6	Quantification of the Decomposition Event Tree	37-13
37.6.1	Node SP	37-13
37.6.2	Node NC	37-14
37.6.3	Node LM	37-15
37.6.4	Node SG	37-15
37.6.5	Node HL	37-16
37.6.6	Node ME	37-16
37.7	Results	37-17
37.8	References	37-17

CHAPTER 38 DECOMPOSITION EVENT TREE - ANALYSIS OF IN-VESSEL STEAM EXPLOSION

38.1	Discussion of the Issue	38-1
38.2	Discussion of Controlling Phenomena and Uncertainties	38-2
38.2.1	Can an Explosion Occur?	38-2
38.2.2	How Much Core Material Would Be Involved?	38-3
38.2.3	How Much Water Would Be Involved?	38-5
38.2.4	What Is Efficiency of Interaction?	38-5
38.2.5	What Is the Likelihood of Forming Slug?	38-7
38.2.6	What Is the Likelihood of Vessel Failure with Consequential Containment Failure?	38-7
38.3	Development of the Decomposition Event Tree	38-9
38.4	Quantification of the Decomposition Event Tree	38-10
38.4.1	Node RP	38-10
38.4.2	Node FR	38-11
38.4.3	Node WA	38-11
38.4.4	Node MX	38-12
38.4.5	Node SX	38-12
38.4.6	Node VF	38-13
38.5	Results	38-13
38.6	References	38-14

CHAPTER 39 DECOMPOSITION EVENT TREE - ANALYSIS OF EX-VESSEL STEAM EXPLOSION

39.1	Discussion of the Issue	39-1
39.2	Discussion of Controlling Phenomena and Uncertainties	39-2
39.2.1	How Much Core Material Would be Involved?	39-3
39.2.2	How Much Water Would be Involved	39-6
39.2.3	What is Efficiency of Interaction?	39-6
39.2.4	What is the Likelihood of Containment Failure Due to Tearing of Containment Penetrations?	39-8
39.2.5	What is the Likelihood of Containment Failure Due to Shock Wave and/or Overpressure?	39-9
39.3	Development of the Decomposition Event Tree	39-9

TABLE OF CONTENTS (continued)

39.4	Quantification of the Decomposition Event Tree	39-10
39.4.1	Node FR	39-10
39.4.2	Node WA	39-11
39.4.3	Node MX	39-11
39.4.4	Node WF	39-12
39.4.5	Node CF	39-12
39.5	Results	39-12
39.6	References	39-13
 CHAPTER 40 DECOMPOSITION EVENT TREE – ANALYSIS OF EX-VESSEL DEBRIS COOLABILITY		
40.1	Discussion of the Issue	40-1
40.2	Discussion of Controlling Phenomena and Uncertainties	40-2
40.2.1	Reactor Vessel Pressure at Vessel Failure	40-2
40.2.2	Debris Mass Expelled from the Reactor Vessel	40-2
40.2.3	Ex-Vessel Steam Explosions	40-3
40.2.4	Debris Configuration	40-3
40.2.5	Debris Spreading	40-4
40.2.6	Long-Term Heat Flux from the Debris to Overlying Water	40-4
40.3	Development of the Decomposition Event Tree	40-5
40.4	Quantification of the Decomposition Event Tree	40-6
40.4.1	Node DM	40-6
40.4.2	Node SE - Steam Explosions	40-8
40.4.3	Node DD - Debris Dispersal	40-8
40.5	Results	40-13
40.6	References	40-13
 CHAPTER 41 DECOMPOSITION EVENT TREE - HYDROGEN COMBUSTION ANALYSIS		
41.1	Discussion of the Issue	41-1
41.2	Controlling Phenomena	41-2
41.3	Assumptions and Phenomenological Uncertainties	41-3
41.3.1	Degree of Cladding Oxidation	41-4
41.3.2	Flammability Limits	41-5
41.3.3	Definition of Global Burn	41-5
41.3.4	Detonation Limits and Loads	41-6
41.3.5	Igniter System	41-6
41.3.6	Other Ignition Sources	41-7
41.3.7	Previous Global Burns	41-8
41.3.8	Effects of Core-Concrete Interactions	41-8
41.4	Hydrogen Combustion during the In-Vessel Phase	41-8
41.4.1	MAAP4 Analyses for Early Hydrogen Combustion	41-9
41.4.2	Decomposition Event Tree Analysis for Early Hydrogen Combustion	41-10

TABLE OF CONTENTS (continued)

41.4.3	Quantification of the Early Hydrogen Combustion Decomposition Event Tree	41-11
41.4.4	Early Hydrogen Combustion Decomposition Event Tree Quantification Results	41-14
41.5	Intermediate and Late Hydrogen Combustion	41-14
41.5.1	MAAP4 Analysis Results and Conclusions for Intermediate and Late Hydrogen Combustion	41-14
41.5.2	Decomposition Event Tree Analysis for Intermediate and Late Hydrogen Combustion	41-16
41.5.3	Quantification of the Intermediate and Late Hydrogen Combustion Decomposition Event Trees	41-17
41.5.4	Intermediate and Late Hydrogen Combustion Decomposition Event Tree Quantification Results	41-22
41.6	References	41-23

CHAPTER 42 CONDITIONAL CONTAINMENT FAILURE PROBABILITY DISTRIBUTION

42.1	Introduction	42-1
42.2	Probabilistic Model	42-1
42.3	Containment Failure Characteristics	42-2
42.3.1	Mean Values for Containment Failure	42-2
42.3.2	Uncertainties in Containment Failure	42-3
42.4	Containment Failure Predictions	42-4
42.4.1	Containment Cylindrical Shell	42-4
42.4.2	Ellipsoidal Upper Head	42-4
42.4.3	Equipment Hatches	42-5
42.4.4	Personnel Airlock	42-5
42.5	Overall Failure Distribution	42-6
42.6	Summary and Conclusions	42-7
42.7	References	42-7

CHAPTER 43 RELEASE FREQUENCY QUANTIFICATION

43.1	Containment Event Tree Quantification	43-1
43.1.1	Containment Event Tree Base Quantification	43-1
43.1.2	In-Vessel Retention Sensitivity Quantification	43-9
43.2	Containment Event Tree Quantification Conclusions	43-9
43.3	References	43-11

LIST OF TABLES

Table 35-1	AP600 Containment Event Tree Nodal Questions	35-19
Table 35-2	AP600 Release Category Definition Summary	35-20
Table 35-3	Summary of Level 1 Accident Sequence Subclasses	35-21
Table 35-4	Summary of CET Accident Sequence Subclasses	35-22
Table 35-5	Summary of Core Damage Frequency by Level 1 Accident Class	35-23
Table 36-1	Combinations of Uncertainties for the IVR DET	36-15
Table 36-2	Material Properties Used for IVR Analysis	36-16
Table 36-3	Input to IVR Analysis	36-16
Table 37-1	Reactor Coolant System Piping Parameters	37-19
Table 37-2	Timing of Key Events in the MAAP4 Analysis	37-19
Table 38-1	Experiments Demonstrating a High-Pressure Cut-Off	38-17
Table 38-2	Sandia Iron-Thermite Test Experiments with an Artificial Trigger	38-18
Table 38-3	Sandia Iron-Thermite and Corium A+R Tests	38-19
Table 39-1	Sandia Iron-Thermite Test Experiments with an Artificial Trigger	39-15
Table 39-2	Sandia Iron-Thermite and Corium A+R Tests	39-16
Table 40-1	Properties of the Main Concrete Types (from Reference 40-11)	40-15
Table 41-1	AP600 Integrated In-Vessel Hydrogen Generation	41-24
Table 41-2	AP600 Hydrogen Combustion Peak Pressure and Temperature Estimates	41-25
Table 41-3	AP600 Hydrogen Combustion Peak Pressure and Temperature Estimates	41-26
Table 41-4	AP600 Early Hydrogen Combustion DET Split Fractions for Node FL	41-27
Table 41-5	Conditional Probability of Deflagration-to-Detonation Transition in the IRWST for Early Hydrogen Combustion in AP600 Containment	41-28
Table 41-6	Conditional Probability of Deflagration-to-Detonation Transition in the Lower Compartments for Early Hydrogen Combustion in AP600 Containment	41-28
Table 41-7	Quantification Results of the Early Hydrogen Combustion DET	41-29
Table 41-8	Summary of MAAP4 Analyses for Loss-of-Feedwater Sequences	41-30
Table 41-9	Summary of MAAP4 Analyses for Hot Leg 2" Small LOCA	41-32
Table 41-10	DET Quantifications for Intermediate Hydrogen Combustion (CET Node HC2)	41-33

LIST OF TABLES (continued)

Table 41-11	DET Quantifications for Late Hydrogen Combustion (CET Node HC3)	41-34
Table 41-12	Analysis of Pressure Peak Due to Intermediate Combustion Event (HC2)	41-35
Table 41-13	Analysis of Pressure Peak Due to Late Combustion Event (HC3)	41-36
Table 41-14	DET Quantifications for Intermediate Hydrogen Combustion (CET Nodes HC2, CF2)	41-37
Table 41-15	DET Quantifications for Late Hydrogen Combustion (CET Nodes HC3, CF3)	41-38
Table 42-1	Parameters Used in the Construction of the AP600 Containment Failure Probability Distribution	42-8
Table 42-2	Cumulative Containment Failure Probability	42-9
Table 43-1	AP600 Containment Event Tree Nodes Quantification Methods	43-12
Table 43-2	AP600 Containment Event Tree Nodal Split Fractions	43-13
Table 43-3	AP600 Containment Event Tree Base Case Quantification Results - Release Category Frequencies (Per Reactor-Year)	43-17
Table 43-4	AP600 Containment Event Tree Base Case Quantification Results - Release Category Frequencies (Per Reactor-Year)	43-18
Table 43-5	Release Category IC Dominant Sequences Release Category IC Frequency = $2.4\text{E-}7$ Per Reactor-Year	43-19
Table 43-6	Release Category ICP Dominant Sequences Release Category ICP Frequency = $1.9\text{E-}11$ Per Reactor-Year	43-20
Table 43-7	Release Category XL Dominant Sequences Release Category XL Frequency = $1.9\text{E-}9$ Per Reactor-Year	43-21
Table 43-8	Release Category BP Dominant Sequences Release Category BP Frequency = $5.9\text{E-}9$ Per Reactor-Year	43-22
Table 43-9	Release Category CI Dominant Sequences Release Category CI Frequency = $2.8\text{E-}9$ Per Reactor-Year	43-22
Table 43-10	Release Category CI-C Dominant Sequences Release Category CI-C Frequency = $1.4\text{E-}11$ Per Reactor-Year	43-23
Table 43-11	Release Category CFE Dominant Sequences Release Category CFE Frequency = $9.5\text{E-}11$ Per Reactor-Year	43-24
Table 43-12	Release Category CFE-C Dominant Sequences Release Category CFE-C Frequency = $6.0\text{E-}11$ Per Reactor-Year	43-24
Table 43-13	Release Category CFI Dominant Sequences Release Category CFI Frequency = $3.6\text{E-}12$ Per Reactor-Year	43-25
Table 43-14	Release Category CFL Dominant Sequences Release Category CFL Frequency = $6.3\text{E-}13$ Per Reactor-Year	43-26
Table 43-15	Release Category CFV Dominant Sequences Release Category CFV Frequency = $1.3\text{E-}10$ Per Reactor-Year	43-27

LIST OF FIGURES

Figure 35-1	Skeleton Containment Event Tree	35-24
Figure 35-2	AP600 Containment Event Tree	35-25
Figure 36-1	In-Vessel Retention Phenomena	36-17
Figure 36-2	In-Vessel Retention Model	36-18
Figure 36-3	AP600 Reactor Vessel Standoff Insulation	36-19
Figure 36-4	AP600 Cavity Flooding System Schematic	36-20
Figure 36-5	AP600 Cavity Flooding Rate	36-21
Figure 36-6	AP600 IVR Decomposition Event Tree	36-22
Figure 36-7	Case IVR.1 - Heat Flux Distribution Through Vessel Wall	36-23
Figure 36-8	Case IVR.1 - Remaining Thickness of Vessel Wall	36-24
Figure 36-9	Case IVR.2 - Heat Flux Distribution Through Vessel Wall	36-25
Figure 36-10	Case IVR.2 - Remaining Thickness of Vessel Wall	36-26
Figure 36-11	Case IVR.3 - Heat Flux Distribution Through Vessel Wall	36-27
Figure 36-12	Case IVR.3 - Remaining Thickness of Vessel Wall	36-28
Figure 36-13	Case IVR.4 - Heat Flux Distribution Through Vessel Wall	36-29
Figure 36-14	Case IVR.4 - Remaining Thickness of Vessel Wall	36-30
Figure 36-15	Case IVR.5 - Heat Flux Distribution Through Vessel Wall	36-31
Figure 36-16	Case IVR.5 - Remaining Thickness of Vessel Wall	36-32
Figure 36-17	Case IVR.6 - Heat Flux Distribution Through Vessel Wall	36-33
Figure 36-18	Case IVR.6 - Remaining Thickness of Vessel Wall	36-34
Figure 36-19	Case IVR.7 - Heat Flux Distribution Through Vessel Wall	36-35
Figure 36-20	Case IVR.7 - Remaining Thickness of Vessel Wall	36-36
Figure 36-21	Case IVR.8 - Heat Flux Distribution Through Vessel Wall	36-37
Figure 36-22	Case IVR.8 - Remaining Thickness of Vessel Wall	36-38
Figure 36-23	Case IVR.9 - Heat Flux Distribution Through Vessel Wall	36-39
Figure 36-24	Case IVR.9 - Remaining Thickness of Vessel Wall	36-40
Figure 36-25	Case IVR.10 - Heat Flux Distribution Through Vessel Wall	36-41
Figure 36-26	Case IVR.10 - Remaining Thickness of Vessel Wall	36-42
Figure 36-27	Case IVR.11 - Heat Flux Distribution Through Vessel Wall	36-43
Figure 36-28	Case IVR.11 - Remaining Thickness of Vessel Wall	36-44
Figure 36-29	Case IVR.12 - Heat Flux Distribution Through Vessel Wall	36-45
Figure 36-30	Case IVR.12 - Remaining Thickness of Vessel Wall	36-46
Figure 36-31	Case IVR.13 - Heat Flux Distribution Through Vessel Wall	36-47
Figure 36-32	Case IVR.13 - Remaining Thickness of Vessel Wall	36-48
Figure 36-33	Case IVR.14 - Heat Flux Distribution Through Vessel Wall	36-49
Figure 36-34	Case IVR.14 - Remaining Thickness of Vessel Wall	36-50
Figure 36-35	Case IVR.15 - Heat Flux Distribution Through Vessel Wall	36-51
Figure 36-36	Case IVR.15 - Remaining Thickness of Vessel Wall	36-52
Figure 36-37	Case IVR.16 - Heat Flux Distribution Through Vessel Wall	36-53
Figure 36-38	Case IVR.16 - Remaining Thickness of Vessel Wall	36-54
Figure 37-1	Time-to-Failure Data for Reactor Coolant System Components	37-20
Figure 37-2	Time-to-Failure Data for AP600 Reactor Coolant System Components	37-20

LIST OF FIGURES (continued)

Figure 37-3	MA/AP Nodalization	37-21
Figure 37-4	Case HP - Base Case with Pressurized Secondary System Primary System and Secondary System Pressure	37-22
Figure 37-5	Case HP - Base Case with Pressurized Secondary System Reactor Vessel Water Level	37-23
Figure 37-6	Case HP - Base Case with Pressurized Secondary System Primary System Core and Gas Temperature	37-24
Figure 37-7	Case HP - Base Case with Pressurized Secondary System Core to Upper Plenum Flow Rate	37-25
Figure 37-8	Case HP - Base Case with Pressurized Secondary System Primary System Natural Circulation Volumetric Flow	37-26
Figure 37-9	Case HP - Base Case with Pressurized Secondary System Reactor Coolant System Component Average Through-Wall Temperature	37-27
Figure 37-10	Case DP - Base Case with Depressurized Secondary System Primary System and Secondary System Pressure	37-28
Figure 37-11	Case DP - Base Case with Depressurized Secondary System Reactor Vessel Water Level	37-29
Figure 37-12	Case DP - Base Case with Depressurized Secondary System Primary System Core and Gas Temperature	37-30
Figure 37-13	Case DP - Base Case with Depressurized Secondary System Core to Upper Plenum Flow Rate	37-31
Figure 37-14	Case DP - Base Case with Depressurized Secondary System Primary System Natural Circulation Volumetric Flow	37-32
Figure 37-15	Case DP - Base Case with Depressurized Secondary System Reactor Coolant System Component Average Through-Wall Temperature	37-33
Figure 37-16	Case NC - Sensitivity Case with Reduced Natural Circulation Primary System and Secondary System Pressure	37-34
Figure 37-17	Case NC - Sensitivity Case with Reduced Natural Circulation Reactor Vessel Water Level	37-35
Figure 37-18	Case NC - Sensitivity Case with Reduced Natural Circulation Primary System Core and Gas Temperature	37-36
Figure 37-19	Case NC - Sensitivity Case with Reduced Natural Circulation Core to Upper Plenum Flow Rate	37-37
Figure 37-20	Case NC - Sensitivity Case with Reduced Natural Circulation Primary System Natural Circulation Volumetric Flow	37-38
Figure 37-21	Case NC - Sensitivity Case with Reduced Natural Circulation Reactor Coolant System Component Average Through-Wall Temperature	37-39
Figure 37-22	Case NC - Sensitivity Case with Reduced Natural Circulation Core Debris in Lower Head	37-40
Figure 37-23	Case FL - Sensitivity Case with Flooded Reactor Cavity Primary System and Secondary System Pressure	37-41
Figure 37-24	Case FL - Sensitivity Case with Flooded Reactor Cavity Reactor Vessel Water Level	37-42

LIST OF FIGURES (continued)

Figure 37-25	Case FL - Sensitivity Case with Flooded Reactor Cavity Primary System Core and Gas Temperature	37-43
Figure 37-26	Case FL - Sensitivity Case with Flooded Reactor Cavity Core to Upper Plenum Flow Rate	37-44
Figure 37-27	Case FL - Sensitivity Case with Flooded Reactor Cavity Primary System Natural Circulation Volumetric Flow	37-45
Figure 37-28	Case FL - Sensitivity Case with Flooded Reactor Cavity Reactor Coolant System Component Average Through-Wall Temperature	37-46
Figure 37-29	Case FL - Sensitivity Case with Flooded Reactor Cavity Core Debris in Lower Head	37-47
Figure 37-30	Case HP - Reactor Coolant System Component Creep Damage Best Estimate Hot Leg Larson-Miller Parameter	37-48
Figure 37-31	Case HP - Reactor Coolant System Component Creep Damage Upper Bound Hot Leg Larson-Miller Parameter	37-49
Figure 37-32	Case DP - Reactor Coolant System Component Creep Damage Best Estimate Hot Leg Larson-Miller Parameter	37-50
Figure 37-33	Case DP - Reactor Coolant System Component Creep Damage Upper Bound Hot Leg Larson-Miller Parameter	37-51
Figure 37-34	Case NC - Reactor Coolant System Component Creep Damage Best Estimate Hot Leg Larson-Miller Parameter	37-52
Figure 37-35	Case NC - Reactor Coolant System Component Creep Damage Upper Bound Hot Leg Larson-Miller Parameter	37-53
Figure 37-36	Case FL - Reactor Coolant System Component Creep Damage Best Estimate Hot Leg Larson-Miller Parameter	37-54
Figure 37-37	Case FL - Reactor Coolant System Component Creep Damage Upper Bound Hot Leg Larson-Miller Parameter	37-55
Figure 37-38	AP600 Thermally Induced Reactor Coolant System Pressure Boundary Failure Decomposition Event Tree	37-56
Figure 38-1	Behavior Modeled in WASH-1400	38-20
Figure 38-2	Schematic Representation of the Deformation of an LWR Vessel Due to an Internal Steam Explosion	38-21
Figure 38-3	Decomposition Event Tree for In-Vessel Steam Explosion	38-22
Figure 38-4	Quantified Decomposition Event Tree for In-Vessel Steam Explosion	38-23
Figure 39-1	Decomposition Event Tree for Ex-Vessel Steam Explosion	39-17
Figure 39-2	Quantified Decomposition Event Tree for Ex-Vessel Steam Explosion	39-18
Figure 40-1	Ex-Vessel Debris Coolability Decomposition Event Tree	40-16
Figure 40-2	MELTSPREAD Nodalization for the AP600, From Reference 40-10	40-17

LIST OF FIGURES (continued)

Figure 41-1	Flammability Limit Fit at Elevated Temperatures (Reference 41-5)	41-39
Figure 41-2	Combustion Completeness for Nevada Test Site Premixed Combustion Tests (Reference 41-6)	41-40
Figure 41-3	Theoretical Adiabatic, Constant-Volume Combustion Pressures of Hydrogen-Air- Mixtures (Reference 41-7)	41-41
Figure 41-4	AP600 Case 1A No Hydrogen Ignition Case Containment Pressure	41-42
Figure 41-5	AP600 Case 1A No Hydrogen Ignition Case Containment Gas Temperature	41-43
Figure 41-6	AP600 Case 1A No Hydrogen Ignition Case In-Vessel Hydrogen Generation	41-44
Figure 41-7	AP600 Case 1A No Hydrogen Ignition Case Best Estimate In-Vessel Hydrogen Generation Containment Compartment Hydrogen Mole Fractions	41-45
Figure 41-8	AP600 Case 1A No Hydrogen Ignition Case Bounding Estimate In-Vessel Hydrogen Generation Containment Compartment Hydrogen Mole Fractions	41-46
Figure 41-9	AP600 Case 1A No Hydrogen Ignition Case Best Estimate In-Vessel Hydrogen Generation Containment Compartment Steam Mole Fractions	41-47
Figure 41-10	AP600 Case 1A No Hydrogen Ignition Case Bounding Estimate In-Vessel Hydrogen Generation Containment Compartment Steam Mole Fractions	41-48
Figure 41-11	AP600 Case 1A No Hydrogen Ignition Case Best Estimate In-Vessel Hydrogen Generation Containment Flammability Limits	41-49
Figure 41-12	AP600 Case 1A No Hydrogen Ignition Case Bounding Estimate In-Vessel Hydrogen Generation Containment Flammability Limits	41-50
Figure 41-13	AP600 Case 1AP No Hydrogen Ignition Case Containment Pressure	41-51
Figure 41-14	AP600 Case 1AP No Hydrogen Ignition Case Containment Gas Temperature	41-52
Figure 41-15	AP600 Case 1AP No Hydrogen Ignition Case In-Vessel Hydrogen Generation	41-53
Figure 41-16	AP600 Case 1AP No Hydrogen Ignition Case Best Estimate In-Vessel Hydrogen Generation Containment Compartment Hydrogen Mole Fractions	41-54
Figure 41-17	AP600 Case 1AP No Hydrogen Ignition Case Bounding Estimate In-Vessel Hydrogen Generation Containment Compartment Hydrogen Mole Fractions	41-55
Figure 41-18	AP600 Case 1AP No Hydrogen Ignition Case Best Estimate In-Vessel Hydrogen Generation Containment Compartment Steam Mole Fractions	41-56

LIST OF FIGURES (continued)

Figure 41-19	AP600 Case 1AP No Hydrogen Ignition Case Bounding Estimate In-Vessel Hydrogen Generation Containment Compartment Steam Mole Fractions	41-57
Figure 41-20	AP600 Case 1AP No Hydrogen Ignition Case Best Estimate In-Vessel Hydrogen Generation Containment Flammability Limits	41-58
Figure 41-21	AP600 Case 1AP No Hydrogen Ignition Case Bounding Estimate In-Vessel Hydrogen Generation Containment Flammability Limits	41-59
Figure 41-22	AP600 Case 3BE No Reflood No Hydrogen Ignition Case Containment Pressure	41-60
Figure 41-23	AP600 Case 3BE No Reflood No Hydrogen Ignition Case Containment Gas Temperature	41-61
Figure 41-24	AP600 Case 3BE No Reflood No Hydrogen Ignition Case In-Vessel Hydrogen Generation	41-62
Figure 41-25	AP600 Case 3BE No Reflood No Hydrogen Ignition Case Best Estimate In-Vessel Hydrogen Generation Containment Compartment Hydrogen Mole Fractions	41-63
Figure 41-26	AP600 Case 3BE No Reflood No Hydrogen Ignition Case Bounding Estimate In-Vessel Hydrogen Generation Containment Compartment Hydrogen Mole Fractions	41-64
Figure 41-27	AP600 Case 3BE No Hydrogen Ignition Case Best Estimate In-Vessel Hydrogen Generation Containment Compartment Steam Mole Fractions	41-65
Figure 41-28	AP600 Case 3BE No Reflood No Hydrogen Ignition Case Bounding Estimate In-Vessel Hydrogen Generation Containment Compartment Steam Mole Fractions	41-66
Figure 41-29	AP600 Case 3BE No Reflood No Hydrogen Ignition Case Best Estimate In-Vessel Hydrogen Generation Containment Flammability Limits	41-67
Figure 41-30	AP600 Case 3BE No Reflood No Hydrogen Ignition Case Bounding Estimate In-Vessel Hydrogen Generation Containment Flammability Limits	41-68
Figure 41-31	AP600 Case 3BE With Reflood No Hydrogen Ignition Case Containment Pressure	41-69
Figure 41-32	AP600 Case 3BE With Reflood No Hydrogen Ignition Case Containment Gas Temperature	41-70
Figure 41-33	AP600 Case 3BE With Reflood No Hydrogen Ignition Case In-Vessel Hydrogen Generation	41-71
Figure 41-34	AP600 Case 3BE With Reflood No Hydrogen Ignition Case Best Estimate In-Vessel Hydrogen Generation Containment Compartment Hydrogen Mole Fractions	41-72
Figure 41-35	AP600 Case 3BE With Reflood No Hydrogen Ignition Case Bounding Estimate In-Vessel Hydrogen Generation Containment Hydrogen Mole Fractions	41-73

LIST OF FIGURES (continued)

Figure 41-36	AP600 Case 3BE With Reflood No Hydrogen Ignition Case Best Estimate In-Vessel Hydrogen Generation Containment Compartment Steam Mole Fractions	41-74
Figure 41-37	AP600 Case 3BE With Reflood No Hydrogen Ignition Case Bounding Estimate In-Vessel Hydrogen Generation Containment Compartment Steam Mole Fractions	41-75
Figure 41-38	AP600 Case 3BE With Reflood No Hydrogen Ignition Case Best Estimate In-Vessel Hydrogen Generation Containment Flammability Limits	41-76
Figure 41-39	AP600 Case 3BE With Reflood No Hydrogen Ignition Case Bounding Estimate In-Vessel Hydrogen Generation Containment Flammability Limits	41-77
Figure 41-40	AP600 Case 3BE With No Reflood, PCS Water Failed - No Hydrogen Ignition Case Containment Pressure	41-78
Figure 41-41	AP600 Case 3BE With No Reflood, PCS Water Failed - No Hydrogen Ignition Case Containment Gas Temperature	41-79
Figure 41-42	AP600 Case 3BE With No Reflood, PCS Water Failed - No Hydrogen Ignition Case In-Vessel Hydrogen Generation	41-80
Figure 41-43	AP600 Case 3BE With No Reflood, PCS Water Failed - No Hydrogen Ignition Case Best Estimate In-Vessel Hydrogen Generation Containment Compartment Hydrogen Mole Fractions	41-81
Figure 41-44	AP600 Case 3BE With No Reflood, PCS Water Failed - No Hydrogen Ignition Case Bounding Estimate In-Vessel Hydrogen Generation Containment Compartment Hydrogen Mole Fractions	41-82
Figure 41-45	AP600 Case 3BE With No Reflood, PCS Water Failed - No Hydrogen Ignition Case Best Estimate In-Vessel Hydrogen Generation Containment Compartment Steam Mole Fractions	41-83
Figure 41-46	AP600 Case 3BE With No Reflood, PCS Water Failed - No Hydrogen Ignition Case Bounding Estimate In-Vessel Hydrogen Generation Containment Compartment Steam Mole Fractions	41-84
Figure 41-47	AP600 Case 3BE With No Reflood, PCS Water Failed - No Hydrogen Ignition Case Best Estimate In-Vessel Hydrogen Generation Containment Flammability Limits	41-85
Figure 41-48	AP600 Case 3BE With No Reflood, PCS Water Failed - No Hydrogen Ignition Case Bounding Estimate In-Vessel Hydrogen Generation Containment Flammability Limits	41-86
Figure 41-49	AP600 Case 3BE With Reflood No Hydrogen Ignition Case, PCS Failed Containment Pressure	41-87
Figure 41-50	AP600 Case 3BE With Reflood No Hydrogen Ignition Case, PCS Failed Containment Gas Temperature	41-88
Figure 41-51	AP600 Case 3BE With Reflood No Hydrogen Ignition Case, PCS Failed In-Vessel Hydrogen Generation	41-89

LIST OF FIGURES (continued)

Figure 41-52	AP600 Case 3BE With Reflood No Hydrogen Ignition Case, PCS Failed Best Estimate In-Vessel Hydrogen Generation Containment Compartment Hydrogen Mole Fractions	41-90
Figure 41-53	AP600 Case 3BE With Reflood No Hydrogen Ignition Case, PCS Failed Bounding Estimate In-Vessel Hydrogen Generation Containment Compartment Hydrogen Mole Fractions	41-91
Figure 41-54	AP600 Case 3BE With Reflood No Hydrogen Ignition Case, PCS Failed Best Estimate In-Vessel Hydrogen Generation Containment Compartment Steam Mole Fractions	41-92
Figure 41-55	AP600 Case 3BE With Reflood No Hydrogen Ignition Case, PCS Failed Bounding Estimate In-Vessel Hydrogen Generation Containment Compartment Steam Mole Fractions	41-93
Figure 41-56	AP600 Case 3BE With Reflood No Hydrogen Ignition Case, PCS Failed Best Estimate In-Vessel Hydrogen Generation Containment Flammability Limits	41-94
Figure 41-57	AP600 Case 3BE With Reflood No Hydrogen Ignition Case, PCS Failed Bounding Estimate In-Vessel Hydrogen Generation Containment Flammability Limits	41-95
Figure 41-58	AP600 Case 3C No Hydrogen Ignition Case Containment Pressure	41-96
Figure 41-59	AP600 Case 3C No Hydrogen Ignition Case Containment Gas Temperature	41-97
Figure 41-60	AP600 Case 3C No Hydrogen Ignition Case In-Vessel Hydrogen Generation	41-98
Figure 41-61	AP600 Case 3C No Hydrogen Ignition Case Best Estimate In-Vessel Hydrogen Generation Containment Compartment Hydrogen Mole Fractions	41-99
Figure 41-62	AP600 Case 3C No Hydrogen Ignition Case Bounding Estimate In-Vessel Hydrogen Generation Containment Compartment Hydrogen Mole Fractions	41-100
Figure 41-63	AP600 Case 3C No Hydrogen Ignition Case Best Estimate In-Vessel Hydrogen Generation Containment Compartment Steam Mole Fractions	41-101
Figure 41-64	AP600 Case 3C No Hydrogen Ignition Case Bounding Estimate In-Vessel Hydrogen Generation Containment Compartment Steam Mole Fractions	41-102
Figure 41-65	AP600 Case 3C No Hydrogen Ignition Case Best Estimate In-Vessel Hydrogen Generation Containment Flammability Limits	41-103
Figure 41-66	AP600 Case 3C No Hydrogen Ignition Case Bounding Estimate In-Vessel Hydrogen Generation Containment Flammability Limits	41-104
Figure 41-67	AP600 Case 3D No Hydrogen Ignition Case Containment Pressure	41-105

LIST OF FIGURES (continued)

Figure 41-68	AP600 Case 3D No Hydrogen Ignition Case Containment Gas Temperature	41-106
Figure 41-69	AP600 Case 3D No Hydrogen Ignition Case In-Vessel Hydrogen Generation	41-107
Figure 41-70	AP600 Case 3D No Hydrogen Ignition Case Best Estimate In-Vessel Hydrogen Generation Containment Compartment Hydrogen Mole Fractions	41-108
Figure 41-71	AP600 Case 3D No Hydrogen Ignition Case Bounding Estimate In-Vessel Hydrogen Generation Containment Compartment Hydrogen Mole Fractions	41-109
Figure 41-72	AP600 Case 3D No Hydrogen Ignition Case Best Estimate In-Vessel Hydrogen Generation Containment Compartment Steam Mole Fractions	41-110
Figure 41-73	AP600 Case 3D No Hydrogen Ignition Case Bounding Estimate In-Vessel Hydrogen Generation Containment Compartment Steam Mole Fractions	41-111
Figure 41-74	AP600 Case 3D No Hydrogen Ignition Case Best Estimate In-Vessel Hydrogen Generation Containment Flammability Limits	41-112
Figure 41-75	AP600 Case 3D No Hydrogen Ignition Case Bounding Estimate In-Vessel Hydrogen Generation Containment Flammability Limits	41-113
Figure 41-76	AP600 DET-EH2 - Early Hydrogen Combustion Decomposition Event Tree	41-114
Figure 41-77	AP600 DET - Intermediate and Late Hydrogen Combustion Decomposition Event Tree	41-115
Figure 42-1	AP600 Containment Fragility	42-10

1 INTRODUCTION

The Westinghouse AP600 Probabilistic Risk Assessment (PRA) team performed a low-power and shutdown risk assessment that is documented in Chapter 54 of the AP600 PRA document. The assessment was conducted to assess the risk (core damage frequency and large release frequency) of operations during shutdown conditions. The assessment examined operations when the reactor is in a subcritical state or is in transition between subcriticality and power operation up to 5 percent of rated power.

The Level 1 (core damage) and Level 2 (large release) PRA shutdown assessments are not being updated beyond Revision 7 of the AP600 PRA document. However, the Level 2 PRA at-power models and analysis are updated in Revision 8 of the PRA to address NRC comments and to credit the benefits of in-vessel retention of molten core debris. An evaluation of the Level 2 analysis for the shutdown core damage sequences shows that the results obtained from the latest at-power Level 2 models are almost identical to the previous Level 2 shutdown analysis. No new PRA insights could be gained from a detailed reassessment of the Level 2 shutdown analysis over those from the previous assessment.

This WCAP report contains the old Level 2 chapters that are still being referenced by the shutdown analysis in the AP600 PRA document. These chapters include Revision 3 of PRA Chapters 35 through 43, which are the following:

- Chapter 35, Containment Event Tree Analysis
- Chapter 36, Decomposition Event Tree - Analysis of In-Vessel Retention of Molten Core Debris
- Chapter 37, Decomposition Event Tree - Analysis of Thermally Induced Failures of the Reactor Coolant System Pressure Boundary
- Chapter 38, Decomposition Event Tree - Analysis of In-Vessel Steam Explosion
- Chapter 39, Decomposition Event Tree - Analysis of Ex-Vessel Steam Explosion
- Chapter 40, Decomposition Event Tree - Analysis of Ex-Vessel Debris Coolability
- Chapter 41, Decomposition Event Tree - Hydrogen Combustion Analysis
- Chapter 42, Conditional Containment Failure Probability Distribution
- Chapter 43, Release Frequency Quantification

CHAPTER 35

CONTAINMENT EVENT TREE ANALYSIS

35.1 Introduction

This chapter describes the containment event tree analysis. A containment event tree (CET) displays the characteristics of the severe accident progression that impact the fission-product source term to the environment. It is used to provide the likelihood, magnitude, and timing of the possible accident progressions and the fission-product releases to the environment for each of the AP600 accident classes.

A containment event tree (CET) has been developed for the AP600 PRA at-power events. The top events considered on the tree are presented in Table 35-1. A detailed description of the containment event tree development and structure follows.

35.2 Containment Event Tree - General Discussion

The containment event tree is a general tool which provides a logical and practical structure for uniting the complex phenomenology of postulated severe accident event sequences. The event tree approach allows the analyst to determine the likelihood of a particular event sequence progression. This approach also permits evaluation of the impact of uncertainty of the event progression on the overall results and conclusions of the study. The comprehensive treatment of severe accidents provided by the containment event tree provides assurance that important contributors to fission-product releases are identified and evaluated in a structured and disciplined approach. The bases for the top events (or nodal questions) on the tree are supported by analyses, evaluations and testing, empirical data from past studies, and the AP600 design.

This section details the preparation of the containment event tree for the AP600 PRA. The following sections lay out the thought process involved in creating the tree structure and present the containment event tree questions.

A containment event tree serves a number of purposes:

- It provides a logical, systematic approach to map the large number of severe accident sequence progressions that may occur. Each path on the tree represents a possible accident sequence progression resulting in some final containment state.
- It provides a convenient method of identifying the fission-product release timing and magnitude. The end-point of each path on the event tree represents a fission-product release.

- It provides a means of quantifying the likelihood of each of the proposed accident sequences. Each node on the tree is assigned a probability of success conditional on upstream event outcomes. The product of all the nodal probabilities on a path is the overall probability of the sequence.
- It provides a means of quantifying the likelihood of fission-product release magnitude and timing. The sum of the probabilities of similar fission-product release "end-points" provides the overall probability of these "release categories."

For example, the containment event tree could simply ask, Does the containment fail? The outcome results in two end-points via failure or success. A tree this simple is impractical since the final end-points are too coarse to reasonably identify all the possible release states. Additionally, the number of different possible sequences and resulting phenomena make the question impossible to quantify. On the other hand, it is possible to ask many questions of phenomena which will affect the containment and release state, resulting in many hundreds of thousands of end-states. This also is impractical as it becomes unmanageable to quantify or comprehend such a large tree. A balance must be found between a sufficient number of top nodes to adequately describe the accident progression and a tree that is practically sized for easy understanding.

Still, a practically-sized containment event tree will result in many end-points which must be accounted for. It is possible, to a first order, to group a number of different sequences into the same release category. Similarities in accident progression, containment failure time, and the containment fission-product source term make it reasonable to do this. In this way, the number of end-points that must be tracked is reduced from tens of thousands to tens.

35.3 Event Tree Construction

The containment event tree is quantified for a number of different end-states in the plant matrix (referred to as accident classes). Likewise, the containment event tree end-points are classified into groups of similar release characteristics called release categories. To provide an initial basic structure for the containment event tree, a simple containment event tree with each branch leading to one potential release category is used (Figure 35-1). This "skeleton" tree addresses timing of containment failure and provides a useful aid to the construction of a more quantifiable tree. The system and phenomenological nodes that can contribute to the containment failure timing or to the fission-product release magnitude are then filled into the skeleton tree.

As an aid to the definition of the additional event tree top events (or nodal questions), a set of criteria were established by which each question could be tested in order to identify irrelevant or unnecessary nodal questions. These were as follows:

1. A phenomenological event will be considered if it can significantly affect the fission-product release characteristics or impact the containment integrity.

2. A phenomenological event will be considered if it can affect a downstream event that satisfies criterion 1.
3. A system functionality event will be considered if it determines the branch of the containment event tree that needs to be considered, or if it is not explicitly defined by the accident class and it significantly affects events satisfying criterion 1.
4. An operator action will be considered if it significantly affects events satisfying criterion 1, and it is not included in the Level 1 PRA analysis.

The normal questions included on the AP600 containment event tree are presented in Table 35-1.

35.4 Fission-Product Release Considerations

The radiological consequences of the core melt accident are largely determined by three major considerations: the time of containment failure relative to the time of major fission-product release from the core or core debris; the mode of containment failure (bypass, isolation failure, enhanced leakage, self-limiting failure, gross failure, or intact containment); and fission-product removal mechanisms.

AP600 does not have active containment fission-product removal mechanisms such as containment sprays. Therefore, natural deposition processes are relied on to scrub aerosols from the containment atmosphere. The natural processes are time dependent, thus the timing of the containment failure and the degree of the fission-product removal are directly related and treated together for the AP600 containment event tree development.

35.4.1 Fission-Product Release Timing

In defining the release categories, the time of containment failure is specified in relation to the time of the fission-product release mechanisms. Two important release times are considered: the onset of core damage and core-concrete interaction.

35.4.1.1 The Onset of Core Damage

During the initial stages of the severe accident, the core uncovers and the fuel temperature rapidly increases because of decay heat and heat of oxidation of the zirconium. This heatup can lead to failure of the fuel rod cladding. If the cladding fails, a fraction of the noble gases and volatile fission products, normally present in the fuel-clad gap, will be released into the reactor coolant system. This is normally called the "gap release."

As the fuel pellet temperature rises toward the melting point, the release of fission products from in the fuel is enhanced. During the melting of the fuel matrix, a large proportion of the



total core inventory of volatile fission products is released from the fuel. This is normally called the "melt release."

The gap release, temperature-enhanced fission-product release and initiation of melt release occur sufficiently close together such that they are considered to occur coincidentally and termed the onset of core damage. Indications of the onset of core damage in the analyses are in-vessel hydrogen generation, and noble gas and volatile fission products in the reactor coolant system.

35.4.1.2 Core-Concrete Interaction

The second release mechanism considered to be of importance occurs if the molten fuel fails the reactor pressure vessel, is released to the containment, and begins attacking the concrete basemat. This yields a release of any remaining noble gas and volatile species, in addition to nonvolatile fission products released by the chemical processes, and agitation of the debris pool, which occur during the core-concrete interaction. Indications of core-concrete interaction are the generation of flammable and noncondensable gases from the debris pool and the degradation of the concrete basemat.

35.4.2 Containment Failure Considerations

The failure mode of the containment determines the area available for fission-product release from the containment and significantly affects the timing with respect to the release of fission products. The containment failure modes considered in the development of the AP600 release categories are intact containment, enhanced leakage, containment bypass, isolation failure, self-limiting failure, and gross failure. The self-limiting containment failure mode applies mainly to concrete containments and, therefore, is ruled out for further consideration for the steel shell AP600 containment. Induced containment structural failures are considered to be gross failures that result in sudden and complete depressurization of the containment. Each of the other failure modes is discussed in more detail in the following sections.

Containment failure can be postulated to occur in one of four periods defined relative to the occurrence of the onset of fuel damage. These time periods are termed early, intermediate, late, and very late and are defined in detail in the following sections. Consideration of the occurrence of the core-concrete interaction affects the release magnitude and can affect the containment integrity.

35.4.2.1 Intact Containment and Enhanced Leakage

If the containment integrity is maintained throughout the accident, then the release of radiation from the containment is due to nominal leakage and is expected to be within the design basis of the containment. This is the "no failure" containment failure mode and is termed intact containment. The main location for fission-product leakage from the containment is into the auxiliary building where significant deposition of aerosol fission products may occur.



Consideration is made for the possibility that the containment leakage is not within the technical specifications, and the resulting 24-hour dose to the environment is not less than 25 rem at the site boundary, a design goal of the AP600. This failure mode is termed enhanced leakage.

35.4.2.2 Containment Bypass

A containment bypass release is postulated to occur if the primary system fluid and/or fission products are released directly from the reactor coolant system to the environment, thus bypassing the containment completely. In such a case, the fission-product release begins approximately at the onset of fuel damage, and there is no attenuation of the magnitude of the source term from natural deposition processes beyond that which occurs in the reactor coolant system and secondary volume. The energy of release of a containment bypass sequence is high, usually associated with the release of steam from the steam generator safety valves at the setpoint pressure.

35.4.2.3 Failure of Containment Isolation

A containment isolation failure occurs because of the postulated failure of the system or valves that close the penetrations between the containment atmosphere and the environment. For such a failure, fission-product releases from the reactor coolant system can leak directly from the containment to the environment with diminished potential for attenuation. Most isolation failures occur at a penetration that connects the containment with the auxiliary building. The auxiliary building may provide additional attenuation of aerosol fission-product releases. However, this is not credited in the containment isolation failure cases. The energy of the release is low (not driven by a high-containment pressure), since the containment is open and does not pressurize significantly.

35.4.2.4 Early Containment Failure

During the core melt and relocation process, several dynamic phenomena can be postulated to result in rapid pressurization of the containment to the point of failure. The combustion of hydrogen generated in-vessel, steam explosions, and reactor vessel failure from high pressure are major phenomena postulated to have the potential to fail the containment. If the containment fails during or soon after the time when the fuel is overheating and starting to melt, the potential for attenuation of the fission product release will diminish because of its short residence time in the containment. In this case, the fission products released to the containment prior to the containment failure will be discharged at high pressure to the environment, as the containment blows down. Subsequent release of fission products can then pass directly to the environment at low energy. The failure of the containment due to dynamic phenomena that occur during core relocation is termed early containment failure.



35.4.2.5 Intermediate Containment Failure

Intermediate containment failure is defined as containment failure postulated to occur after the period of dynamic in-vessel related phenomena and before 24 hours after the onset of fuel damage. One of the design goals of the AP600 containment is to limit the likelihood of large releases to the environment at 24 hours after core damage to a frequency less than 1.0×10^{-6} per reactor-year. Therefore, the intermediate containment failure category provides a bin for quantifying the large releases that may occur before 24 hours after the onset of fuel damage. Since the AP600 passive containment cooling system has the capability to maintain quasi-static containment pressure increases to a level below that required to fail the containment, intermediate containment failure generally results from a high-energy phenomenon, such as hydrogen combustion, rapidly pressurizing the containment.

35.4.2.6 Late Containment Failure

Late containment failure is defined as containment failure postulated to occur between 24 and 72 hours after the onset of core damage. One of the design goals of the AP600 containment is to show that there is essentially no probability of containment failure before 72 hours for any severe accident. This category addresses sequences that are outliers to this goal to show that their frequency is a negligible fraction of the core-damage frequency. Since the AP600 passive containment cooling system can maintain quasi-static containment pressure increases to a level below that required to fail the containment, late containment failure generally results from a high-energy phenomenon, rapidly pressurizing the containment. Therefore, this is a high-energy release.

35.4.2.7 Very Late Containment Failure

Very late containment failure is defined as a potential containment failure postulated to occur after 72 hours after the onset of core damage. This category addresses sequences that have not been postulated to fail the containment or result in enhanced leakage, but that have not achieved a stable condition after 72 hours. This category generally contains sequences with noncoolable ex-vessel debris beds with an intact containment at 72 hours. The main purpose for this category is as input to the accident management guidance and, along with the late containment failure category, to show that the containment provides a reliable fission-product barrier after the 24-hour challenges per SECY-93-087 (Reference 35-1).

35.5 AP600 Release Categories

The endpoints of the containment event tree paths are grouped into appropriate source term categories based on similar fission-product releases. Different endpoints for AP600 are defined, depending on the type and timing of containment failure (bypass, isolation failure, late basemat penetration due to core-concrete interaction). If the containment does not fail, the availability of the passive containment cooling system water has a strong influence on the containment pressure and, therefore, is used to determine the release category. The source term for a representative sequence in each important accident class is calculated with the

Modular Accident Analysis Program, version 4.0 (MAAP4) code (Reference 35-2) described in Chapter 44.

The release categories for AP600 are defined in Table 35-2.

35.5.1 Release Category IC

Release category IC is defined for an intact containment with passive containment cooling system water operating. The fission-product source term associated with this release category is due to nominal containment leakage within the technical specification limits. The containment is not pressurized over the design pressure for the long term because of the heat removal capability of the passive containment cooling system with a wet containment shell. The low containment leakage and long fission product residence times allow for significant retention of fission products.

35.5.2 Release Category ICP

Release category ICP is defined for an intact containment with passive containment cooling system water failed. The fission-product source term associated with this release category is due to nominal containment leakage area within the technical specification limits. The containment is pressurized over the design pressure, however, because of the reduced dry shell heat removal capability of the passive containment cooling system. The increased pressure in the containment results in greater leakage than in the IC release category. Noble gas releases are increased. However, high steam concentrations may enhance aerosol deposition over the IC release category.

35.5.3 Release Category XL

Release category XL is defined for excessive leakage from an intact containment with no core-concrete interaction. The fission-product source term associated with this release category is due to leakage from an intact containment that exceeds the technical specifications and may result in doses exceeding 25 man-rem at the site boundary 24 hours after the onset of core damage. This release category includes both wet- and dry-shell passive cooling cases.

35.5.4 Release Category BP

Release category BP is defined for containment bypass. The fission-product source term associated with this release category is due to the direct release of primary system fluid from the reactor coolant system to the environment. For AP600, this applies specifically to steam generator tube rupture cases. There is no fission-product scrubbing associated with this release category other than the natural retention in the reactor coolant system piping and steam generator volume.



35.5.5 Release Category CI

Release category CI is defined for containment isolation failure with no core-concrete interaction. The fission-product source term associated with this release category is due to the discharge of fission products released in-vessel from a containment with an open penetration from the containment atmosphere to the environment. The containment volume provides some scrubbing for aerosol fission products.

35.5.6 Release Category CI-C

Release category CI-C is defined for containment isolation failure with core-concrete interaction release. The fission-product source term associated with this release category is due to the discharge of fission products released in-vessel and ex-vessel from a containment with an open penetration from the containment atmosphere to the environment. The containment volume provides some scrubbing of aerosol fission products.

35.5.7 Release Category CFE

Release category CFE is defined for early containment failure induced by high-energy in-vessel or vessel failure phenomena. The fission-product source term associated with this release category is due to the discharge of fission products released in-vessel from a containment that fails during the dynamic phase of the core relocation process. High-energy phenomena that can occur at this time can be postulated to rapidly pressurize the containment with a potential for failure before any significant aerosol deposition has occurred.

35.5.8 Release Category CFE-C

Release category CFE-C is defined for early containment failure induced by high-energy in-vessel or vessel failure phenomena with later core-concrete interaction release. The fission-product source term associated with this release category is due to the discharge of fission products released in-vessel from a containment that fails during the dynamic phase of the core relocation process. High-energy phenomena that can occur at this time can be postulated to rapidly pressurize the containment to the point of failure before any significant aerosol deposition has occurred. Later in the accident, core-concrete interaction results in the release of nonvolatile fission products into a containment that is open to the environment.

35.5.9 Release Category CFI

Release category CFI is defined for intermediate containment failure. The fission-product source term associated with this release category is due to the discharge of fission products released in-vessel and ex-vessel from a containment that fails in 24 hours after the initial core damage. Since quasi-static pressurization of the AP600 containment by steam is not a credible failure mode due to the passive containment heat removal, the containment failure is associated with a high-energy event which rapidly pressurizes the containment.



35.5.10 Release Category CFL

Release category CFL is defined for late containment failure without core-concrete interaction. The fission-product source term associated with this release category is due to the discharge of fission products released in-vessel from a containment that fails between 24 and 72 hours after the initial core damage. Since quasi-static pressurization of the AP600 containment by steam is not a credible failure mode due to the passive containment heat removal, the containment failure is associated with a high-energy event that rapidly pressurizes the containment.

35.5.11 Release Category CFV

Release category CFV is defined for potential very late containment failure with core-concrete interaction release. This release category is reserved for sequences with core-concrete interaction which have not been postulated to fail the containment before 72 hours. The containment would be pressurized with noncondensable gases and the basemat significantly eroded. Since fission-product releases are evaluated to 72 hours, the source term for this release category will essentially be the same as the ICP release category. The frequency of this category is calculated for future accident management and informational purposes.

35.6 Containment Event Tree Nodes

This section describes the questions considered at each of the AP600 containment event tree nodes; their success criteria; and the dependencies associated with them, both upstream and downstream on the paths. The manner in which the nodal split fractions will be determined will also be discussed. In the quantification of the containment event tree, the split fractions for nodes associated with plant systems are linked to fault trees to ensure consistent treatment within any given sequence. Split fractions associated with phenomenological nodes will be determined using decomposition event trees. The probability of containment failure is determined based on peak pressure predicted for the sequence and the conditional containment failure probability distribution.

35.6.1 Node DP

The question "Does the operator depressurize the reactor coolant system after core damage has occurred?" is asked at node DP. This question applies only to accident sequences that are not fully depressurized and are binned into accident classes 1A, 1AP, and 3D. Depressurization prior to core damage is considered in the core damage frequency analysis, so this question applies to operator actions that may occur after core damage. Success at node DP is defined as the manual operation of the automatic depressurization system opening at least one train of one stage prior to any failure of the reactor coolant system piping or reactor vessel. The time available between core damage and imminent reactor vessel, hot leg, surge



line, or steam generator tube failure is an important consideration in determining success at this node. The failure probability of this node is determined by linking the node to a fault tree.

Success at node DP ensures that any vessel failure occurs at low pressure and allows the tree structure to bypass the hot leg and steam generator tube creep rupture failure nodes (accident class 1A), since it implies that the piping integrity is no longer challenged by high temperature and pressure natural circulation of hot gases in the primary system. Depressurization of the reactor coolant system after core damage results in high-temperature hydrogen and steam being released into the containment.

35.6.2 Node SG

The question "Do the steam generator tubes remain intact during high pressure and temperature reactor coolant system natural circulation?" is asked at node SG. This question applies only to accident sequences binned into accident class 1A in which the operator fails to depressurize the reactor coolant system (node DP). Success is defined as not exceeding the time/temperature Larsen-Miller failure criterion or high-pressure and high-temperature burst strength for Inconel 690.

Considerations for uncertainties such as tube degradation must also be taken into account. A decomposition event tree is used to examine high-temperature failures of reactor coolant system piping and to assign the failure probabilities (Chapter 37).

Failure of the steam generator tubes at high primary system pressure will open the secondary system safety valves and provide a direct pathway for fission-product release to the environment. Therefore, failure of node SG leads directly to release category BP on the containment event tree structure.

35.6.3 Node CR

The question "Does the hot leg nozzle or surge line fail because of high-temperature creep rupture?" is asked at node CR. This question only applies to high-pressure accident sequences binned into accident class 1A in which the operator has failed to manually depressurize (node DP). Success is defined as the hot leg or surge line exceeding the time/temperature Larsen-Miller failure criterion for 316 stainless steel prior to a failure of the steam generator tubes or the reactor vessel. A decomposition event tree is used to examine high temperature failures of reactor coolant system piping and assign the failure probabilities (Chapter 37).

A creep rupture failure of the hot leg or surge line ensures that any vessel failure would occur at low pressure. Failure and depressurization of the reactor coolant system after core damage results in high-temperature hydrogen and steam being released into the containment. This release will impact the considerations made at the early hydrogen combustion node downstream.



Failure of node CR implies that the reactor vessel fails prior to hot leg nozzle, surge line, or steam generator tube failure. Therefore, considerations of high-pressure reactor vessel failure must be made. The AP600 containment event tree conservatively assumes that high-pressure melt ejection results in an early containment failure.

35.6.4 Node IS

The question "Is the containment isolated?" is asked at node IS. Success at this node is defined as the automatic or manual generation of a containment isolation signal and the successful closure of the valves at the penetrations that join the containment atmosphere to the environment. Success leads to the examination of severe accident phenomena which may later fail the containment. The failure probability at node IS is determined by linking the node to a fault tree.

Failure of node IS leads to a containment isolation failure release category, CI, or CI-C; depending on the downstream outcomes of reactor vessel failure (node VF), cavity flooding (node IR), and debris coolability (nodes DQ and RW). The amount of water available in the containment for debris cooling can be affected by the failure of node IS due to inventory loss through to the environment.

35.6.5 Node PC

The question "Is the passive containment cooling system operating?" is asked at node PC. Success at this node is defined as the automatic or manual actuation of the system which provides water for cooling the containment shell. The failure probability of node PC is determined by linking the node to a fault tree.

The heat removal from the containment directly determines the containment pressurization for the accident sequence. Success of the passive containment cooling water condenses more steam out of the containment atmosphere, providing more water for debris cooling (node RW) and less inerting of containment hydrogen (node HC1 and HC2); and lowers containment pressure over the long term, which can determine the release category and probability of excessive leakage.

35.6.6 Node IG

The question "Is the hydrogen control system operating?" is asked at node IG. Success at this node is defined as the manual actuation of the containment hydrogen igniters. The failure probability of node IG is determined by linking to a fault tree.

The consideration of global hydrogen combustion is affected by the outcome of this node. Operation of the igniters allows the hydrogen to be consumed at low concentrations to prevent global burning or detonation (nodes HC1, HC2, and HC3).



35.6.7 Node IR

The question "Is the water from the in-containment refueling water storage tank flooding the reactor cavity?" is asked at node IR. Success is defined as the gravity draining of the in-containment refueling water storage tank water through the vessel or manual actuation of the cavity flooding valves prior to the relocation of molten core debris to the lower plenum. The failure probability of node IR is determined by linking the node to a fault tree.

The outcome of flooding the reactor cavity affects considerations of the reactor vessel failure. Emergency procedures for AP600 instruct the operators to flood the reactor cavity as a last resort if the core exit thermocouple readings are indicative of significant core damage. The effect of vessel flooding over the hot leg nozzles, preventing high-temperature failure of the hot leg, is not considered since the time after core damage required to flood the reactor vessel up to the hot leg nozzles to cool them is much greater than the time required to fail the hot leg or the steam generator tubes.

In high-pressure sequences (accident class 1A), node IR is dependent on the outcome of manual depressurization (node CR) and hot leg/surge line high-temperature failure. Successful depressurization of the primary system could allow the in-containment refueling water storage tank water to inject via gravity and flood the containment. In other sequences, operator action would be required to flood.

35.6.8 Node SE

The question "Does the molten core relocation to the lower plenum fail to produce a steam explosion that could fail the reactor vessel?" is asked at node SE. Success is defined as the inability to mix sufficient molten core debris mass with coolant or the inability to trigger a steam explosion in the reactor coolant system that fails the reactor vessel. The steam explosion phenomenon is analyzed with a decomposition event tree (Chapter 38). The outcome of node SE affects downstream considerations of vessel failure (node VF), containment failure (node CF1), and ex-vessel debris quench (node DQ).

35.6.9 Node VF

The question "Does the reactor vessel remain intact?" is asked at node VF. Success is defined as the capability of transferring sufficient heat from the lower head to water in the containment to prevent creep failure of the vessel wall. A decomposition event tree is used to examine external reactor vessel cooling preventing vessel failure and assign probability at this node (Chapter 36).

The outcome of node VF affects downstream considerations of ex-vessel fuel coolant interaction and coolability (node DQ), and containment integrity (node CF1). If the vessel does not fail, then debris is not released to the containment, and further containment event tree questions concerning ex-vessel debris (nodes DQ, SCC, and RW) can be bypassed.

35.6.10 Node HC1

The question "Does the hydrogen generated in-vessel fail to burn globally?" is asked at node HC1. Success at this node is defined as the inerting of hydrogen by steam concentration or controlled combustion of the hydrogen at the igniters (node IG). A decomposition event tree is used to examine hydrogen combustion phenomena and determine the failure probability at this node (Chapter 41).

Success of node HC1 results in a benign situation for the early threat to containment integrity from hydrogen combustion. Upstream phenomena affecting the release rate of hydrogen to the containment (nodes DP and CR) can influence the outcome at this node. If hydrogen is released to the containment because of sudden blowdown of the reactor coolant system, the containment atmosphere may become globally flammable, even if the igniters are operating.

The failure of this node affects consideration of the early containment integrity (node CF1) and future hydrogen combustion (node HC2).

35.6.11 Node DQ

The question "Does the ex-vessel core debris quench in the reactor cavity?" is asked at node DQ. Success is defined as sufficient water in the cavity to remove the latent and sensible heat from the core debris and the ability to transfer the heat to the water at a rate that prevents significant core-concrete interaction. A decomposition event tree is used to examine debris coolability and to assign probability at this node (Chapter 40).

The amount of water in the cavity is dependent on the available water sources (primary system, core makeup tanks, accumulators, in-containment refueling water storage tank water), defined by the accident sequence and containment heat removal (node PC). The outcome of node DQ affects the debris coolability issue, containment integrity (node CF1), and hydrogen combustion considerations (node HC2).

35.6.12 Node SCC

The question "Does short-term core-concrete interaction not occur as a result of core debris relocation to the reactor cavity?" is asked at node SCC. Success at node SCC is defined as a reactor cavity debris bed thickness less than 25 centimeters at reactor vessel failure. If the vessel fails below the elevation of the in-vessel debris pool and all of the core debris is ejected into the reactor cavity at once, then the debris bed may be thick enough to allow core-concrete interaction to occur for a time during quenching. If only a portion of the debris is released to the cavity and the debris does not spread, then core-concrete interaction would be expected for a duration until the debris melted and spread to a coolable configuration. A decomposition event tree is used to address core-concrete interaction and to quantify the failure probability of node SCC (Chapter 40).



The outcome of node SCC affects the amount of hydrogen in the containment and considerations at downstream hydrogen combustion nodes (HC2 and HC3).

35.6.13 Node CF1

The question "Do the dynamic processes that occur because of core melting and relocation fail to threaten the containment integrity?" is asked at node CF1. Success of node CF1 is defined by the failure of the phenomena to pressurize the containment past the ultimate failure pressure as defined by the containment failure probability distribution (Chapter 42).

The outcome of node CF1 affects the release category to which the path is assigned. Failure of node CF1 leads to early release categories CFE and CFE-C, depending on debris coolability.

Many upstream considerations can affect the peak pressure that occurs during the dynamic phase of core relocation. The outcome of node CF1 is dependent on reactor coolant system pressure at the time of vessel failure (nodes DP, CR, and SG), containment heat removal (node PC), hydrogen combustion (node HC1), vessel failure (nodes SE and VF), and ex-vessel fuel-coolant interaction (node DQ). The combined effects of more than one phenomenon occurring in a short time frame is considered.

35.6.14 Node RW

The question "Is containment water recirculated into the cavity for long-term debris cooling?" is asked at node RW. Success is defined as sufficient water overflowing from the refueling canal into the cavity to maintain water coverage to remove decay heat from an ex-vessel debris bed. The failure probability for node RW is determined by linking a fault tree to the node.

Consideration of this node implies that the vessel is failed (node VF). Injection of the in-containment refueling water storage tank water into the cavity guarantees sufficient water for recirculation. If the containment is not isolated and the in-containment refueling water storage tank water is not injected, water inventory loss to the outside environment will prevent success of node RW. If the debris is not quenched, then this node is bypassed and the debris bed is considered to be noncoolable for the duration of the sequence. If the debris is quenched (node DQ), then the availability of cooling water determines debris coolability. The outcome of node RW affects downstream hydrogen combustion and containment integrity events.

35.6.15 Node HC2

The question "Does the hydrogen in the containment fail to burn globally before 24 hours?" is asked at node HC2. Success is defined as not reaching global flammability conditions prior to 24 hours after the onset of core damage. A decomposition event tree is used to examine hydrogen combustion phenomena and to assign probability at this node (Chapter 41).



Hydrogen combustion at this time can be a result of previously unburned hydrogen generated in-vessel or hydrogen generated during core-concrete interaction. The outcome of node HC2 is affected by the upstream outcomes of the operation of the hydrogen igniter system (node IG), previous hydrogen combustion (node HC1), and debris coolability (node DQ and RW). The outcome of node HC2 affects containment integrity prior to 24 hours.

35.6.16 Node CF2

The question "Does the containment remain intact to 24 hours after the onset of core damage?" is asked at node CF2. Success of node CF2 is defined by the failure to pressurize the containment past the ultimate failure pressure as defined by the containment failure probability distribution (Chapter 42.) The outcome of node CF2 determines the release category selection for the sequence. Failure leads to intermediate release categories CFI and CFI-C, depending on the state of the ex-vessel debris coolability. Success continues on to investigate future containment integrity. The outcome of node CF2 is dependent on upstream nodes determining debris coolability (nodes DQ and RW) and hydrogen combustion.

35.6.17 Node HC3

The question "Does the hydrogen in the containment fail to burn globally between 24 and 72 hours?" is asked at node HC3. Success is defined as not reaching global flammability conditions between 24 and 72 hours after the onset of core damage. A decomposition event tree is used to examine hydrogen combustion phenomena and to assign probability at this node (Chapter 41).

Hydrogen combustion at this time can be a result of previously unburned hydrogen generated in-vessel or hydrogen generated during core-concrete interaction. The outcome of node HC3 is affected by the upstream outcomes of the operation of the hydrogen igniter system (node IG), previous hydrogen combustion (nodes HC1 and HC2), and debris coolability (nodes DQ and RW). The outcome of node HC3 affects containment integrity prior to 72 hours.

35.6.18 Node CF3

The question "Does the containment remain intact to 72 hours after the onset of core damage?" is asked at node CF3. Success of node CF3 is defined by the failure to pressurize the containment past the ultimate failure pressure as defined by the containment failure probability distribution (Chapter 42). The outcome of node CF3 determines release category selection for a sequence. Failure leads to late release categories CFL and CFL-C, depending on the state of debris coolability (nodes DQ and RW). Success continues on to investigate the final potential for containment failure.



35.6.19 Node CF4

The question "Is the containment integrity not threatened after 72 hours after the onset of core damage?" is asked at node CF4. Success of node CF4 is defined as an intact containment with an intact vessel or a coolable debris bed (VF success, DQ success, or RW success). If VF is failed and DQ or RW is also failed, the failure probability of node CF4 is 1.

The outcome of node CF4 determines release category selection for a sequence. Failure leads to very late release category CFV. Success indicates intact containment in a controlled, stable condition with no lasting phenomenological threats from core-concrete interaction.

35.6.20 Node EX

The question "Does the containment not leak excessively?" is asked at node EX. Success is defined as intact containment leakage low enough to limit the 24-hour whole-body dose to less than 25 rem at the site boundary. The probability at this node is estimated from existing data on containment leakage and considerations of AP600 designed to reduce the likelihood of excessive leakage.

The leak-tightness of the AP600 containment is expected to be better than that of existing plants for the following reasons:

- AP600 has approximately 50 percent fewer penetrations, thereby reducing the number of potential leak pathways by a factor of two
- Large purge valves (48 to 54 in.) prone to leakage are replaced with smaller valves (12 in.)
- Check valves are used only in mild service conditions where wear and service-related problems would not challenge successful valve operation
- Solenoid valves that have had high failure rates are used only on very small lines (3/8 in.) which are expected to plug with particulates during severe accidents
- Each personnel air lock door has two gaskets. The doors can be tested individually for leak-tightness

For sequences in which the containment does not fail (release categories IC and ICP), the dose evaluation presented in Chapter 49 shows that, with a leak area corresponding to the technical specification limit of 0.12 percent per day at the design pressure, the mean whole-body doses for the IC and ICP release categories are less than 1 rem at 24 hours after core damage. Assuming the dose increases proportionally to the leak rate, the leak rate would have to exceed on the order of 10 times the technical specification limit. The probability that AP600 containment leakage exceeds more than 10 times the technical specification limit is estimated

to be 8×10^{-3} based on Reference 35-3 and the considerations of the design improvements described above.

Examination of excess containment leakage is performed for all cases in which the containment is intact out to 72 hours. The outcome of node EX determines the final release category. Failure leads to release category XL. Success leads to release categories IC and ICP, depending on the containment heat removal (node PC).

35.7 AP600 Containment Event Tree Structure

The overall structure of the AP600 containment event tree is presented in Figure 35-2. The structure of the tree employs the nodal questions and release category end-states described in the previous sections.

35.8 Core Damage Sequence Grouping

The plant event trees quantified in the Level 1 PRA analysis identify all of the plant event sequences that lead to core damage. Many of the core damage sequences have common characteristics with respect to the reactor system and containment system response. Such sequences can be grouped together into accident classes (plant damage states) to reduce the number of containment event trees that need to be quantified. The accident classes form the link between the plant event tree and the containment event tree. The process of grouping the core damage sequences from the event trees is described in the following paragraphs.

The core damage sequences are binned together into accident classes or plant damage states on the basis of similarities in the following characteristics:

- The initiating event type, such as loss-of-coolant accident, transient, and anticipated transient without scram leading to core damage
- The primary system pressure at the time of initial core damage (high or low)
- Timing of core damage (early or late)
- Containment integrity at the time of core damage (intact or impaired)
- Availability of safety systems at the time of core damage
- Disposition of water in the containment at the time of core damage
- Containment pressure and temperature at the time of core damage

Table 35-3 defines the various accident classes defined for AP600. For the Level 2 PRA containment event tree analysis, accident classes 1A, 1AP, and 3D are further categorized to



define if manual actuation of the automatic depressurization system is not successful. The revised accident class categories for the containment event tree quantification are defined in Table 35-4. For each accident class, an equation made up of the Boolean sum of the minimal cutsets for all sequences combined into that class is prepared. The cutset equation for the accident class, along with the frequency of core damage from the individual sequences, is used as input for the quantification of the containment event trees. The Level 1 PRA core damage frequencies of the accident classes as quantified in the plant analysis event trees are presented in Table 35-5.

35.9 References

- 35-1 SECY-93-087, "Policy, Technical, and Licensing Issues Pertaining to Evolutionary and Advanced Light-Water Reactor (ALWR) Designs," April 2, 1993.
- 35-2 "EPRI MAAP 4.0 Users Manual," EPRI NP-xxxx, [to be published].
- 35-3 *Technical Findings and Regulatory Analysis for Generic Safety Issue II.E.4.3, 'Containment Integrity Check'*, NUREG-1273, April 1988.

Table 35-1

AP600 CONTAINMENT EVENT TREE NODAL QUESTIONS

Node DP	Does the operator depressurize the RCS after core damage has occurred?
Node SG	Do the steam generator tubes remain intact? (accident class 1A only)
Node CR	Does the hot leg nozzle/surge line fail due to high temperature creep rupture? (accident class 1A only)
Node IS	Is the containment isolated?
Node PC	Is the passive containment cooling system operating?
Node IG	Is the hydrogen control system operating?
Node IR	Is the IRWST water flooding the reactor cavity?
Node SE	Does the molten core relocation to the lower plenum fail to produce a steam explosion that fails the reactor vessel?
Node VF	Does the reactor vessel remain intact?
Node HC1	Does the hydrogen generated in-vessel fail to burn globally?
Node DQ	Does the ex-vessel core debris quench in the reactor cavity?
Node SCC	Does short-term core-concrete interaction not occur as a result of core debris relocation to the reactor cavity?
Node CF1	Does the containment remain intact during the dynamic phase of core relocation?
Node RW	Is containment water recirculated into the cavity for long-term debris cooling?
Node HC2	Does the hydrogen in the containment fail to burn globally before 24 hours?
Node CF2	Does the containment remain intact 24 hours after the onset of core damage?
Node HC3	Does the hydrogen in the containment fail to burn globally between 24 and 72 hours?
Node CF3	Does the containment remain intact 72 hours after the onset of core damage?
Node CF4	Is the containment integrity not threatened after 72 hours after the onset of core damage?
Node EX	Does the containment not leak excessively?



Table 35-2

AP600 RELEASE CATEGORY DEFINITION SUMMARY

RC Name	Description
IC	Intact containment with nominal leakage, wet PCS heat removal
ICP	Intact containment with nominal leakage, dry PCS heat removal
XL	Intact containment with excessive leakage
BP	Containment bypass
CI	Containment isolation failure with no CCI
CI-C	Containment isolation failure with CCI
CFE	Early containment failure induced during dynamic phase of core relocation with no CCI
CFE-C	Early containment failure induced during dynamic phase of core relocation with CCI
CFI	Intermediate containment failure before 24 hours after the onset of core damage
CFL	Late containment failure before 72 hours after the onset of core damage
CFV	Potential very late containment failure (basemat) after 72 hours with CCI

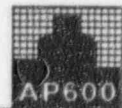


Table 35-3

SUMMARY OF LEVEL 1 ACCIDENT SEQUENCE SUBCLASSES

Accident Class	Subclass	Definition
1	A	Core damage with RCS at high pressure following transient or very small LOCA
	AP	Core damage following small LOCA and very small LOCA with no depressurization but with passive residual heat removal operating
	B	Core damage following loss of offsite power not recovered in 24 hours
	C	Core damage following loss of all dc power supply
	D	Core damage with partial depressurization of RCS following transient
2E, 2L		Loss of containment integrity -- potential core damage following loss of containment water inventory
3	A	Core damage with RCS at high pressure following anticipated transient without scram or main steam line break inside containment
	BR	Core damage following LOCA or other events with full RCS depressurization, but CMT and accumulator failed
	BA	Medium LOCA without CMT and accumulator, core melt is arrested by normal residual heat removal injection
	BE	Core damage following large LOCAs or other event with full depressurization
	BL	Core damage at long term following failure of water recirculation to RPV after successful gravity injection
	EE, ER, EL	Same as III BE, III BR, III BL with SBO initiating event
	C	Core damage following vessel rupture
	D	Core damage following LOCA (except large) with partial depressurization
5		Core damage sequences with containment already bypassed, except steam generator tube rupture sequences
6		Core damage following steam generator tube rupture. The containment is bypassed



Table 35-4

SUMMARY OF CET ACCIDENT SEQUENCE SUBCLASSES

Accident Class	Subclass	Definition
1	AC	Core damage with RCS at high pressure following transient or very small LOCA; manual actuation of ADS fails
	APC	Core damage following small LOCA and very small LOCA with passive residual heat removal operating; manual actuation of ADS fails
	B	Core damage following loss of offsite power not recovered in 24 hours
	C	Core damage following loss of all dc power supply
	D	Core damage with partial depressurization of RCS following transient
2E, 2L		Loss of containment integrity -- potential core damage following loss of containment water inventory
3	A	Core damage with RCS at high pressure following anticipated transient without scram or main steam line break inside containment
	BRC	Core damage following LOCA or other events with full RCS depressurization, but CMT and accumulator failed (includes accident classes 1A, 1AP, and 3D sequences when manual actuation of ADS is successful)
	BA	Medium LOCA without CMT and accumulator, core melt is arrested by normal residual heat removal injection
	BE	Core damage following large LOCAs or other event with full depressurization
	BL	Core damage at long term following failure of water recirculation to RPV after successful gravity injection
	EE, ER, EL	Same as III BE, III BR, III BL with SBO initiating event
	C	Core damage following vessel rupture
	DC	Core damage following LOCA (except large) with partial depressurization; manual actuation to fully depressurize fails
5		Core damage sequences with containment already bypassed, except steam generator tube rupture sequences
6		Core damage following steam generator tube rupture. The containment is bypassed

Table 35-5

**SUMMARY OF CORE DAMAGE FREQUENCY BY
LEVEL 1 ACCIDENT CLASS**

Accident Class	Subclass	Core Damage Frequency (Events Per Year)
1	A	5.4E-8
	AP	7.9E-9
	B	-
	C	-
	D	-
2	E	-
	L	-
3	A	-
	BA	-
	BE	1.2E-7
	BL	-
	BR	7.9E-9
	C	1.0E-8
	D	3.5E-8
5		-
6	E	5.7E-9
	L	-

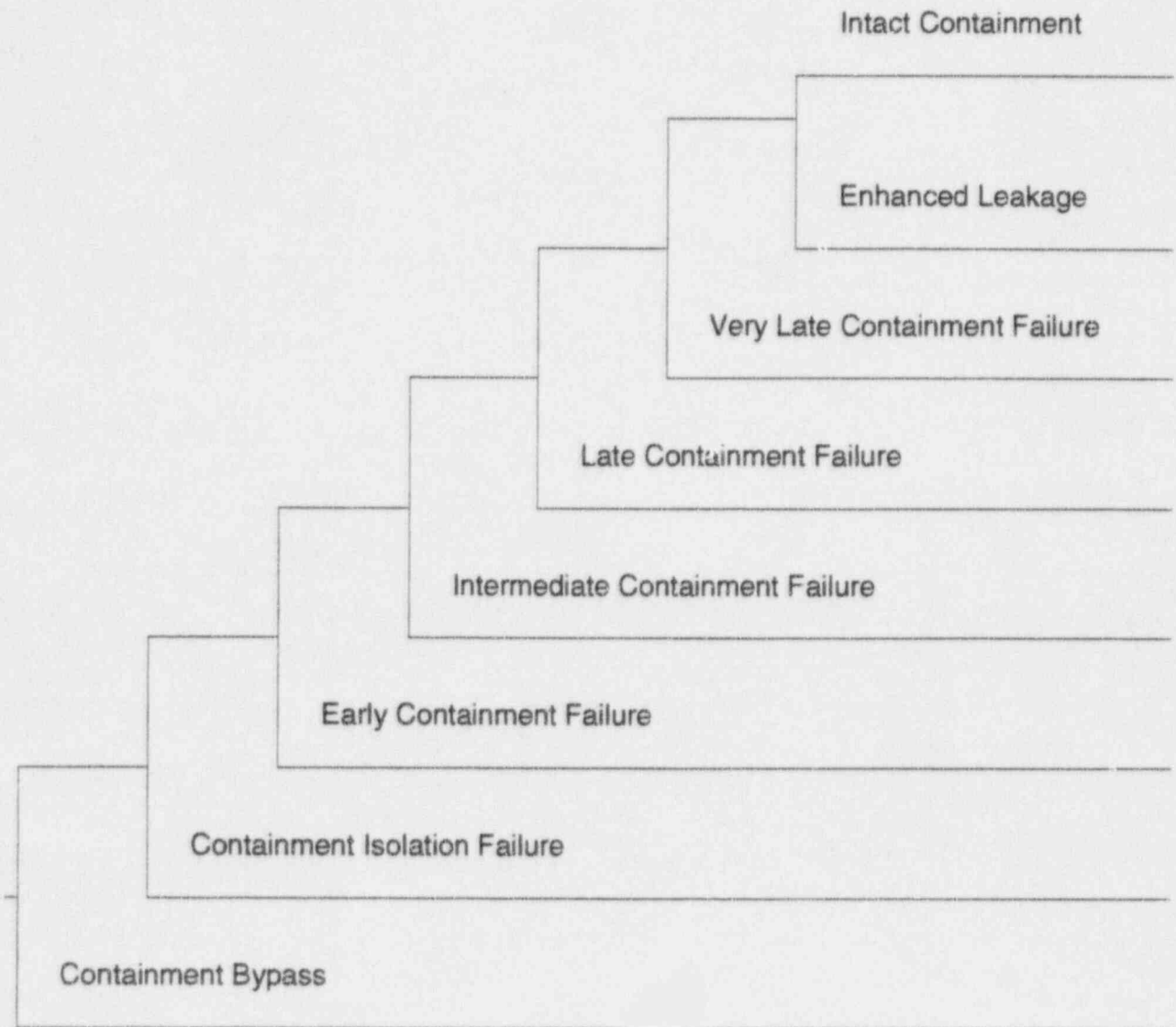


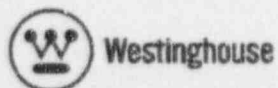
Figure 35-1

Skeleton Containment Event Tree



Figure 35-2 (Sheet 1 of 20)

AP600 Containment Event Tree



04/29/94 13:38:26 File: 03/13/92 15:02:00 186218 Path: C:\CODES\CADET.EXE
 edfiles\tree_hp.ed
 AP600 Containment Event Tree - Tree_HP High Pressure Entry Tree
 List of top events

Event	Description
1A	DAMAGE STATE 1A
DP	Does op act depress the RCS after core damage? (AC1A)
SG	Do the SG tubes remain intact? (AC1A)
CR	Does HL/SL fail due to creep rupture? (AC1A)

Figure 35-2 (Sheet 2 of 20)

AP600 Containment Event Tree

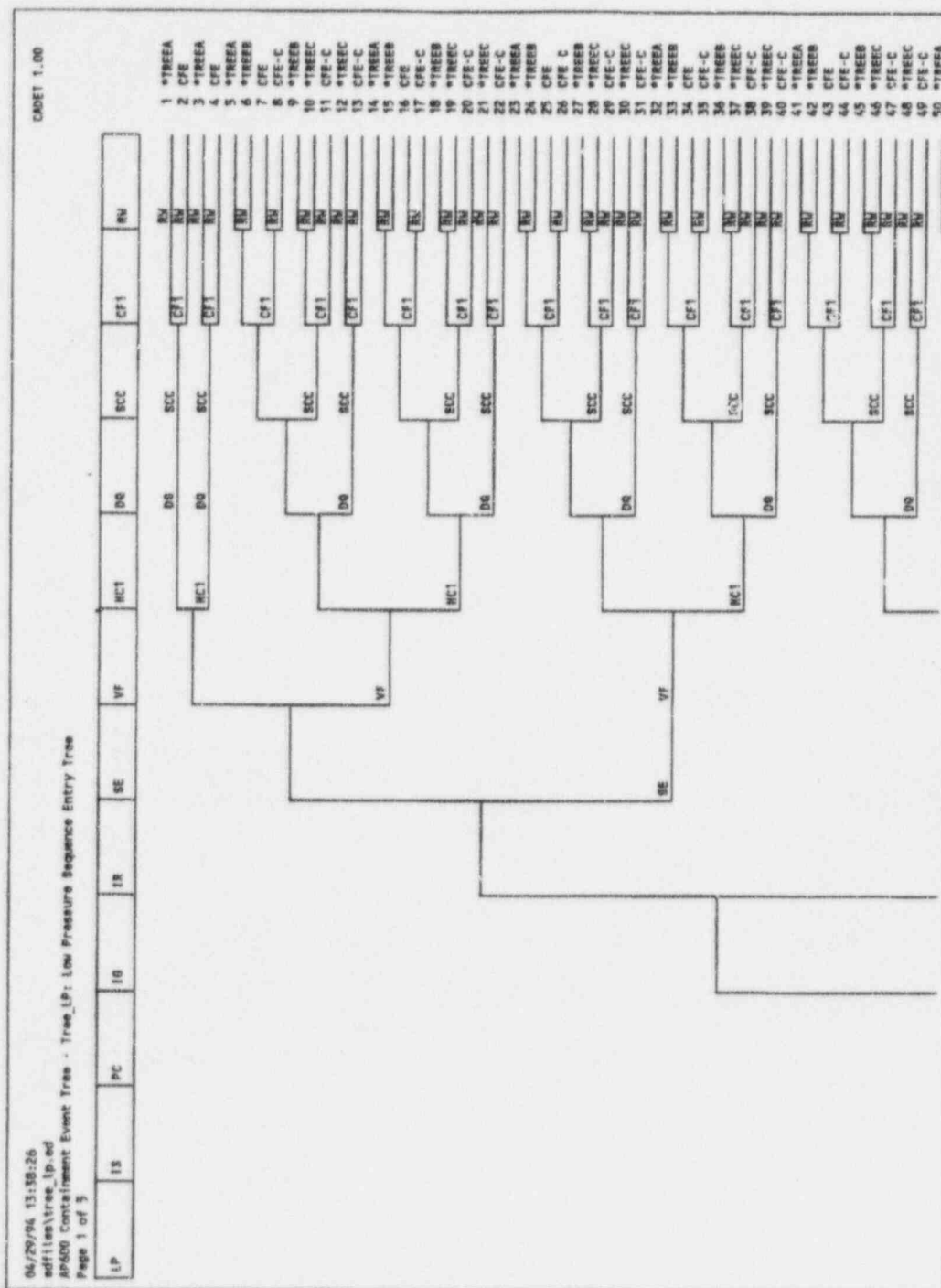


Figure 35-2 (Sheet 3 of 20)

AP600 Containment Event Tree

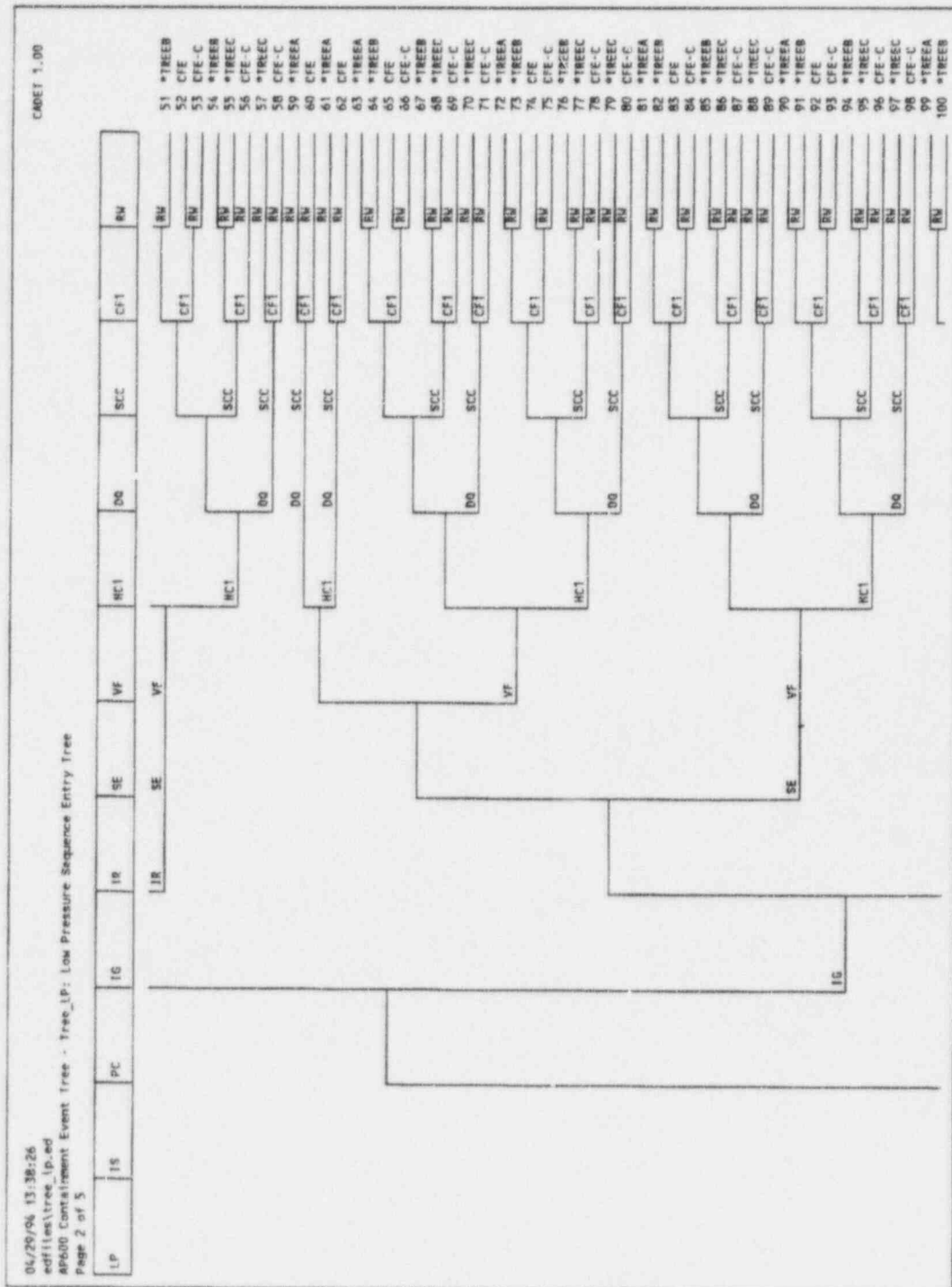


Figure 35-2 (Sheet 4 of 20)

AP600 Containment Event Tree

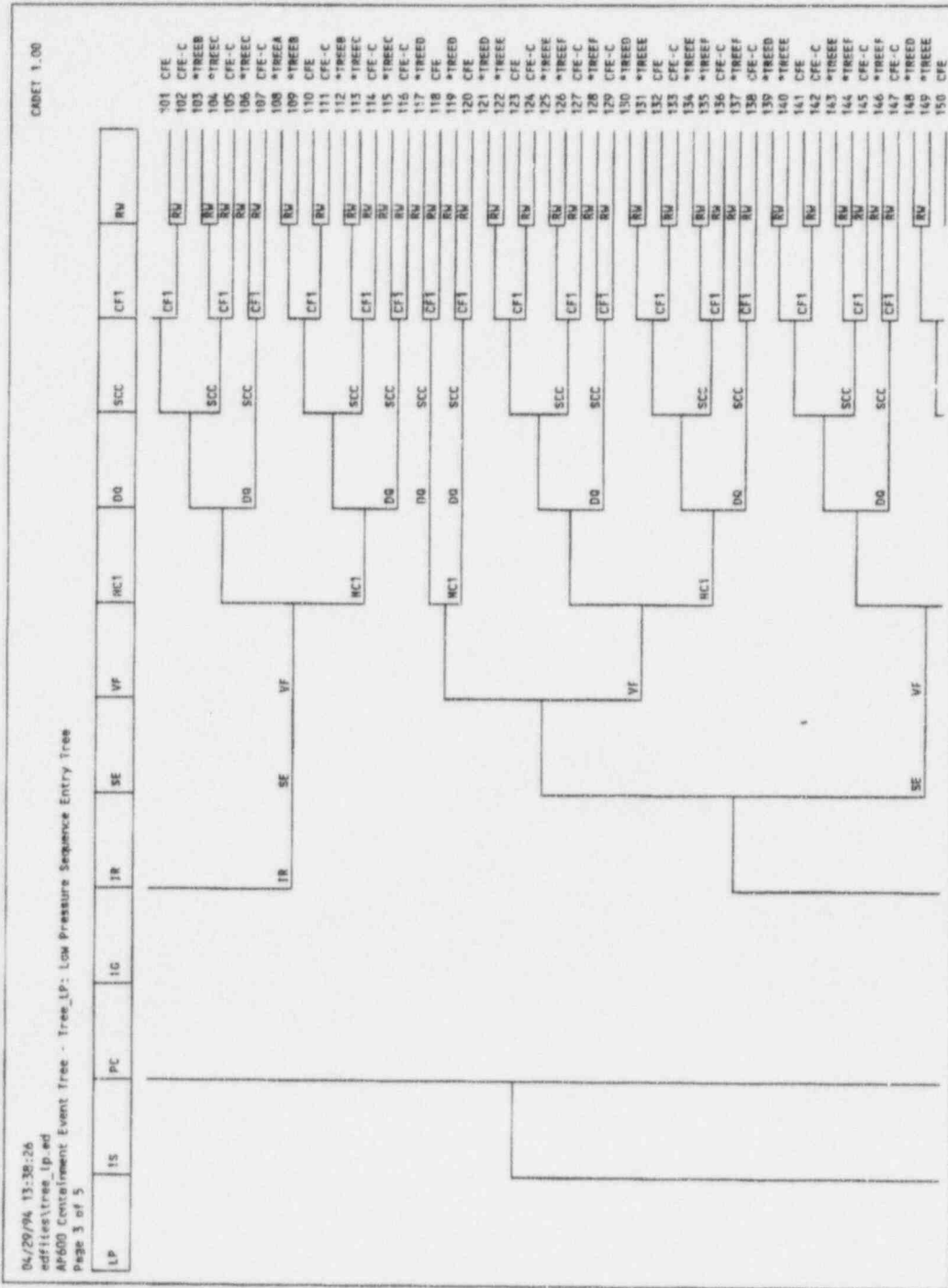


Figure 35-2 (Sheet 5 of 20)

AP600 Containment Event Tree

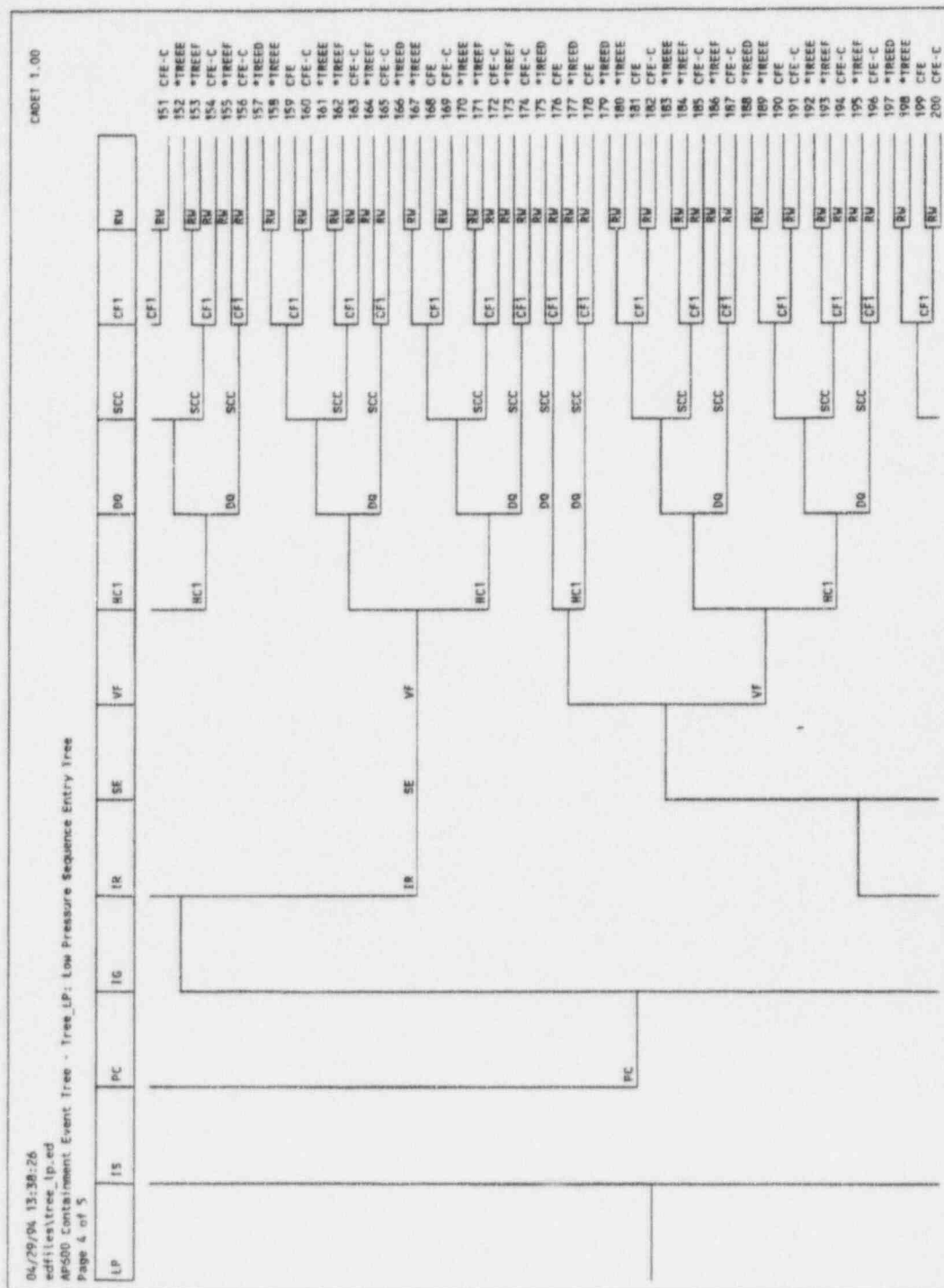


Figure 35-2 (Sheet 6 of 20)

AP600 Containment Event Tree

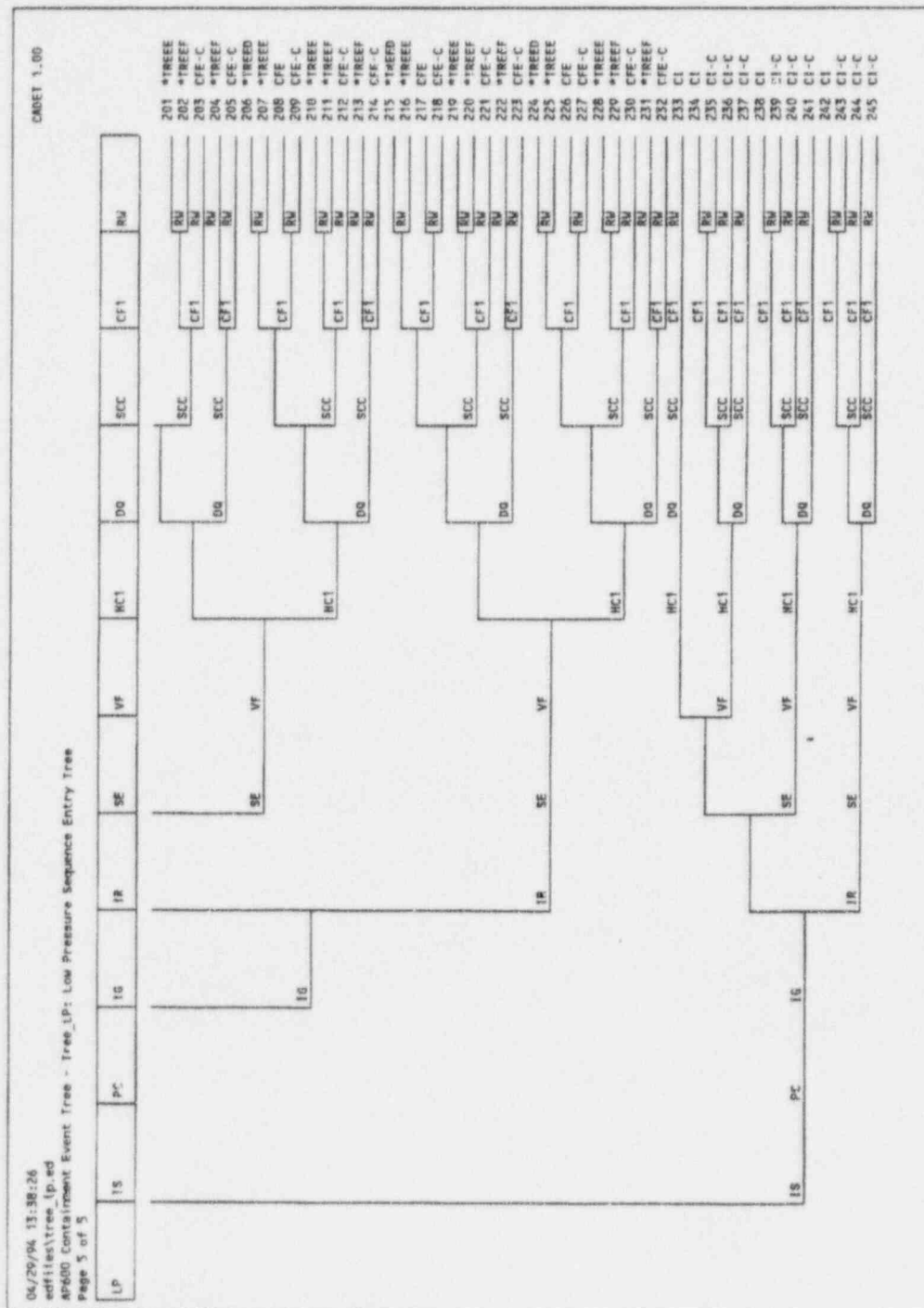


Figure 35-2 (Sheet 7 of 20)

AP600 Containment Event Tree

04/29/94 13:38:26 File: 03/13/92 15:02:00 186218 Path: C:\CODES\CADET.EXE
 edfiles\tree_lp.ed
 AP600 Containment Event Tree - Tree_LP: Low Pressure Sequence Entry Tree
 List of top events

Event	Description
LP	Low Pressure Accident Sequences
IS	Is the containment isolated?
PC	Is the passive containment cooling water operating?
IG	Is the hydrogen control system operating?
IR	Is the IRWST water flooding the reactor cavity?
SE	Does an in-vessel steam explosion not occur?
VF	Does the reactor vessel remain intact?
HC1	Does the in-vessel gen H2 fail to burn globally?
DQ	Does the core debris quench in the reactor cavity?
SCC	Does short term CCI fail to occur during quench?
CF1	Does cont remain intact through core relocation?
RW	Is water recirc to the cavity for debris cooling?

Figure 35-2 (Sheet 8 of 20)

AP600 Containment Event Tree

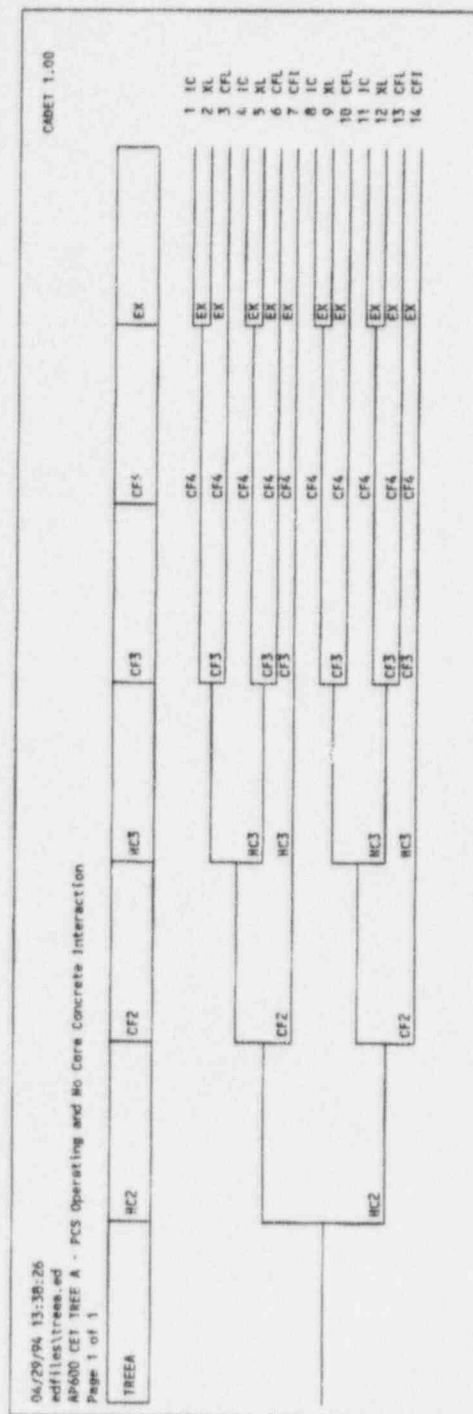


Figure 35-2 (Sheet 9 of 20)

AP600 Containment Event Tree

04/29/94 13:38:26 File: 03/13/92 15:02:00 186218 Path: C:\CODES\CADET.EXE
 edfiles\treea.ed
 AP600 CET TREE A - PCS Operating and No Core Concrete Interaction
 List of top events

Event	Description
TREEA	Transfer from Entry Tree
HC2	Does the H2 in the cont fail to burn globally to 24 hr?
CF2	Does the containment remain intact to 24 hours?
HC3	Does the H2 in the cont fail to burn globally to 72 hr?
CF3	Does the containment remain intact to 72 hours?
CF4	Is the cont integrity not threatened after 72 hours?
EX	Does the containment not leak excessively?

Figure 35-2 (Page 10 of 20)

AP600 Containment Event Tree

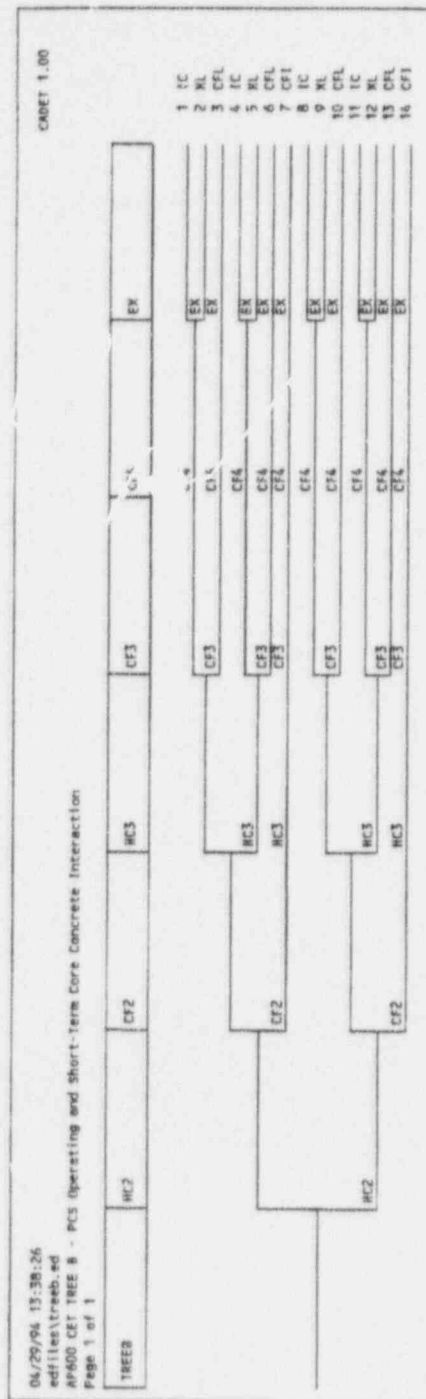
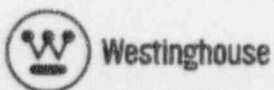


Figure 35-2 (Sheet 11 of 20)

AP600 Containment Event Tree



Revision 3
February 28, 1995

04/29/94 13:38:26 File: 03/13/92 15:02:00 186218 Path: C:\CODES\CADET.EXE
 edfiles\treeb.ed
 AP600 CET TREE B - PCS Operating and Short-Term Core Concrete Interaction
 List of top events

Event	Description
TREEB	Transfer from Entry Tree
HC2	Does the H2 in the cont fail to burn globally to 24 hr?
CF2	Does the containment remain intact to 24 hours?
HC3	Does the H2 in the cont fail to burn globally to 72 hr?
CF3	Does the containment remain intact to 72 hours?
CF4	Is the cont integrity not threatened after 72 hours?
EX	Does the containment not leak excessively?

Figure 35-2 (Sheet 12 of 20)

AP600 Containment Event Tree

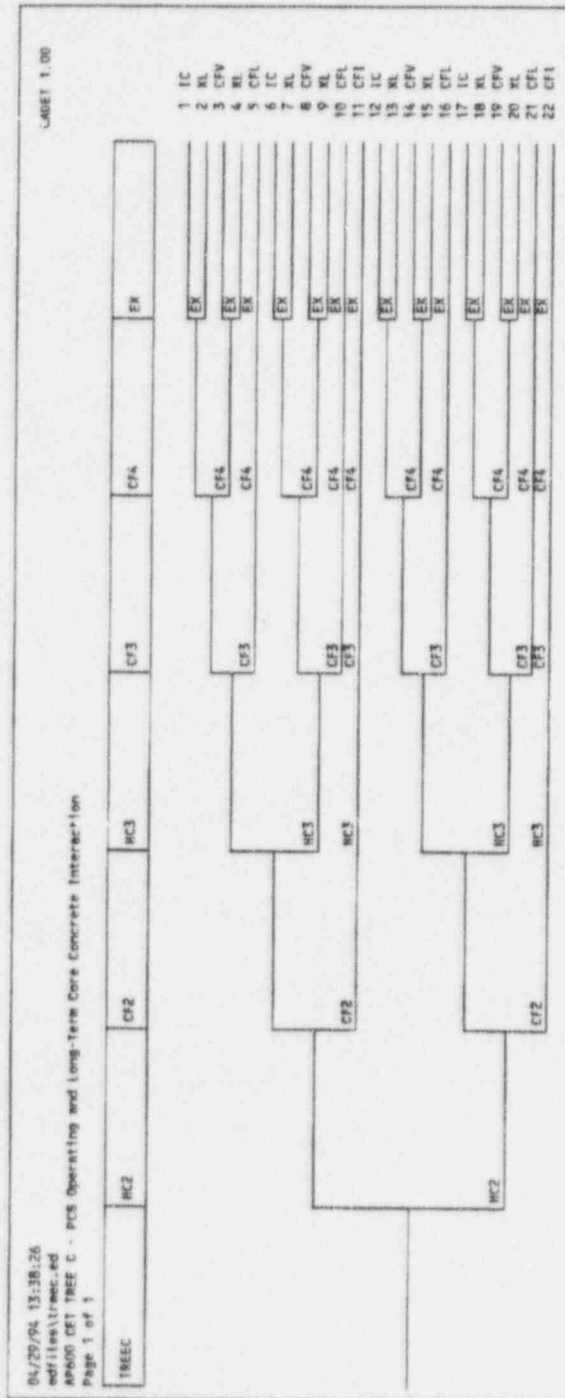


Figure 35-2 (Sheet 13 of 20)

AP600 Containment Event Tree

04/29/94 13:38:26 File: 03/13/92 15:02:00 186218 Path: C:\CODES\CADET.EXE
edfiles\treec.ed
AP600 CET TREE C - PCS Operating and Long-Term Core Concrete Interaction
List of top events

Event	Description
TREEC	Transfer from Entry Tree
HC2	Does the H2 in the cont fail to burn globally to 24 hr?
CF2	Does the containment remain intact to 24 hours?
HC3	Does the H2 in the cont fail to burn globally to 72 hr?
CF3	Does the containment remain intact to 72 hours?
CF4	Is the cont integrity not threatened after 72 hours?
EX	Does the containment not leak excessively?

Figure 35-2 (Sheet 14 of 20)

AP600 Containment Event Tree

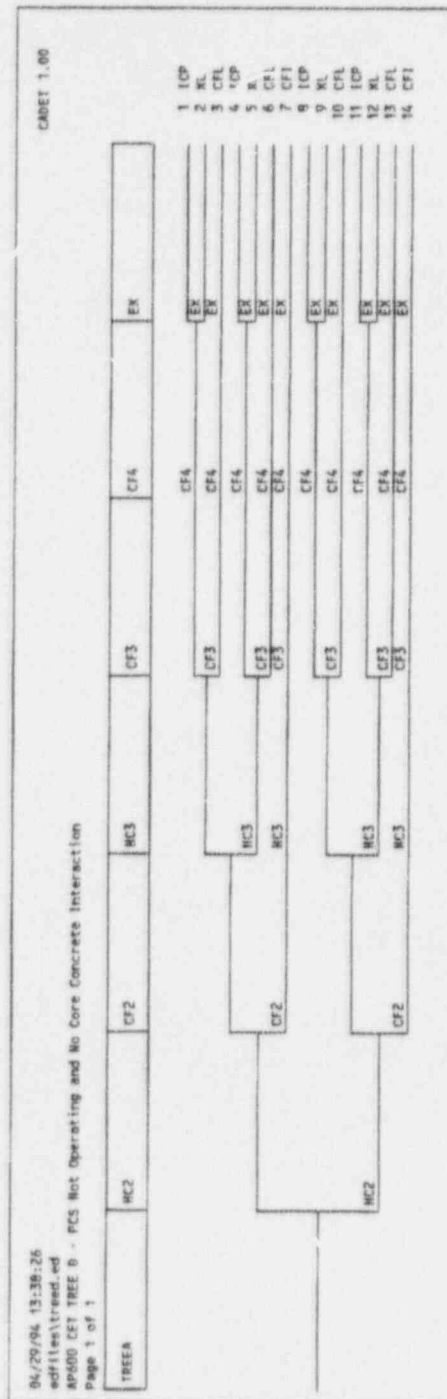


Figure 35-2 (Sheet 15 of 20)

AP600 Containment Event Tree

04/29/94 13:38:26 File: 03/13/92 15:02:00 186218 Path: C:\CODES\CADET.EXE
edfiles\treed.ed
AP600 CET TREE D - PCS Not Operating and No Core Concrete Interaction
List of top events

Event	Description
TREEA	Transfer from Entry Tree
HC2	Does the H2 in the cont fail to burn globally to 24 hr?
CF2	Does the containment remain intact to 24 hours?
HC3	Does the H2 in the cont fail to burn globally to 72 hr?
CF3	Does the containment remain intact to 72 hours?
CF4	Is the cont integrity not threatened after 72 hours?
EX	Does the containment not leak excessively?

Figure 35-2 (Sheet 16 of 20)

AP600 Containment Event Tree

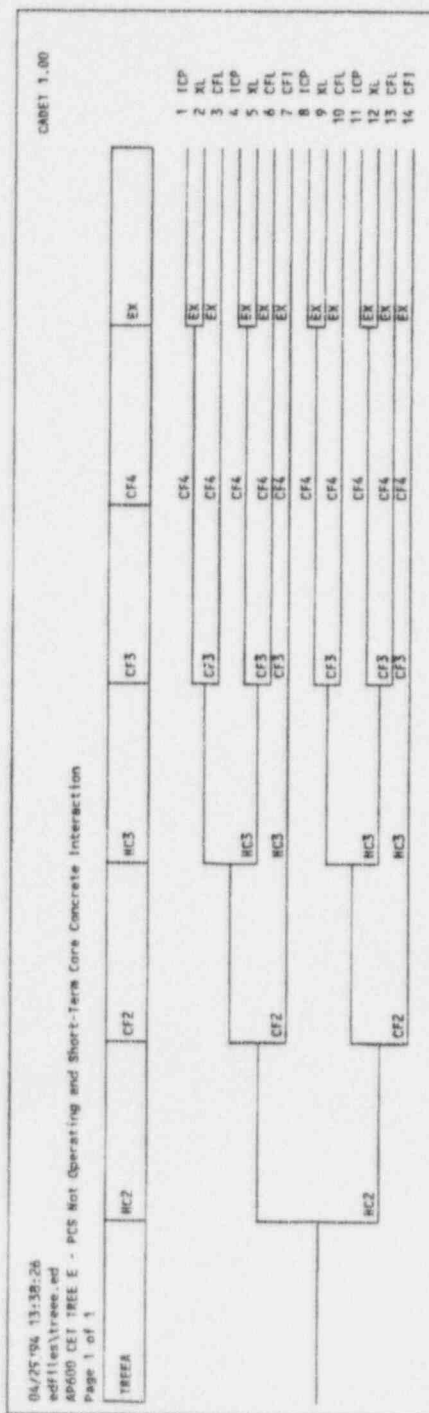


Figure 35-2 (Sheet 17 of 20)

AP600 Containment Event Tree

04/29/94 13:38:26 File: 03/13/92 15:02:00 186218 Path: C:\CODES\CADET.EXE
edfiles\treee.ed
AP600 CET TREE E - PCS Not Operating and Short-Term Core Concrete Interaction
List of top events

Event	Description
TREEA	Transfer from Entry Tree
HC2	Does the H2 in the cont fail to burn globally to 24 hr?
CF2	Does the containment remain intact to 24 hours?
HC3	Does the H2 in the cont fail to burn globally to 72 hr?
CF3	Does the containment remain intact to 72 hours?
CF4	Is the cont integrity not threatened after 72 hours?
EX	Does the containment not leak excessively?

Figure 35-8 (Sheet 18 of 20)

AP600 Containment Event Tree

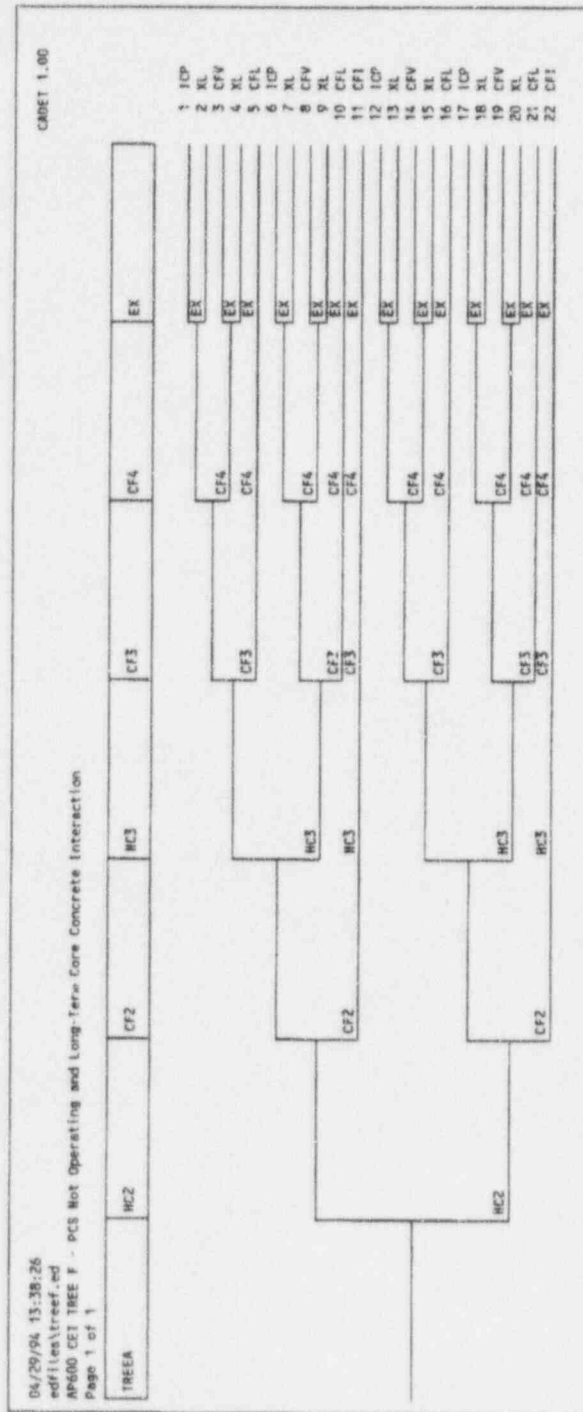
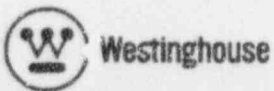


Figure 35-2 (Sheet 19 of 20)

AP600 Containment Event Tree



Revision 3
February 28, 1995

04/29/94 13:38:26 File: 03/13/92 15:02:00 186218 Path: C:\CODES\CADET.EXE
 edfiles\treef.ed
 AP600 CET TREE F - PCS Not Operating and Long-Term Core Concrete Interaction
 List of top events

Event	Description
TREEA	Transfer from Entry Tree
HC2	Does the H2 in the cont fail to burn globally to 24 hr?
CF2	Does the containment remain intact to 24 hours?
HC3	Does the H2 in the cont fail to burn globally to 72 hr?
CF3	Does the containment remain intact to 72 hours?
CF4	Is the cont integrity not threatened after 72 hours?
EX	Does the containment not leak excessively?

Figure 35-2 (Sheet 20 of 20)

AP600 Containment Event Tree



CHAPTER 36

DECOMPOSITION EVENT TREE - ANALYSIS OF IN-VESSEL RETENTION OF MOLTEN CORE DEBRIS

This chapter presents a decomposition event tree analysis of the phenomena related to preventing reactor vessel failure by flooding the reactor cavity and cooling the outside of the vessel with water. The AP600 design provides the operators with the ability to drain the in-containment refueling water storage tank (IRWST) water into the reactor cavity in the event that the core has uncovered and is melting. The objective of this cavity flooding action is to prevent vessel failure and subsequent relocation of molten core debris into the containment. Retention of the debris in the vessel significantly reduces the uncertainty in the assessment of containment failure and radioactive release to the environment due to ex-vessel severe accident phenomena. These postulated phenomena include ex-vessel fuel-coolant interaction, direct containment heating, and core-concrete interaction.

Separate analysis, discussed below, has shown that at the time of core relocation to the lower head of the reactor vessel in all sequences of interest, the reactor coolant system pressure is expected to be very near containment pressure. This is because of the reliable and diverse primary system depressurization capability consisting of the safety-related automatic depressurization system and the safety-related passive residual heat removal system. In postulated events in which no planned reactor coolant system depressurization occurs, the thermally induced failure of the pressure boundary is expected to occur well before molten core debris relocates to the lower head (see Chapter 37). This results in a depressurized reactor coolant system. The analysis presented in this section assumes that the reactor coolant system pressure is very low at the time of the challenge to the vessel integrity. The analysis also assumes that the operator action to flood the reactor cavity with in-containment refueling water storage tank water is successful, and that the vessel does not fail from an in-vessel steam explosion. Otherwise, vessel failure is assumed in the containment event tree.

36.1 Discussion of the Issue

Given the presence of molten core debris in the reactor vessel lower head, the debris constituents separate to form two layers based on the relative densities of the materials. A metallic pool layer forms on top of an oxidic pool layer. The oxidic pool is heated by the presence of the mainly non-volatile fission products remaining in the molten fuel. The heat is transferred from the debris by radiation from the top of the metal pool to the surrounding structures and by convection from the pools to the reactor vessel wall.

The contact of the debris with the inside surface of the vessel wall causes a crust to form at the melt-wall interface. The crust helps protect the wall from the high temperature debris and limits the heat flux, which can be transferred to the wall. This behavior was observed in the Three Mile Island accident in which the crust effectively insulated most of the vessel wall from the molten debris (Reference 36-1). The temperature at the crust-melt interface is



equivalent to the melting temperature of the core debris, so the heat transfer to the crust is driven by the superheat in the core debris. This heat flux determines the temperature profile through the vessel wall, which is essentially linear, assuming that the heat can also be transferred from the outside surface. Natural convection currents in the molten debris (Figure 36-1) cause the heat flux to be a function of the angular position on the hemispherical head such that the heat flux at the intersection of the top of the debris pool and the vessel wall is substantially larger than the heat flux at the bottom of the vessel (References 36-2, 36-3, 36-4, and 36-11).

Submergence of the reactor vessel in water results in substantial heat removal capability from the vessel wall via boiling on the outside surface (References 36-5, 36-6, and 36-12). In AP600, the operator has the capability to flood the reactor cavity by opening motor-operated valves that allow the in-containment refueling water storage tank water to drain into the lower containment. Fully injected, the in-containment refueling water storage tank water submerges the vessel up to the flange of the upper head.

Since the heat flux at the top of the oxidic pool is high, the crust is not as thick, so it provides less insulating capability than the crust at the bottom of the vessel. The metal pool melting temperature is essentially the same as the melting temperature of the vessel wall. At these angular positions in the oxide pool and at the molten metal pool boundaries, thinning of the vessel wall is expected to occur.

Structural analyses of the vessel wall at these thermal conditions indicate that virtually complete melt-through of the wall is required to fail the vessel (Reference 36-7) via wall thinning if the heat flux at the outer surface is maintained below the critical heat flux. If the heat flux exceeds the critical heat flux, then film boiling would occur on the outside surface of the vessel. In the film-boiling regime, the outside surface temperature of the wall required to transfer the heat flux to the water would exceed the wall-melting temperature. Therefore, the vessel would fail.

36.2 Analysis Methodology

In this analysis, the AP600 is analyzed for the steady-state conditions in a submerged reactor vessel with the lower head filled with molten core debris. In this section, a one-dimensional heat transfer model (Figure 36-2) is described, which is used to analyze the severe accident conditions in which molten debris relocates to the lower head and the outside surface of the vessel is being cooled by water. Analyses have been performed previously (References 36-4, 36-7, and 36-11), and the analysis presented here draws extensively from these reports.

Considering the presence of a crust at the interface of the vessel wall and the oxide pool, the heat flux from the molten pool to the crust both upward and downward has been described (References 36-4 and 36-11) by incorporating the correlations of Mayinger (Reference 36-8). In Reference 36-7, the data for the downward and upward heat fluxes from the COPO (Reference 36-2) and UCLA (Reference 36-3) experiments have been incorporated into the

Mayinger correlations. This results in the following Nussult number correlations for the upward and downward average heat fluxes:

$$Nu_d = \frac{\bar{q}_d R}{k \Delta T} = 0.54 Ra_c^{0.2} \left(\frac{H}{R} \right)^{0.25} \quad (1)$$

and

$$Nu_u = \frac{\bar{q}_u R}{k \Delta T} = 0.345 Ra_c^{0.233} \quad (2)$$

where:

Nu_d and Nu_u	= the downward and upward Nussult numbers, respectively
\bar{q}_d and \bar{q}_u	= the downward and upward average heat fluxes, respectively
R	= the radius of the vessel
k	= the thermal conductivity of the oxide pool
ΔT	= the pool superheat
Ra_c	= the Rayleigh number of the oxide pool
H	= height of the debris

The Rayleigh number for the oxide pool is given by:

$$Ra_c = \frac{g \beta Q R^5}{\alpha \nu k} \quad (3)$$

where:

g	= the acceleration due to gravity
β	= the volumetric expansion coefficient of the oxide pool
Q	= the volumetric heat rate in the corium pool
α	= the thermal diffusivity of the oxide pool
ν	= the kinematic viscosity of the oxide pool

The superheat of the pool can be found by performing a heat balance on the pool. Once the superheat of the pool is known, the average heat fluxes are also known.



The local heat fluxes to the crust at the angular positions are found by employing the UCLA correlation (Reference 36-3) for the flux distribution over a hemisphere.

$$\frac{q(\Theta)}{\bar{q}_d} = C_1 \left(\frac{\Theta}{\phi} \right)^2 + C_2 \quad (4)$$

where:

- θ = the angular position on the lower head
- ϕ = the angle to the top of the oxide pool surface (90° for full hemisphere)
- C_1 = 0.83 and $C_2 = 0.28$ for $0.0 < \theta/\phi < 0.6$ and,
- C_1 = $-1.76 \cos\phi + 2.75$ and $C_2 = 0.7 \cos\phi - 0.45$ for $0.6 < \theta/\phi < 1.0$
- $q(\theta)$ = the heat flux into the crust at angular position θ

The heat transfer to the crust is limited (Reference 36-7) by the sideward heat transfer in the Maying correlations.

$$q_{\max} = 0.85 Ra_c^{0.19} \left(\frac{k}{R} \right) \Delta T \quad (5)$$

The thickness of the oxide crust is found by simultaneously solving the conduction through the vessel wall (equation 6) and the temperature difference (equation 7) through the crust:

$$q(\Theta) + Q \delta_{cr}(\theta) = k_s \frac{T_w - T^*}{\delta_w} \quad (6)$$

and

$$T_{cm} - T_w = \frac{Q \delta_{cr}^2(\theta)}{2k_{cr}} + \frac{\delta_{cr}}{k_{cr}} q(\Theta) \quad (7)$$

where:

- $\delta_{cr}(\theta)$ = the crust thickness at angular position θ
- δ_w = the thickness of the vessel wall
- k_s = the thermal conductivity of the vessel wall
- k_{cr} = the thermal conductivity of the crust
- T_{cm} = the melting temperature of the oxide
- T_w = the temperature at the crust wall interface
- T^* = the nucleate boiling temperature on the outside surface of the vessel

The local heat flux into the wall is then given by:

$$q_w(\Theta) = q(\Theta) + Q\delta_{cr}(\Theta) \quad (8)$$

The upward and sideward heat fluxes through the metal pool are described by (Reference 36-7):

$$Nu_{m,u} = 0.067Ra_{m,u}^{(1/3)} \quad (9)$$

and

$$Nu_{m,s} = 0.1Ra_{m,s}^{(1/3)} \quad (10)$$

The Rayleigh number for the upward heat flux (equation 9) is found from the temperature difference between the upper and lower surface of the metal pool layer. The Rayleigh number for the sideward heat flux correlation (equation 10) is found from the temperature difference between the bulk temperature of the metal pool and the melting temperature of the vessel wall.

The Rayleigh number for the metal pool is given by:

$$Ra = \frac{g\beta (\Delta T) x^3}{\nu\alpha} \quad (11)$$

where:

ΔT = the appropriate driving temperature difference

x = the thickness of the metal pool

The heat fluxes through the metal pool are found by simultaneously solving equations 9 and 10 with the heat balance in the pool (equation 12), the radiative heat transfer to the inside vessel surfaces above the pool (equation 13), and the conduction through the vessel upper wall to the boiling surface on the outside wall (equation 14).

$$\overline{q}_u * A_u = \overline{q}_{m,u} * A_m + \overline{q}_{m,s} * A_s \quad (12)$$

$$\overline{q}_{m,u} = \epsilon \alpha (T_o^4 - T_{uw}^4) \quad (13)$$

$$\overline{q}_{m,s} = k_s \frac{2H_{uw}}{R} \frac{T_{uw} - T^*}{\sigma_{uw}} \quad (14)$$

where:

A_u , A_m , and A_s	=	the surface areas of the top of the oxide pool, the top of the metal pool, and the side of the metal pool, respectively
ϵ	=	the emissivity of the top of the metal pool
σ	=	the Stefan-Boltzmann constant
T_o	=	the temperature of the top of the metal pool
T_{uw}	=	the temperature of the upper walls
H_{uw}	=	the height of the upper walls

The thickness of the vessel wall (δ_w) is calculated from the conduction of the local heat flux through the wall at the melting temperature of the wall (T_{sm}) in equation 15.

$$q(\theta) = k_s \frac{T_{sm} - T^*}{\delta_w(\theta)} \quad (15)$$

36.3 Discussion of Uncertainties

Uncertainties in the boundary conditions and the modeling of the in-vessel retention are discussed in this section. Best estimates and bounding estimates of the uncertainties are developed, and combinations of these estimates are evaluated in the model described above to assess the likelihood of vessel failure.

36.3.1 Behavior of the Reactor Vessel Insulation

It can be postulated that the insulation surrounding the reactor vessel may prevent water from wetting the outside surface of the vessel or prevent steam from escaping from the reactor cavity annulus, thus significantly attenuating the heat removal capability. This is not expected to occur in AP600, since there are provisions in the design of the insulation to allow the water in and steam out to cool the outside surface of the vessel.

The insulation surrounding the AP600 reactor vessel is of the reflective panel variety. It is placed in the annulus between the vessel wall and the biological shield. There is a typical gap of 9 in. between the insulation and the vessel wall (Figure 36-3). The insulation is made up of numerous panels mounted to a frame. The bottom panels are held in place by their own weight. The side panels are clipped together. Each panel is estimated to weigh less than 50 pounds (23 kilograms), based on the design requirement that they can be installed by one person. Neither the panels or the frame is designed for seismic events, nor are they intended to be leak-tight or to withstand forces other than gravity.

Testing of prototypical reflective insulation leak-tightness for accident management purposes has been performed by Fauske and Associates, Incorporated (References 36-4 and 36-9). The tests conclude that more than sufficient water can pass through the cracks between the panels



to provide cooling water to the outside of the vessel, and to relieve steam under conditions expected in the severe accident.

Additionally, if the crack between the panels is assumed to be leak-tight, only a few inches of water is required to cause the bottom panels to move, allowing water inside the insulation. Likewise, by assuming that steam cannot be vented from the insulation, the pressure inside the insulation boundary would be equivalent to a head of 9 in. of water that would have to be displaced to vent the steam at the bottom of the insulation. The forces exerted on the insulation panels and frame due to pressurization by steam generated inside the insulation are estimated to be capable of blowing out panels, allowing both water in and steam out.

The possibility of the panels maintaining or moving into positions that block the water and steam flow outside the vessel is highly unlikely. Insulation blockage of the cooling of the outside of the reactor vessel is not considered to be a failure mode for in-vessel retention of core debris.

36.3.2 Cavity Flooding Rate

The reliability of cavity flooding is addressed on the containment event tree node IR. The cavity flooding system of AP600 consists of two parallel lines, one 10-in. diameter and one 4-in. diameter, which connect the in-containment refueling water storage tank to the steam generator compartments. There are two motor-operated valves in each line (Figure 36-4). When the valves are opened, the water drains from the in-containment refueling water storage tank and spills from the loop compartments directly into the cavity. The rate at which the cavity level rises is dependent on the number of lines that open (Figure 36-5). If both of the lines, or only the 10-in. line, is opened, the cavity fills quickly. If only the 4-in. line is opened, the cavity flooding rate is relatively slow. The elevation of the water on the vessel at the time of the challenge to the vessel integrity can have an impact on the determination of the vessel failure by affecting the rate at which heat can be removed from the top of the debris by radiation.

Flooding of the cavity is a severe accident management action that would be taken by the operator only in the event that core damage is occurring and the in-containment refueling water storage tank injection into the vessel cannot be recovered. The action is assumed to be initiated at 2000°F (1370 K) core-exit thermocouple temperature since this would indicate oxidation of the cladding. A review of the analyses for each accident class in Chapters 34 and 45 indicate the time available between the time of cavity flooding initiation and the time that the vessel integrity is challenged. Based on these times and the cavity flooding rates (Figure 36-5), the cavity will be completely filled with water to the 102-ft. elevation in the containment if the 10-in. line is available. If one of the two motor-operated valves in the 10-in. line fails to open and only the 4-in. line is available, the cavity may be only partially full of water at the time that the vessel integrity is challenged. Based on the analysis results, several of the cases had fully flooded cavities at the time that the debris in the lower head reached 2500 K, with only the 4-in. line injecting into the cavity. All of these cases had at least several feet of water above the top of the debris. As a bounding value, the water level

on the outside of the vessel wall is estimated to be 8.2 ft. (2.5 meters) above the top of the in-vessel debris.

The conditional probability of the failure of the 10-in. line, given successful operation of the cavity flooding system, is equivalent to the failure of one of the two motor-operated valves in the 10-in. line. The operation of the 10-in. line is the best estimate value, resulting in a water level on the outside reactor vessel wall of 19.7 ft. (6 meters) above the top of the in-vessel core debris. The bounding estimate is operation of the 4-in. line only, resulting in an outside water level of 8.2 ft. (2.5 meters) above the top of the in-vessel debris.

36.3.3 Debris Pool Characteristics

The characteristics of the debris pool are mainly determined by the masses of the oxide and metal layers. This analysis assumes that 100 percent of the core relocates into the lower head of the reactor vessel. The bulk of the oxide layer is uranium-dioxide. The rest of the oxide layer is metal, mainly zircaloy, which was oxidized during the core heatup. The metal layer is made up of unoxidized zircaloy and stainless steel from the portion of the core reflector, the core support plate, and the lower internals, which are melted in the core relocation.

Based on a review of the analysis results presented in Chapters 34 and 45, 75 percent oxidation of the fuel-rod cladding in the active core region is used to determine the best-estimate values of the mass of metal (40.9 metric tons) and oxide (90.5 metric tons) in the debris pools. For the bounding estimate, 100 percent oxidation of the cladding in the active core region is used to determine the values of 37.3 metric tons of metal and 95.3 metric tons of oxide.

In the one-dimensional model presented in Section 36.2, a larger oxide pool results in more heat that has to be taken out of the vessel since the decay heat is evaluated as a volumetric heat rate that is not adjusted based on the size of the pool. A smaller metal pool results in a larger thermal load at the metal pool side boundary since the heat is focused over a smaller area. In reality, the development of internal radial gradients is expected to at least partially counteract this effect. Preliminary testing with stimulant fluids at one-quarter scale geometry heated from below and cooled from above and from the side confirms this expectation (Reference 36-7). Nevertheless, internal radial gradients are not credited here in order to maintain a conservative estimate of the sideward heat flux.

36.3.4 Decay Power in the Debris Pool

The decay power in the debris determines the volumetric heat generation rate in the oxide pool, which is a boundary condition in the determination of the heat fluxes at the vessel wall. The main uncertainty in the decay power in the debris pool is a function of the timing of the accident sequences and the release of the volatile fission products from the debris. A review of the analysis presented in Chapters 34 and 45 for AP600 and consideration that 30 percent of the fission-product heating is provided by the volatile fission products results in a best-estimate decay power in the debris pool of 1.0 megawatts per cubic meter. This agrees with

base values presented in References 36-4 and 36-7. Based on the probability distribution for decay heating presented in Reference 36-7 and on the review of MAAP4 results, the bounding estimate of decay power is taken to be 1.3 megawatts per cubic meter.

36.3.5 Radiation Heat Transfer to the Upper Vessel

The heat flux from the top of the metal pool to the structures of the upper vessel is an important consideration in determining the heat flux at the side of the metal pool to the vessel. The highest heat flux in the system is expected to be at the side of the metal pool in the debris-vessel interface. The controlling parameter in the radiation heat flux from the metal pool to the upper vessel is the emissivity of the upper surface of the pool. Emissivity of the pool surface is dependent on the composition of the pool (Reference 36-7). The emissivity of carbon steel and pure molten iron at 1770°C (3200°F) is determined to be 0.45 in Reference 36-10. The effects of adding zirconium and other impurities as well as oxidation are unknown, but are expected to increase the emissivity (Reference 36-7). Considering the high temperature and the presence of steam in the atmosphere, the best-estimate value for the emissivity is taken to be 0.55. The value of 0.4 is taken as the bounding estimate based on the probability distribution for the molten metal pool emissivity presented in Reference 36-7.

36.4 In-Vessel Retention Decomposition Event Tree

The decomposition event tree used to evaluate the likelihood of in-vessel retention is presented in Figure 36-6. It has four nodes at which the uncertainties are evaluated and one node that evaluates the vessel integrity. The decomposition event tree nodes follow:

- Node FL - Is the in-containment refueling water storage tank water fully injected into the reactor cavity at the time of challenge to the reactor vessel integrity?
- Node MD - Is less than 75 percent of the active zircaloy cladding oxidized?
- Node DK - Is the volumetric heat rate of the pool less than 1.0 MW/m³?
- Node QUP - Is the emissivity of the metal pool greater than 0.5?
- Node IVR - Is the debris retained in the vessel?

The upward path at each node indicates a positive response to the question, and the downward path indicates a negative response. The end-points of the paths represent the outcome of the combinations of the uncertainties along the path and are assigned either end-state VI (vessel intact) or end-state VF (vessel failed) based on the outcome at node IVR.

The decomposition event tree is used to quantify the likelihood of each of the combinations of the uncertainties. The outcome of each of the combinations in terms of vessel failure is analyzed in the following section.

36.4.1 Analysis of the Combined Uncertainties

The decomposition event tree shows that there are 16 combinations of the uncertainties for which vessel failure needs to be evaluated. These combinations are summarized in Table 36-1. The methodology described in subsection 36.2 is applied to the combined uncertainties. The input to the analyses is presented in Tables 36-2 and 36-3, and the heat flux distributions and the wall thickness distribution results are presented in Figures 36-7 through 36-38.

36.5 Quantification of the Decomposition Event Tree

This section presents the split fractions at each of the event tree nodes and the overall quantification of the tree.

36.5.1 Node FL

Is the in-containment refueling water storage tank water fully injected into the reactor cavity at the time of challenge to the reactor vessel integrity?

Success Criteria:

Successful opening of both motor-operated valves in the 10-in. cavity flooding line.

The failure probability of node FL is based on the failure of one out of two motor-operated valves in the 10-in. cavity flooding line given that some amount of cavity flooding is successful. The failure of motor-operated valves from the AP600 Level 1 PRA is 1.1×10^{-2} per demand. Therefore, the failure of either of the valves in the line is 2.2×10^{-2} per demand. The following split fraction values are assigned to node FL:

Probability of success = 9.78×10^{-1}
Probability of failure = 2.2×10^{-2}

36.5.2 Node MD

Is less than 75 percent of the active zircaloy cladding oxidized?

Success Criteria:

Less than 75 percent of the cladding of the active fuel region is oxidized after the core relocation to the lower head is completed.

The best estimate analysis of the accident sequences result in less than 75 percent cladding reaction for each of the accident classes. However, there is sufficient uncertainty in the in-vessel phenomena that a finite probability is assigned to reflect the likelihood of oxidation of more than 75 percent of the active cladding. The following split fraction values are assigned to node MD:

Probability of success = 0.90

Probability of failure = 0.10

36.5.3 Node DK

Is the volumetric heat rate of the pool less than 1.0 MW/m³?

Success Criteria:

Less than 1.0 MW/m³ volumetric heating in the oxide pool.

The best-estimate analyses results predict that at the time of significant challenge to the reactor vessel, the decay heat rates, considering 30 percent heat reduction due to the loss of the volatile fission products, are less than 1.0 MW/m³. However, the uncertainty in predicting decay heat and the transport of volatile fission products is such that a finite probability of decay power greater than 1.0 MW/m³ must be considered. The following split fraction values are assigned to node DK:

Probability of success = 0.90

Probability of failure = 0.10

36.5.4 Node QUP

Is the emissivity of the metal pool greater than 0.5?

Success Criteria:

Metal pool emissivity greater than 0.5

The best-estimate value of the emissivity of the top of the metal pool is considered to be greater than the emissivity for pure molten iron (0.45), considering the oxidation and the effects of zirconium, chromium, and nickel. Therefore, the following split fractions are assigned to node QUP based on the probability distribution for the molten pool emissivity developed in Reference 36-7:

Probability of success = 0.99

Probability of failure = 0.01



36.5.5 Node IVR

Is the debris retained in the vessel?

Success Criteria:

Heat flux less than critical heat flux at all points on the surface.

In Reference 36-7, a structural analysis of the reactor vessel under these thermal loading conditions and vessel wall thinning concludes that the thinned vessel wall is capable of sustaining the load from the weight of the vessel and debris as well as a significant pressure load as long as the heat transferred through the vessel wall can be removed at the outside surface below the critical heat flux. Therefore, in this analysis, the critical heat flux is used to determine the success of the reactor vessel integrity.

Based on the results of the ULPU testing (Reference 36-7), the critical heat fluxes at the bottom of the reactor vessel and at the sidewall ($60^\circ < \theta < 90^\circ$) are 276 kW/m^2 and 1100 kW/m^2 , respectively. The critical heat flux on the vertical wall (above 90°) is 1300 kW/m^2 . Interpolation of the data at the angles between 0 and 60 degrees provides a reasonable estimate of the other critical heat fluxes. Based on the results of the analysis of the combinations of the uncertainties, two cases fail to meet the success criteria: IVR.8 and IVR.16. Both cases fail the vessel at the side of the metal pool, and in both cases, nodes MD, DK, and QUP are failed. Based on this result, the following split fractions have been assigned to node IVR:

Given (MD=F, DK=F, and QUP=F) - Probability of failure = 1.0

Otherwise - Probability of failure = 0.0

36.6 Results

The overall result of the analysis is that the conditional probability of the failure of the reactor vessel into a cavity which has been successfully flooded is 1.0×10^{-4} . The contribution to this probability is from the uncertainty in the phenomena controlling the amount of heat that must be removed from the vessel wall.

This conditional probability is applied at node VF (vessel failure) on the containment event tree given successful outcomes at nodes IR (cavity flooding) and SE (in-vessel steam explosion). Failure of node VF under these conditions represents the release of molten debris into a fully flooded cavity. As shown in this analysis, the best-estimate (assigned a probability of 0.9) vessel failure mode is above the debris oxide pool elevation which would significantly limit the mass of debris that would relocate to the containment. However, if the vessel were postulated to fail below the debris, a large debris mass would relocate to the containment and could possibly participate in an ex-vessel steam explosion. If the debris quench (node DQ) is successful, then the sequence is assumed to result in early containment failure with a probability of 0.1, the split fraction assigned to node MX of the ex-vessel steam

explosion event tree (see Chapter 39). The failure of node MX indicates that the premixing of the debris in the water would produce a steam explosion in the cavity. This sequence is treated in this way in order to account for the uncertainties in the containment response to a steam explosion in a fully flooded cavity. The treatment conservatively assumes that, given reactor vessel failure below the debris pool and a steam explosion in a fully flooded reactor cavity, the conditional probability of containment failure is 1.0.

36.7 References

- 36-1 Vessel Investigation Project Integration Report, TMI V(93)EG10, OECD-NEA-TMI-2, October 1993.
- 36-2 Kymalainen, O., et. al, "Heat Flux Distribution from a Volumetrically Heated Pool with High Rayleigh Number," Proceedings of NURETH-6, Grenoble, France, October 5-8, 1993.
- 36-3 Frantz, B. and V.K. Dhir, "Experimental Investigation of Natural Convection in Spherical Segments of Volumetrically Heated Pools," ASME Proceeding 1992 National Heat Transfer Conference, San Diego, CA, August 9-12, 1992.
- 36-4 *AP600 Phenomenological Evaluation Summaries*, WCAP-13388 (Proprietary) Rev. 0, June, 1992 and WCAP-13389 (Nonproprietary), Rev. 1, 1994.
- 36-5 Chu, T.Y., et. al, Quick Look Report for NE1 Experiment, Sandia National Laboratories, November 1993.
- 36-6 Chu, T.Y., et. al, Quick Look Report for NE2 Experiment, Sandia National Laboratories, November 1993.
- 36-7 Theofanous, T. G., et al, "Experience from the First Two Integrated Approaches to In-Vessel Retention Through External Cooling," OECD/CSNI/NEA Workshop on Large Molten Pool Heat Transfer, Grenoble, France, March 9 - 11, 1994.
- 36-8 Mayinger, F., et. al., "Examination of Thermal-hydraulic Processes and Heat Transfer in a Core Melt," BMFT RS 48/1, Institute fur Verfahrenstechnik der T. U. Hanover, 1976.
- 36-9 Henry, R. E., et. al., "Cooling of Debris Within the Reactor Vessel Lower Head," ANS Topical Meeting, June, 1991.
- 36-10 VDI-Warmeatlas, Berechnungsblätter für den Wärmenbergang, Sechste Auflage, VDI-Verlag, Dusseldorf, 1991.



- 36-11 O'Brien, J. E., Hawkes, G. L., "ARSAP AP600 In-Vessel Coolability Thermal Analysis Final Report," DOE/ID-10369, December 1991.
- 36-12 Theofanovs, T. G., et. al., "Critical Heat Flux Through Curved, Downward Facing, Thick Walls, Int'l Conf.," New Trends in Nuclear System Thermohydraulics, PSIA, May 30 - June 2, 1994.



Table 36-1

COMBINATIONS OF UNCERTAINTIES FOR THE IVR DET

Case Name	Cavity Flooding	Debris Character	Decay Power	Pool Emissivity	Max. Side Heat Flux (kW/m ²)
IVR.1	S	S	S	S	608
IVR.2	S	S	S	F	721
IVR.3	S	S	F	S	896
IVR.4	S	S	F	F	1020
IVR.5	S	F	S	S	696
IVR.6	S	F	S	F	823
IVR.7	S	F	F	S	1022
IVR.8	S	F	F	F	1162
IVR.9	F	S	S	S	647
IVR.10	F	S	S	F	739
IVR.11	F	S	F	S	946
IVR.12	F	S	F	F	1043
IVR.13	F	F	S	S	742
IVR.14	F	F	S	F	844
IVR.15	F	F	F	S	1080
IVR.16	F	F	F	F	1189



Table 36-2

MATERIAL PROPERTIES USED FOR IVR ANALYSIS

	Metal Pool	Oxide Pool
Density (kg/m ³)	6930	7270
Thermal Conductivity (W/m/K)	20	5.7
Spec. Ht. Capacity (J/kg/K)	560	618
Viscosity (kg/m/s)	2.3×10^{-2}	7.14×10^{-3}
Thermal Expansion (1/K)	1.3×10^{-4}	1.1×10^{-4}
Melting Temperature (K)	1600	2600

Table 36-3

INPUT TO IVR ANALYSIS

	Best Estimate	Bounding Estimate
Water Level Above Debris (m)	6	2.5
Mass of Oxide Pool (metric tons)	90.5	95.3
Mass of Metal Pool (metric tons)	40.9	37.3
Decay Power (MW/m ³)	1.0	1.3
Emissivity of Metal Pool	0.55	0.40

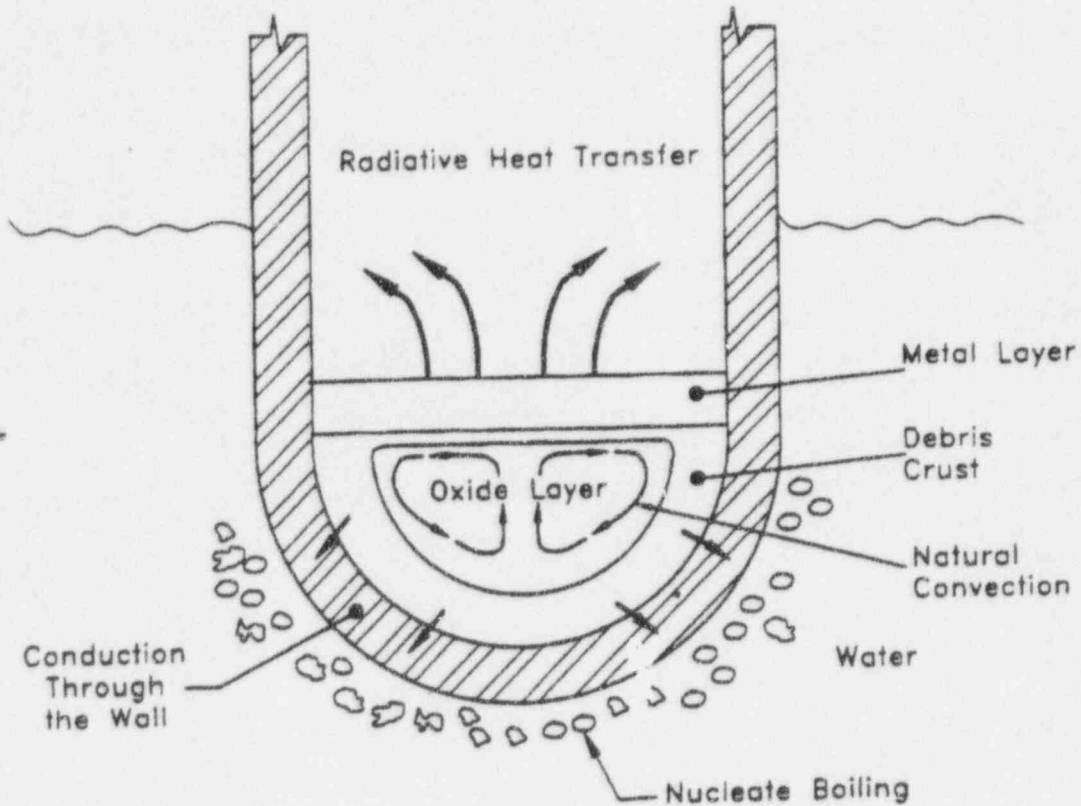


Figure 36-1

In-Vessel Retention Phenomena

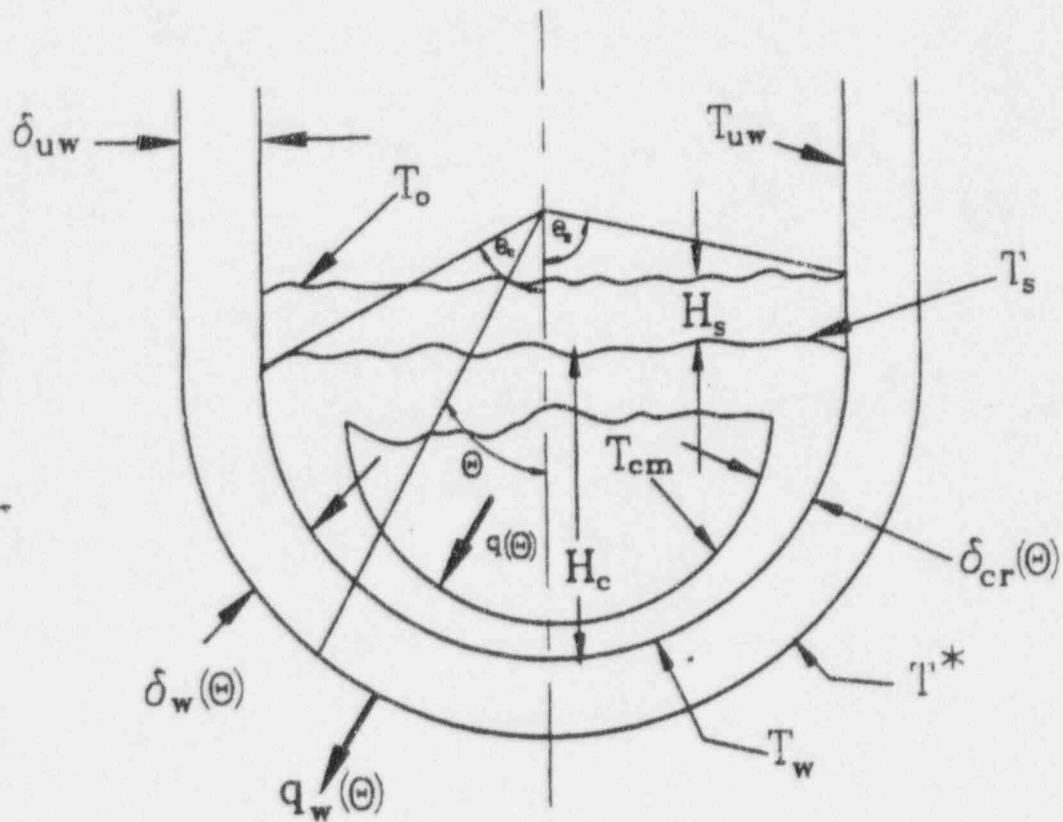


Figure 36-2

In-Vessel Retention Model

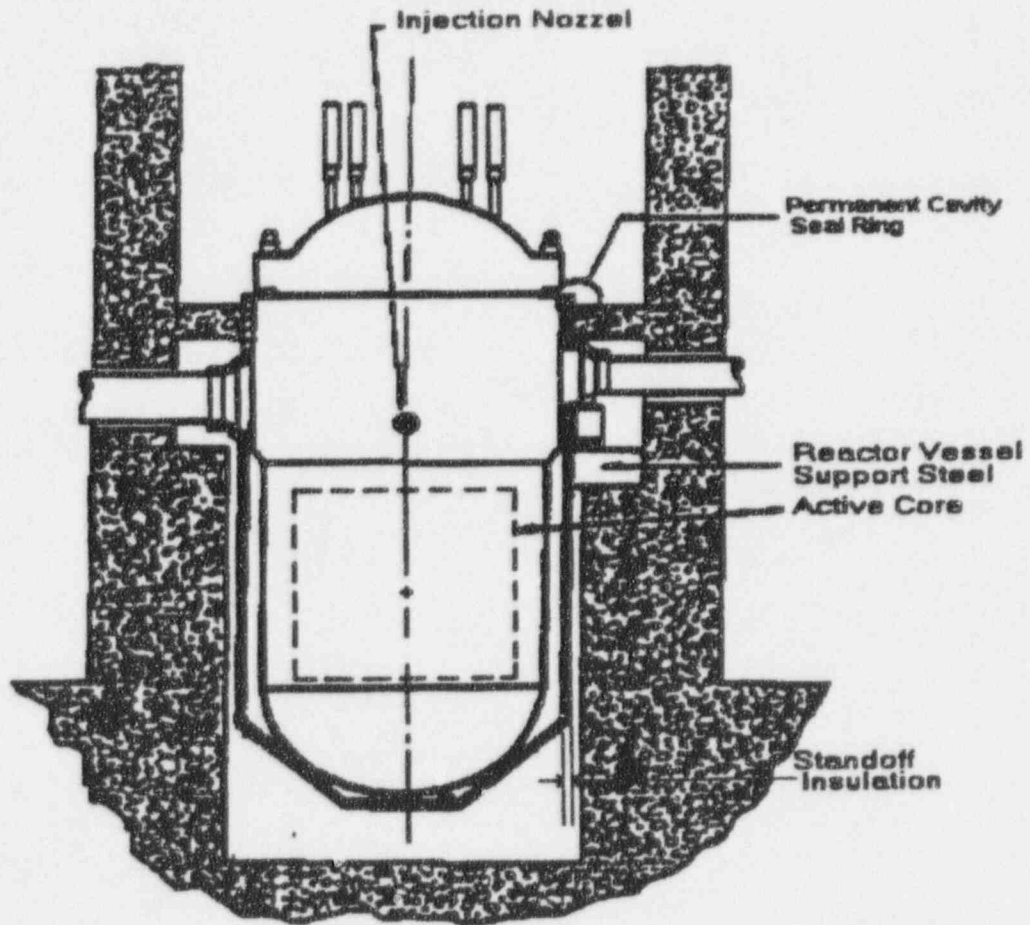


Figure 36-3

AP600 Reactor Vessel Standoff Insulation

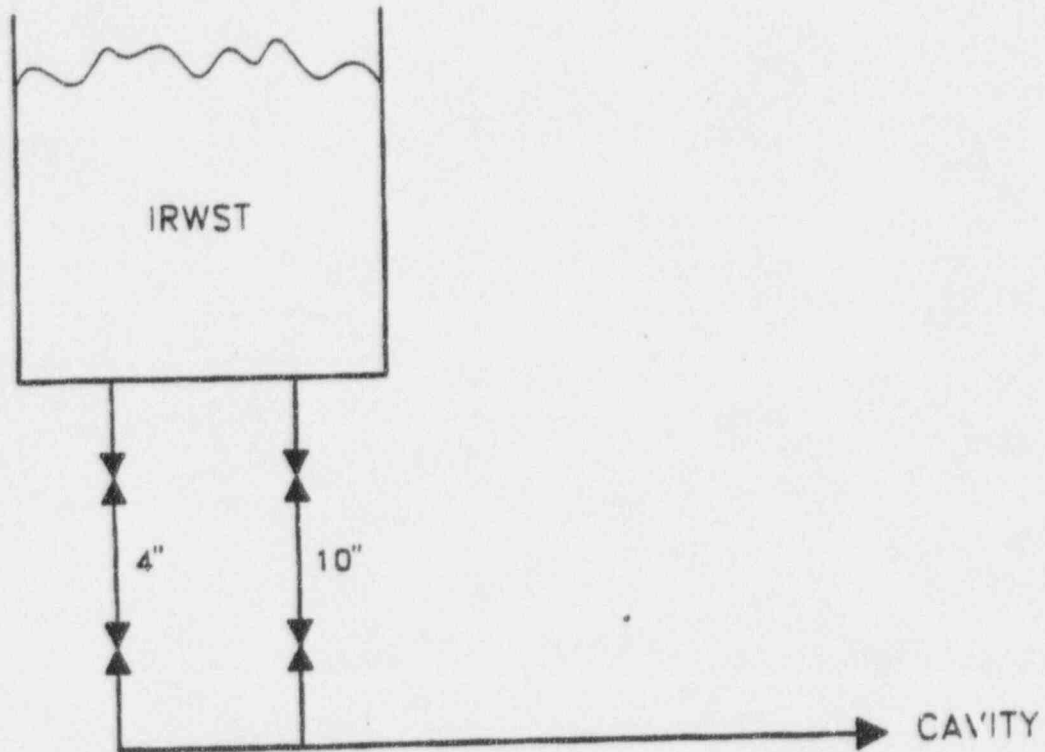


Figure 36-4

AP600 Cavity Flooding System Schematic

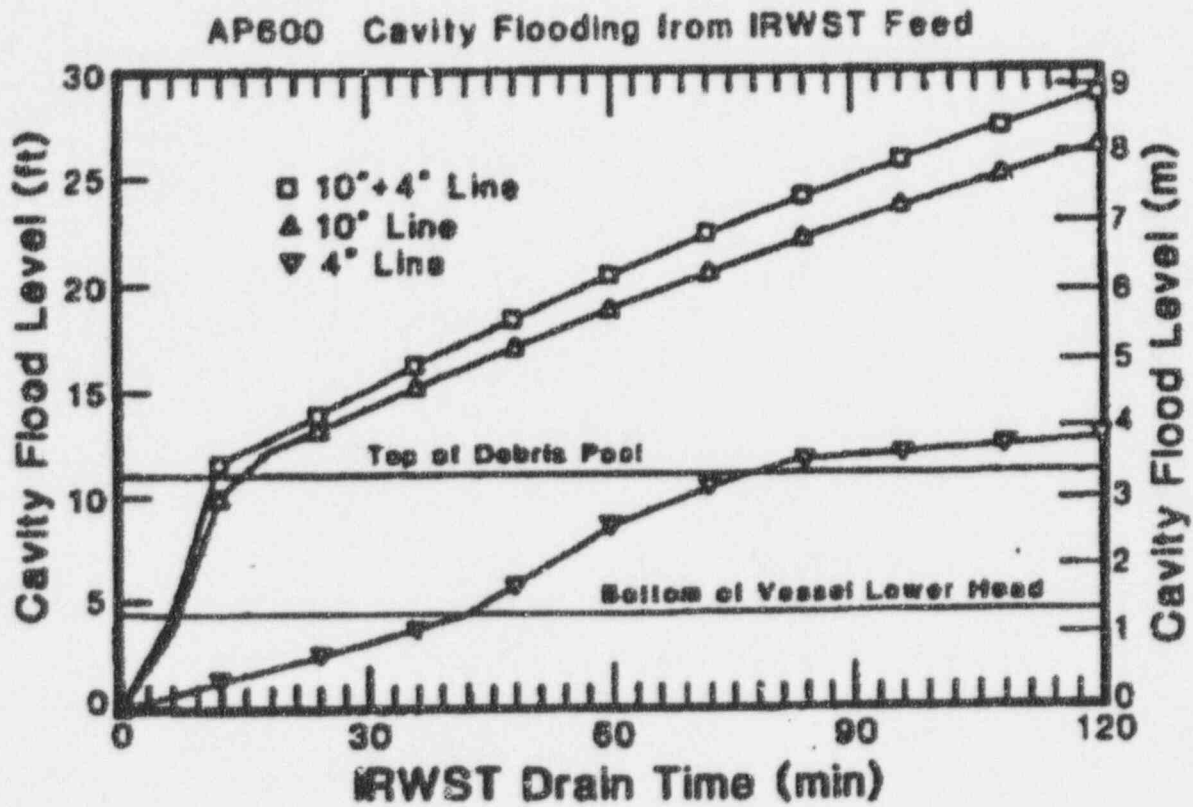
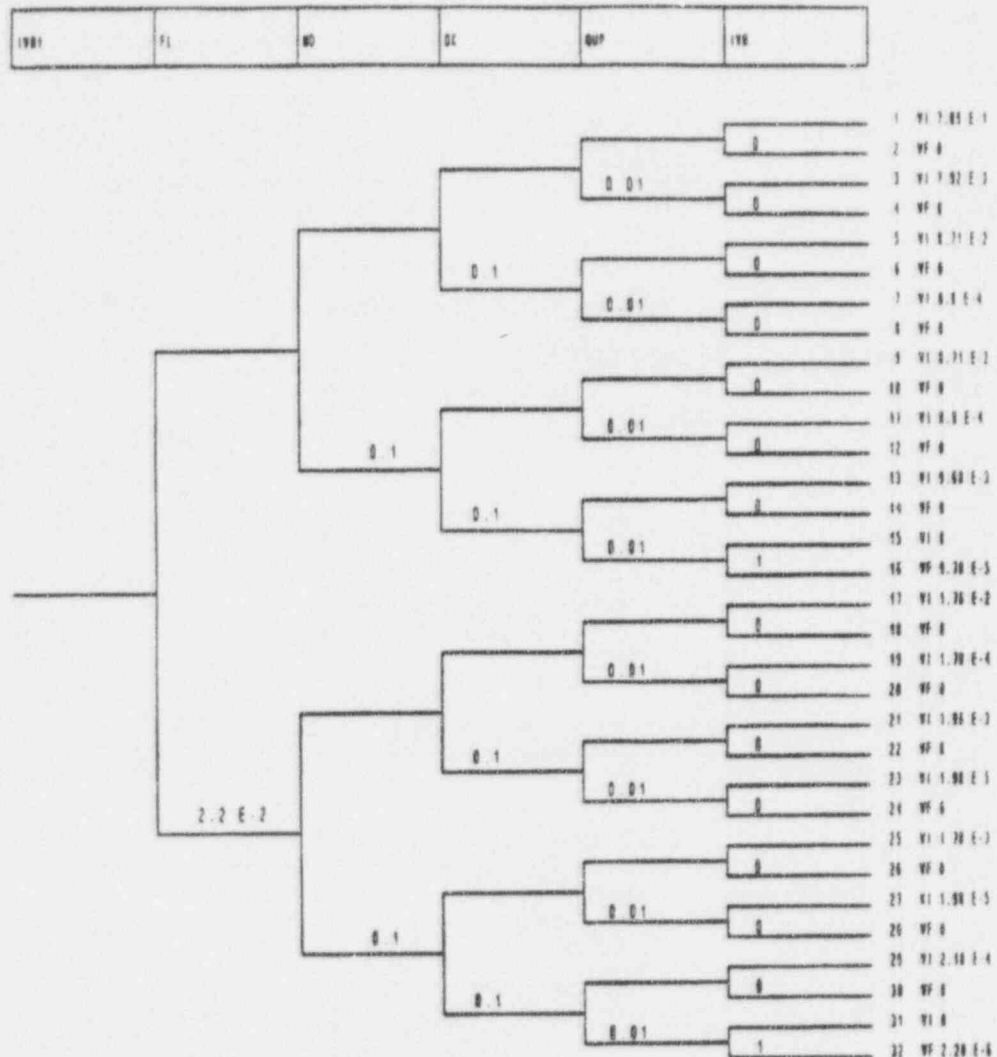


Figure 36-5

AP600 Cavity Flooding Rate



36. Decomposition Event Tree - Analysis of In-Vessel Retention of Molten Core Debris



DET IVR - In-Vessel Retention of Molten Core Debris
List of top events

Event	Description
IVR	Core Filled and Intact Vessel
FL	Degree of Flooding of Lower Head
MO	Mass of Molten and Oxide in the Debris
DC	Amount of Decay Heat in the Debris
QUP	Upward Heat Transfer (Radiation Limited)
IVR	CMF Escaped as Debris Shell

Figure 36-6

AP600 IVR Decomposition Event Tree

Case IVR.1 - FL=S, MD=S, DK=S, QUP=S
Heat Flux Distribution Through Vessel Wall

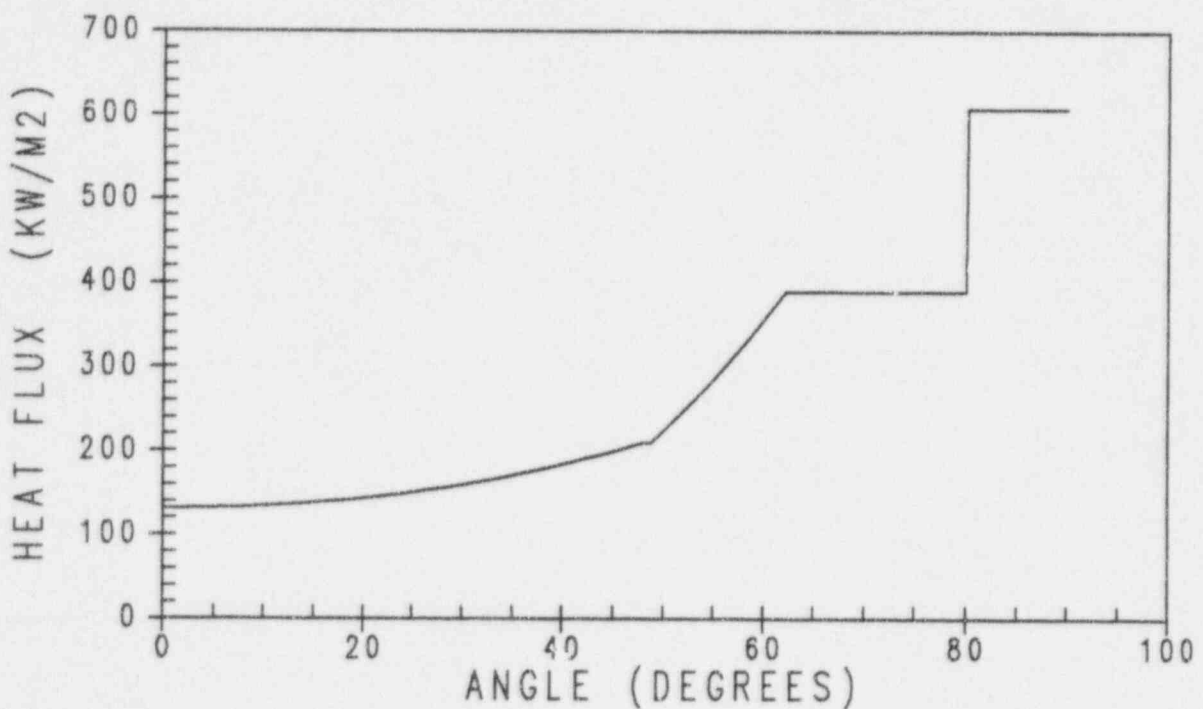


Figure 36-7

Case IVR.1 - Heat Flux Distribution Through Vessel Wall

Case IVR.1 - FL=S, MD=S, DK=S, QUP=S
Remaining Thickness of Vessel Wall

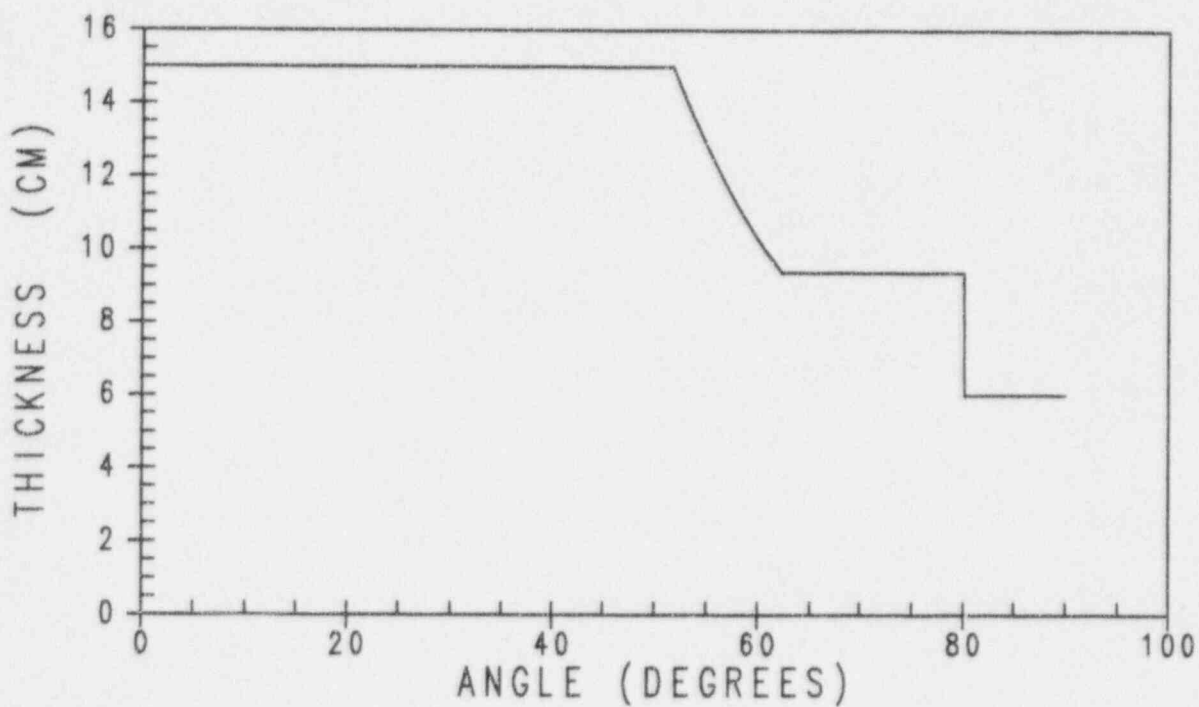


Figure 36-8

Case IVR.1 - Remaining Thickness of Vessel Wall

Case IVR.2 - FL=S, MD=S, DK=S, QUP=F
Heat Flux Distribution Through Vessel Wall

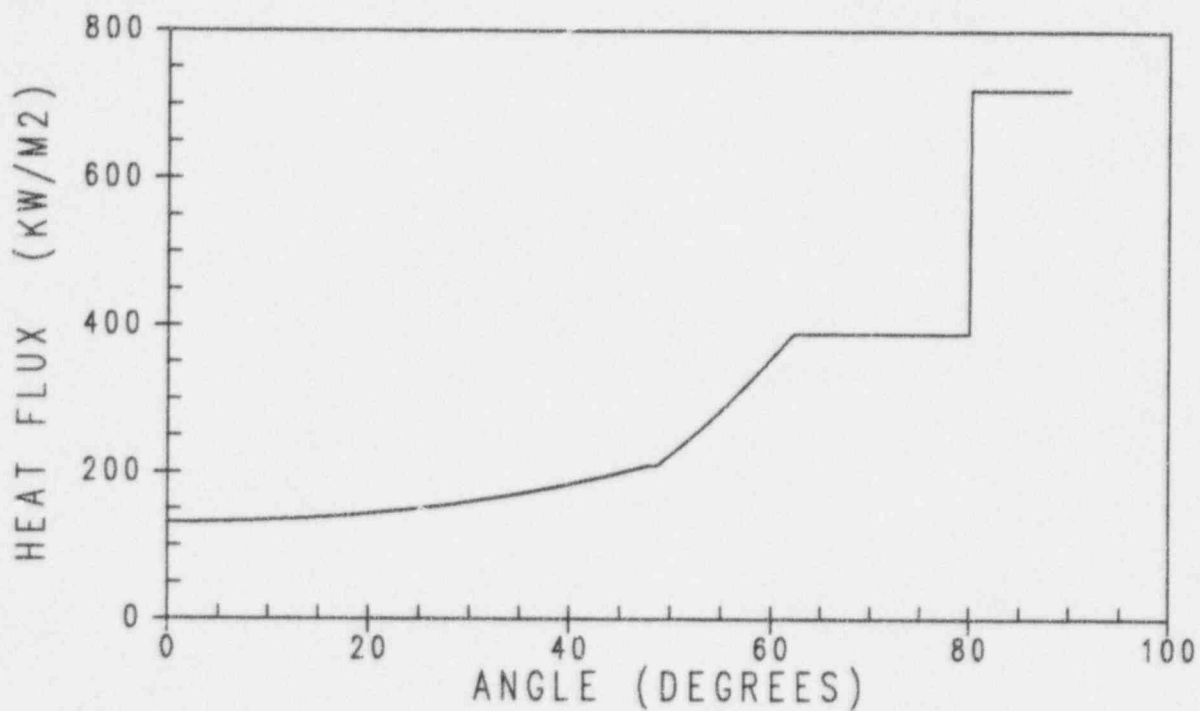


Figure 36-9

Case IVR.2 - Heat Flux Distribution Through Vessel Wall

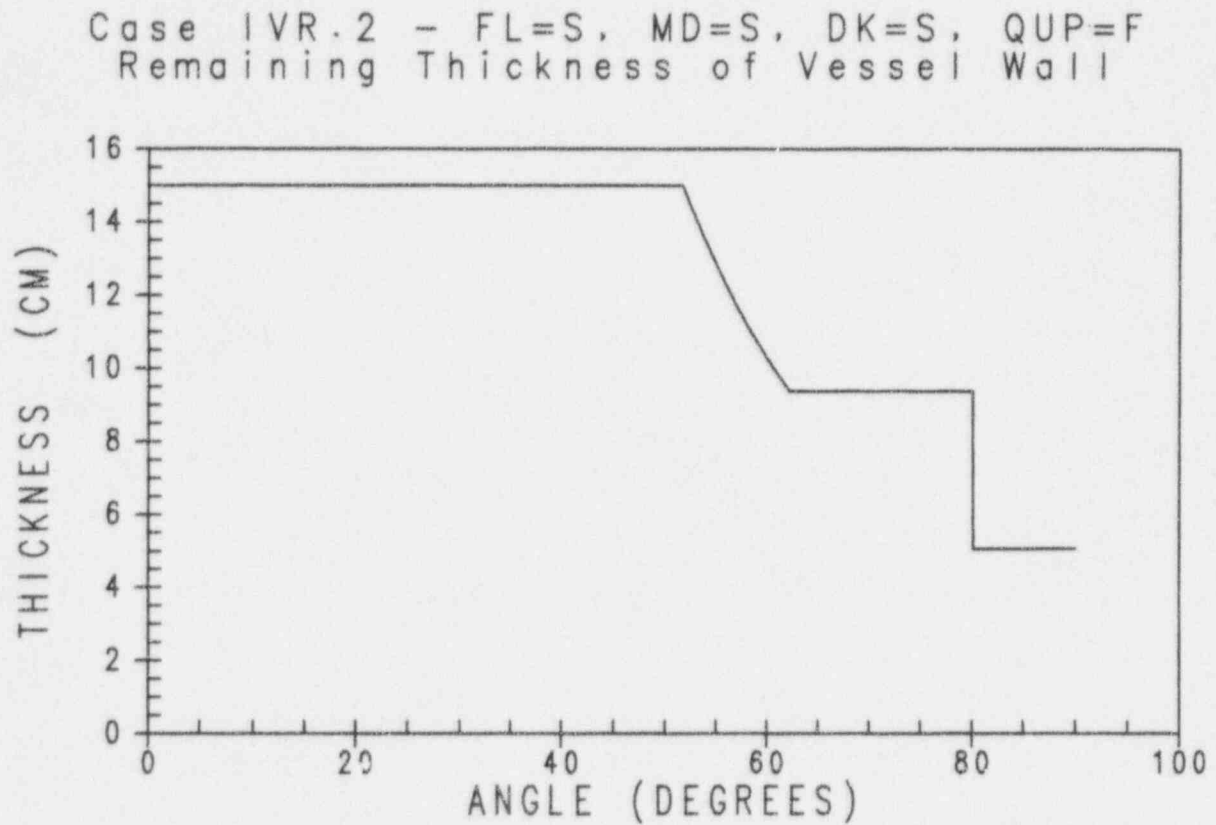


Figure 36-10

Case IVR.2 - Remaining Thickness of Vessel Wall

Case IVR.3 - FL=S, MD=S, DK=F, QUP=S
Heat Flux Distribution Through Vessel Wall

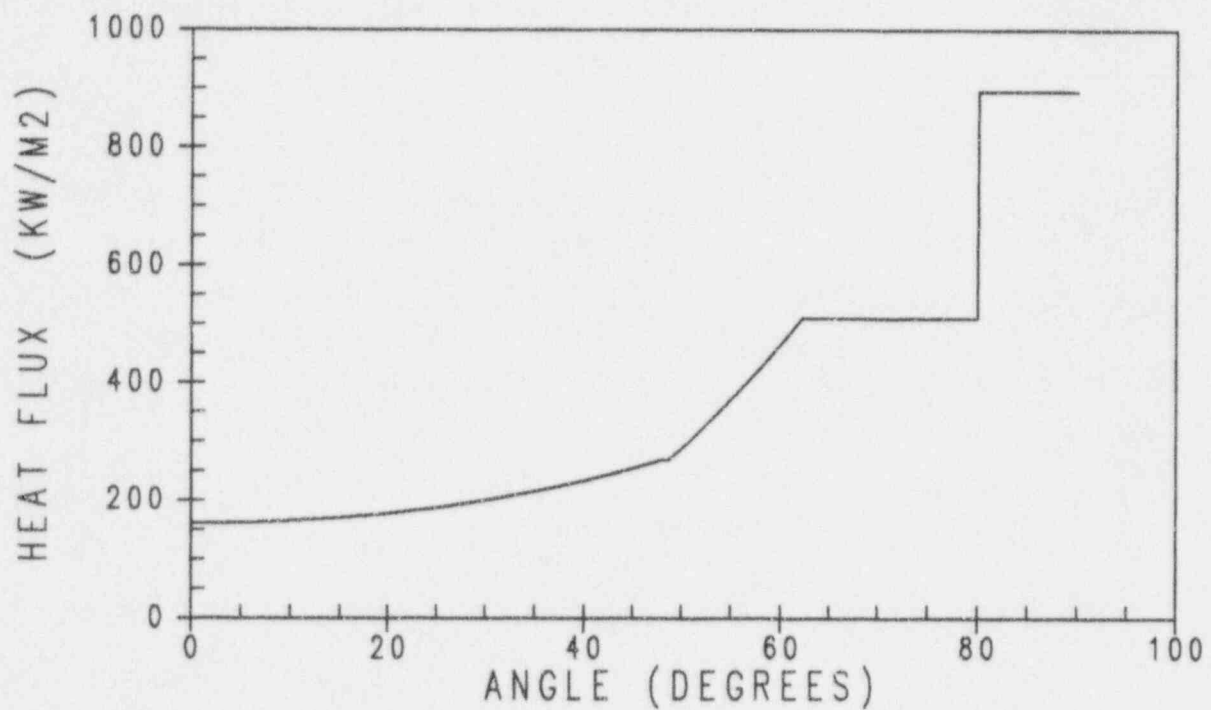


Figure 36-11

Case IVR.3 - Heat Flux Distribution Through Vessel Wall

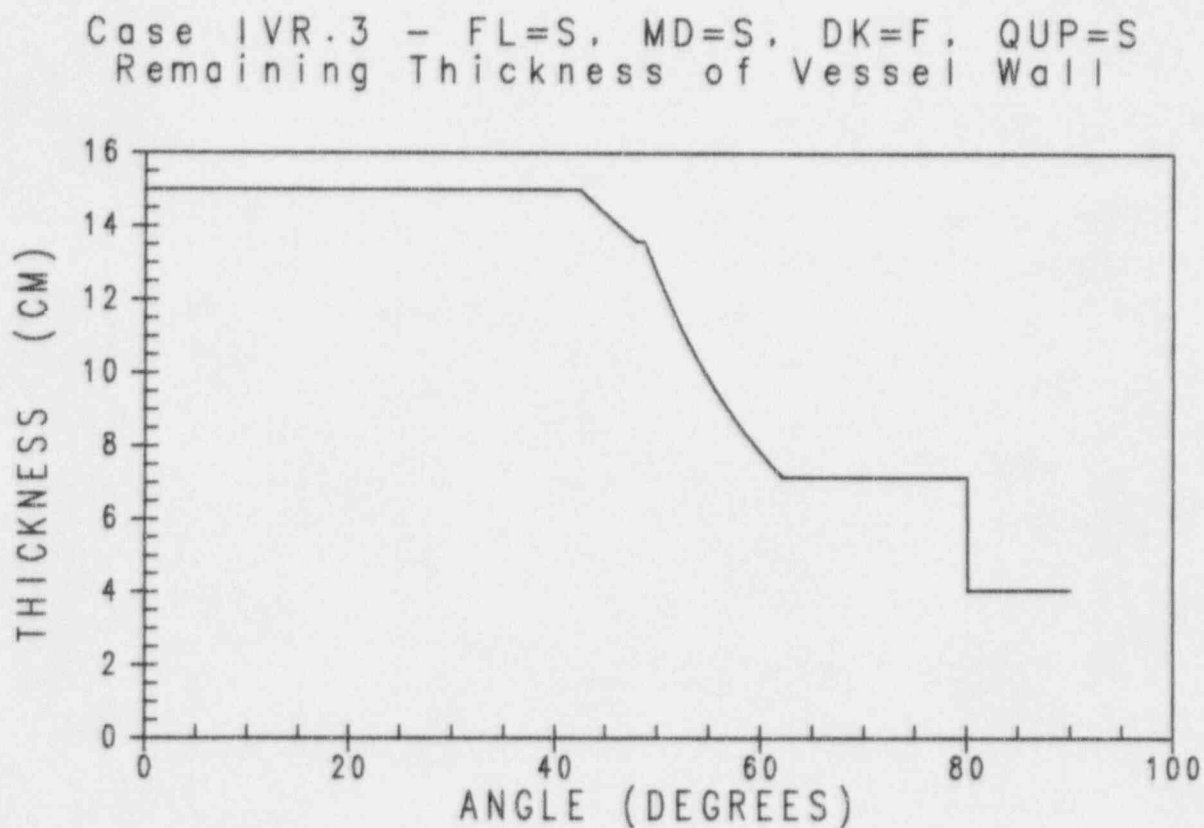


Figure 36-12

Case IVR.3 - Remaining Thickness of Vessel Wall

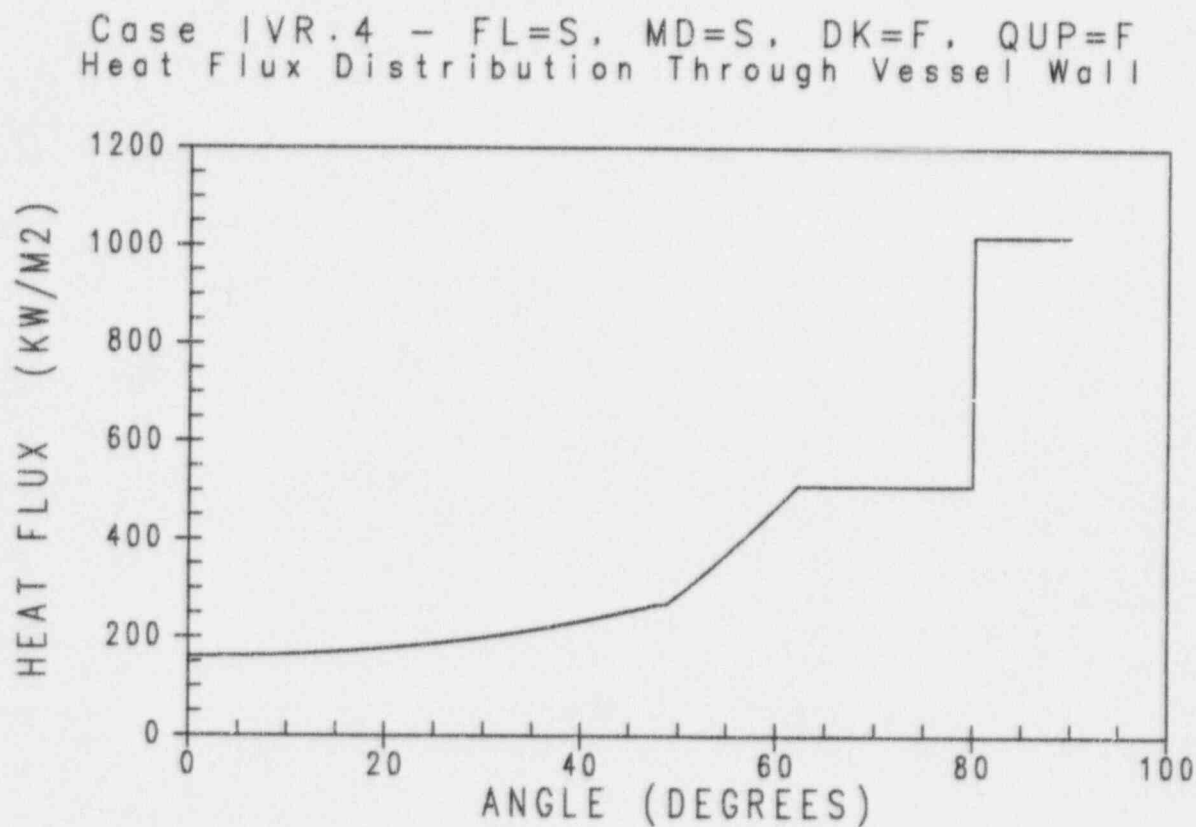


Figure 36-13

Case IVR.4 - Heat Flux Distribution Through Vessel Wall

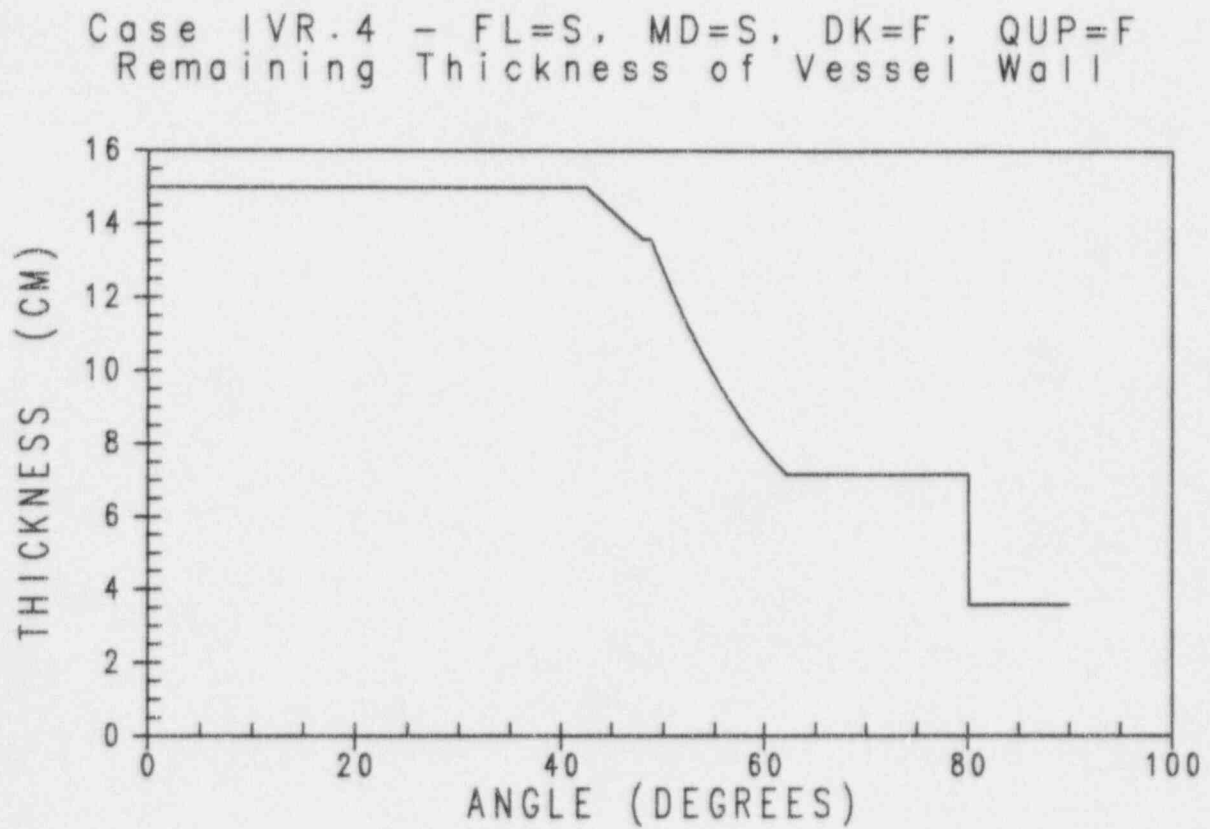


Figure 36-14

Case IVR.4 - Remaining Thickness of Vessel Wall

Case IVR.5 - FL=S, MD=F, DK=S, QUP=S
Heat Flux Distribution Through Vessel Wall

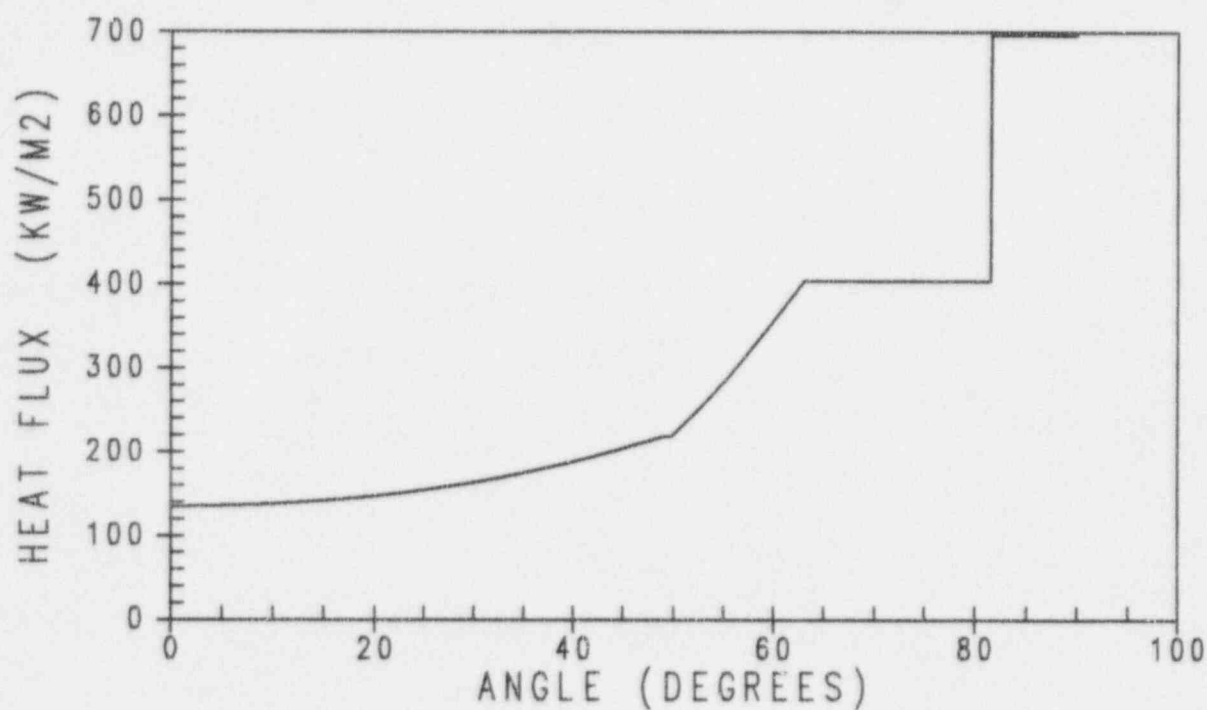


Figure 36-15

Case IVR.5 - Heat Flux Distribution Through Vessel Wall

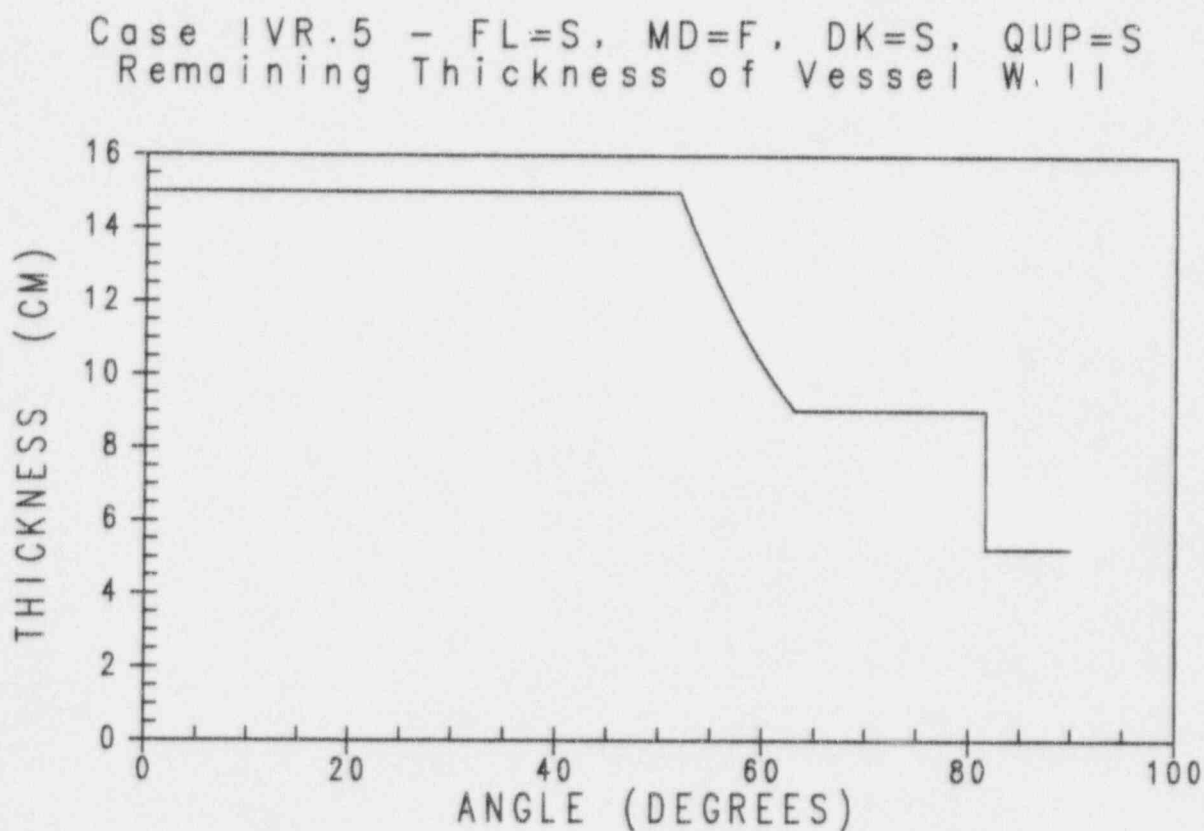


Figure 36-16

Case IVR.5 - Remaining Thickness of Vessel Wall

Case IVR.6 - FL=S, MD=F, DK=S, QUP=F
Heat Flux Distribution Through Vessel Wall

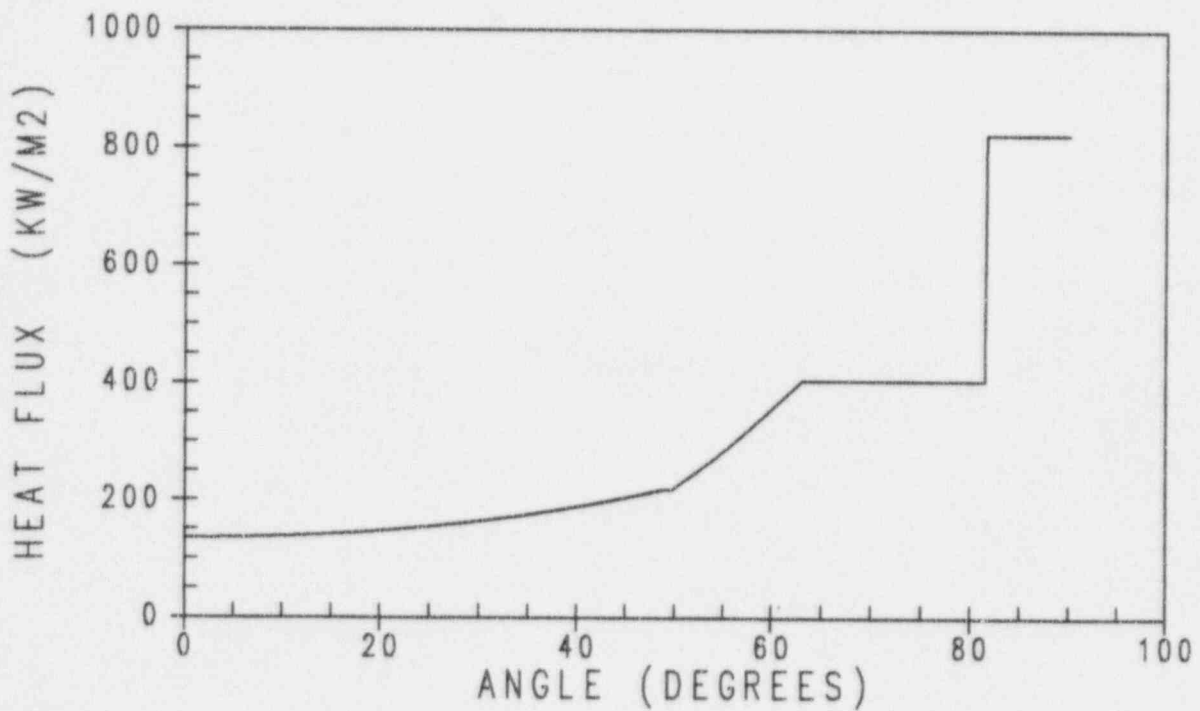


Figure 36-17

Case IVR.6 - Heat Flux Distribution Through Vessel Wall

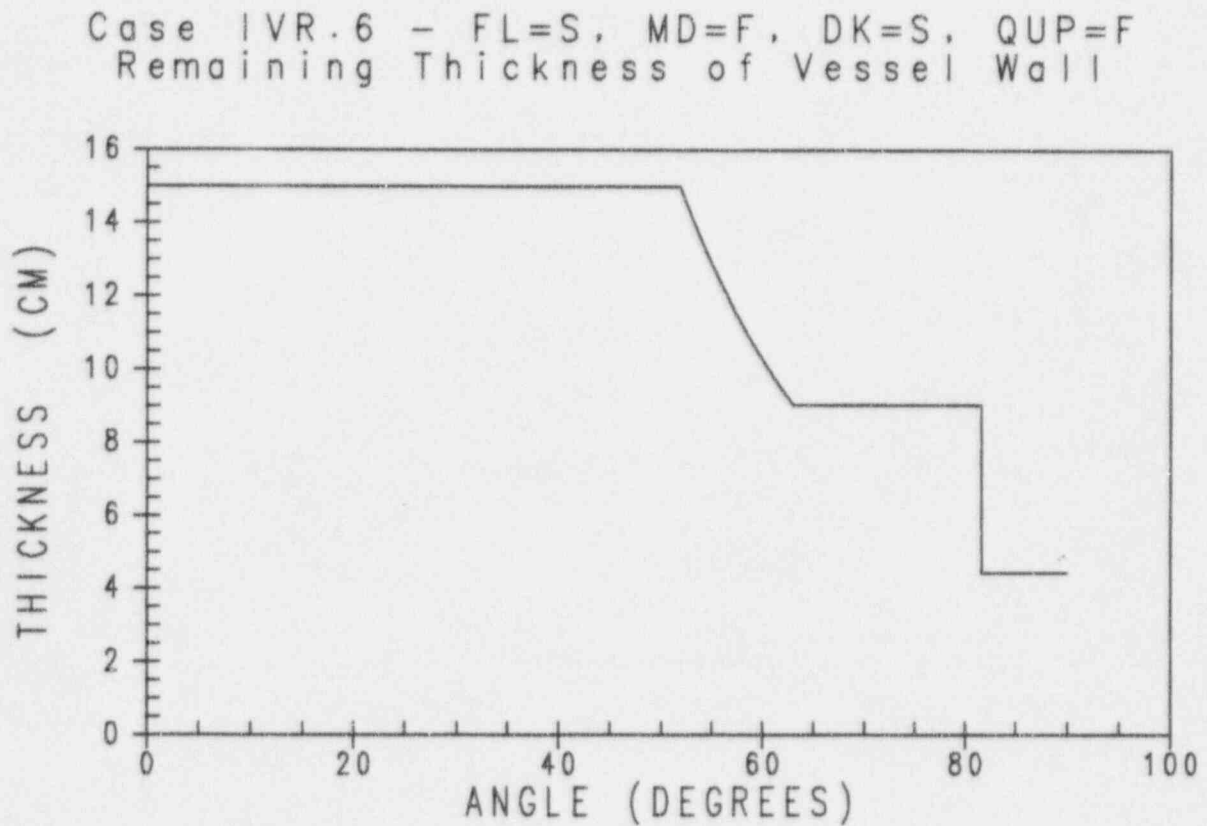


Figure 36-18

Case IVR.6 - Remaining Thickness of Vessel Wall

Case IVR.7 - FL=S, MD=F, DK=F, QUP=S
Heat Flux Distribution Through Vessel Wall

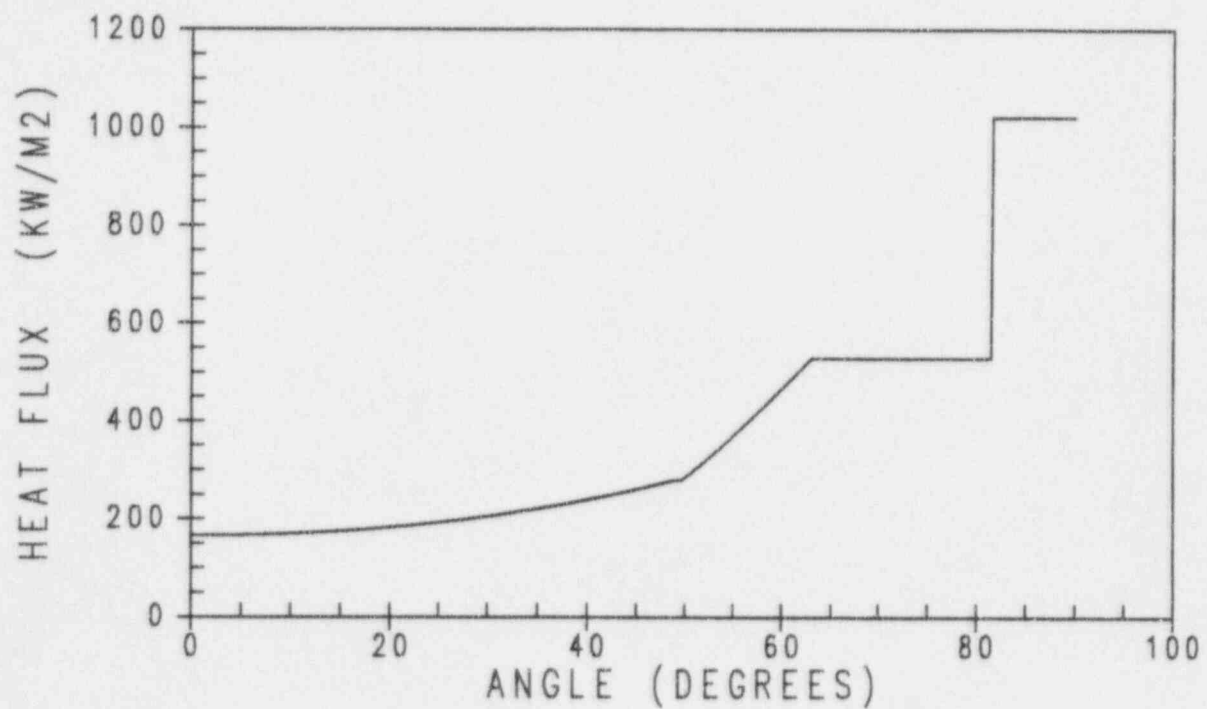


Figure 36-19

Case IVR.7 - Heat Flux Distribution Through Vessel Wall

Case IVR.7 - FL=S, MD=F, DK=F, QUP=S
Remaining Thickness of Vessel Wall

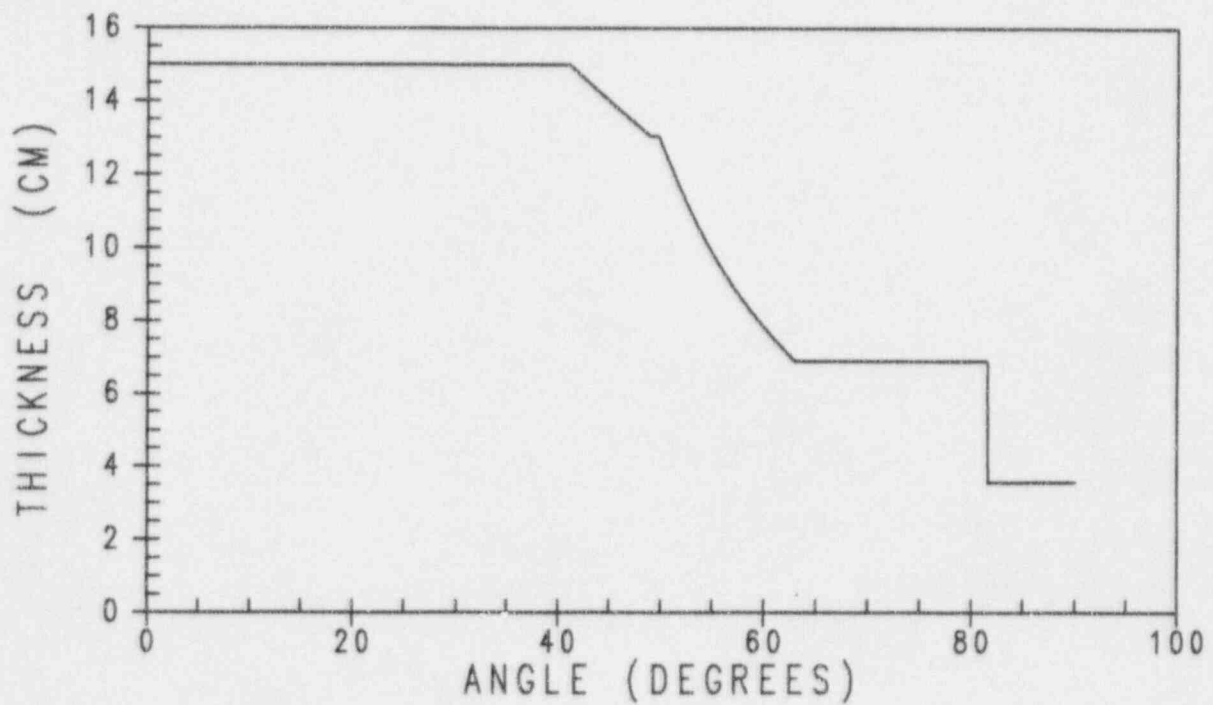


Figure 36-20

Case IVR.7 - Remaining Thickness of Vessel Wall

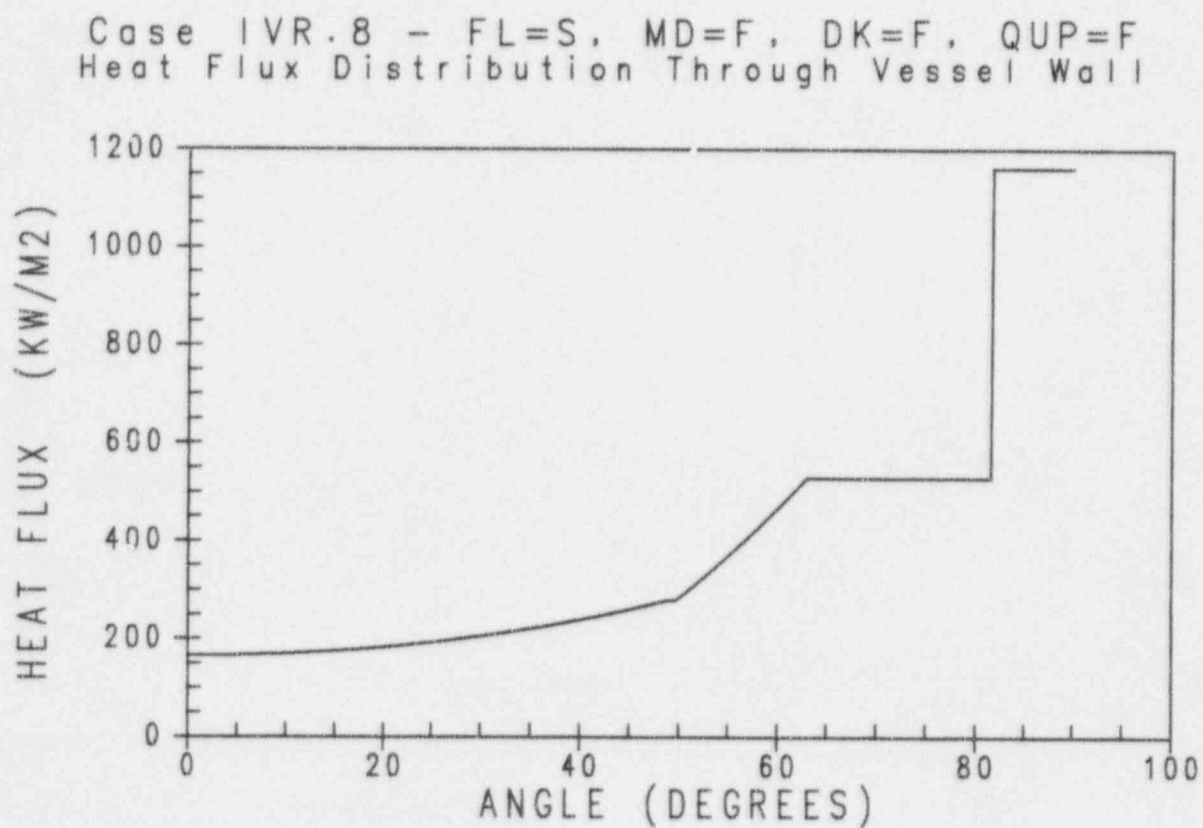


Figure 36-21

Case IVR.8 - Heat Flux Distribution Through Vessel Wall



Westinghouse

ENEL
ENTE NAZIONALE
PER L'ENERGIA ELETTRICA

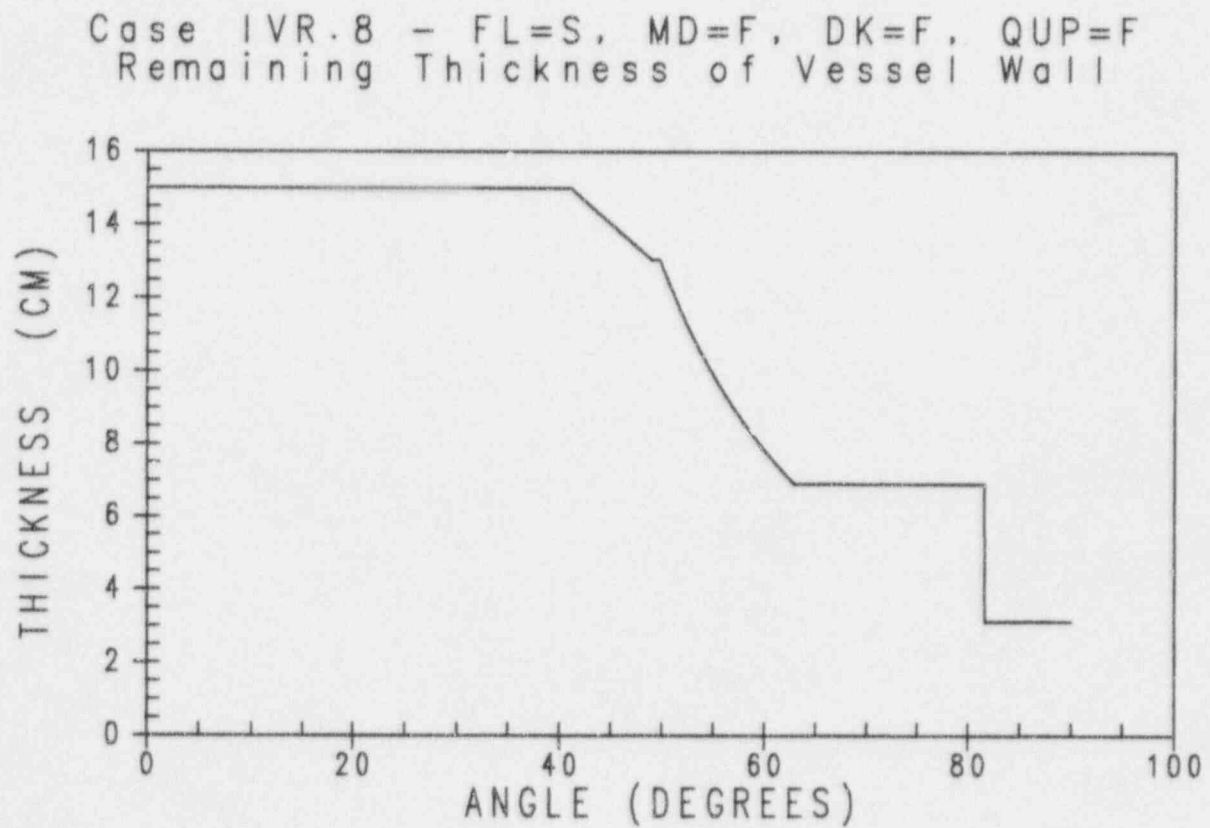


Figure 36-22

Case IVR.8 - Remaining Thickness of Vessel Wall

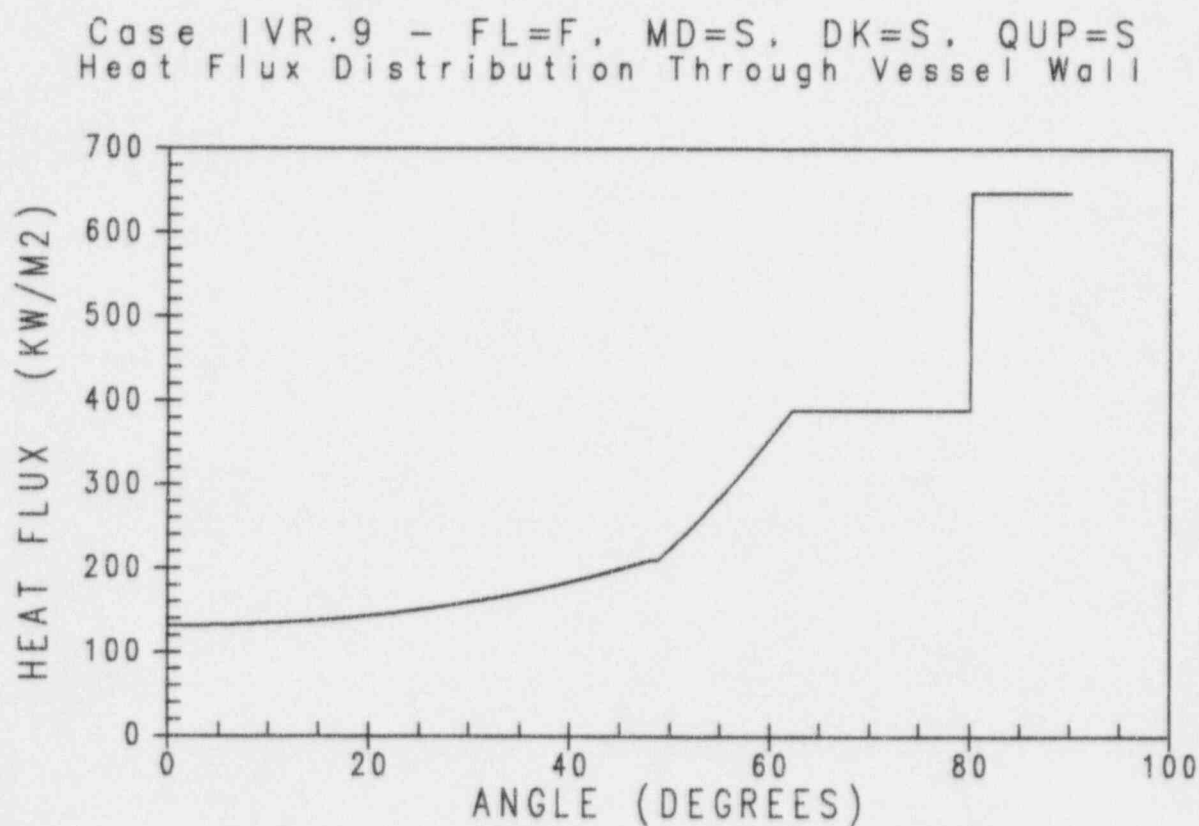


Figure 36-23

Case IVR.9 - Heat Flux Distribution Through Vessel Wall



Westinghouse

ENEL
ENTE NAZIONALE
PER L'ENERGIA ELETTRICA

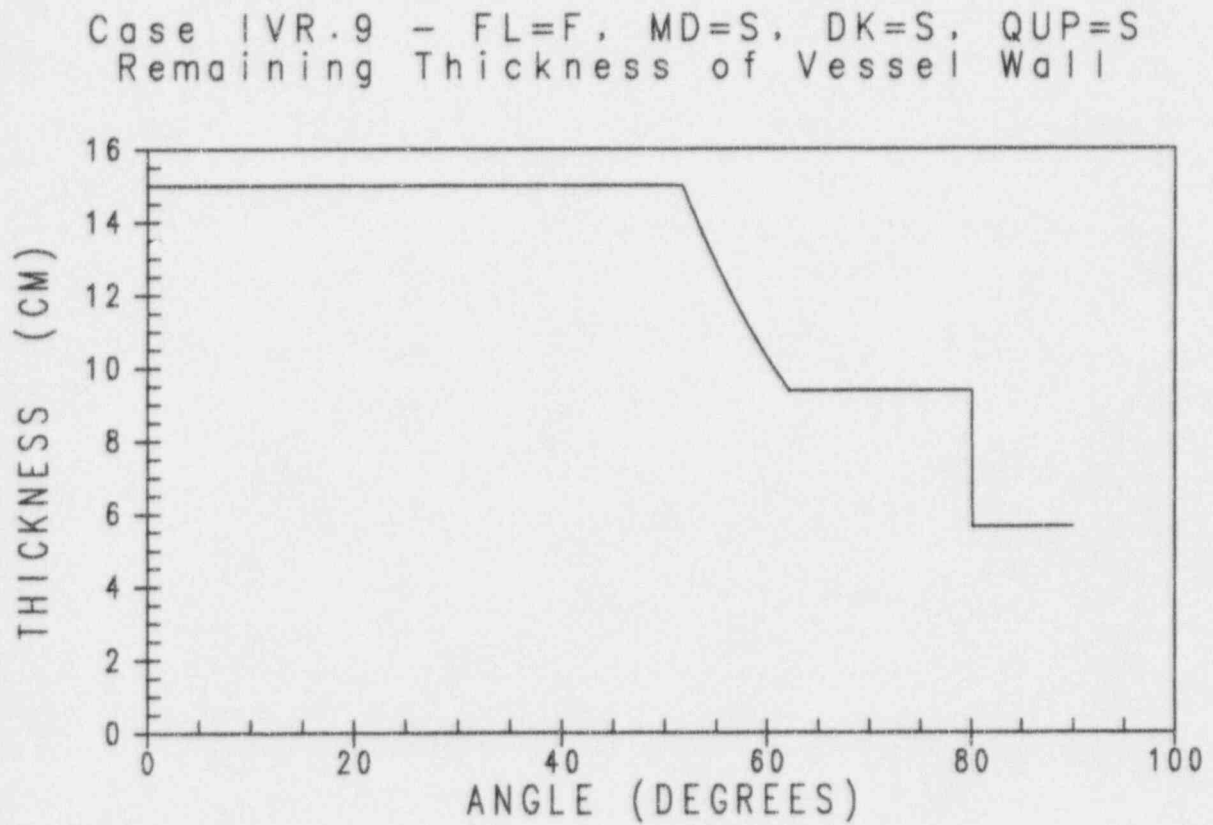


Figure 36-24

Case IVR.9 - Remaining Thickness of Vessel Wall

Case IVR.10 - FL=F, MD=S, DK=S, QUP=F
Heat Flux Distribution Through Vessel Wall

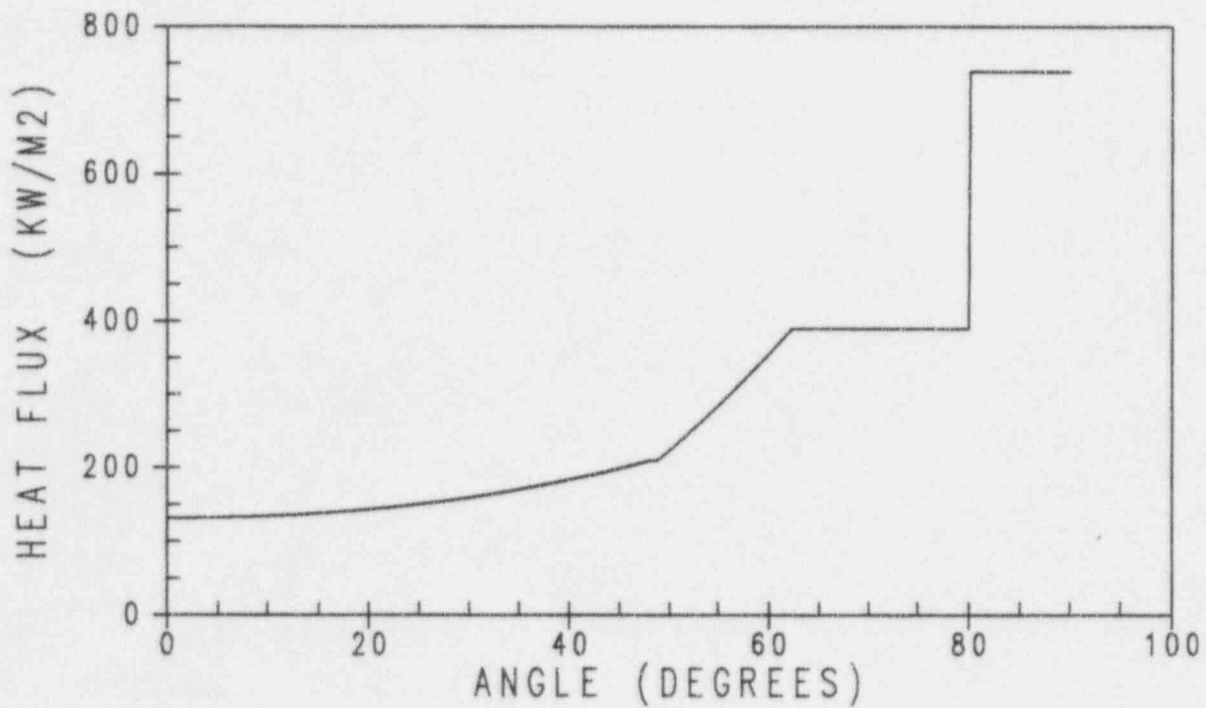


Figure 36-25

Case IVR.10 - Heat Flux Distribution Through Vessel Wall



Westinghouse

ENEL
ENTE NAZIONALE
PER L'ENERGIA ELETTRICA

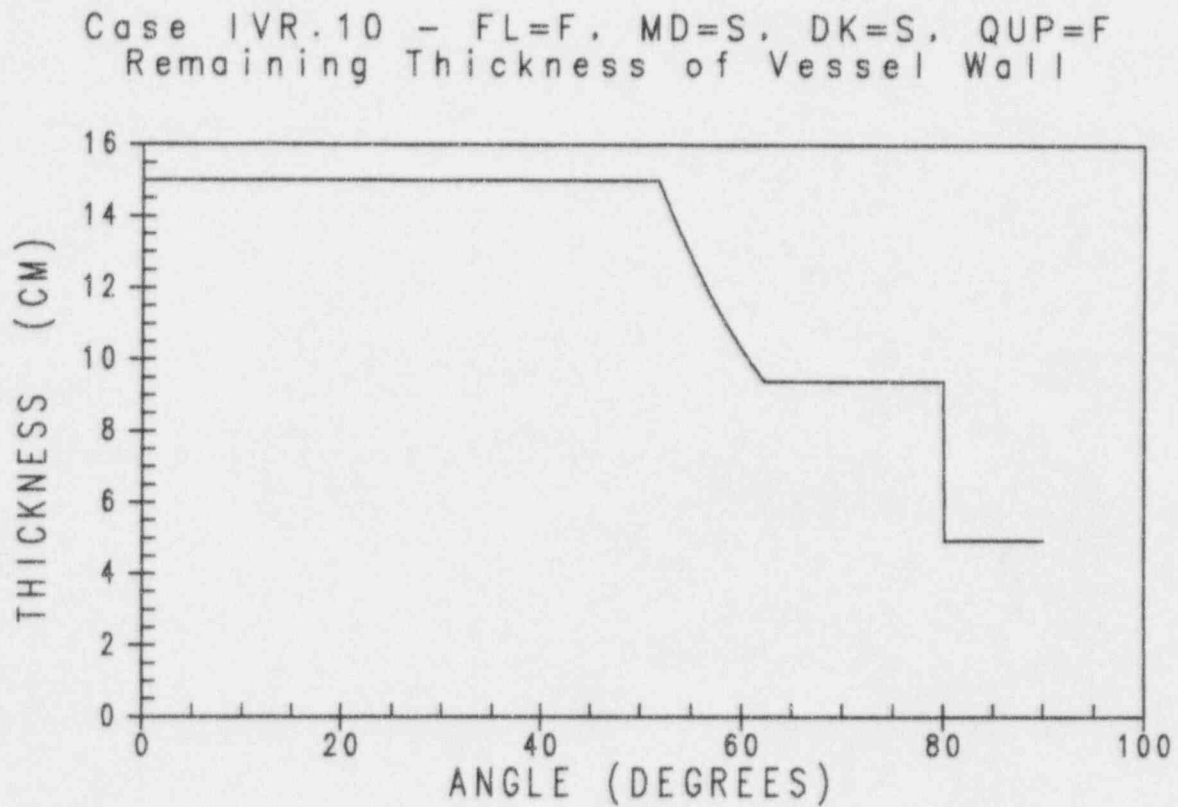


Figure 36-26

Case IVR.10 - Remaining Thickness of Vessel Wall

Case IVR.11 - FL=F, MD=S, DK=F, QUP=S
Heat Flux Distribution Through Vessel Wall

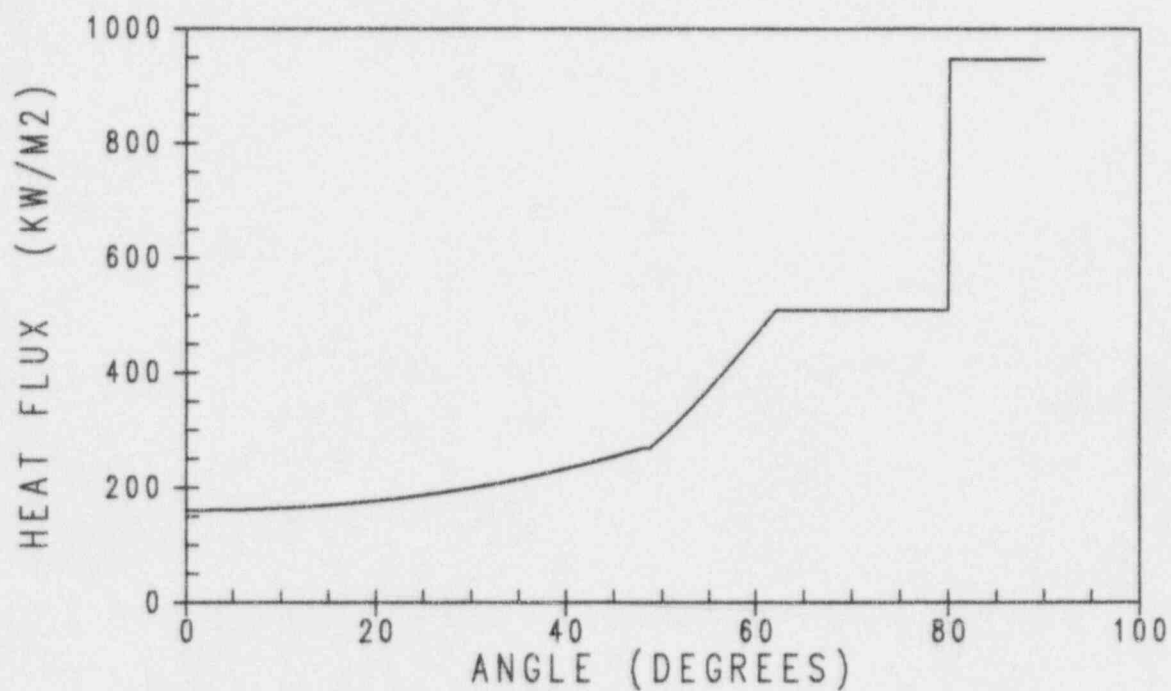


Figure 36-27

Case IVR.11 - Heat Flux Distribution Through Vessel Wall

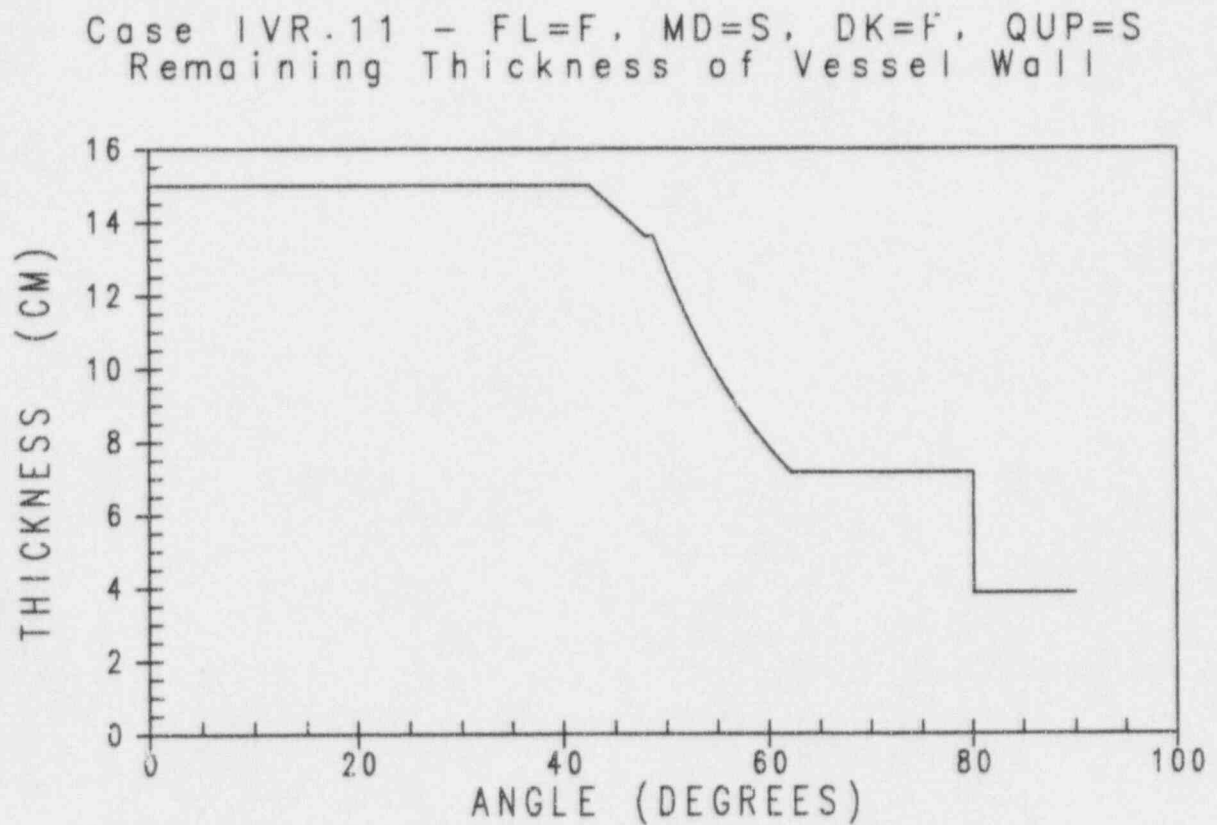


Figure 36-28

Case IVR.11 - Remaining Thickness of Vessel Wall

Case IVR.12 - FL=F, MD=S, DK=F, QUP=F
Heat Flux Distribution Through Vessel Wall

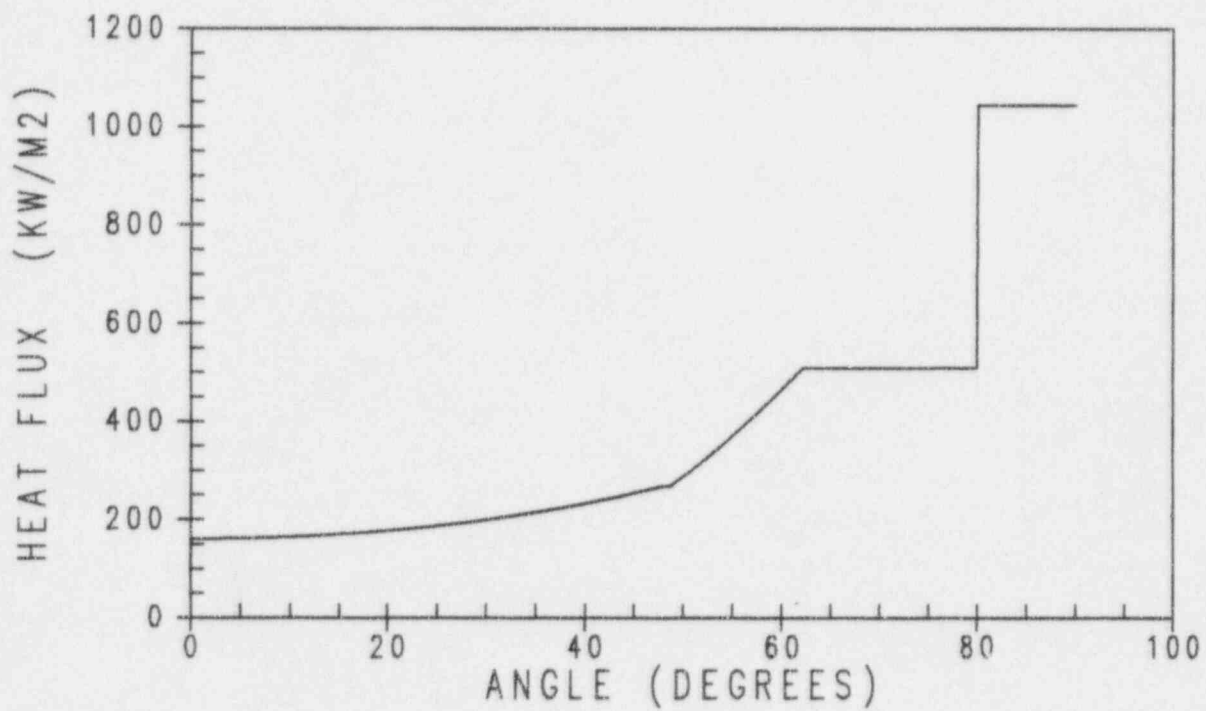


Figure 36-29

Case IVR.12 - Heat Flux Distribution Through Vessel Wall



Westinghouse

ENEL
ENTE NAZIONALE
PER L'ENERGIA ELETTRICA

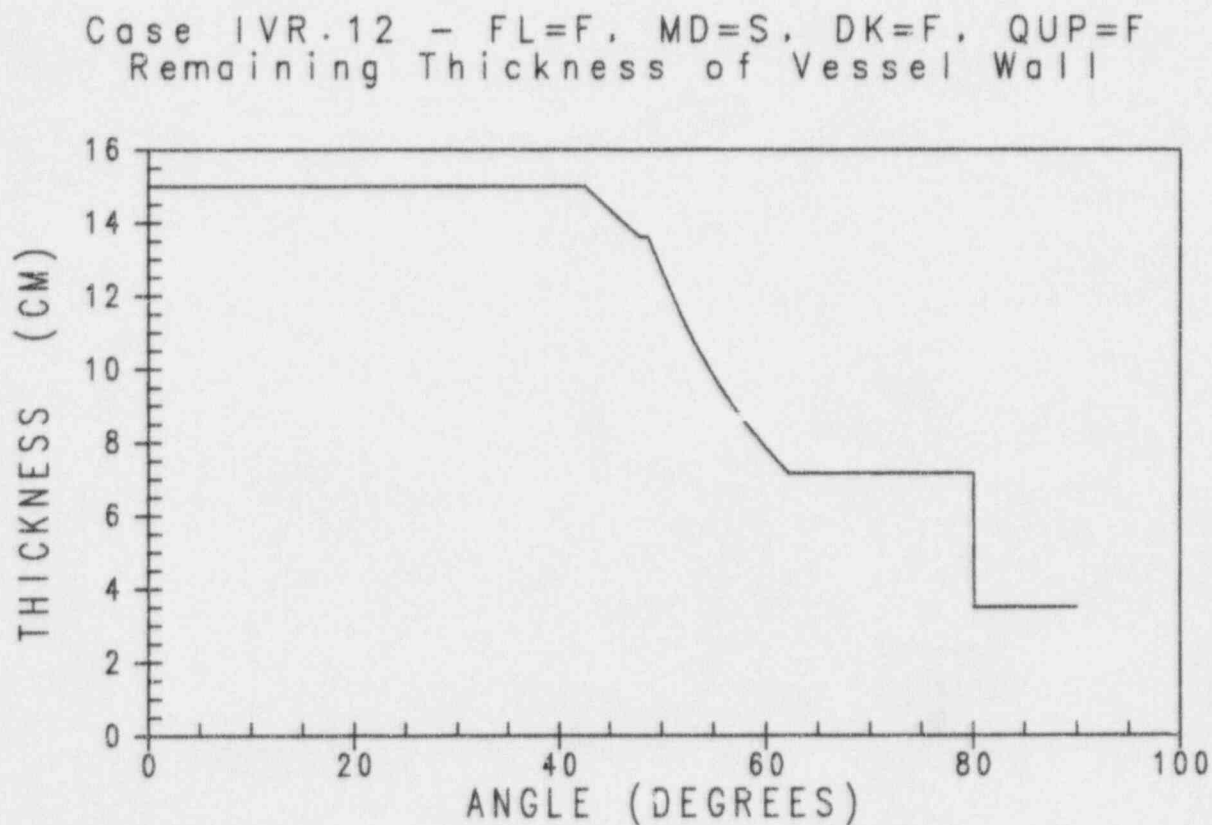


Figure 36-30

Case IVR.12 - Remaining Thickness of Vessel Wall

Case IVR.13 - FL=F, MD=F, DK=S, QUP=S
Heat Flux Distribution Through Vessel Wall

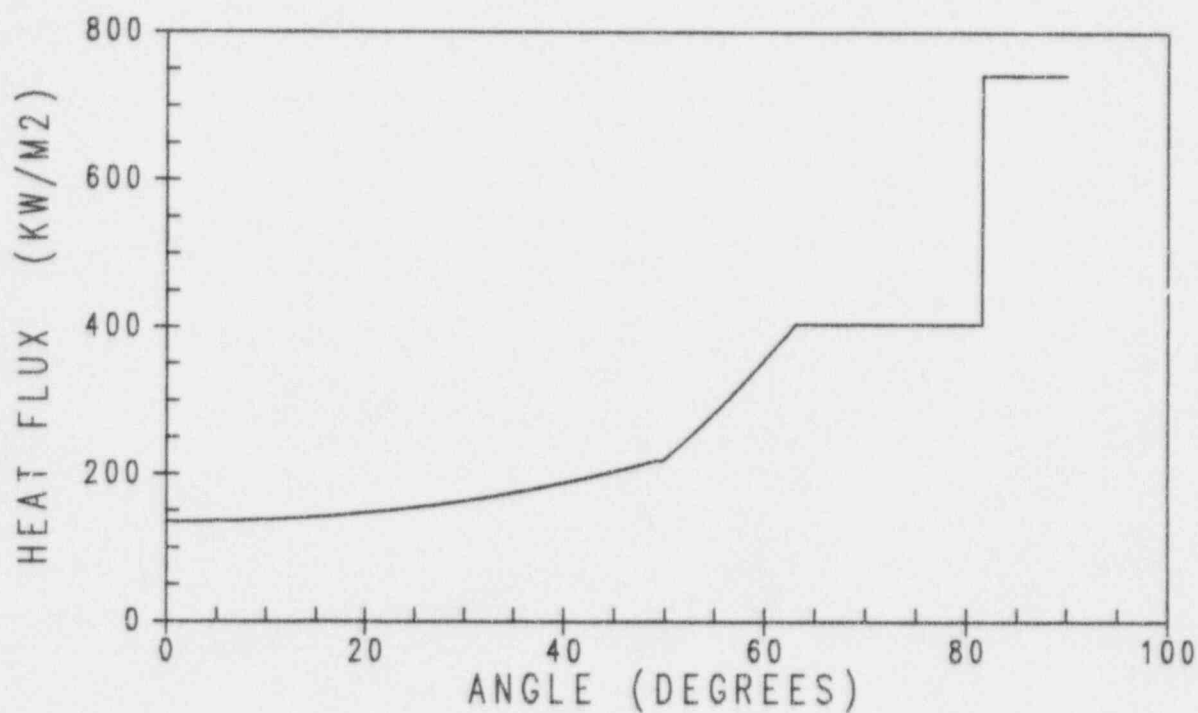


Figure 36-31

Case IVR.13 - Heat Flux Distribution Through Vessel Wall



Westinghouse

ENEL
ENTE NAZIONALE
PER L'ENERGIA ELETTRICA

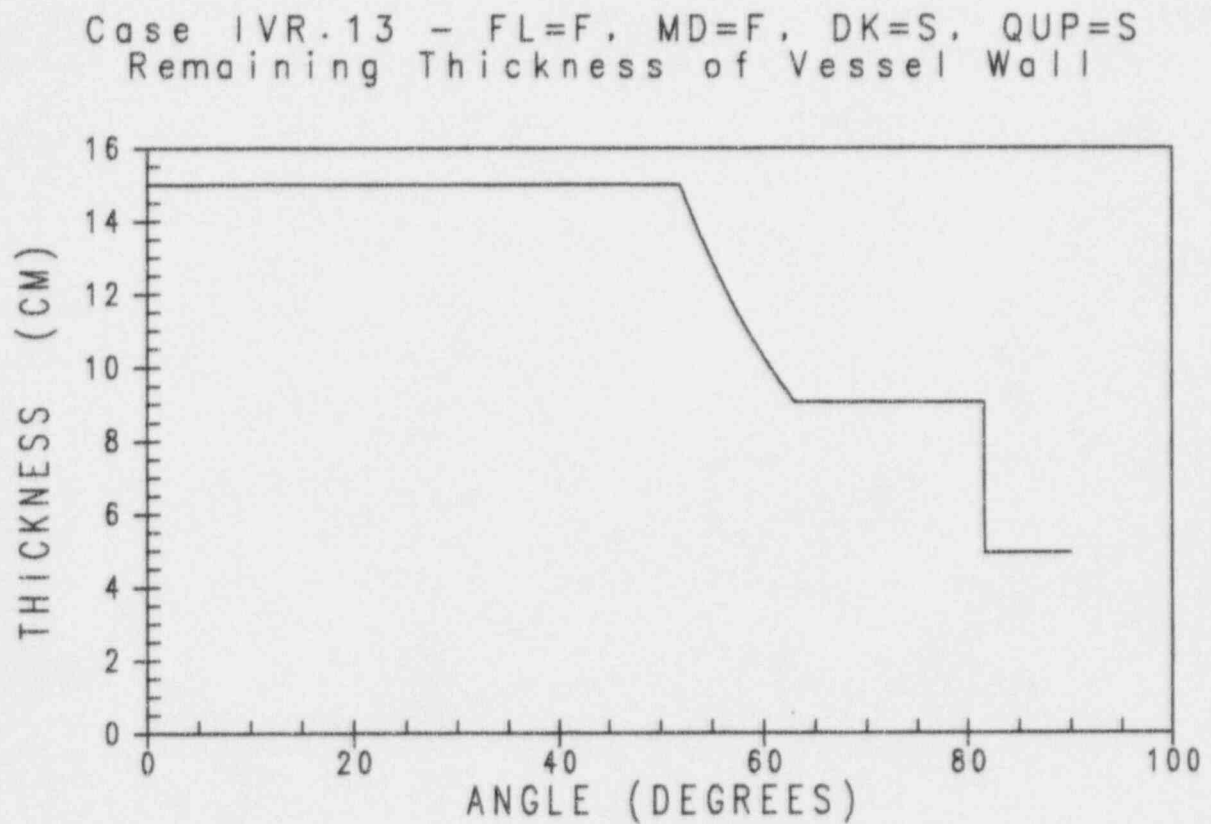


Figure 36-32

Case IVR.13 - Remaining Thickness of Vessel Wall

Case IVR.14 - FL=F, MD=F, DK=S, QUP=F
Heat Flux Distribution Through Vessel Wall

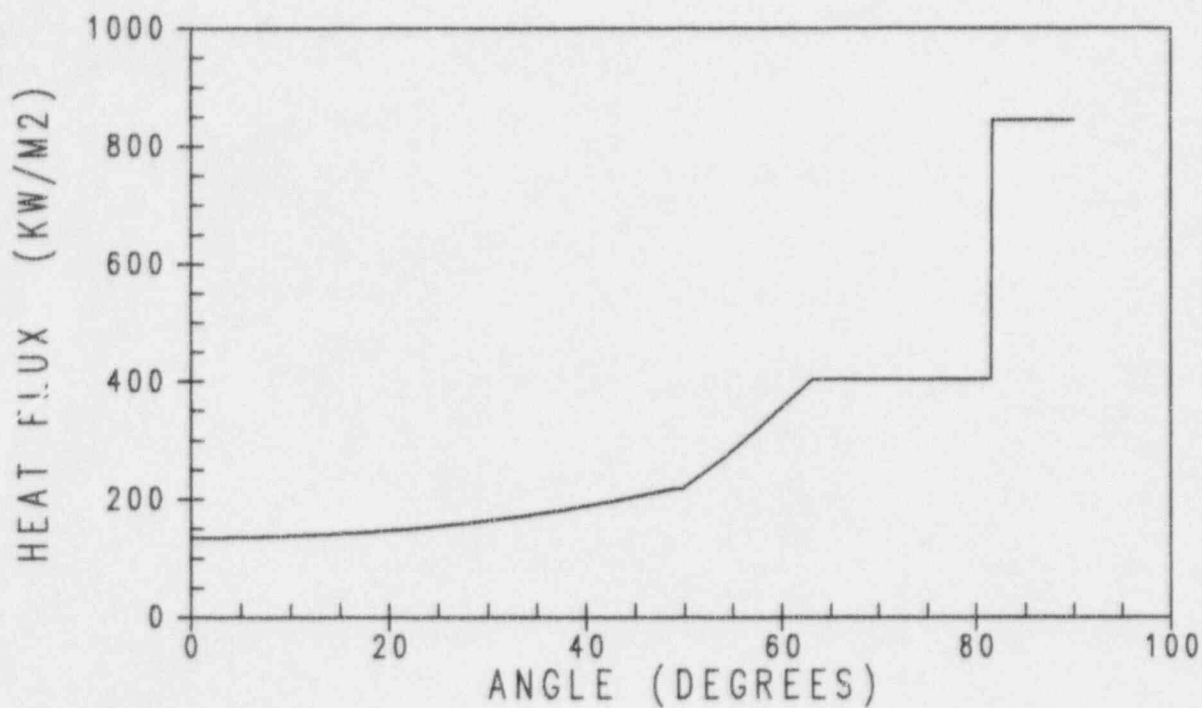


Figure 36-33

Case IVR.14 - Heat Flux Distribution Through Vessel Wall



Westinghouse

ENEL
ENTE NAZIONALE
PER L'ENERGIA ELETTRICA

Case IVR.14 - FL=F, MD=F, DK=S, QUP=F
Remaining Thickness of Vessel Wall

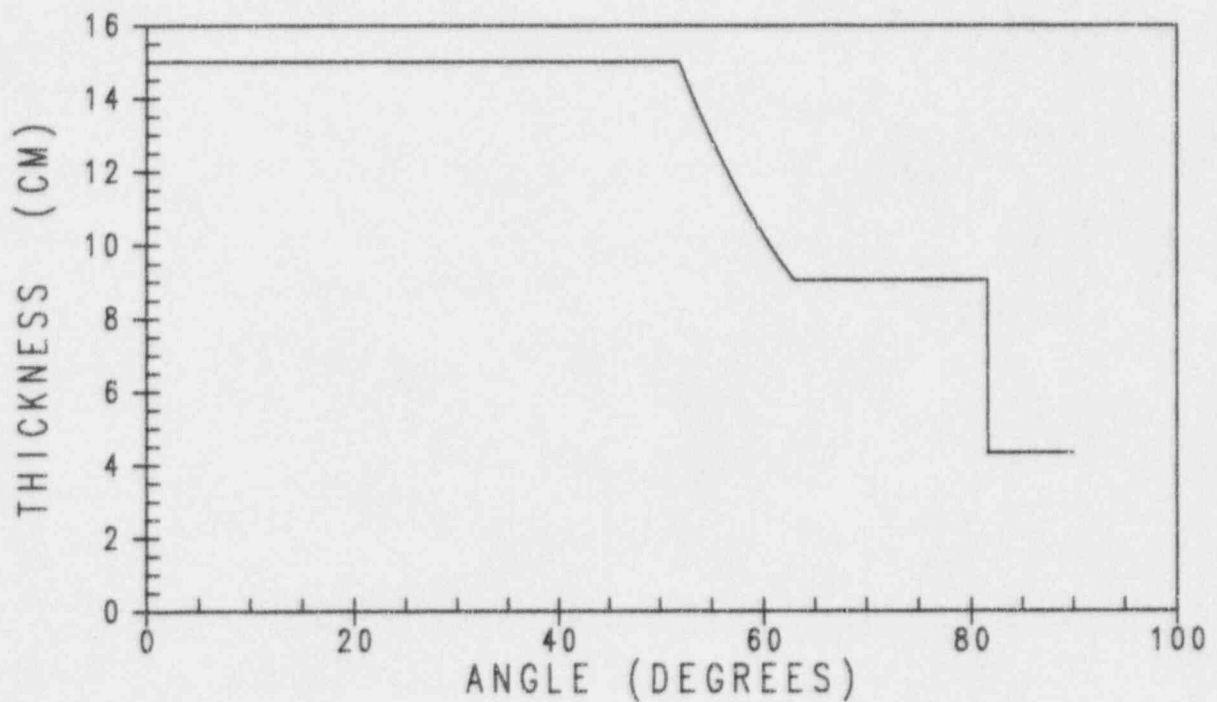


Figure 36-34

Case IVR.14 - Remaining Thickness of Vessel Wall

Case IVR.15 - FL=F, MD=F, DK=F, QUP=S
Heat Flux Distribution Through Vessel Wall

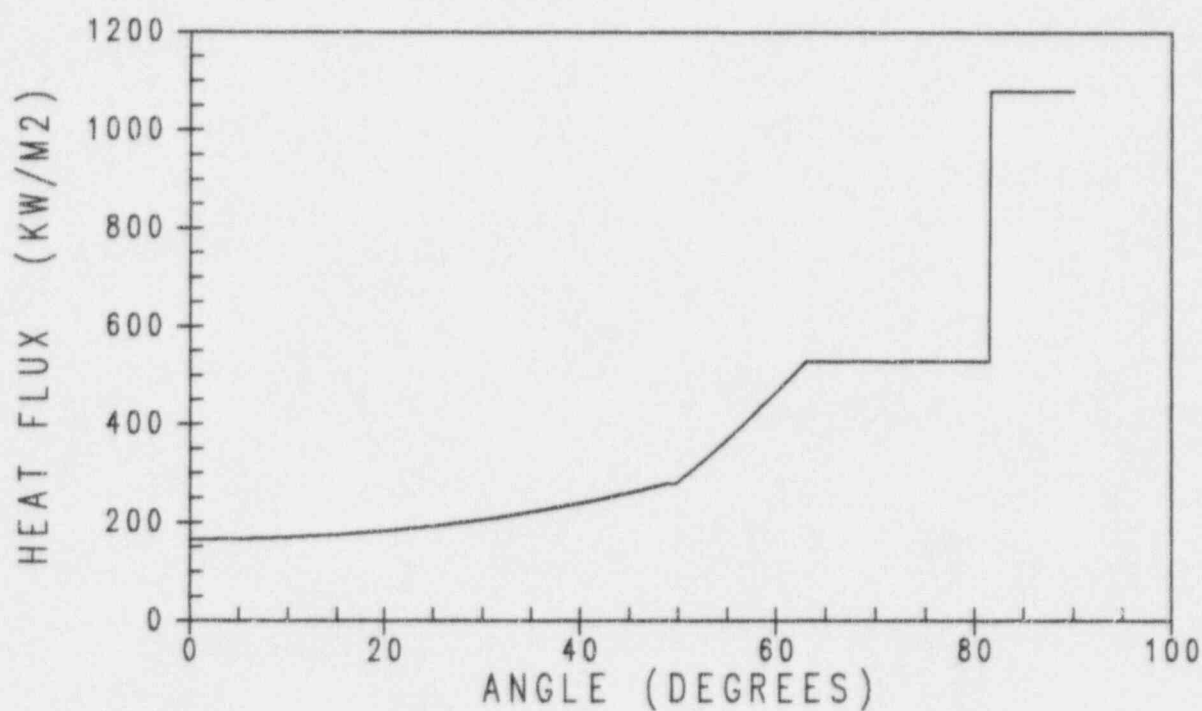


Figure 36-35

Case IVR.15 - Heat Flux Distribution Through Vessel Wall



Westinghouse

ENEL
ENTE NAZIONALE
PER L'ENERGIA ELETTRICA

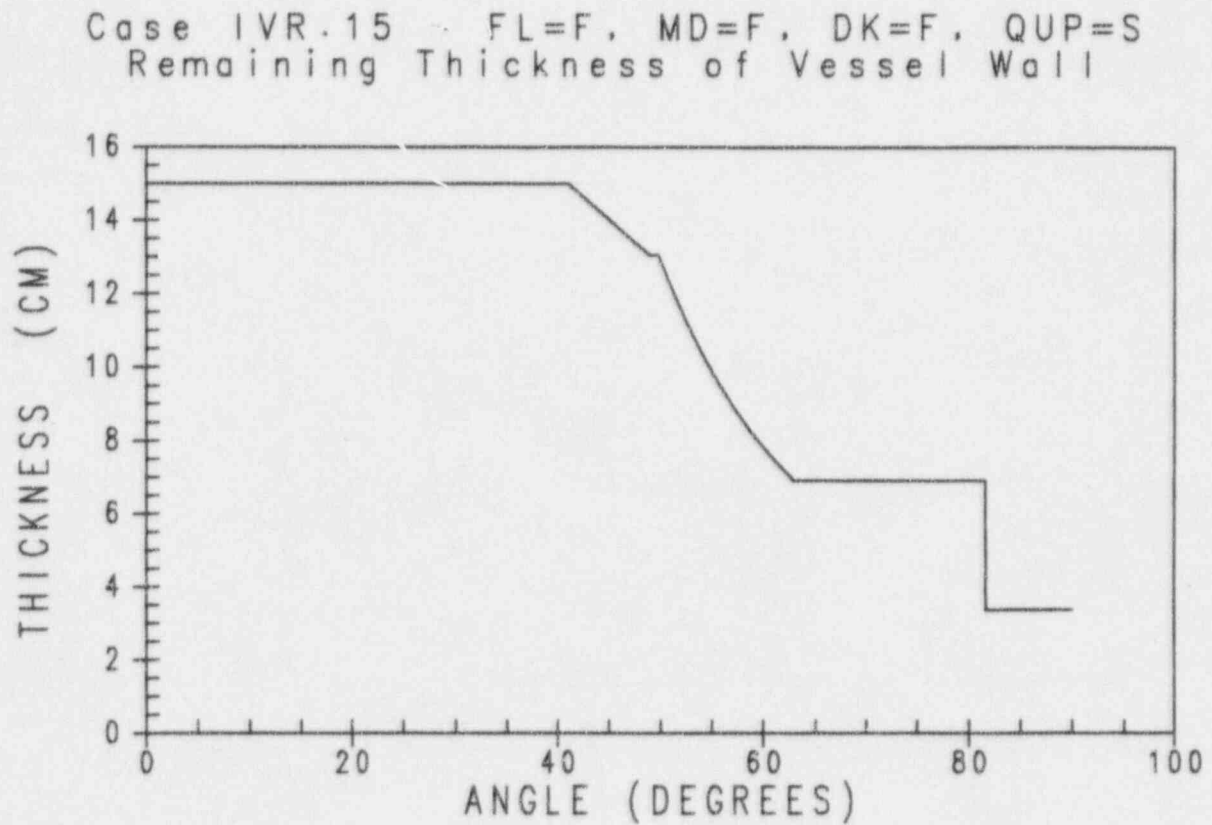


Figure 36-36

Case IVR.15 - Remaining Thickness of Vessel Wall

Case IVR.16 - FL=F, MD=F, DK=F, QUP=F
Heat Flux Distribution Through Vessel Wall

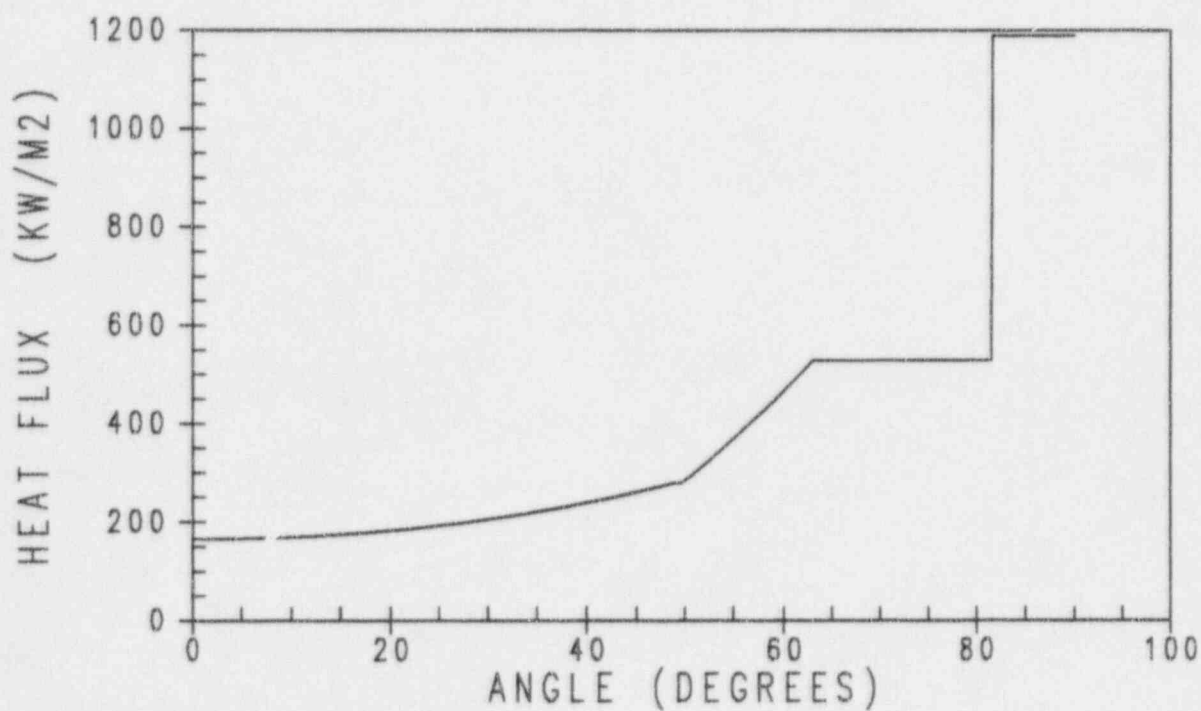


Figure 36-37

Case IVR.16 - Heat Flux Distribution Through Vessel Wall

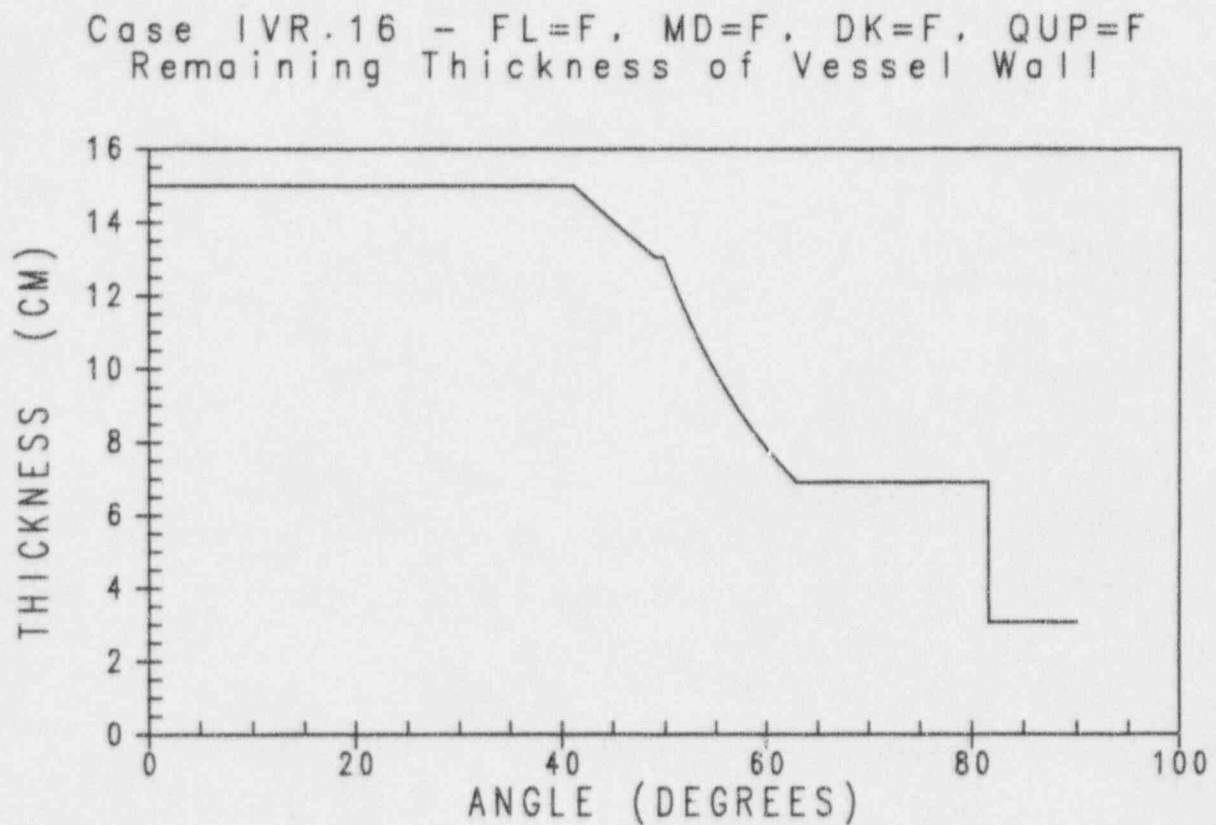


Figure 36-38

Case IVR.16 - Remaining Thickness of Vessel Wall

CHAPTER 37

DECOMPOSITION EVENT TREE - ANALYSIS OF THERMALLY INDUCED FAILURES OF THE REACTOR COOLANT SYSTEM PRESSURE BOUNDARY

This analysis quantifies the likelihood and location of thermally induced failures of the reactor coolant system (RCS) pressure boundary. These types of failures are postulated to occur in high-pressure accident sequences that appear in AP600 accident class 1A, defined as transients and very small loss-of-coolant accidents with no automatic or manual depressurization and no passive heat removal. The frequency of accident class 1A, from the Level 1 PRA results, is 6.3×10^{-8} per reactor year, 15.4 percent of the overall core damage frequency.

The quantification process involves several steps, outlined below:

- The investigation of the thermally induced failures to identify those variables that can affect the probability of failure of the reactor coolant system pressure boundary
- The development of a decomposition event tree (DET) to define the minimum set of events and variable attributes that determine the possible failure modes and likelihood
- The determination of the probability of occurrence of the events and variable attributes included in the decomposition event tree
- The quantification of the probability of thermally induced failures of the reactor coolant system boundary using the results of the previous steps

The results of the quantification of this decomposition event tree provide input to nodes SG and CR on the AP600 containment event tree.

37.1 Background

To be at the conditions in which temperature-induced failure of the reactor coolant system piping is credible, startup feedwater must be failed and the steam generators must have dried out, causing a loss of heat removal from the reactor coolant system. Failures of the passive residual heat removal and the core makeup tanks would, in turn, fail the emergency heat removal and activation of the automatic depressurization of the reactor coolant system. Manual depressurization must also have failed. The primary pressure would then increase to the setpoint of the pressurizer safety valve because of the loss of decay heat removal. The loss of primary coolant through the safety valve would result in core uncover. The natural circulation of superheated gases through the reactor coolant system after core uncover could produce temperatures in the primary system piping and steam generator tubes that could challenge the integrity of the pressure boundary. The determination of the location of the first failure of the pressure boundary is an important consideration of the accident progression

which significantly affects the final release of fission products to the environment. The primary system can be postulated to fail at one of several locations:

- The reactor vessel bottom, induced by high temperature core debris relocated into the lower head
- A hot or cold leg reactor vessel nozzle, induced by hot gases circulating through the reactor coolant system
- A hot or cold leg reactor coolant pipe, induced by hot gases circulating through the reactor coolant system
- The pressurizer surge line, induced by hot gases being relieved through the pressurizer relief and/or safety valves
- The steam generator tubes, induced by the circulation of hot gases through the reactor coolant system

The types of pressure boundary failures postulated to occur in these types of accident sequences and the consequences of the failures are discussed in the following subsections.

37.1.1 Vessel Failure Induced by Molten Core Debris

If molten core debris is relocated to the bottom head of the reactor pressure vessel, the vessel walls in contact with the molten core material will begin to heat up as energy is transferred from the core debris to the vessel walls. If there is insufficient heat removal on the external surface of the reactor vessel walls, the wall temperature will begin to approach the temperature at which its structural properties deteriorate significantly. Additionally, the inner surfaces of the wall may be eroded by the high temperature molten core material, thereby reducing the vessel wall thickness and, consequently, its structural capability. Vessel failure can be postulated to occur at the top of the debris pool, discharging the gas from the reactor coolant system before the debris is expelled to the containment. Or the vessel failure can be postulated to occur near the bottom of the vessel, discharging the debris into the containment at high pressure prior to the gas discharge.

Failure of the reactor vessel by molten core debris in the lower head can be postulated to produce several high-energy phenomena that can challenge containment integrity. If the molten debris is expelled from the vessel before the blowdown of the gas, the breakup and entrainment of the debris in the high-velocity flow down the reactor vessel can result in the oxidation of unreacted metal in the debris, releasing hydrogen and reaction heat to the containment atmosphere. The hot debris can provide an ignition source for the hydrogen, and the resultant combustion event can be postulated to challenge the containment integrity. Latent and sensible heat in the debris can be transferred directly from the airborne debris fragments to the containment gas, a process called direct containment heating. The rapid heating of the containment air can result in a significant pressurization of the containment.

The expulsion of the debris from the vessel can also result in thrust forces that may be postulated to move the vessel in such a way as to tear containment penetrations or create missiles that may impact the containment pressure boundary.

37.1.2 Primary System Piping Failures into Containment

As hot gases from the reactor vessel are circulated through the reactor coolant system piping, the pipe wall temperatures will increase. The increased pipe wall temperatures, in conjunction with a high-pressure differential across the pipe wall, can lead to creep failure of the piping.

The failure of a primary system pressure boundary (either the reactor vessel nozzles, the reactor coolant system piping, or the pressurizer surge line) results in a high-energy blowdown of superheated steam and hydrogen into the containment. The blowdown decreases primary system pressure and can produce a significant pressure and temperature transient in the containment. Given significant core damage (based on cladding reaction) prior to the piping failure, a significant mass of hydrogen can be rapidly released to the containment. The combustion of the hydrogen can result in a challenge to the containment integrity.

37.1.3 Steam Generator Tube Failures into the Secondary System

As hot gases from the reactor vessel are circulated through the steam generator tubes, the tube wall temperatures will increase. The increased tube wall temperatures, in conjunction with a high-pressure differential across the tube wall, can lead to creep failure of the piping. In addition, the potential exists for tube burst at these conditions at any tube defect locations.

Failure of the steam generator tubes into the secondary system results in a reduction of primary system pressure to the pressure of the steam generator safety/relief valve setpoint and provides a direct pathway for fission-product release to the environment through the safety/relief valves. Given significant core damage (fission-product gap release) prior to the failure, the steam generator tube failure can result in a release of radiation to the environment producing doses greater than the large release criterion.

37.2 Controlling Phenomena and Uncertainties

37.2.1 Natural Circulation of High Temperature Gases in the Reactor Coolant System

The threat of reactor coolant system pressure boundary failures is driven by the heating of the loops and steam generator tubes by natural circulation flows. In high-pressure accident sequences, natural circulation in the reactor coolant system is a very efficient mechanism by which heat is transferred from the core to the reactor coolant system piping and steam generators (Reference 37-1). After core uncover, heat from the core is carried to the upper plenum by steam and hydrogen flowing through the fuel assemblies. The gas is cooled by heat transfer to the internal structures in the upper plenum and by mixing with gases that are



circulating into the upper plenum from other regions of the reactor coolant system. The cooled gases flow down into the core, then circulate through the vessel.

The upper internals transfer heat to the cooler gas in the upper plenum, which circulates into one of the reactor coolant system loops. The gas transfers its heat to the reactor coolant system piping and steam generator tubes, cooling the gas and causing it to flow back down through the cold legs into the reactor vessel downcomer, where it is again heated by the vessel structures. The gas is then predicted to flow backwards through the other reactor coolant system loop and into the upper plenum of the reactor vessel, where the cycle begins again. This pattern develops because the AP600 reactor coolant loop has no intermediate leg to trap water in the loop to form a seal preventing gas flow from the steam generator to cold leg.

As the water inventory in the reactor pressure vessel is boiled off, it eventually uncovers the entire length of the active core. At this point, continued water inventory loss from the reactor vessel is predicted to occur as a result of heat transfer from the core and vessel structures to the water remaining below the core. When sufficient water inventory is boiled off to the level of the bottom of the core barrel, a new natural circulation pathway is created between the downcomer and the bottom of the core. Since this flow path has a smaller resistance compared to the previous pathway, a new natural circulation pattern is developed with both loops circulating gases through the core, the hot leg, the steam generator, the cold legs, the downcomer, and back through the core. When this pattern is first developed, the hot gases in the upper plenum region of the reactor vessel are rapidly swept into the hot legs. This results in a significant temperature transient in the reactor coolant system piping and steam generator tubes.

37.2.1.1 Natural Circulation Uncertainties

There are a number of uncertainties in the modeling of the natural circulation flows in the reactor vessel and coolant system that can impact the overall results, as identified in Reference 37-2.

If the core overheats so that melting of the fuel occurs, the molten fuel will relocate and refreeze in the core. The relocated debris can form blockages which may attenuate the natural circulation which carries the heat away from the core to the upper plenum. The reduction in the heat transfer from the core causes the core to heat up more rapidly and the natural circulation flow rates to decrease. The degree of core relocation, the formation of core blockages, and the efficiency of the core blockages in attenuating the heat transfer are subject to uncertainty in estimating the natural circulation flow rates and heat transfer from the core to the upper plenum.

Uncertainty in the natural circulation through the coolant loops is dominated by the determination of whether the intermediate leg is cleared of water to the extent that gas can flow through the pump bowl from the steam generator to the cold leg. This uncertainty does not apply directly to the AP600 since the coolant loop has no intermediate leg, and there is nowhere for a loop seal to form in the loop. However, a water seal does form in the vessel

at the bottom of the core barrel, preventing the gas from flowing directly through the bottom of the core and completely around the loop. Circulation of gases directly through the core can transfer the heat from the core more efficiently, cooling the core, but more rapidly heating the reactor coolant system piping.

Reference 37-2 recommends uncertainty analyses for natural circulation calculations with MAAP3B to investigate the sensitivity to core blockage and clearing loop seals. The natural circulation model in MAAP4 is the same as the model in MAAP3B, except that MAAP4 does not include the IDCOR core blockage model discussed in Reference 37-2. The MAAP4 model allows core channels to block when sufficient debris relocates and refreezes to reduce the flow area in the lower core nodes. A sensitivity analysis on relocation timing (case NC) is performed by reducing the natural circulation flow from the core, thus retaining more heat in the core, to address blockage uncertainty. The timing of reactor coolant system failures with respect to the clearing of the bottom of the core barrel is also investigated to address the sensitivity of reactor coolant system piping temperatures to the presence of a loop seal.

37.2.2 Creep Rupture Failure of Hot Leg Nozzle, Surge Line, and Steam Generator Tubes

Under high-temperature, high-stress conditions, such as are expected for accident class 1A transients, a material may fail well below its yield strength if the severe conditions are maintained over a long enough duration. This is known as creep failure. Larson and Miller (Reference 37-3) developed an analytical methodology for estimating the time required to fail a material at a given stress and temperature. The methodology involves the application of a Larson-Miller parameter (LMP) to determine the creep rupture time.

Based on the natural circulation flow pattern described above, and considering the loop with the positively flowing circulation to be loop 1 and the loop with the reverse flow to be loop 2, the likely locations for creep rupture failure in the reactor coolant system are considered to be at the loop 1 hot leg nozzle safe-end, the loop 2 cold leg nozzle safe-end, the pressurizer surge line, and steam generator tubes. Table 37-1 provides the parameters for these components used for the AP600 creep rupture analysis for the 1A accident class, including geometries, materials, stress levels, and Larson-Miller parameters. Stress levels and Larson-Miller parameters are presented for steam generator tubes given pressurized and depressurized secondary conditions, since both may exist for the 1A accident class. The geometries and materials are well known for each of the components and are not subject to uncertainty.

Creep failure of the stainless steel hot and cold legs at a location near the reactor vessel was considered, but was not included in the detailed analyses. Evaluation of the material properties of the stainless steel versus carbon steel, with respect to creep failure, and consideration of the geometries of the nozzles and reactor coolant system piping indicate that the nozzles are always predicted to fail by creep failure before the loop piping. The differences in the creep predictions between the nozzles and the piping are large enough that any uncertainties in the creep predictions for carbon steel versus stainless steel are not significant.

Creep rupture is caused by the maximum principal stress due to primary loading in this case, the pressure loading. Although the reactor coolant system components piping may be subject to additional stress during severe accident conditions (such as, from the thermal expansion of the reactor coolant system piping), the stress level contributing to creep rupture failure is not subject to significant uncertainty since the internal pressures are the only dominant stress. Therefore, the loading used to determine the stress in the piping is the hoop stress, which is defined by the primary and secondary safety valve pressure setpoints (2500 psia and 1085 psia, respectively). Therefore, the major uncertainty in the creep rupture analysis is in the selection of the Larson-Miller parameter.

The Larson-Miller parameters for the AP600 reactor coolant system components are determined using the master creep rupture curves presented in Reference 37-4 and the hoop stress in the component. The data for steam generator tubes presented is for Inconel 600. The use of the Larson-Miller parameters may introduce significant uncertainties since the predicted times to failure can vary by a factor of 2 to 10, when compared to the observed experimental times to failure. The large variations in the predicted Larson-Miller parameters versus the experimental observations are a result of the scatter in creep data due to the heat-to-heat variation and the differences in chemical composition within a heat of material, and due to the large stress exponent of power creep law at high temperatures wherein a large variation in time is predicted for small variations in stress.

It is assumed that the use of the Inconel 600 master creep rupture curve for Inconel 690 is reasonable, given the high temperature yield strength and ultimate strength are comparable, with Inconel 690 being the stronger of the two materials (Reference 37-5). Lower bound Larson-Miller parameters are used for the steam generator tubes, since tubes exhibiting minimum material properties are expected to be present in the plant at some location in each of the steam generators, given the large population of tubes and considering the weakest tube in the analysis. The nominal Larson-Miller parameters for the stainless steel surge line is used given that there is only one surge line, and it is not expected to be the limiting component. A nominal Larson-Miller parameters is used for the base case analysis of the hot leg nozzle since there is a small population of hot legs in the design. An upper bound Larson-Miller parameters is used for sensitivity cases since a hot leg nozzle failure may preclude the failure of a steam generator tube. The upper bound Larson-Miller parameters is based on the upper bound curve for carbon steel in Reference 37-4 and will extend the time to failure of the hot leg in the calculation, thus subjecting the steam generator tube to longer durations at the adverse conditions, increasing the creep damage and likelihood of failure. The time-to-failure curves for the reactor coolant system components are calculated based on the selected Larson-Miller parameters and are presented in Figures 37-1 and 37-2.

The sizing of the hot leg and cold leg nozzles result in higher stress levels in the hot leg nozzle at the given conditions. The reactor coolant system loop 1 hot leg nozzle temperature response is expected to be more challenging than the other nozzles because of its close proximity to the initial flow of hot gases from the core. The stress in the surge line is lower. Because of the difference in materials (such as, stainless steel surge line versus carbon steel nozzles), the difference in stress levels, and the lower predicted pipe temperatures, the surge

line will have a significantly longer time-to-failure. The reactor coolant system loop 1 hot leg nozzle response will be presented as the bounding analysis, or the "weakest link," for the timing of all the primary system to containment failures.

37.2.3 Degradation of Steam Generator Tubes

Tube degradation can occur over the course of the life of the tubes and may be present as tube defects (such as cracking) under the support plates and tubesheet, as tube thinning due to corrosion or as abrasive wear at the antivibration bar locations. Tube thinning and abrasive wear affect the stress level in the tube walls by providing a reduced wall thickness over a significant area and thereby may increase the likelihood of creep rupture failure. Tube defects impact only the likelihood of tube bursting since the area of concern is very limited.

In the time and temperature ranges where creep of steam generator tubes is negligible, tube bursting may occur at defect locations, depending on the conditions and defect characteristics. Small cracks in the tubes may be present under the support plates and, therefore, may not be exposed to the steam generator tube differential pressure. Under severe accident conditions, the thermal expansion of the tubes with respect to the support plate structure may result in these cracks becoming exposed to the full steam generator tube differential pressure. The tube may burst at the crack location if the differential tube pressure exceeds the empirically determined bursting pressure for the crack characteristic profile.

The high temperatures expected in the sequences in accident class 1A are predicted to result in significant thermal growth of steam generator tubes, thereby exposing cracks under the upper support plates. However, the expected frequency of cracking in thermally treated Inconel is negligibly small. Currently, there are over 800 reactor years of operating experience with Model F and F-type steam generators employing thermally treated Inconel 600. There have been no (zero) incidents of the tube cracking with crack characteristics that would lead to bursting under severe accident conditions. Thus, it is assumed that the probability of tube burst is negligibly small under severe accident conditions for thermally treated Inconel.

Therefore, only tube thinning over the life of the steam generator is considered in this analysis. Tubes are predicted to thin no more than three mils over the life of the plant. Therefore, the tube wall thickness for the creep rupture analysis is considered to be the nominal tube thickness less the three mils due to thinning over the life of the plant.

37.3 MAAP4 Analyses

The MAAP4 (Reference 37-6) analyses of high pressure transient sequences are used to define the pressure and temperature transients for the reactor coolant system piping caused by the natural circulation. The accident sequences analyzed are initiated by a loss of all feedwater to the steam generators, followed by failures of both passive residual heat removal heat exchangers, both core makeup tanks, and all automatic and manual reactor coolant system



depressurization. It is assumed that no failures of the reactor coolant system pressure boundary occur at any time in the transient in order to develop the bounding temperature transients for the reactor coolant system components that may be subject to creep failure.

The MAAP4 reactor coolant system nodalization is presented in Figure 37-3. The component temperatures are taken from the hot leg node closest to the reactor vessel and the steam generator tube nodes at the tubesheet. The steam generator tube temperature from loop 1 is taken from the hot side of the tube bundle. The steam generator tube temperature from loop 2 is taken from the cold side since the flow in loop 2 is reversed. These component temperature transients are used to determine the timing of expected hot leg nozzle creep rupture failure with respect to the timing of the failure of the steam generator tubes. In the MAAP4 model, the hot legs are divided into three nodes through the wall; the middle node temperature is used to estimate the average through-wall temperature. Since the steam generator tubes have a very small temperature gradient through the wall thickness, the primary side temperature of the steam generator tubes is used for the tube temperature.

Four MAAP4 analyses are performed to investigate the variations in component temperatures, as described below in detail. Table 37-2 presents the resultant timing of key events from each of the analyses.

37.3.1 Base Cases

Two base cases are analyzed, one with the secondary side pressurized (case HP) and one with the secondary side depressurized at the time of accident initiation (case DP).

37.3.1.1 Case HP - Pressurized Secondary System

The results of the case HP are presented in Figures 37-4 through 37-9. The loss of feedwater to the steam generators leads to a loss of primary system heat sink due to the drying out of the steam generator. The reactor coolant system and secondary systems are pressurized to the setpoints of their safety valves (Figure 37-4). The loss of primary coolant through the safety valve leads to core uncover at 4800 seconds (Figure 37-5), causing the core to heat up (Figure 37-6). Natural circulation of the hot gases through the reactor coolant system loops (Figures 37-7 and 37-8) transfers the heat to reactor coolant system pressure boundary walls, causing them to heat up (Figure 37-9). After approximately 10,000 seconds, the water level in the vessel is below the bottom of the active fuel. Radiation heat transfer from the bottom of the core and the gas to the water in the lower plenum causes the water level to continue to fall. At 14,895 seconds, the bottom of the core support plate uncovers, allowing the natural circulation flow of gas to pass directly through the core. No significant melting of the fuel has occurred. The heat transfer to the gas cools the core. Increased circulation through the core at the time that the lower core support plate uncovers causes a spike in the vessel upper plenum gas and the reactor coolant system component temperatures. No core relocation to the lower head is predicted to occur prior to failure of the hot leg nozzle from creep due to the high pressure and temperature gases.

37.3.1.2 Case DP - Depressurized Secondary System

The results of case DP are presented in Figures 37-10 through 37-15. This sequence is the same as case HP except that the relief valve of one steam generator is stuck open from time zero. The blowdown of the affected steam generator cools the system until the reduced water level on the tubes attenuates the heat transfer from the primary system. The affected steam generator dries out at 10,217 seconds, and the secondary pressure (Figure 37-10) falls to approximately atmospheric pressure. The unaffected steam generator then removes heat from the reactor coolant system until the reduced secondary inventory uncovers the tubes and the heat transfer is insufficient to remove all of the decay heat from the primary system. The reactor coolant system pressure (Figure 37-10) then increases to the pressurizer safety valve setpoint. The unaffected steam generator dries out at 14,871 seconds. The core uncovers at 17,042 seconds, and the sequence then proceeds similarly to the sequence described in case HP.

37.3.2 Sensitivity Cases

MAAP4 sensitivity cases to examine the effect of change in the natural circulation flow and the operator action to flood the reactor cavity on the component temperature transients are presented. The reduction in natural circulation increases the core temperature and can result in core relocation and potential blockage. The flooding of the reactor cavity has the potential to cool the reactor coolant system components and change the temperature response.

37.3.2.1 Case NC - Natural Circulation Sensitivity

To examine uncertainties recommended in Reference 37-2, the natural circulation flow rate from the core to the upper plenum is reduced in case NC. This is accomplished in MAAP4 by using case HP and increasing the friction factor in the core to upper plenum flow causing the core to heat up faster. This results in increased cladding oxidation and significant fuel melting prior to reaching reactor coolant system piping temperatures where creep rupture failure could occur.

Increasing the natural circulation removes more heat from the core and results in slightly higher transient temperatures of the reactor coolant system components. However, the time at which the various reactor coolant system components reach the temperature required for consideration of creep failure is not substantially altered with respect to each other. Therefore, increased natural circulation is not specifically analyzed as part of this sensitivity analysis.

The MAAP4 results are presented in Figures 37-16 through 37-22. The sequence proceeds much like the sequence in case HP. However, the core to upper plenum natural circulation (Figure 37-19) is reduced by more than 10 percent. Rapid oxidation of the cladding begins at approximately 13,000 seconds as indicated by the rapid temperature increase in the core (Figure 37-18). The heat of reaction released by the oxidation results in significant melting in the core, which causes the core to relocate and block heat transfer from the fuel to the passing steam. This blockage is indicated by the noncoolable core debris (Figure 37-18) in



the core region at the time of support plate uncover. The reduced heat transfer to the steam and lower natural circulation flow to the upper plenum cause the temperature in the upper plenum gas to stabilize (Figure 37-18). The temperature of the reactor coolant system components follows (Figure 37-21). Core debris relocates to the lower head of the reactor vessel at 17,200 seconds (Figure 37-22).

37.3.2.2 Case FL - Flooding the Reactor Cavity Sensitivity

Flooding the reactor cavity can affect the high-pressure and temperature transient by removing heat from the reactor coolant system through the vessel walls and cooling the hot leg nozzle wall after it is flooded. To examine the effect that flooding the reactor cavity may have on the transient, the sequence examined in case HP is repeated with the operator action to flood the cavity, initiated at the time that the core exit temperatures reach 2000°F.

The MAAP4 results for case FL are presented in Figures 37-23 through 37-29. Case FL proceeds much like case HP until 11,624 seconds, when the operator action to flood the reactor cavity is initiated. The effect of the flooding of the vessel results in cooler temperatures in the reactor coolant system. The cooler temperatures extend to time to support plate uncover to 16,632 seconds, so cooldown of the core before rapid oxidation does not occur as it does in case HP. Core melting and relocation occurs and forms blockages in the core region as indicated by the noncoolable geometry and the stabilization of the upper plenum gas temperature. Core debris relocates to the lower head of the vessel at 17,200 seconds (Figure 37-29). At 17,500 seconds, the cavity is flooded above the hot leg elevation. The hot leg nozzle wall temperatures (Figure 37-28) fall rapidly because of the heat transfer to the containment water.

37.4 Reactor Coolant System Piping and Steam Generator Tube Failure

37.4.1 Creep Rupture Timing

The reactor coolant system components are analyzed for the timing of creep rupture failure, with respect to each other. The temperature transients for the hot leg nozzle and steam generator tubes developed in MAAP4 analyses, described above, provide the input to the analyses. The temperature transients representing the average through-wall temperatures at the hottest point for each component are selected for use in this portion of the analysis. The hottest points are the following:

- Loop 1 hot leg nozzle
- Loop 1 hot side steam generator tubes at the tubesheet
- Loop 2 cold side steam generator tubes at the tubesheet

The timing of creep rupture failure is estimated by calculating the creep damage in each component. This method is used in Reference 37-4 to determine the timing of creep rupture failure of reactor coolant system components in the Surry plant. The temperature transient is divided into small time-steps; the time-to-failure based on the Larson-Miller parameter is

calculated for the average temperature over the time-step. The duration of time-step divided by the time-to-failure found for the temperatures in that time-step gives the incremental damage incurred over the time-step. The summation of the incremental damage terms gives the overall damage to the component. The component is considered to be failed when the overall damage term is equal to 1.0.

37.4.2 Results of the Component Failure Analysis

The methodology to calculate creep damage is applied to the average through-wall temperature transients for each of the components in the four MAAP4 cases. Creep damage is calculated for the hot leg nozzle and for tubes from both steam generators. The base case for creep damage calculation uses the best-estimate hot leg nozzle Larson-Miller parameter to determine the creep damage. A sensitivity case, using the upper bound Larson-Miller parameters for the hot leg nozzle, was also performed for each of the MAAP4 cases. In both cases, the lower bound steam generator tube Larson-Miller parameters are used to estimate the creep damage for the steam generator tubes.

37.4.2.1 Case HP Creep Damage Results

Results of the creep damage analysis for case HP are presented in Figures 37-30 and 37-31. Failure of the hot leg nozzle is predicted to occur prior to the failure of the steam generator tubes for both the best-estimate and the upper bound hot leg Larson-Miller parameter cases. The hot leg nozzle failures occur well before core debris is relocated to the lower head of the vessel.

37.4.2.2 Case DP Creep Damage Results

Results of the creep damage analysis for case DP are presented in Figures 37-32 and 37-33. Failure of the steam generator tubes is predicted to occur prior to the failure of the hot leg for both the best-estimate and the upper bound hot leg Larson-Miller parameter cases. The steam generator tube failure occurs well before core debris is relocated to the lower head of the vessel.

37.4.2.3 Case NC Creep Damage Results

Results of the creep damage analysis for case NC are presented in Figures 37-34 and 37-35. Failure of the reactor vessel due to the relocation of core debris is predicted to occur before creep damage leads to failure of the hot leg or the steam generator tubes.

37.4.2.4 Case FL Creep Damage Results

Results of the creep damage analysis for case FL are presented in Figures 37-36 and 37-37. Failure of the hot leg nozzle is predicted to occur prior to the failure of the steam generator tubes for both the best-estimate and the upper bound hot leg Larson-Miller parameter cases.

The hot leg nozzle failures occur before core debris is relocated to the lower head of the vessel.

37.4.3 Conclusions from the Component Failure Analysis

The major conclusions of the creep damage analysis are as follows:

- Creep rupture failure of the hot leg nozzle or the steam generator tubes occurs before relocation of core debris to the lower head of the vessel challenges the vessel integrity for the HP, DP, and FL cases.
- For a pressurized secondary system, the hot leg nozzle is expected to fail by creep sooner than the steam generator tubes.
- For a depressurized secondary system, creep rupture failure is predicted to occur in the affected steam generator tubes prior to hot leg nozzle failure.
- Core blockage (case NC) has a significant effect on the timing of creep rupture failure and can lead to high-pressure failure of the reactor vessel.
- Flooding of the reactor cavity affects the timing of the core support plate uncover and of the core melt progression prior to the creep failure, but does not significantly affect the timing of creep rupture failure.
- The effect of the uncertainty in the hot leg nozzle Larson-Miller parameter on the timing of the hot leg nozzle creep rupture failure does not significantly affect the creep rupture results.

37.5 Development of the Decomposition Event Tree

The decomposition event tree is developed to examine the uncertainties that may have an affect on the likelihood of thermally induced failures of the reactor coolant system. The decomposition event tree structure developed for quantifying the likelihood of thermally induced primary system boundary failures is presented in Figure 37-38. To answer the questions posed at each node on the tree, the examination and quantification of the uncertainties identified in the analysis presented in the previous sections are required. The upward path at each node indicates a positive response to the question; the downward path indicates a negative response. The nodes chosen for the decomposition event tree are as follows:

Node SP - Is the secondary system pressurized?

Node NC - Is the natural circulation rate high enough to prevent significant core blockage prior to a pressure boundary failure?

- Node LM - Does the hot leg nozzle exhibit nominal creep rupture properties?
- Node SG - Do the steam generator tubes not fail because of creep rupture prior to hot leg nozzle creep rupture failure?
- Node HL - Does the hot leg nozzle creep rupture failure occur before vessel integrity is challenged by molten debris in the lower head?
- Node ME - Does a reactor vessel failure occur above the debris such that the reactor coolant system pressure is relieved prior to ejection of the core debris?

The end-states of the tree represent the types of reactor coolant system failures that are postulated:

- HLC - Hot leg nozzle creep rupture failure prior to steam generator tube or vessel failures
- SGC - Steam generator tube creep rupture failure prior to hot leg nozzle or vessel failures
- VF - Vessel failure due to molten debris in the lower head prior to hot leg nozzle or steam generator tube failures; core debris ejected at low pressure
- HPME - Vessel failure due to molten debris in the lower head prior to hot leg nozzle or steam generator tube failures; core debris ejected at high pressure

37.6 Quantification of the Decomposition Event Tree

This section discusses the assignment of the split fractions at each of the nodes on the decomposition event tree. Multiplication of each of the split fractions along a path of the tree results in the probability of the accident following that particular path. The summation of the probabilities of the paths that result in a particular end-state is the probability of that end-state.

37.6.1 Node SP

Is the secondary system pressurized?

Success Criteria:

Steam generator secondary side integrity maintained.

If feedwater is unavailable for secondary cooling, it is assumed that the AP600 emergency operating procedures will instruct the operator to skip the steps that would depressurize the secondary system. For accident class 1A, the secondary system is expected to be pressurized



unless a safety valve or relief valve sticks open, or a main steamline break upstream of the isolation valve occurs. These types of valve failures are analyzed in the Level 1 PRA analysis and accounted for in the core damage frequency of accident class 1A. Therefore, the probability of the failure of decomposition event tree node SP is the conditional probability of these equipment failures defined in accident class 1A sequences, plus the frequency of a main steamline break upstream of the main steam isolation valve.

Probability of depressurization in accident class 1A = 3.34×10^{-2}

Downstream Considerations:

Depressurization of the secondary side of a steam generator is assumed to result in creep failure of the steam generator tubes in all cases (MAAP4 case DP). Therefore, failure of node SP leads directly to end-state SGC.

37.6.2 Node NC

Is the natural circulation rate high enough to prevent significant core blockage prior to a pressure boundary failure?

Success Criteria:

Significant core blockage does not attenuate heat transfer from the fuel rods.

The MAAP4 base case analysis (cases HP and DP) results show no relocation of the core prior to lower support plate uncover. The natural circulation uncertainty analysis (case NC) results in relocation and blockage of the core prior to the uncover of the support plate. This is indicated by the formation of noncoolable debris in the core region for case NC (Figure 37-18) and attenuation of the heat removed from the core to the reactor coolant system metal. The base cases use the recommended default value (Reference 37-2) for the friction in the core to upper plenum natural circulation, which is the lower bound of the recommended range (Reference 37-8). Case NC uses the upper bound of the recommended range (Reference 37-8). The geometrical design of the AP600 core is not significantly different from that of a current plant, and there is no reason that the range of the value for the friction factor should be different than that recommended in Reference 37-8. The base case friction parameter recommended for use in the MAAP4 code is based on the benchmarking with the one-seventh scale natural circulation testing (Reference 37-1) and is, therefore, considered to be more representative than the bounding value.

Probability of NC Success = 0.90

Probability of NC Fail = 0.10

Downstream Considerations:

The degree of natural circulation has a significant effect on the tube temperature, and can affect the probability of tube failure before hot leg failure at node SG.

37.6.3 Node LM

Does the hot leg nozzle exhibit nominal creep rupture properties?

Success Criteria:

Does the hot leg nozzle fail first if the upper bound Larson-Miller parameter is used to assess creep damage?

The creep damage was analyzed for all of the cases with a best estimate and an upper bound Larson-Miller parameter, as shown in Figures 37-30 through 37-37. In all cases, the use of the upper bound Larson-Miller parameters did not change the conclusion that the hot leg nozzle would accumulate creep damage at a much faster rate than the steam generator tubes, for all cases with the steam generator secondary side pressurized. As shown in Figures 37-30 through 37-37, there is a significant margin in the time between predicted hot leg nozzle failure (using the upper bound Larson-Miller parameters) and the predicted steam generator tube failure. Even if the upper bound Larson-Miller parameters, which bounds all of the applicable test data for creep failure, was shifted in a more bounding direction, the overall conclusion would still be applicable.

Probability of nominal Larson-Miller parameters LM Success = 1.0

Downstream Considerations:

The probability that the hot leg nozzle has significantly greater strength creep resistance than indicated by upper bound Larson-Miller parameters affects the probability that the steam generator tube fails before the hot leg nozzle (node SG) and the probability of vessel failure before hot leg nozzle failure (node HL).

37.6.4 Node SG

Do the steam generator tubes not fail because of creep rupture prior to hot leg nozzle creep rupture failure?

Success Criteria:

Steam generator tube creep damage less than 1.0 at the time of expected hot leg nozzle creep rupture failure.

The creep damage for the steam generator tubes in each case is presented in Figures 37-30 through 37-37. In all cases, with the secondary system pressurized, significant creep damage does not occur in the steam generator tubes prior to the time of hot leg nozzle creep failure. This includes the cases in which the upper bound Larson-Miller parameter value for the hot leg nozzle is used, as well as the best estimate value.

Probability of tube creep failure = 0.0

Downstream Considerations:

Failure at node SG leads directly to end-state SGC.

37.6.5 Node HL

Do the hot leg nozzles not fail because of creep rupture before vessel integrity is challenged by molten debris in the lower head?

Success Criteria:

Relocation of core debris to the lower head of the reactor vessel prior to the time the hot leg nozzle creep damage equals 1.0.

The creep damage for the hot leg nozzle for each case is presented in Figures 37-30 through 37-37. In no case with best-estimate natural circulation has any core relocation to the lower head occurred prior to hot leg nozzle creep failure. If the natural circulation is insufficient and the core heat transfer from the core is blocked by relocated debris, then relocation to the lower head of the vessel occurs prior to predicted creep failure of either the hot leg nozzle or the steam generator tubes.

Given success at node NC, probability of hot leg nozzle creep failure = 1.0

Given failure at node NC, probability of hot leg nozzle creep failure = 0.0

Downstream Considerations:

Failure at node HL lead directly to end-state HLC. Success of node HL leads to consideration of high-pressure melt ejection.

37.6.6 Node ME

Does a reactor vessel failure occur above the debris such that the reactor coolant system pressure is relieved prior to ejection of the core debris?

Success Criteria:

Vessel failure occurs at a location that does not allow a large debris mass to be entrained into the containment prior to blowdown of the reactor coolant system.

The discussion presented in Reference 37-7 and the analysis for the retention of debris in the reactor vessel (Chapter 24) show that the likely location of the failure of the reactor vessel is at the top of the debris bed at the metal pool. Failure at the top of the pool would allow the reactor coolant system to depressurize without entraining a significant debris mass to the containment prior to the blowdown (Reference 37-7). Therefore, success at node ME is the best-estimate response, and uncertainty in the high-pressure vessel failure mode is accounted for by applying a 10 percent failure probability.

Probability of success at node ME = 0.90

Probability of failure at node ME = 0.10

Downstream considerations:

Failure of node ME results in end-state HPME which represents a high-pressure discharge of the molten core debris. On the AP600 containment event tree structure, this is assumed to result in containment failure.

37.7 Results

The results of the quantification of the decomposition event tree are shown in Figure 37-38. The results show that the conditional probability of a steam generator tube failure induced by high gas temperatures after core damage for accident class 1A is 1.0 for those accident sequences that result in a depressurized steam generator secondary side and 0.0 for those accident sequences in which secondary side isolation is maintained. The likelihood of high-pressure melt ejection is estimated to be approximately 1 percent of the cases in which the steam generators are not depressurized. These results are used to quantify the split fractions at nodes SG and CR on the AP600 containment event tree.

On the AP600 containment event tree, high-pressure melt ejection (end-state HPME) is assumed to lead to early containment failure with a probability of unity. This is a conservative assumption with respect to direct containment heating, which is not considered to be a credible containment failure mechanism for the AP600 (Reference 37-7). The likelihood of containment failure from a high-pressure melt ejection is mostly attributed to possible vertical movement of the reactor vessel from the thrust forces and pressurization of the reactor cavity. The direct vessel injection lines connected to the reactor vessel also have a direct connection to a penetration at the containment wall. In actuality, the likelihood of containment failure from movement of the vessel is not considered to be guaranteed. However, since this failure mechanism occurs in less than 1 percent of the accident class and is several times less likely than the containment bypass failure for high-pressure sequences, the probability is conservatively lumped into the early containment failure release category.

37.8 References

- 37-1 W. A. Stewart, et. al., "Experiments on Natural Circulation Flows in Steam Generators During Severe Accidents," Procedures of the International ANS/ENS Meeting on Thermal Reactor Safety, San Diego, CA, February 2 - 6, 1986.
- 37-2 "Recommended Sensitivity Analyses for an Individual Plant Examination Using MAAP 3.0B," EPRI TR-100167, 1990.
- 37-3 Larson, F.R., Miller, J., "A Time-Temperature Relationship for Rupture and Creep Stress," Transactions of the American Society of Mechanical Engineers, pp 765 - 775, July 1952.
- 37-4 "Creep Rupture Failure of Three Components of the Reactor Primary Coolant System During the TMLB Accident," EGG-EA-7431, EG&G Idaho, November 1986.



- 37-5 Harrold, D.L., et. al., "The Temperature Dependence of the Tensile Properties of Thermally Treated Alloy 690 Tubing," Fifth International Symposium on Environmental Degradation of Materials in Nuclear Power Systems - Water Reactors, Monterey, CA, August 25-29, 1991.
- 37-6 "EPRI MAAP 4.0 User's Manual," EPRI NP-xxxx, [to be published].
- 37-7 *AP600 Phenomenological Evaluation Summaries*, WCAP-13388 (Proprietary), Rev. 0, June 1992, and WCAP-13389 (Nonproprietary), Rev. 1, 1994.
- 37-8 "MAAP 3.0b PWR Large Dry User's Guide," Fauske and Associates, Inc., prepared for EPRI, April 19, 1991.

Table 37-1

REACTOR COOLANT SYSTEM PIPING PARAMETERS

Pipe	Inner Dia. (in.)	Thickness (in.)	Material	σ_{2500} (ksi)	σ_{1415} (ksi)	LMP ₂₅₀₀ (x 10 ⁻³)	LMP ₁₄₁₅ (x 10 ⁻³)
HL Nozzle	31	3.25	SA-508	11.9	-	35.7 / 36.0	-
CL Nozzle	22	2.56	SA-508	10.7	-	35.7 / 36.0	-
Surge Line	14.44	1.78	SS-316	10.1	-	41.8	-
SG Tubes	0.607	0.036	Inconel 690	21.1	11.9	25.7	29.2

Table 37-2

TIMING OF KEY EVENTS IN THE MAAP4 ANALYSIS

Event	MAAP4 Case			
	HP (sec.)	DP (sec.)	NCL (sec.)	FL (sec.)
Core Uncovery	4792	17042	4792	4788
Rapid Oxidation	-	-	13000	14600
Sup Plate Uncovery	14895	26762	14381	16632
Debris in Low Head	-	-	17200	17200
Hot Leg Flooding	-	-	-	17500



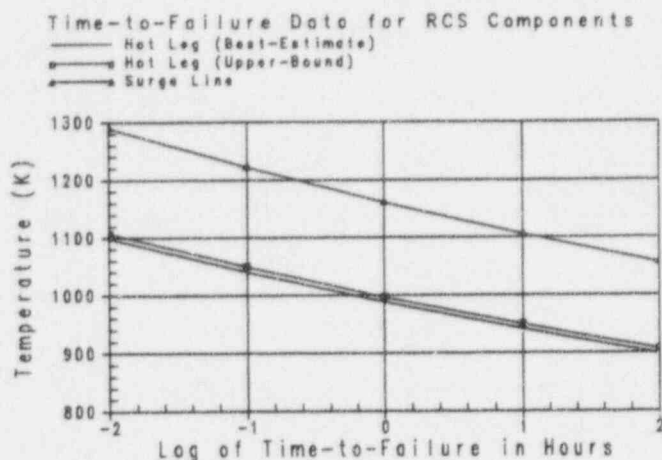


Figure 37-1

Time-to-Failure Data for Reactor Coolant System Components

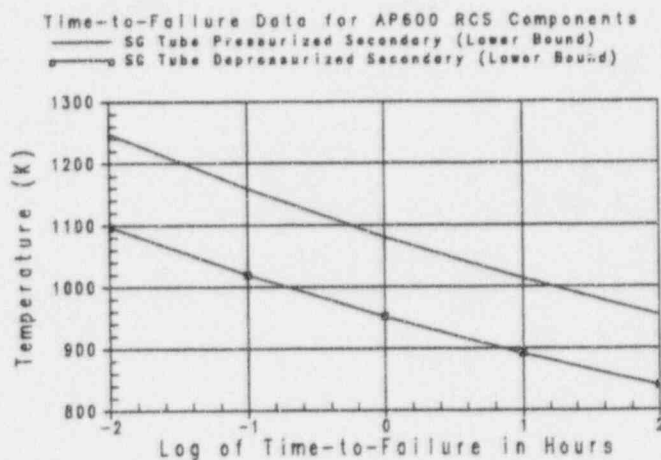


Figure 37-2

Time-to-Failure Data for AP600 Reactor Coolant System Components

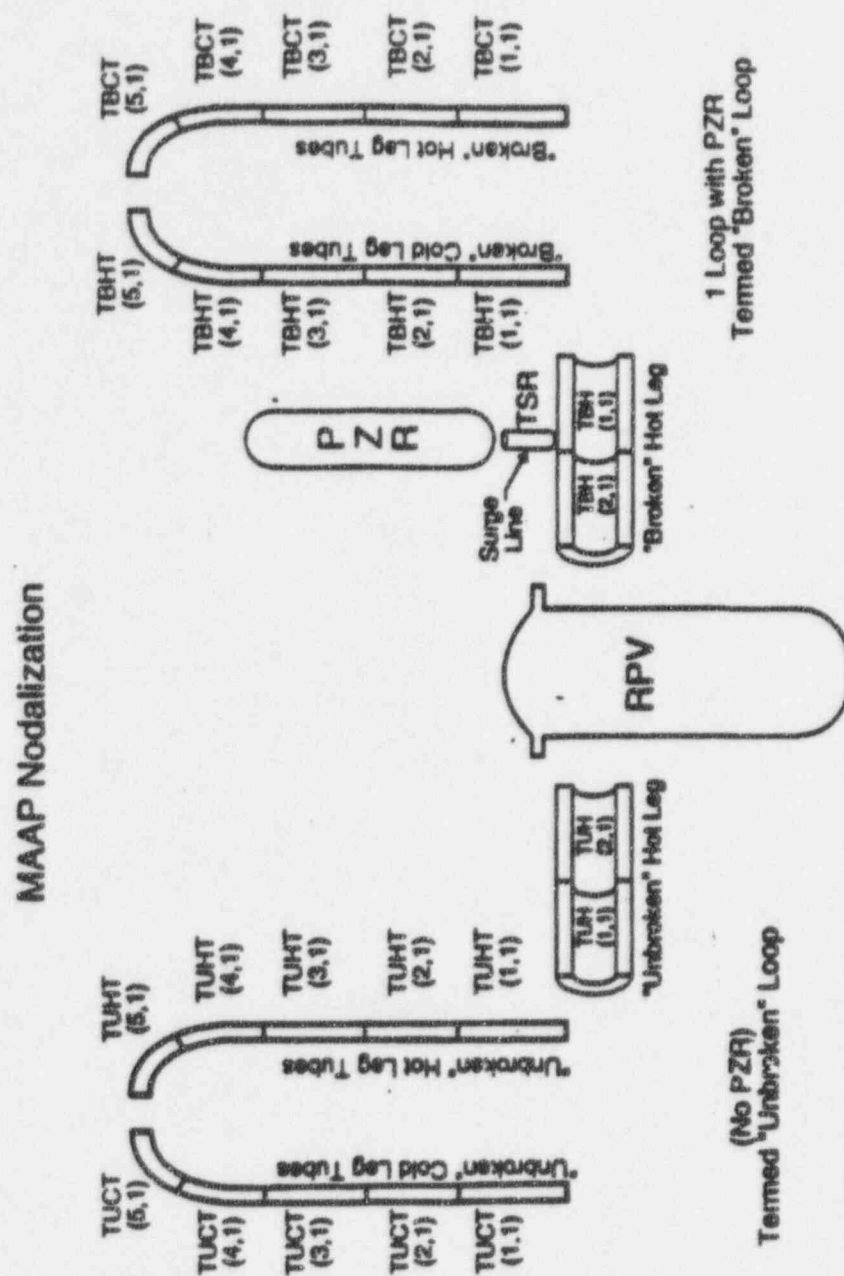


Figure 37-3

MAAP Nodalization

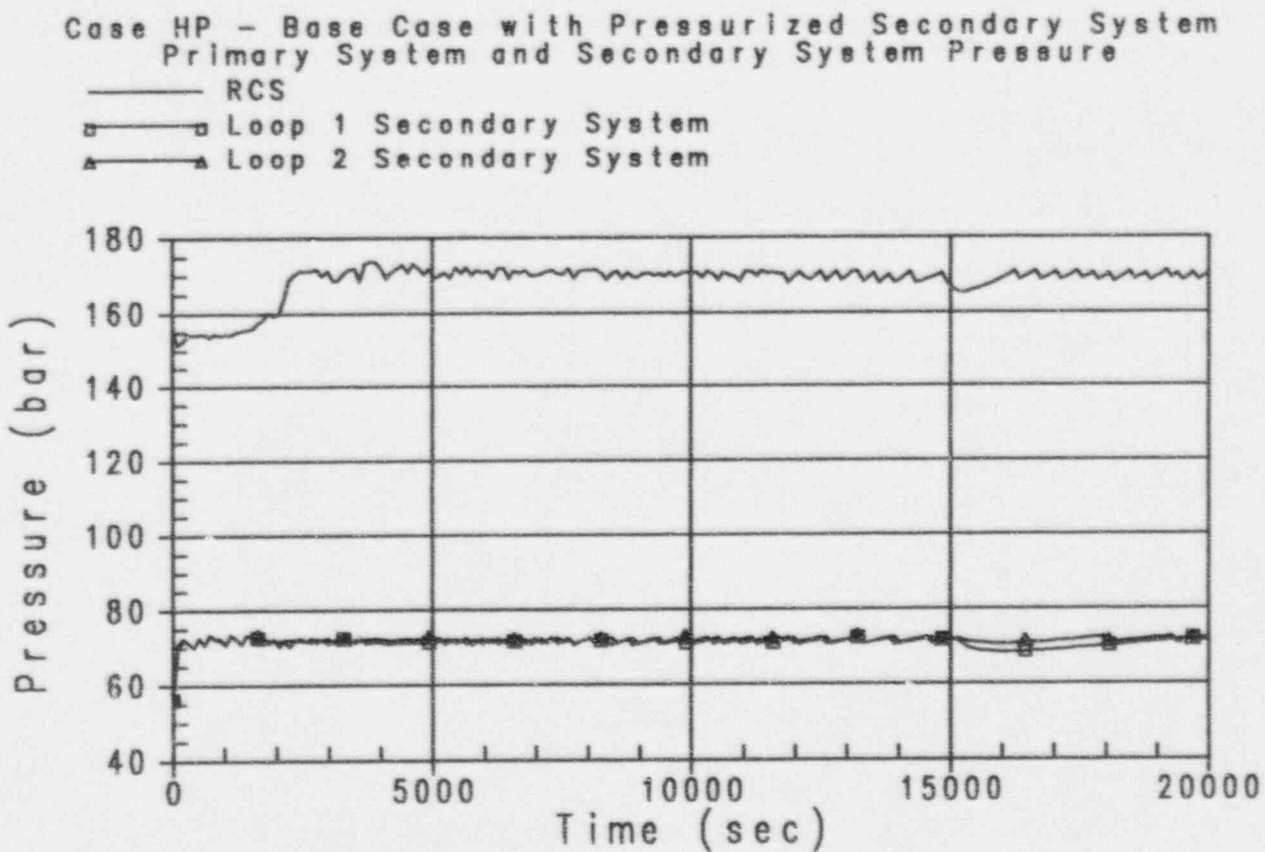


Figure 37-4

Case HP - Base Case with Pressurized Secondary System
Primary System and Secondary System Pressure

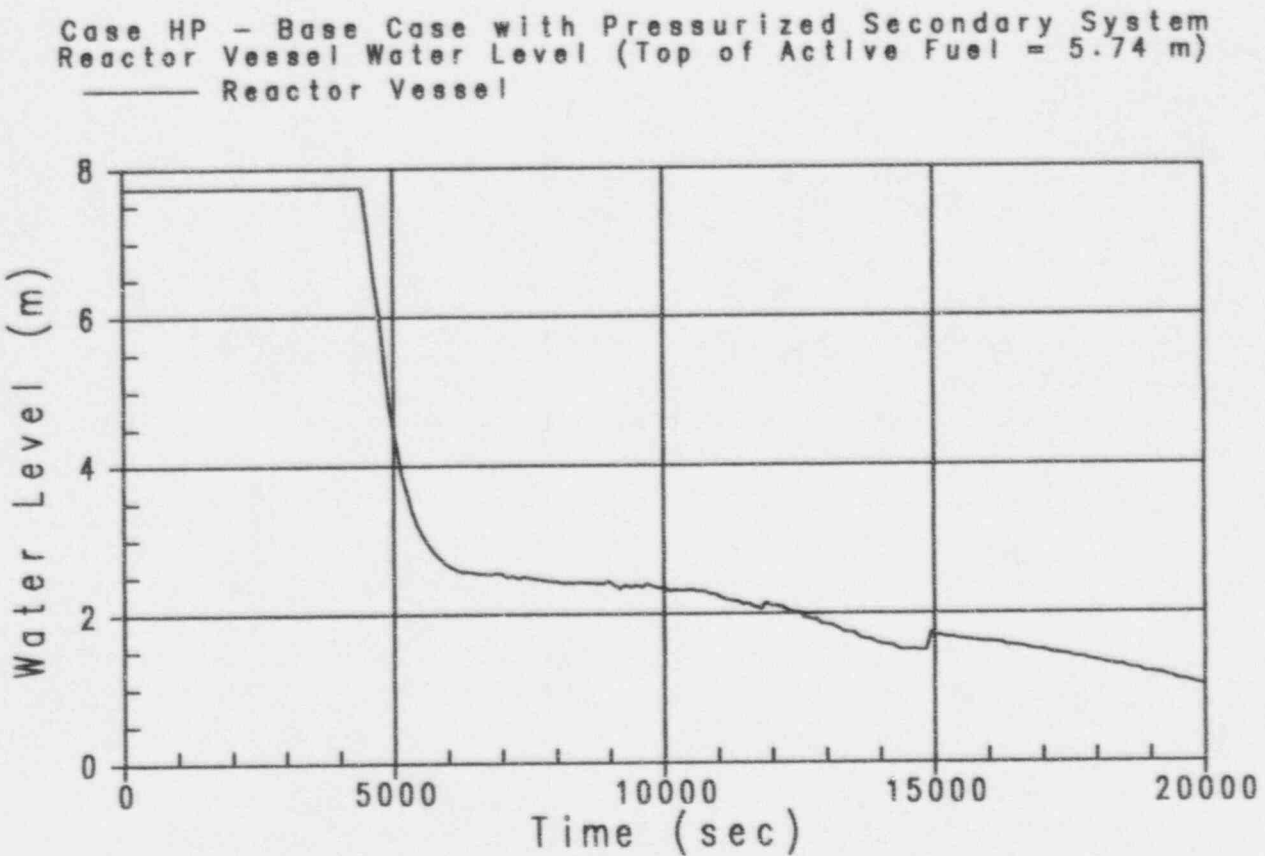


Figure 37-5

Case HP - Base Case with Pressurized Secondary System
Reactor Vessel Water Level



Westinghouse

ENEL
EDF, MAGNOL
PO, L'ESPOIR, ELETTRICA

37-23

Revision: 3
February 28, 1995
u:\ap600\apra\sec37.wpd:lb

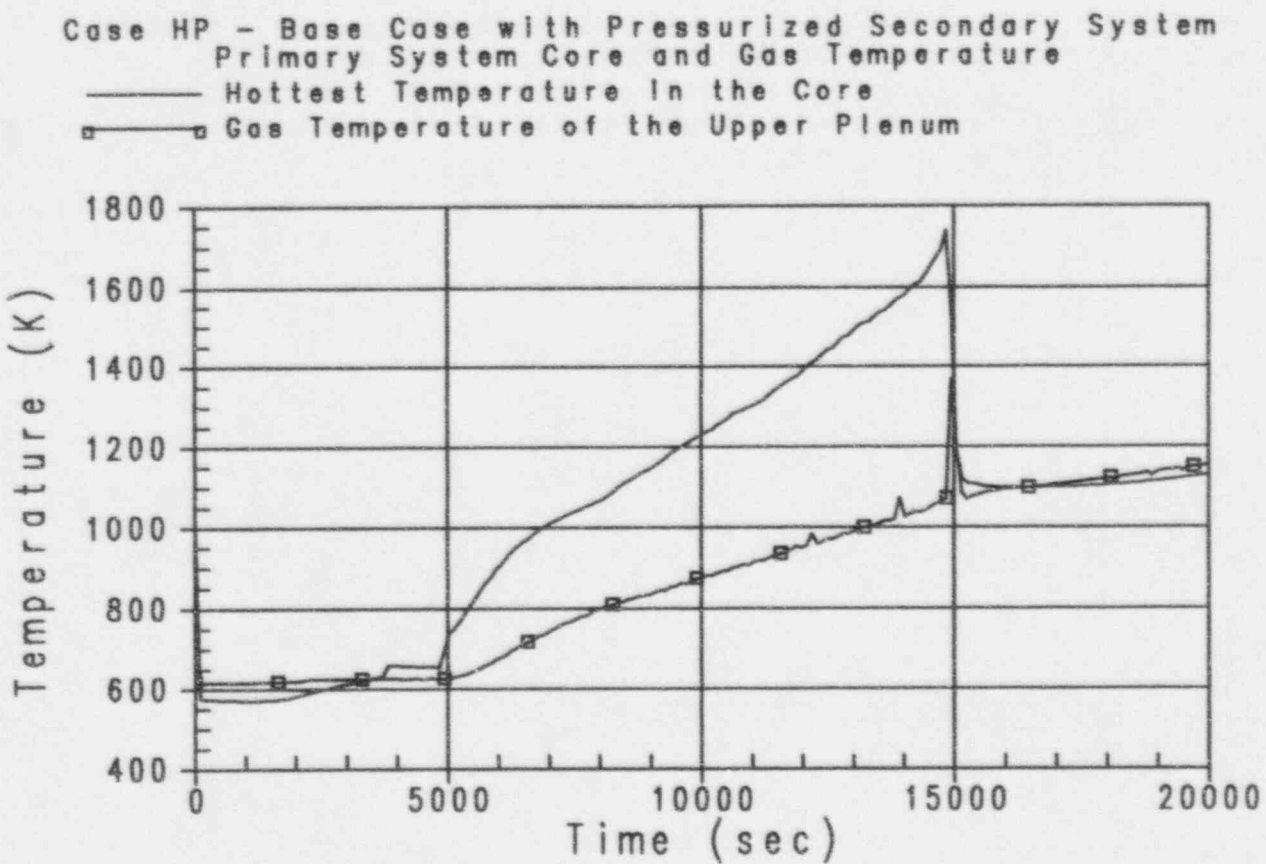


Figure 37-6

Case HP - Base Case with Pressurized Secondary System
Primary System Core and Gas Temperature

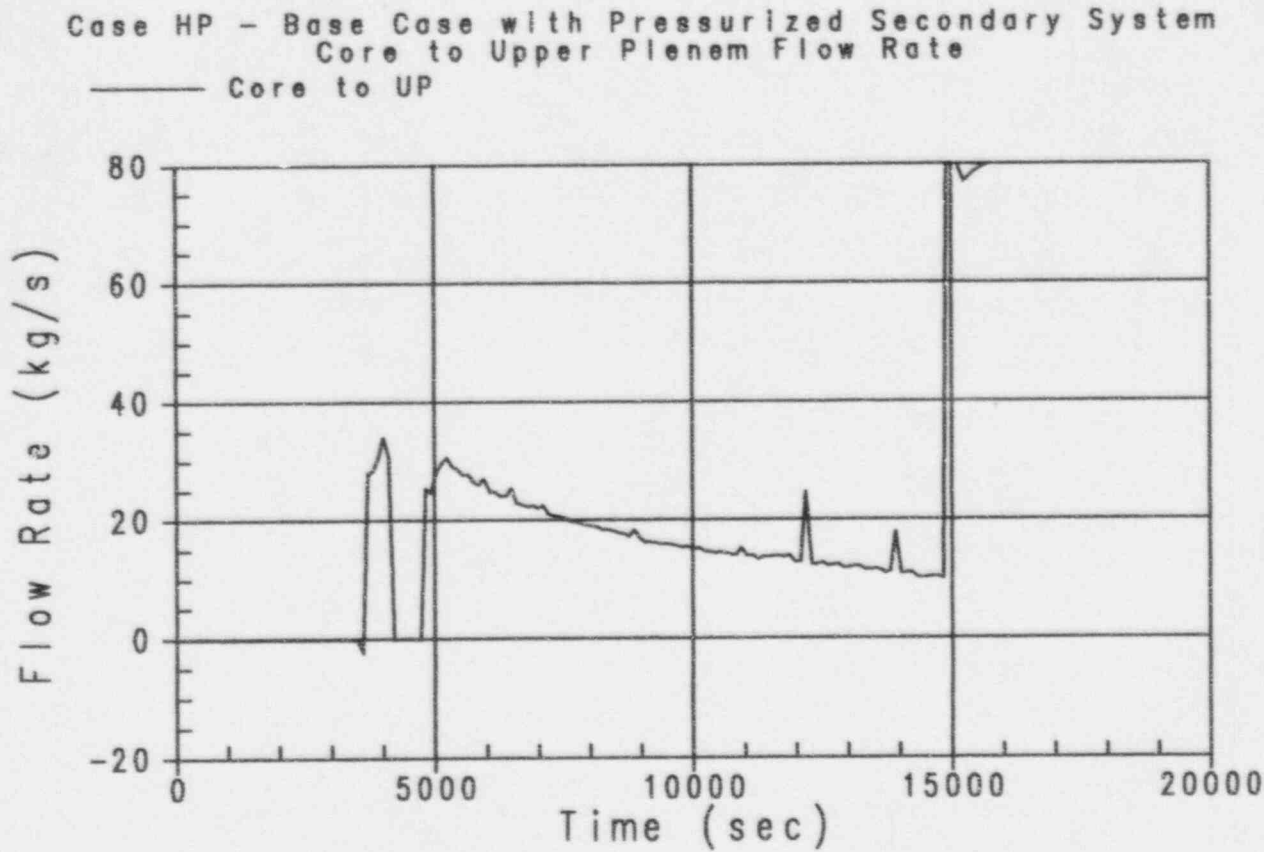


Figure 37-7

Case HP - Base Case with Pressurized Secondary System
Core to Upper Plenum Flow Rate



Westinghouse

ENEL
ENEL NUCLEARE
PER L'ENERGIA ELETTRICA

37-25

Revision: 3
February 28, 1995
u:\ap600\pna\ec37.wpf:lb

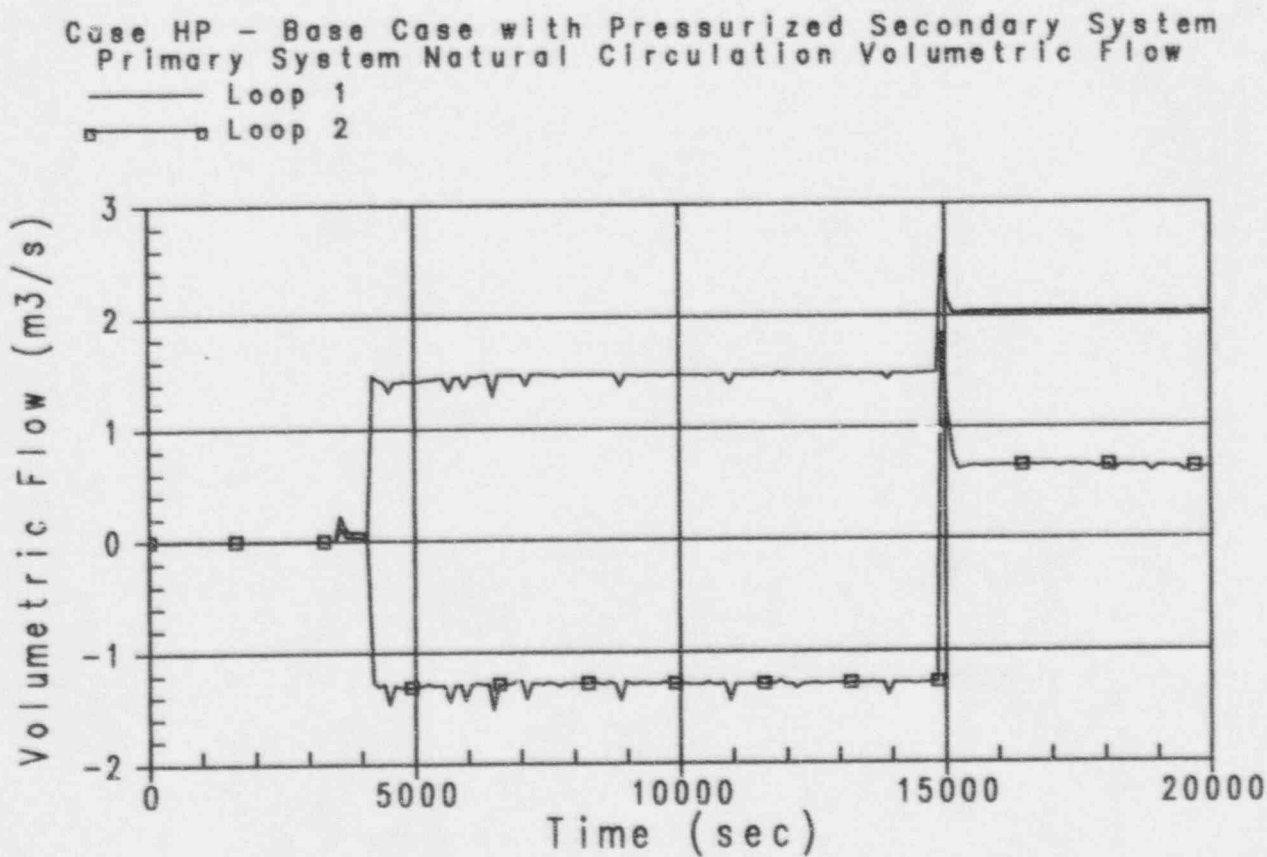


Figure 37-8

Case HP - Base Case with Pressurized Secondary System
Primary System Natural Circulation Volumetric Flow

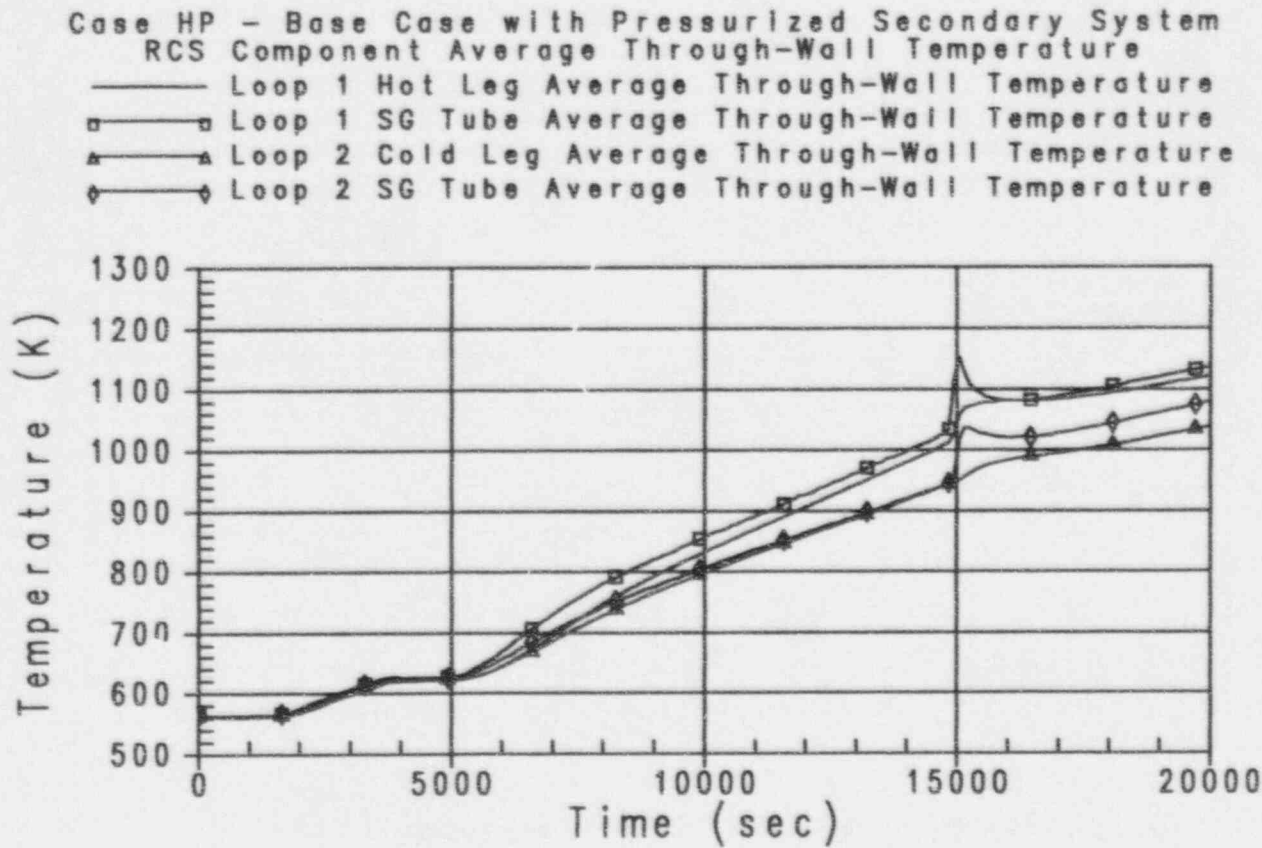


Figure 37-9

Case HP - Base Case with Pressurized Secondary System
Reactor Coolant System Component Average Through-Wall Temperature



Westinghouse

ENEL
ENVIRO NUCLEAR
FOR LONDON, ELECTRONICS

37-27

Revision: 3
February 28, 1995
u:\ap600\prra\ec37.wpf:1b

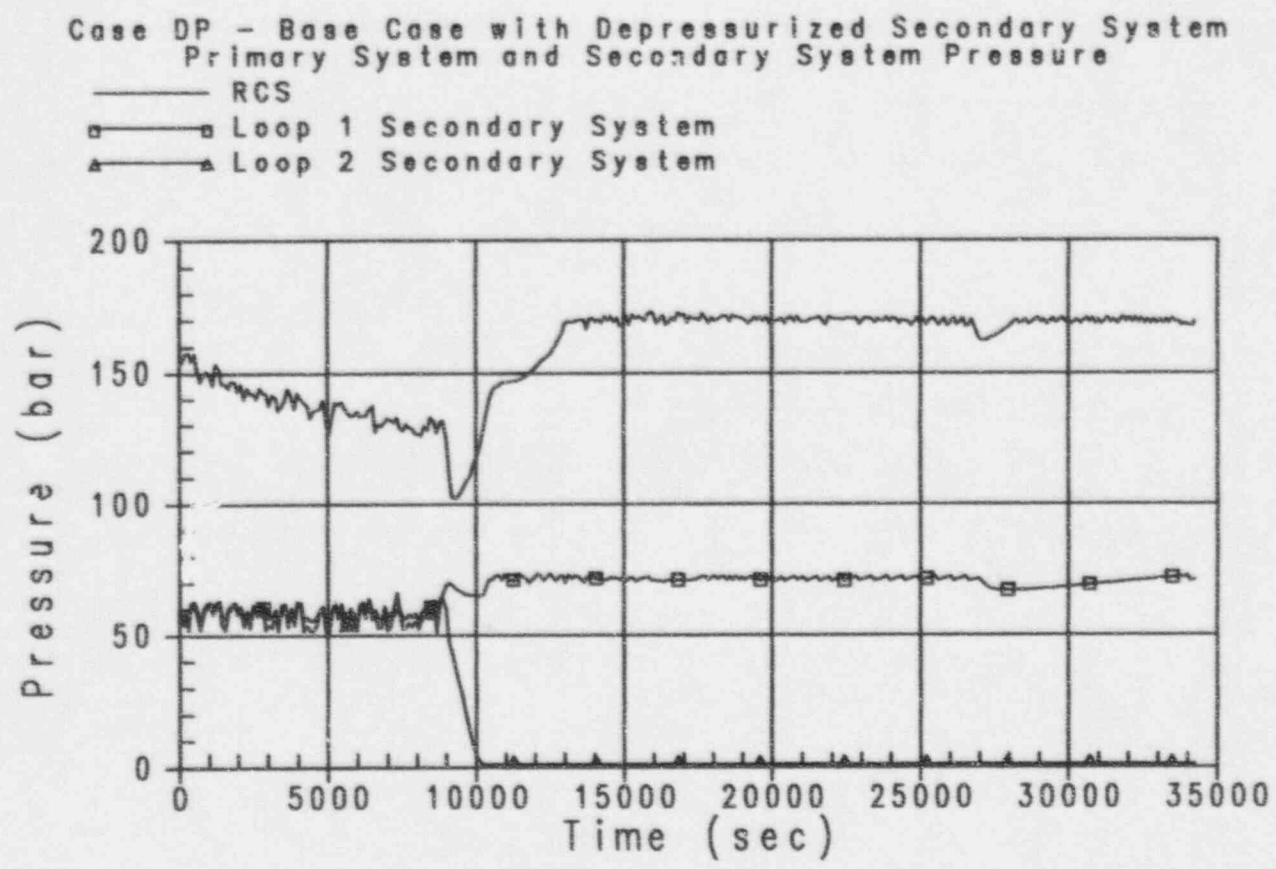


Figure 37-10

Case DP - Base Case with Depressurized Secondary System
Primary System and Secondary System Pressure

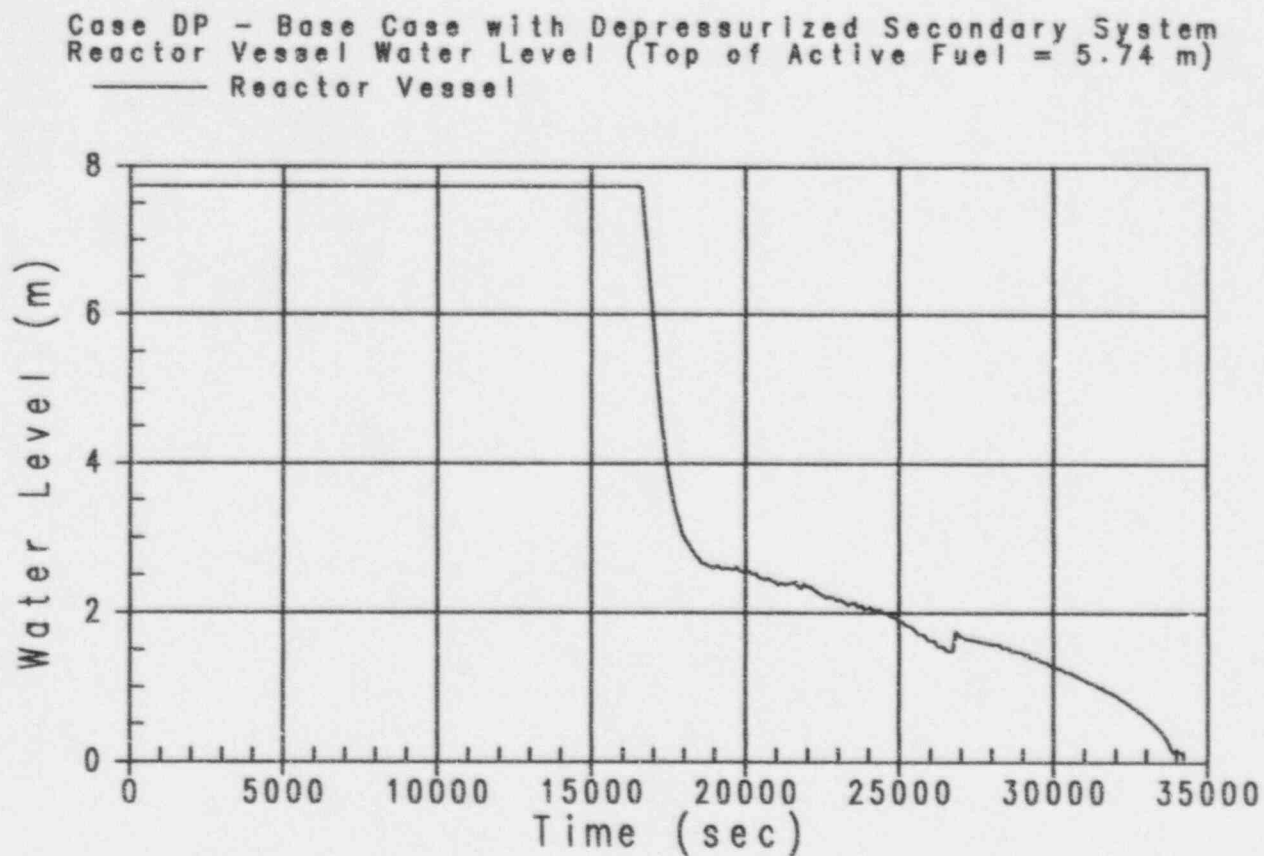


Figure 37-11

Case DP - Base Case with Depressurized Secondary System
Reactor Vessel Water Level



Westinghouse

ENEL
SISTEMI
PER LA
PRODUZIONE
ELETTRICA

37-29

Revision: 3
February 28, 1995
u:\ap600\pna\ee37.wpl:1b

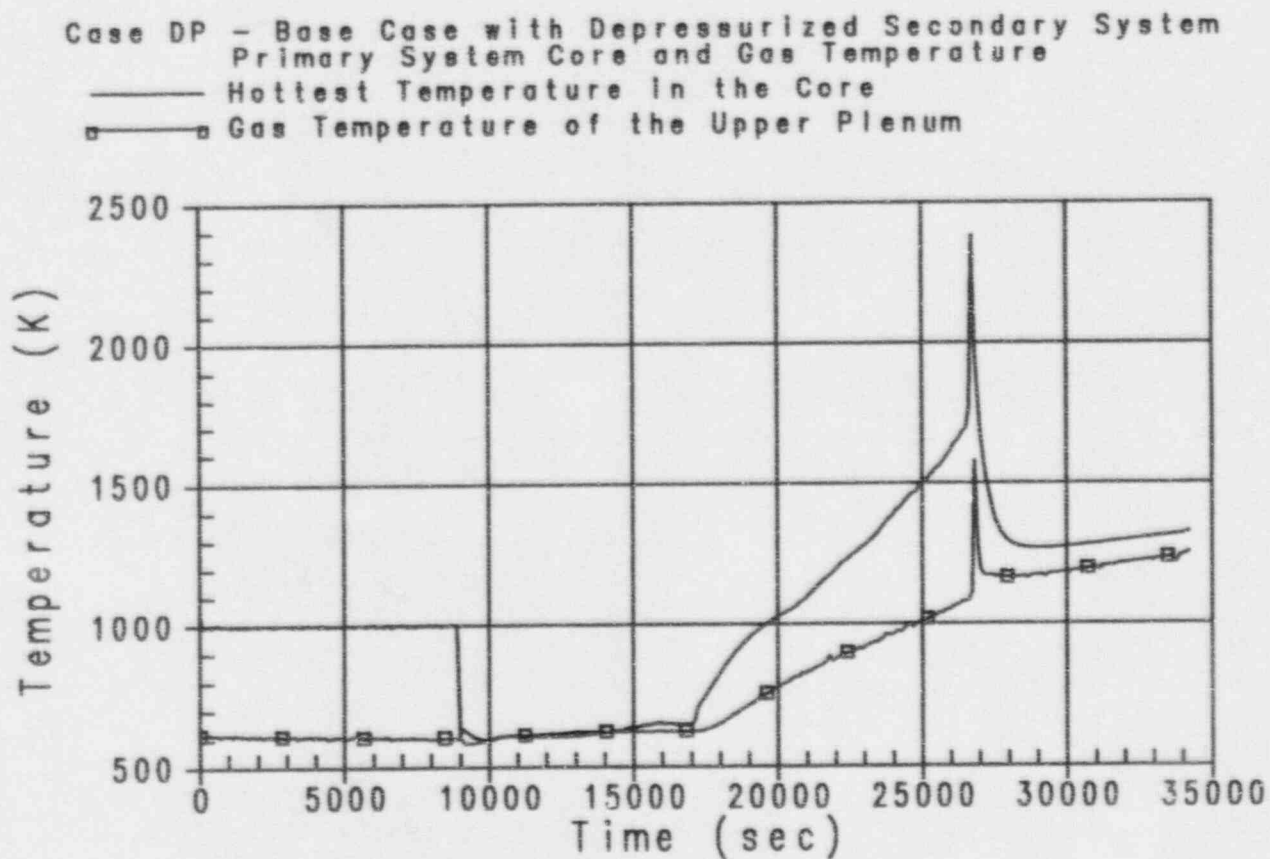


Figure 37-12

Case DP - Base Case with Depressurized Secondary System
Primary System Core and Gas Temperature

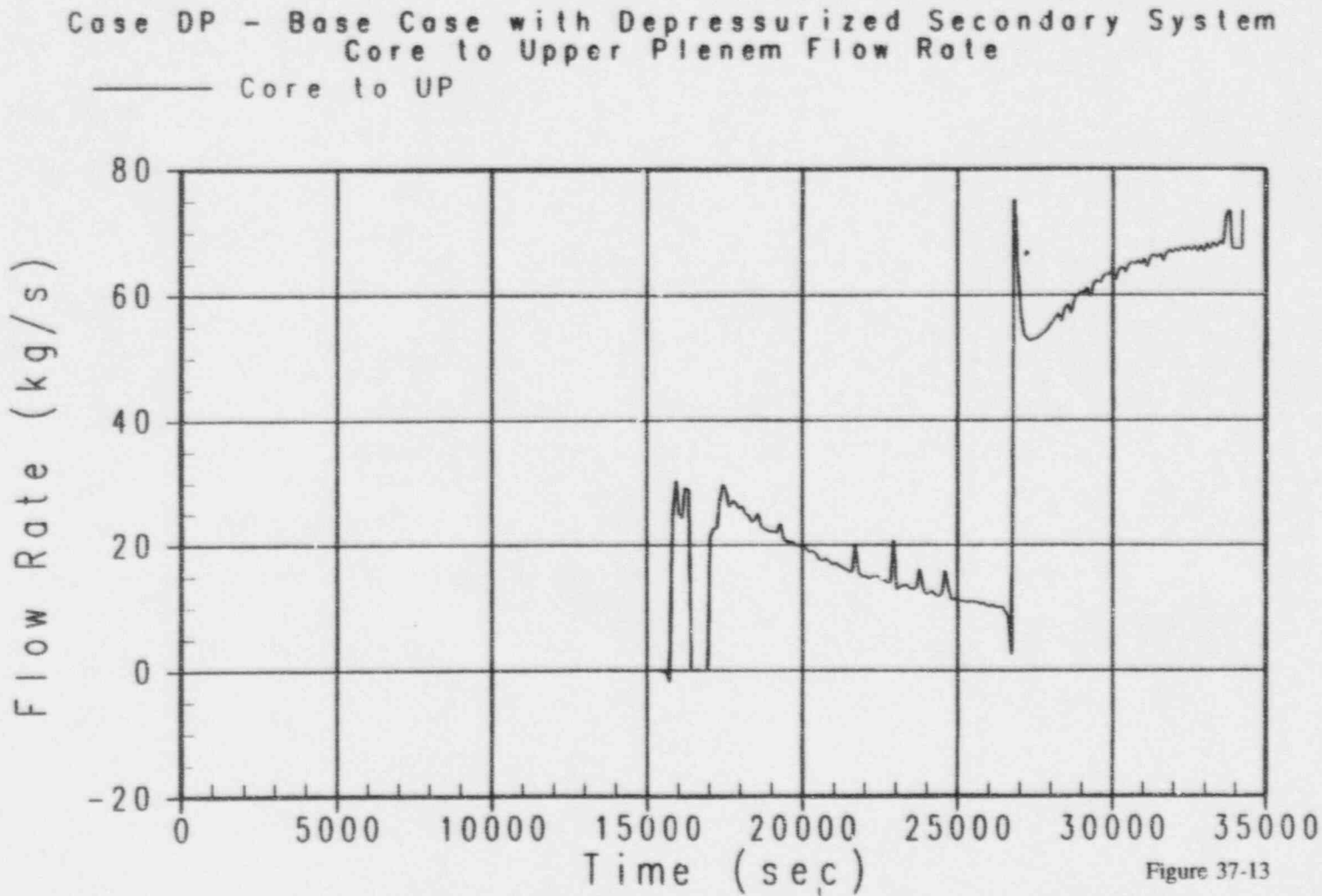


Figure 37-13

Case DP - Base Case with Depressurized Secondary System
Core to Upper Plenum Flow Rate



Westinghouse

ENEL
ELECTRONIC SYSTEMS
DIVISION

37-31

Revision: 3
February 28, 1995
u:\ap600\pna\ec37.wpf:1b

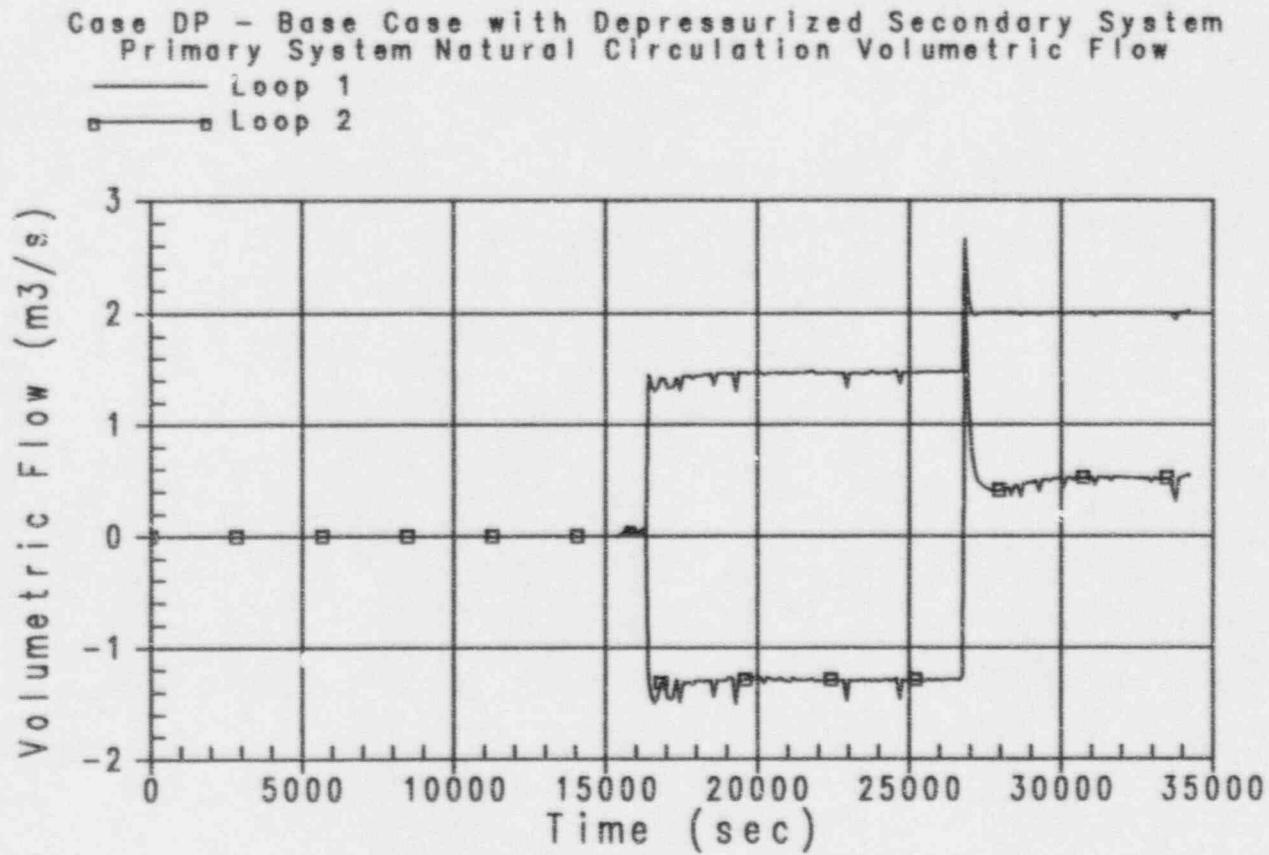


Figure 37-14

Case DP - Base Case with Depressurized Secondary System
Primary System Natural Circulation Volumetric Flow

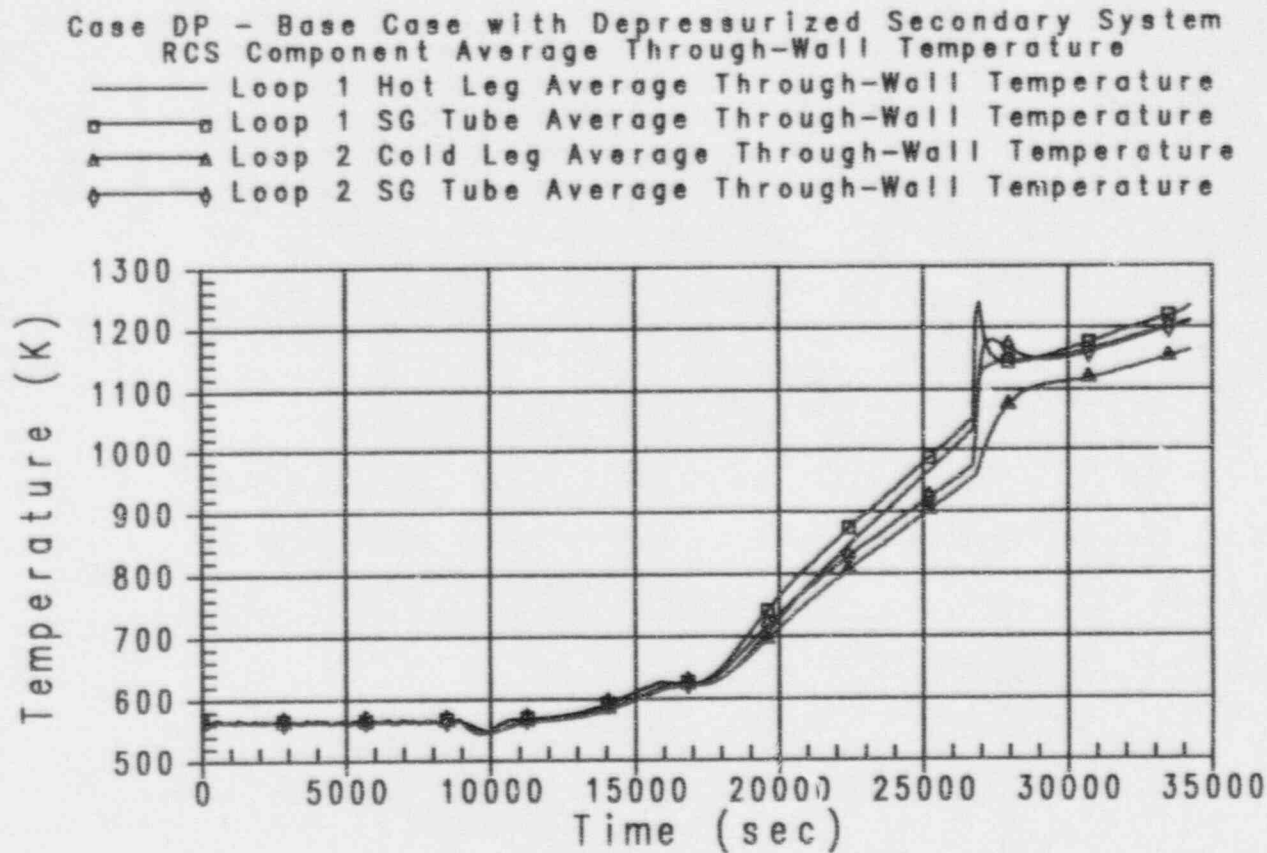


Figure 37-15

Case DP - Base Case with Depressurized Secondary System
Reactor Coolant System Component Average Through-Wall Temperature



Westinghouse

ENEL
ENEL NUCLEONALE
PER L'ENERGIA ELETTRICA

37-33

Revision: 3
February 28, 1995
u:\ap600\pna\sec37.mpf:1b

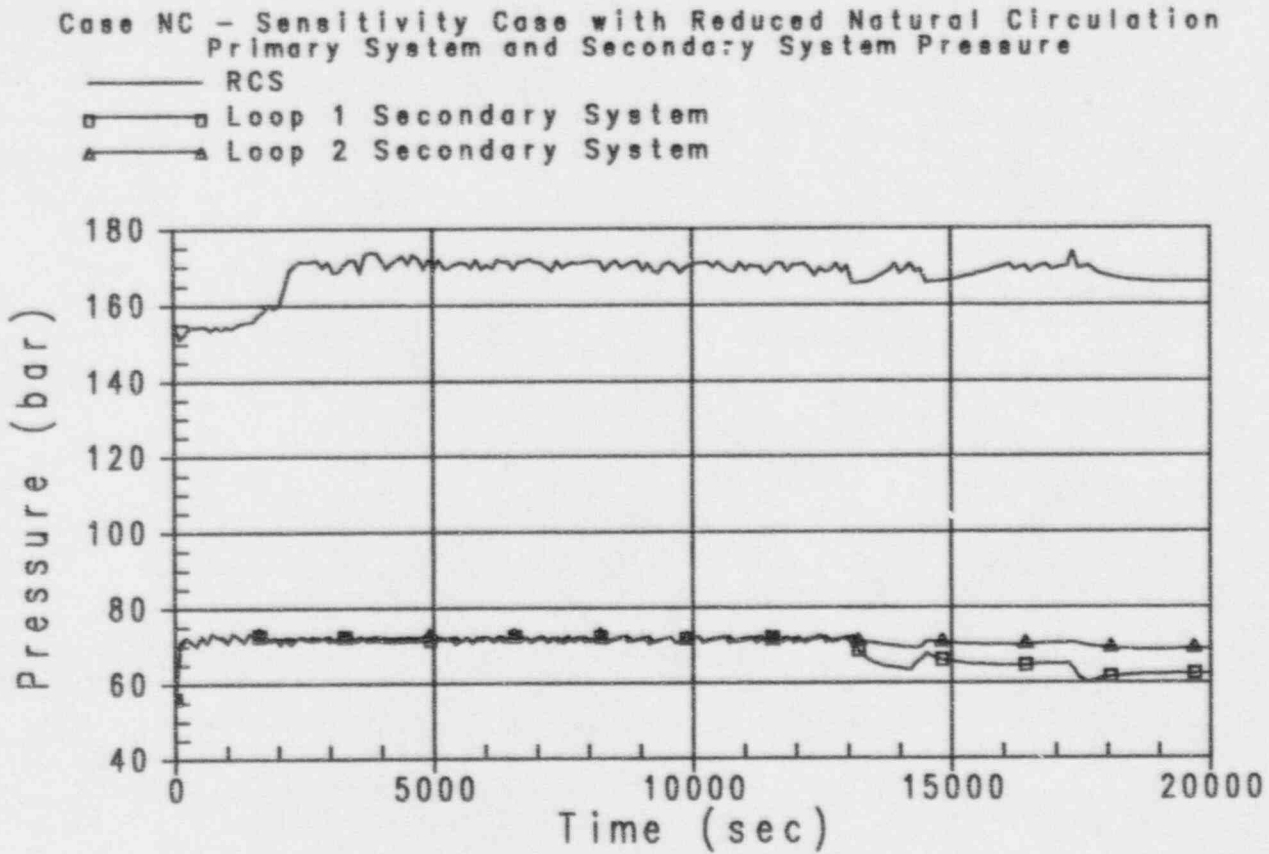


Figure 37-16

Case NC - Sensitivity Case with Reduced Natural Circulation
Primary System and Secondary System Pressure

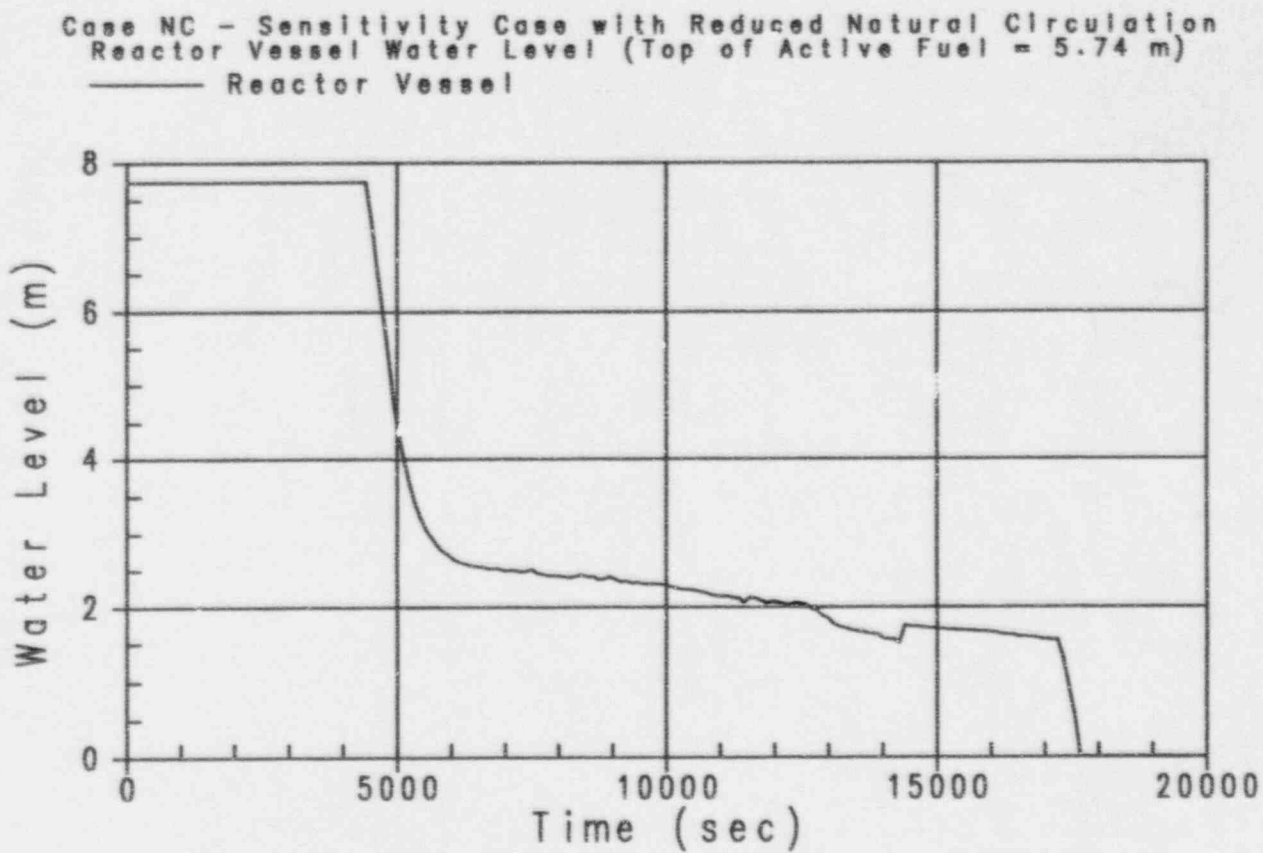


Figure 37-17

Case NC - Sensitivity Case with Reduced Natural Circulation
Reactor Vessel Water Level



Westinghouse

ENEL
ENERGIA NUCLEARE
PER L'ENERGIA ELETTRICA

37-35

Revision: 3
February 28, 1995
u:\ap600\pwr\vec37.wpf:1b

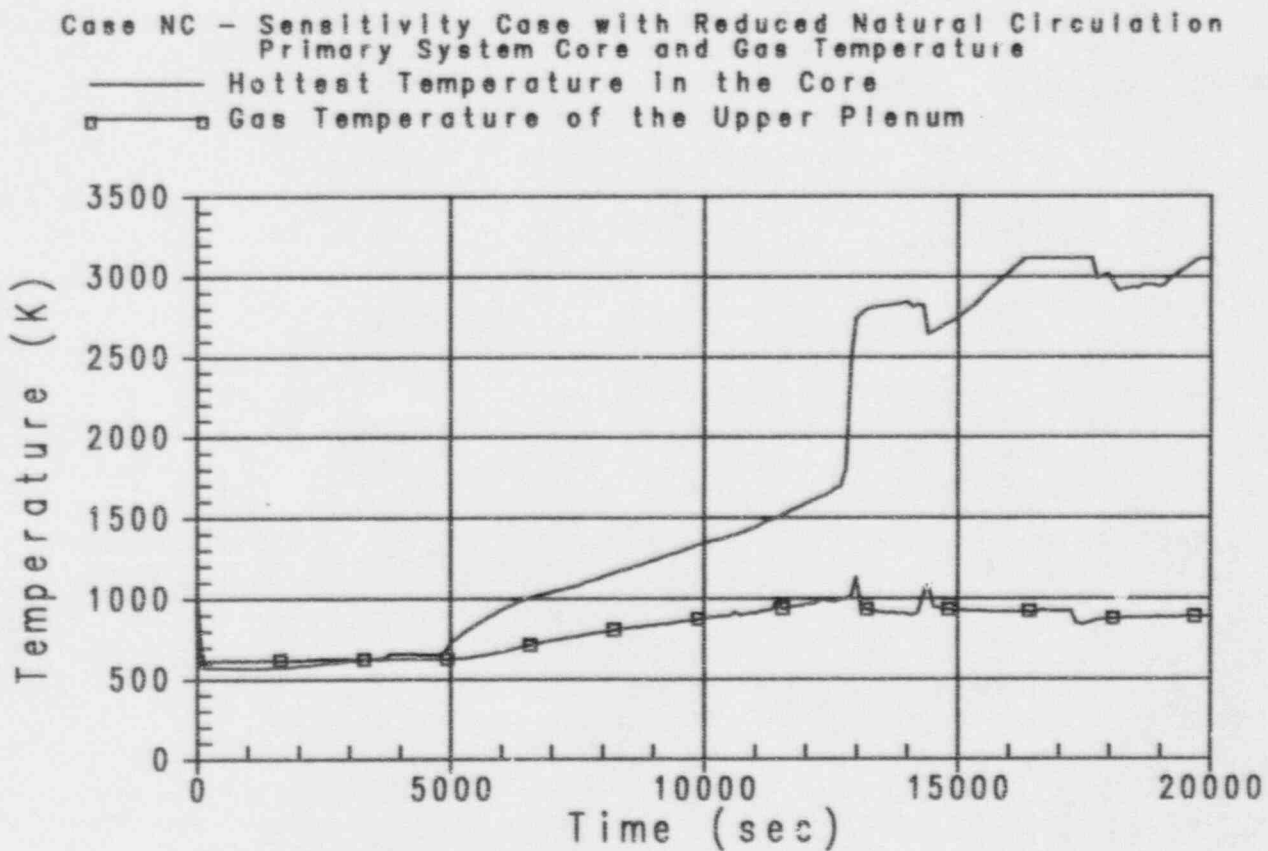


Figure 37-18

Case NC - Sensitivity Case with Reduced Natural Circulation
Primary System Core and Gas Temperature

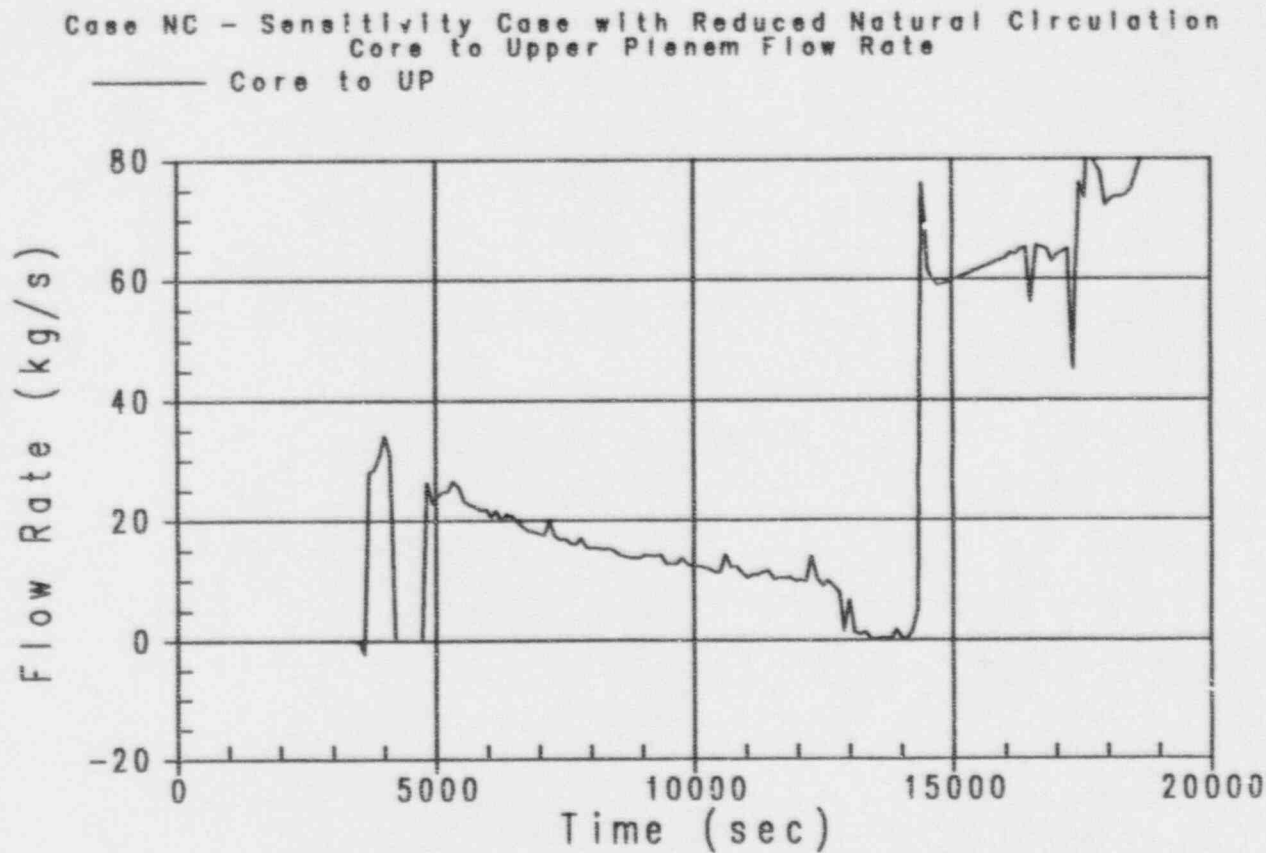


Figure 37-19

Case NC - Sensitivity Case with Reduced Natural Circulation
Core to Upper Plenum Flow Rate



Westinghouse

ENEL
ENERGIA NUCLEARE
PER L'ENERGIA ELETTRICA

37-37

Revision: 3
February 28, 1995
u:\ap600\gna\sec37.wpi:lb

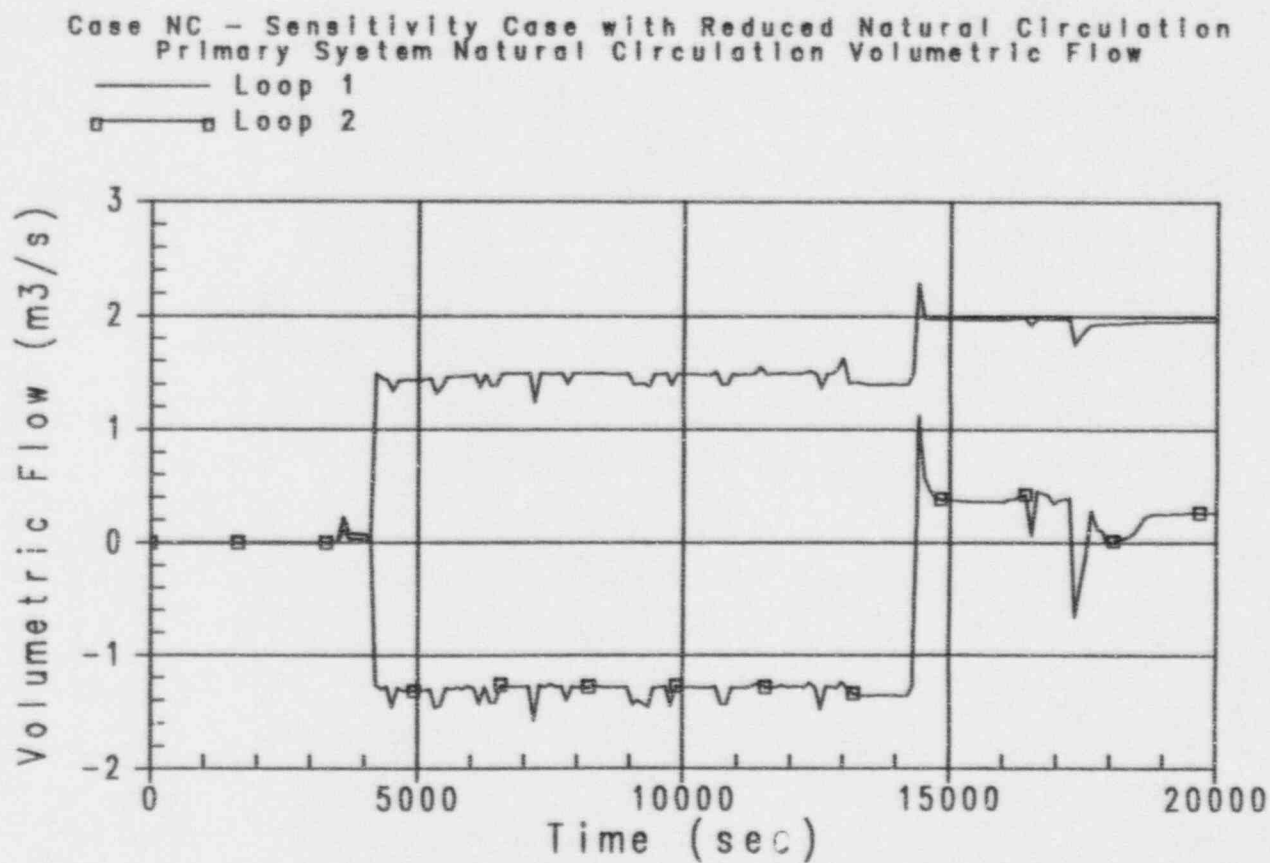


Figure 37-20

Case NC - Sensitivity Case with Reduced Natural Circulation
Primary System Natural Circulation Volumetric Flow

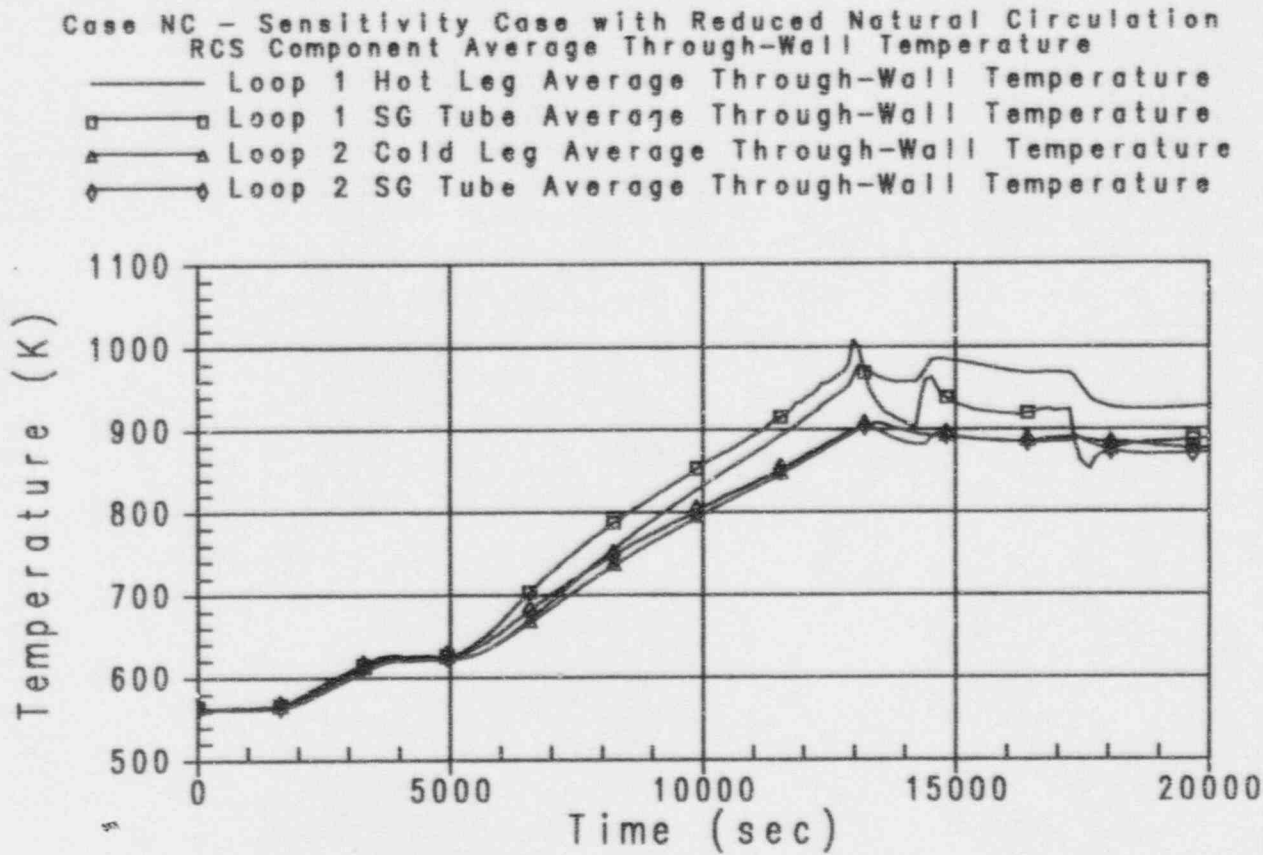


Figure 37-21

Case NC - Sensitivity Case with Reduced Natural Circulation
Reactor Coolant System Component Average Through-Wall Temperature



Westinghouse

ENEL
ENEL NUCLEAR
PCI L'ENERGIA ELETTRICA

37-39

Revision: 3
February 28, 1995
u:\ap600\pna\vec37.wpf:1b

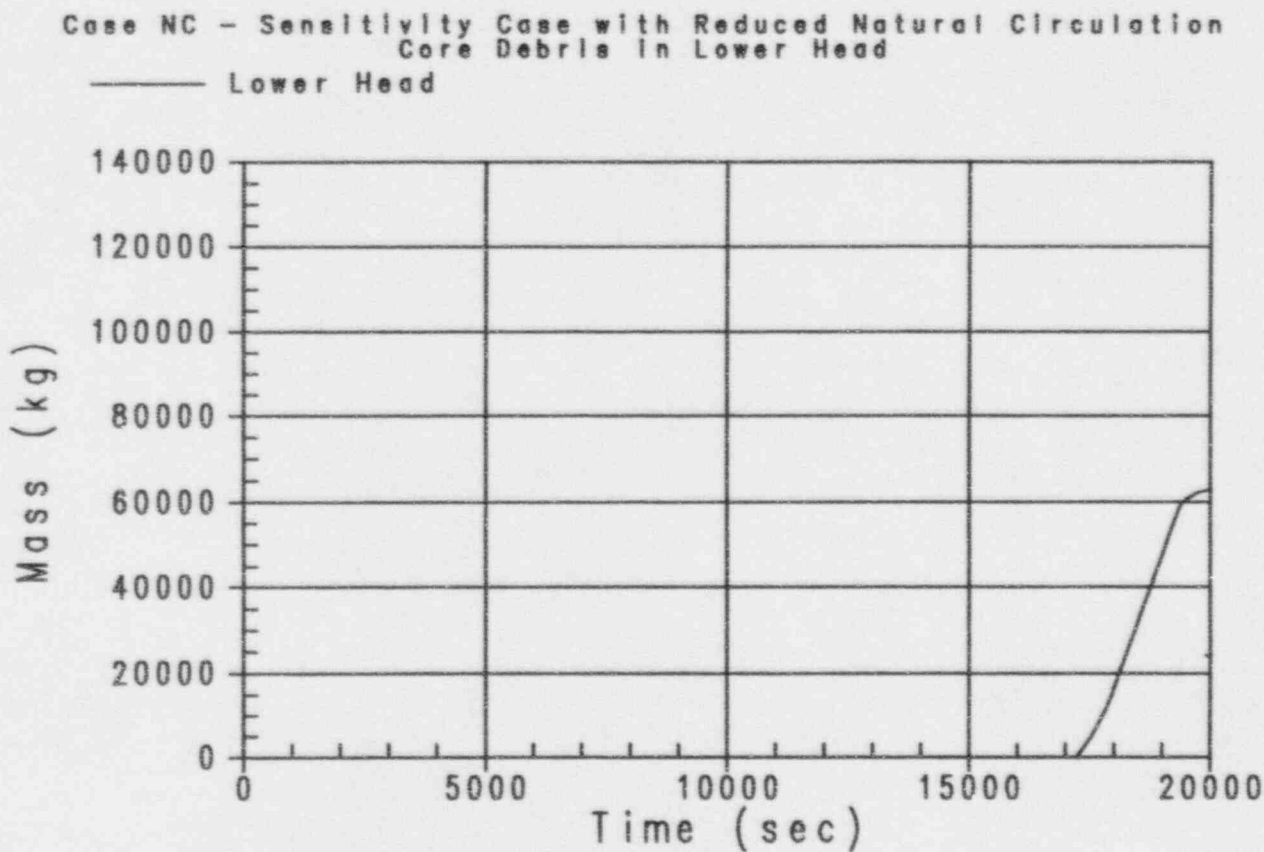


Figure 37-22

Case NC - Sensitivity Case with Reduced Natural Circulation
Core Debris in Lower Head

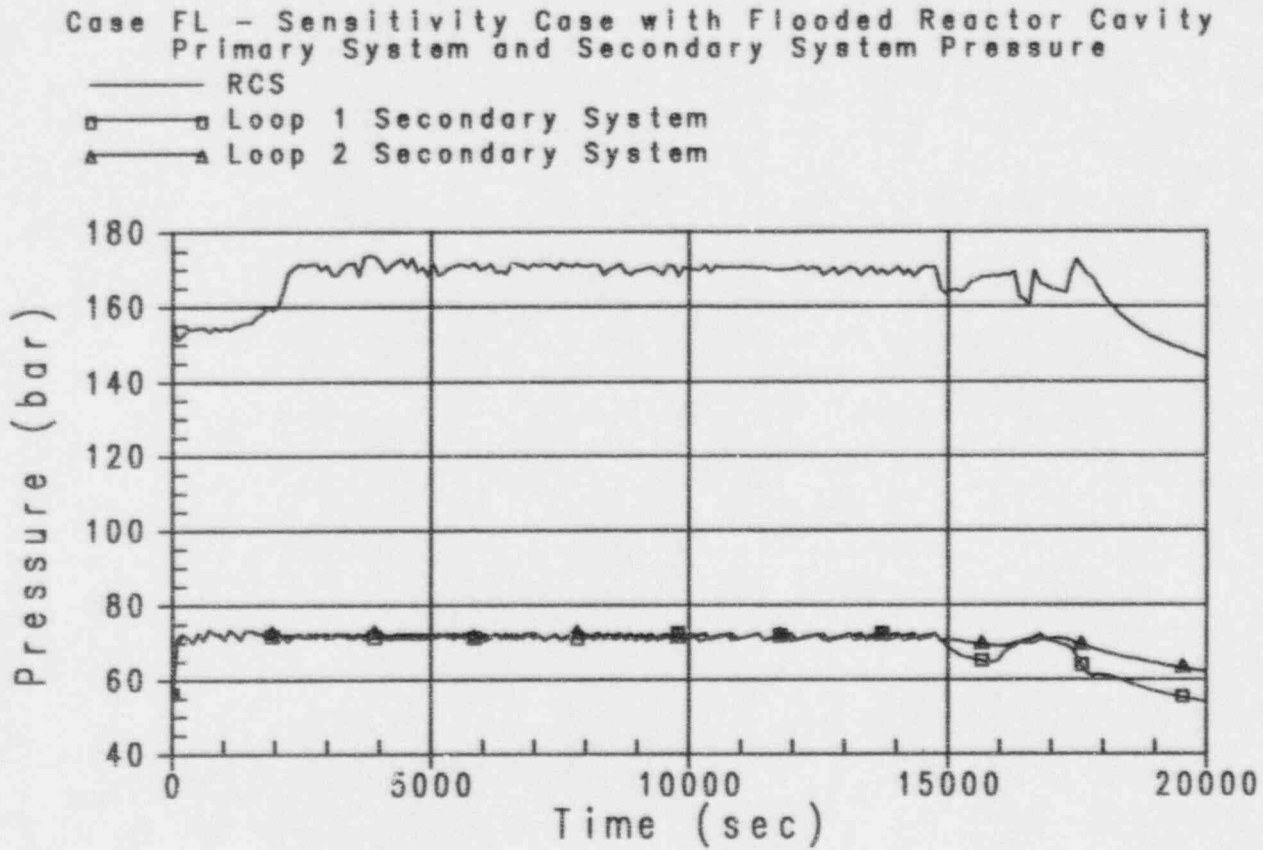


Figure 37-23

Case FL - Sensitivity Case with Flooded Reactor Cavity
Primary System and Secondary System Pressure



Westinghouse

ENEL
ENERGIA NUCLEARE
PER L'INDUSTRIA ELETTRICA

37-41

Revision: 3
February 28, 1995
u:\ap600\gras\sec37.wpf:1b

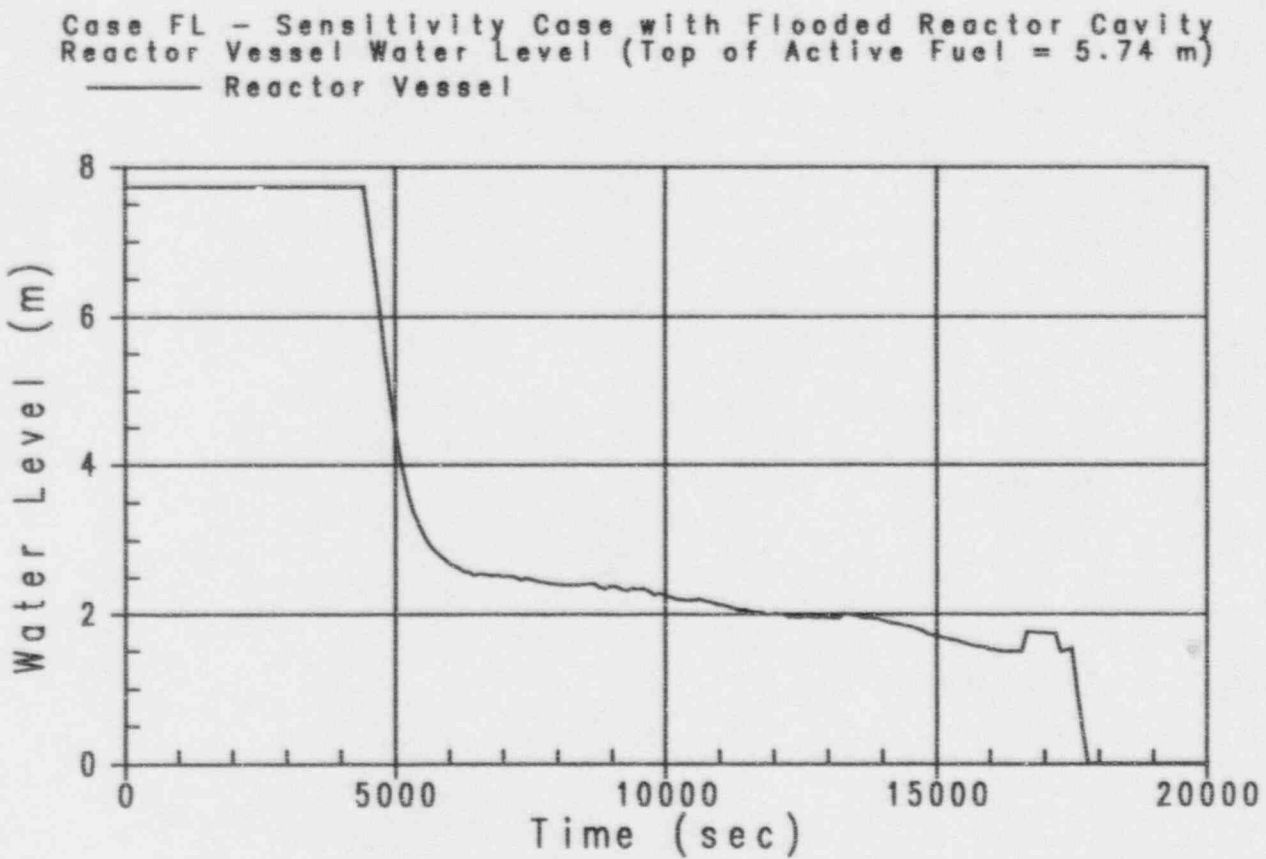


Figure 37-24

Case FL - Sensitivity Case with Flooded Reactor Cavity
Reactor Vessel Water Level

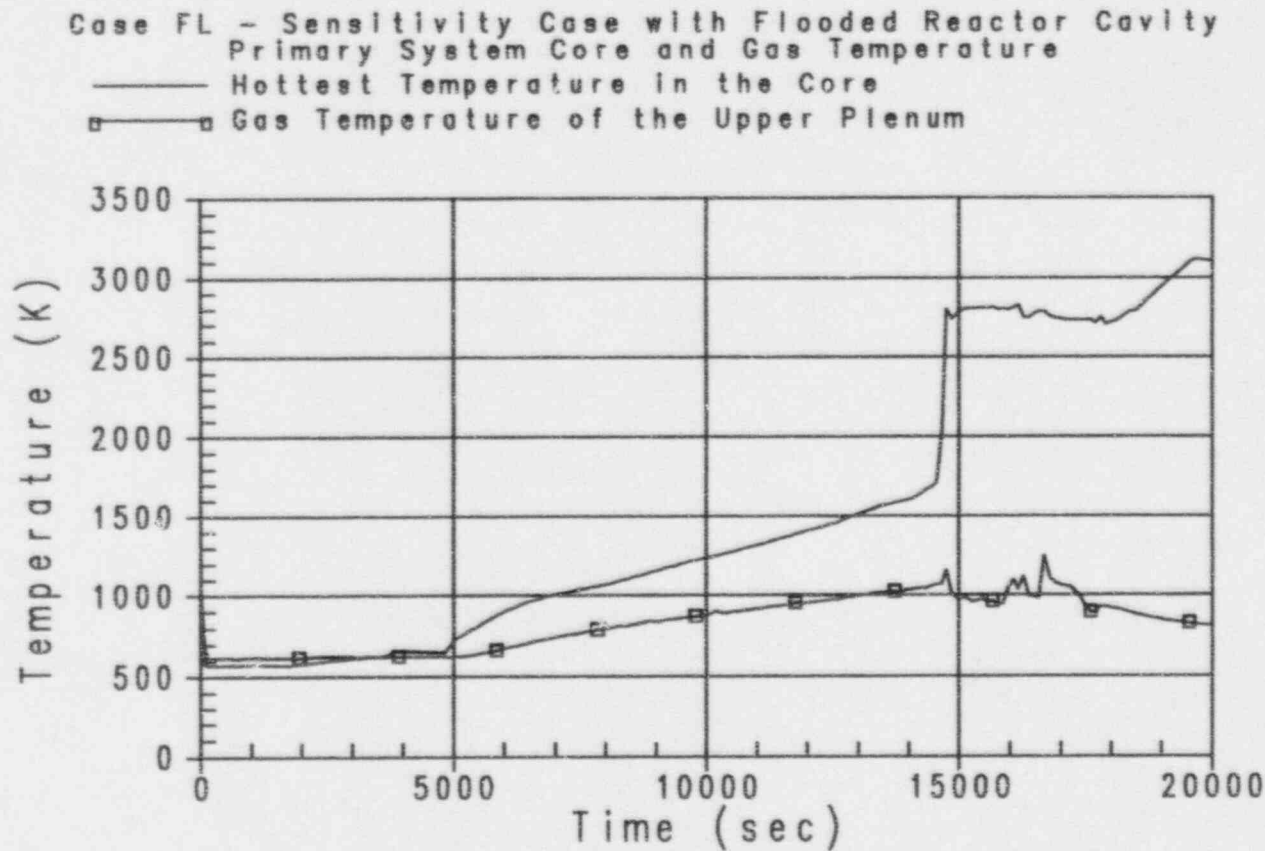


Figure 37-25

Case FL - Sensitivity Case with Flooded Reactor Cavity
Primary System Core and Gas Temperature



Westinghouse

ENEL
FOR NUCLEAR &
FOR LOW-POWER ELECTRONICS

37-43

Revision: 3
February 28, 1995
u:\ap600\gralvec37.wpf:1b

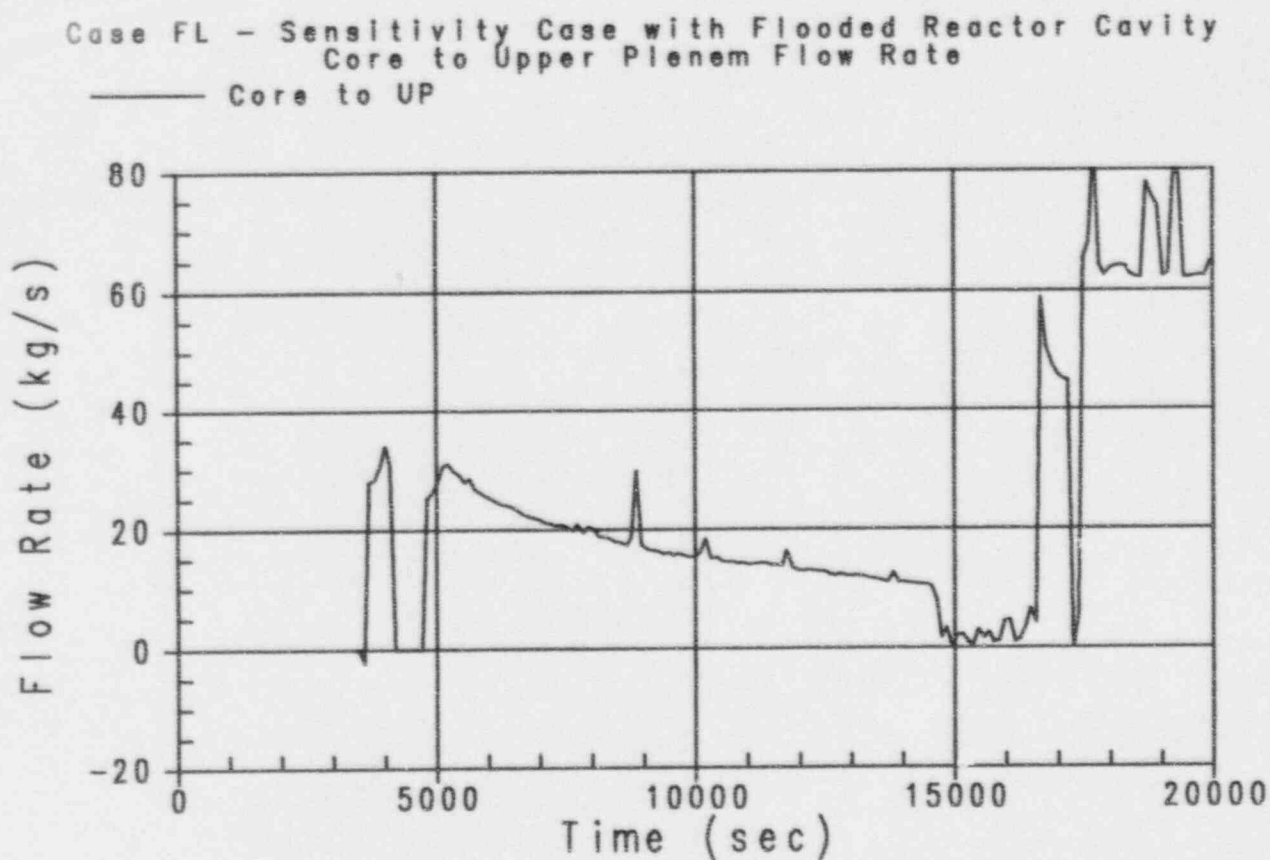


Figure 37-26

Case FL - Sensitivity Case with Flooded Reactor Cavity
Core to Upper Plenum Flow Rate

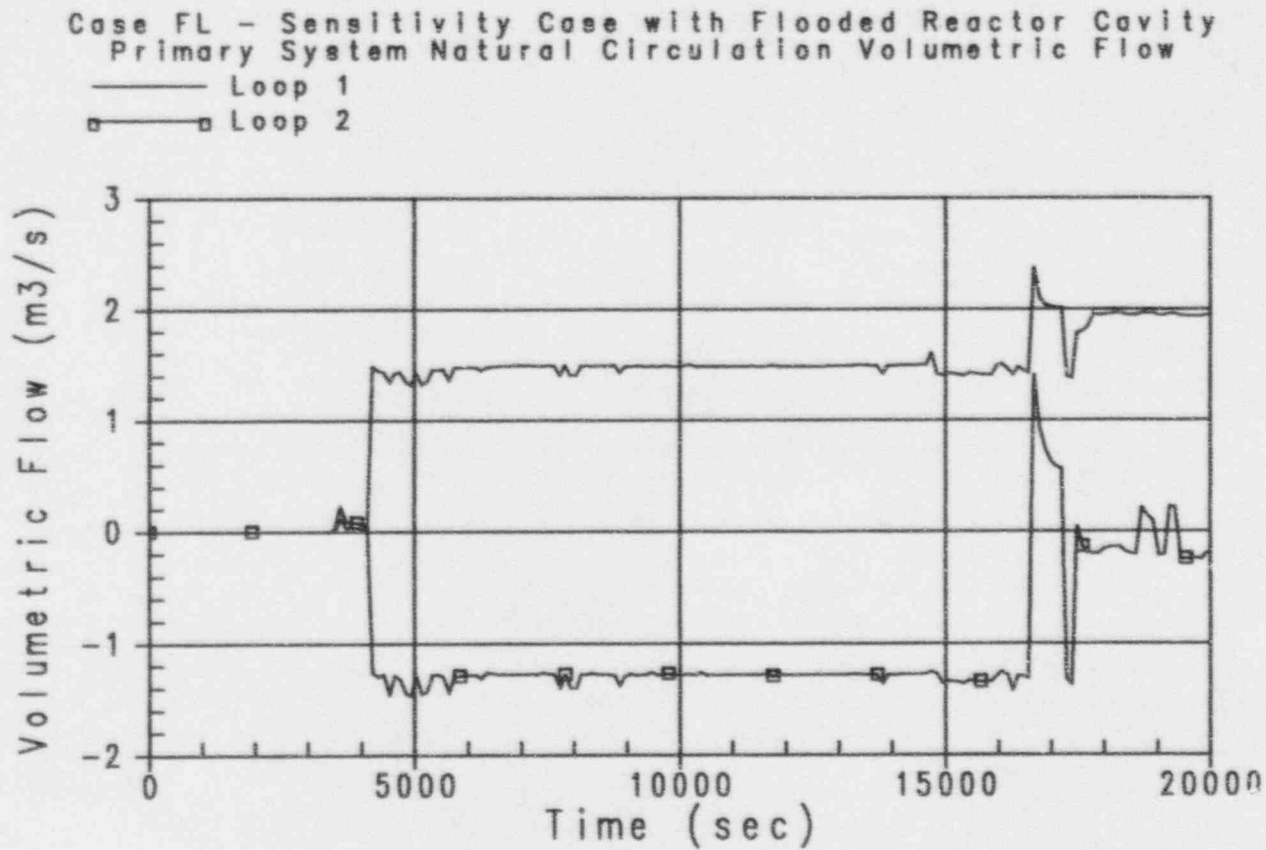


Figure 37-27

Case FL - Sensitivity Case with Flooded Reactor Cavity
Primary System Natural Circulation Volumetric Flow



Westinghouse

ENEL
ENR. MAGAZINE
PER L'ESPRESSO LETTERA

37-45

Revision: 3
February 28, 1995
u:\ap600\pna\sec37.mpf:1b

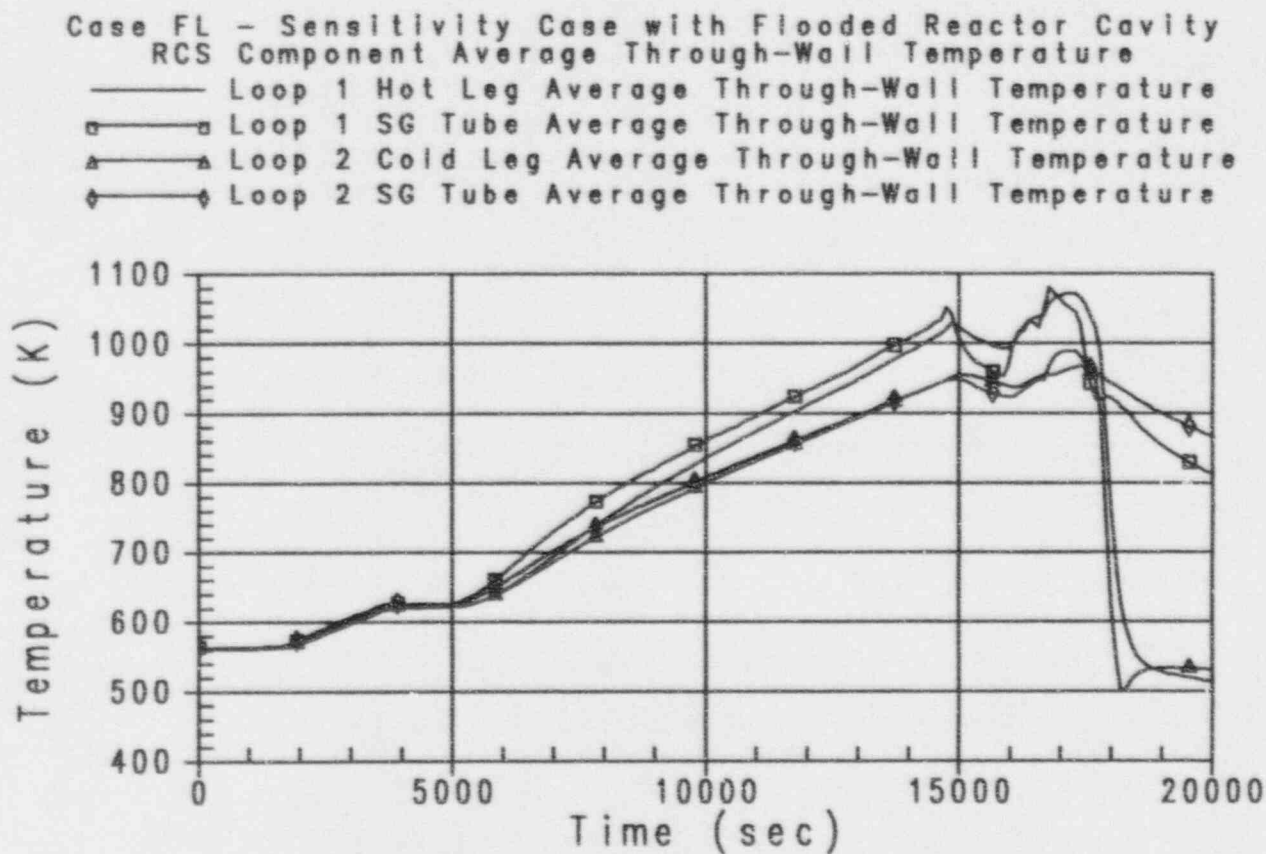


Figure 37-28

Case FL - Sensitivity Case with Flooded Reactor Cavity
Reactor Coolant System Component Average Through-Wall Temperature

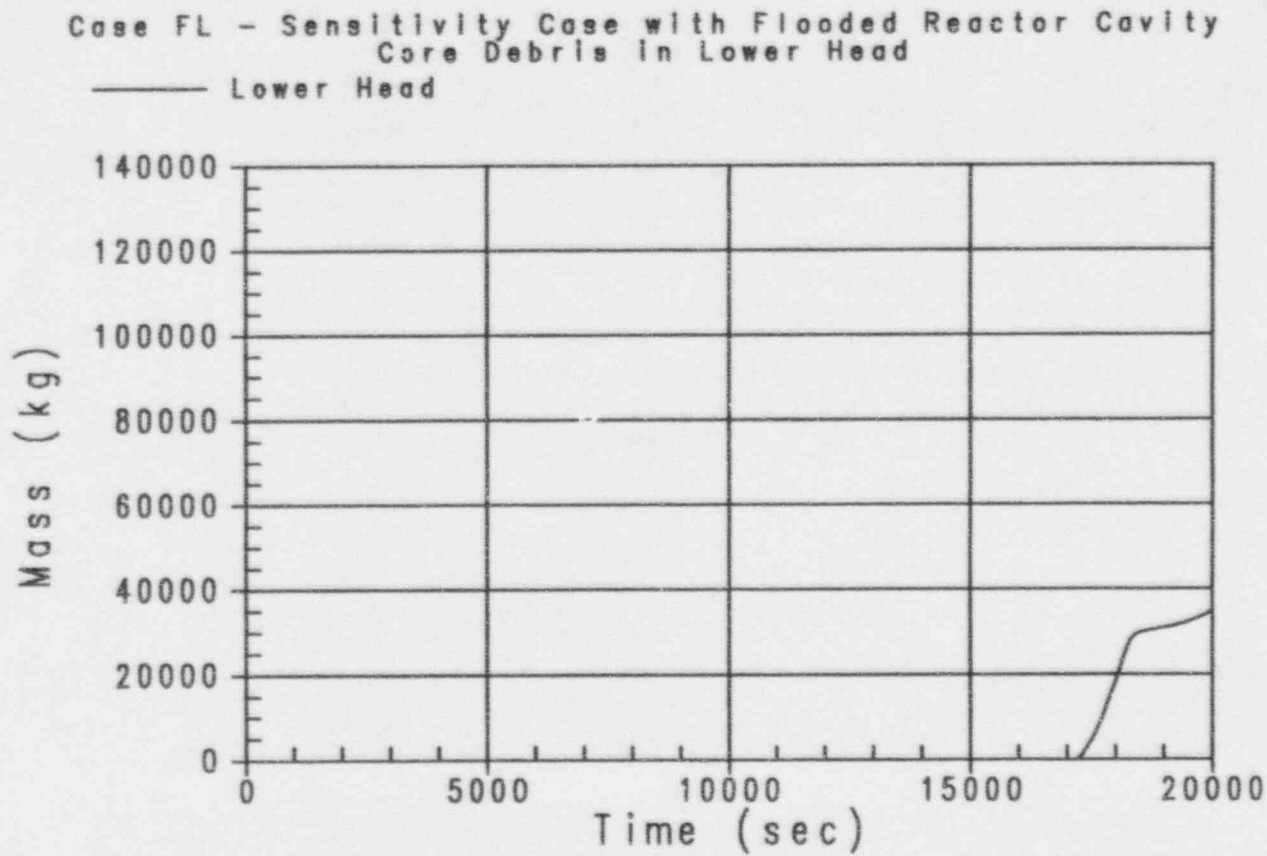


Figure 37-29

Case FL - Sensitivity Case with Flooded Reactor Cavity
Core Debris in Lower Head



Westinghouse

ENEL
ENEL NUCLEARE
PER LAVORAZIONE ELETTRICA

37-47

Revision: 3
February 28, 1995
u:\ap600\ptra\vec37.wpl:1b

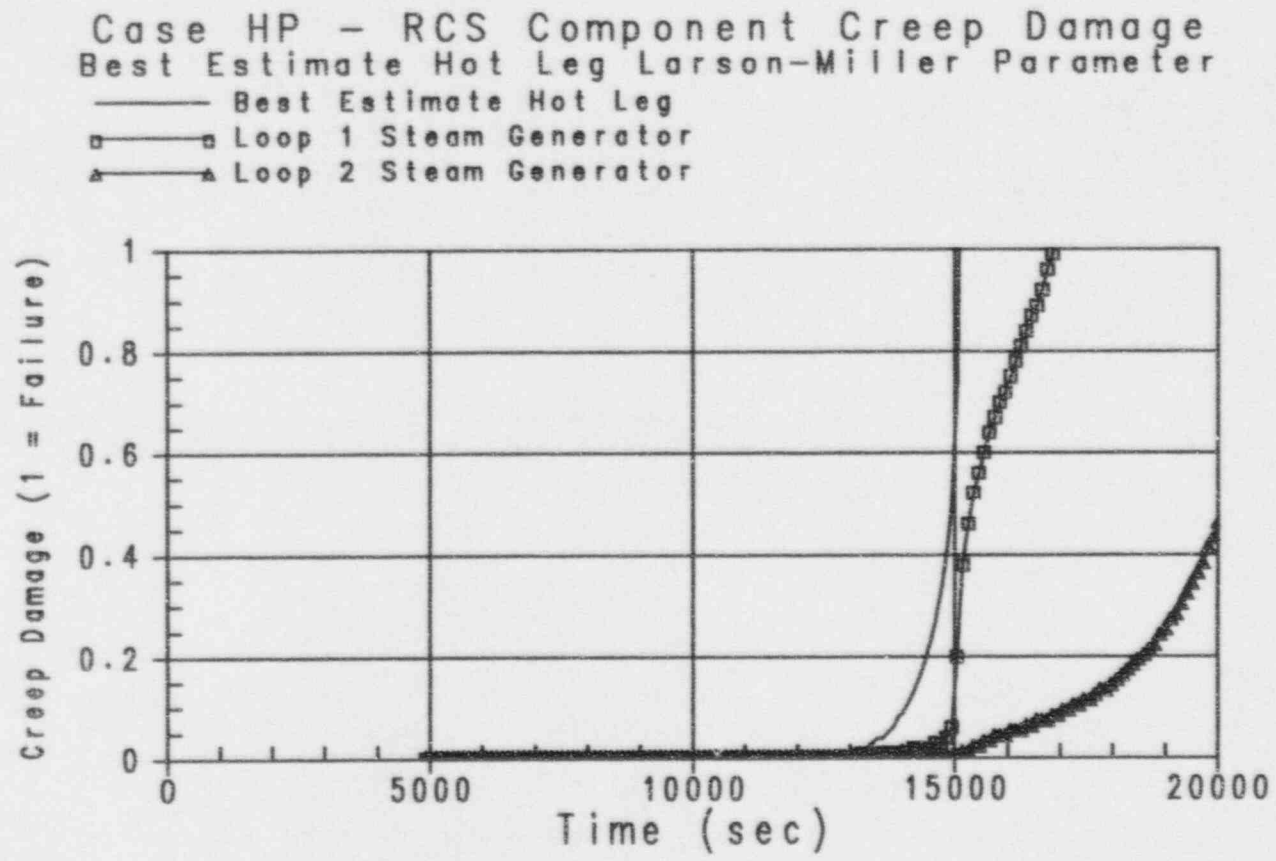


Figure 37-30

Case HP - Reactor Coolant System Component Creep Damage Best Estimate Hot Leg Larson-Miller Parameter

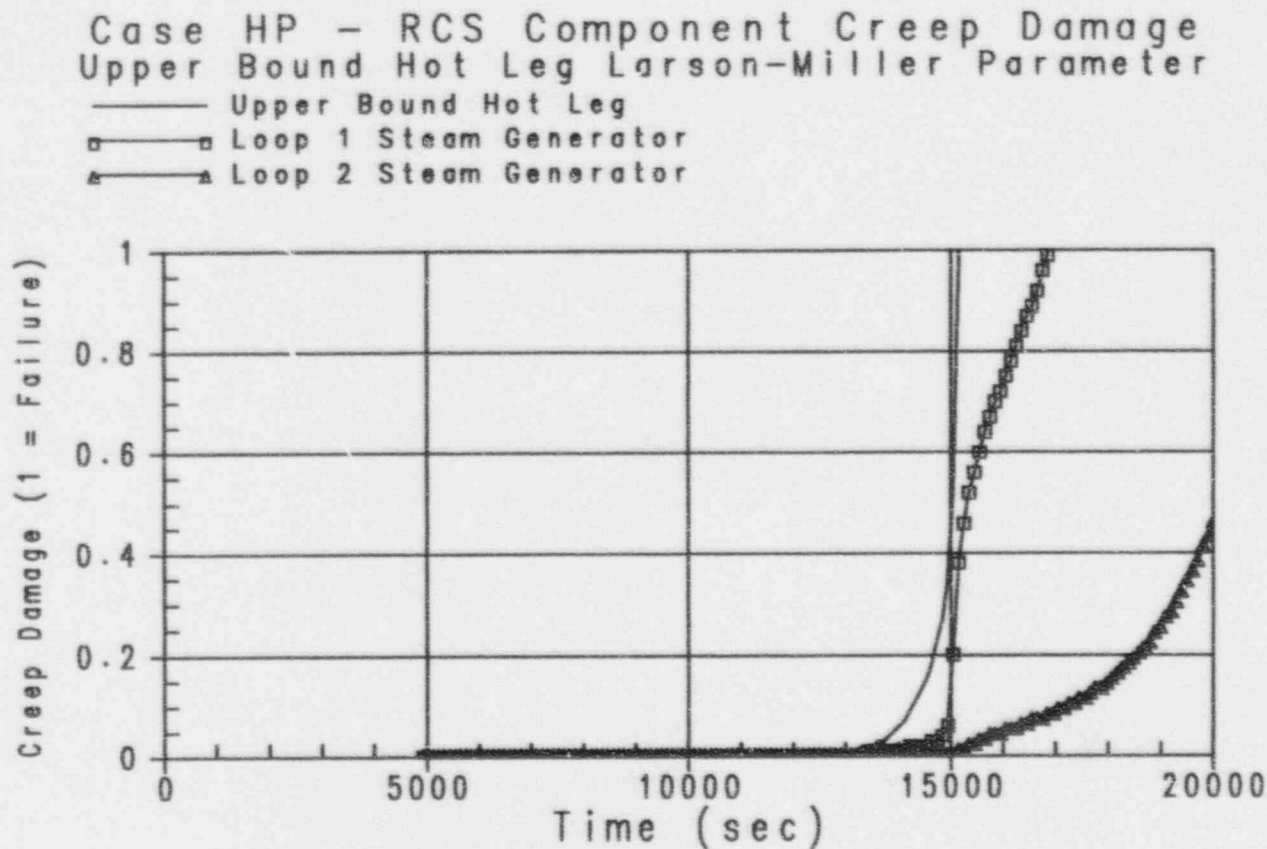


Figure 37-31

Case HP - Reactor Coolant System Component Creep
Damage Upper Bound Hot Leg Larson-Miller Parameter



Westinghouse

ENEL
ENEL NUCLEAR
FOR ENERGY ELECTRONICS

37-49

Revision: 3
February 28, 1995
u:\ap600\pva\sec37.mpf:1b

Case DP - RCS Component Creep Damage
Best Estimate Hot Leg Larson-Miller Parameter

- Best Estimate Hot Leg
- Loop 1 Steam Generator
- ▲ Loop 2 Steam Generator

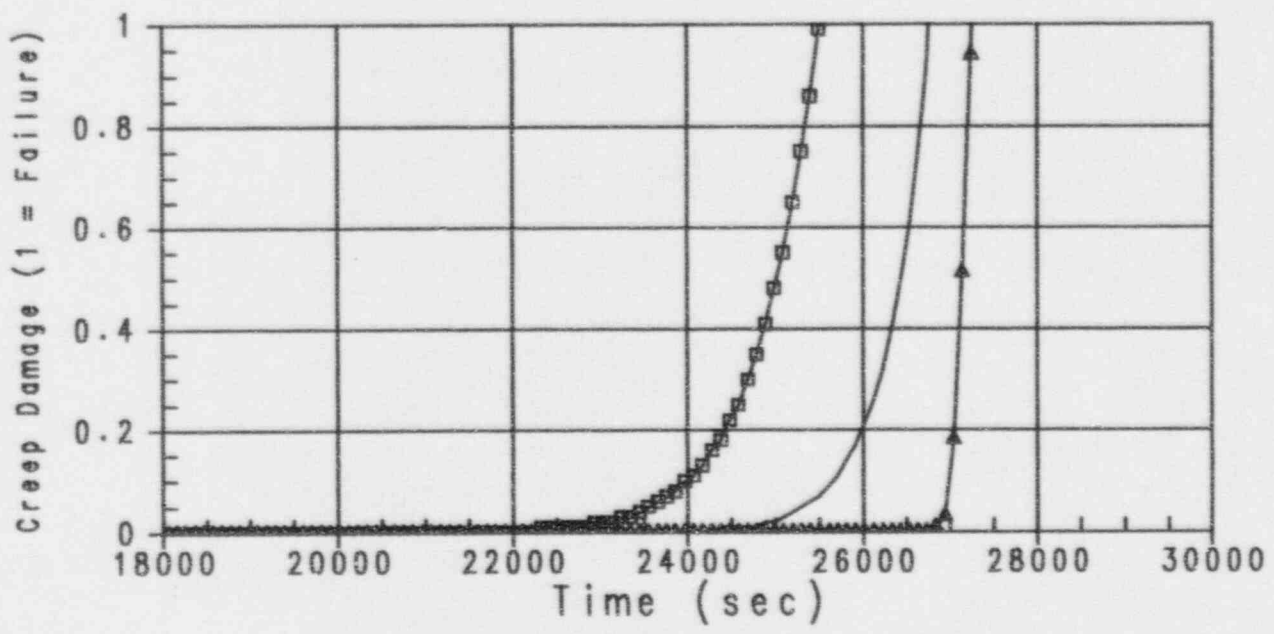


Figure 37-32

Case DP - Reactor Coolant System Component Creep Damage Best Estimate Hot Leg Larson-Miller Parameter

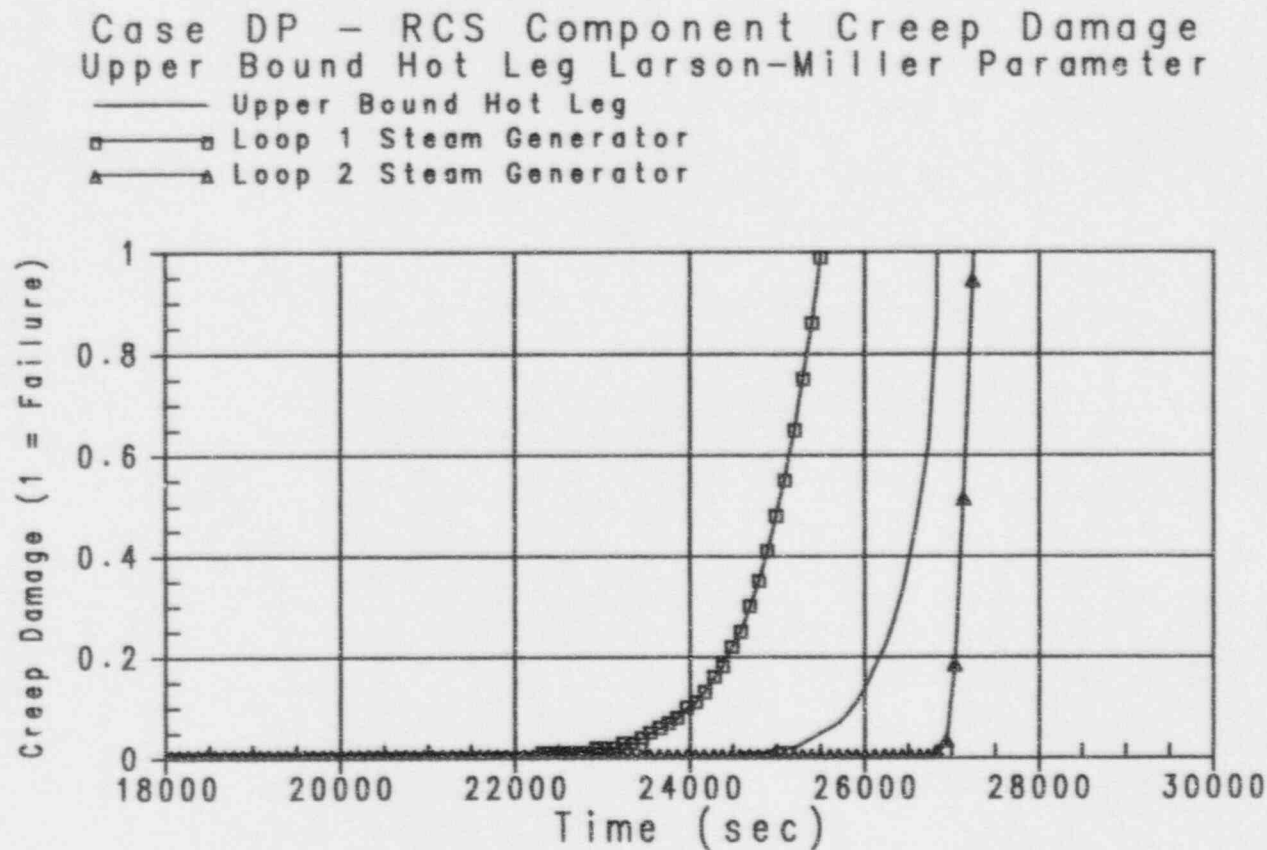


Figure 37-33

Case DP - Reactor Coolant System Component Creep
Damage Upper Bound Hot Leg Larson-Miller Parameter



Westinghouse

ENEL
ENEL NUCLEARE
PER L'ENERGIA ELETTRICA

37-51

Revision: 3
February 28, 1995
u:\ap600\yna\vec37.wpf:1b

Case NC - RCS Component Creep Damage Best Estimate Hot Leg Larson-Miller Parameter

— Best Estimate Hot Leg
 □ Loop 1 Steam Generator
 ▲ Loop 2 Steam Generator

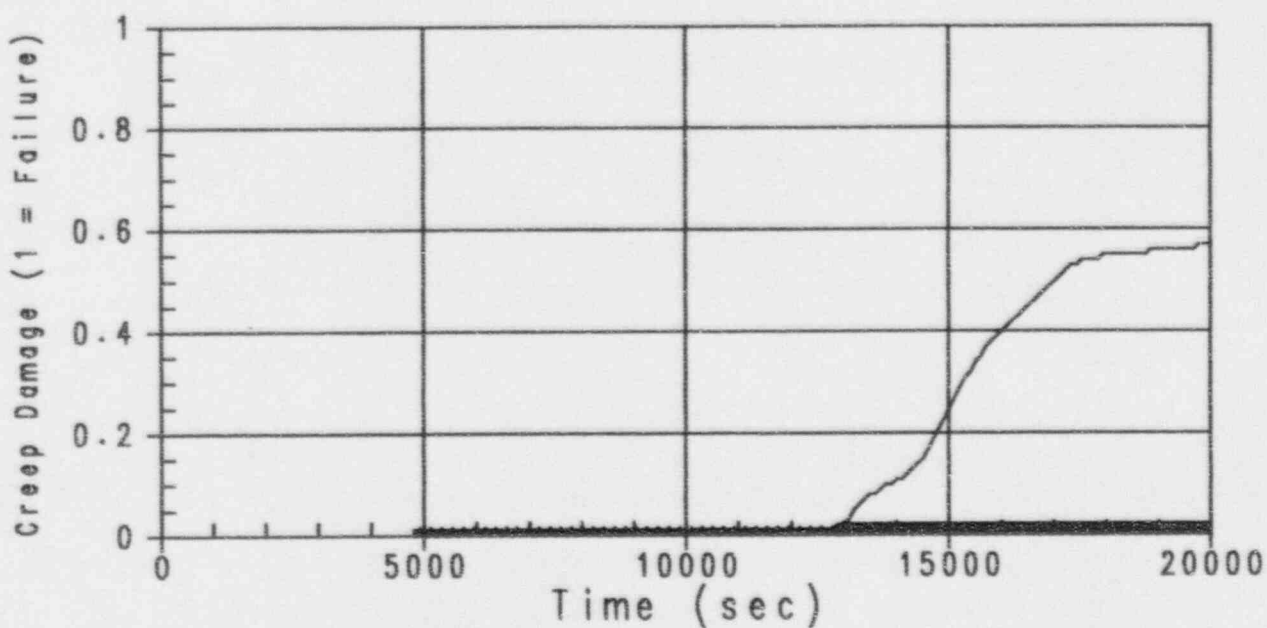


Figure 37-34

Case NC - Reactor Coolant System Component Creep
Damage Best Estimate Hot Leg Larson-Miller Parameter

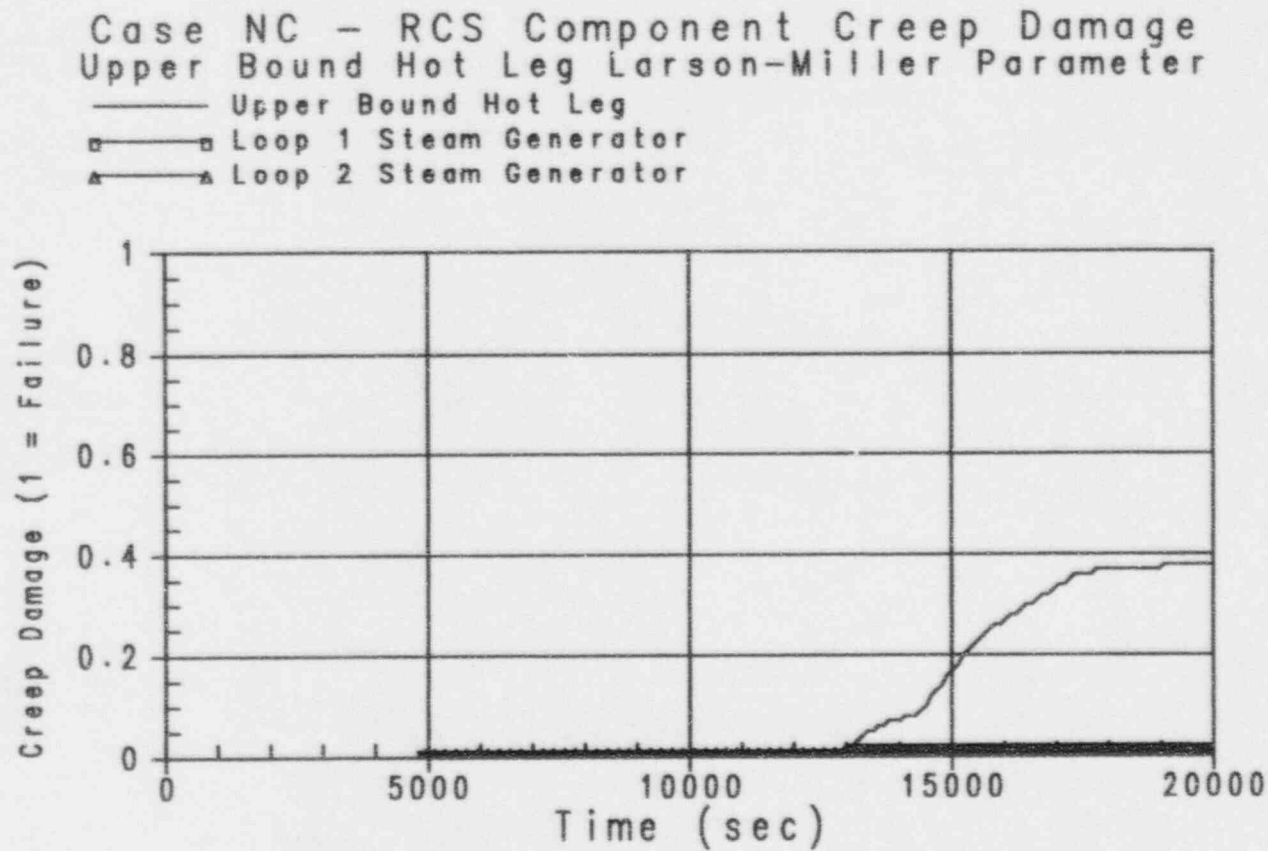


Figure 37-35

Case NC - Reactor Coolant System Component Creep
Damage Upper Bound Hot Leg Larson-Miller Parameter



Westinghouse

ENEL
FOR NUCLEAR ELECTRICITY

37-53

Revision: 3
February 28, 1995
u:\ap600\pna\sec37.wpf:1b

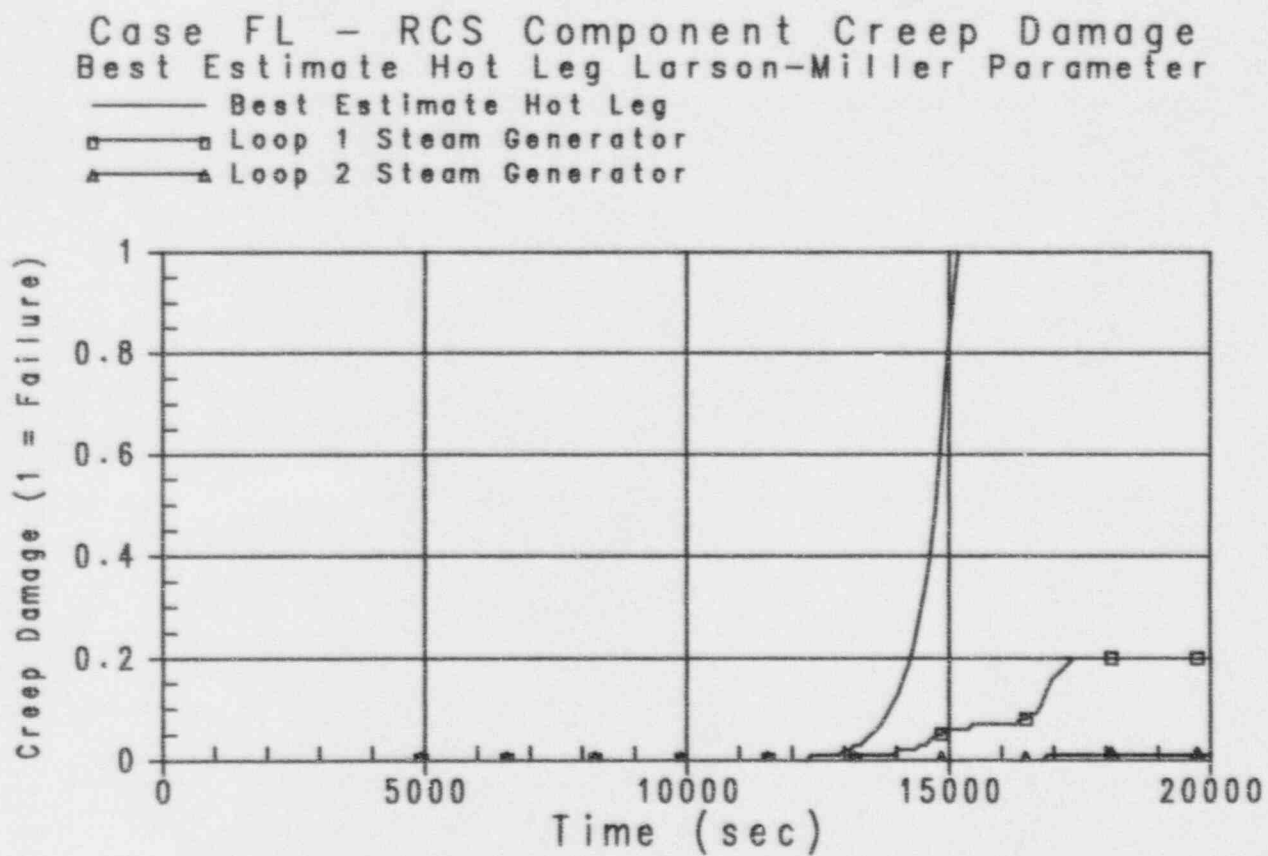


Figure 37-36

Case FL - Reactor Coolant System Component Creep
Damage Best Estimate Hot Leg Larson-Miller Parameter

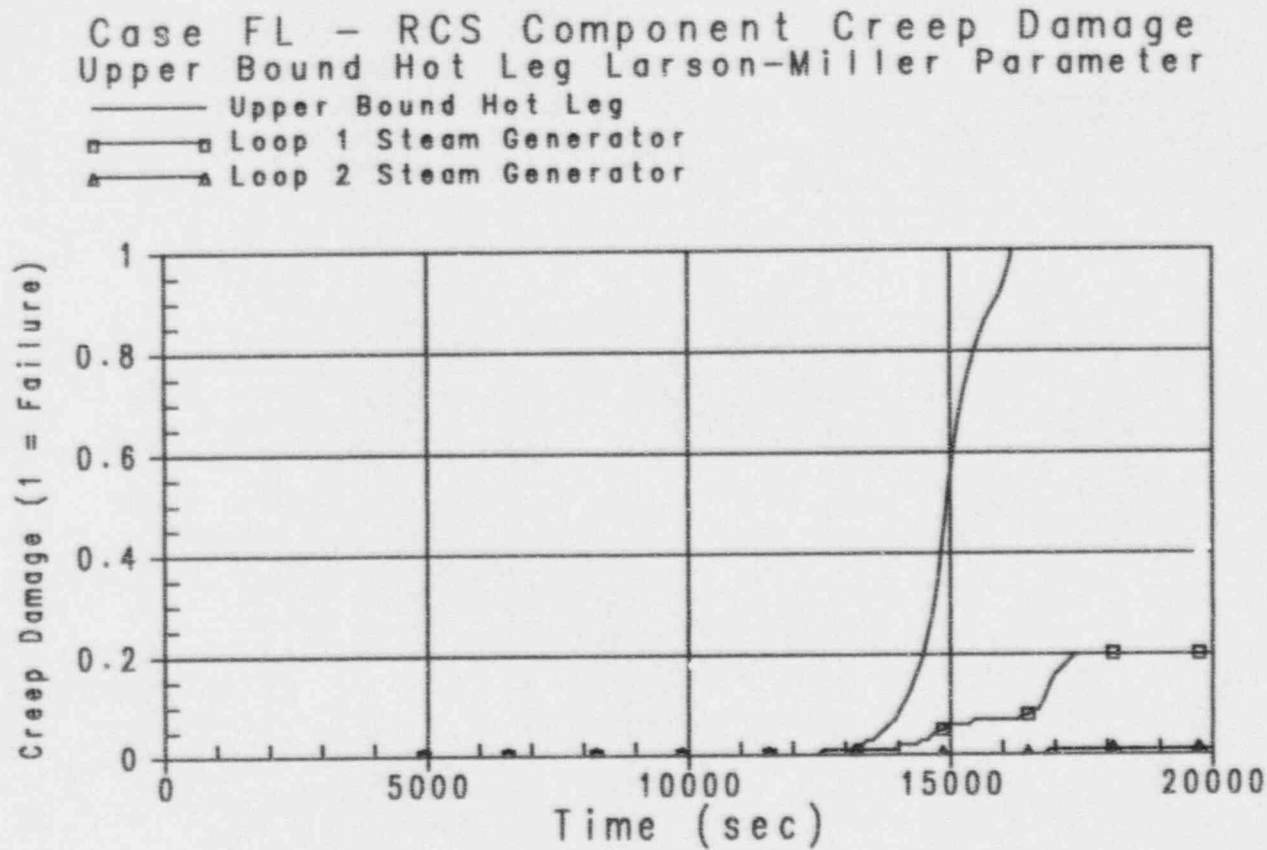


Figure 37-37

Case FL - Reactor Coolant System Component Creep Damage Upper Bound Hot Leg Larson-Miller Parameter



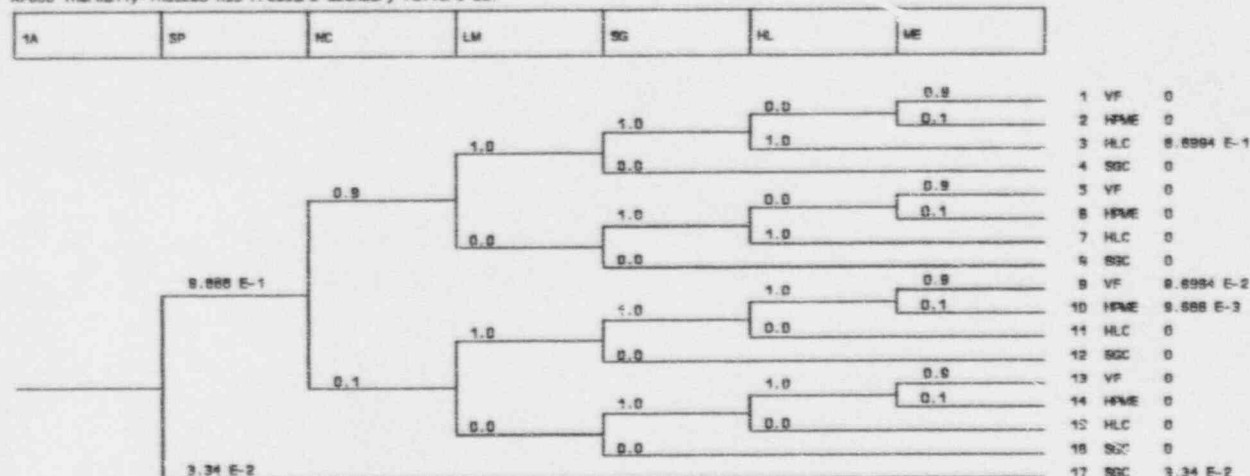
Westinghouse

ENEL
ENVI. NUCLEON. ELETTRICA

37-55

Revision: 3
February 28, 1995
u:\ap600\pna\sec37.wpf:1b

AP600 Thermally-Induced RCS Pressure Boundary Failure DET



AP600 Thermally-Induced RCS Pressure Boundary Failure DET
List of top events

Event	Description	END STATE	PROBABILITY
1A	Accident Class 1A	VF	8.6884 E-2
SP	Secondary Side Pressure	HLC	8.6884 E-1
NC	Natural Circulation of Hot Gas thru RCS	SGC	3.34 E-2
LM	Hot Leg Material Properties	HPME	8.688 E-3
SG	Steam Generator Tube Creep Rupture Failure		
HL	Hot Leg/Surge Line Creep Rupture Failure		
ME	Debris Ejected Prior to Blowdown		

Figure 37-38

AP600 Thermally Induced Reactor Coolant System Pressure Boundary Failure Decomposition Event Tree



CHAPTER 38

DECOMPOSITION EVENT TREE - ANALYSIS OF IN-VESSEL STEAM EXPLOSION

Thermally induced steam explosions within the reactor vessel (in-vessel steam explosions) have been postulated to occur in core damage severe accident sequences with low primary system pressure. The decomposition event tree quantifies the contribution to the overall likelihood of containment failure due to in-vessel steam explosions. Results of the quantification of the decomposition event tree provide input to nodes CF1 and SE on the AP600 containment event tree.

38.1 Discussion of the Issue

Vapor explosions must be considered any time two molten materials may come into contact and the temperature of one of the materials is far above that which would cause rapid vaporization of the second fluid. A steam explosion is a vapor explosion in which the rapidly vaporized fluid is water. Such phenomena must be considered in evaluations of accidents for water-cooled reactors where the core materials could become molten as a result of the accident condition.

This section decomposes the phenomenological chain of events that determine the condition for explosive interactions in-vessel, the energy release from such events, and the damage potential for the interactions once an explosion has occurred. These are represented as a series of events, hence, the designation of decomposition event tree. Of particular interest for reactor safety evaluations is the damage that could occur following an explosive event. Consequently, the decomposition event tree is structured toward an assessment of whether an in-vessel explosive interaction can:

- Be initiated
- Involve substantial material
- Propagate in a manner to release the energy stored in the high temperature molten material
- Transmit the energy release effectively to the reactor vessel wall with sufficient energy to cause failure of this boundary with consequential failure of the containment through ejection of the reactor vessel head as a missile with sufficient velocity to fail the containment wall on impact

38.2 Discussion of Controlling Phenomena and Uncertainties

Typically, steam explosions have been divided into four major phases. These are:

- Premixing
- Triggering (initiation)
- Propagation
- Expansion (sometimes called the energetics)

Figure 38-1 illustrates how these phases were considered in WASH-1400 (Reference 38-1). For the decomposition event tree associated with in-vessel explosions, the four phases form the foundation for the assessment. Additional events are considered to represent the likelihood that an explosion could occur, and also that a mechanism could be created whereby an energetic explosion could efficiently transfer energy to the reactor vessel and then to the containment boundary through ejection of a ruptured reactor vessel head as a missile with sufficient velocity to fail the containment wall on impact.

The major phenomenological questions are:

- Are the conditions consistent with those where steam explosions can occur?
- If an explosion can occur, how much core material could be coarsely mixed with water when the event would be initiated?
- If an explosion can occur, how much water mass would be available in the interaction zone (how much water could explode)?
- How efficient are interactions with large masses of materials?
- What is the likelihood of forming a continuous liquid "slug" over the top of the interaction zone?
- What is the likelihood that the energy impact of the slug would exceed the structural integrity of the reactor vessel upper head to the extent that the head would rupture and be ejected as a missile with sufficient velocity to fail the containment wall on impact?

Each of these is discussed in terms of conditions relevant to the specific question in the following sections.

38.2.1 Can an Explosion Occur?

Are the conditions consistent with those where explosions can occur?

The particular condition of interest is the reactor coolant system pressure when molten material comes into contact with the water. Numerous references have demonstrated that explosive interactions are suppressed by elevated system pressures. These include experiments

with molten sodium chloride in water (References 38-2 and 38-3), Freon-22 in mineral oil (References 38-4 and 38-5), molten core debris in water (Reference 38-6), iron thermite in water (Reference 38-7) as well as limited scale experiments on individual phenomena such as those by Henry and Miyazaki (Reference 38-8) and Avedisian (Reference 38-9). These experimental studies clearly show that pressures in the range of 5 percent of the critical pressure are sufficient to preclude explosive interactions in the absence of an energetic trigger contained in the experiment. This is best illustrated by the extent of experimental information shown in Table 38-1, which summarizes the results of 17 years of experimental work by different investigators and illustrates that the reduced pressure (the ratio of the system pressure to the thermodynamic critical pressure of the exploding fluid) is less than 0.05 for all systems without an external trigger added to the system. Since large explosive triggers would be absent in an accident situation, the occurrence of a steam explosion can be considered to be of negligible likelihood for conditions where the reactor coolant system is pressurized above this level, which corresponds to 1 MPa (145 psia). It is noted here that this behavior is consistent with the Three Mile Island Unit 2 accident where molten material drained into the water filled reactor vessel lower plenum when the pressure was ~10 MPa (1450 psia) and there was no indication of an explosive interaction.

Therefore, on a sequence-specific basis, the conditions for an initiating explosive interaction is considered as the first fundamental question in the in-vessel steam explosion decomposition event tree.

38.2.2 How Much Core Material Would Be Involved?

If a steam explosion could occur, how much core material would be available to coarsely mix with water when the event is triggered?

Of particular interest in this question is how much of the molten material could be in a particulated form within the reactor vessel lower plenum. This is represented by the material which would be in the process of draining from an in-core location into the lower head, but would not include material that would be accumulated on the lower head as a stratified continuous layer of debris. Hence, the focus in these calculations is the extent of material that would be molten, particulated, and in the process of settling in the lower head.

In the source term analysis of the AP600 PRA, the debris mass which that to the reactor vessel lower head is 1.3E5 kg in the worst two cases (Figures 38-28 and 38-131), about 40,000 kg slumps instantaneously at any one time. However, considerations of particulation (which provides a significant limitation) must be taken into account to determine if there is enough core material within the reactor vessel lower plenum to potentially fail the vessel through a steam explosion in the case of a core damage sequence.

The Steam Explosion Review Group (SERG) (Reference 38-13) concluded that the occurrence of a steam explosion of sufficient energetics that could lead to alpha-mode reactor vessel failure has a low probability given a core melt accident. Relevant new experimental and theoretical information presented at a Committee on the Safety of Nuclear Installations Fuel



Coolant Interactions Specialist meeting held at the University of California in Santa Barbara, California, on January 5-8, 1993 provided further confirmatory support for this conclusion.

A central feature of the quantitative responses in the SERG assessment was a mechanistic treatment of various stages of the steam explosion sequence, with emphasis on estimation of the mass of melt participating in the explosion. It follows that the low probability of early containment failure suggested by the SERG stems largely from the belief that the fuel mass participating in a potential steam explosion in the reactor vessel lower plenum following fuel relocation from the core region is quite limited.

The limited potential for premixing of fuel and water prior to triggering and propagation was first outlined by Henry and Fauske (Reference 38-15). The need for the premixing step in order to produce an energetic large-scale steam explosion is clearly demonstrated by the limited mixing observed in triggered experiments with an initially stratified flow regime. As illustrated by previous studies as well as papers presented at the CSNI-FCI specialist meeting, the resulting mixing depth in the molten layer following triggered vapor collapse is limited to less than 1 centimeter (Reference 38-14). Quasi-steady one-dimensional analyses accounting for radiative and convective heat transfer from capillary size fuel particles suggested sufficient steam generation rates to "flood" or deplete the water and, therefore, limiting a potentially explosive premixture to a few hundred kilograms.

Subsequently, more detailed calculations related to the water depletion phenomenon have been performed and reported in the open literature and the latest results were reported at the CSNI-FCI specialist meeting (References 38-16, 38-17, 38-18, 38-19, and 38-20).

The most advanced calculations (three fluid formulation) as well as hot particle experiments were presented by Theofanous (Reference 38-16), demonstrating excellent agreement between measured and calculated void distributions. Utilizing a water depletion criterion corresponding to a void fraction of 0.7 along with a fuel pour area or core support failure area of 2 m² (fuel pour diameter about 1.6 meters) and a fuel particle size of 2 centimeters, Theofanous' calculations suggest a peak premixing value of about 1.5 tonnes at atmospheric pressure condition. This value is a factor of about three lower than earlier calculations (two fluid formulation) (Reference 38-21).

A related issue is the fuel particle size to be used in the premixing calculations. Relevant quenching experiments (Reference 38-6) suggest that the capillary size, $d \sim (\sigma/g\rho)^{1/2}$, is a good representation of the average measured particle size for the fraction of corium jet experiencing breakup. Since radiative heat transfer would appear of prime importance (as clearly illustrated by Theofanous' comparison between the CHYMES and PM-ALPHA calculations), to a first order the premixing fuel mass would be proportional to the assumed premixture fuel dimension. Theofanous' calculation of 1.5 tonnes based on a 2-centimeter fuel particle is reduced to about 300 kg when the capillary size of 0.4 centimeter is used, even when a very large fuel pour diameter of 1.6 meters is assumed.

Furthermore, as indicated by Turland and Fletcher (Reference 38-22), Theofanous' example, utilizing a pour diameter of 1.6 meters, can be considered an outlier. A more reasonable fuel

pour diameter would be of the order of 0.1 meter, as suggested by the Three Mile Island Unit 2 fuel relocation process (Reference 38-23). As such, consideration of hydrodynamic breakup in the absence of thermal considerations leads to a fuel premixture of a few hundred kilograms.

In summary, excellent progress has been made toward improving the quantification, as well as experimental confirmation, of the water depletion phenomenon in limiting the fuel mass in the premixing stage of an energetic steam explosion. For pour diameters of the order of 0.1 meter, the premixing would be largely independent of pressure. This is consistent with the Three Mile Island Unit 2 estimate of a few hundred kilograms at a pressure of about 7 MPa (Reference 38-23).

38.2.3 How Much Water Would Be Involved?

If an explosion can occur, how much water mass would be available in the interaction zone?

Water is always available in the lower plenum when the core debris slumps into it. From the source term analysis, the water mass available in the lower plenum when the core slumps is about 30,000 kg. However, considerations of interaction zone, as discussed in subsection 38.2.2, show that a void fraction of 50 to 70 percent would be expected to enable water and molten core debris to mix. Therefore, considering an interaction zone of about 1 meter in diameter and 2 meters deep with a void fraction of 50 percent (and discounting the core debris) results in a water mass of approximately 3000 kg. Thus, only a fraction of the water in the lower plenum would participate in the interaction.

38.2.4 What Is Efficiency of Interaction?

How efficient are interactions with large masses of materials?

Explosion efficiency is defined as the fraction of stored thermal energy in the melt material which is converted to explosion mechanical energy. Large scale steam explosion efficiency experiments have been carried out at Sandia Laboratories in two different test series, one using an iron thermite mixture (Reference 38-24) to simulate the degraded core material and the other incorporating both an iron-thermite and a corium-thermite (Reference 38-25) which had a higher melting temperature and was a more realistic simulant of the anticipated debris character.

In the first set of experiments (Reference 38-24), the iron thermite melt had a temperature of about 3000 K as it left the melt generator and was discharged directly into a 0.9 meter diameter vessel filled with water. For all those experiments carried out with an artificial trigger, the water was at the ambient temperature, assumed to be 295 K. The reported conditions for the various experiments of interest are listed in Table 38-2 for the melt quantity, the water temperature, the time to explosion, and the reported explosion efficiency (as compared to the stored energy in the melt material). Given the mass of material discharged into the test vessel, the water temperature, and the melt temperature, the pre-



explosion fragmentation sizes can be evaluated from the film boiling fragmentation model. (In these experiments the ambient pressure was always slightly less than 0.1 MPa.) The melt temperature resulting from the thermite reaction is about 3000 K and results in reaction products of metallic iron (Fe) and aluminum trioxide (Al_2O_3). The melting temperature for the aluminum trioxide is about 2300 K and 1800 K for metallic iron. Consequently, solidification of either of these constituents requires a substantial decrease in temperature and the resulting fragmentation process could continue as the melt cools, i.e., lower temperatures reduce the film boiling steam generation rate and allow finer particulation. The various levels predicted for melt temperatures of 3000 K and 1800 K are illustrated in Table 38-2, and as shown, the lower temperature predicts a radius 1/5 of that typical of the higher temperature fragmentation condition. These calculated values bracket the coarse prefragmentation states which could be rapidly dispersed on an explosive time scale by the mixing energy from the explosive detonator. However, the salient point displayed in the table is not the explosive detonator. The most important point shown in the table is that the combination of (the magnitude of the melt, the subcooled water temperature, and the large vessel cross-sectional area allows significant coarse prefragmentation of the melt prior to the onset of an explosive interaction. The largest fragmentation sizes prior to the explosion are 1.6 centimeters in diameter (in close agreement with the pre-explosion sizes reported for the Sandia experimenters in other publications) (Reference 38-26). These sizes were deduced from movies taken in similar-sized vessels with transparent viewing ports.

To externally trigger an explosive interaction, a 0.64 gram charge of high explosives was used. Assuming this detonator to be PETN or an equivalent material, the explosive reaction products are essentially all gaseous and the work delivered to the corium-water mixture by the detonator can be equated to the heat of explosion. For PETN this is about 5800 J/gm of material. This can be treated as the energy available to intermix materials prior to the explosive energy transfer. To achieve such intermixing on an explosive time scale, it is assumed that it occurs within a 1 ms interval with a final particle size sufficiently small to enable an efficient thermal energy transfer, i.e., about 500 μm in diameter. This particle size range is also in general agreement with the post-explosion particle sizes found in these experiments.

A second test series was performed at Sandia with a different test vessel (1.2 meters internal diameter) and molten material generated from both iron-aluminum oxide thermite and a corium-A+R thermite. This latter reaction had products of uranium dioxide, zirconium dioxide, nickel oxide, stainless steel, and molybdenum. The minimum liquidus temperature for this mixture is reported to be 2770 K, which is considerably greater than the 2300 K temperature for aluminum oxide. Boiling steel limited the maximum temperature for the corium reaction to 3070 K.

In this second test series, external triggering was also induced by explosive detonators, but two different sizes were used. One was the same as that employed in the first iron-thermite test (0.64 gram of PETN), and the other was a detonator plus a lead-covered explosive core 0.76 meter in length, containing 6 grams of PETN. This second method represented a much more energetic trigger than that used in the thermite tests. In fact, the pulse duration for the corium A+R event in run 59, which used this larger trigger, was not much different than that

represented by the trigger alone. Also the measured work (about 30 kJ) was less than the work released by the high explosive (about 35 kJ).

Table 38-3 lists the experimental conditions and observations for the tests in which molten material was successfully discharged into the interaction vessel. As illustrated, explosions were observed with the iron thermite as initiated by both spontaneous and artificial triggers. However, with the corium A+R melt, only one mild explosion was reported, and this was triggered by the 6 gram PETN external trigger.

From these results, then, it can be concluded that the efficiency of interactions involving degraded core material and water is less than about 0.5 percent, even with artificial triggers.

38.2.5 What Is the Likelihood of Forming Slug?

What is the likelihood of forming a continuous liquid "slug" over the top of the interaction zone?

Turland et al, in their assessment of the probability of containment failure due to in-vessel steam explosions for the Sizewell B PWR (Reference 38-22), had difficulty in identifying a continuous liquid slug tamping an in-vessel steam explosion. Calculations indicate that there is much steam in the region above the explosive mixture. There may be relatively intact fuel assemblies at the periphery of the core. The downcomer is expected to contain highly voided water. In addition, the core debris is unlikely to be a single liquid, but could contain substantial solid remains (remains of the lower crust, upper and lower fuel pins). Although Turland et al (Reference 38-22) have developed a concept of leakage to study this question, they have been unable to quantify whether a coherent slug forms.

The energy required to crush and fail structures on the path to the upper head, the remains of the core itself, the core support plate, the upper core tie plate, the upper core plate, and the upper plenum structures will further impact slug energy and the continuity of the slug (References 38-21 and 38-22), although, if it does stay together as a continuous slug, it will now include the remains of the internals as a single upwardly moving mass.

These considerations make formation of a continuous overlying slug unrealistic.

38.2.6 What Is the Likelihood of Vessel Failure with Consequential Containment Failure?

What is the likelihood that the energy impact of the slug would exceed the structural integrity of the reactor vessel upper head to the extent that the head would rupture and be ejected as a missile with sufficient velocity to fail the containment wall on impact?

38.2.6.1 Vessel Energy Absorption Capability

For the postulated energetic thermal interactions considered in WASH-1400 (Reference 38-1), the primary coolant system could be breached at some point. The required conditions in the calculational model included a strong fluid-structural coupling between the energy source and the reactor vessel walls. This coupling resulted from the vessel being either fully or partially filled with water such that a coherent water slug can be driven against the upper vessel head (such as a mechanism like that created in the SL-1 accident). The ability of the pressure boundary to absorb the energy generated will depend on many factors, including the magnitude and time scale of the energy release; the amount of fluid-structure coupling present; the directionality, if any, of the event; the presence of in-vessel structures that can both absorb energy and disrupt a coherent slug; and the material properties and condition of the vessel and bolts at the time of the event.

The determination of the energy absorption capabilities of nuclear reactor vessel components has been the subject of numerous experimental programs and analytical studies for over 15 years. These include the early experimental work of Proctor and Wise (References 38-27 and 38-28) and the more sophisticated computer techniques developed at Argonne National Laboratory (References 38-29 and 38-30) and Sandia (Reference 38-31). An analysis of the energy absorption capability for the Zion and Indian Point reactor vessels in response to in-vessel steam explosions was performed (References 38-32 and 38-33) by Sandia and Los Alamos. These results were then extended by Carlsson (Reference 38-34) to Swedish pressurized water reactors (PWR) and boiling water reactors (BWR) using scaling laws to account for a range of vessel diameters, thickness, and boiling systems.

The Sandia estimate of the work potential possible from an in-vessel steam explosion, given an assumed intimate dispersion of corium and water, ranged from 300 MJ to 3000 MJ. The force from the steam explosion was assumed to accelerate a water slug to a velocity corresponding to an energy of the same magnitude. Slug impact then caused vessel head deformation along with stud elongation and upper vessel deformation, which was evaluated using the HONDO II code. It was estimated that structural failure would probably occur at the top of the head (where maximum strains occur) for slug energies in 300 MJ to 1200 MJ range while a 3000 MJ slug would fail the head and possibly the studs. Although this study was interesting in the sense that failure was related to slug and steam explosion work energy, it was based on vague assumptions concerning slug mass. This parameter is important in assessing the response of the vessel. (For example, doubling the slug mass would cause the impact pressure to drop to only 70 percent of its initial value.) Further, no estimates were given for the partitioning of the slug energy between the vessel head, studs, and upper vessel. Nor was there an estimate of the maximum strain energy absorbed in the various components, (such as, head, bolts, vessels) at the time of failure.

The energy-absorbing capability of the various vessel components can be related to the volume of material. With this in mind, Carlsson (Reference 38-34) estimated the slug impact energies required to fail various Swedish pressurized water reactors and boiling water reactors vessels – or at least give the same amount of deformation as calculated by LASL and Sandia

in References 38-32 and 38-33. Again, this analysis is predicated on a given slug mass, shape, and energy (1200 MJ), and assumes there is a linear relationship between slug energy and energy absorbed in the structure.

Perhaps a better approach to estimating vessel energy absorption capability would be to use the experience gained in evaluating the response of liquid metal fast breeder reactor (LMFBR) containment vessels (References 38-35, 38-36, and 38-37). These analyses were essentially based on similar hypothetical energy source terms (molten fuel coolant interactions) under the "ideal" conditions which provided for good coolant-structure coupling and a mass of coolant above the core which would act as a slug. It should be pointed out, however, that there are also dissimilarities. For example, the L/D rate for LMFBR vessels is somewhat smaller than those of LWRs and the vessel top heads are flat rather than hemispherical. Also, the vessel heads are generally more massive and stiffer than in LMFBRs which have a tendency to cause more deformation of the upper vessel walls. However, based on the calculated response for a LMFBR vessel under postulated explosive interactions, it can be expected that an assumed large scale FCI in the core region would initially deform the vessel horizontally while the slug would deform the upper vessel and head as shown schematically in Figure 38-2. The vessel wall deformations are roughly sinusoidal along the length of the vessel while the head can be expected to deform in a manner similar to that calculated by Sandia (Reference 38-32). Thus, it is possible to give a rough estimate of the energy absorption capability of LWR reactor vessels.

38.2.6.2 Energy Yield of In-Vessel Steam Explosion

Theofanous et al. (Reference 38-16), in a continuation of the calculations that led to the fuel premix of 1.5 tonnes (see subsection 38.2.2), attempted to quantify the threat to the vessel. Even with a conservatively bounding explosion efficiency of 20 percent, the 1.5-tonne premixture led to a mechanical energy release value much too small to threaten the upper head. It is concluded there that accumulating enough fuel mass for an energy yield to threaten the upper head cannot be anticipated to be physically possible under any circumstances relevant to reactor conditions.

38.2.6.3 Containment Failure

For the purposes of the analysis, it is assumed as a conservatism that, if the energy impact of the slug exceeds the structural integrity of the reactor vessel upper head, containment failure results due to impact of the reactor vessel upper head as a missile on the containment wall.

38.3 Development of the Decomposition Event Tree

The decomposition event tree structure developed for quantifying the contribution of this decomposition event tree to the probability of containment failure is presented in Figure 38-3. The questions posed at each node on the tree examine and quantify the phenomenological questions and uncertainties identified in the analysis presented in the previous sections. The

upward path at each node indicates a positive response to the question; the downward path indicates a negative response. The nodes chosen for the decomposition event tree are:

- Node RP - Is the initial system pressure elevated above the level where initiation of steam explosions is prevented?
- Node FR - Is there less molten core material being coarsely mixed in the water in the lower plenum than is needed to provide the energy release required to rupture the reactor vessel?
- Node WA - Is insufficient water mass available in the interaction zone in the lower plenum to create an explosion of enough magnitude to rupture the reactor vessel?
- Node MX - Is the efficiency of the interaction less than required to cause an explosion of enough magnitude to rupture the reactor vessel?
- Node SX - Is there either no long, coherent, continuous water slug overlying the reaction zone or insufficient energy transfer from the steam explosion delivered to the slug to transmit the energy from the expansion of the steam in a coherent fashion?
- Node VF - Does the liquid slug fail to impact the reactor vessel upper head with sufficient energy to fail the reactor vessel?

The end-states of the tree represent the state of the containment due to postulated in-vessel steam explosions.

- SC - Success; both the vessel and the containment remain intact
- CF - Containment failure

38.4 Quantification of the Decomposition Event Tree

This section discusses the assignment of the split fractions at each of the nodes on the decomposition event tree. Multiplication of the split fractions along a path of the tree results in the probability of the accident following that particular path. The summation of the probabilities of the paths that result in a particular end-state is the probability of that end-state.

38.4.1 Node RP

Is the initial system pressure elevated above the level where initiation of steam explosions is prevented?

Success Criteria:

Per subsection 38.2.1, the occurrence of a steam explosion is of negligible likelihood for conditions where the reactor coolant system is pressurized above 0.5 MPa.

In the PRA analysis for all core damage sequences, drainage of the molten core material into the lower plenum essentially always occurs at low reactor system pressure.

Probability of initial system pressure below 0.5 MPa (failure of node) = 1.0

Downstream Considerations:

Success of Node RP leads directly to end-state SC. If initial system pressure is below 0.5 MPa, in-vessel steam explosions can potentially occur. This potential is examined further in subsequent nodes of this decomposition event tree.

38.4.2 Node FR

Is there less molten core material being coarsely mixed in the water in the lower plenum than is needed to provide the energy release required to rupture the reactor vessel?

Success Criteria:

Less mass of corium than that needed to threaten reactor vessel integrity must be premixed in the water in the lower plenum.

Per subsection 38.2.2, the maximum mass of molten debris that could be particulated and mixed is about 1000 kg. This is far less than the quantity necessary to challenge the reactor vessel. Since vessel failure is then considered to be unrealistic, the likelihood of having a sufficient molten mass coarsely mixed will be set at 10^{-3} . This value was used to characterize those postulated behaviors which are found to be unrealistic in the ROAAM process applied to the Mark I liner melt-through (Reference 38-38).

Probability of enough core material being coarsely mixed (failure of node) = 0.001

Downstream Considerations:

Success of node FR leads directly to end-state SC. If there is enough molten core material draining into the lower plenum to challenge the reactor vessel, the potential exists for the debris to actually rupture the vessel and fail containment through an in-vessel steam explosion. This potential is examined further in subsequent nodes of this decomposition event tree.

38.4.3 Node WA

Is insufficient water mass available in the interaction zone in the lower plenum to create an explosion of enough magnitude to rupture the reactor vessel?

Success Criteria:

Less than 1000 kg premixed in the interaction zone.

Per subsection 38.2.3, sufficient water mass is always available in the lower plenum when the core debris drains into it.

Probability of sufficient water mass being available (failure of node) = 1.0

Downstream Considerations:

Success of node WA leads directly to end-state SC. If the debris drains into a sufficient pool of water, the potential exists for an in-vessel steam explosion of enough magnitude to rupture the reactor vessel. This potential is examined further in subsequent nodes of this decomposition event tree.

38.4.4 Node MX

Is the efficiency of the interaction less than required to cause an explosion of enough magnitude to rupture the reactor vessel?

Success Criteria:

Efficiency of interaction less than required.

Per discussion of this issue in subsection 38.2.4, an interaction with an efficiency which would challenge the vessel is unrealistic, so, like node FR, the likelihood will be set to 0.001.

Probability of interaction with more than required efficiency = 0.001

Downstream Considerations:

Success of node MX leads directly to end-state SC. If the efficiency of the interaction is large enough, the potential exists for an explosion of enough magnitude to rupture the reactor vessel. This potential is examined further in subsequent nodes of this decomposition event tree.

38.4.5 Node SX

Is there either no long, coherent, continuous water slug overlying the reaction zone or insufficient energy transfer from the steam explosion delivered to the slug to transmit the energy from the expansion of the steam in a coherent fashion?

Success Criteria:

No water slug or insufficient coherent energy transmission.

Per discussion of this issue in subsection 38.2.5, formation of a continuous overlying slug is unrealistic, so, here again, the likelihood will be set to 0.001.

Probability of coherent transmission of energy to liquid slug = 0.001

Downstream Considerations:

Success of node SX leads directly to end-state SC. If energy can be transmitted to a water slug in a coherent fashion, the potential exists that the slug can impact the reactor vessel head with sufficient energy to rupture the head. This potential is examined further in a subsequent node of this decomposition event tree.

38.4.6 Node VF

Does the liquid slug fail to impact the reactor vessel upper head with sufficient energy to fail the reactor vessel?

Success Criteria:

The liquid slug breaks up and dissipates in the upper plenum and fails to impact the reactor vessel upper head with sufficient energy to fail the reactor vessel.

Per discussion in subsections 38.2.6, 38.2.2, and 38.4.2, the failure of the reactor vessel with consequential failure of the containment due to impact of a liquid slug formed by an in-vessel steam explosion is unrealistic, so, as before, the likelihood will be set to 0.001.

Probability of slug impacting head = 0.001

Downstream Considerations:

Success of node VF leads to end-state SC. As previously discussed, failure of the reactor vessel is assumed to lead to containment failure through the impact of the reactor vessel upper head as a missile on the containment wall. Therefore, failure at node VF leads directly to end-state CF.

38.5 Results

The decomposition event tree is quantified using the split fractions outlined above (Figure 38-4). Given a core damage severe accident, the conditional probability of containment failure due to in-vessel steam explosions is an extremely small number. This is due to the fact that several elements in the chain of events are found to be physically unrealizable. This number is so small that it loses physical meaning. Hence, it is suggested that ϵ be used in the event tree instead of the number. An alternate means of showing this is to show less than 10^{-6} . This is how the conditional probability is used in the split fraction for containment event tree nodes CF1 and SE.



38.6 References

- 38-1 *Reactor Safety Study*, WASH-1400, NUREG/75-0114, 1975.
- 38-2 Hohmann, H., et al., "The Effect of Pressure on NaCl-H₂O Explosions", 4th CSNI Specialists Meeting on Fuel-Coolant Interactions and Nuclear Reactor Safety, Bournemouth, U.K., CSNI Report No. 37, pp. 308-323, 1979.
- 38-3 Hohmann, H., et al., "Experimental Investigations of Spontaneous and Triggered Vapour Explosions in the Molten Salt/Water Systems," Paper presented at the ANS/ENS Topical Meeting on Thermal Reactor Safety, Chicago, IL, 1982.
- 38-4 Henry, R. E. and McUmbler, L. M., "Vapor Explosion Experiments With an External Trigger," 2nd CSNI Experts Meeting on the Science of Vapor Explosions, Grenoble, France, 1978.
- 38-5 Henry, R. E. and Fauske, H. K., "Nucleation Processes in Large-Scale Vapor Explosions," *ASME Journal of Heat Transfer*, Vol. 101, p. 280, 1979.
- 38-6 Magallon, D. and Hohmann, H., "High Pressure Corium Melt Quenching Tests in FARO," CSNI-FCI Specialists Meeting, Santa Barbara, CA, 1993.
- 38-7 Yamano, N., et al., 1993, "Studies on Fuel Coolant Interactions During Core Melt Accident of Nuclear Power Plants," CSNI-FCI Specialists Meeting, Santa Barbara, CA.
- 38-8 Henry, R. E. and Miyazaki, K., "Effects of System Pressure on the Bubble Growth from Highly Superheated Water Droplets," Paper presented at the ASME Winter Annual Meeting, San Francisco, CA, 1978.
- 38-9 Avedisian, C. T., "Effect of Pressure on Bubble Growth Within Liquid Droplets at the Superheat Limit," *ASME Journal of Heat Transfer*, Vol. 104, pp. 750-757, 1982.
- 38-10 Nelson, L. S. and Buxton, L. D., "Effects of Pressure on Steam Explosion Triggering in Corium-E Simulants," *Trans. ANS*, Vol. 18, p. 448, June, 1978.
- 38-11 Bird, M. J. and Millington, R. A., "Fuel-Coolant Interaction Studies with Water and Thermite Generated Molten Uranium Dioxide," 4th CSNI Specialist Mtg. on Fuel-Coolant Interaction in Nucl. Reactor Safety, Bournemouth, United Kingdom, CSNI Report No. 37, pp. 420-448, April, 1979.
- 38-12 Corradini, M. L., Mitchell, D. E. and Nelson, L. S., "Recent Experiments and Analysis Regarding Steam Explosions with Simulant Molten Reactor Fuels," ASME Symp. on Fuel-Coolant Interactions, Winter Annual Mtg., Washington, pp. 49-63, November, 1981.



- 38-13 *A Review of the Current Understanding of the Potential for Containment Failure From In-Vessel Steam Explosions*, NUREG-1116, June 1985.
- 38-14 Frost, D. L., Bruckert, B., and Ciccarelli, G., "Effect of Boundary Conditions on the Propagation of a Vapor Explosion in Stratified Molten Tin/Water Systems," CSNI-FCI Specialist Meeting, Santa Barbara, CA, January 5-8, 1993.
- 38-15 Henry, R. E. and Fauske, H. K., "Required Initial Conditions for Energetic Steam Explosions," Fuel-Coolant Interactions, HTD-V19, American Society of Mechanical Engineers, 1981.
- 38-16 Theofanous, T. G. and Yuen, W. W., "The Probability of Alpha-Mode Containment Failure Updated," CSNI-FCI Specialist Meeting, Santa Barbara, CA, Jan. 5-8, 1993.
- 38-17 Jacobs, H., "Analysis of Large-Scale Melt-Water Mixing Events," CSNI-FCI Specialist Meeting, Santa Barbara, CA, January 5-8, 1993.
- 38-18 Berthoud, G., and Valette, M., "Calculations of the Premixing Phase of an FCI with the TRIO Code," CSNI-FCI Specialist Meeting, Santa Barbara, CA, January 5-8, 1993.
- 38-19 Hall, R. W., "Validation of CHYMES: Simulant Studies," CSNI-FCI Specialist Meeting, Santa Barbara, CA, January 5-8, 1993.
- 38-20 Fletcher, D. F., and Denham, M. K., "Validation of the CHYMES Mixing Model," CSNI-FCI Specialist Meeting, Santa Barbara, CA, January 5-8, 1993.
- 38-21 *An Assessment of Steam Explosion Induced Containment Failure*, NUREG/CR-5030, 1989.
- 38-22 Turland, B. D., et al., "Quantification of the Probability of Containment Failure Caused by an In-Vessel Steam Explosion for the Sizewell B PWR," CSNI-FCI Specialist Mtg., Santa Barbara, CA, Jan. 5-8, 1993.
- 38-23 Epstein, M. and Fauske, H. K., "The Three Mile Island Unit 2 Core Relocation - Heat Transfer and Mechanism," *Nuclear Technology*, Vol. 87, 1989.
- 38-24 *Steam Explosion Efficiency Studies*, NUREG/CR-0947, SAND 79-1399, November, 1979.
- 38-25 *Steam Explosion Efficiency Studies: Part II Corium Experiments*, NUREG/R-1746, SAND 80-1324, October, 1980.



- 38-26 *Report of the Zion/Indian Point Study: Volume 1*, NUREG/CR-1410, SAND 80-0617/1, 1980.
- 38-27 Naval Ordinance Laboratory Report NOLTR 63-140, Explosion Containment Laws for Nuclear Reactor Vessels, August 1965.
- 38-28 Proctor, J. F., "Adequacy of Explosion-Response Data in Estimating Reactor-Vessel Damage," *Nuclear Safety*, 8, pp. 565-572, 1967.
- 38-29 "REXCO-HEP: A Two-Dimensional Computer Code for Calculating the Primary System Response in Fast Reactors," Argonne National Laboratory Report ANL-75-19, June 1975.
- 38-30 "Analysis of Non-Linear Fluid-Structure Interaction Transients in Fast Reactors," Argonne National Laboratory Report ANL-78-103, November 1978.
- 38-31 "HONDO II, A Finite Element Computer Program for the Large Deformation Dynamic Response of Axisymmetric Solids," Sandia National Laboratories Report SAND 78-0422, October 1978.
- 38-32 *Appendix 2A, Reactor Vessel Failure and Missile Generation Due to In-Vessel Steam Explosion, to Report of the Zion/Indian Point Study: Volume I*, SAND80-0617/1 or NUREG/CR-1410, April 1980.
- 38-33 *Report of the Zion/Indian Point Study: Volume II*, Los Alamos National Scientific Laboratory, April 1980.
- 38-34 Carlsson, J., "The Effect of a Steam Explosion on a Reactor Pressure Vessel," Steam Explosions in Light Water Reactors, Report of the Swedish Government Committee on Steam Explosions, Ministry of Industry Report DsI 1981:3, Appendix 3, 1981.
- 38-35 "An Overview of Pool-Type LMFBRs: General Characteristics," Argonne National Laboratory Report ANL 76-61, May 1976.
- 38-36 "Analysis of FFTF Primary-Containment Complex Model Experiments," Argonne National Laboratory Report ANL-8062, January 1974.
- 38-37 "Supplement 1, Comparison of a Two-Dimensional Hydrodynamics Code (REXCO) to Excursion Experiments for Fast Reactor Containments," Argonne National Laboratory Report ANL-7911, July 1972.
- 38-38 *The Probability of Liner Failure in a Mark-I Containment*, NUREG/CR-5423, 1991.

Table 38-1

EXPERIMENTS DEMONSTRATING A HIGH-PRESSURE CUT-OFF

Laboratory	Materials Used	Explosive Pressures Measured (MPa/psia)	System Pressure Required to Eliminate Explosion (MPa/psia)	Reduced Pressure Ratio
Argonne (Reference 38-5)	Freon-22 and mineral oil	2.5/363	0.2/29	0.04
Argonne ⁽¹⁾ (Reference 38-4)	Freon-22 and mineral oil	2.0/290	0.5/73	0.10
Isp ^a (Reference 38-2)	Water and molten sodium chloride	6.0/870	1.0/145	0.05
Isp ^a ¹ (Reference 38-3)	Water and molten sodium chloride	4.0/580	3.1/450	0.15
Sandia ¹ (Reference 38-10)	Water and molten corium	1.5/218	0.75/109	0.04
Winfrith (Reference 38-11)	Water and molten uranium dioxide	3.0/435	0.9/131	0.05
Sandia (Reference 38-12)	Water and molten iron thermite	3.5/508	> 1.01/> 147	> 0.0
Avedisian (Reference 38-9)	η -Octane and glycerin	Not measured	> 0.101/14.7 < 0.687/100	> 0.04 < 0.27
Magallon and Hohmann (Reference 38-6)	Molten UO ₂ and water	No explosion observed	Pressure = 5/725	Consistent with 0.5
Yamano, et al. (Reference 38-7)	Molten iron thermite and water	10/1450	Explosions observed when: P = 0.1/15 No explosions for P = 1.6/232	Consistent with 0.05

Note:

- Externally triggered systems

Table 38-2

**SANDIA IRON-THERMITE TEST
EXPERIMENTS WITH AN ARTIFICIAL TRIGGER**

Run	Melt Quantity kg	Water Temperature K	Time to Explosion sec.	Efficiency %	Pre-Trigger	
					Particle	Diameter
					3000 K	1800 K
27	4.2	~ 295	1.17	0.42	5.0	1.0
29	3.4	~ 295	0.92	0.47	4.0	0.8
30	3.2	~ 295	0.95	0.36	3.7	0.7
35	12.0	~ 295	3.34	0.20	14.0	2.8
38	13.0	~ 295	3.45	0.19	16.0	3.0
41	9.4	~ 295	2.34	0.26	10.8	2.2

Table 38-3

SANDIA IRON-THERMITE AND CORIUM A+R TESTS

Run	Melt	Melt Quantity kg	Water Temperature K	Water Mass kg	Time to Explosion sec.	Efficiency %	Comments
54	Fe-Al ₂ O ₃	13.6	~ 295	3500		0.5	Spontaneous explosion
55	Fe-Al ₂ O ₃	13.6	~ 295	3500		0.56	Spontaneous explosion, triggered explosion later -0.64 g PETN
56	Corium A+R	13.6	~ 295	3500	-	-	No explosion -0.64 g PETN
57	Corium A+R	13.6	~ 295	3500	1.3	<< 0.01	Weak interaction -0.64 g PETN
58	Corium A+R	19.4	~ 295	3500	0.3	-	No explosion 6 g PETN
59	Corium A+R	19.4	~ 295	3500	1.3	0.05	Mild explosion -6 g PETN



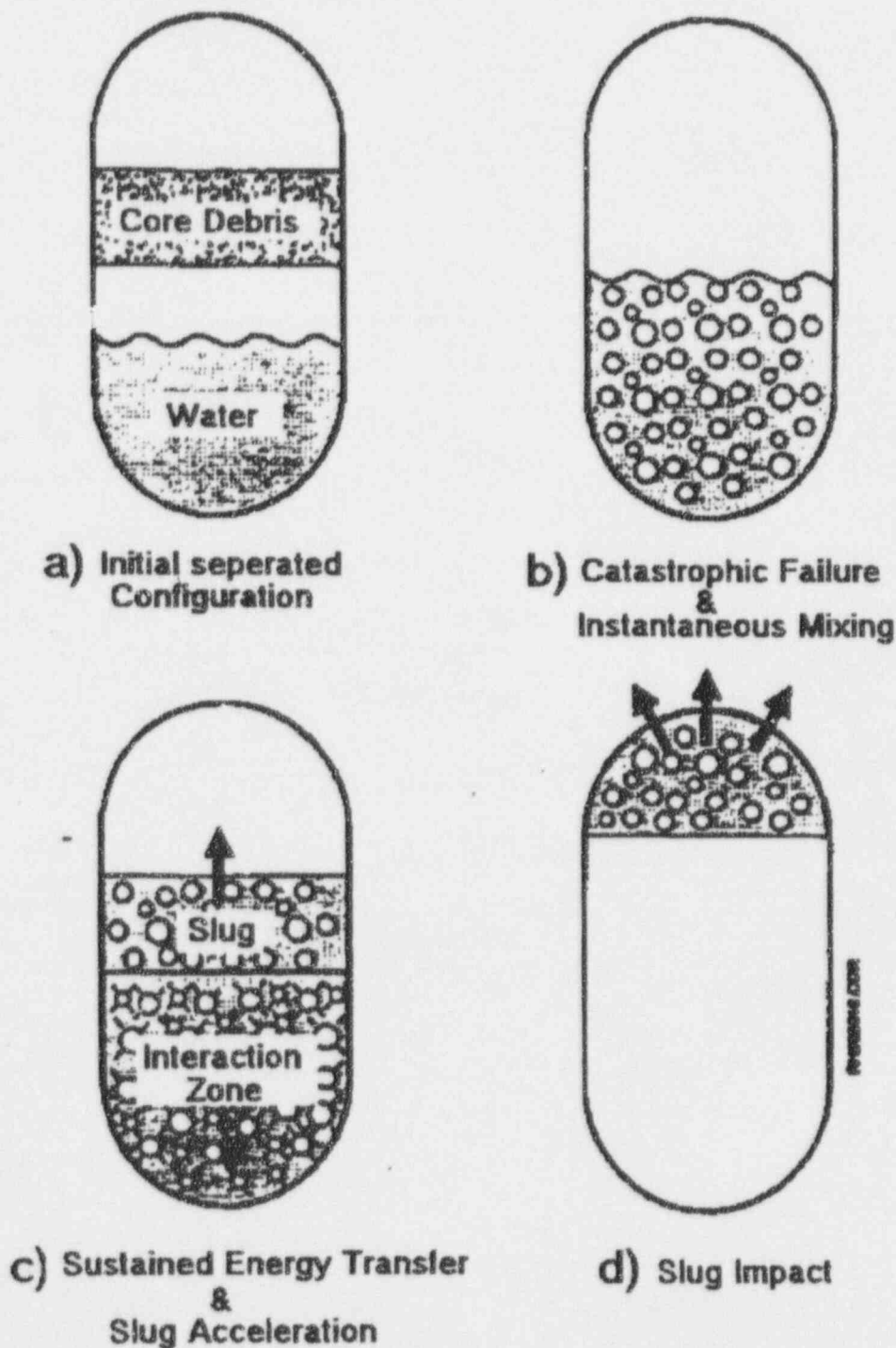


Figure 38-1

Behavior Modeled in WASH-1400

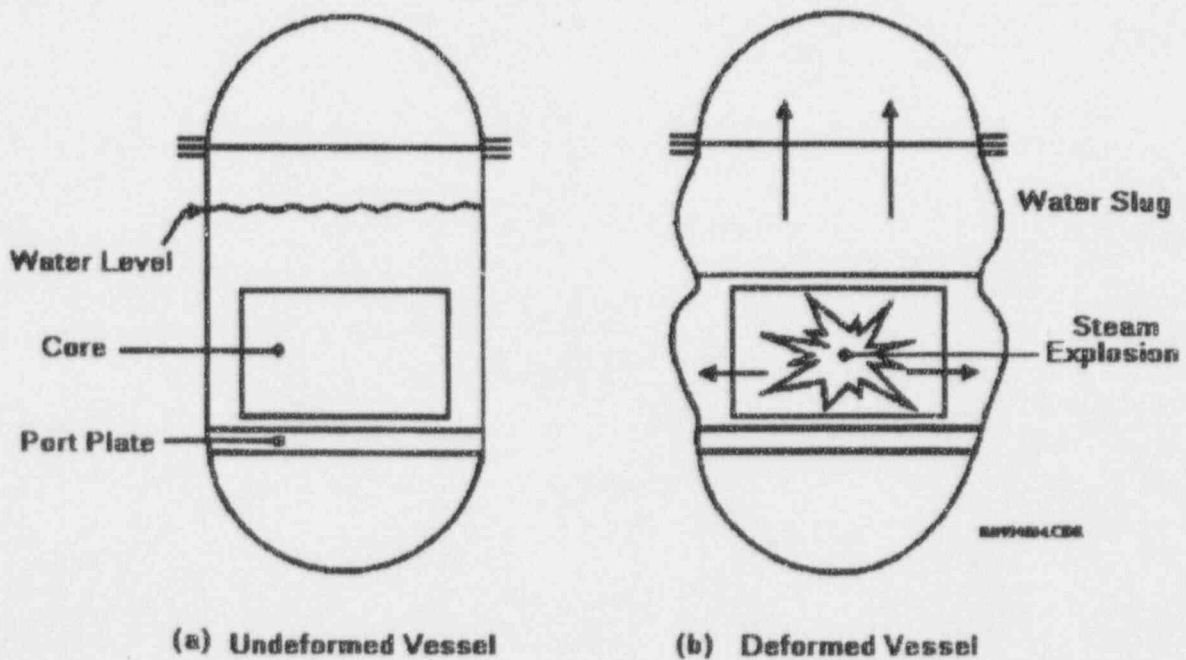


Figure 38-2

Schematic Representation of the Deformation of an LWR Vessel Due to an Internal Steam Explosion

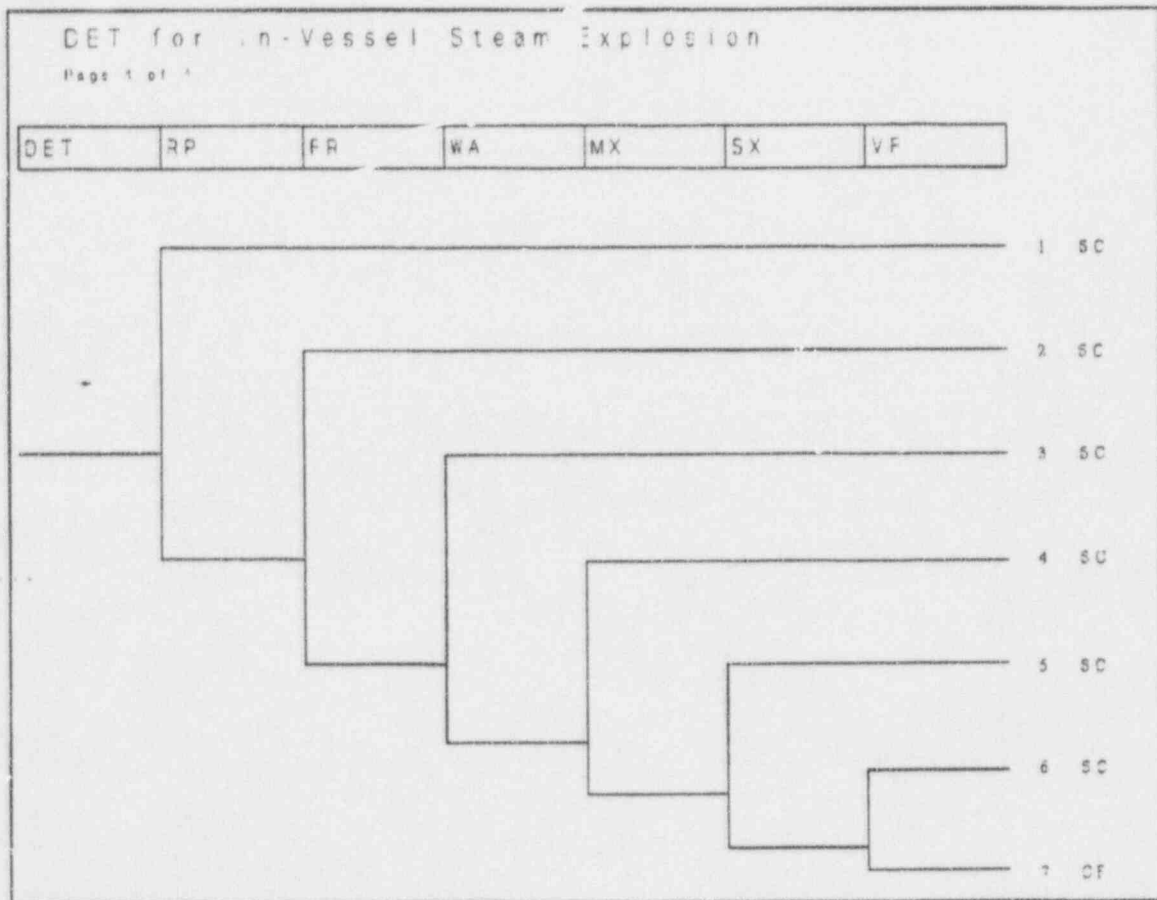


Figure 38-3

Decomposition Event Tree for In-Vessel Steam Explosion

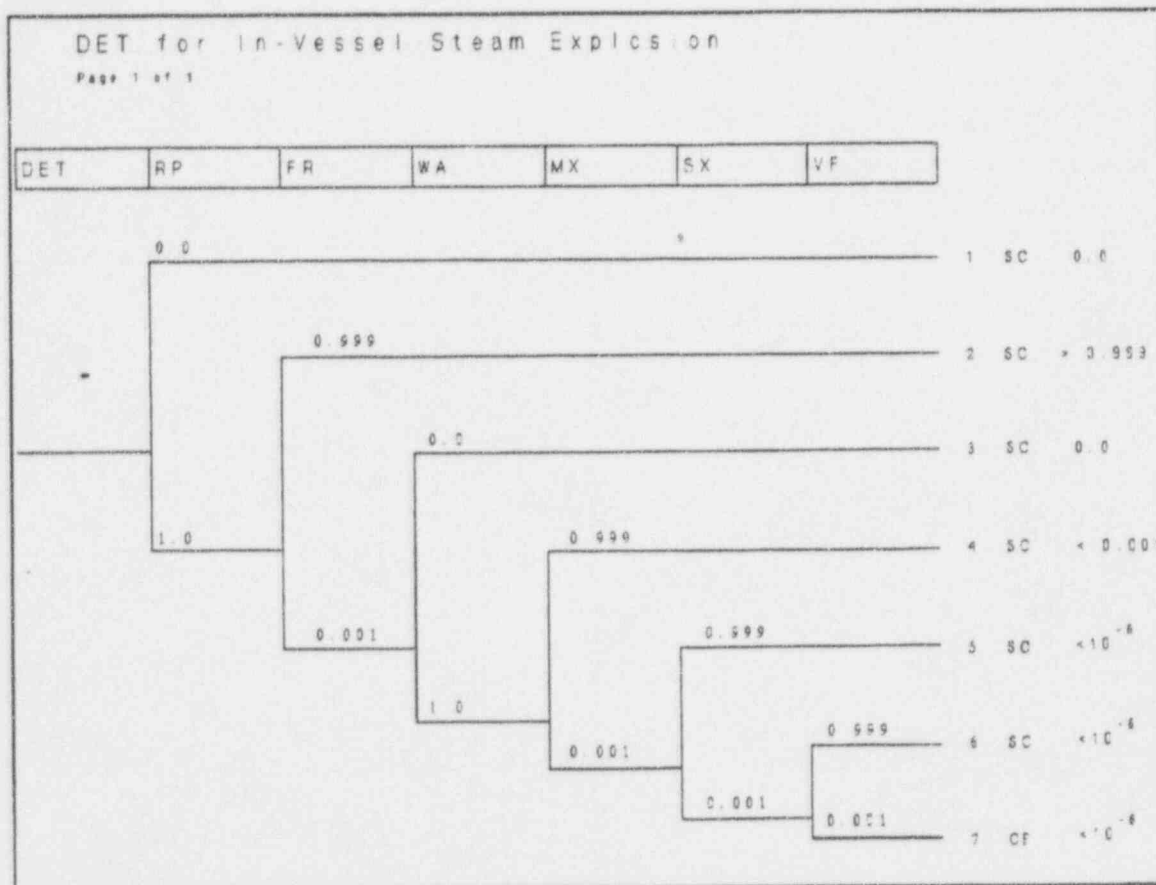


Figure 38-4

Quantified Decomposition Event Tree for In-Vessel Steam Explosion



CHAPTER 39

DECOMPOSITION EVENT TREE - ANALYSIS OF EX-VESSEL STEAM EXPLOSION

Thermally-induced steam explosions outside the reactor vessel (ex-vessel steam explosions) have been postulated to occur in core damage severe accident sequences in which debris may be discharged from the reactor vessel into a pool of water. This happens only on failure of in-vessel retention which, in turn, happens only on failure to submerge the lower head. The decomposition event tree (DET) quantifies the contribution to the overall likelihood of containment failure because of ex-vessel steam explosions given core damage and failure of in-vessel retention. Results of the quantification of the decomposition event tree provide input to node CF1 on the AP600 containment event tree.

39.1 Discussion of the Issue

Ex-vessel steam explosions could occur in the reactor cavity if molten core debris is discharged from the reactor vessel into the flooded cavity on failure of in-vessel retention. Studies evaluating the risk of severe accident sequences have considered ex-vessel steam explosions as a potential mechanism for early containment failure. Results of analyses performed in accordance with significant scale experiments and expansion characteristics of shock waves form the basis for treatment of ex-vessel steam explosions. Specifically, ex-vessel steam explosions are addressed by considering the potential for overpressure in the containment because of rapid steam generation as a result of explosive interactions and the shock waves that could be created by the interactions and imposed on subcompartment and containment walls. Since the energy released from a thermal explosion increases with increasing mass of molten material, the largest threat to containment integrity from a steam explosion would be a core melt sequence with a relatively coherent release of molten material at vessel failure.

The first systematic evaluation of steam explosions was performed by an ad hoc panel of experts, the Steam Explosions Review Group (SERG) (Reference 39-1). Although this evaluation was carried out for in-vessel steam explosions, there are insights for ex-vessel steam explosions in Reference 39-1 in terms of fragmentation, intermixing, heat transfer, and triggering. The NUREG-1150 expert panel on steam explosions (Reference 39-2) agreed that the SERG assessments were appropriate, and made use of them (based on arithmetic averaging) in their quantification. A specialist meeting on fuel coolant interactions sponsored by the Committee on the Safety of Nuclear Installations was held at the University of California in Santa Barbara, California on January 5-8, 1993 to provide a forum to discuss recent progress regarding steam explosions. The meeting included integral assessments of risk due to steam explosions; none of these indicated that the SERG conclusions were overstated (optimistic). The available information provided at the meeting either validated the opinions generated by the SERG, or demonstrated that there was substantial conservatism in the SERG assessments and reduced these conservatisms. More explicit Risk-Oriented Accident Analysis Methodology (ROAAM) quantifications are currently under way (Reference 39-3).



39.2 Discussion of Controlling Phenomena and Uncertainties

For large-scale steam explosions to occur in a containment, large fractions of hot molten core material must be first premixed with the water prior to the explosion as it is released from the reactor vessel, then finely fragmented and intermixed with the water on the time scale of the explosion.

The key factors that determine the likelihood, magnitude, and significance of steam explosions within a containment include:

- The energy required to fail the containment
- The transmission of this energy from the explosion to the containment boundary
- The amount of core material needed to provide such an energy release
- The fragmentation of the hot material in the water
- The mixing energy requirements when the material is finely fragmented and rapidly intermixed during the explosion
- The size of an external trigger to initiate the explosion
- The propagation characteristics of the coarsely fragmented system

Each of these factors must be sufficient to create an event of sufficient magnitude to fail the containment. The failure of a single link in this chain to achieve the proper conditions will preclude an event of such magnitude.

The major phenomenological questions that control these factors are:

- How much core material could be coarsely mixed with water when an explosion event could be initiated?
- How much water mass would be available in the interaction zone (how much water could explode)?
- How efficient are interactions with large masses of materials?
- What is the likelihood of the shock waves resulting from an explosion weakening the cavity walls such that the vessel moves and tears one or more containment penetrations?
- What is the likelihood that the pressure resulting from the explosion shock wave and the longer-term steam overpressure would fail the containment?



Each of these is discussed in terms of conditions relevant to the specific question in the following sections.

39.2.1 How Much Core Material Would Be Involved?

How much core material would be available to coarsely mix with water when a steam explosion event is triggered?

Of particular interest in this question is how much of the molten material could be in a particulated form within the reactor cavity. Hence, the focus in these calculations is the extent of material that would be molten, particulated, and in the process of settling in the cavity.

An order-of-magnitude estimation of the amount of core material needed to provide an energy release sufficient to fail containment can be performed. case 3BE.cc1 in the source term analysis of the PRA can be taken as a typical vessel failure case. The containment gas pressure and temperature just prior to vessel failure in case 3BE.cc1 are $1.3\text{E}5$ Pa and 400 K, respectively (see Figures 34-152, 34-153, and 34-162). The containment volume is $48,000\text{ m}^3$. Treating the air in the containment as an ideal gas and taking the gas constant as $8314\text{ Pa m}^3/\text{kgmole-K}$ leads to an amount of air in the containment of 2000 kgmoles. Per Chapter 42, the mean containment failure pressure is 137.1 psig ($1.0\text{E}6$ Pa). Raising 2000 kgmoles of an ideal gas in a volume of $48,000\text{ m}^3$ from a pressure of $1.3\text{E}5$ Pa to $1.0\text{E}6$ Pa requires a temperature increase of 2800 K. Air has a molecular weight of 29 kg/kgmole and a specific heat at constant volume of 716 J/kg K (Reference 39-4). The energy needed to raise the temperature of 2000 kgmoles of air 3000 K is $1.3\text{E}11\text{ J}$. Therefore, the expected energy deposition required to fail the AP600 containment would be about $1.1\text{E}11\text{ J}$.

The mechanical work delivered by a completely efficient thermal interaction is considered in Reference 39-5; this shows a specific work term of 815 kJ/kg of water vaporized with a final pressure of 3 atmospheres, which in turn requires almost 2800 kJ/kg of thermal energy transfer. As a result, the necessary corium mass undergoing a complete reaction from 2500 K to the coolant saturation temperature to fail containment would be about $3.0\text{E}5\text{ kg}$. However, typical steam explosion measurements show large scale interactions to be less than 1 percent efficient (Reference 39-6). For conservatism in this analysis it is assumed that the interactions are of the order of 10 percent efficient. Thus, a mass of about $3.0\text{E}6\text{ kg}$ would be required.

In the source term analysis of the AP600 PRA, the debris mass in the reactor cavity is just over $1.3\text{E}5\text{ kg}$ in case 3BE.cc1. Even without considerations of particulation (which provides a significant limitation), there is significantly less core material within the reactor cavity than is needed to fail the containment through a steam explosion in the case of a vessel failure sequence. However, particulation will still be considered.

39.2.1.1 Water Depletion during Pre-Mixing

Water depletion refers to the formation of a voided (high steam fraction) region when melt pours into water. Water depletion (voiding) during premixing was postulated (Reference 39-7) as a mechanism that limits the amount of debris mass that can participate in a steam explosion. This mechanism has been investigated analytically (Reference 39-8) and demonstrated experimentally (Reference 39-9). A coarse premixed configuration is a prerequisite condition for a steam explosion. Steam is produced by the radiative and convective heat transfer from capillary size melt (fuel) particles during the premixing of these two fluids. High steam generation rates would drive water out of the mixing region, thereby depleting the water and limiting the size of the potentially explosive interaction. Specifically, large quantities of high temperature melt cannot coexist with large quantities of water in such a coarsely mixed configuration. Furthermore, largely voided premixtures are very inefficient for energy transfer should an explosion be initiated (triggered).

39.2.1.2 Multi-Dimensional Venting of the Interaction Zone

Multi-dimensional venting of the explosion or interaction zone may occur in open pool geometries or shallow pools for configurations with large aspect ratios (Reference 39-10). This phenomenon is particularly important when dynamic pressure loads are quantified on structures adjacent to steam explosions. Direct venting of the explosion zone reduces the peak dynamic pressure. Furthermore, reflections of pressure waves off the free surface of the pool mitigate the transmitted component of the load on affected structures such as the reactor cavity walls.

39.2.1.3 Limited Debris Jet Penetration into Cold (Sub-Cooled) Water Pools

Limited debris jet penetration for high-velocity jets entering highly subcooled pools may lead to highly dynamic breakup patterns. The high-velocity jet could result from high-pressure melt ejection or long "free-fall" distances for gravity-driven draining of melt from depressurized reactor pressure vessels. (High-pressure sequences themselves are very unlikely because of the large depressurization capability for the design, and because of hot leg creep rupture if the core should be overheated at high pressures.) The dynamic and localized rapid pressure generation would lead to melt fragmentation and quenching and the destruction of the coarse melt premixed configuration. This destruction by fragmentation and quenching of the coarse melt masses by forced, small-scale, but intense interactions is called "penetration cutoff" (Reference 39-10). This localized breakup would tend to prevent deep pool penetration.

39.2.1.4 Triggering

Given that a coarse premixed configuration can be produced, an event that triggers the initiation and propagation of a steam explosion is required. Spontaneous triggering of a steam explosion may occur when molten debris contacts the water pool surface, when debris contacts structures or piping submerged in the water, or when debris contacts the submerged concrete

surface (floor or wall). In any case, only a limited amount of debris is likely to be available to participate in the steam explosion due to the difference in time scales for the leading edge of the debris to contact the wetted surfaces compared to the time to discharge the molten debris mass from the failed reactor vessel. The steam explosion will disperse the available core debris and water, and disrupt the required premixed configuration and quench (solidify) at least a portion of the core debris. Since only a fraction of the molten debris would participate, this limits the amount of energy available to participate in the steam explosion.

39.2.1.5 Core Material Available

The limited potential for premixing of fuel and water prior to triggering and propagation was first outlined by Henry and Fauske (Reference 39-7). Quasi-steady one-dimensional analyses accounting for radiative and convective heat transfer from capillary size fuel particles suggested sufficient steam generation rates to "flood" or deplete the water and, therefore, limit a potentially explosive premixture to a few hundred kilograms.

The most advanced calculations (three fluid formulation) as well as hot particle experiments were presented by Theofanous (Reference 39-3), demonstrating excellent agreement between measured and calculated void distributions. Utilizing a water depletion criterion corresponding to a void fraction of 0.7 along with a fuel pour area of 2 m² (fuel pour diameter about 1.6 m) and a fuel particle size of 2 centimeters, Theofanous' calculations suggest a peak premixing value of about 1.5 tonnes at atmospheric pressure condition.

A related issue is the fuel particle size to be used in the premixing calculations. Relevant quenching experiments (Reference 39-11) suggest that the capillary size is a good representation of the average measured particle size for the fraction of corium jet experiencing breakup. Since radiative heat transfer would appear of prime importance (as clearly illustrated by Theofanous' comparison between the CHYMES and PM-ALPHA calculations), to a first order the premixing fuel mass would be proportional to the assumed premixture fuel dimension. Theofanous' calculation of 1.5 tonnes based on a 2 centimeters fuel particle is reduced to about 300 kg when the capillary size of 0.4 centimeters is used, even when a very large fuel pour diameter of 1.6 meters is assumed.

In summary, excellent progress has been made toward improving the quantification, as well as experimental confirmation, of the water depletion phenomenon in limiting the fuel mass in the premixing stage of an energetic steam explosion. For pour diameters of the order of 0.1 meter, the premixing would be largely independent of pressure. This is consistent with the Three Mile Island Unit 2 estimate of a few hundred kilograms at a pressure of about 7 MPa (Reference 39-12).





39.2.2 How Much Water Would Be Involved?

How much water mass would be available in the interaction zone if an explosion could occur?

This decomposition event tree assesses the potential for an ex-vessel steam explosion challenging the integrity of the containment given that vessel failure has occurred. The conditional state of vessel failure assumes that drainage of the in-containment refueling water storage tank inventory to the reactor cavity has failed. Therefore, at most the successful operation of the passive injection capability (core makeup tank and accumulators) and primary system inventory would be available to flood the cavity. This total inventory would be sufficient to temporarily submerge the lower vessel head and provide cooling. However, as this water was boiled away it would eventually collect in the in-containment refueling water storage tank. Given the failure of the in-containment refueling water storage tank drainage paths, the water would not return to the cavity and maintain a submerged reactor pressure vessel condition. This process could leave a water pool in the reactor cavity approximately 1.4 meters deep. This is the vertical displacement between the bottom of the lower head and the reactor cavity floor. For those non-loss-of-coolant accident sequences where neither primary system inventory nor the passive injection could collect in the reactor cavity, only condensation on surfaces beneath the condensate collection system elevation (approximately at the level of the operating deck) would collect in the reactor cavity. This could result in a water pool in the reactor cavity a fraction of a meter deep. Thus, water would always be expected to be present in the reactor cavity, although in some cases it would be expected to be a shallow pool. Furthermore, the AP600 plant design assures that the reactor cavity will be flooded. It is assumed there is always sufficient water in the reactor cavity to cause a steam explosion.

39.2.3 What is Efficiency of Interaction?

How efficient are interactions with large masses of materials?

Explosion efficiency is defined as the fraction of stored thermal energy in the melt material that is converted to explosion mechanical energy. Large-scale steam explosion efficiency experiments have been carried out at Sandia Laboratories in two different test series, one using an iron thermite mixture (Reference 39-6) to simulate the degraded core material and the other incorporating both an iron-thermite and a corium-thermite (Reference 39-13), which had a higher melting temperature and was a more realistic simulant of the anticipated debris character.

In the first set of experiments (Reference 39-6), the iron thermite melt had a temperature of about 3000 K as it left the melt generator and was discharged directly into a 0.9 meter diameter vessel filled with water. For all those experiments carried out with an artificial trigger, the water was at the ambient temperature, assumed to be 295 K. The reported conditions for the various experiments of interest are listed in Table 39-1 for the melt quantity, water temperature, time to explosion, and reported explosion efficiency (as compared to the stored energy in the melt material). Given the mass of material discharged into the test



vessel, the water temperature, and the melt temperature, the pre-explosion fragmentation sizes can be evaluated from the film boiling fragmentation model. (In these experiments the ambient pressure was always slightly less than 0.1 MPa.) The melt temperature resulting from the thermite reaction was about 3000 K and results in reaction products of metallic iron (Fe) and aluminum trioxide (Al_2O_3). The melting temperature of the aluminum trioxide is about 2300 K and that of metallic iron is about 1800 K. Consequently, solidification of either of these constituents requires a substantial decrease in temperature and the resulting fragmentation process could continue as the melt cools (lower temperatures reduce the film boiling steam generation rate and allow finer particulation). The various levels predicted for melt temperatures of 3000 K and 1800 K are illustrated in Table 39-1, and as shown, the lower temperature predicts a radius 1/5 of that typical of the higher temperature fragmentation condition. These calculated values bracket the coarse prefragmentation states that could be rapidly dispersed on an explosive time scale by the mixing energy from the explosive detonator. However, the salient point displayed in the table is not the explosive detonator. The most important point shown in the table is that the combination of the magnitude of the melt, the subcooled water temperature, and the large vessel cross-sectional area allow significant coarse prefragmentation of the melt prior to the onset of an explosive interaction. It should also be noted, that the largest fragmentation sizes prior to the explosion are 1.6 centimeters in diameter (in close agreement with the pre-explosion sizes reported for the Sandia experimenters in other publications) (Reference 39-14). These sizes were deduced from movies taken in similar-sized vessels with transparent viewing ports.

To externally trigger an explosive interaction, a 0.64 gram charge of high explosives was used. Assuming this detonator to be PETN, or an equivalent material, the explosive reaction products are essentially all gaseous and the work delivered to the corium-water mixture by the detonator can be equated to the heat of explosion. For PETN, this is about 5800 J/gm of material. This can be treated as the energy available to intermix materials prior to the explosive energy transfer. To achieve such intermixing on an explosive time scale, it is assumed that it occurs in an ms interval with a final particle size sufficiently small to enable an efficient thermal energy transfer (about 500 μm in diameter). This particle size range is also in general agreement with the post-explosion particle sizes found in these experiments.

A second test series was performed at Sandia with a different test vessel (1.2 meters internal diameter) and molten material generated from both iron-aluminum oxide thermite and a corium-A+R thermite. This latter reaction had products of uranium dioxide, zirconium dioxide, nickel oxide, stainless steel, and molybdenum. The minimum liquidus temperature for this mixture is reported to be 2770 K, which is considerably greater than the 2300 K temperature for aluminum oxide. Boiling steel limited the maximum temperature for the corium reaction to 3070 K.

In this second test series, external triggering was also induced by explosive detonators, but two different sizes were used. One was the same as that employed in the first iron-thermite test (0.64 gram of PETN), and the other was a detonator plus a lead-covered explosive core 0.76 meter in length and containing 6 grams of PETN. This second method represented a much more energetic trigger than that used in the thermite tests. In fact, the pulse duration



for the corium A+R event in run 59, which used this larger trigger, was not much different than that represented by the trigger alone. Additionally, the measured work (about 30 kJ) was less than the work released by the high explosive (about 35 kJ).

Table 39-2 lists the experimental conditions and observations for the tests in which molten material was successfully discharged into the interaction vessel. As illustrated, explosions were observed with the iron thermite as initiated by both spontaneous and artificial triggers. However, with the corium A+R melt, only one mild explosion is reported and this was triggered by the 6 gram PETN external trigger.

From these results, it can be concluded that the efficiency of interactions involving degraded core material and water is less than about 0.5 percent, even with artificial triggers.

39.2.4 What is the Likelihood of Containment Failure Due to Tearing of Containment Penetrations?

What is the likelihood of the shock waves resulting from an explosion weakening the cavity walls such that the vessel moves and tears one or more containment penetrations?

Since a steam explosion would occur in the confines of the cavity, the shock wave would impact the cavity floor and walls. The severity of the shock wave would be mitigated somewhat by the shallowness of the water pool in the cavity (Reference 39-15). The shock wave impact will not have a significant effect on the massive reinforced concrete structure of the cavity. If the sonic velocity of a concrete wall 1 meter thick is taken to be 1000 m/s, the far side of the wall would not experience any change due to the initiation of a shock wave imposed on it for at least 1 millisecond. At this time, the outer surface of the wall would experience the arrival of a compression wave and the transmittal of a rarefaction wave back toward the explosive source. This would indicate a velocity in the wall of about 4 m/s if the density of the wall is assumed to be 2000 kg/m³. Movement of the wall due to this induced velocity would be counteracted by the tensile strength of the wall, which is principally the steel reinforcement within the wall. Forces developed by straining the reinforcement would reduce the velocity in the wall. Since the loadings associated with the shock wave have a duration of a few milliseconds, velocities induced by the transmittal of the wave through the wall would only result in a few millimeters displacement. Experiments with reinforced concrete walls have demonstrated that substantially greater displacements would be required to structurally fail such members (Reference 39-16). Therefore, the dynamic response of the cavity wall is so small that the concrete structure, and ultimately the containment, can be assumed not to respond.



39.2.5 What is the Likelihood of Containment Failure Due to Shock Wave and/or Overpressure?

What is the likelihood that the pressure resulting from the explosion shock wave and the longer term steam overpressure would fail the containment?

A significant ex-vessel steam explosion could occur only in the reactor cavity of the AP600. The plant design provides that the cavity will accumulate water before any other compartments. For low-pressure vessel failure, the debris-water interaction is limited to the cavity because debris will not be transported to other parts of the containment. For a high pressure sequence, the debris can be transported to other compartments in the containment, but not before passing through the cavity pool. The AP600 design is such that it cannot have an isolated pool outside the cavity that can be contacted by molten debris if the cavity is dry. High-pressure sequences are very unlikely because of the large depressurization capability for the design, and because of hot leg creep rupture if the core should be overheated at high pressures which will probably fall under the residual risk (negligible). There is little chance of damaging equipment required for recovery, since no essential equipment is located in the cavity. Shock waves created in the cavity by the steam explosion would dissipate in a few meters.

Due to the distance between the cavity and the containment wall, a shock wave created by an ex-vessel steam explosion would not challenge the integrity of the containment wall. The amplitude of the impulsive pressure loading that could occur on the containment shell because of a steam explosion in the reactor cavity would be on the order of a few psi (Reference 39-17).

Case 3BE.ccl in the source term analysis of the PRA shows a containment gas pressure spike right after vessel failure to $3.2E5$ Pa (46 psia). Per Reference 39-17, the ex-vessel steam explosion contribution to this is 0.3 psi from steam generation and 1.3 psi from shock wave. Per Chapter 42, the containment failure probability at 46 psia is much less than $6.12E-8$.

39.3 Development of the Decomposition Event Tree

The decomposition event tree structure developed for quantifying the contribution of this decomposition event tree to the probability of containment failure is presented in Figure 39-1. The questions posed at each node on the tree examine and quantify the uncertainties identified in the analysis presented in the previous sections. The upward path at each node indicates a positive response to the question; the downward path indicates a negative response. The nodes chosen for the decomposition event tree are:

Node FR - Is there less molten core material being coarsely mixed in the water in the reactor cavity than is needed to provide the energy release required to fail the containment?



- Node WA - Is insufficient water mass available in the interaction zone in the reactor cavity to create an explosion of enough magnitude to fail the containment?
- Node MX - Is the efficiency of the interaction less than required to cause an explosion of enough magnitude to fail the containment?
- Node WF - Are the resulting shock waves insufficient to weaken the cavity walls such that the vessel moves and tears out one or more containment penetrations?
- Node CF - Is the pressure resulting from the explosion shock wave and the longer-term steam overpressure less than that required to fail containment?

The end-states of the tree represent the state of the containment due to postulated ex-vessel steam explosions.

- SC - Success; the containment remains intact
- CF - Containment failure following an ex-vessel steam explosion

39.4 Quantification of the Decomposition Event Tree

This section discusses the assignment of the split fractions at each of the nodes on the decomposition event tree. Multiplication of the split fractions along a path of the tree results in the probability of the accident following that particular path. The summation of the probabilities of the paths that result in a particular end-state is the probability of that end-state.

39.4.1 Node FR

Is there less molten core material being coarsely mixed in the water in the reactor cavity than is needed to provide the energy release required to fail the containment?

Success Criteria:

Per subsection 39.2.1, a minimum of 3.0E6 kg of corium must undergo a complete reaction from 2500 K to the coolant saturation temperature to challenge containment integrity.

Per subsection 39.2.1, the maximum mass of molten debris that could be particulated and mixed is about 1000 kg. This is far less than the quantity necessary to challenge the containment. Since containment failure is then considered to be unrealistic, the likelihood of having a sufficient molten mass coarsely mixed will be set at 10^{-3} . This value was used to characterize those postulated behaviors which are found to be unrealistic in the Risk-Oriented Accident Analysis Methodology process applied to the Mark I liner melt-through (Reference 39-18).

Probability of enough core material being coarsely mixed (failure of node) = 0.001

Downstream Considerations:

Success of node FR leads directly to end-state SC. If there is enough molten core material draining into the reactor cavity to challenge the containment, the potential exists for the debris to actually fail containment through an ex-vessel steam explosion. This potential is examined further in subsequent nodes of this decomposition event tree.

39.4.2 Node WA

Is insufficient water mass available in the interaction zone in the reactor cavity to create an explosion of enough magnitude to fail the containment?

Success Criteria:

Insufficient water in reactor cavity to cause a steam explosion which could fail the containment.

Per subsection 39.2.2, sufficient water is always available in the reactor cavity when the core debris drains into it.

Probability of sufficient water mass being available (failure of node) = 1.0

Downstream Considerations:

Success of node WA leads directly to end-state SC. If the debris drains into a sufficient pool of water, the potential exists for an ex-vessel steam explosion of enough magnitude to fail the containment. This potential is examined further in subsequent nodes of this decomposition event tree.

39.4.3 Node MX

Is the efficiency of the interaction less than required to cause an explosion of enough magnitude to fail the containment?

Success Criteria:

Efficiency of interaction less than required.

Per discussion of this issue in subsection 39.2.3, an interaction with an efficiency which would challenge the containment is unrealistic, so, like node FR, the likelihood will be set to 0.001.

Probability of interaction with more than required efficiency = 0.001

Downstream Considerations:

Success of node MX leads directly to end-state SC. If the efficiency of the interaction is large enough, the potential exists for an explosion of enough magnitude to fail the containment. This potential is examined further in subsequent nodes of this decomposition event tree.



39.4.4 Node WF

Are the resulting shock waves insufficient to weaken the cavity walls such that the vessel moves and tears one or more containment penetrations?

Success Criteria:

Loads resulting from steam explosion does not challenge integrity of reactor cavity (interior) walls.

Per discussion of this issue in subsection 39.2.4, the probability of the load resulting from a steam explosion directly challenging the integrity of the reactor cavity (interior) walls is unrealistic, so, like node FR, the likelihood will be set to 0.001.

Probability of challenging integrity of interior walls = 0.001

Downstream Considerations:

Failure of node WF leads directly to end-state CF. Even if there is success of node WF, the potential exists for the explosion to fail the containment directly. This potential is examined further in the next node of this decomposition event tree.

39.4.5 Node CF

Is the pressure resulting from the explosion shock wave and the longer term steam overpressure less than that required to fail containment?

Success Criteria:

Loads resulting from explosion do not challenge integrity of containment boundary.

Per discussion of this issue in subsection 39.2.5, the probability of the load resulting from a steam explosion directly challenging the integrity of the containment boundary is unrealistic, so, here again, the likelihood is set to 0.001.

Probability of challenging integrity of containment = 0.001

Downstream Considerations:

Failure at node CF leads directly to end-state CF. Success of node CF leads to end-state SC.

39.5 Results

The decomposition event tree is quantified using the split fractions outlined above (Figure 39-2). Given a core damage severe accident and vessel failure, the conditional probability of containment failure due to ex-vessel steam explosions is an extremely small number. This is because several elements in the chain of events are found to be physically unrealizable. This number is so small that it loses physical meaning. Hence, it is suggested that ϵ be used in the event tree instead of the number. An alternate means of showing this

is to show less than 10^{-6} . This is how the conditional probability is used in the split fraction for containment event tree node CF1.

39.6 References

- 39-1 *A Review of the Current Understanding of the Potential for Containment Failure from In-Vessel Steam Explosions*, NUREG-1116, June 1985.
- 39-2 *Reactor Risk Reference Document*, NUREG-1150, February 1987.
- 39-3 Theofanous, T. G. and Yuen, W. W., "The Probability of Alpha-Mode Containment Failure Updated," CSNI-FCI Specialist Meeting, Santa Barbara, CA, Jan. 5-8, 1993.
- 39-4 Reynolds, W. C., *Thermodynamics*, McGraw-Hill Book Company, New York, 1968.
- 39-5 Assessment of Steam Explosion Potential in Hypothetical LWR Core Meltdown Accidents, FAI/92-25, Fauske and Associates, Draft Report Submitted to EPRI, June 1992.
- 39-6 *Steam Explosion Efficiency Studies*, NUREG/CR-0947, SAND 79-1399, November 1979.
- 39-7 Henry, R. E., and Fauske, H. K., "Required Initial Conditions for Energetic Steam Explosions," Fuel-Coolant Interactions, HTD-V19, American Society of Mechanical Engineers, 1981.
- 39-8 Angelini, S., et al., "Premixing-Related Behavior of Steam Explosions," CSNI-FCI Specialist Meeting, Santa Barbara, CA, January 5-8, 1993.
- 39-9 Fletcher, D. F., and Denham, M. K., "Validation of the CHYMES Mixing Model," CSNI-FCI Specialist Meeting, Santa Barbara, CA, January 5-8, 1993.
- 39-10 Theofanous, T. G., "The Study of Steam Explosions in Nuclear Systems," Proceedings, International Seminar on Physics of Vapor Explosions, Hokkaido, Japan, October 25-28, 1993.
- 39-11 Magallon, D. and Hohmann, H., "High Pressure Corium Melt Quenching Tests in FARO," CSNI-FCI Specialists Meeting, Santa Barbara, CA, 1993.
- 39-12 Epstein, M. and Fauske, H. K., "The Three Mile Island Unit 2 Core Relocation -Heat Transfer and Mechanism," *Nuclear Technology*, Vol. 87, 1989.
- 39-13 *Steam Explosion Efficiency Studies: Part II Corium Experiments*, NUREG/CR-1746, SAND 80-1324, October 1980.



- 39-14 *Report of the Zion/Indian Point Study: Volume 1*, NUREG/CR-1410, SAND 80-0617/1, 1980.
- 39-15 Theofanous, T. G., and Yuen, W. W., "The Prediction of Dynamic Loads from Ex-Vessel Steam Explosions," Proceedings, International Conference "New Trends in Nuclear System Thermodynamics," Pisa, May 30 - June 2, 1994.
- 39-16 MacGregor, J. G., Simmonds, S. H., and Rixkalla, S. H., "Test of a Pre-Stressed Concrete Secondary Containment Structure," University of Alberta, Department of Civil Engineering Report, 1980.
- 39-17 *AP600 Phenomenological Evaluation Summaries*, WCAP-13388 (Proprietary) and WCAP-13389 (Non-proprietary), Rev. 0, 1992.
- 39-18 *The Probability of Liner Failure in a Mark-I Containment*, NUREG/CR-5423, 1991.



Table 39-1

**SANDIA IRON-THERMITE TEST
EXPERIMENTS WITH AN ARTIFICIAL TRIGGER**

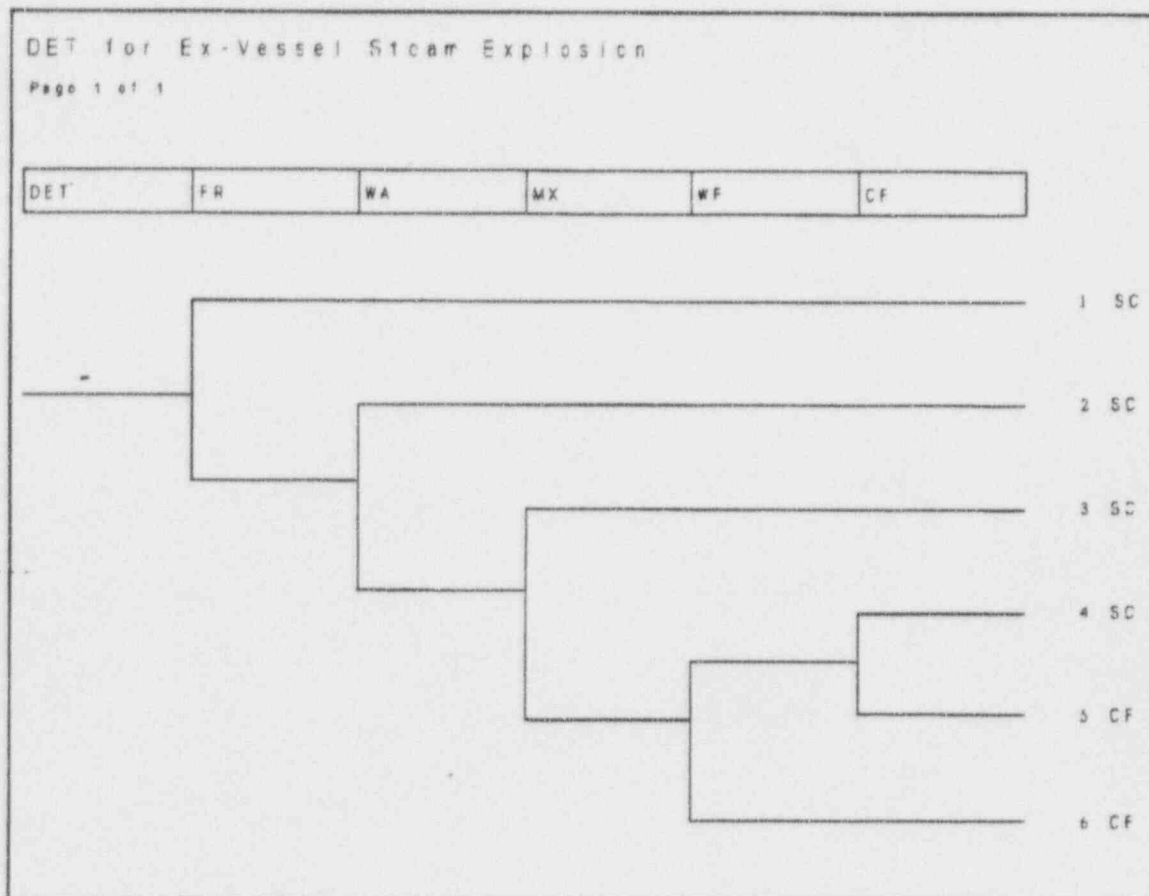
Run	Melt Quantity kg	Water Temperature K	Time to Explosion sec.	Efficiency %	Pre-Trigger	
					Particle	Diameter
					3000 K	1800 K
27	4.2	~ 295	1.17	0.42	5.0	1.0
29	3.4	~ 295	0.92	0.47	4.0	0.8
30	3.2	~ 295	0.95	0.36	3.7	0.7
35	12.0	~ 295	3.34	0.20	14.0	2.8
38	13.0	~ 295	3.45	0.19	16.0	3.0
41	9.4	~ 295	2.34	0.26	10.8	2.2



Table 39-2

SANDIA IRON-THERMITE AND CORIUM A+R TESTS

Run	Melt	Melt Quantity kg	Water Temperature K	Water Mass kg	Time to Explosion sec.	Efficiency %	Comments
54	Fe-Al ₂ O ₃	13.6	~ 295	3500		0.5	Spontaneous explosion
55	Fe-Al ₂ O ₃	13.6	~ 295	3500		0.56	Spontaneous explosion, triggered explosion later -0.64 g PETN
56	Corium A+R	13.6	~ 295	3500	-	-	No explosion -0.64 g PETN
57	Corium A+R	13.6	~ 295	3500	1.3	<< 0.01	Weak interaction -0.64 g PETN
58	Corium A+R	19.4	~ 295	3500	0.3	-	No explosion 6 g PETN
59	Corium A+R	19.4	~ 295	3500	1.3	0.05	Mild explosion -6 g PETN



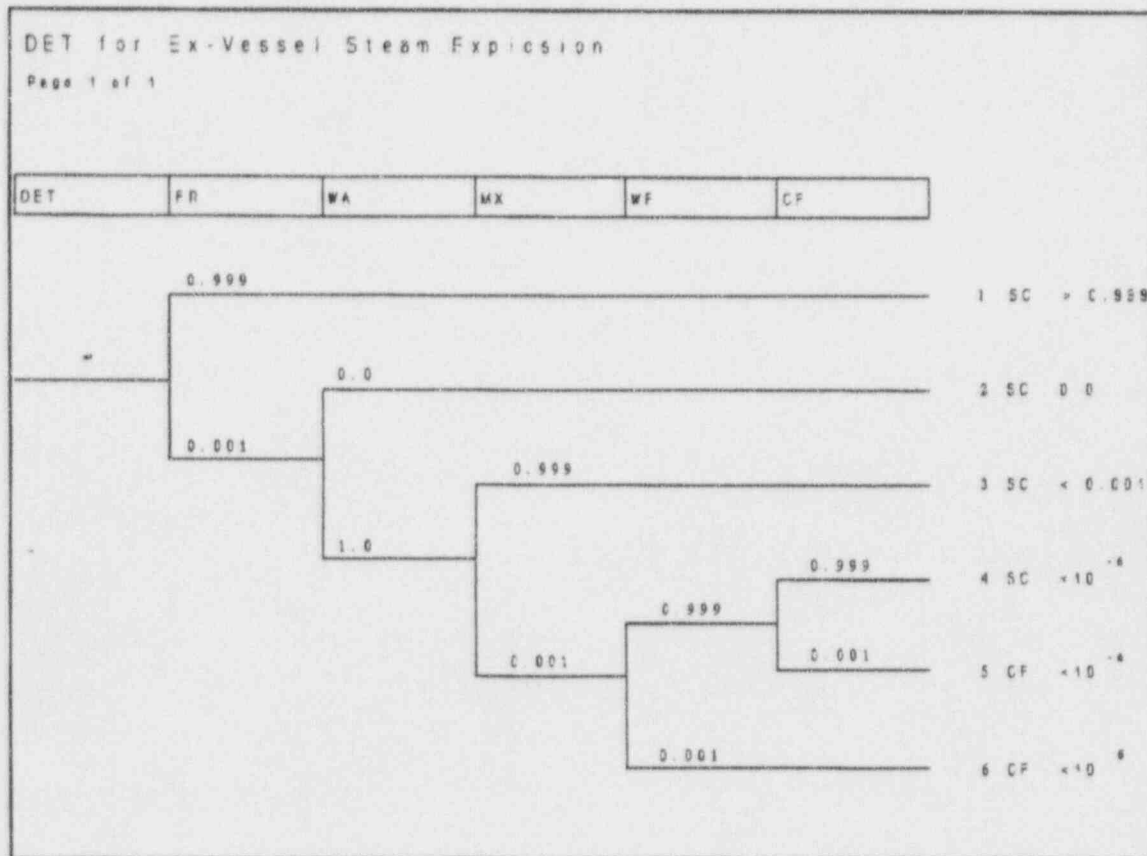


Figure 39-2

Quantified Decomposition Event Tree for Ex-Vessel Steam Explosion



CHAPTER 40

DECOMPOSITION EVENT TREE – ANALYSIS OF EX-VESSEL DEBRIS COOLABILITY

This decomposition event tree (DET) quantifies the likelihood of ex-vessel debris coolability in the reactor cavity. Ex-vessel debris coolability must be established to prevent molten core-concrete interaction (MCCI) which can threaten containment integrity by noncondensable gas generation and concrete ablation. The purpose of the decomposition event tree is to provide a structured, AP600 design-specific assessment of the phenomenological uncertainties related to debris coolability and to provide input to the DQ and SCC nodes of the AP600 containment event tree.

40.1 Discussion of the Issue

To assure ex-vessel debris coolability, the necessary water inventory must be maintained in the cavity, and the debris must remain in a coolable geometry. The cavity can be flooded prior to vessel failure by gravity draining of the in-containment refueling water storage tank (IRWST) (automatic or manual actuation of the cavity flooding valves), as specified in the AP600 containment event tree. If this is successful, debris coolability is relevant only in the event that submerging the reactor vessel is unable to prevent vessel failure. In accident sequences where the in-containment refueling water storage tank is unavailable, accumulators and core make-up tanks can provide water to the cavity. To maintain cavity water inventory, steam created by debris quenching must be recirculated back to the cavity. The passive containment cooling system provides cooling of the steel containment shell and thereby recirculates steam from the containment atmosphere back to the cavity. The long-term cavity water inventory is considered in both the PC and RW nodes of the AP600 containment event tree. Since sufficient initial inventory is always present in the AP600 reactor cavity to quench the debris and because maintenance of the inventory is addressed in other nodes of the containment event tree, coolant inventory considerations are not addressed in the quantification of node DQ.

Even with the necessary water inventory, the debris may not be coolable if the cavity geometry or debris configuration does not promote sufficient heat transfer from the debris to the water. For a fixed volume, debris thickness (or surface area) can limit the total heat transfer rate if the debris cannot disperse. The debris is most likely coolable if it is dispersed into a thin layer. Debris dispersal is addressed in the AP600 design by the large cavity area and absence of unguarded cavity sumps where debris can accumulate in a thick layer. The debris configuration affects the heat flux to water as well. Two configurations, debris bed or continuous slab, are possible. The continuous slab might limit water ingress into the debris because fissures or cracks may not be present.



40.2 Discussion of Controlling Phenomena and Uncertainties

40.2.1 Reactor Vessel Pressure at Vessel Failure

If vessel failure results in high-pressure melt ejection, gas flow from the vessel disperses debris, in the form of discrete particles or a thin coherent wave, throughout the cavity and other containment compartments. High-pressure melt ejection occurs if the reactor coolant system is not depressurized and the reactor vessel fails by debris impingement and ablation of the lower head. If the vessel fails in this mode, the debris is expelled first and the exiting gases entrain debris as particles or coherent waves. A reactor vessel pressure of several hundred psi is required to entrain debris. In the case of low-pressure melt ejection, the debris remains in the cavity and debris dispersal must be assessed, assuming the cavity is flooded. High-pressure melt ejection will not occur if the initiating event is a large loss-of-coolant accident; the automatic depressurization system is successful; the operator depressurizes the reactor coolant system after core damage has occurred; the hot leg or surge line fails due to high temperature creep rupture; or the reactor vessel fails due to creep rupture above the debris bed in the lower plenum, which allows the gas to exit before the debris and prevents entrainment. The decomposition event tree analysis for thermally-induced failures of the reactor coolant system pressure boundary (Section 37) demonstrates that hot leg creep generally occurs prior to reactor vessel lower head failure for high pressure sequences and the containment event tree conservatively assumes containment failure for all high-pressure melt ejection events. Therefore, no high-pressure melt ejection events are considered in the quantification of the ex-vessel debris coolability decomposition event tree.

40.2.2 Debris Mass Expelled from the Reactor Vessel

The thickness of the debris bed depends on the extent of the debris dispersal, the debris spreading area, and the mass of debris expelled. For a low-pressure sequence where the debris is essentially limited to the cavity area, the minimum debris thickness is determined by the amount of debris that is expelled from the reactor vessel. A value of 25 centimeters has been used as a criterion for debris coolability (Reference 40-1), although coolability might also depend on the configuration. Experiments suggest that a molten pool of 15 centimeters is coolable and may be coolable up to 25 centimeters (Reference 40-2). Assessments of condensed debris thickness were made by assuming that the debris is dispersed throughout the AP600 cavity (Reference 40-3). An upper bound of 43 centimeters results from assuming that the debris includes the mass of UO_2 zirconium, the core support plate, and the reactor vessel lower head. This value overstates the debris thickness because the reactor vessel lower head may not be part of the debris, especially if the cavity is flooded or partially flooded. If the reactor vessel lower head is excluded, the condensed debris thickness becomes 25 centimeters. If any part of the core remains in-vessel, or if the entire core support plate is not molten, the uniform, condensed debris thickness would be less than 25 centimeters.

40.2.3 Ex-Vessel Steam Explosions

If the reactor vessel fails and the cavity is flooded or partially flooded, there is the potential for a steam explosion in the cavity. A steam explosion promotes coolability by fragmenting debris and dispersing it throughout the cavity and perhaps other parts of the containment. Therefore, debris dispersal is likely if a steam explosion occurs. The likelihood of an ex-vessel steam explosion is the subject of a separate decomposition event tree.

40.2.4 Debris Configuration

The potential debris configuration must also be considered in the event that a high-pressure melt ejection or steam explosion does not occur. Two configurations are possible: a continuous phase underlying coolant and a fragmented debris bed. A continuous phase, or slab, is expected whenever there is insufficient water to quench and fragment the debris initially. A fragmented debris bed can become continuous if decay heat cannot be removed and the debris re-melts.

Debris coolability can be limited in the slab configuration if the heat transfer mechanism is one-dimensional conduction. One-dimensional conduction occurs if cracking and water ingression into the debris does not occur. A large stable crust across the top of the debris might prevent cracking and water ingression, but stable crusts on the AP600 scale have not been observed experimentally. Stable crusts have been observed in small-scale molten core-concrete interaction experiments (References 40-4 and 40-5). Argonne National Laboratory performed similar, but dry, experiments for the Aerosol Containment Experiments program, but stable continuous crusts were not observed in the 50 cm square test apparatus. Evaluations of crust phenomenology (suspended or floating) suggest that the crust phenomenology varies with increasing scale. The results may indicate that a stable crust is less likely in the AP600 cavity design, which is much larger than any test apparatus used to date.

The debris bed will be fragmented if any of the following occur: a steam explosion in the cavity, high-pressure melt ejection, or the debris falls through a deep water pool. The depth of the water pool required for jet break-up is given by (Reference 40-6):

$$\frac{L}{D} = 6.25 (\rho_j / \rho_o)^{1/2}$$

where:

- L = the break-up length
- D = the initial jet diameter
- ρ_j = the corium density
- ρ_o = the water density





Using a corium density of 8000 kg/m^3 and a water density of 1000 kg/m^3 , the break-up length (or pool depth) is 18 times the initial debris jet diameter. This result suggests that the required break-up length for a corium debris jet would be on the order of a few meters, with an exact value depending on the initial jet diameter and the pool temperature. The pool depth in AP600 is more or less limited by the 1.34 meters between the cavity floor and the reactor vessel lower head bottom. If the pool depth is much larger than 1.34 meters, ex-vessel cooling will, in all likelihood, prevent vessel failure. Therefore, partial debris fragmentation is expected in the absence of steam explosions or high-pressure melt ejection. Part of the debris bed may be fragmented, while other parts may be continuous pools. Partial debris fragmentation should still prevent the formation of a continuous slab that inhibits water ingress.

40.2.5 Debris Spreading

Debris must spread over the cavity floor to provide heat transfer surface area and reduce the debris thickness. High-pressure melt ejection or an ex-vessel steam explosion results in debris fragmentation and debris spreading. For other sequences, debris spreading may be limited by freezing, although debris spreading might occur even in low-pressure sequences with cavity flooding. Nonuniformly distributed debris that is not coolable will ultimately heat up, melt, and spread further. Gas sparging by concrete ablation aids in spreading of molten or partially molten debris.

40.2.6 Long-Term Heat Flux from the Debris to Overlying Water

To maintain debris coolability, the heat flux from the debris to overlying water must be large enough to remove decay heat in the long term. The AP600 cavity design meets the advanced light water reactor Utility Requirements Document design requirement (References 40-2 and 40-7). This requirement is based on a debris bed with water ingress and heat transfer capability equal to or greater than saturated flat plate critical heat flux. (The requirement also states that the sump depths must be kept to a minimum, or else sumps must be built with curbs or obstructions to keep debris out.) A heat flux of 1 MW/m^2 , which is actually slightly less than flat plate critical heat flux, but typical of 2 to 3 millimeters particle debris beds, is used as a reference. This reference heat flux is justified because film boiling is unstable for low thermal conductivity oxides and irregular surfaces. Also, a stable crust cannot be maintained, and water will ingress and contact the debris.

Several conservatisms are built into the advanced light water reactor requirement. A decay power of 1 percent and a design factor of 0.5 are both assumed. In the long term, a decay power of 1 percent is conservative because it corresponds to decay heat at about two or three hours into the accident - a very early vessel failure time for the AP600 design. The design factor states that the heat flux necessary to remove decay heat must really be less than 0.5 MW/m^2 . This requirement takes no credit for debris ejection from the cavity or debris retention within the vessel. The effective decay power would be reduced to 0.5 percent if vessel failure occurs at two or three hours, but 50 percent of the debris remains in-vessel. The





advance light water reactor requirement also takes no credit for vaporization of volatile fission products that can amount to 30 percent of decay heat (Reference 40-3).

The AP600 cavity area of 53 m² provides conservatism over and above the advance light water reactor requirement. The required heat flux for debris coolability in AP600 is given by:

$$q'' = \frac{0.01 (1933 \text{ MWth})}{53 \text{ m}^2} = 0.37 \text{ MW/m}^2$$

The required heat flux is reduced even further if vessel failure occurs well after two hours, or if volatile fission product vaporization is credited because of the reduced decay heat in the debris. If vessel failure occurs at, say, eight hours, (decay heat is 0.67 percent of rated power) and volatile fission product vaporization is credited, the required heat flux would be 0.17 MW/m².

Given debris dispersal and spreading over the full cavity area, the necessary heat flux for decay heat removal (0.37 MW/m² as an upper bound) is far less than the reference heat flux of 1.0 MW/m². Therefore, long-term heat flux is given no further consideration for the decomposition event tree. The decomposition event tree is concerned primarily with establishing debris dispersal or spreading.

40.3 Development of the Decomposition Event Tree

A number of assumptions are used to develop and quantify the ex-vessel debris coolability decomposition event tree:

- Vessel failure with cavity flooding is the initiating event for the decomposition event tree.
- High-pressure melt ejection does not occur.
- Partial debris fragmentation occurs if the cavity is initially flooded. The debris forms a continuous slab if the cavity is not initially flooded.
- The long-term heat flux from debris to overlying water will be large enough to remove decay heat if the debris is fragmented and covers the entire cavity area.

The decomposition event tree structure developed for quantifying the likelihood of ex-vessel debris coolability is presented in Figure 40-1. The questions posed at each node on the tree examine and quantify the uncertainties identified in the analysis presented in the previous sections. decomposition event tree nodes are as follows:

Node DM - Is the debris mass high (or low)?



Node SE - Do steam explosions occur?

Node DD - Is the debris dispersed and/or does it spread throughout the cavity?

End-states can be defined as follows:

NCC - No short-term molten core-concrete interaction; debris is coolable long-term.

SCC - Short-term molten core-concrete interaction occurs initially; debris is coolable long-term.

LCC - Short-term molten core-concrete interaction occurs; debris is not coolable long-term.

End-states NCC and SCC are successes while end-state LCC is not.

40.4 Quantification of the Decomposition Event Tree

This section discusses the assignment of the split fractions at each of the nodes of the decomposition event tree. Multiplication of each of the split fractions along a path of the tree results in the probability of the accident following that particular path. The summation of the probabilities of the paths that result in a particular end-state is the probability of the end-state.

40.4.1 Node DM

Is the debris mass high?

Success Criteria:

The mass of debris expelled at vessel failure is roughly the entire mass of the core. The mass of debris expelled is "low" if in-vessel debris retention is significant, (such as 30 to 50 percent).

The AP600 design suggests that most of the core will melt prior to vessel failure. The AP600 core is not segmented and fuel pins heat up fairly uniformly during an accident progression. There are no spots in the core that could stay relatively cool (as in a boiling water reactor core) until vessel failure. Because the AP600 design has no reactor vessel lower head penetrations and in many cases may be submerged in water for a period of time, the time between core relocation to the lower plenum and reactor vessel failure can be several hours. This allows continued heat transfer from the debris in the lower plenum to the damaged core region, instead of rapid vessel failure and relocation to the containment cavity. Debris accumulates and heats up continually in the lower plenum until vessel failure finally occurs and the debris relocates to the containment cavity.

MAAP4 analyses in Chapter 34 show that all of the core relocates to the lower plenum before vessel failure, and relocation to the containment cavity can occur. The same analyses also

show that the debris temperature increases steadily between relocation to the lower plenum and vessel failure. The MAAP4 analysis case 3BE.cc1 from Chapter 34 is considered here to illustrate. Case 3BE.cc1 is a severed direct vessel injection line with in-containment refueling water storage tank failure. Both accumulators and one core make-up tank are available, and at least one train of the automatic depressurization systems is operational. Passive containment cooling water is also available to cool the containment shell. The entire core relocates to the lower plenum prior to vessel failure, which occurs at about 11 hours. MAAP4 assumes the reactor vessel lower head fails at the bottom by creep rupture.

The debris mass expelled from the reactor vessel depends on the vessel failure mode (Reference 40-3). Jet ablation or impingement is not likely to fail the reactor vessel lower head because the AP600 design has no lower head penetrations. Analyses using the THIRMAL code developed by Argonne National Laboratory indicate complete corium jet breakup, droplet solidification, and particle quenching prevent or mitigate jet ablation and impingement on the reactor vessel lower head (Reference 40-8). Two other scenarios are possible. Initial reactor vessel failure might occur due to creep rupture of the reactor vessel wall, in the form of a local "blister" at or just above the debris surface. This failure mode prevents high-pressure melt ejection because the reactor coolant system gas exits and does not entrain debris; a crust forms on the top of the debris and prevents contact between the exiting gas and the liquid debris (Reference 40-3). This failure mode limits the amount of debris expelled from the vessel. Solid debris and perhaps some molten debris would remain in the vessel. On this reasoning, the MELTSPREAD analysis (discussed below) presented in (Reference 40-9) assumed that 25 percent of the debris remains in-vessel, although there was no strong support for this value. Moody states that the in-vessel debris retention could be somewhere between 30 to 50 percent (Reference 40-8), and suggests that water or steam entering the failed reactor vessel can cool debris and prevent it from relocating. An alternative scenario states that reactor vessel lower head fails globally (around the entire circumference of the lower head), and releases all the debris in the lower head to the cavity. This scenario has been analyzed by Rempe, et al. (Reference 40-10), but Rempe makes no judgment about the likelihood of global failure relative to local creep rupture failure.

Based on the discussion of vessel failure for the AP600 design in WCAP-13388 (Reference 40-3) and the calculation of vessel wall thinning in the in-vessel retention of core debris decomposition event tree Chapter 36, the best-estimate vessel failure mode for the AP600 is a local failure at the top of the debris pool accumulated in the lower plenum. Such a vessel failure would result in a low debris mass being ejected. Thus, the split fraction for expelling a low debris mass at vessel failure is assigned a value of 0.9.

Probability of high debris mass: 0.1
Probability of low debris mass: 0.9



40.4.2 Node SE - Steam Explosions

Do steam explosions occur?

Success Criteria:

Steam explosions sufficient to disperse debris, given cavity flooding and vessel failure.

The probability of ex-vessel steam explosions, given vessel failure and cavity flooding, is included as part of the steam explosions decomposition event tree. For the ex-vessel cooling decomposition event tree, the intermixing of finely fragmented core debris and water causes a sufficient steam explosion to disperse the debris. This probability is 0.1, based on the results of node MX in the ex-vessel steam explosion decomposition event tree.

Probability of ex-vessel steam explosion: 0.1

Probability of no ex-vessel steam explosion: 0.9

40.4.3 Node DD - Debris Dispersal

Is the debris dispersed and/or does it spread throughout the cavity?

Success Criteria:

In the absence of high-pressure melt ejection or steam explosions, the debris spreads to cover the entire cavity and assumes a coolable (thin) layer.

Corium spreading with an overlying pool has been considered through several different approaches (References 40-2 and 40-8) and in Chapter 36, although for the AP600 design, results seem consistent. The different approaches are considered here for the AP600 cavity design. Debris spreading in water pools has been considered experimentally by Greene (Reference 40-13). Greene characterized debris spreading by a spreading number N_{sp} and dimensionless thickness t^* as follows:

$$N_{sp} = \frac{(M/\rho)^{1/3} h_s}{H h_{tg}^*}$$

$$t^* = (M/\rho)^{1/3} t$$

where:

M	=	debris mass (kg)
ρ	=	debris density (kg/m ³)
h_s	=	debris enthalpy, including superheat (J/kg)
h_{tg}^*	=	water enthalpy, including subcooling (J/kg)
H	=	water depth (m)
t	=	debris thickness (m)

A correlation for the dimensionless thickness and spreading number is given by:

$$t^* = 0.026 N_{sp}^{-1/2}$$

The following values are appropriate for the AP600 design (References 40-2 and 40-3):

M	=	120,000 kg
ρ	=	8000 kg/m ³
A	=	53 m ²
h_s	=	1.25E6 J/kg
H	=	2 m
h_{fg}^*	=	2.56E6 J/kg

This results in the following:

N_{sp}	=	0.62
t^*	=	0.0331
t	=	0.08 m

The actual debris thickness would be 25 centimeters, assuming the debris spread uniformly about the cavity. Because the thickness predicted by Greene's correlation is less than 25 centimeters, the debris would be expected to spread uniformly throughout the cavity. Note that Greene's experiments did not include molten debris-concrete interaction, which suggests that this correlation underpredicts the actual debris spreading expected under severe accident conditions.

Moody considered molten core debris spreading in advanced light water reactors (Reference 40-8). Moody did not feel that Greene's experiments could be applied to the AP600 design. Moody presented results from the MELTSPREAD code, analytical calculations, and scaling analyses of corium spreading. MELTSPREAD was developed by Argonne National Laboratory to predict corium spreading (Reference 40-9). MELTSPREAD treats the phenomena of spreading, puddling, freezing, remelting, core-concrete interaction, convective heat transfer, and internal heat generation. Two key uncertainties in corium spreading are the debris viscosity and debris temperature at which spreading stops. For the calculations presented in (Reference 40-8), MELTSPREAD assumes Newtonian variation of viscosity with temperature and debris immobilization when the debris temperature reaches the solidus value. In one case, MELTSPREAD was applied to the cavity design shown in Figure 40-2, subject to these assumptions:

- The vessel is submerged.
- The release rate is 8200 kg/s for 10 seconds.
- The debris superheat is 12 K, and the debris temperature must decrease 92 K to freeze.



- d.) The initial water subcooling is 30 K.
- e.) The concrete is limestone.

The calculation included a detailed representation of the AP600 circular cavity, rectilinear keyway, doorway to the reactor coolant drain tank, and the reactor coolant drain tank compartment. One-dimensional spreading was calculated using 25 nodes to represent the complicated cavity geometry (Figure 40-2).

The geometry considered for the MELTSPREAD analysis presented in Reference 40-9 is not the current AP600 cavity design. It is similar in size and configuration to the current AP600 design, however, and the results of the MELTSPREAD analysis are still worthwhile. MELTSPREAD results for the selected cavity design show little "maldspreading" or concrete ablation. MELTSPREAD predicts that by 60 seconds, the melt layer within the cavity is approximately uniform. A second case was considered with a debris superheat of 0 K. MELTSPREAD still predicts uniform spreading over the full cavity region. MAAP4 results show that the debris superheat can be much greater than 12 K and suggest that both MELTSPREAD results may be conservative for most AP600 accident sequences.

Melt spreading was considered by Kazimi (Reference 40-11) for the Mark I boiling water reactor containment liner melt-through concern. Kazimi considered semi-circular debris spreading on a dry floor. This approach is adapted here to consider the case with overlying water. The AP600 cavity geometry is not modeled, but circular debris spreading is assumed instead.

A heat balance for the leading edge can be written as:

$$\rho c \frac{dT}{dt} (2\pi r \delta) = q''' (2\pi r \delta) - q_D^* 2\pi r - q_u^* 2\pi r \quad (1)$$

where:

- ρ = the debris density
- c = the debris specific heat
- r = the outermost radius
- δ = the debris depth
- q''' = the volumetric heat source
- q_D^* = the heat loss to concrete
- q_u^* = the heat loss to water

The volumetric heat source must include chemical reaction rates that can dominate decay heat. Gases liberated during core-concrete interaction react with zirconium. The heat generation rate is limited by the rate at which concrete can be decomposed. In turn, the rate at which concrete can be decomposed is limited by the downward heat flux. If Q_c is the maximum chemical reaction rate per unit weight of the concrete, then:

$$q''' \delta = Q_r \frac{q_D}{H_{sf}} \quad (2)$$

where H_{sf} is the decomposition enthalpy. If f is the fraction of the decomposed gases that react within the melt, then the heat balance can be written as:

$$\rho c \frac{dT}{dt} (2\pi r \delta) = q_D 2\pi r \left\{ 1 - f \frac{Q_r}{H_{sf}} \right\} - q_u 2\pi r \quad (3)$$

Assuming:

$$\dot{m} = \rho 2\pi r \delta \frac{dr}{dt} \quad (4)$$

and:

$$\psi = 1 - f \frac{Q_r}{H_{sf}} \quad (5)$$

then:

$$\dot{m} c \frac{dT}{dr} = - q_D 2\pi r \psi - q_u 2\pi r \quad (6)$$

Heat fluxes q_D and q_u must be specified. Before melt solidification, q_D can be approximated by:

$$q_D = 20 (T - T_D)^2 \text{ W/m}^2 \quad (7)$$

where T_D is the concrete decomposition temperature. The reference heat flux of 1 MW/m² is used for q_u . Substituting these assumptions into equation 6:

$$\frac{dT}{dr} = - \frac{(20 (T - T_D)^2 \psi + q_u) 2\pi r}{\dot{m} c} \quad (8)$$

Values for ψ , \dot{m} , and c must be specified, as well as initial conditions for the debris temperature and spreading radius, to evaluate equation 8. Kazimi used the data presented in Table 40-1. Limestone/common-sand properties are used here. Values of $Q_r = 2.2$ MJ/kg and $H_{sf} = 3.6$ MJ/kg are used, and $f = 0.5$, by assumption. Therefore, $\psi = 0.69$. The specific heat



used by Kazimi is 600 J/kg for an oxidic pour. The pour rate \dot{m} is uncertain, but the discussion presented for node DM shows that entire core debris mass can relocate from the lower plenum to containment cavity. AP600 pour rates should be large, relative to the pour rates used in (Reference 40-12) to evaluate the Mark I boiling water reactor liner melt-through issue (i.e. 100 to 800 kg/s). For the MELTSPREAD analysis discussed above, 8200 kg/s was applied for 10 seconds. To account for uncertainties, pour rates between 1000 kg/s and 10000 kg/s are considered here. A value of 0.2 meters is assumed for the initial pour radius and 2600 K is assumed for the initial debris temperature.

To evaluate equation 8, approximate the final spreading radius by:

$$A_c = \pi r_f^2$$

where A_c is the cavity area and r_f is the spreading radius. For a cavity area of 53 m², $r_f = 4.1$ m. Equation 8 is evaluated to find the temperature at the debris spreading front, T_f . If T_f is greater than 2200 K, debris spreading to r_f occurs. Equation 8 was integrated numerically to yield the following results:

\dot{m}	r_f	T_f
1000 Kg/s	4.1 m	1920 K
2000 Kg/s	4.1 m	2117 K
8200 Kg/s	4.1 m	2432 K
10000 Kg/s	4.1 m	2458 K

Although the application of Kazimi's analysis to the AP600 is approximate, these results suggest that for high pour rates (greater than 3000 Kg/s) the leading edge of the debris will not cool to immobilization before spreading throughout the cavity. At reactor vessel failure, the debris mass in the lower plenum relocates quickly to the containment cavity. The debris pour rate is very large if the lower head fails globally due to creep rupture around the reactor vessel circumference.

The foregoing analyses demonstrate that the debris should spread about the AP600 containment cavity. None of these analyses consider the AP600 cavity design exactly and each is subject to uncertainty. The probability of debris spreading throughout the cavity is assigned a value of 0.9. This reflects a lack of conclusive analysis for the AP600 cavity design, rather than any randomness in the debris spreading process. This probability could increase, so as to approach 1.0, if further analyses are performed for the AP600 design.

Probability of debris spreading throughout the cavity: 0.9
Probability of "malspreading": 0.1



40.5 Results

The results of the AP600 ex-vessel debris coolability decomposition event tree are summarized below.

The amount of debris released from the vessel is highly uncertain. Vessel failure could occur locally due to creep rupture in the lower head, and some fraction of the debris could remain in-vessel. Vessel failure could occur globally due to creep rupture along the diameter of the reactor vessel lower head, and the entire contents of the lower head could relocate to the cavity.

Debris spreading is likely even for low pressure sequences with cavity flooding. The long-term heat flux to overlying water will be large enough to remove decay heat because debris dispersal and spreading create the necessary heat transfer surface area.

End-states with a high debris mass expelled could show short-term concrete ablation, but significant molten core-concrete interaction will not occur if the debris spreads throughout the containment cavity. End-states with a low debris mass could show short-term concrete ablation, but significant molten core-concrete interaction will not occur.

End-state frequencies are summarized as follows:

End-state SCC - 0.162

End-state LCC - 0.009

End-state NCC - 0.829

40.6 References

- 40-1 NRC letter to All Licensees Holding Operating Licenses and Construction Permits for Nuclear Power Reactor Facilities, "Individual Plant Examination for Severe Accident Vulnerabilities - 10 CFR 50.54(f)," Generic Letter No. 88-20, dated November 23, 1988.
- 40-2 *Technical Support for the EPRI Debris Coolability Requirement for Advanced Light Water Reactors (Task 8.3.5.6)*, Fauske & Associates, Inc., December 1988.
- 40-3 *AP600 Phenomenological Evaluation Summaries*, WCAP-13388 (Proprietary) Rev. 0, June 1992, and WCAP-13389 (Non-proprietary), Rev. 1, 1994.
- 40-4 Tarbell, W. W., "Core/Concrete Experiments at Sandia National Laboratories," U.S. NRC LWR Safety Meeting, Gaithersburg, MD, 1981.



- 40-5 Blose, R. E., et al., *SWISS: Sustained Heated Metallic Melt/Concrete Interactions with Overlying Water Pools*, NUREG/CR-4727, SAND85-1546, Sandia National Laboratories, July 1987.
- 40-6 Epstein, M. and H. K. Fauske, "The Three Mile Island Unit 2 Core Relocation - Heat Transfer and Mechanism," *Nuclear Technology*, Vol. 87, pp 1021-1035.
- 40-7 *Advanced Light Water Reactor Requirements Document*, Vol. III, Revs. 5 and 6, December, 1993.
- 40-8 Levy, S., et al., *Assessment of Ex-vessel Debris Coolability*, September 30, 1991.
- 40-9 Chu, C. C., and J. J. Sienicki, *MELTSPREAD-1 Calculations of the Transient Spreading of Core Materials in the AP600 and SBWR Containments*, ANL/RE/LWR91-3, July 1991.
- 40-10 Rempe, J. L., et al., *Light Water Reactor Lower Head Analysis (Draft)*, NUREG/CR-5642, EGG-2618, December, 1990.
- 40-11 Kazimi, M. S., "On the Liner Failure Potential in Mark-I Boiling Water Reactors," *Nuclear Technology*, V. 103, pp. 59-69.
- 40-12 Frost, D. L., B. Bruckert, G. Ciccarelli, "Effect of Boundary Conditions on the Propagation of a Vapor Explosion in Stratified Molten Tin/Water Systems," CSNI-FCI Specialist is Meeting Santa Barbara, CA, January 1993.
- 40-13 Greene, G. A., et al., "Experimental Studies on Melt Spreading, Bubbling Heat Transfer, and Coolant Layer Boiling," 16th Water Reactor Safety Information Meeting, Gaithersburg, MD, October 24-27, 1988.

Table 40-1

PROPERTIES OF THE MAIN CONCRETE TYPES (FROM REFERENCE 40-11)

	Limestone	L/CS	Basaltic
Solidus Point, T_{sol} (K)	1690	1420	1350
Liquidus Point, T_{liq} (K)	1875	1670	1650
Decomposition Point, ^a T_D (K)	1750	1500	1450
Decomposition Enthalpy, H_D (MJ/kg)	2.5	1.8	0.83
Effective Heating Enthalpy, ^b H_{st} (MJ/kg)	5.0	3.6	2.75
Water Content, H_2O (wt%)	6.0	4.7	2.0
Gas Content, CO_2 (wt%)	36	21	1.5
Gas Reaction Energy, ^c Q_r (MJ/kg)	3.2	2.2	0.42

$$^a T_D = T_{sol} + 0.33 (T_{liq} - T_{sol})$$

$$^b H_{st} = H_D + \int_{300}^{T_D} c_p dT$$

$$^c Q_r = \frac{1}{100} \left(\frac{\text{wt}\%}{18} Q_{H_2O} + \frac{\text{wt}\%}{44} Q_{CO_2} \right)$$

$$Q_{H_2O} = 300 \text{ MJ/kg mol } H_2O$$

$$Q_{CO_2} = 270 \text{ MJ/kg mol } CO_2$$





40. Decomposition Event Tree - Analysis of Ex-Vessel Debris Coolability

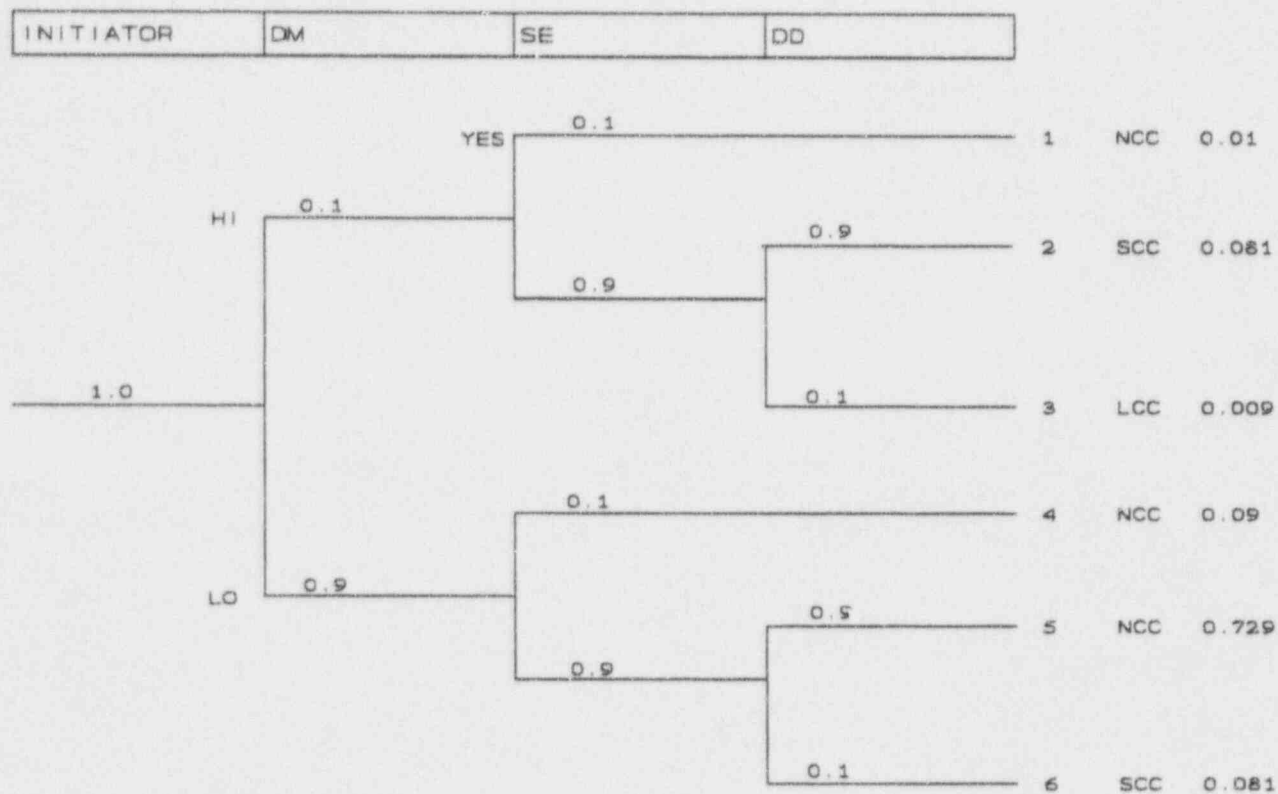


Figure 40-1

Ex-Vessel Debris Coolability Decomposition Event Tree

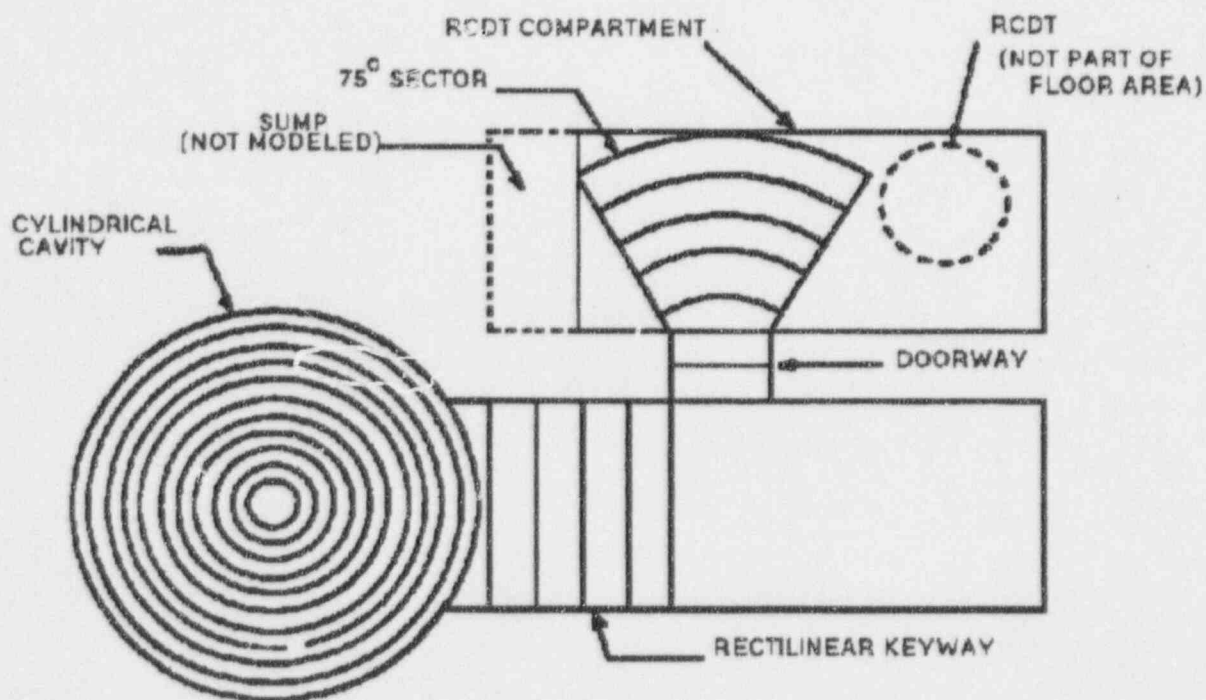


Figure 40-2

MELTSPREAD Nodalization for the AP600, From Reference 40-10



Westinghouse

ENEL
ENTE NAZIONALE
PER L'ENERGIA ELETTRICA



CHAPTER 41

DECOMPOSITION EVENT TREE - HYDROGEN COMBUSTION ANALYSIS

The likelihood of a global burning of combustible gases in the containment and the challenge to the containment integrity are considered in this analysis. A global burn is defined as a combustion event that occurs containment-wide with a hydrogen (and a carbon monoxide) concentration at or above the lean downward flame propagation limits and includes deflagrations and detonations. The probability of such an event is quantified using decomposition event trees (DETs). The results of the quantification of the decomposition event tree provide input to nodes HC1, HC2, and HC3 on the AP600 containment event tree (CET). In the containment event tree, node HC1 indicates the likelihood of a global burn during the in-vessel phase of the accident, node HC2 indicates the probability of a global burn prior to 24 hours after the onset of core damage, while node HC3 indicates the probability between 24 and 72 hours after the onset of core damage. This analysis also provides input to the quantification of the containment failure nodes CF1, CF2, and CF3 on the containment event tree.

41.1 Discussion of the Issue

In the course of a severe accident in the AP600 plant, a substantial amount of hydrogen and carbon monoxide can be generated because of the oxidation of metals. The AP600 containment is provided with glow plug igniters to control the concentration of the combustible gases. However, combustible gas can accumulate in the containment at flammable concentrations if the igniter system fails to function. The amount and type of combustible gases produced depends on the progression of the accident.

If vessel failure does not occur, the amount of hydrogen in the containment is limited to the in-vessel generation only. If vessel failure occurs with water in the cavity, an additional amount of hydrogen may be generated from ex-vessel fuel-coolant interactions. Furthermore, if the debris layer in the cavity is not coolable or if insufficient water is available in the containment to cool the debris, and subsequent thermal attack of concrete occurs, an additional amount of hydrogen and other combustible gas, such as carbon monoxide, can be generated.

Since the pressure rise or dynamic loads associated with a large energy release from a combustion event in the containment could be substantial, the containment integrity depends on the likelihood of combustion and the containment pressure at the time of the burn. Hydrogen combustion is evaluated during three time frames: early, intermediate, and late. The early time frame is from the onset of core damage until vessel failure (or until complete core relocation to the lower head of the vessel if no vessel failure occurs). The intermediate time frame is from vessel failure (or until complete core relocation if no vessel failure occurs) to 24 hours after the onset of core damage. The late time frame is from 24 to 72 hours after the onset of core damage.



Westinghouse

ENEL
ENTE NAZIONALE
PER L'ENERGIA ELETTRICA

Revision: 3
February 28, 1995

41.2 Controlling Phenomena

Conditions required for combustion in the containment are the flammability limits of the containment gas mixtures and the presence of an ignition source. Typically, a spark is sufficient to cause ignition. If the mixture temperature is above ~1000 K, auto-ignition can occur without the presence of an ignition source. The flammability limits are determined by the concentrations and temperature of the combustible gas-air-inertant mixture. Hydrogen, carbon monoxide, and the oxygen in the air are the reactants in the combustion reaction. Steam, carbon dioxide, and excess nitrogen in the mixture act as inertants that may inhibit the reaction.

Hydrogen-air-steam mixtures can burn in several modes: diffusion flames, slow and accelerated deflagrations, and detonations (Reference 41-1). Burning of unmixed hydrogen near the source results in a diffusion flame. Diffusion flames are stationary and result primarily in thermal loads on nearby structures or equipment. Deflagrations or detonations are burning of premixed mixtures. In practical terms, a slow deflagration is a flame that travels at a speed much slower than the speed of sound such that the pressure inside the containment equilibrates during the combustion. No dynamic loads are generated. Accelerated deflagrations or accelerated flames travel fast enough to generate shock waves and dynamic loads. Detonations travel at supersonic velocities and also generate significant dynamic loads. The static loads that result from deflagrations can be predicted and bounded. The maximum dynamic loads from accelerated flames and detonations are difficult to calculate.

The static loads associated with deflagrations are limited by thermodynamics. If all of the chemical energy available in the mixture is converted to temperature and pressure, then the maximum pressure is limited by the adiabatic isochoric (constant volume) complete combustion (AICC) pressure. The actual pressure would drop over time from this peak because of heat losses to water, structures, and equipment in containment. Dynamic pressure loads are not limited by the adiabatic isochoric complete combustion value because the local pressure is due to very rapid, nonequilibrium combustion.

The mode of combustion depends on the mixture concentrations, initial conditions and boundary conditions (Reference 41-1). Near the hydrogen source, hydrogen will not be mixed significantly with the air in the containment. If ignition occurs there, then a diffusion flame may be formed. Further downstream from the hydrogen source, mixing will have occurred and a deflagration or detonation may result, depending on the hydrogen concentration and geometric boundary factors. In some cases, accelerated flames may also develop to detonations and are usually called deflagration-to-detonation transition (DDT). The degree of flame acceleration and occurrence of deflagration-to-detonation transition depend in complex and incompletely understood ways on a number of parameters. These include hydrogen and oxygen concentrations; nature and concentration of inertants; gas temperature and pressure before ignition; ignition source; the size and shape of the compartment in which the combustion occurs; and the number, size, and shape of any obstacles in the compartment.



In AP600, the likelihood of direct initiation of detonation by sufficiently high energy sources from equipment in containment does not exist (Reference 41-2), but mechanisms to amplify a flame to a detonation may occur. Deflagration-to-detonation transition is considered the most likely mechanism. Transition to detonation is considered in several sections of the containment (Reference 41-2) for accident sequences that result in hydrogen concentrations greater than 10 volume percent, including the tunnel connecting the two steam generator compartments, the core makeup tank and equipment bay, in-containment refueling water storage tank gas space, steam generator compartments, and steam generator annulus.

Standing diffusion flames on the in-containment refueling water storage tank pool or at the in-containment refueling water storage tank vents can be postulated early into an accident following core uncover for sequences where the automatic depressurization system provides a primary depressurization mechanism. A standing diffusion flame at the vent could present a significant thermal load to the containment steel shell, which is close to some of the vents. However, a stable, standing flame at the vent exit is difficult to produce and is considered to be highly unlikely. Hydrogen released to the in-containment refueling water storage tank is expected to mix with containment air in the gas space above the water such that, when ignited by a glow plug at the vent exit, the flame front flashes back and consumes the bulk of the hydrogen in the tank. Depending on the amount of hydrogen released and the duration, this could result in periodic deflagrations in the in-containment refueling water storage tank. This type of burning does not result in a significant thermal loading on the containment shell since the burn lasts for only a short time (on the order of seconds), and the thermal inertia of the containment wall would prevent the temperature from increasing more than several degrees.

Hydrogen mixing analyses and, if needed, adjustment to the vent design, will be used to assure that the diffusion flame induced containment failure mode makes an insignificant contribution to the large release frequency in the AP600 PRA. Diffusion flames at the in-containment refueling water storage tank vent exits are not considered as a containment failure mode in this analysis.

In an unlikely event of reactor vessel lower head failure accompanied by debris dryout and severe core-concrete attack of the reactor cavity floor, gases in the cavity would be at high temperatures as well as rich in hydrogen. Such a scenario would require failure of most of the safety injection features. Combustion may occur in the cavity because of auto-ignition. Standing diffusion flames above the debris or at the cavity exit may also be possible. This mode of combustion has negligible effects on containment pressures, but could be significant in reducing the unburned amount of combustible gases and oxygen in the containment (Reference 41-3). Thermal loads from such diffusion flames are inside the containment compartments and do not present a threat to the containment shell.

41.3 Assumptions and Phenomenological Uncertainties

Because of phenomenological uncertainties, a number of assumptions are necessary in the construction and quantification of the decomposition event tree.



41.3.1 Degree of Cladding Oxidation

The degree to which the cladding is oxidized during the in-vessel phase of the accident sequence determines the amount of hydrogen released to the containment during the early time phase. The mass of hydrogen produced is an important parameter in determining the hydrogen concentration and the flammability limits of the gas mixtures in the containment compartments.

For each of the accident classes examined on the containment event tree, a best-estimate and a bounding-estimate of the integrated hydrogen mass produced during the in-vessel phase have been made. These estimates are based on MAAP4 analysis of the accident sequences, consideration of the uncertainties in the MAAP4 models, the events that occurred during the Three Mile Island Unit 2 accident, and a review of the expert opinion elicitation for in-vessel issues performed for NUREG-1150 (Reference 41-4). The estimate also considers the effect of water addition to the core pre- and post-relocation and to debris in the lower head of the reactor vessel.

The estimates for hydrogen production for each accident class are presented in Table 41-1. The best-estimate hydrogen production for each accident class is the mass of hydrogen produced in the MAAP4 analysis of the accident sequence that represents the accident class. The upper bound-estimate for each accident sequence is based on the review of the hydrogen production described above. A brief description of the events contributing to the hydrogen production for each accident class is provided below.

Accident class 1A, high pressure sequence: the core is uncovered and initially heats up until the hot leg nozzle fails because of creep. The accumulators inject, reflood, and quench the overheated but intact core. A second heatup occurs, and the core relocates to the lower head. A small amount of in-containment refueling water storage tank water can inject into the vessel when the debris dries out.

Accident class 1AP, small loss-of-coolant accident (LOCA) with passive residual heat removal and no depressurization: the core uncovers, heats up, and relocates to the lower head. A small amount of in-containment refueling water storage tank water can inject into the vessel when the core debris dries out.

Accident class 3BE with no reflood, fully depressurized with gravity injection failure: the core uncovers, heats up, and relocates to the lower head. No water addition can occur.

Accident class 3BE/3BR with reflood, operator floods cavity: the core uncovers, heats up, and begins to form a molten pool in the core region. When the water level in the cavity reaches the break elevation, water refloods into the vessel. A significant portion of the core is blocked by the formation of the molten pool and remains hot after the reflood. Zirconium in the crust of the debris and in relocating pool material oxidizes, and hydrogen production continues for a time, even after the reflood has covered the core region. Accident class 3BR

cases are lumped into this category because of the post-core damage reflood and potential for additional hydrogen production.

Accident class 3C, vessel rupture: the core uncovers very rapidly at the accident initiation, heats up rapidly, and relocates. Water injection cannot reflood the core until the cavity is filled. After that time, the injection rate cannot keep pace with the quench rate. Hydrogen production is limited by the core relocation.

Accident class 3D, partial depressurization: the core uncovers, heats up, and relocates to the lower head. A small amount of in-containment refueling water storage tank water can inject into the vessel when the core debris dries out.

41.3.2 Flammability Limits

A flammable condition is determined by flammability limits. Flammability limits of a combustible gas mixture are defined as the limiting gas compositions at a given temperature and pressure in which a deflagration once ignited will propagate. There is relatively good information on flammability limits of hydrogen-air-steam mixtures at temperatures less than 149°C. At higher temperatures, such information is lacking. For this reason, extrapolation of flammability limits to higher temperature, as in the model developed by the Advanced Reactor Severe Accident Program for use in the MAAP4 code (Reference 41-5), and shown in Figure 41-1, is considered to be a reasonable approach.

For hydrogen, there are two lean propagation limits considered, upward and downward. At lean upward propagation limits, flames will propagate upward because of buoyancy. At lean downward propagation limits, flames will propagate upward and downward throughout the volume by their own reaction kinetics. Hence, the extent of flame propagation (or combustion completeness) for combustion at lean flammability limits is determined by the hydrogen concentration. This relation is clearly shown in Figure 41-2, which is a result from the Nevada Test Site (Reference 41-6). For decomposition event tree quantification, the gas compositions obtained from MAAP4 runs and the MAAP4 flammability limits curves are used to determine the flammability conditions of an accident.

41.3.3 Definition of Global Burn

Combustion initiated by igniters occurs at lean upward flammability limits with a small pressure rise. However, with the failure of igniters, combustion of much larger pressure and temperature consequences at a hydrogen concentration above the lean downward propagation limits may result. For this reason, the global burn considered in the decomposition event tree evaluation is defined as combustion at or above the lean downward propagation limits. This definition includes the possibility that a global burn becomes a detonation, since the occurrence of a detonation requires a hydrogen concentration much above the lean downward propagation limits. Combustion regimes and associated adiabatic isochoric complete



combustion pressure are approximately demonstrated in Figure 41-3 for certain conditions (Reference 41-7).

41.3.4 Detonation Limits and Loads

A detonation is a supersonic combustion front that produces a dynamic load in excess of the adiabatic isochoric complete combustion value. The energy release from the combustion of the hydrogen-air-steam mixture sustains the shock structure that ignites and burns the mixture. The detonation limits cannot currently be predicted by any first-principles theory. Engineering correlations used to predict the limits have been developed based on a measurable quantity called the detonation cell width. For simplified discussion, the detonation cell width can be considered a characteristic length that describes the sensitivity of the mixture to detonation. The smaller the detonation width, the easier it is to get the mixture to detonate and sustain propagation. For the decomposition event tree quantification, it is assumed that the likelihood of direct initiation of detonation by sufficiently high energy sources from any objects in the containment during accident conditions does not exist (Reference 41-2). Only deflagration-to-detonation transition is considered, and the method of NUREG/CR-4803 (Reference 41-8) is used for deflagration-to-detonation transition evaluation. This method is summarized in Reference 41-2.

Deflagration-to-detonation transition evaluations for hydrogen burns during intermediate and late time frames (after the in-vessel phase) may also involve a significant volume fraction of carbon monoxide generated ex-vessel. Deflagration-to-detonation transition due to carbon monoxide in air is relatively unknown because the burning velocity of carbon monoxide in air is much smaller than that of hydrogen. Hence, it is expected that the contribution of carbon monoxide to deflagration-to-detonation transition is small.

For decomposition event tree quantification, it is assumed in the deflagration-to-detonation transition evaluation method that the hydrogen concentration used in the calculation is the sum of the concentrations of hydrogen and carbon monoxide. This conservatively bounds the effects of carbon monoxide on the likelihood of deflagration-to-detonation transition. Since the lowest hydrogen concentration for which deflagration-to-detonation transition has been observed in an intermediate scale FLAME facility at Sandia is 15 percent (Reference 41-9), the likelihood of deflagration-to-detonation transition is assumed to be zero if the combined combustible gas concentration is less than 10 percent.

To evaluate deflagration-to-detonation transition loads, it is assumed that the detonation peak pressure is given as 4.5 adiabatic isochoric complete combustion pressure which is the maximum reflected peak pressure in one-dimensional geometry (Reference 41-10).

41.3.5 Igniter System

The AP600 igniter system, if operational during a severe accident, will burn hydrogen as soon as the lean upward flammability limits are met. Thus, the concentration of hydrogen is maintained, on average, at the lean upward flammability limits. However, depending on the

hydrogen release rate and location, a locally high concentration may exist in the in-containment refueling water storage tank or in the subcompartment where the pipe break occurs. According to the analysis to demonstrate the AP600 compliance with 10 CFR 50.34(f) (Chapter 47), hydrogen combustion due to the operation of the igniter system results in low hydrogen concentrations during the transients even with artificially high hydrogen generation rates assumed in the analysis. Therefore, for accident scenarios in which the igniter system is operational, a zero conditional probability of having a global burn is assumed, if the igniter system is operational from the onset of the accident.

41.3.6 Other Ignition Sources

The scenarios with large uncertainties in an occurrence of a combustion event are those in which the igniter system fails to function. A flammable mixture will not burn without an ignition source unless the temperature of the mixture is raised up so high (~1000 K) that auto-ignition becomes possible. An unquenched debris in a relatively dry cavity can be defined as an ignition source. The highest, but still low, likelihood of having ignition sources (other than the igniter system) for less extreme conditions where the core relocates to the lower head but the lower head remains intact, or vessel failure occurs but the debris is quenched in cavity, is from the following:

- High temperature core debris remaining on the reactor pressure vessel wall or high temperature internal structures following vessel failure
- High temperature gas exiting the reactor coolant system into the containment such as from the pipe break or the reactor pressure vessel lower head break

The ignition difficulty associated with the first source is that it is in the environment of high steam content. However, the chance increases with time (late into an accident) as the global steam concentration drops because of global pressure reduction from an operating passive containment cooling system. The initial ~60 percent steam concentration in the cavity following a short transient period, as shown in MAAP4 runs, approaches ~45 percent over the accident time. Although the debris cools off to some degree, an ignition can be postulated from the contact of high-temperature objects and a reasonably burnable mixture near the bottom of the broken reactor pressure vessel.

The difficulty associated with the second ignition source is that the exiting gas stream may not have enough momentum to entrain the surrounding flammable mixture to cause a reasonable level of mixing. The lack of jet mixing reduces the likelihood of ignition, which must rely on a less efficient heat transfer mode. Local auto-ignition due to high temperature at the break location may result in extensive flame propagation.

For decomposition event tree quantification, the likelihood of having ignition sources is assumed to be 0.5 during the in-vessel phase of the accident. For cases with intact vessel, the probability of a random ignition source is assumed to be 0.4 for an intermediate burn and 0.1

for a late burn. For combustion with vessel failure, the probability of a random ignition source is 0.3 for an intermediate burn and 0.4 for a late burn. This is based on a subjective judgment that the possibility exists but less than 0.5 after the in-vessel phase. The probability increases with time because of decaying cavity steam concentration for cases with vessel failure and decreases with time as the reactor coolant system cools down for cases with intact vessel.

41.3.7 Previous Global Burns

A global burn can consume a substantial amount of hydrogen generated in-vessel from the containment atmosphere. If a global burn has been determined to occur in the previous hydrogen combustion node or nodes on the containment event tree, the likelihood that hydrogen will build up to the flammable level again would depend on whether there is any significant generation of hydrogen and a sufficient amount of oxygen remaining after the burn. If the vessel remains intact, it would be unlikely to form even a slightly flammable mixture again, not to mention a concentration required for a global burn. If vessel failure occurs and the debris is not quenched or not immediately quenched, ex-vessel generation of hydrogen and carbon monoxide due to core-concrete interactions (CCI) could produce a flammable mixture of high combustible gas concentrations. Therefore, for the case in which the vessel remains intact or no core-concrete interaction occurs, the conditional probability of having a global burn, given that a global burn has occurred previously, is assumed to be zero.

41.3.8 Effects of Core-Concrete Interactions

Following the vessel failure event in which molten core debris falls onto the cavity floor, there are potential ex-vessel sources of hydrogen and carbon monoxide generation. These ex-vessel sources include the molten core-water interactions and core-concrete interactions in the reactor cavity. Because of the nature of the much longer time scale of core-concrete interactions (if debris is not cooled or is uncoolable), the combustible gas generation would be dominated by core-concrete interactions. If a global burn has occurred previously and no core-concrete interactions occur, as discussed in subsection 41.3.7, the probability that a global burn will occur again is considered to be zero. However, if core-concrete interactions occur, it would be necessary to consider an intermediate potential global burn regardless of the occurrence of an early global burn. If two global burns have occurred, the likelihood of another late global burn will also depend on the availability of oxygen, which may be too little to support a large burn.

41.4 Hydrogen Combustion during the In-Vessel Phase

When the reactor core is uncovered, the heat transfer from the cladding is significantly attenuated, and the cladding heats up. At temperatures above approximately 1200 K (1700°F), the zirconium in the cladding chemically reacts with passing steam, stripping the oxygen from the water molecules, producing hydrogen. This is commonly called the in-vessel hydrogen production. The likelihood of hydrogen combustion, deflagration and detonation, and the

threat to containment integrity during the early, in-vessel phase of the accident is investigated in this section.

41.4.1 MAAP4 Analyses for Early Hydrogen Combustion

MAAP4 analyses for each of the AP600 PRA accident classes with the hydrogen combustion models turned off provide information on the hydrogen mixing in the containment and possible peak pressures from randomly ignited burns. This section presents the results and conclusion of the MAAP4 analysis for each of the "no ignition" cases with respect to hydrogen combustion. For each of these cases, bounding hydrogen release sensitivities are also presented. A complete description of each of the accident sequences for these accident classes appears in Chapters 34 and 45.

The following "no ignition" cases are presented:

- Accident class 1A, loss of feedwater (Figures 41-4 through 41-12)
- Accident class 1AP, small loss-of-coolant accident with passive residual heat removal and failure to depressurize (Figures 41-13 through 41-21)
- Accident class 3BE, loss-of-coolant accident with fully depressurized reactor coolant system and gravity injection failure and no core reflood (Figures 41-22 through 41-30)
- Accident class 3BE, core not reflooded and passive containment cooling water failed (Figures 41-31 through 41-39)
- Accident class 3BE, core reflooded and passive containment cooling water failed (Figures 41-40 through 41-48)
- Accident class 3BE, core reflooded through break (Figures 41-49 through 41-57)
- Accident class 3C, vessel rupture (Figures 41-58 through 41-66)
- Accident class 3D, partial depressurization case (Figures 41-67 through 41-75)

A summary of the results of these sequences with respect to hydrogen combustion can be found in Table 41-2 for the best-estimate hydrogen generation cases and Table 41-3 for the bounding-estimate hydrogen generation cases.

The conclusions from the analyses with respect to early hydrogen combustion are summarized below.

- In cases in which the automatic depressurization system operates fully or partially, hydrogen is released to the in-containment refueling water storage tank through the

depressurization system spargers. The hydrogen concentration becomes high for a time, given the small volume of the tank and the no-ignition assumption. If the igniters are assumed to be operating, this concentration is held to the lower flammability limits and does not accumulate in the tank. If the igniters are not operational, a burn in the tank could undergo transition to detonation if a burn in the upper compartment could propagate to the in-containment refueling water storage tank (IRWST). The potential of deflagration-to-detonation transition in the in-containment refueling water storage tank for each case are presented in Tables 41-2 and 41-3. The potential for deflagration-to-detonation transition in the in-containment refueling water storage tank is determined based on the in-containment refueling water storage tank gas space conditions at the times that the containment is globally flammable.

- For the best-estimate hydrogen generation, accident classes 1A and 3BE/3BR with reflood are globally flammable and have the potential to undergo transition to detonation in the lower compartments of the containment.
- For the bounding estimate hydrogen generation, accident classes 1A, 3BE/3BR with reflood, and 3C are globally flammable and have the potential to transition to detonation.
- Failure of the passive containment cooling water causes the containment pressure to increase significantly, and only the bounding-estimate 3BE/3BR case with core reflood becomes globally flammable.
- For each of the cases that become globally flammable, the adiabatic isochoric complete combustion peak pressure and temperature for deflagration of the hydrogen are presented in Tables 41-2 and 41-3. None of the deflagration cases fail the containment based on the conditional containment probability distribution presented in Chapter 42.

41.4.2 Decomposition Event Tree Analysis for Early Hydrogen Combustion

The decomposition event tree structure for quantifying the likelihood of deflagrations and detonations in the containment during the in-vessel phase of the accident is presented in Figure 41-76. To answer the questions posed at each node on the tree, the examination and quantification of each of the uncertainties identified previously are required. Except for node DF/DT, the upward path at each node indicates a positive response to the question; the downward path indicates a negative response. The nodes chosen for the decomposition event tree are as follows:

- | | | |
|---------|---|---|
| Node OX | - | Is the hydrogen generation represented by the best-estimate hydrogen generation? |
| Node FL | - | Is the containment not globally flammable during the in-vessel phase of the accident? |

- Node IGS - Is there no ignition source present?
- Node DF/DT - Is the combustion initiated as a deflagration (upward branch) or a detonation (downward branch)?
- Node DDT1 - Does a burn fail to undergo transition to detonation in the in-containment refueling water storage tank?
- Node DDT2 - Does a burn fail to undergo transition to detonation below the operating deck?

The end-states of the tree represent the hydrogen combustion event that occurs during the in-vessel phase of the accident for the particular path. The end-states are as follows:

- NB - No global combustion
- GB - Global deflagration
- DD - Detonation by direct energy deposition
- DT - Deflagration-to-detonation transition

End-states DD and DT are assumed to lead to containment failure with a probability of 1.0.

A sequence of questions asked by the decomposition event tree is a logical check for the requirement of combustion. First, the amount of hydrogen generated and flammability limits are verified. Then the ignition source is checked. If both requirements are met, a combustion event will occur. Combustion will take place in the form of either deflagration or detonation depending on the hydrogen concentration and strength of the ignition source. If combustion results in deflagration, the possibility of deflagration-to-detonation transition is further checked.

41.4.3 Quantification of the Early Hydrogen Combustion Decomposition Event Tree

This section discusses the assignment of the split fractions at each of the nodes on the decomposition event tree. Multiplication of each of the split fractions along a path results in the probability of the accident following that particular path. The summation of the probabilities of the paths that result in a particular end state is the probability of that end-state.

41.4.3.1 Node OX

Is the hydrogen generation represented by the best-estimate hydrogen generation?

Success Criteria:

MAAP4 hydrogen generation representative of the accident class hydrogen generation.

The bounding-estimate hydrogen value is assumed to represent the hydrogen generation at three standard deviations on a normal distribution. Therefore, the failure of node OX is assigned the following value for all cases:

Failure Probability of Node OX = 0.025

Downstream Considerations:

The amount of hydrogen in the containment directly influences the flammability limits and likelihood of transition to detonation.

41.4.3.2 Node FL

Is the containment not globally flammable during the in-vessel phase of the accident?

Success Criteria:

Hydrogen concentration less than the downward flammability limit.

This node is assigned a value of either 0 or 1, based on the gas compositions and the containment temperatures for the best-estimate and bounding-estimate cases. The failure probabilities (containment globally flammable) for node FL for each case are summarized in Table 41-4.

Downstream Considerations:

If the containment gases are not flammable, then no combustion can occur.

41.4.3.3 Node IGS

Is there no ignition source present?

Success Criteria:

Flammable hydrogen not ignited in the containment.

As discussed in subsection 41.3.6, during the in-vessel phase, the probability of a random ignition source is assumed to be 0.5 in all cases. Therefore, the following failure probability is assigned to node IGS:

Failure Probability of Node IGS = 0.5

Downstream Considerations:

If there is no ignition source, hydrogen cannot burn regardless of the flammability of the gas mixture.

41.4.3.4 Node DF/DT

Is the combustion initiated as a deflagration or a detonation?

Success Criteria:

No source of sufficient energy to trigger detonation.

A review of the AP600 (Reference 41-2) concluded that no triggers of sufficient energy to trigger a direct detonation exist in the containment. Therefore, the following failure probability is assigned to node DF/DT:

Failure Probability of Node DF/DT = 0.0

Downstream Considerations:

A detonation in the containment leads to end-state DT and is assumed to fail the containment.

41.4.3.5 Node DDT1

Does a burn fail to undergo transition to detonation in the in-containment refueling water storage tank?

Success Criteria:

Upper compartment not globally flammable, or in-containment refueling water storage tank hydrogen mole fraction less than 0.1 or steam fraction greater than 0.4 or deflagration-to-detonation transition not predicted by methodology of Reference 41-8.

Given that the igniters are not functioning, the only ignition source for the in-containment refueling water storage tank gas space is a propagated flame from the upper compartment. If the upper compartment is not flammable, then no deflagration-to-detonation transition can occur in the in-containment refueling water storage tank. If the hydrogen mole fraction is less than 0.1 or if the steam mole fraction is greater than 0.4, then the detonation cell width is too large to consider detonation.

Based on the above success criteria and the methodology for calculating the likelihood of deflagration-to-detonation transition, there are four cases in which the failure probability of node DDT1 is non-zero. These cases and the failure probability of node DDT1 are presented in Table 41-5.

Downstream Considerations:

A detonation in the containment leads to end-state DT and is assumed to fail the containment.



41.4.3.6 Node DDT2

Does a burn fail to transition to detonation in the lower compartment?

Success Criteria:

Hydrogen mole fraction less than 0.10 or steam mole fraction greater than 0.40 or deflagration-to-detonation transition not predicted by methodology of Reference 41-8.

Based on the success criteria, there are six cases that have a non-zero probability of undergoing a transition to detonation. These cases and the failure probabilities are presented in Table 41-6.

Downstream Considerations:

A detonation in the containment leads to end-state DT and is assumed to fail the containment.

41.4.4 Early Hydrogen Combustion Decomposition Event Tree Quantification Results

The results of the quantification of the early hydrogen combustion decomposition event trees for each of the cases are presented in Table 41-7. For each case, the table shows the probability for each decomposition event tree end-state and the split fraction applied to the containment event tree node HC1 (early hydrogen combustion), and the split fraction applied to containment event tree node (early containment failure) CF1, given failure of HC1. Local detonations in the in-containment refueling water storage tank are conservatively assumed to result in containment failure with a probability of unity. Accident class 3BE/3BR with a reflooded core has the highest likelihood of containment failure since this case produces the most hydrogen and releases a portion of it through the in-containment refueling water storage tank, increasing the likelihood of local detonation.

41.5 Intermediate and Late Hydrogen Combustion

Following vessel failure, or after the in-vessel hydrogen production is completed, the hydrogen behavior in the containment must be assessed to determine impact on containment integrity in time frames out to 24 hours after core damage and from 24 to 72 hours after core damage. Containment event tree node HC2 and CF2 assess the hydrogen combustion and containment failure up to 24 hours after core damage, and nodes HC3 and CF3 assess the hydrogen combustion and containment failure probabilities to 72 hours. The split fractions for these nodes are determined in the following section.

41.5.1 MAAP4 Analysis Results and Conclusions for Intermediate and Late Hydrogen Combustion

The results of MAAP4 analysis are used to support the decomposition event tree construction and quantification of intermediate and late hydrogen combustion. A set of MAAP4 analyses have been performed to examine long-term hydrogen combustion and phenomena that may contribute to the likelihood of combustion and containment failure.



The accidents analyzed are initiated by a loss of all feedwater to the steam generators and by a 2-in. loss-of-coolant accident. Based on these two initiating events, sensitivities on in- and ex-vessel hydrogen production and flammability were performed so that a variety of accident conditions considered in the AP600 containment event tree would be covered. This includes cases in which the vessel remains intact, vessel failure occurs, passive containment cooling system operates or does not operate, igniter system functions or not, and core-concrete interactions occur to varying degrees. The MAAP4 case descriptions and results are presented in Tables 41-8 and 41-9.

These MAAP runs do not represent typical AP600 specific accident class sequences from the PRA results. Rather, they examine a wide range of long-term combustion phenomena in the containment. The conclusions of the MAAP4 analyses with respect to post-in-vessel phase hydrogen combustion are summarized as follows:

- If all of the core debris is released from the lower head to the containment at the time of vessel failure, there is a minimum ex-vessel generation of combustible gases that occurs during the short-term core-concrete interaction. This combustible gas generation occurs even if water is present in the cavity prior to the drainage of core debris and is recirculated for debris cooling by the passive containment cooling system. The mole number of gases (H_2 and CO) generated ex-vessel is at least a factor of 1.5 of the in-vessel portion. The ex-vessel generation of combustible gases is a result of uncoolable debris for a period of time following vessel failure. After this period, the debris may eventually become coolable.
- Vessel failure occurs when cavity flooding by the in-containment refueling water storage tank fails. The degree of ex-vessel generation of combustible gases is inversely proportional to the number of water (core makeup tanks and accumulators) sources available for injection.
- For cases in which vessel failure occurs and passive containment cooling system is operational, an early global burn may not prevent the containment atmosphere from meeting the flammability conditions required for a second global burn again later in time. An early global burn can consume all of the in-vessel hydrogen. However, the remaining ex-vessel portion is at least 1.5 times the in-vessel portion.
- When the igniter system operates, hydrogen combustion occurs locally where hydrogen is released (in-containment refueling water storage tank and pipe break location). Hydrogen is maintained below the lower flammability limits during an early phase of core melt. The same observation is supported by analyses presented in Chapter 47. A global burn does not occur at any time during accident sequences analyzed even if an artificially high rate of in-vessel hydrogen generation is used.
- In some cases in which debris is quenched in the cavity or remains in the vessel lower head, gas temperatures in the reactor coolant system remain high, above 1000 K.

(1340°F), even if the containment gas temperatures are lower, 400 K (260°F). The reactor coolant system gas temperatures decline slowly over time. A drop of a few hundred degrees Kelvin is typical over a 72-hour period. The reactor coolant system high temperature gas could be a potential ignition source.

- With safety injection from at least three out of four tanks (two accumulators and two core makeup tanks), debris will quench if vessel failure occurs. The debris surface temperature for most of the time will be relatively low (about the cavity gas temperature). Such debris does not show a sign of being an ignition source. There is only a relatively short time frame when the debris surface temperature is above 1000 K. This time frame is immediately after vessel failure.
- Debris can not be quenched when less than three out of four tanks (two accumulators and two core makeup tanks) injection is available due to the inability to recirculate water to the cavity. A large amount of ex-vessel generation of hydrogen and carbon monoxide accompanies severe core-concrete interactions. Steam inerting does not occur under these conditions because of a limited amount of containment water. The debris surface temperature is above 1000 K, and is a potential ignition source.

41.5.2 Decomposition Event Tree Analysis for Intermediate and Late Hydrogen Combustion

The decomposition event tree structure developed for quantifying the likelihood of intermediate and late hydrogen combustion is presented in Figure 41-77. The questions posed at each node on the tree examine and quantify the uncertainties identified in subsection 41.2. The upward path at each node (except node DF/DT) indicates a positive response to the question; the downward path indicates a negative response. For node DF/DT, the upward path indicates deflagration, while the downward path indicates detonation by direct energy deposition. The nodes chosen for the decomposition event tree are the following:

Node FL:

Does the containment atmosphere fail to become flammable?

Node IGS:

Are there no sources capable of ignition?

Node DF/DT:

Does combustion take place in the form of deflagrations, or does it take place in the form of detonations?

Node DDT:

Does deflagration-to-detonation transition fail to occur, given an occurrence of deflagration?



The end-states of the tree represent the modes of combustion:

- NB - No global combustion
- GB - Global deflagration
- DT - Deflagration-to-detonation transition

The sequence of questions asked by the decomposition event tree is a logical check for the requirement of combustion. First,

<u>Split Fraction</u>	<u>Node</u>
x	FL
y	IGS
1	DF/DT
z	DDT

The split fraction node DF/DT is predetermined at this step to be unity according to the evaluation that no high energy sources exist in the containment to cause detonation by direct-energy deposition (Reference 41-2).

Second, the flammability limits are verified. Then the ignition source is checked. If both requirements are met, a combustion event will occur. Combustion will take place in the form of either deflagration or detonation, depending on the hydrogen concentration and the strength of the ignition source. If combustion results in deflagration, the possibility of deflagration-to-detonation transition is further checked.

41.5.3 Quantification of the Intermediate and Late Hydrogen Combustion Decomposition Event Trees

In this subsection, the decomposition event tree quantification is presented for AP600 containment event tree nodes HC2 (for intermediate combustion) and HC3 (for late combustion). Assignment of the split fractions at each of the nodes on the decomposition event tree will be made. Multiplication of each of the split fractions along a path of the tree results in the probability of the phenomena following that particular path. The summation of the probabilities of the paths that result in a particular end-state is the probability of that end-state. The success criteria and the split fractions for each decomposition event tree node are defined as follows:

- The containment atmosphere does not satisfies the flammability limits



- Surface temperatures of debris in cavity or gas temperatures at reactor coolant system break do not exceed 1000 K
- The occurrence of deflagration
- No occurrence of deflagration-to-detonation transition

Based on these success criteria, the value of split fractions (x, y, and z) will be assigned. In terms of the decomposition event tree node split fractions (see Figure 41-77), the probability for each end-state can be represented as:

- Probability for occurrence of detonation = xyz
- Probability for occurrence of deflagration = $xy(1-z)$
- Probability for no combustion = $1 - xy$
- Probability for combustion = xy

Since the likelihood of intermediate and late hydrogen combustion depends strongly on accident progression states, quantification of the decomposition event tree has to be performed for each progression state. The accident progression states are defined in terms of a set of containment event tree nodes that are in front of nodes HC2 and HC3. Only containment event tree nodes that affect the flammability conditions and the generation and consumption of hydrogen need to be considered. With this approach, the accident progression states are grouped into eight cases. These are shown in Tables 41-10 and 41-11.

41.5.3.1 Intermediate Hydrogen Combustion (CET Node HC2)

Quantifications of the decomposition event tree for an intermediate hydrogen burn event (containment event tree node HC2) are presented in this section. The results are shown in Table 41-10. In assigning the split fractions for node FL (gas composition flammability), the results of MAAP4 analyses are used. Values for the flammability limits and hydrogen concentration result in either zero or one split fraction. The split fractions for node IGS (ignition source) are assigned 0.4 for cases in which debris is in-vessel and 0.3 if debris is quenched in the cavity, as discussed in Section 41.3. The split fractions for node DDT are determined based on gas compositions obtained from MAAP4 runs using the method described in Reference 41-8. It is noted that a burn in case 6 will be the most challenging to containment integrity. Because of the limited amount of containment water, all accident progression states with unquenched debris can be lumped together regardless of the status of the passive containment cooling system. Steam inerting (at least 55 percent steam) dominates the flammability conditions only for cases with quenched debris and non-operating passive containment cooling water. Descriptions for each case are given below. The meaning of symbols used for identifying entry conditions for each case is given in Table 41-10.

**Case 1: IG**

This case involves an operation of the igniter system. As discussed previously, the igniter system keeps the containment atmosphere below the lower flammability limits unless the containment is steam-inerted. A global burn for this case is extremely unlikely.

Case 2: No IG, PCCS, PB, No VF

This case involves only in-vessel hydrogen generation. The amount of in-vessel generation can lead to the flammability limits required for a global burn if the passive containment cooling system operates. However, since a large portion of this hydrogen inventory burns previously, the remaining hydrogen will be much lower than the requirement.

Case 3: No IG, PCCS, PB, DQ

This case involves vessel failure with short-term core-concrete interaction in which the debris is eventually quenched. There is a certain amount of ex-vessel generation sufficient to reach the flammability limits required for a global burn even if an early global burn has occurred.

Case 4: No IG, PB, No DQ

This case involves severe core-concrete interactions that generate a tremendous amount of combustible gases. Hence, even if a burn has occurred previously, a second burn is still very likely both in terms of flammability limits and ignition sources. Severe core-concrete interactions are a result of too little water in the containment (cavity flooding failure and injection of two out of four tanks or fewer). Because of this limited amount of water, the differences between cases with and without passive containment cooling water operating in terms of combustion likelihood are negligible. Therefore, this case is applied regardless of the status of the passive containment cooling water.

Case 5: No IG, PCCS, No PB, No VF

This case involves only in-vessel hydrogen generation with passive containment cooling water operating. The probabilities calculated for flammability and for deflagration-to-detonation transition in the containment in the early time frame (node HC1) are used to quantify the intermediate hydrogen combustion probabilities.

Case 6: No IG, No PB, No DQ

This case, similar to case 4, involves severe core-concrete interactions. The likelihood and consequence for combustion are greater than case 4 because no burn has occurred previously.

Case 7: No IG, PCCS, No PB, DQ

This case, similar to case 3, involves vessel failure with quenched debris. Because of the no previous burn condition, the combustion consequence is greater than case 3.

Case 8: No IG, No PCCS, No VF or DQ

This case involves failure of the passive containment cooling system with no vessel failure or quenched debris. The amount of containment water injected is at least three of four tanks (accumulator and core makeup tanks) in order to quench the debris. This amount of water is sufficient to maintain steam concentration above 55 percent. Hence, the atmosphere is inerted throughout the sequence.

The quantification of the decomposition event tree for each of these cases is presented in Table 41-10.

41.5.3.2 Late Hydrogen Combustion (CET Node HC3)

Quantification of the decomposition event tree for a late hydrogen burn event (containment event tree node HC3) is presented in this section. The results of the quantification are shown in Table 41-11. Assignment of split fractions is done similar to that of a intermediate hydrogen burn event (containment event tree node HC2). In assigning the split fractions for node FL, values for the flammability limits are obtained or can be anticipated resulting in either zero or one split fractions.

The split fractions for node IGS (ignition source) is assigned 0.1 for cases in which debris is in vessel (intact vessel) and 0.4 if the debris is quenched in the cavity as discussed in subsection 41.3.6. The split fractions for node DDT are determined based on gas compositions using the method described in Reference 41-8. It is noted that the existence of case 4 depends on whether containment failure has occurred previously because of a previous global burn.

If a previous global burn occurs at an early hydrogen combustion node (containment event tree HC1), containment will remain intact, but the combustible gas inventory will be reduced. If a burn occurs at an intermediate hydrogen combustion node (containment event tree HC2), there will be no oxygen to support further combustion.

The meaning of symbols used for identifying entry conditions for each case is provided in Table 41-11. Descriptions for each case are given below.

Case 1: IG

This case involves an operation of the igniter system. As discussed previously, the igniter system keeps the containment atmosphere below the lower flammability limits, unless the containment is steam-inerted. A global burn for this case is extremely unlikely.

Case 2: No IG, PCCS, PB, No VF

This case involves only in-vessel hydrogen generation. The amount of in-vessel generation can lead to the flammability limits required for a global burn if the passive containment cooling system operates. However, since a large portion of this hydrogen inventory burns previously, the remaining hydrogen will be much lower than the requirement.

Case 3: No IG, PCCS, PB, DQ

This case involves vessel failure in which the debris is eventually quenched. There is a certain amount of ex-vessel generation sufficient to reach the flammability limits required for a global burn even if an early global burn has occurred. However, if an intermediate global burn has occurred, the likelihood of reaching the flammability limits again is zero. The value of x in this case is equal to the probability of no burn at containment event tree node HC2 for cases with quenched debris (case 3 or 7 of Table 41-9).

Case 4: No IG, PB, No DQ

This case involves severe core-concrete interactions that generate a tremendous amount of combustible gases. Even if an early burn has occurred, another burn is still possible both in terms of flammability limits and ignition sources. Severe core-concrete interactions are a result of too little water in the containment (failure to flood the cavity and injection of only two out of four tanks or less). Because of this limited amount of water, the differences between cases with and without passive containment cooling system operating in terms of combustion likelihood are negligible. Therefore, this case is applied regardless of the status of the passive containment cooling system. However, if an intermediate global burn has occurred previously, the likelihood of reaching the flammability limits again is zero because of insufficient availability of oxygen. For this case, x is equal to the probability of no burn at containment event tree node HC2 for unquenched debris (case 4 or 6 of Table 41-10).

Case 5: No IG, PCCS, No PB, No VF

This case involves only in-vessel hydrogen generation with passive containment cooling system operating. The probabilities calculated for flammability and for deflagration-to-detonation transition in the containment in the early time frame (node HC1) are used to quantify the late hydrogen combustion probabilities.

Case 6: No IG, No PB, No DQ

This case, similar to case 4, involves severe core-concrete interactions. The likelihood and consequence for combustion are greater than case 4 because no burn has occurred previously.



Case 7: No IG, PCCS, No PB, DQ

This case, similar to case 3, involves vessel failure with quenched debris. Because of the no previous burn condition, the combustion consequence is greater than case 3.

Case 8: No IG, No PCCS, No VF or DQ

This case involves failure of the PCCS with no vessel failure or quenched debris. The amount of containment water injected is at least three of four tanks in order to quench the debris. This amount of water is sufficient to maintain steam concentration above 55 percent. Hence, the atmosphere is inerted throughout the sequence.

41.5.4 Intermediate and Late Hydrogen Combustion Decomposition Event Tree Quantification Results

The results of the quantification for intermediate combustion and late combustion are presented in Tables 41-10 and 41-11, respectively. These tables show the conditional probabilities of each end-state, given one of the eight cases discussed in the sections above.

Four of eight cases identified have a potential to challenge the containment by deflagration. They are cases 3, 4, 6, and 7. A global burn in these cases involves combustible gases generated both in and ex-vessel. MAAP 4 analyses of deflagration pressure peaks for these cases were performed in addition to those described previously. The results are summarized in Table 41-12 for an intermediate combustion event and in Table 41-13 for late combustion event. Other cases do not have a global burn (cases 1, 2, and 8) or burn only the in-vessel hydrogen (case 5), which produces a pressure peak too low to produce a non-zero containment failure probability. Based on the deflagration pressures and the AP600 containment fragility curve, the split fractions for containment failure due to deflagrations and detonations were determined and listed in the tables. To obtain detonation loads, it was assumed that the loads are equal to the deflagration pressures multiplied by 4.5. This results in a split fraction of 1 for containment failure due to detonations in all these cases. The likelihood of containment failure due to a burn is given in Table 41-14 for an intermediate combustion event, and in Table 41-15 for a late combustion event. In case 6 for both intermediate and late combustion events, all oxygen gas was consumed by the burn. Case 6 represents the most severe (upper bound) combustion event that could be postulated. It is noted that the deflagration-to-detonation transition loads dominate the conditional probability of containment failure due to combustion. The zero conditional probability for HC3 case 4 (Table 41-15) implies that, for accident sequences with unquenched debris in cavity, there would be no oxygen to support a later burn if a previous intermediate burn has already occurred. The previous global burn at node HC2 would have consumed most oxygen present in the containment.

The split fractions applied to containment event tree nodes HC2, CF2, HC3, and CF3 are presented in Tables 41-14 and 41-15 as well.

41.6 References

- 41-1 Tieszen, S. R., et al., "Hydrogen Distribution and Combustion," in Ex-Vessel Severe Accident Review for the Heavy Water New Production Reactor (ed. by K. D. Bergeron), SAND90-0234, NPRW-SA90-3, Sandia National Laboratories, 1993.
- 41-2 AP600 *Phenomenological Evaluation Summaries*, WCAP-13388 (Proprietary) Rev. 0, June 1992 and WCAP-13389 (Nonproprietary) Rev. 1, 1994.
- 41-3 Luangdilok, W., et al., "Conditions for Oxygen-Deficient Combustion During Accidents with Severe Core Concrete Thermal Attack," Proceeding 2nd ASME/JSME Nuclear Eng. Conference, Vol. 1, pp 349-355, 1993.
- 41-4 *Evaluation of Severe Accident Risks: Quantification of Major Input Parameters, Expert Opinion Elicitation on In-Vessel Issues*, NUREG/CR-4551, Vol. 2, Rev. 1, Part 1, December 1990.
- 41-5 "Modification for the Development of MAAP-DOE Code, A Mechanistic Model for Combustion in Integrated Analysis," Task 3.4.5, DOE/ID-10216, Vol. III, November 1988.
- 41-6 Ratze, A.C., *Data Analysis for Nevada Test Site (NTS) Premixed Combustion Tests*, NUREG/CR-4138, SAND85-0135, Sandia National Laboratories, 1985.
- 41-7 Sherman, M.P., et al., *Deliberate Ignition and Water Fogs as H₂ Control Measures for Sequoyah*, Proc. Workshop on the Impact of Hydrogen on Water Reactor Safety, Volume IV, NUREG/CR-2017, SAND81-0661, Sandia National Laboratories, 1981.
- 41-8 Sherman, M. P., and Berman, M., *The Possibility of Local Detonation During Degraded Core Accidents in the Bellefonte Nuclear Plant*, NUREG/CR-4803, SAND86-1180, Sandia National Laboratories, 1987.
- 41-9 Sherman, M. P., et al., *FLAME Facility*, NUREG/CR-5275, SAND85-1264, Sandia National Laboratories, 1989.
- 41-10 Kevin, W. B., et al., "Loads from the Detonation of Hydrogen-Air-Steam Mixtures," SAND92-0541, Sandia National Laboratories, 1992.

Table 41-1

AP600 INTEGRATED IN-VESSEL HYDROGEN GENERATION

Accident Class	Best-Estimate		Bounding-Estimate	
	Mass H ₂ (kg)	Active Clad Reacted (%)	Mass H ₂ (kg)	Active Clad Reacted (%)
1A	482	77	610	98
1AP	397	64	530	85
3BE No Reflood	288	46	440	70
3BE/3BR Reflood	614	98	740	118
3C	360	58	518	83
3D	365	58	530	85

Table 41-2

AP600 HYDROGEN COMBUSTION PEAK PRESSURE AND TEMPERATURE ESTIMATES

	Best-Estimate Hydrogen Generation Cases							
	1A	1AP	3BE No Reflood	3BE/ 3BR Reflood	3BE No Reflood PCS Fail	3BE/3BR Reflood PCS Fail	3C	3D
Pre-Burn Gas Comp								
mole fraction H ₂	0.115	0.07	0.06	0.135	0.05	0.10	0.08	0.07
mole fraction steam	0.16	0.28	0.25	0.20	0.50	0.40	0.25	0.35
Mass of H ₂ (kg)	482	397	288	614	378	614	325	380
Pre-Burn								
Press (bar)	1.4	1.5	1.5	1.5	2.5	2.1	1.6	1.8
Temp (K)	400	375	375	370	390	380	360	365
Post-Burn								
Press (bar) ⁽¹⁾	4.5	-	-	5.3	-	-	-	-
Temp (K) ⁽¹⁾	1330	-	-	1440	-	-	-	-
Cond Prob CF due to Deflagration ⁽²⁾	0	0	0	0	0	0	0	0
Cond Prob of DDT in IRWST ⁽³⁾	0	0	0	0.01	0	0	0	0
Cond Prob of DDT in Lower Compt ⁽³⁾	0.01	0	0	0.01	0	0	0	0

Note:

- (1) AICC peak pressure and temperature
 (2) Based on conditional containment failure probability distribution (Chapter 42)
 (3) Based on methodology outlined in Reference 41-6



Westinghouse

ENEL
 ENTE NAZIONALE
 PER L'ENERGIA ELETTRICA

Table 41-3

AP600 HYDROGEN COMBUSTION PEAK PRESSURE AND TEMPERATURE ESTIMATES

	Bounding-Estimate Hydrogen Generation Cases							
	1A	1AP	3BE No Reflood	3BE/ 3BR Reflood	3BE No Reflood PCS Fail	3BE/ 3BR Reflood PCS Fail	3C	3D
Pre-Burn Gas Comp								
mole fraction H ₂	0.14	0.09	0.09	0.17	0.06	0.115	0.12	0.08
mole fraction steam	0.16	0.28	0.25	0.20	0.50	0.40	0.25	0.35
Mass of H ₂ (kg)	610	530	440	740	440	740	520	440
Pre-Burn								
Press (bar)	1.4	1.5	1.5	1.5	2.5	2.1	1.6	1.8
Temp (K)	400	375	375	370	390	380	360	365
Post-Burn								
Press (bar) ⁽¹⁾	5.3	-	-	5.8	-	7.0	4.6	-
Temp (K) ⁽¹⁾	1500	-	-	1675	-	1155	1310	-
Cond Prob CF due to Deflagration ⁽²⁾	0	0	0	0	0	0	0	0
Cond Prob of DDT in IRWST ⁽³⁾	0	0	0	0.01	0	0.01	0.1	0
Cond Prob of DDT in Lower Comp ⁽³⁾	0.01	0	0	0.1	0	0	0.01	0

Note:

- (1) AICC peak pressure and temperature
- (2) Based on conditional containment failure probability distribution (Chapter 42)
- (3) Based on methodology outlined in Reference 41-6



Table 41-4

AP600 EARLY HYDROGEN COMBUSTION DET SPLIT FRACTIONS FOR NODE FL

Failure Probabilities for Node FL - Early Hydrogen Combustion DET

Case	Best-Estimate Hydrogen Generation	Bounding-Estimate Hydrogen Generation
Igniters On	0	0
PCS Off (All Except 3BE Reflood)	0	0
1A	1	1
1AP	0	0
3BE No Reflood	0	0
3BE/3BR Reflood PCS On	1	1
3BE/3BR Reflood PCS Off	0	1
3C	0	1
3D	0	0



Westinghouse

ENEL
 ENTE NAZIONALE
 PER L'ENERGIA ELETTRICA

Table 41-5

**CONDITIONAL PROBABILITY OF DEFLAGRATION-TO-DETONATION
TRANSITION IN THE IRWST FOR EARLY HYDROGEN COMBUSTION
IN AP600 CONTAINMENT**

Case	Node DDT1 Failure Probability
3BE/3BR With Reflood, PCS On, Best-Estimate H ₂	0.01
3BE/3BR With Reflood, PCS On, Bounding-Estimate H ₂	0.01
3BE/3BR With Reflood, PCS Failed, Bounding-Estimate H ₂	0.01
3C, PCS On, Bounding-Estimate H ₂	0.10
All Others	0.0

Table 41-6

**CONDITIONAL PROBABILITY OF DEFLAGRATION-TO-DETONATION
TRANSITION IN THE LOWER COMPARTMENTS FOR EARLY
HYDROGEN COMBUSTION IN AP600 CONTAINMENT**

Case	Node DDT2 Failure Probability
1A PCS On, Best-Estimate H ₂	0.01
1A, PCS On, Bounding-Estimate H ₂	0.01
3BE/3BR With Reflood, PCS On, Best-Estimate H ₂	0.01
3BE/3BR With Reflood, PCS On, Bounding-Estimate H ₂	0.10
3C, PCS On, Bounding-Estimate H ₂	0.01
All Others	0.0

Table 41-7

**QUANTIFICATION RESULTS OF THE
EARLY HYDROGEN COMBUSTION DET**

Case	NB	GB	DT	DD	P _{HCl}	P _{CFI}
Igniters On (All Cases)	1.0	0.0	0.0	0.0	0.0	0.0
PCS Fail, Ign Fail (All cases, Except 3BE Reflood)	1.0	0.0	0.0	0.0	0.0	0.0
1A Ign Fail, PCS Suc	0.5	0.495	5.E-3	0.0	0.5	0.01
1AP Ign Fail, PCS Suc	1.0	0.0	0.0	0.0	0.0	0.0
3BE No Reflood Ign Fail, PCS Suc	1.0	0.0	0.0	0.0	0.0	0.0
3BE/3BR Reflood Ign Fail, PCS Suc	0.5	0.489	0.011	0.0	0.5	0.022
3BE/3BR Reflood Ign Fail, PCS Fail	0.9875	0.0124	1.25E-4	0.0	0.0125	0.01
3C Ign Fail, PCS Suc	0.9875	0.0111	1.36E-3	0.0	0.0125	0.11
3D Ign Fail, PCS Suc	1.0	0.0	0.0	0.0	0.0	0.0



Table 41-8 (Sheet 1 of 2)

SUMMARY OF MAAP4 ANALYSES FOR LOSS-OF-FEEDWATER SEQUENCES

Key Parameters	MAAP RUN #				
	LF3	LF4 ⁽⁵⁾	LF4A ^(5,9)	LF5	LF5A ^(5,9)
Core Uncovery (hr.)	4.8	3.5	3.4	4.9	4.9
Core Relocation (hr.)	6.9	5.5	5.4	6.6	6.7
Lower Head Failure (hr.)	No	8.9	8.9	21.3	No
In-Vessel Clad Ox. (%)	42	34.8	35	34.8	40
Production: In-Vessel H ₂ (kg)	390	325	330	325	370
Ex-Vessel H ₂ (kg)	No	205	370	240	No
Ex-Vessel CO (kg)	No	4950	12500	6300	No
Early H ₂ (%)	>8% ⁽¹⁾	>8%	<8.3	<4.9% ⁽³⁾	<6.8
Late ⁽⁶⁾ H ₂ /CO (%)	-4.1/0	-8.6/5.7	-9.3/12.3 ⁽²⁾	<2.5/2.5 ⁽⁴⁾	<4.6/0 ⁽⁸⁾
Ignition Source	See ⁽¹⁴⁾	See ⁽¹¹⁾	See ⁽¹⁰⁾	See ⁽¹²⁾	See ⁽¹³⁾
Very Late ⁽⁷⁾ H ₂ /CO (%)	-4.3/0	-9.0/6.0	---	<2.4/2.0	<4.6/0
Ignition Source	See ⁽¹⁴⁾	See ⁽¹¹⁾	---	See ⁽¹²⁾	See ⁽¹³⁾
Safety Features					
Accumulators (2)	2	2	1	2	2
CMT (2)	2	1	1	2	2
ADS (Stages)	3	3	3	3	3
Feedwater (Ail)	No	No	No	No	No
PRHR Functional	No	No	No	No	No
PCS Functional	Yes	Yes	Yes	No	No
Igniters Operational	No	No	No	No	No
IRWST Injection	No	No	No	No	No

Note:

- | | |
|--|--------------------------------------|
| (1) Globally burned; containment pres. = 2.64×10^5 Pa | (8) Steam > 55% |
| (2) Globally burned at 33% steam; containment failed | (9) Burn allowed at 24 hr |
| (3) Local burns in IRWST | (10) Debris in cavity |
| (4) Steam >80% | (11) Up Plen Temp = 650 K to 700 K |
| (5) Burning suppressed initially | (12) Up Plen Temp = 1200 K |
| (6) Up to 24 hr. | (13) Up Plen Temp = 1300 K to 1400 K |
| (7) Up to 72 hr. | (14) Up Plen Temp = 1400 K to 1500 K |

Table 41-8 (Sheet 2 of 2)

SUMMARY OF MAAP4 ANALYSES FOR LOSS-OF-FEEDWATER SEQUENCES

Key Parameters	MAAP RUN #			
	LF5A ⁽⁴⁾	LF5B ⁽⁴⁾	LF5C ⁽⁴⁾	LF5D ⁽⁴⁾
Core Uncovery (hr.)	4.9	3.55	3.4	2.3
Core Relocation (hr.)	6.7	5.3	5.1	3.75
Lower Head Failure (hr.)	No	8.8	8.8	7.56
In-Vessel Clad Ox. (%)	40	33.8	35	28.2
Production: In-Vessel H ₂ (kg)	370	317	326	265
Ex-Vessel H ₂ (kg)	No	210	1400	850
Ex-Vessel CO (kg)	No	4360	54000	31000
Early H ₂ (%)	<6.8	<6.3	<6.7	<5.4
Intermediate H ₂ /CO/H ₂ O (%)	<4.6/0/>55	<4.6/<2.8/>64	<11/<24/>38	<13/<24/>26 ⁽²⁾
Ignition Source	Steam inerted	Steam-inerted	Debris ⁽¹⁾	Debris ⁽¹⁾
Late H ₂ /CO/H ₂ O (%)	<4.6/0/>55	<5.4/<3.4/>58	<13/<28/>34	---
Ignition Source	Steam-inerted	Steam-inerted	Debris ⁽³⁾	---
Safety Features				
Accumulators (2)	2	2	1	0
CMT (2)	2	1	1	1
ADS (Stages)	3	3	3	3
Feedwater (All)	No	No	No	No
PRHR Functional	No	No	No	No
PCS Functional	No	No	No	No
Igniters Operational	No	No	No	No
IRWST Injection	No	No	No	No

Note:

- (1) Debris surface temperature > 1000 K
- (2) Containment failure occurred (globally burned; cont. pres. > 1.037 MPa)
- (3) Debris surface temperature > 700 K
- (4) Burning suppressed initially; allowed for 1/2 hour at 24 hours

Table 41-9

SUMMARY OF MAAP4 ANALYSES FOR HOT LEG 2" SMALL LOCA

Key Parameters	MAAP RUN #		
	SLO2	SLO6	SLO5A ⁽⁷⁾
Core Uncovery (hr.)	1.85	1.8	1.8
Core Relocation (hr.)	3.35	3.29	3.36
Lower Head Failure (hr.)	8.3	8.6	8.35
In-Vessel Clad Ox. (%)	34	37	36.5
In-Vessel H ₂ Production (kg)	318	345	340
Ex-Vessel H ₂ Production (kg)	220	216	220
Ex-Vessel CO Production (kg)	5600	5500	5600
Early H ₂ (%)	>8% ⁽¹⁾	See ⁽²⁾	<6.8% ⁽³⁾
Intermediate (Up to 24 hr.) H ₂ /CO (%)	6.4/6.0 ⁽⁶⁾	<3.6 ⁽⁴⁾ / \leq 2.8	<5/ \leq 3.5 ⁽⁴⁾
Gas Temp in Broken Loop (K)	\approx 1100	<900	<1000
Late (Up to 72 hr.) H ₂ /CO (%)	0.0/0.0	<3.5/ \leq 2.7	\approx 5/5.6 ⁽⁵⁾
Gas Temp in Broken Loop (K)	< 800	<5.0	<600
Safety Features			
Accumulators (2)	1	1	1
CMT (2)	2	2	2
ADS (Stages)	3	3	3
Feedwater (All)	No	No	No
PRHR Functional	No	No	No
PCCS Functional	Yes	No	No
Igniters Operational	No	Yes	No
IRWST Injection	No	No	No

Note:

- (1) Local burns in IRWST, upper comp., SG comp.
- (2) Local burns in SG, IRWST
- (3) Local burns in upper comp.
- (4) Steam > 65%, T < 410 K
- (5) Steam > 55%, T < 410 K
- (6) Globally burned; containment pressure $\approx 7.96 \times 10^5$ Pa
- (7) Burning suppressed

Table 41-10

**DET QUANTIFICATIONS FOR
INTERMEDIATE HYDROGEN COMBUSTION
(CET NODE HC2)**

Case #	Conditions	x	y	z	NB (1-xy)	GB xy(1-z)	DT (xyz)	DD
1	IG	0	1	0	1	0	0	0
2	No IG, PCS, PB, No VF	0	--	--	1	0	0	0
3	No IG, PCS, PB, DQ	1	0.3	0.01	0.7	0.297	3.0E-3	0
4	No IG, PB, No DQ	1	1	0.1	0	0.9	0.1	0
5	No IG, PCS, No PB, No VF							
	1A	1	0.4	0.01	0.6	0.396	4.0E-3	0
	1AP	0	0.4	0	1	0	0	0
	3BE/3BR Reflood	1	0.4	0.012	0.6	0.3952	4.8E-3	0
	3C	0.025 ⁽¹⁾	0.4	0.01	0.99	9.9E-3	1.0E-4	0
	3D	0	0.4	0	1	0	0	0
6	No IG, No PB, No DQ	1	1	0.5	0	0.5	0.5	0
7	No IG, PCS, No PB, DQ	1	0.3	0.01	0.7	0.297	3.0E-3	0
8	No IG, No PCS, DQ or No VF	0	--	--	1	0	0	0

IG = Igniter system operates

PCS = PCCS operates

PB = Global burn has occurred previously

VF = Vessel failure occurs

DQ = Debris in cavity is quenched, short-term CCI occurs

Note:

(1) Only bounding-estimate hydrogen generation case is flammable



Westinghouse

ENEL
 ENTE NAZIONALE
 PER L'ENERGIA ELETTRICA

Table 41-11

**DET QUANTIFICATIONS FOR
LATE HYDROGEN COMBUSTION
(CET NODE HC3)**

Case #	Conditions	x	y	z	NB (1-xy)	GB xy(1-z)	DT xyz	DD
1	IG	0	1	--	1	0	0	0
2	No IG, PCS, PB, No VF	0	--	--	1	0	0	0
3	No IG, PCS, PB, DQ	0.7 ⁽¹⁾	0.4	0.01	0.72	0.2772	2.8E-3	0
4	No IG, PB, No DQ	~0 ⁽²⁾	1	0.5	~1	~0	~0	0
5	No IG, PCS, No PB, No VF							
	1A	1	0.1	0.01	0.9	0.099	1.0E-3	0
	1AP	0	0.1	0	1	0	0	0
	3BE/3BR-Reflood	1	0.1	0.01	0.9	0.0988	1.2E-3	0
	3C	0.025 ⁽³⁾	0.1	2	0.998	1.975E-	2.5E-5	0
	3D	0	0.1	0.01	1	3	0	0
				0		0		
	No IG, No PB, No DQ							
6		1	1		0		0.5	0
	No IG, PCS, No PB, DQ			0.5		0.5		
7		1	0.4		0.6		4.0E-3	0
	No IG, No PCS, DQ or No			0.01		3.96E-1		
8	VF	0	--	--	1		0	0
						0		

IG = Igniter system operates

PCS = PCCS operates

PB = Global burn has occurred previously

VF = Vessel failure occurs

DQ = Debris in cavity is quenched, short term CCI occurs

Note:

(1) Equal to a split fraction of no burn (1-xy) for case 3 or 7 of Table 41-10

(2) Equal to a split fraction of no burn (1-xy) for case 4 or 6 of Table 41-10

(3) Only bounding-estimate hydrogen generation case is flammable

Table 41-12

ANALYSIS OF PRESSURE PEAK DUE TO INTERMEDIATE COMBUSTION EVENT (HC2)

	Case 3 ⁽²⁾	Case 4 ⁽³⁾	Case 6 ⁽⁴⁾	Case 7 ⁽⁵⁾
Early H ₂ Burn	Yes	Yes	No	No
Pre-burn Gas Comp.				
H ₂ /CO (vol.%)	6.4/6.0	6.7/11.4	9.7/12.5	8.6/5.6
H ₂ O/CO ₂ (vol.%)	40/0	36/0	33/0	34/0
Amount Burned				
H ₂ (kg-mole)	215	205	288	268
CO (kg-mole)	200	346	368	178
Pre-Burn				
Temp. (K)	440	380	380	380
Pres. (MPa)	0.26	0.23	0.24	0.21
Post-Burn				
Temp. (K)	1554	1809	1952	1569
Pres. (MPa)	0.796 ⁽⁶⁾	0.946 ⁽⁶⁾	1.064 ⁽⁶⁾	0.767 ⁽⁶⁾
Containment Failure Probability ⁽¹⁾ Due to Deflagrations	0	2.36E-2	6.67E-1	0
Containment Failure Probability ⁽¹⁾ Due to Detonations	1	1	1	1

Note:

- (1) Based on the AP600 containment failure probability distribution (Chapter 42)
- (2) Based on MAAP run #SLO2
- (3) Based on MAAP analysis similar to run # LF4A except that ignition sources are also assume from 8.7 to 8.9 hr. in addition to, from 24 to 24.5 hr. (run # LF4A-4A)
- (4) Based on MAAP analysis to run # LF4A except that containment failure is not allowed (run # LF4A-6A); all oxygen was consumed by the burn
- (5) Based on MAAP analysis similar to run # LF4, except that ignition sources are assumed from 24 hr. (run # LF4-7A)
- (6) Containment failure does not occur or is not allowed for this calculation

Table 41-13

ANALYSIS OF PRESSURE PEAK DUE TO LATE COMBUSTION EVENT (HC3)

	Case 3 ⁽²⁾	Case 4 ⁽³⁾	Case 6 ⁽⁴⁾	Case 7 ⁽⁵⁾
Early H ₂ Burn	Yes	Yes	No	No
Pre-burn Gas Comp.				
H ₂ /CO (vol.%)	>6.4/6.0	7.8/13	10.8/13.6	9.2/6.1
H ₂ O/CO ₂ (vol.%)	<40/0	28/0	26/0	28/0
Amount Burned				
H ₂ (kg-mole)	215	205	290	268
CO (kg-mole)	200	393	364	178
Pre-Burn				
Temp. (K)	440	370	370	370
Pres. (MPa)	0.26	0.196	0.22	0.18
Post-Burn				
Temp. (K)	>1554	1995	2110	1679
Pres. (MPa)	<0.796 ⁽⁶⁾	0.901 ⁽⁶⁾	1.01 ⁽⁶⁾	0.745 ⁽⁶⁾
Containment Failure Probability ⁽¹⁾ Due to Deflagrations	0	2.21E-3	2.19E-1	0
Containment Failure Probability ⁽¹⁾ Due to Detonation	1	1	1	1

Note:

- (1) Based on the AP600 containment failure probability distribution (Chapter 42)
- (2) Based on MAAP run # SLO2
- (3) Based on MAAP analysis similar to run # LF4A except that ignition sources are assumed from 8.7 to 8.9 hr. and from 65 hr. (run # LF4A-4B)
- (4) Based on MAAP analysis similar to run # LF4A except that ignition sources are assumed from 65 hr. (run # LF4A-6B); all oxygen was consumed by the burn
- (5) Based on MAAP analysis similar to run # LF4, except that ignition sources are assumed from 65 hr. (run # LF4-7B)
- (6) Containment failure does not occur or is not allowed for the calculation

Table 41-14

**DET QUANTIFICATIONS FOR
INTERMEDIATE HYDROGEN COMBUSTION
(CET NODES HC2, CF2)**

Case #	Conditions	GB	DT	CF _{GB}	CF _{DT}	ΣCF	P(HC2) CET Node	P(CF2) CET Node
1	IG	0	0	0	0	0	0	0
2	No IG, PCS, PB, No VF	0	0	0	0	0	0	0
3	No IG, PCS, PB, DQ	0.297	3.0E-3	0	3.0E-3	3.0E-3	0.3	0.01
	No IG, PB, No DQ	0.9	0.1	2.1E-2	0.1	1.21E-1	1	1.21E-1
5	No IG, PCS, No PB, No VF							
	1A	0.396	4.0E-3	0	4.0E-3	4.0E-3	0.4	0.01
	1AP	0	0	0	0	0	0	0
	3BR/3BE-Reflood	0.3952	4.8E-3	0	4.8E-3	4.8E-3	0.4	0.012
	3C	9.9E-3	1.0E-4	0	1.0E-4	1.0E-4	0.01	0.01
	3D	0	0	0	0	0	0	0
6	No IG, No PB, No DQ	0.5	0.5	3.3E-1	0.5	8.3E-1	1	8.3E-1
7	No IG, PCS, No PB, DQ	0.297	3.0E-3	0	3.0E-3	3.0E-3	0.3	0.01
		0	0	0	0	0	0	0
8	No IG, No PCS, DQ or No VF							

IG = Igniter system operates

PCS = PCCS operates

PB = Global burn has occurred previously

VF = Vessel failure occurs

DQ = Debris in cavity is quenched

GB = Conditional probability of global deflagration

DT = Conditional probability of detonation

CF_{GB} = Conditional probability of containment failure due to deflagration = GB*split fraction for CF due to deflagration (Table 41-12)CF_{DT} = Conditional probability of containment failure due to detonation = DT*split fraction for CF due to detonation (Table 41-12)

Westinghouse

ENEL
 ENTE NAZIONALE
 PER L'ENERGIA ELETTRICA

Table 41-15

**DET QUANTIFICATIONS FOR
LATE HYDROGEN COMBUSTION
(CET NODE HC3, CF3)**

Case #	Conditions	GB	DT	CF _{GB}	CF _{DT}	ΣCF	P(HC3) CET Node	P(CF3) CET Node
1	IG	0	0	0	0	0	0	0
2	No IG, PCS, PB, No VF	0	0	0	0	0	0	0
3	No IG, PCS, PB, DQ	0.2772	2.8E-3	0	2.8E-3	2.8E-3	0.3	9.33E-3
4	No IG, PB, No DQ	~0	~0	0	0	0	0	0
5	No IG, PCS, No PB, No VF	0.099	1.0E-3	0	1.0E-3	1.0E-3	0.01	0.1
	1A	0	0	0	0	0	0	0
	1AP	0.0988	1.2E-3	0	1.2E-3	1.2E-3	0.1	0.012
	3BR/3BE Reflood	1.975E-3	2.5E-5	0	2.5E-5	2.5E-5	2.0E-3	0.0125
	3C	0	0	0	0	0	0	0
	3D							6.1E-1
6	No IG, No PB, No DQ	0.5	0.5	1.1E-1	0.5	6.1E-1	1	0.01
7	No IG, PCS, No PB, DQ	0.396	4.0E-3	0	4.0E-3	4.0E-3	0.4	0
8	No IG, No PCS, DQ or No VF	0	0	0	0	0	0	

IG = Igniter system operates

PCS = PCCS operates

PB = Global burn has occurred previously

VF = Vessel failure occurs

DQ = Debris in cavity is quenched

GB = Conditional probability of global deflagration

DT = Conditional probability of detonation

CF_{GB} = Conditional probability of containment failure due to deflagration = GB*Split Fraction for CF due to deflagration (Table 41-13)

CF_{DT} = Conditional probability of containment failure due to detonation = DT*Split Fraction for CF due to detonation (Table 41-13)

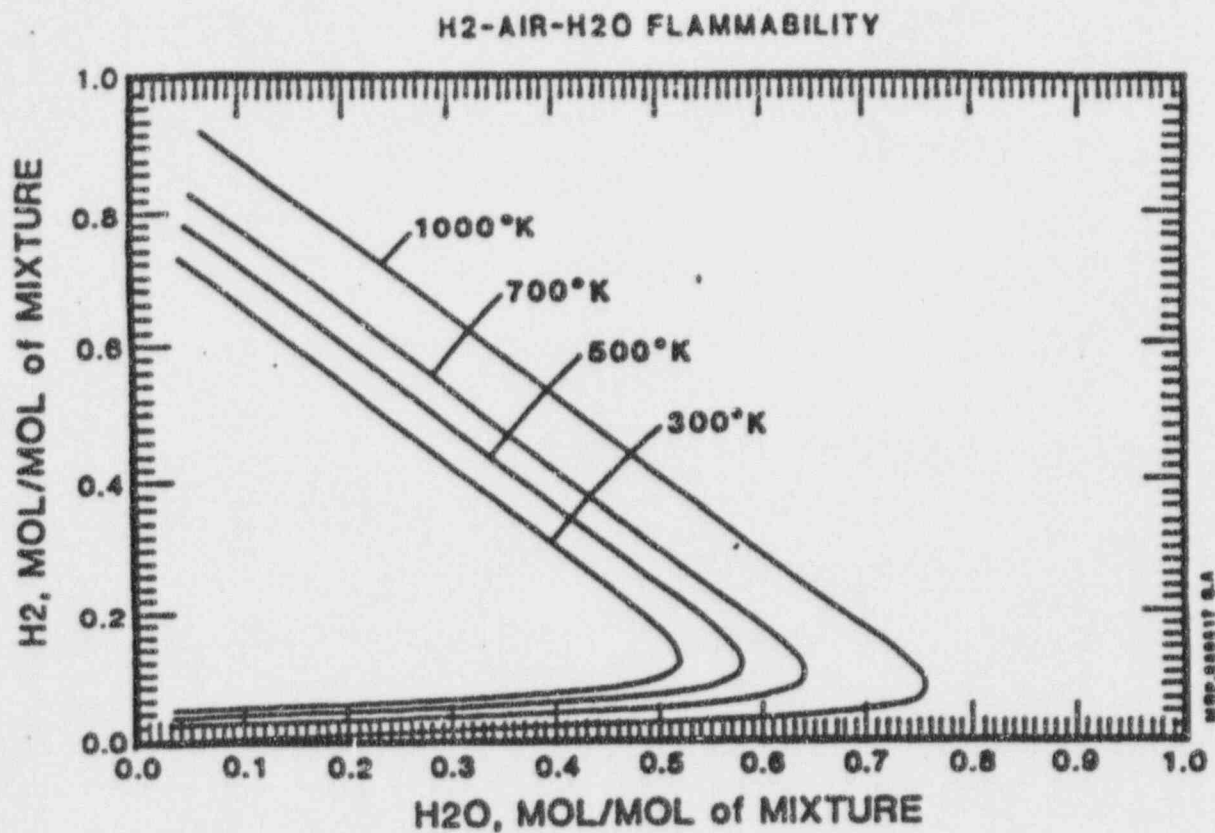


Figure 41-1

Flammability Limit Fit at Elevated Temperatures (Reference 41-5)



Westinghouse

ENEL
ENTE NAZIONALE
PER L'ENERGIA ELETTRICA

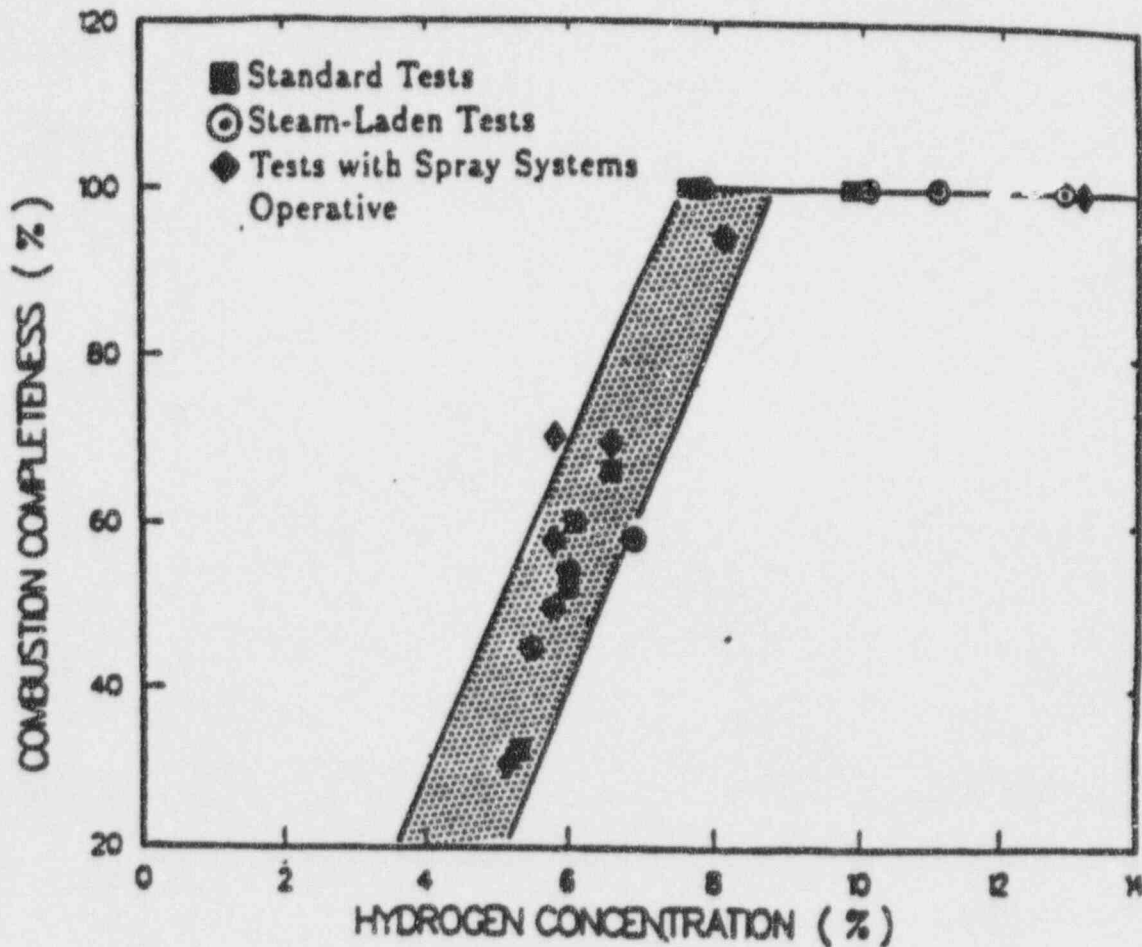


Figure 41-2

Combustion Completeness for Nevada Test Site
Premixed Combustion Tests (Reference 41-6)

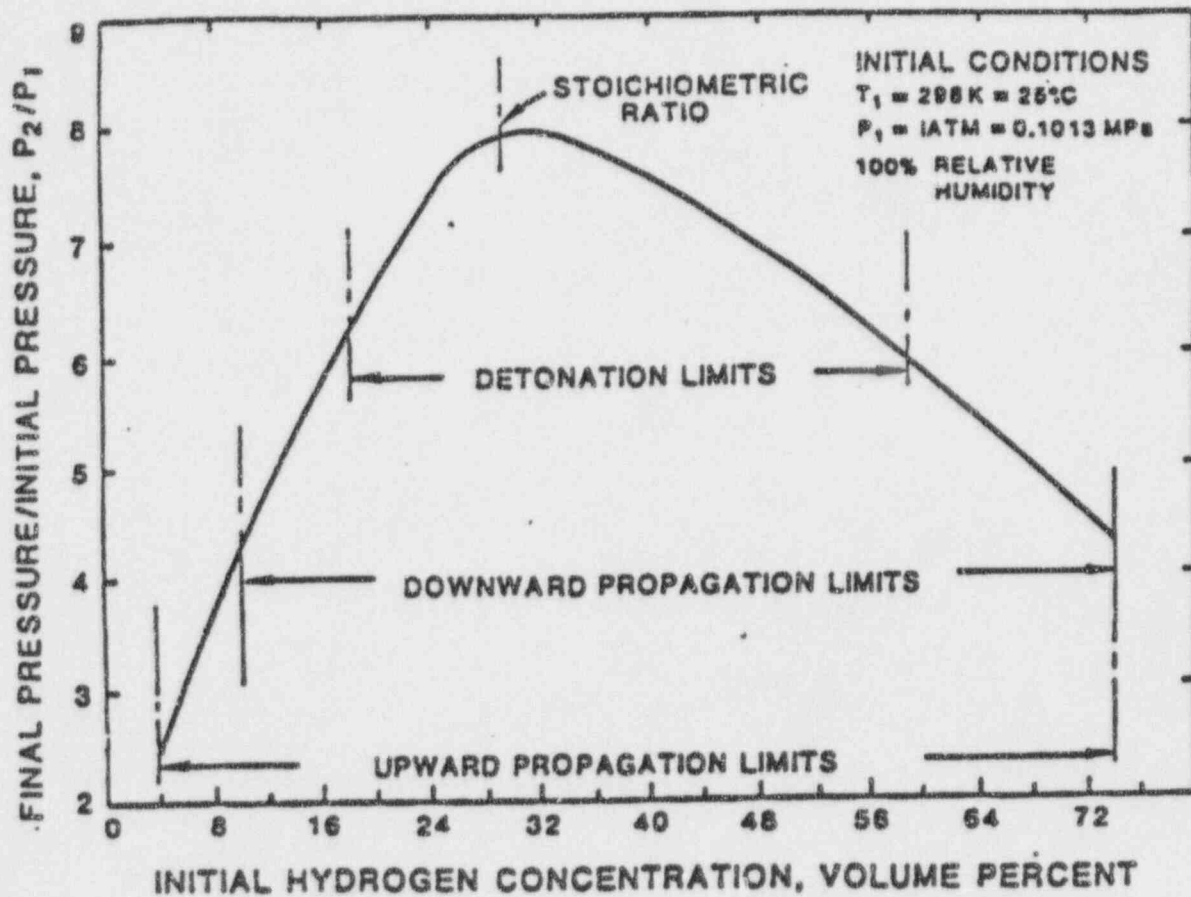


Figure 41-3

Theoretical Adiabatic, Constant-Volume Combustion Pressures of
Hydrogen-Air Mixtures (Reference 41-7)

AP600 Case 1A No Hydrogen Ignition Case Containment Pressure

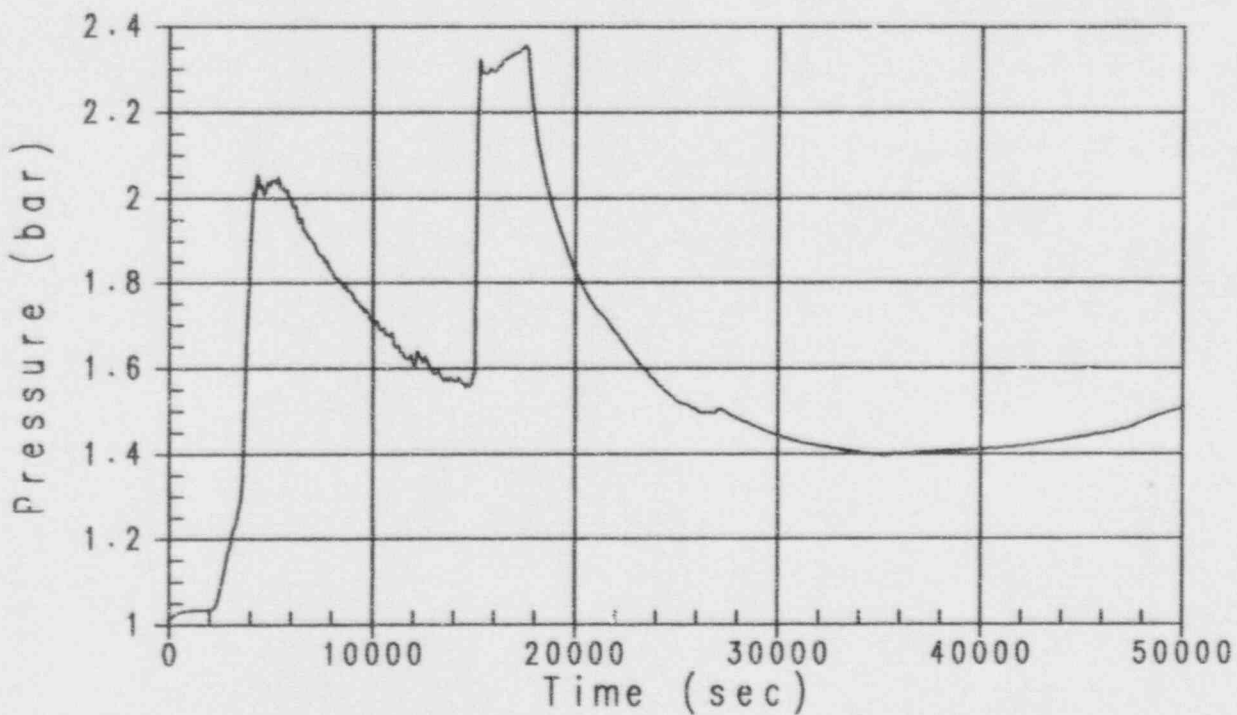


Figure 41-4

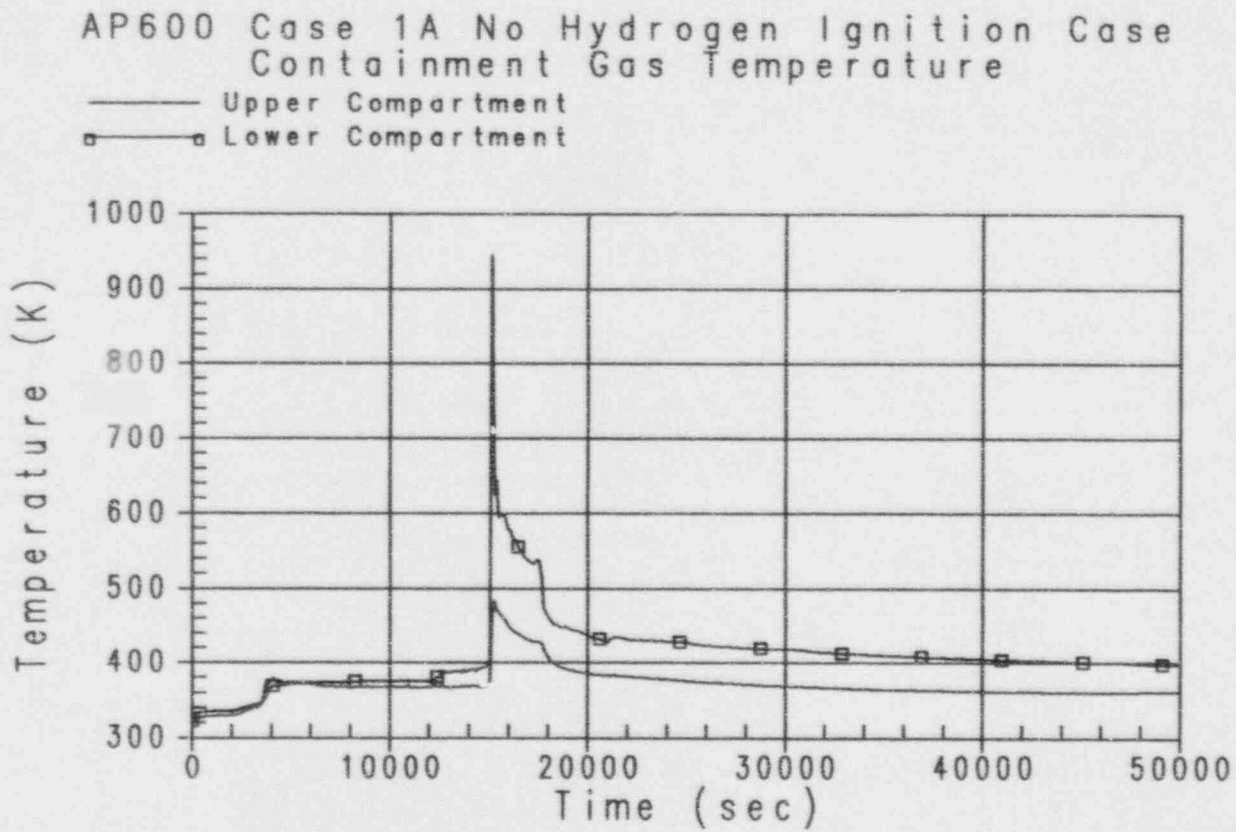


Figure 41-5



Westinghouse

ENEL
ENEL NUCLEARE
PER L'ENERGIA ELETTRICA

41-43

Revision: 3
February 28, 1995
u:\ap600\prj\sec41-1.wpf:lb

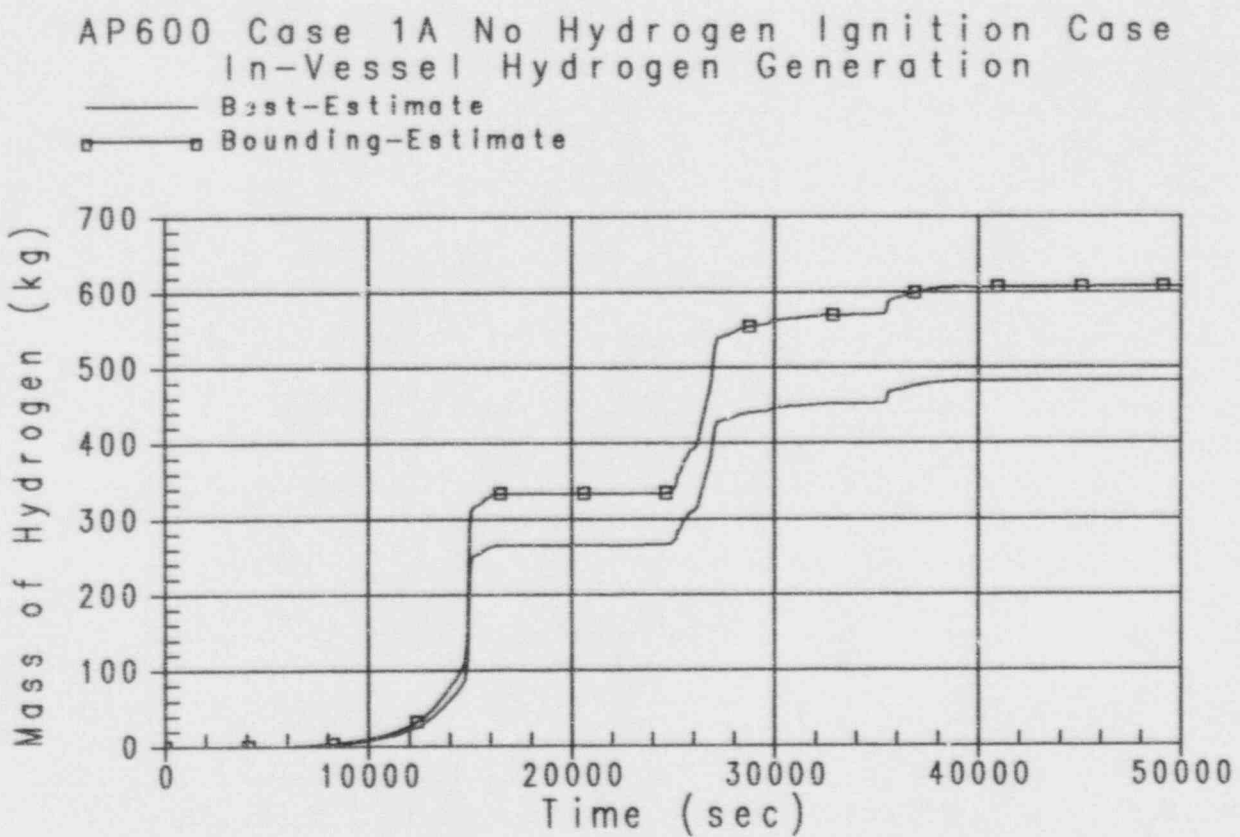


Figure 41-6

AP600 Case 1A No Hydrogen Ignition Case
 Best Estimate In-Vessel Hydrogen Generation
 Containment Compartment Hydrogen Mole Fractions

— Loop Compt
 □ Dead-Ended Region
 △ IRWST
 ◇ Upper Compt

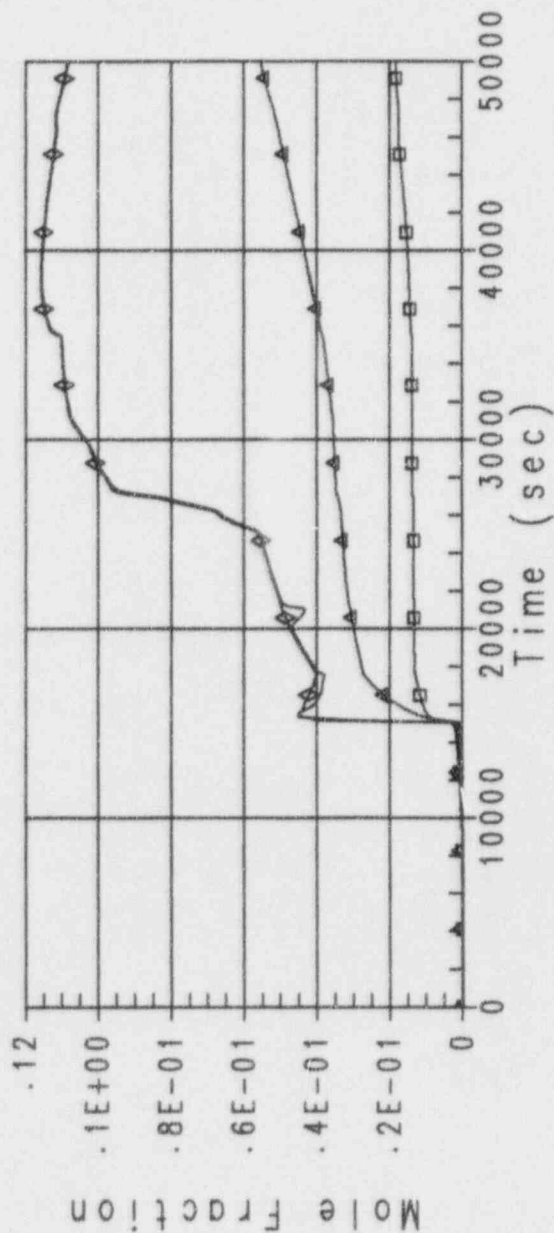


Figure 41-7



Westinghouse

ENEL
 ENTE NAZIONALE
 PER L'ENERGIA ELETTRICA

AP600 Case 1A No Hydrogen Ignition Case
Bounding Estimate In-Vessel Hydrogen Generation
Containment Compartment Hydrogen Mole Fractions

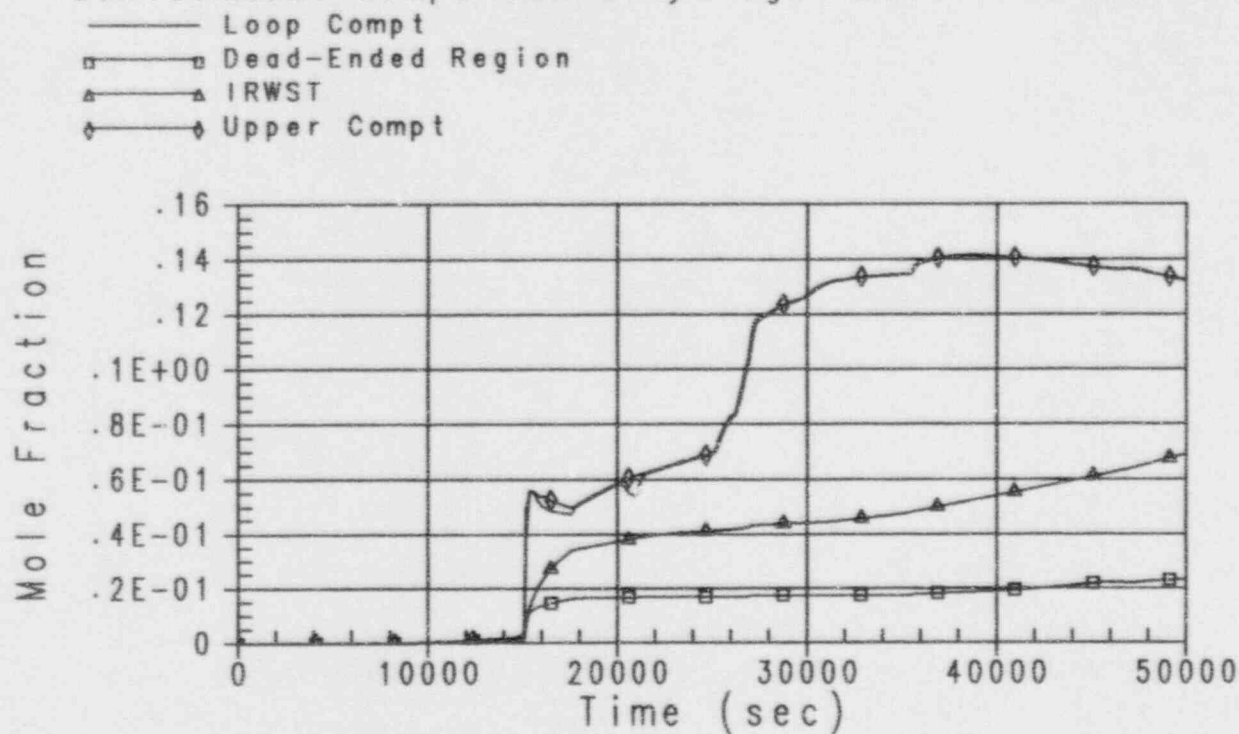


Figure 41-8

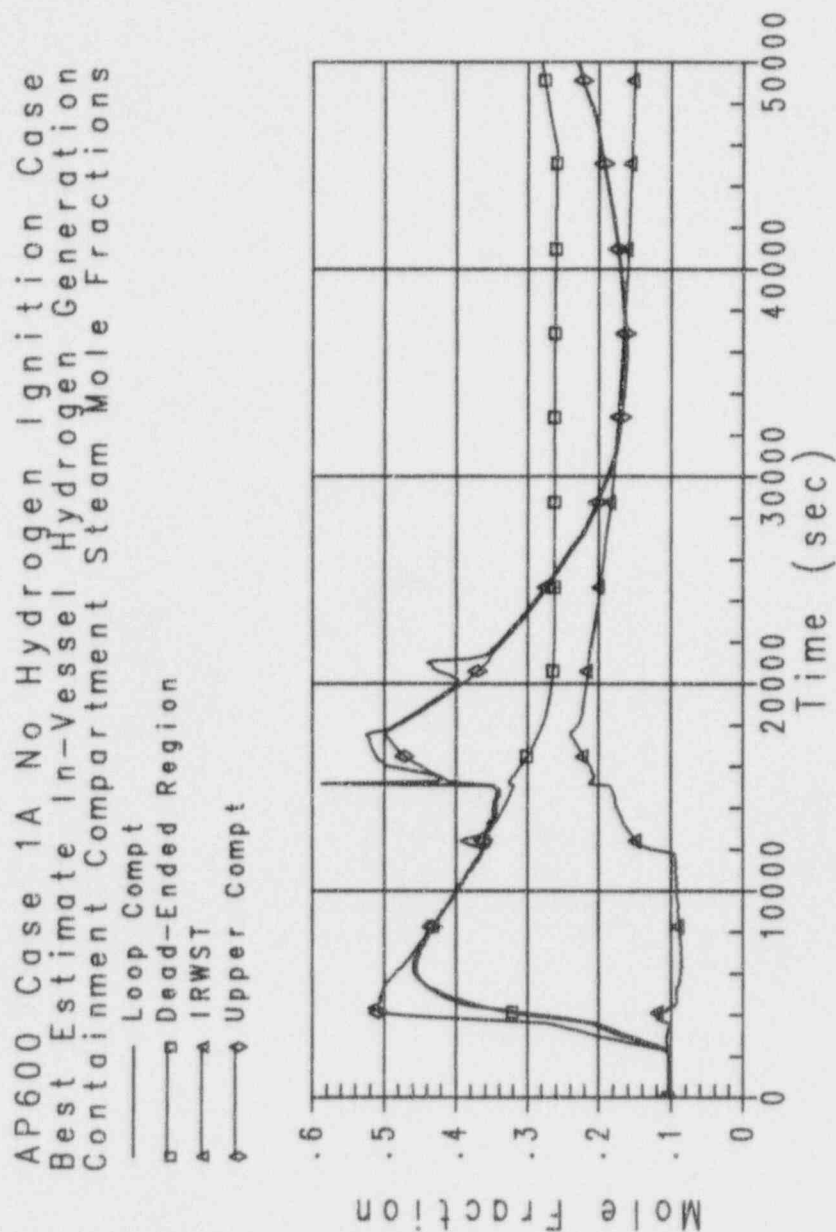


Figure 41-9



Westinghouse

ENEL
 ENTE NAZIONALE
 PER L'ENERGIA ELETTRICA

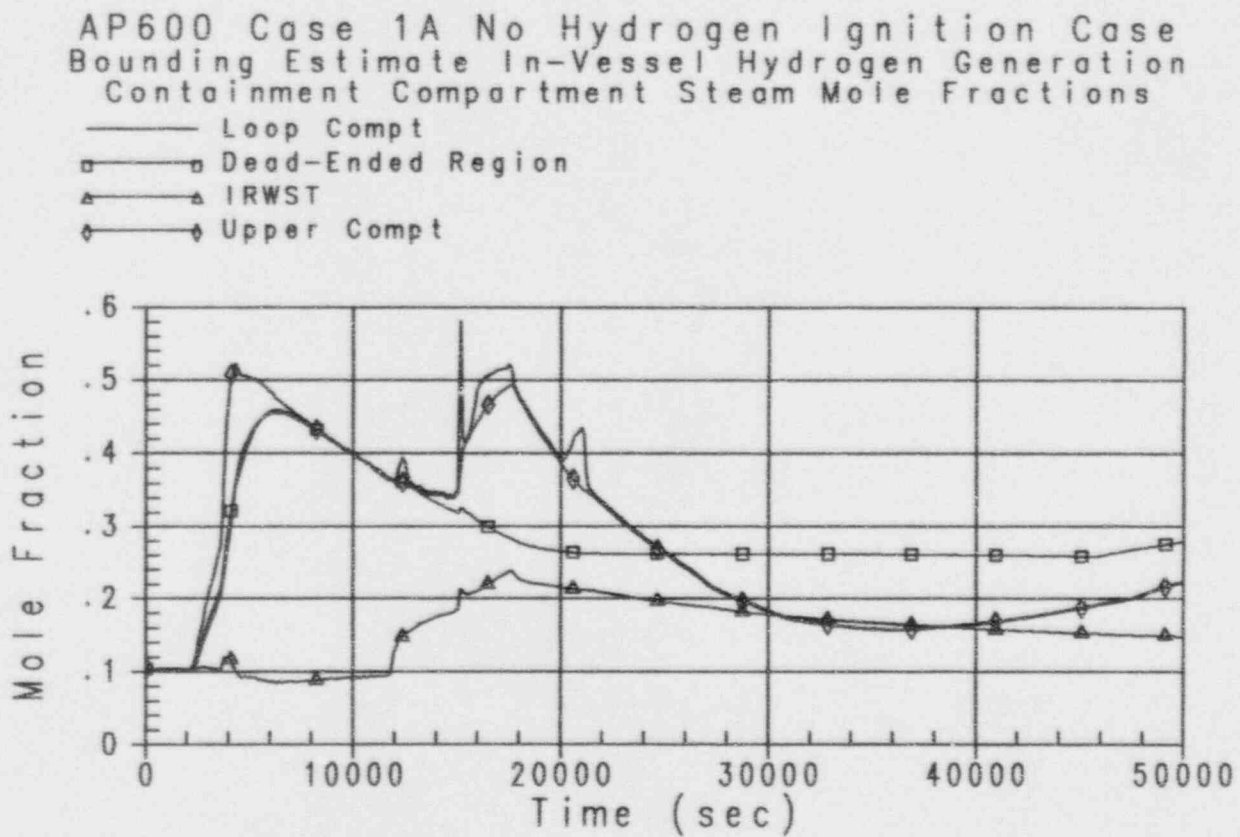


Figure 41-10

AP600 Case 1A No Hydrogen Ignition Case
Best Estimate In-Vessel Hydrogen Generation
Containment Flammability Limits

- Flammability Limit for Upward Combustion
 □ Flammability Limit for Downward Combustion
 ▲ Hydrogen Concentration

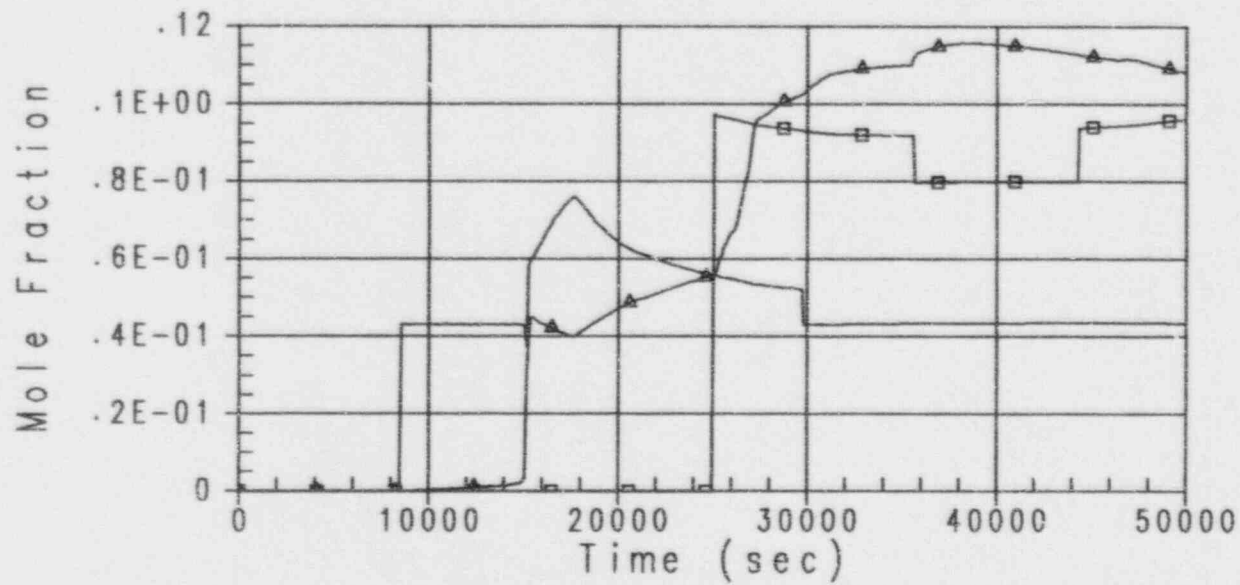


Figure 41-11



Westinghouse

ENEL
 ENVIROMENTAL
 FOR LICENSING EXTENSION

41-49

 Revision: 3
 February 28, 1995
 u:\ap600\prasecd1-1.wpf:lb

AP600 Case 1A No Hydrogen Ignition Case
Bounding Estimate In-Vessel Hydrogen Generation
Containment Flammability Limits

— Flammability Limit for Upward Combustion
□ Flammability Limit for Downward Combustion
△ Hydrogen Concentration

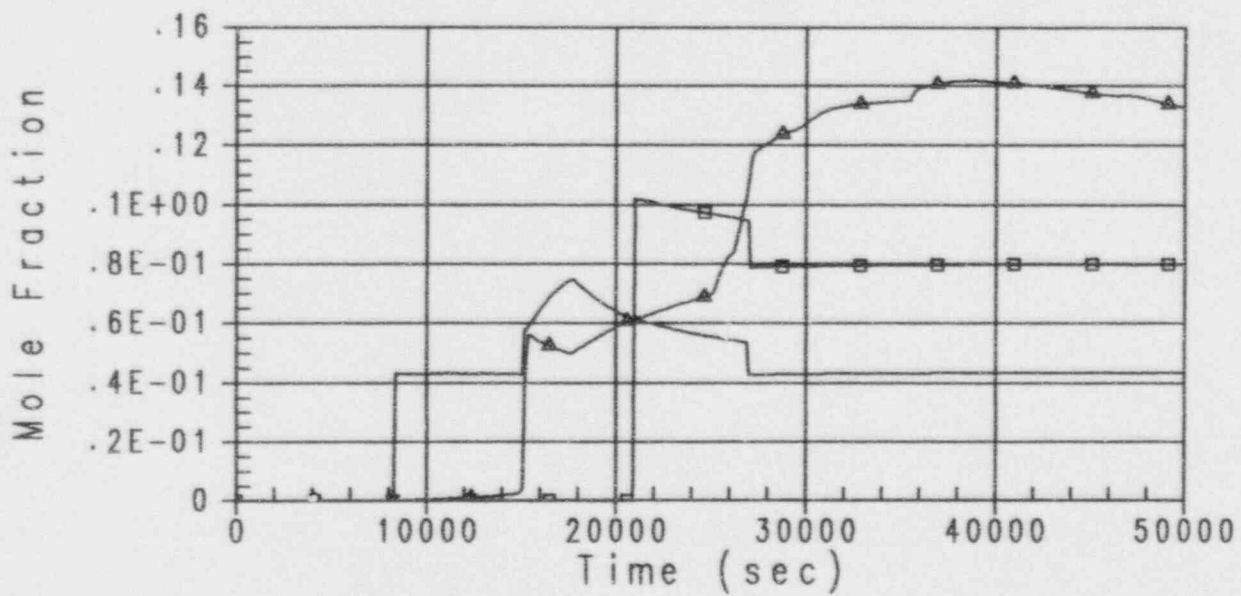


Figure 41-12

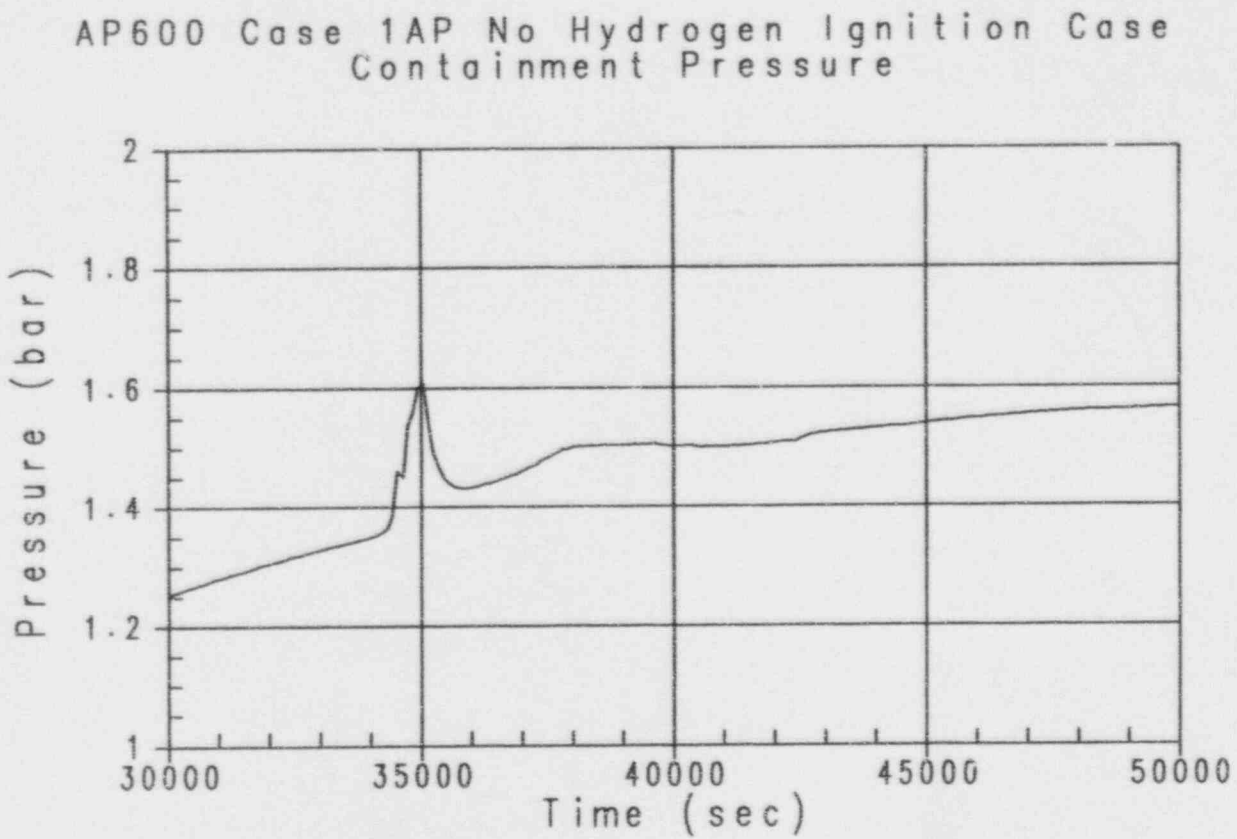


Figure 41-13



Westinghouse

ENEL
ENEL NUCLEAR
P.O. BOX 10000
LONDON, ENGLAND

41-51

Revision: 3
February 28, 1995
u:\ap600\prelsec-1-1.wpf:lb

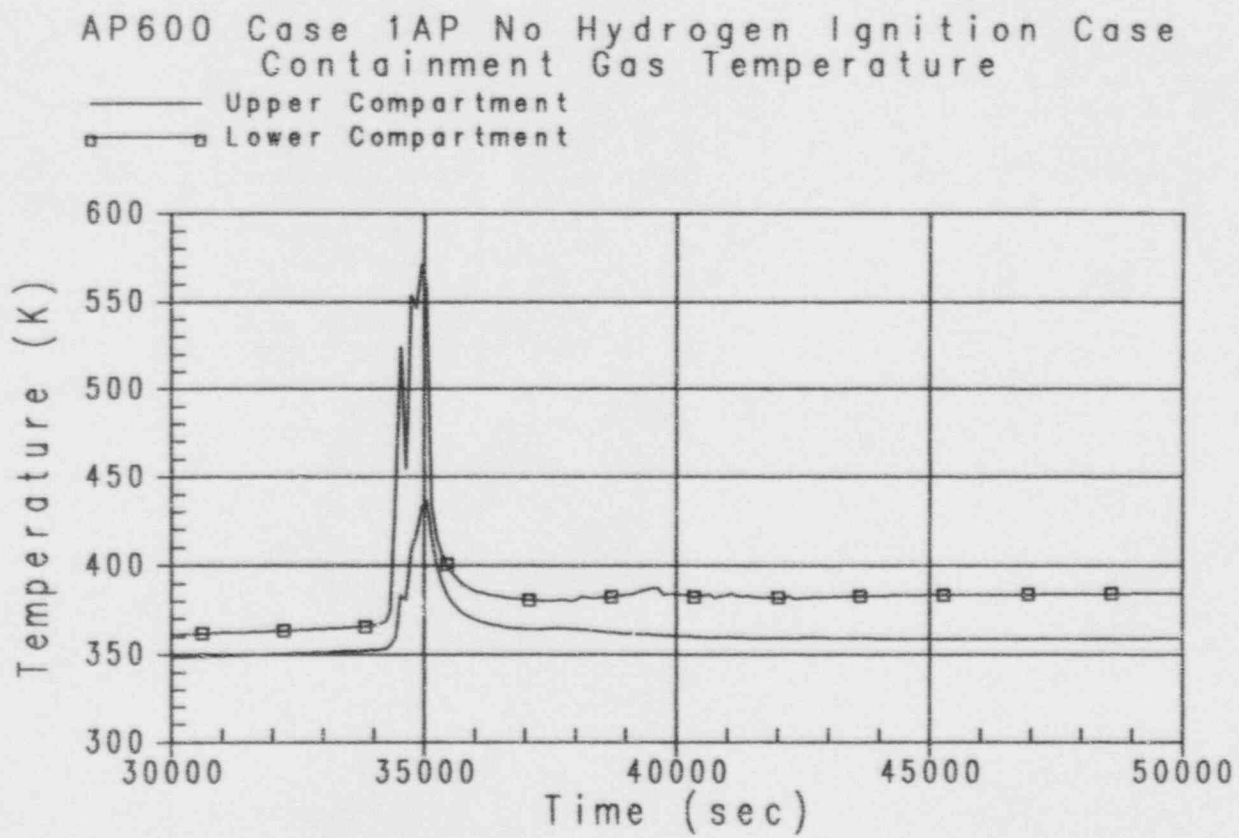


Figure 41-14

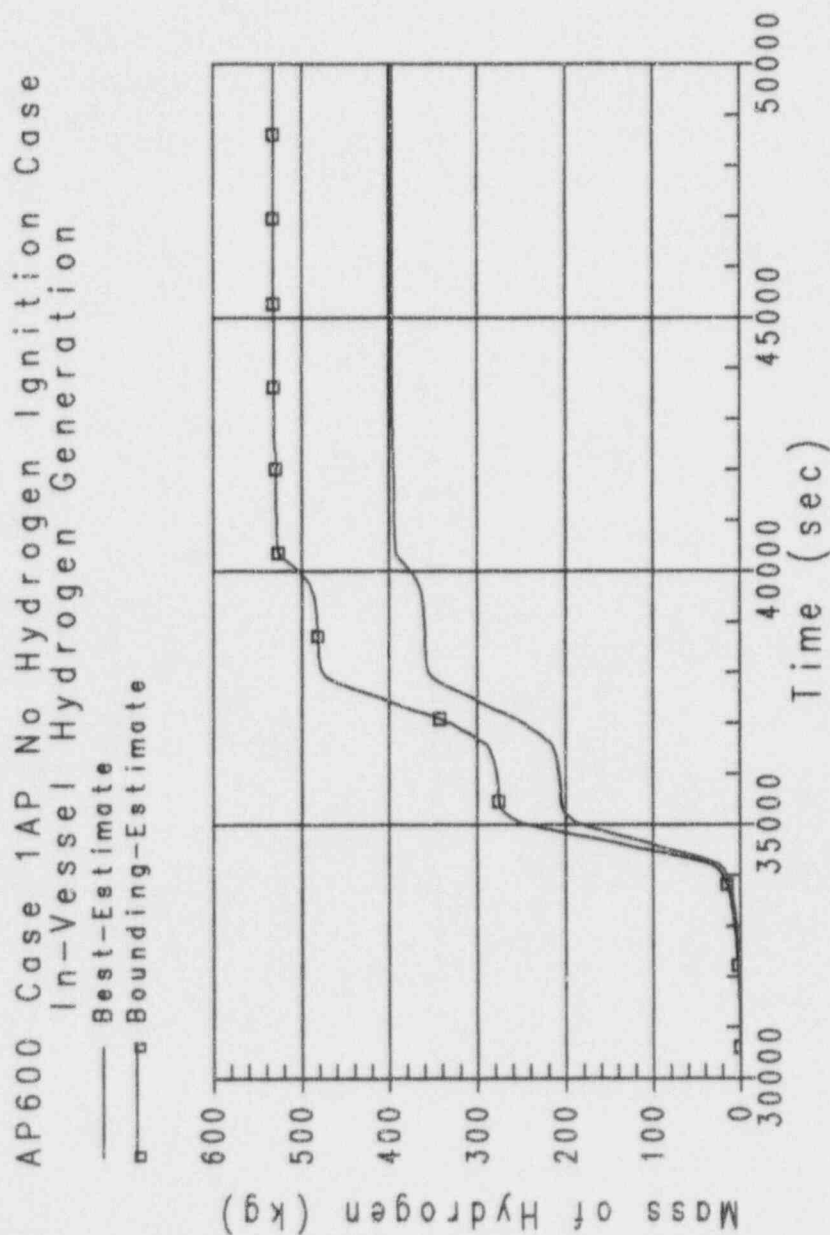


Figure 41-15



Westinghouse

ENEL
ENTE NAZIONALE
PER L'ENERGIA ELETTRICA

AP600 Case 1AP No Hydrogen Ignition Case Best Estimate In-Vessel Hydrogen Generation Containment Compartment Hydrogen Mole Fractions

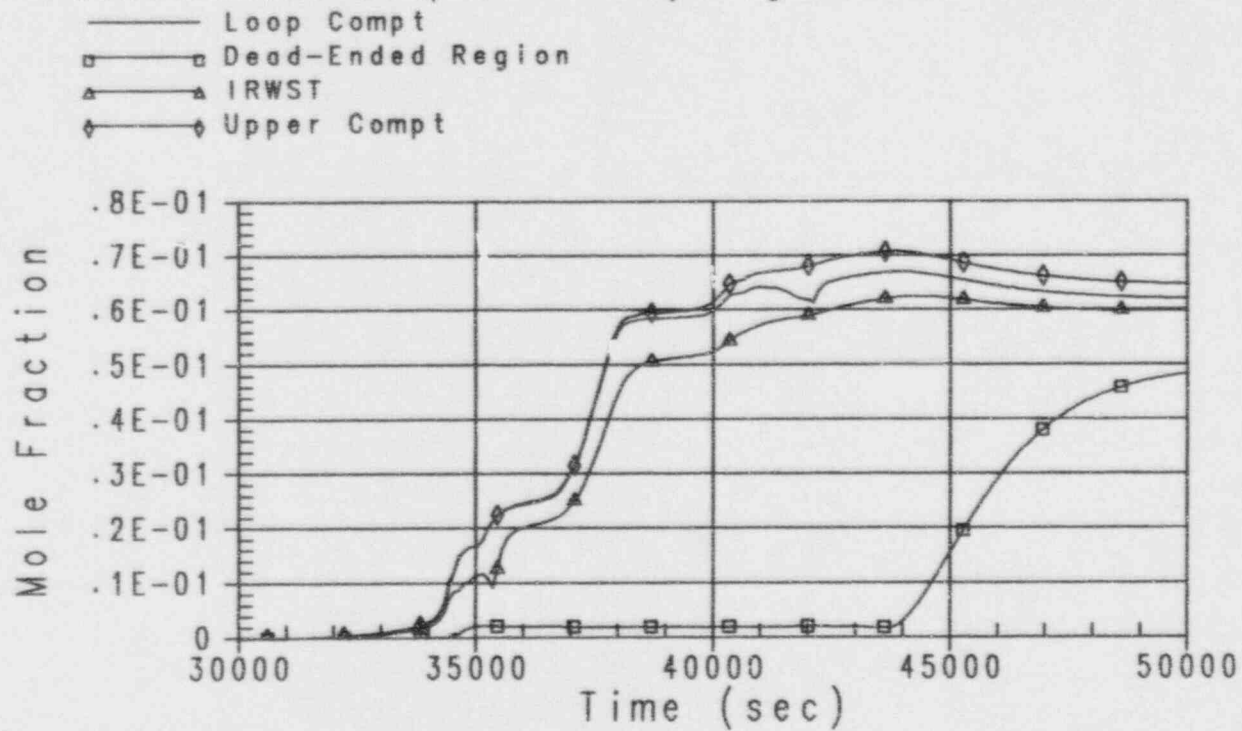


Figure 41-16

AP600 Case 1AP No Hydrogen Ignition Case
Bounding Estimate In-Vessel Hydrogen Generation
Containment Compartment Hydrogen Mole Fractions

— Loop Compt
□ Dead-Ended Region
△ IRWST
◇ Upper Comp

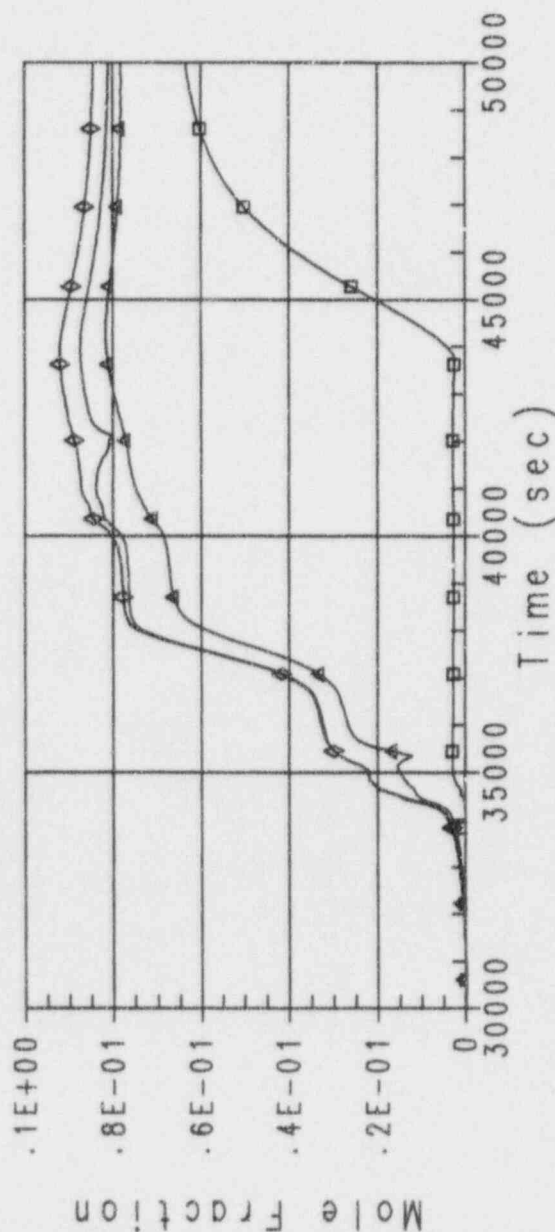


Figure 41-17

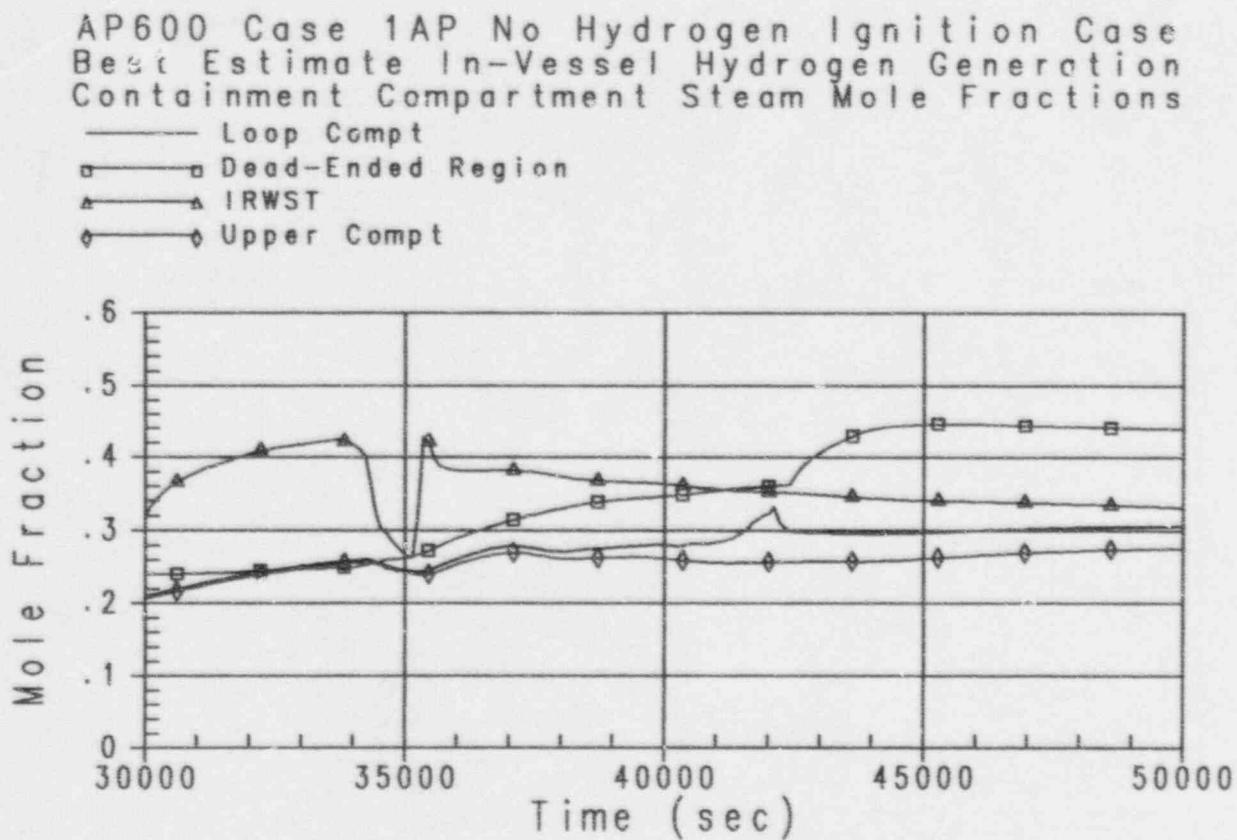


Figure 41-18

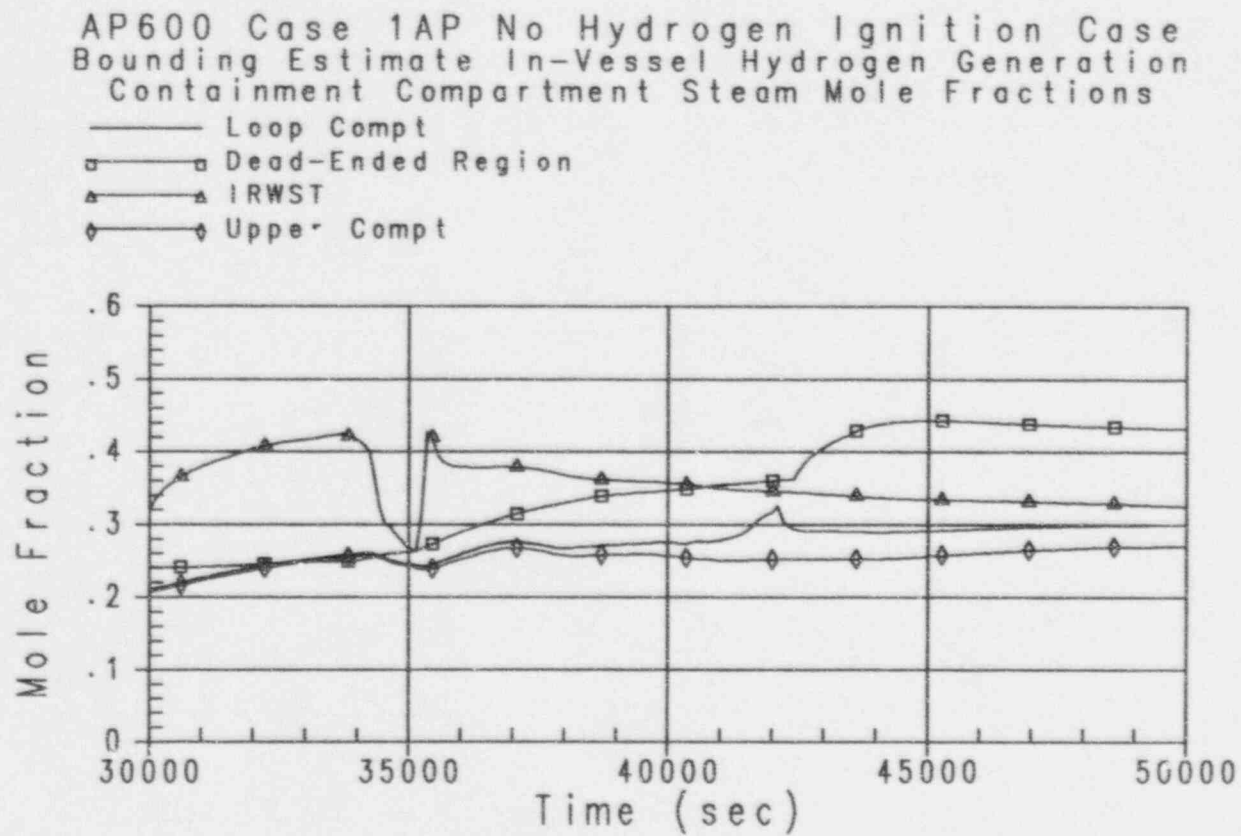


Figure 41-19



Westinghouse

ENEL
 ENEL NUCLEARE
 PER L'ELETTRICITA'

41-57

 Revision: 3
 February 28, 1995
 u:\ap600\pra\sec41-1.wpf:1b

AP600 Case 1AP No Hydrogen Ignition Case
 Best Estimate In-Vessel Hydrogen Generation
 Containment Flammability Limits

— Flammability Limit for Upward Combustion
 □ Flammability Limit for Downward Combustion
 ▲ Hydrogen Concentration

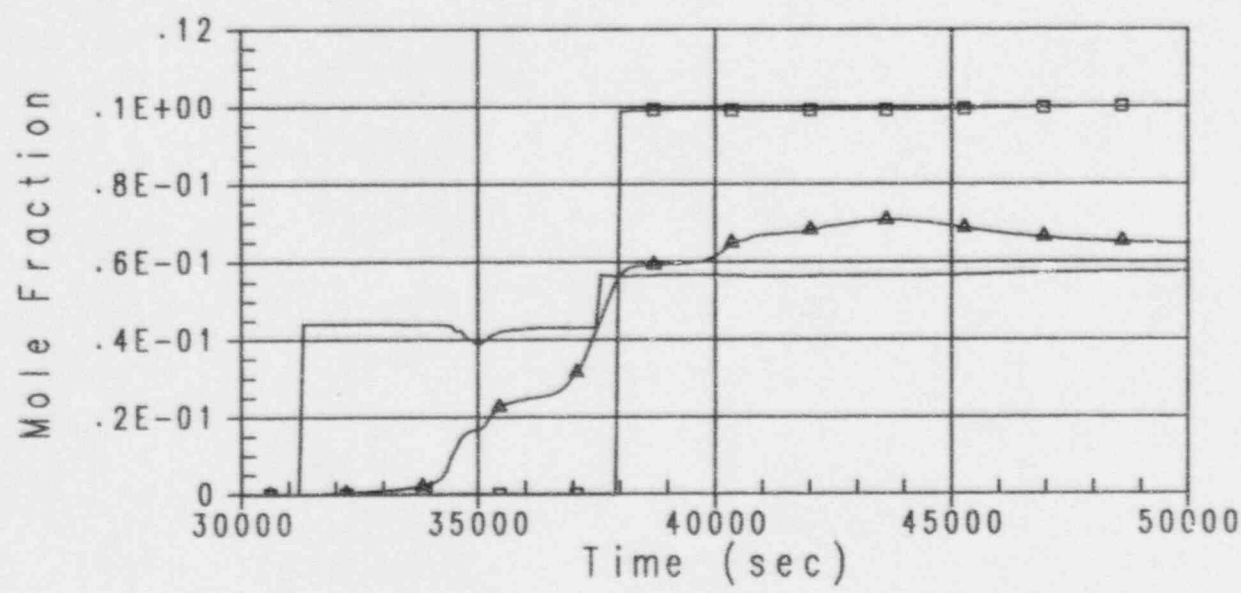


Figure 41-20



AP600 Case 1AP No Hydrogen Ignition Case
Bounding Estimate In-Vessel Hydrogen Generation
Containment Flammability Limits

- Flammability Limit for Upward Combustion
□ Flammability Limit for Downward Combustion
▲ Hydrogen Concentration

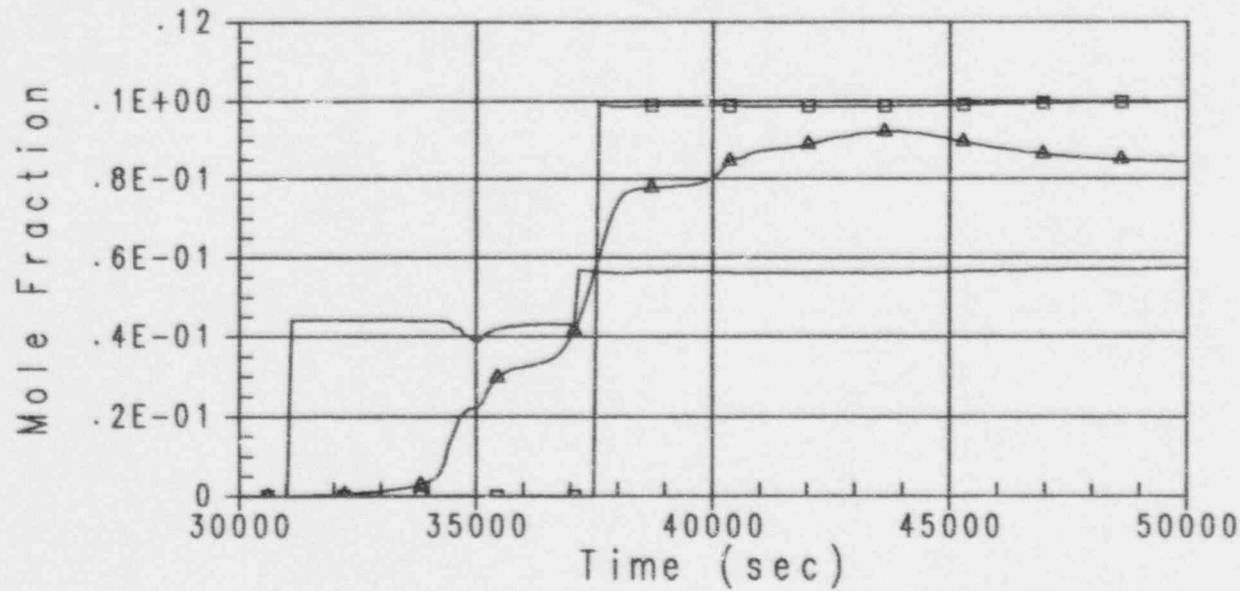


Figure 41-21



Westinghouse

ENEL
ENR NATIONAL
FOR L'ESPRESSO EDITORIA

AP600 Case 3BE No Reflood No Hydrogen Ignition Case
Containment Pressure

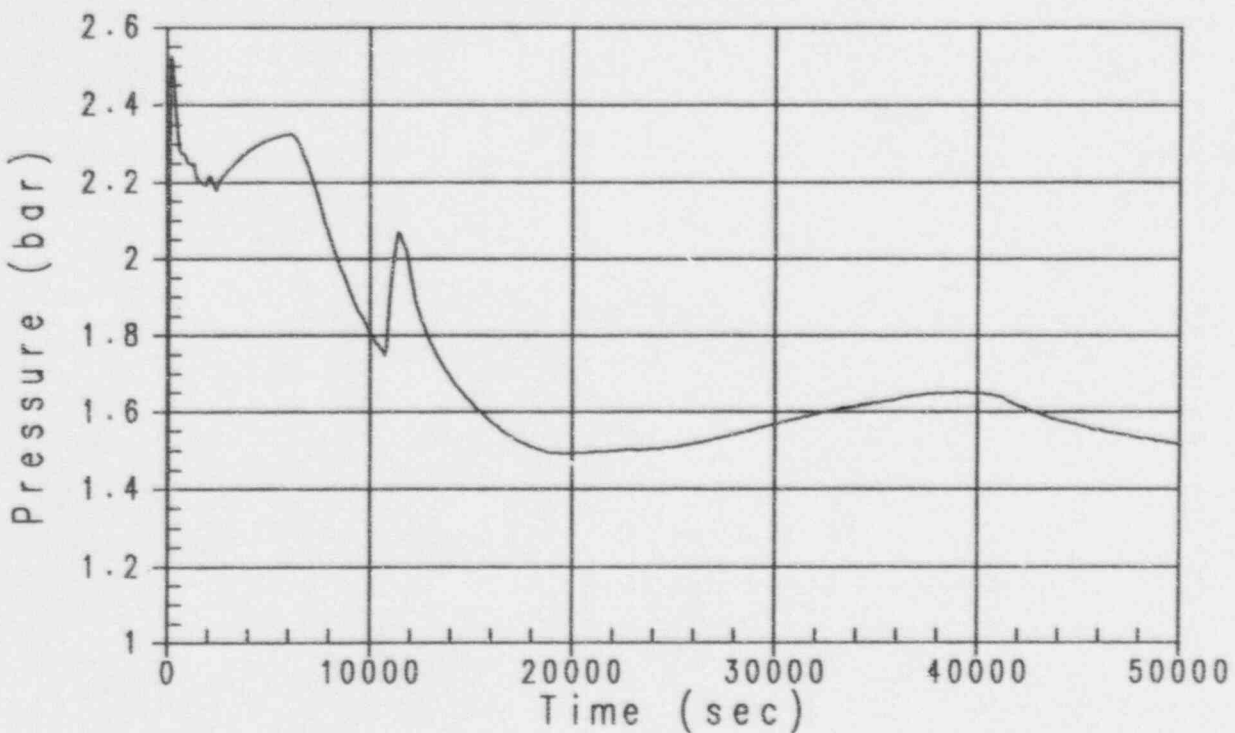


Figure 41-22

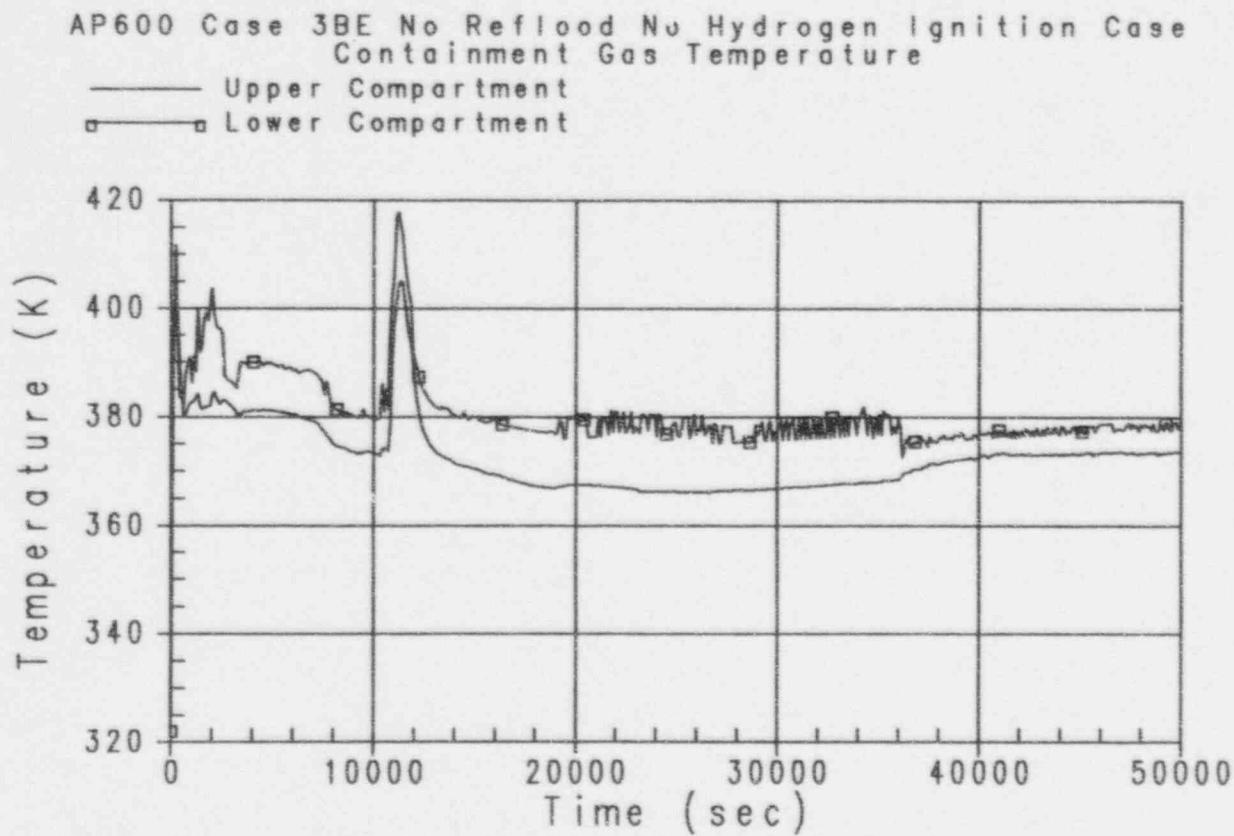


Figure 41-23



Westinghouse

ENEL
ENTE NAZIONALE
PER L'ENERGIA ELETTRICA

41-61

Revision: 3

February 28, 1995

u:\ap600\pralwcd41-1.wpl:1b

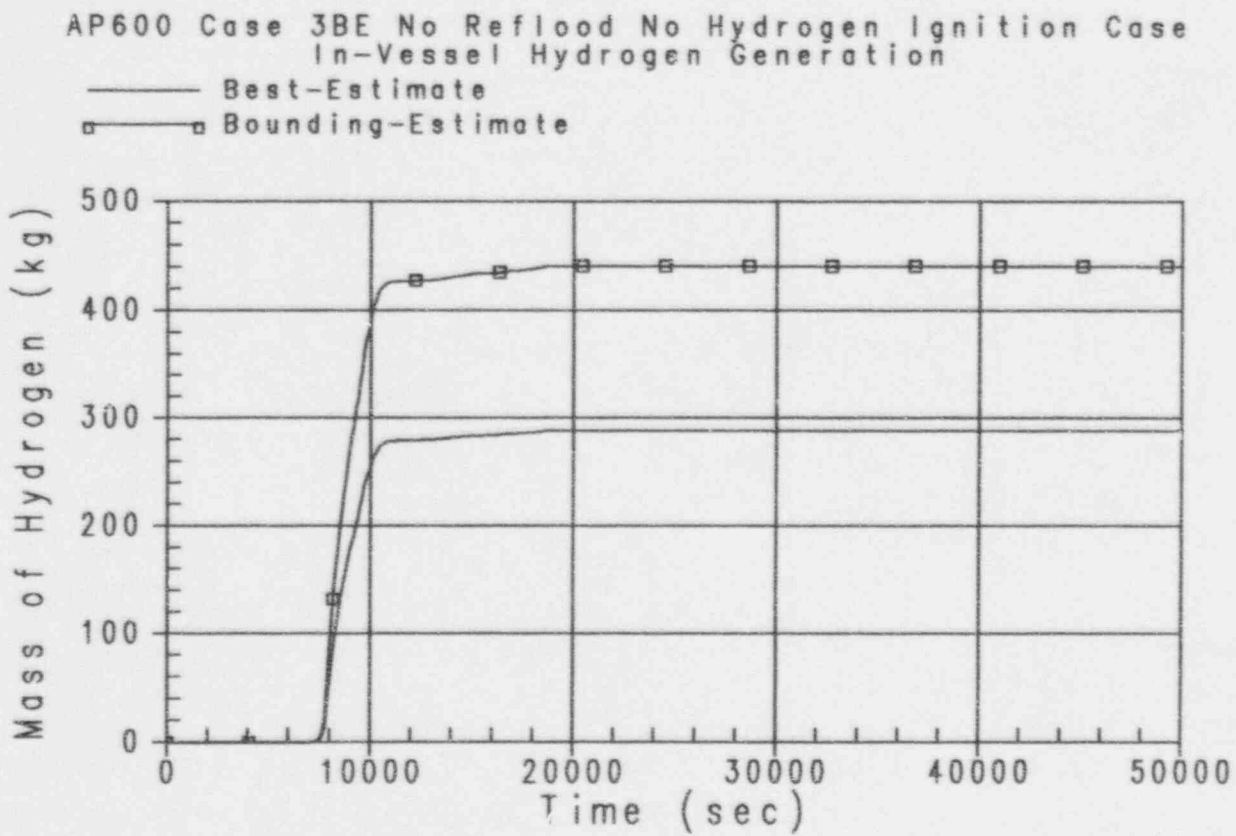


Figure 41-24

AP600 Case 3BE No Reflood No Hydrogen Ignition Case
 Best Estimate In-Vessel Hydrogen Generation
 Containment Compartment Hydrogen Mole Fractions

— Loop Compt
 □ Dead-Ended Region
 ▲ IRWST
 ◇ Upper Compt

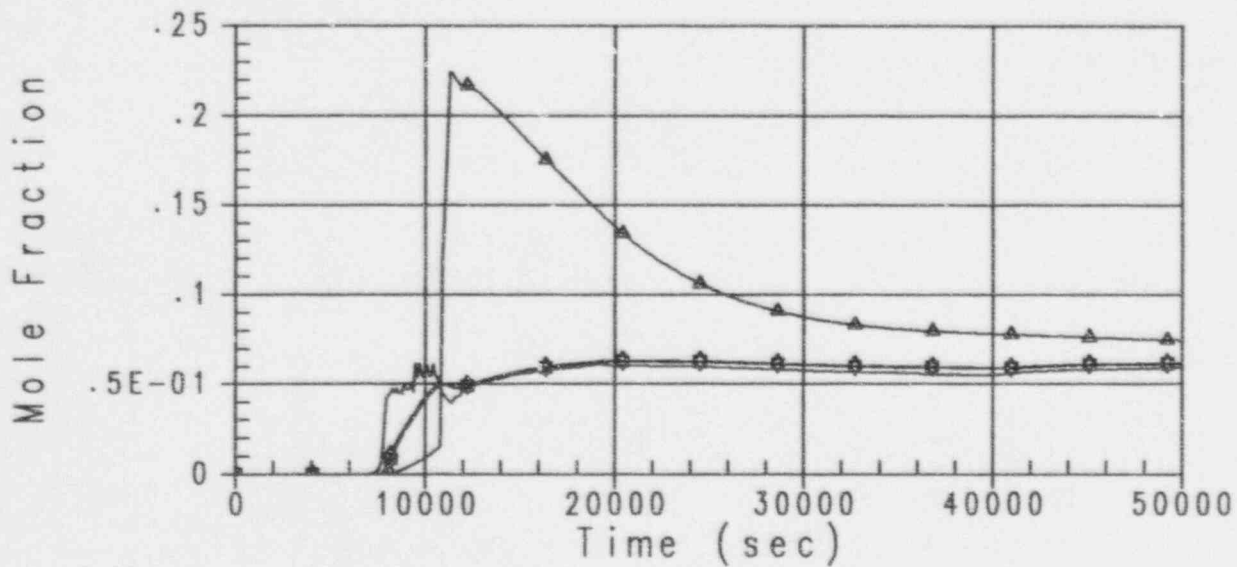


Figure 41-25



Westinghouse

ENEL
 ENEL NUCLEARE
 PER L'ENERGIA ELETTRICA

41-63

Revision: 3
 February 28, 1995
 u:\ap600\pra\sec41-1.wpf:lb

AP600 Case 3BE No Reflood No Hydrogen Ignition Case
 Bounding Estimate In-Vessel Hydrogen Generation
 Containment Compartment Hydrogen Mole Fractions

- Loop Compt
- Dead-Ended Region
- △ IRWST
- ◇ Upper Compt

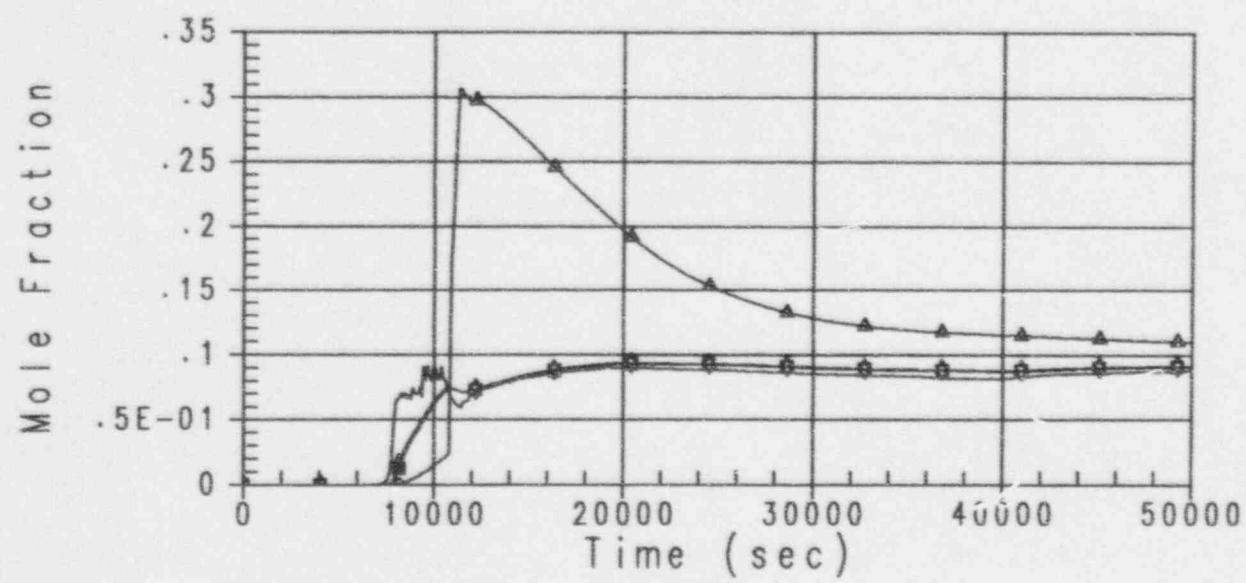


Figure 41-26

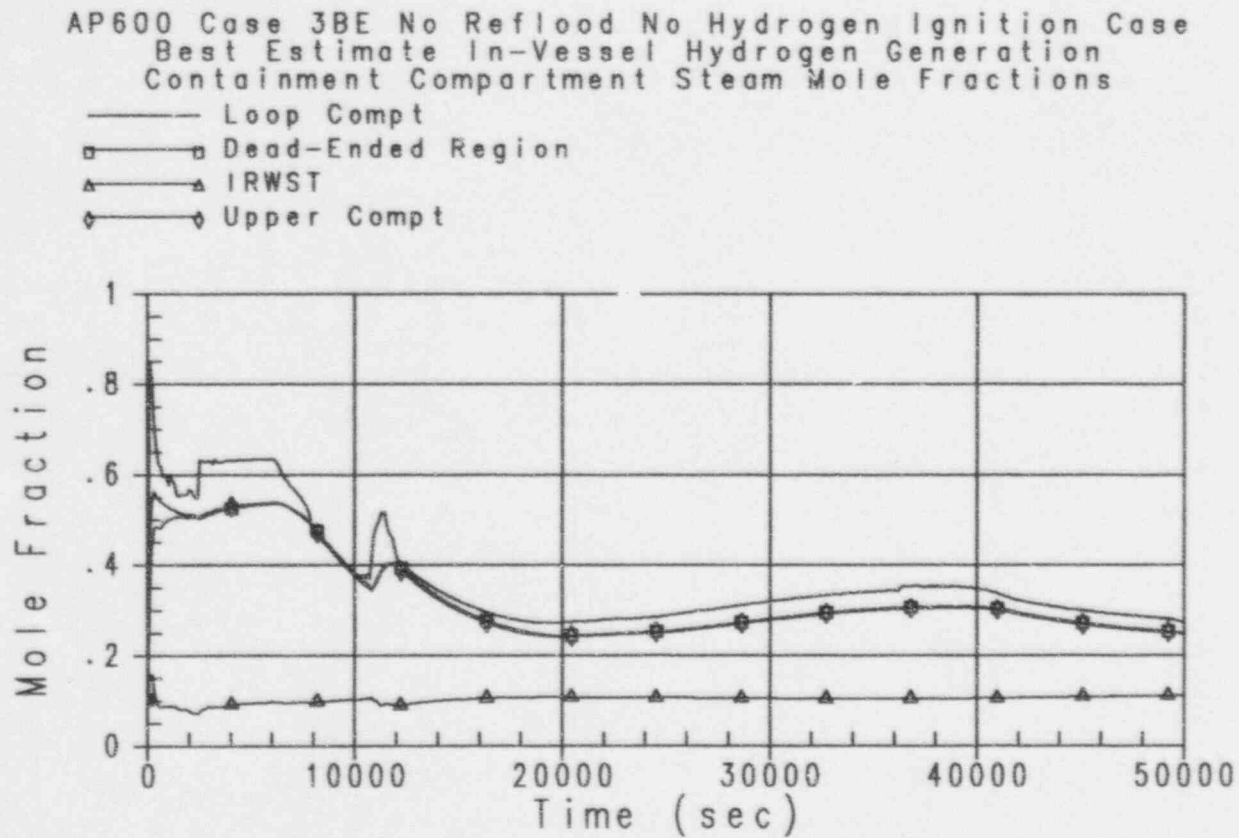


Figure 41-27



Westinghouse

ENEL
 ENTE NAZIONALE
 PER L'ELETTRICITA'

41-65

 Revision: 3
 February 28, 1995
 u:\ap600\gra\sec41-2.wpf:1b

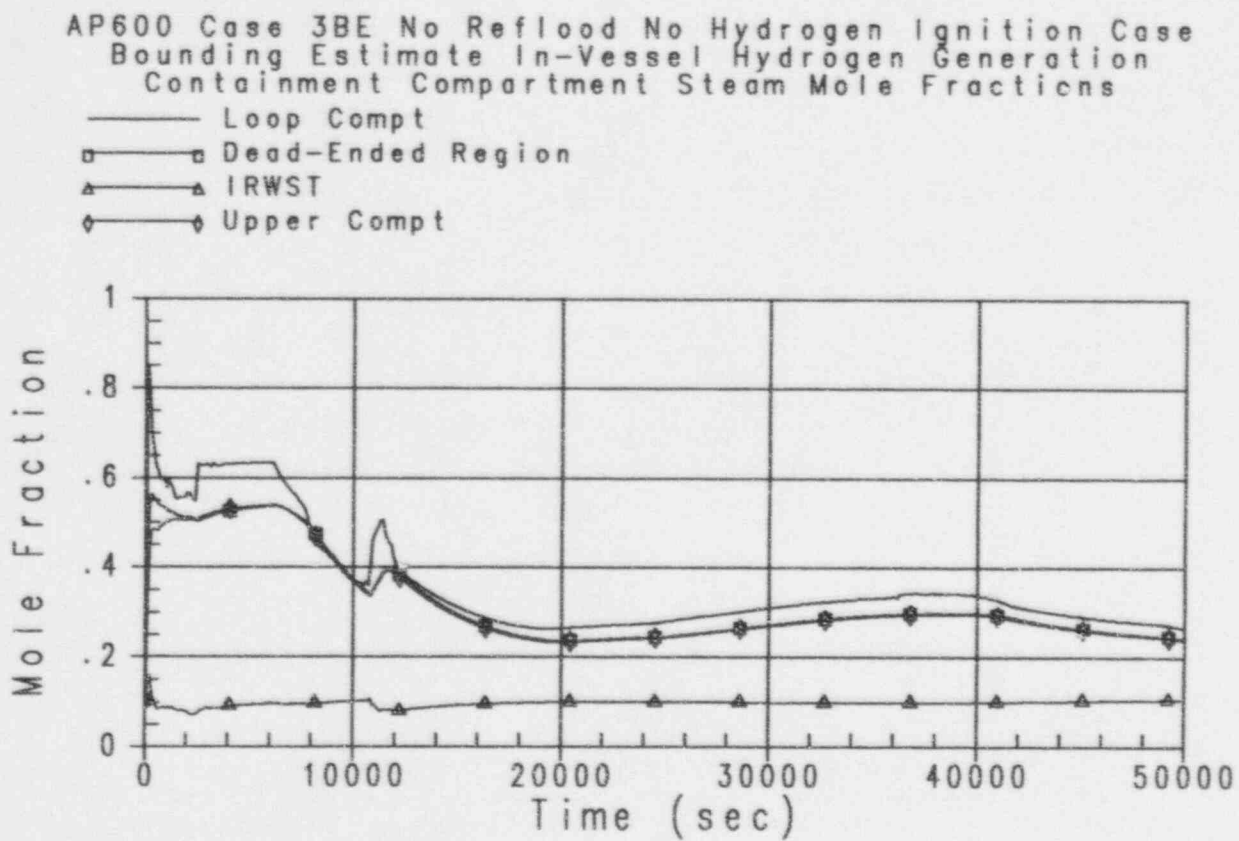


Figure 41-28

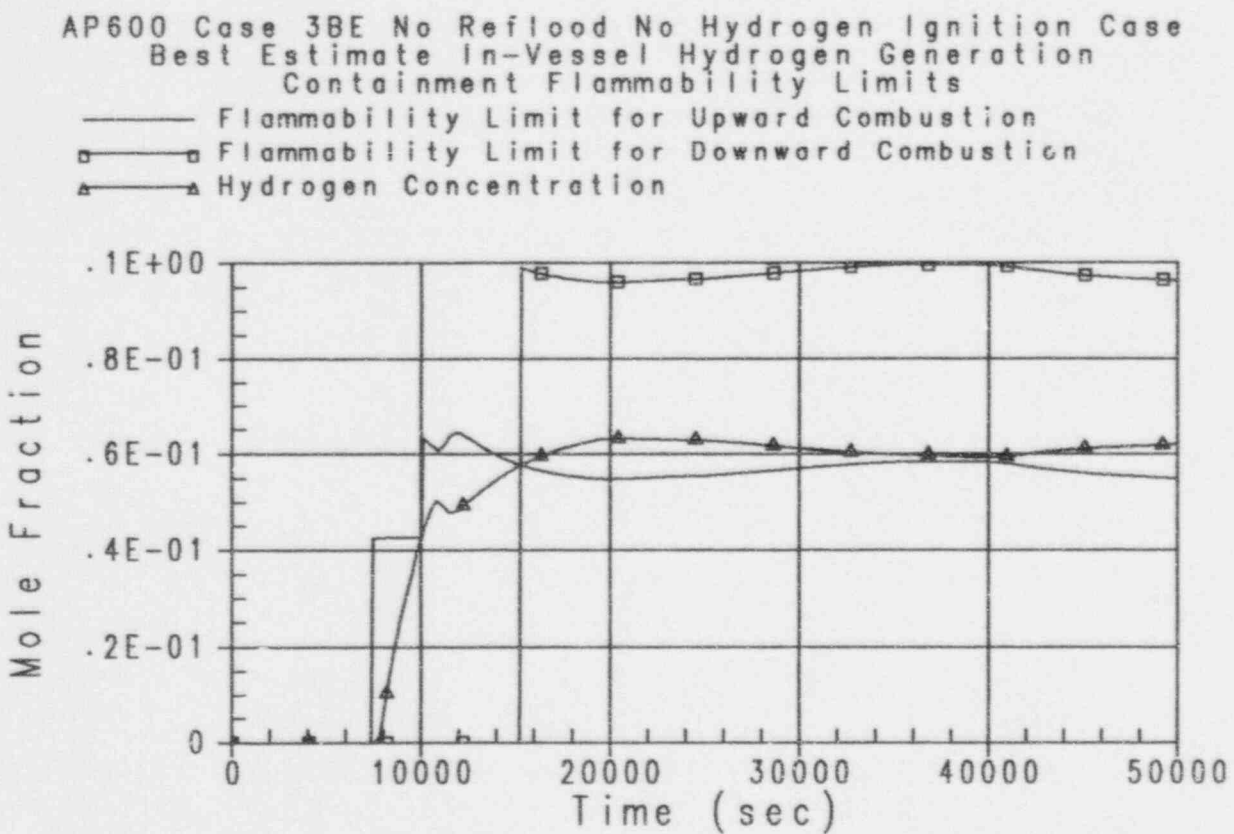


Figure 41-29



Westinghouse

 ENEC
 EAST MANASSAS
 FOR L. CORDON, S. LITVIN

41-67

 Revision: 3
 February 28, 1995
 u:\ap600\grahsec41-2.wpf:lb

AP600 Case 3BE No Reflood No Hydrogen Ignition Case
 Bounding Estimate In-Vessel Hydrogen Generation
 Containment Flammability Limits

— Flammability Limit for Upward Combustion
 □ Flammability Limit for Downward Combustion
 ▲ Hydrogen Concentration

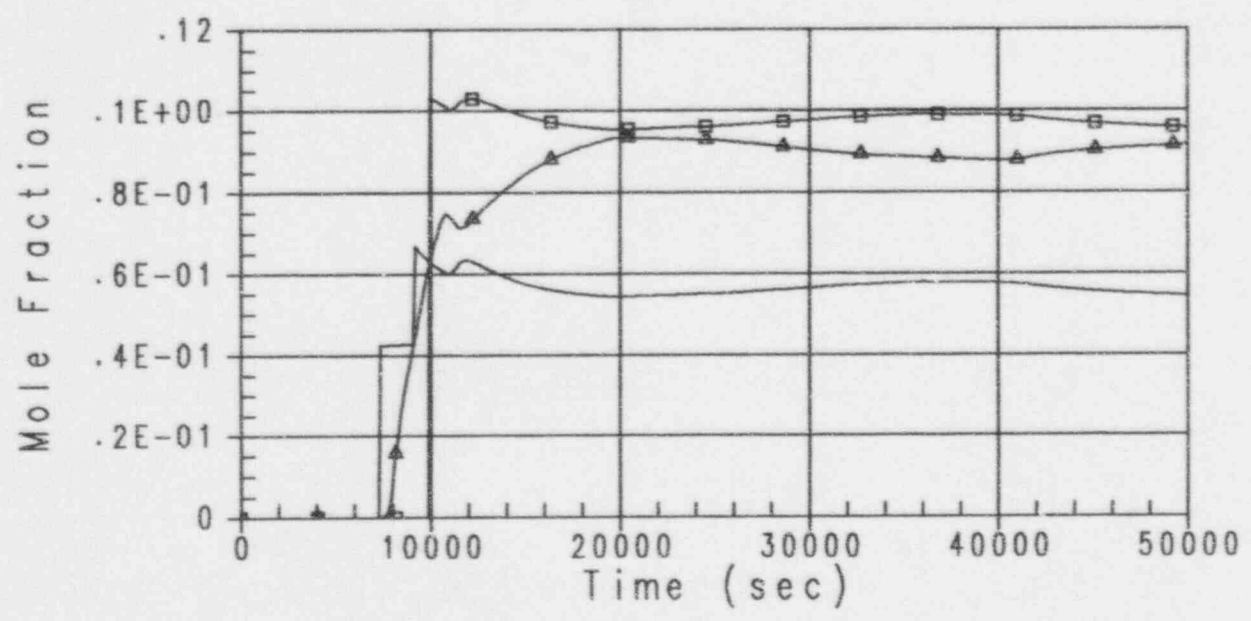


Figure 41-30

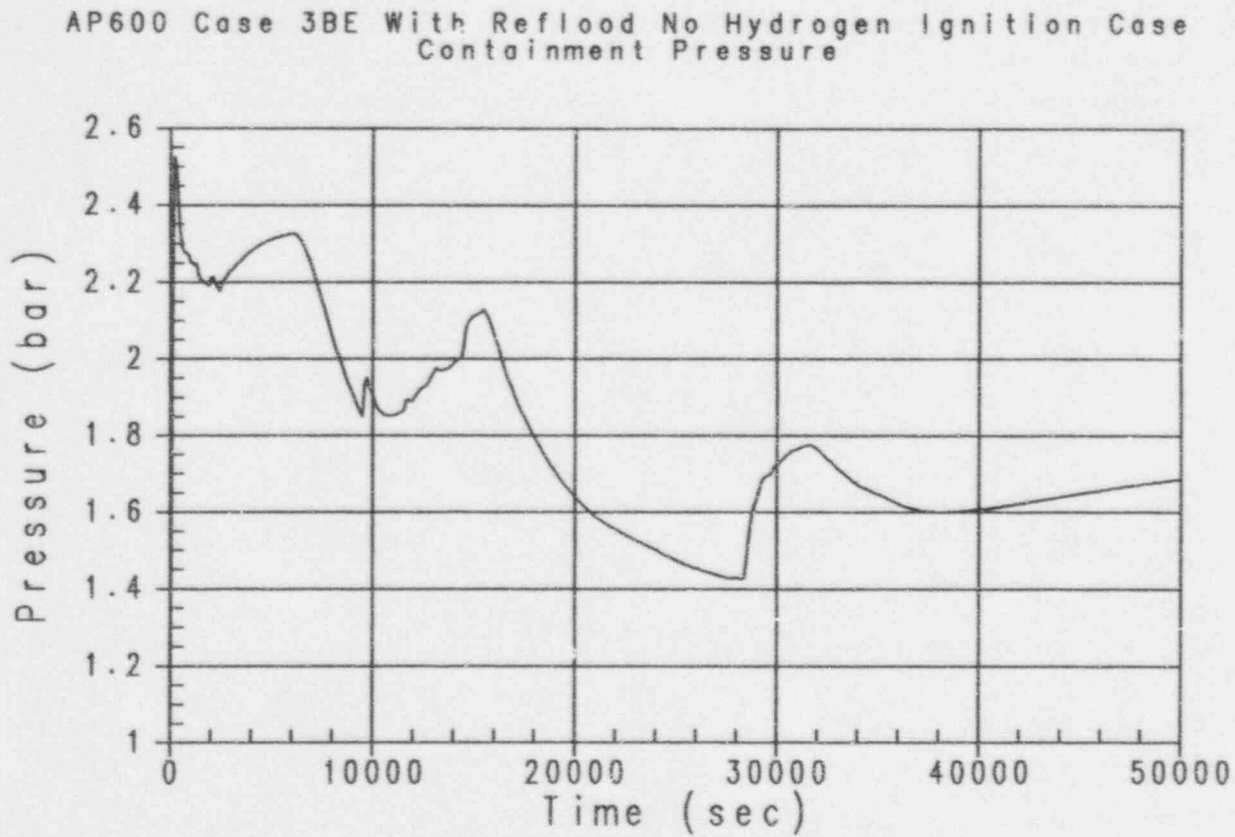


Figure 41-31



Westinghouse

ENEL
ENR. MAGAZINE
PER L'ENERGIA ELETTRICA

41-69

Revision: 3
February 28, 1995
u:\ap600\pra\sec41 2.wpf:1b

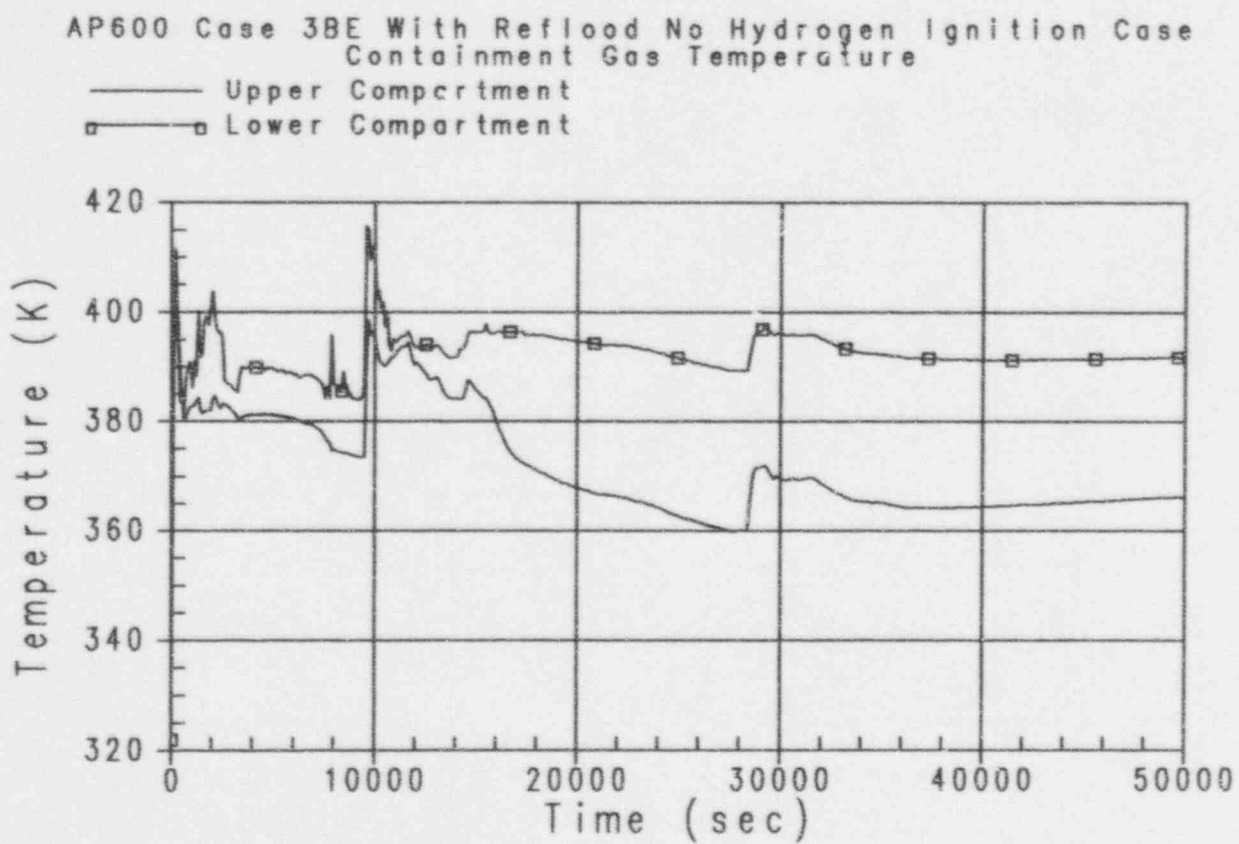


Figure 41-32

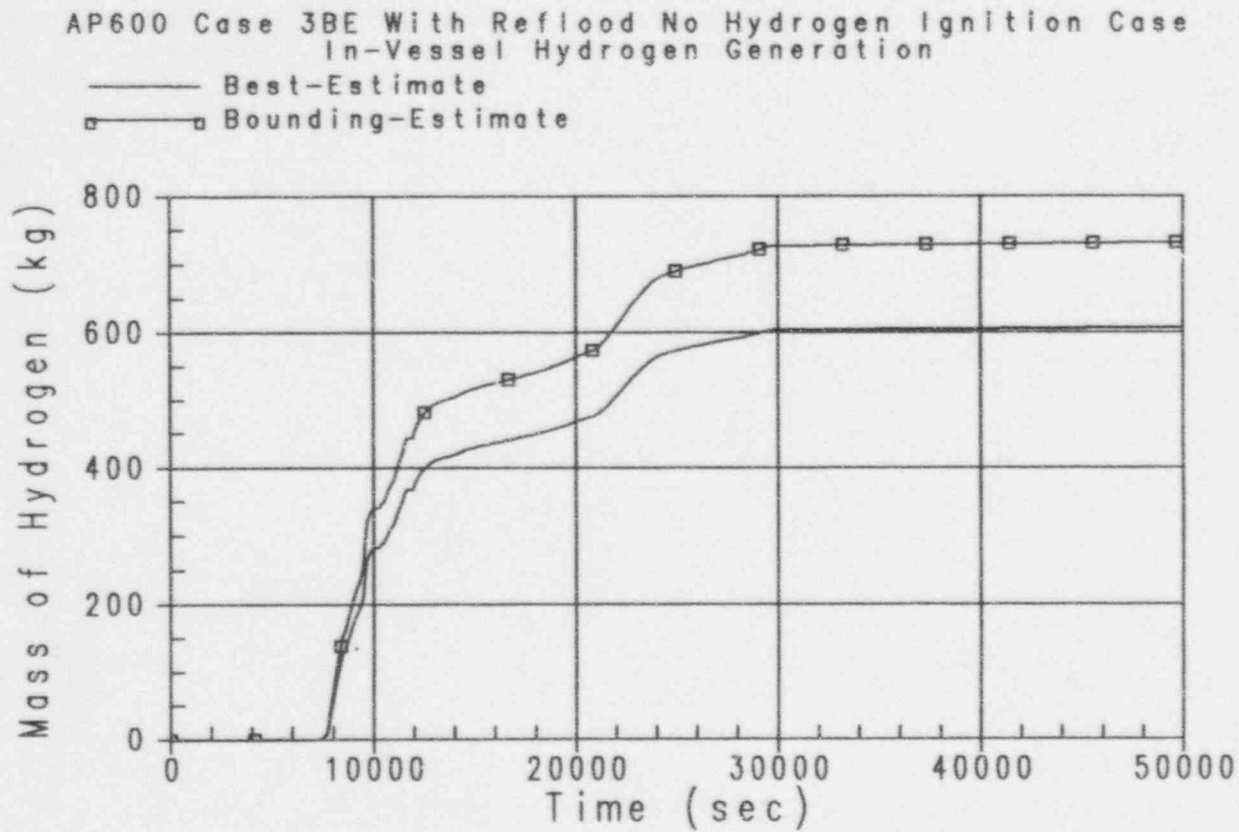


Figure 41-33



Westinghouse

ENEL
 ENEL NUCLEARE
 PER L'ENERGIA ELETTRICA

41-71

 Revision: 3
 February 28, 1995
 u:\ap600\pralvecd1-2.wpf:lb

AP600 Case 3BE With Reflood No Hydrogen Ignition Case
 Best Estimate In-Vessel Hydrogen Generation
 Containment Compartment Hydrogen Mole Fractions

— Loop Compt
 □ Dead-Ended Region
 △ IRWST
 ◇ Upper Compt

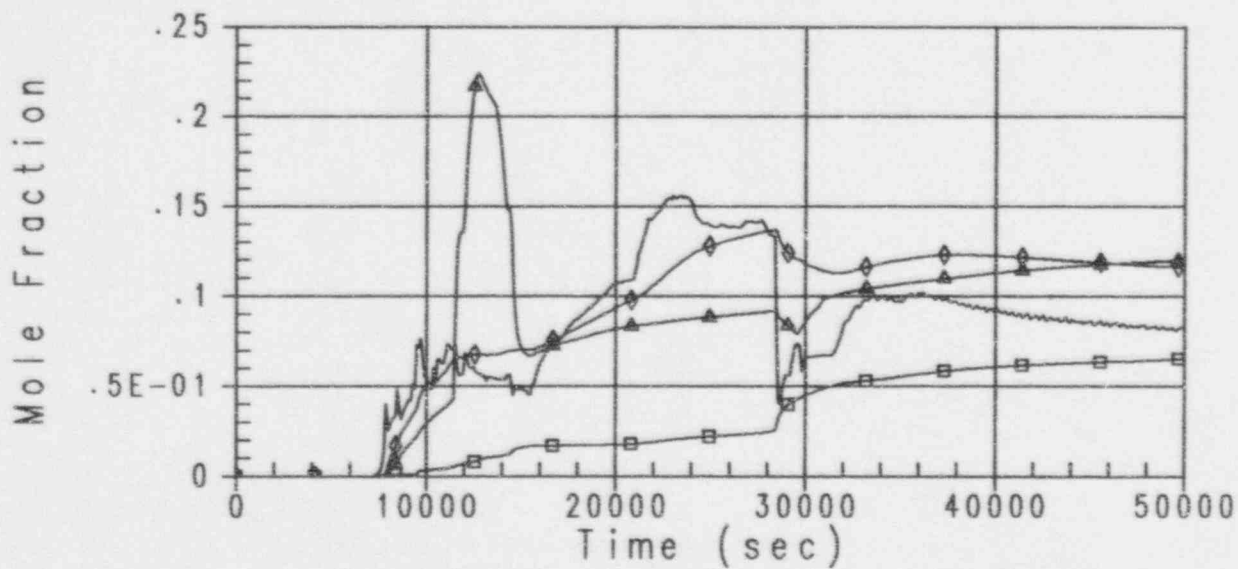


Figure 41-34

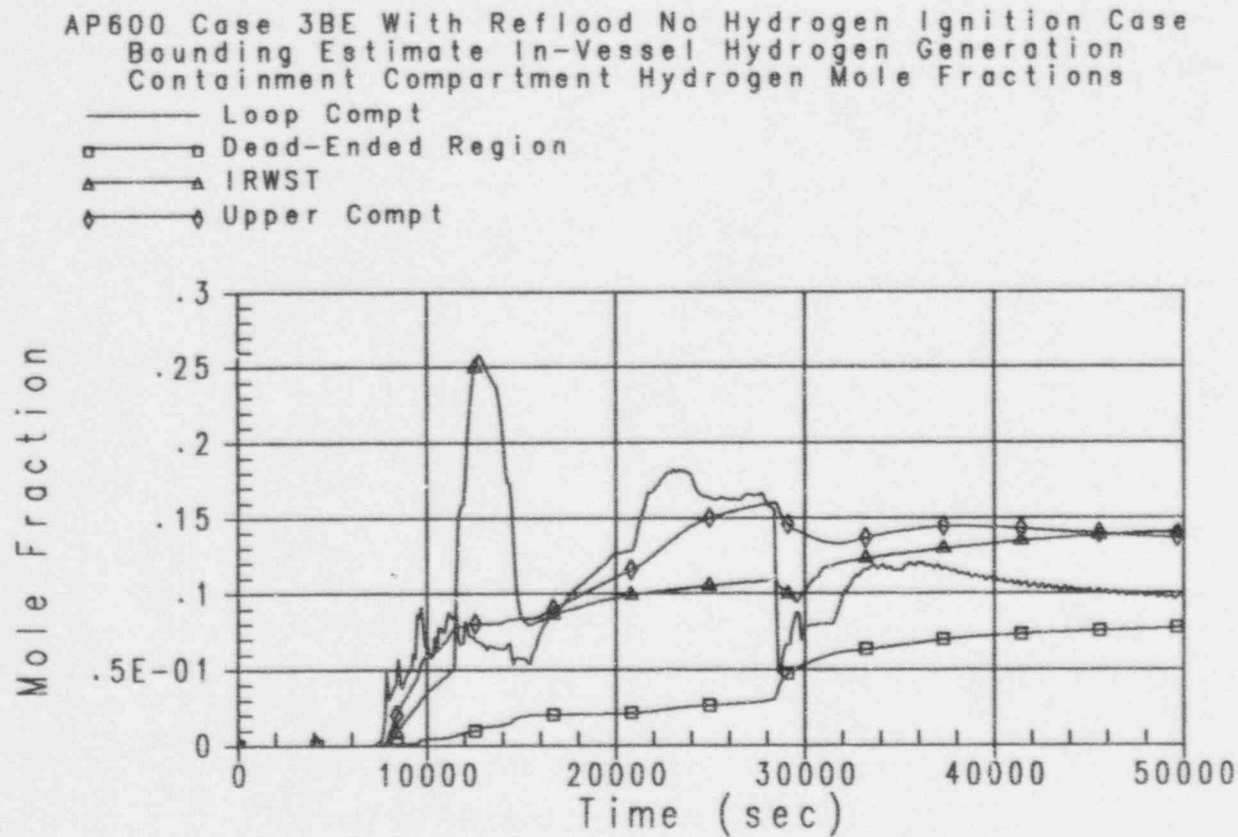


Figure 41-35



Westinghouse

ENEL
 ENEL NUCLEARE
 PER L'ELETTRICITA'

41-73

 Revision: 3
 February 28, 1995
 u:\ap600\pra\sec41-2.wpf:1b

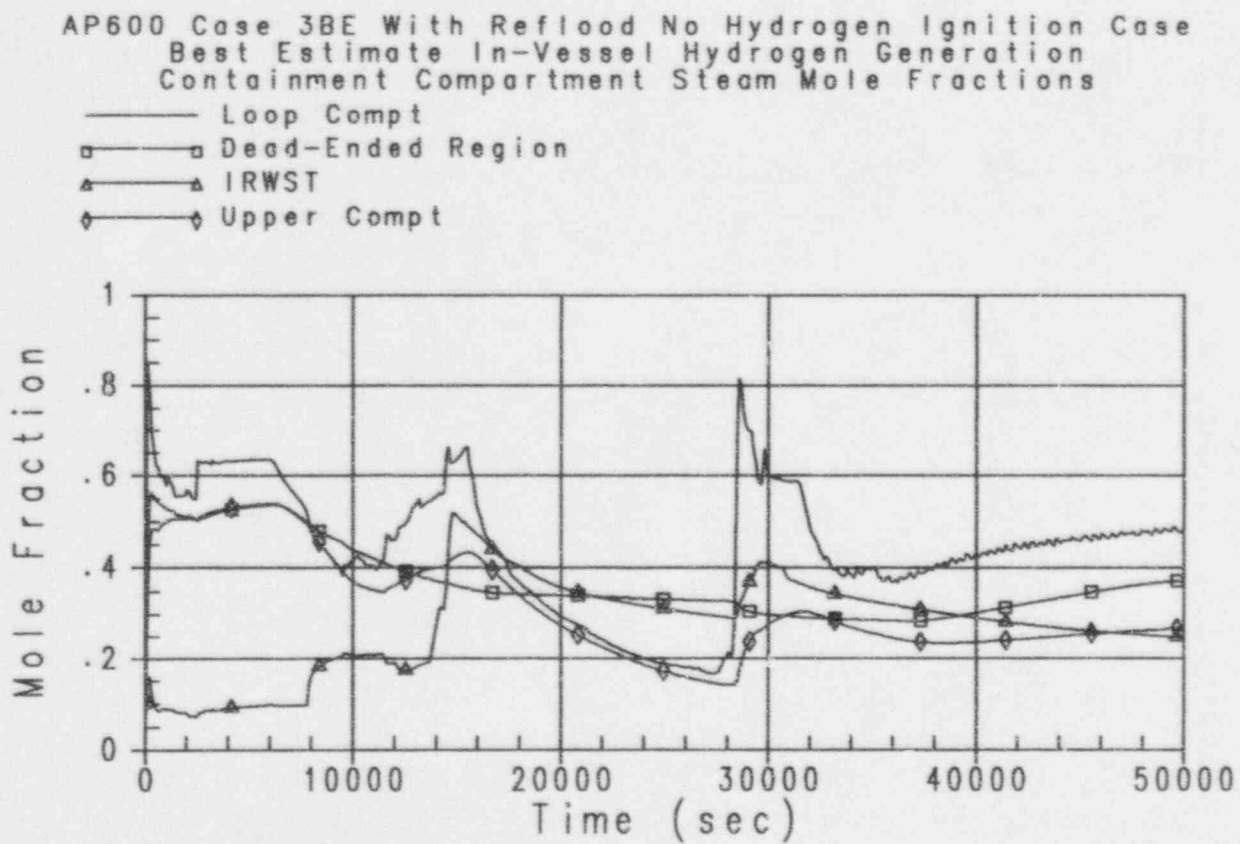


Figure 41-36

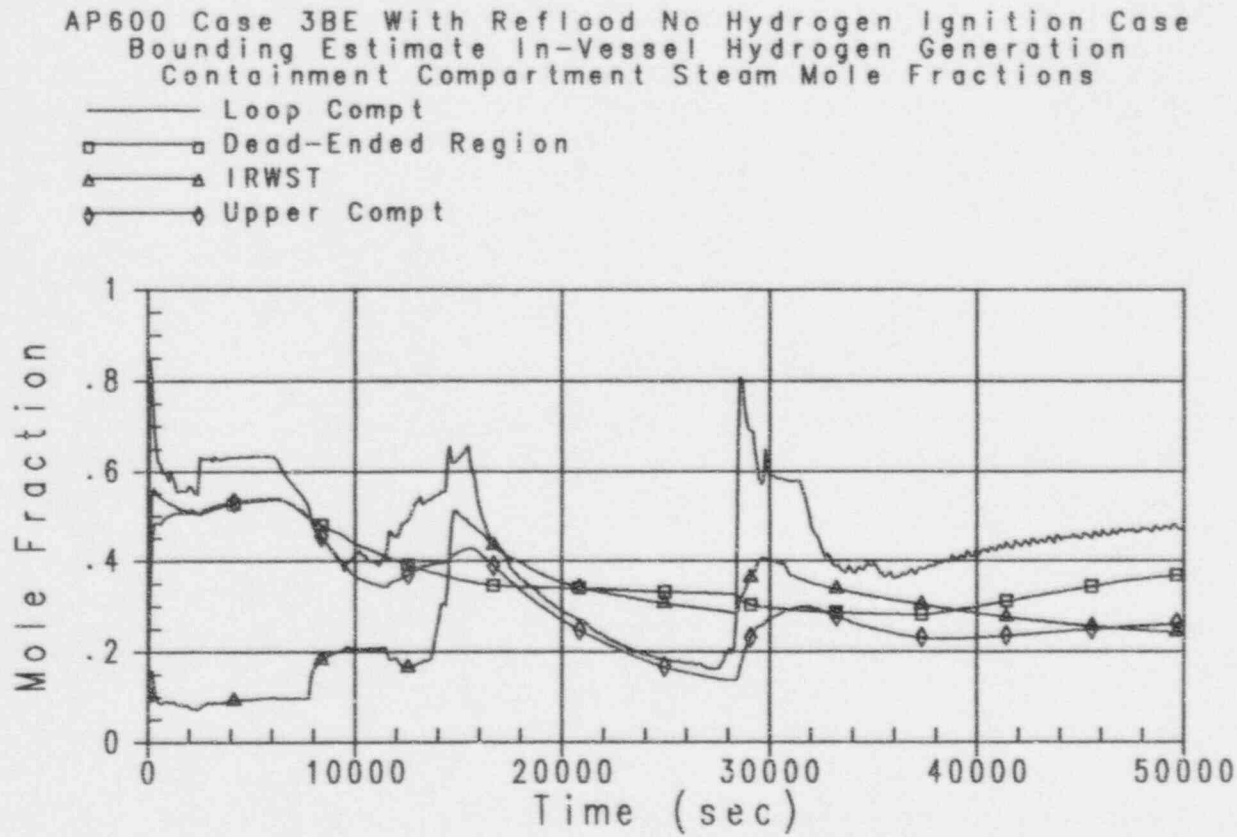


Figure 41-37



Westinghouse

ENEL
 ENERGETIC
 PER L'ESERCIZIO

AP600 Case 3BE With Reflood No Hydrogen Ignition Case
Best Estimate In-Vessel Hydrogen Generation
Containment Flammability Limits

— Flammability Limit for Upward Combustion
□ Flammability Limit for Downward Combustion
▲ Hydrogen Concentration

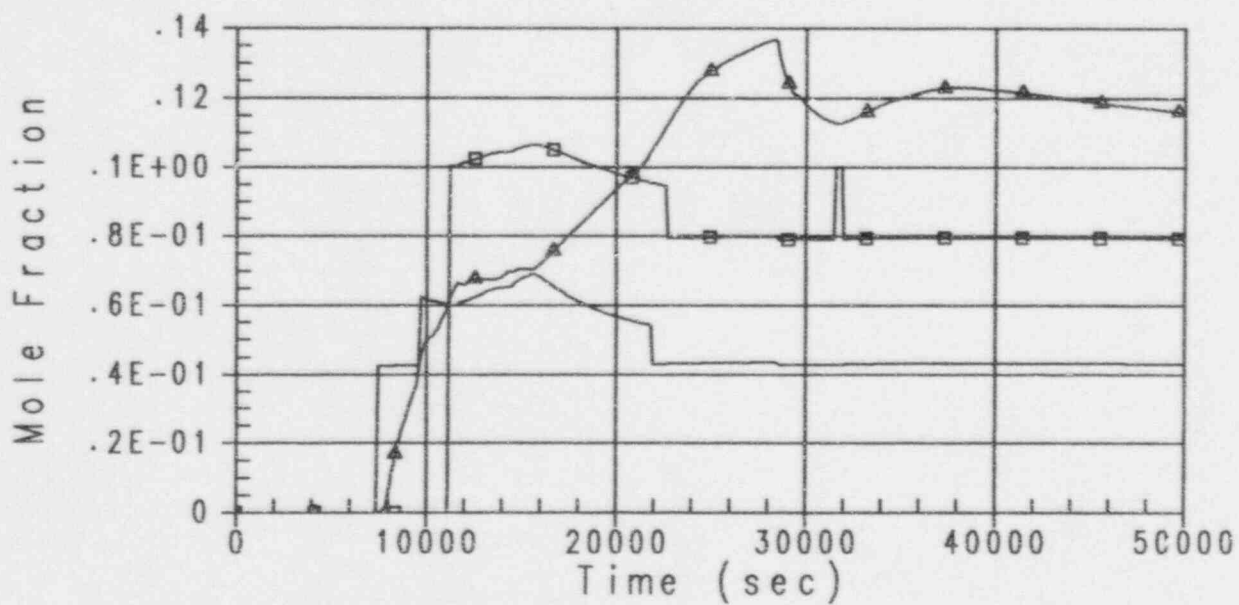


Figure 41-38

AP600 Case 3BE With Reflood No Hydrogen Ignition Case
 Bounding Estimate In-Vessel Hydrogen Generation
 Containment Flammability Limits

— Flammability Limit for Upward Combustion
 □ Flammability Limit for Downward Combustion
 ▲ Hydrogen Concentration

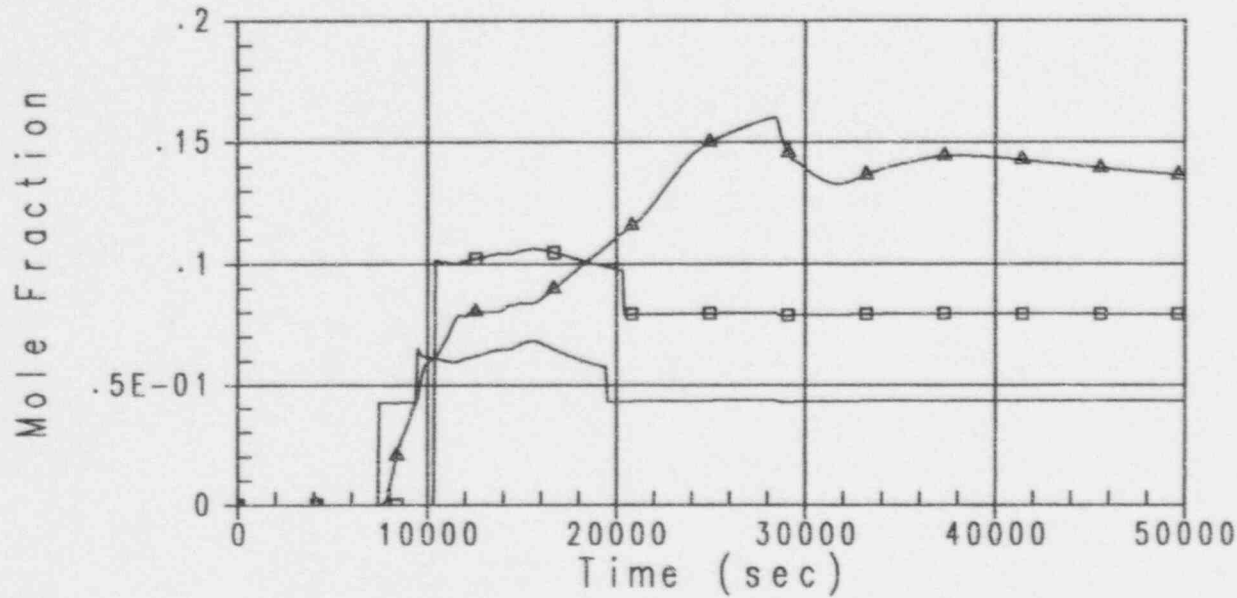


Figure 41-39



Westinghouse

ENEL
 ENERGETICA NUCLEARE
 PER L'ENERGIA ELETTRICA

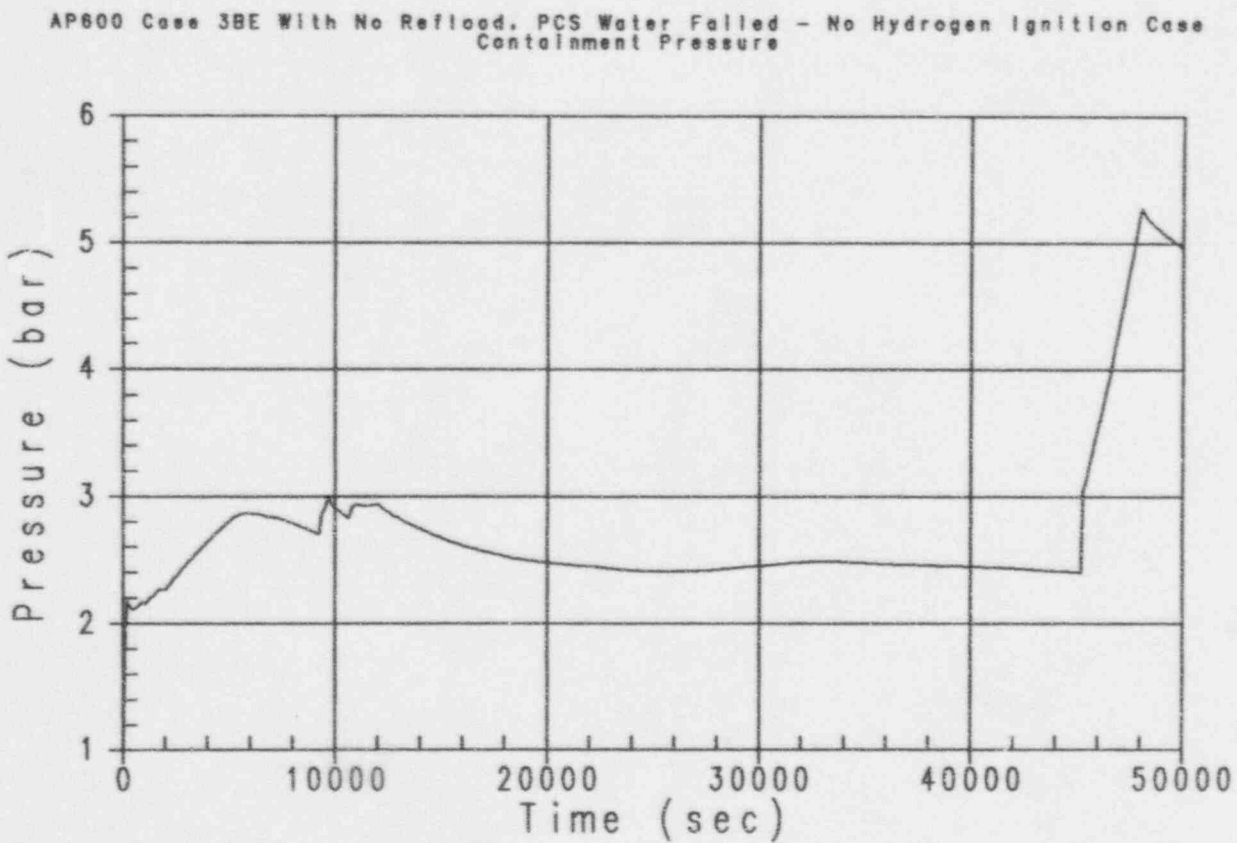


Figure 41-40

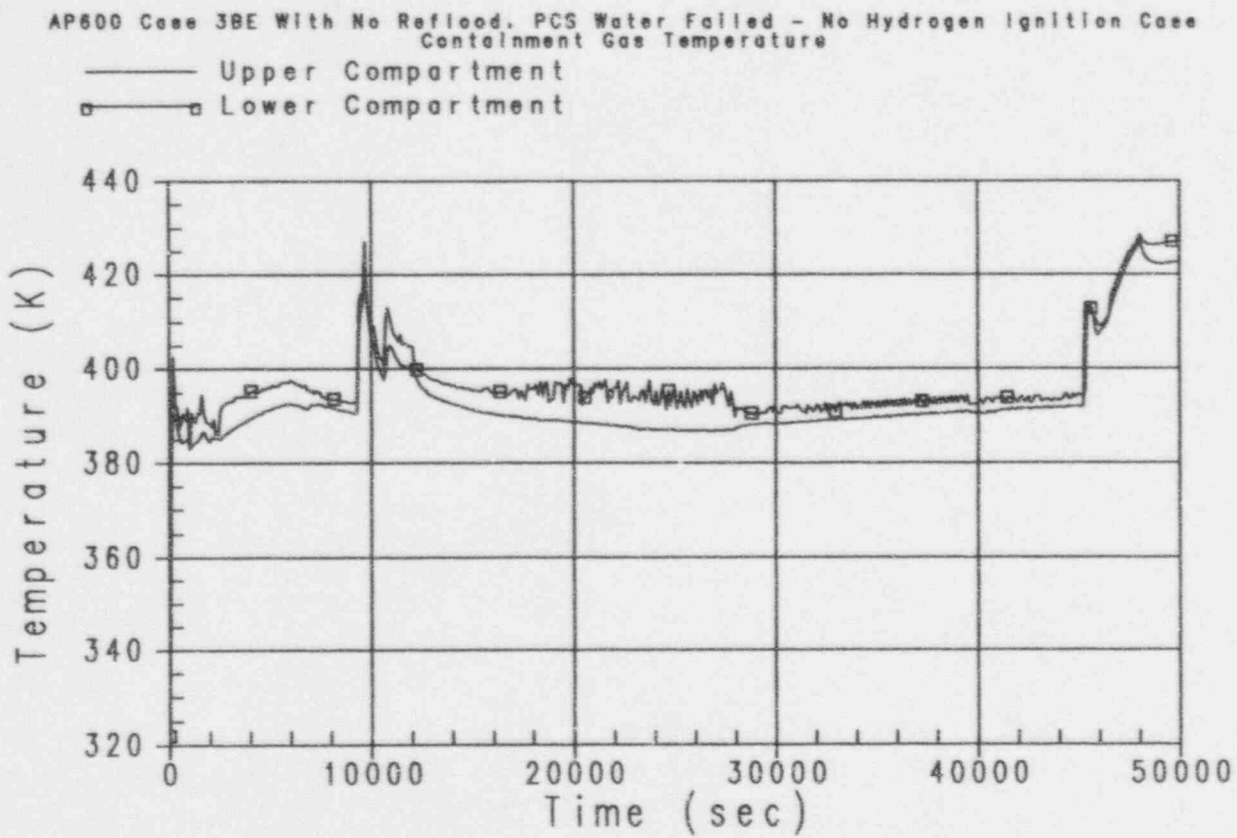


Figure 41-41



Westinghouse

ENEL
 ENEL NUCLEARE
 PER L'ENERGIA ELETTRICA

41-79

 Revision: 3
 February 28, 1995
 u:\ap600\gra\sec41-2.wpf:1b

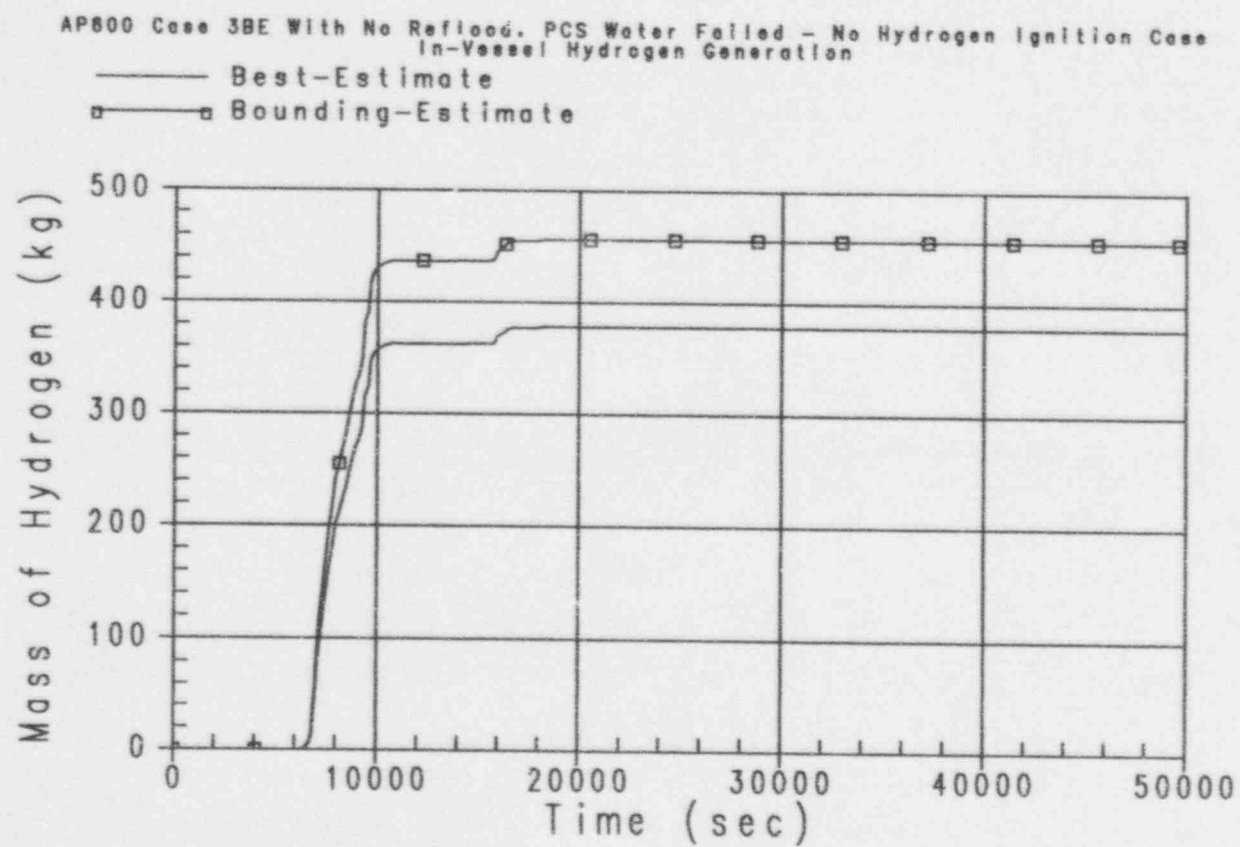


Figure 41-42

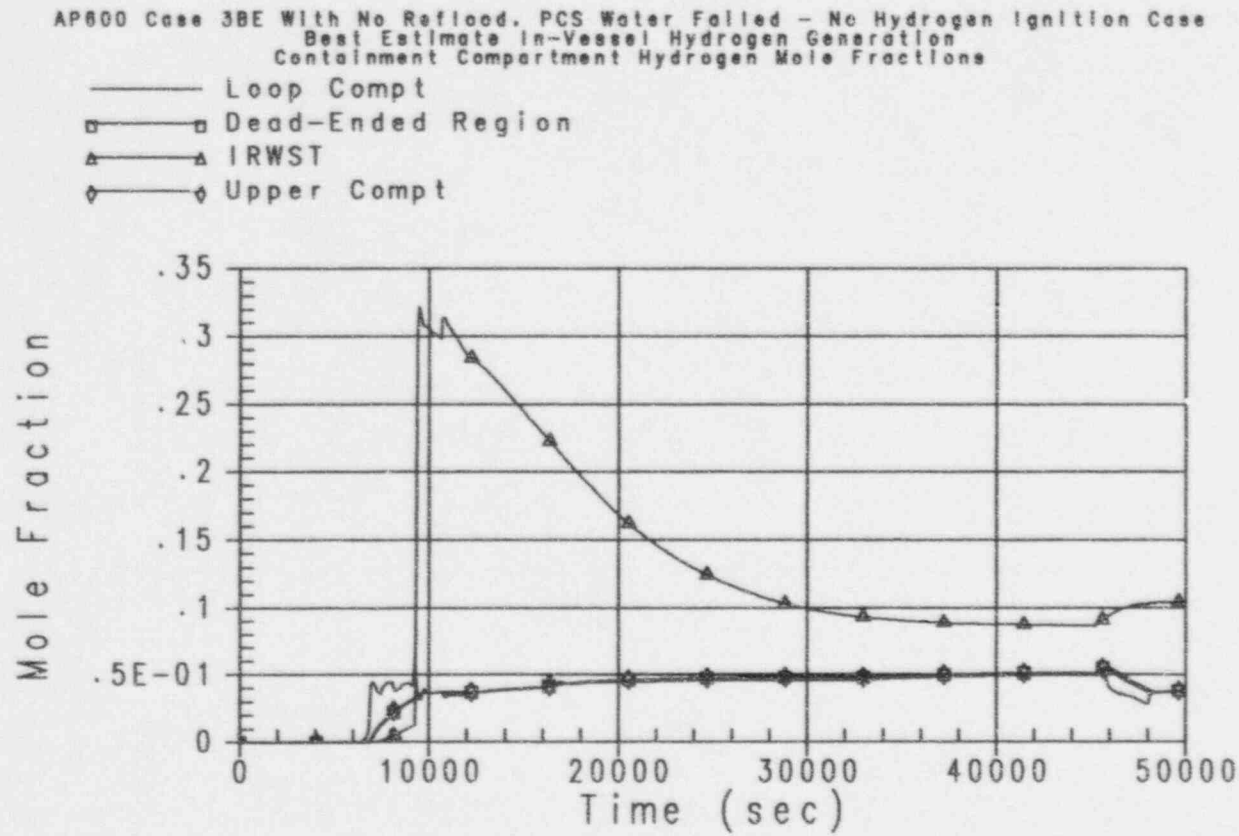


Figure 41-43



Westinghouse

ENEL
ENR NATIONAL
FOR LONDON ELECTRONICS

41-81

Revision: 3
February 28, 1995
u:\ap600\prasec41-2.wpf:lb

AP600 Case 3BE With No Reflood. PCS Water Failed - No Hydrogen Ignition Case
 Bounding Estimate In-Vessel Hydrogen Generation
 Containment Compartment Hydrogen Mole Fractions

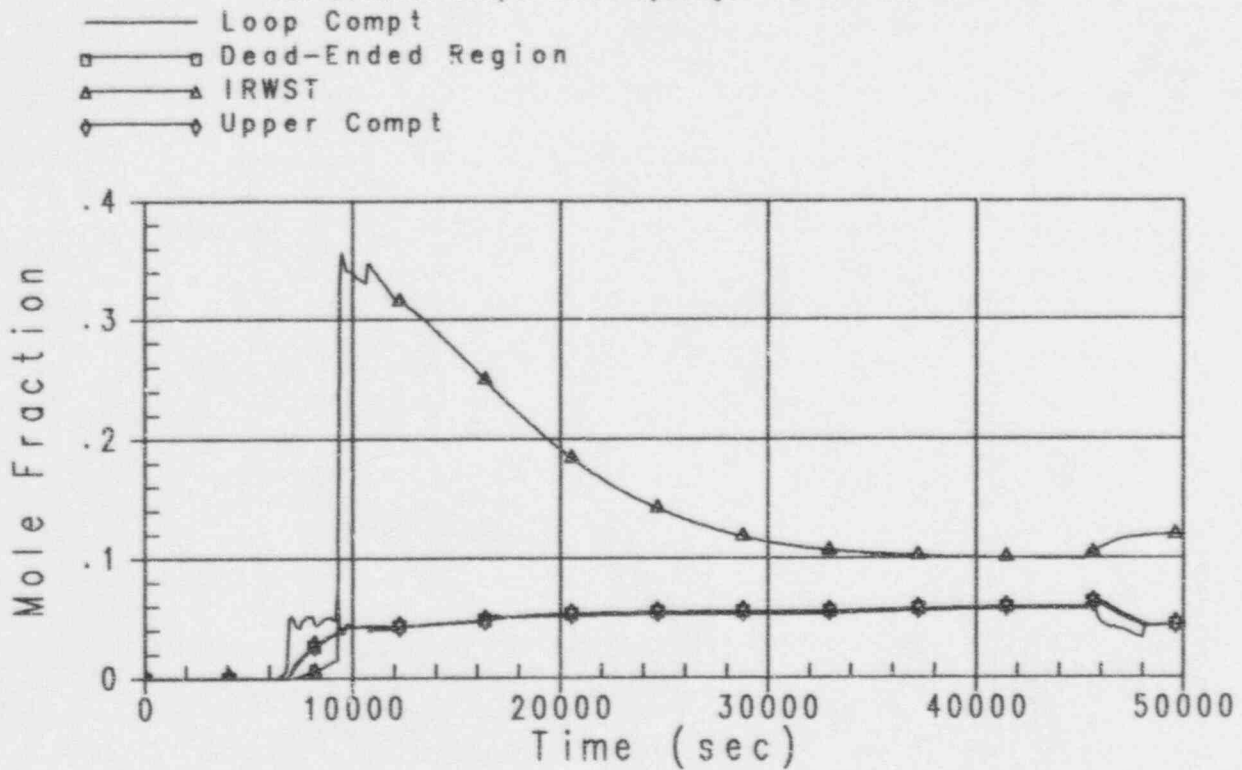


Figure 41-44

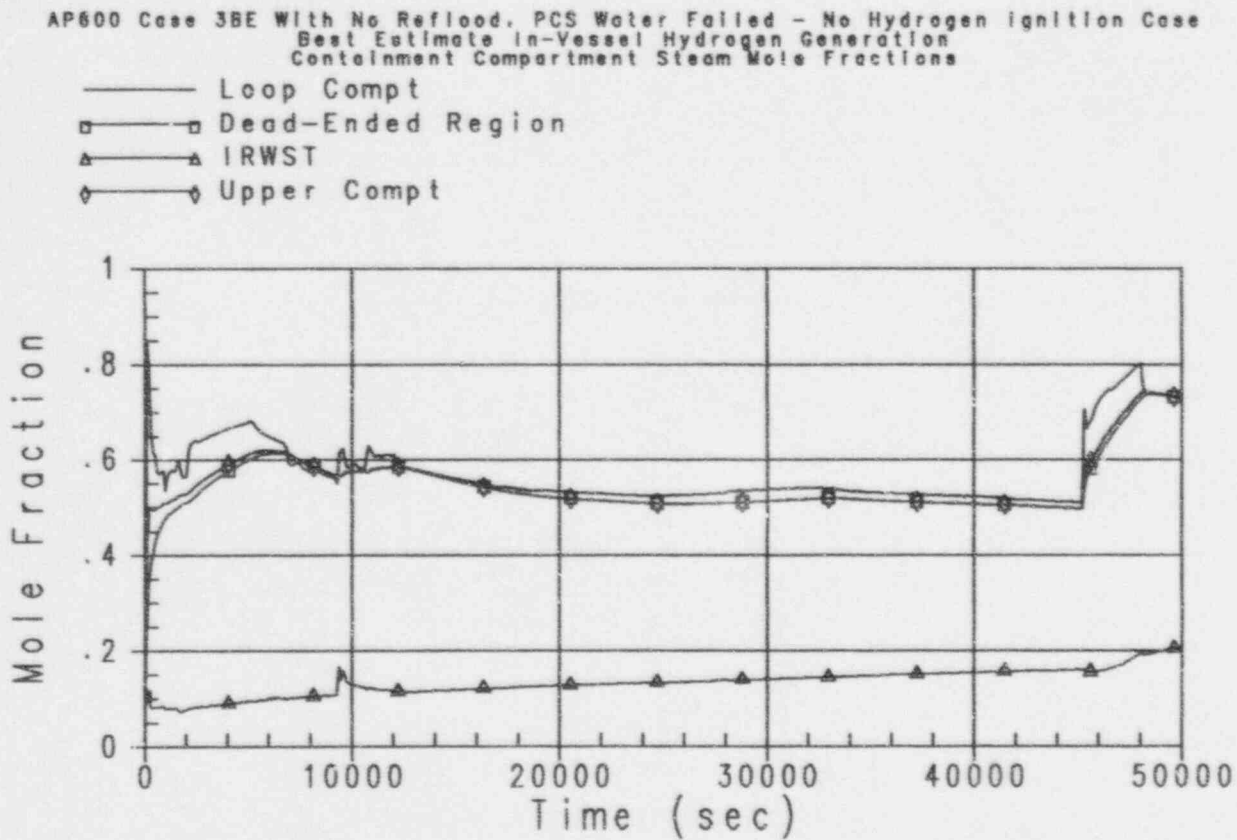


Figure 41-45



Westinghouse

ENEL
 ENVI. NUCLEON. L.
 PER. L. ENERGIA ELETTRICA

41-83

 Revision: 3
 February 28, 1995
 u:\ap600\gra\sec41-2.wpf:1b

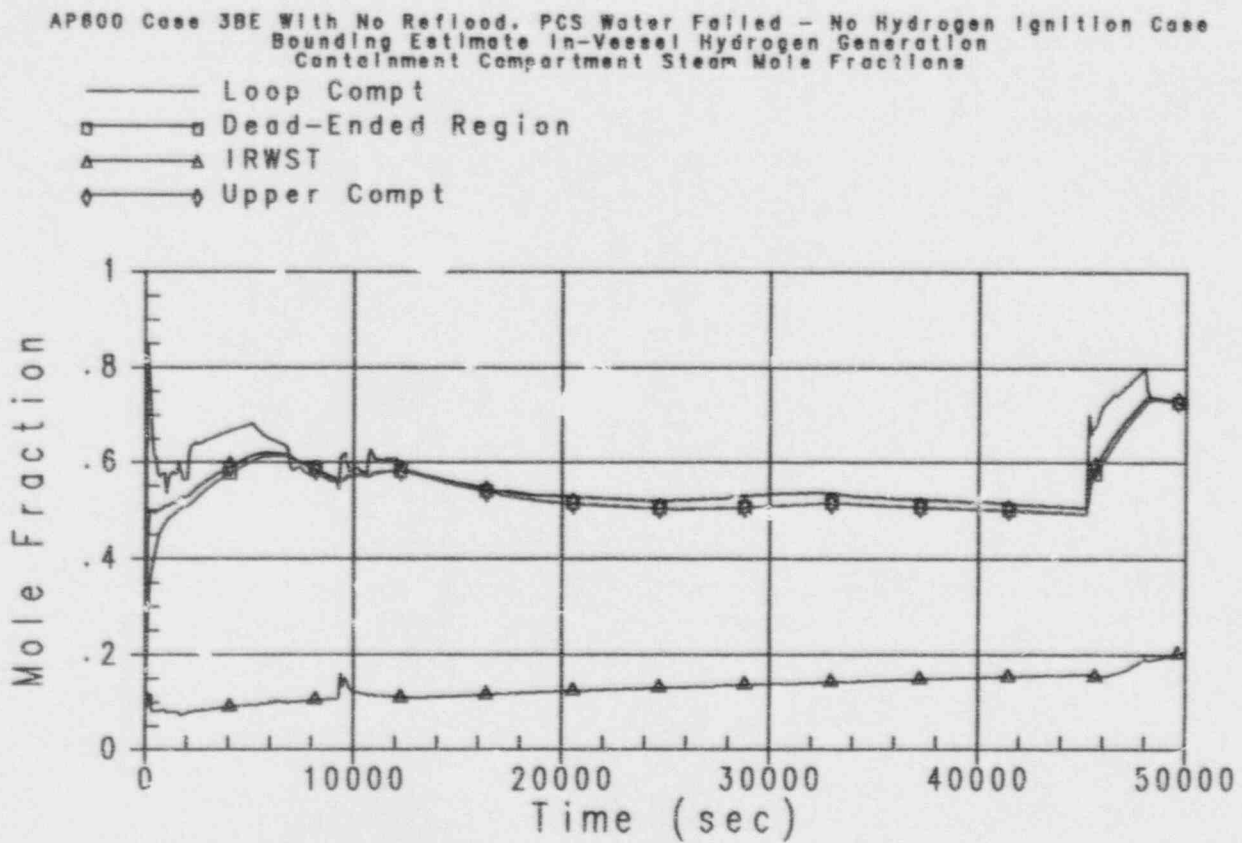


Figure 41-46

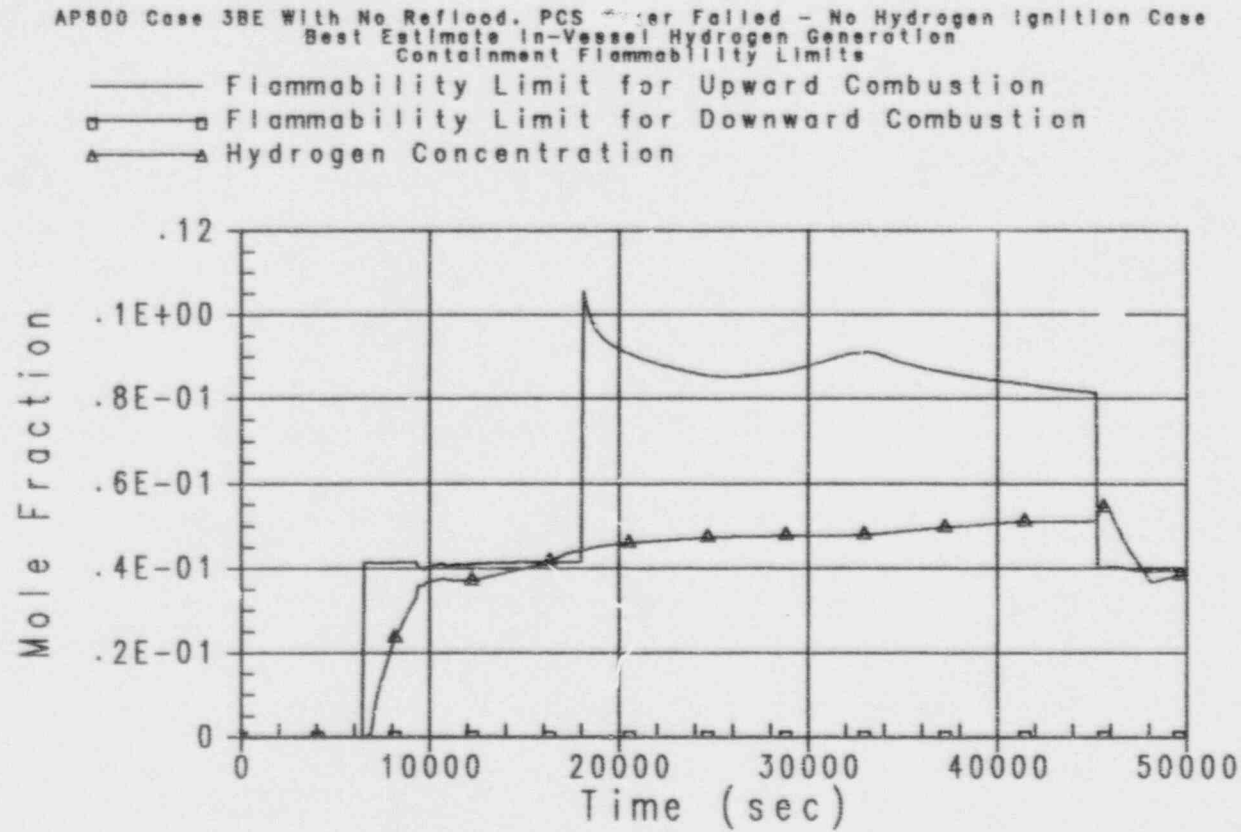


Figure 41-47



Westinghouse

ENEL
 ENEL NUCLEARE
 ENEC LAVORAZI ELETTRICI

41-85

 Revision: 3
 February 28, 1995
 u:\ap600\grawec41-2.wpf 1b

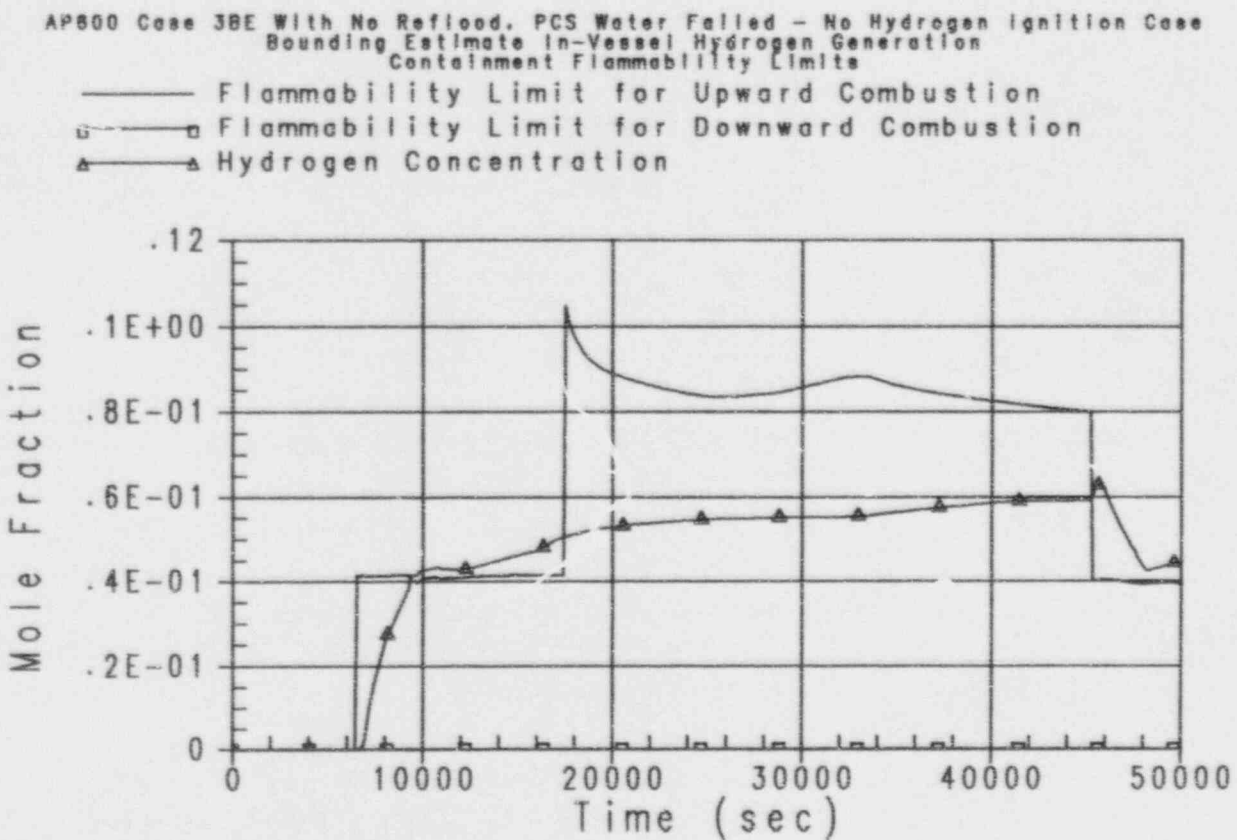


Figure 41-48

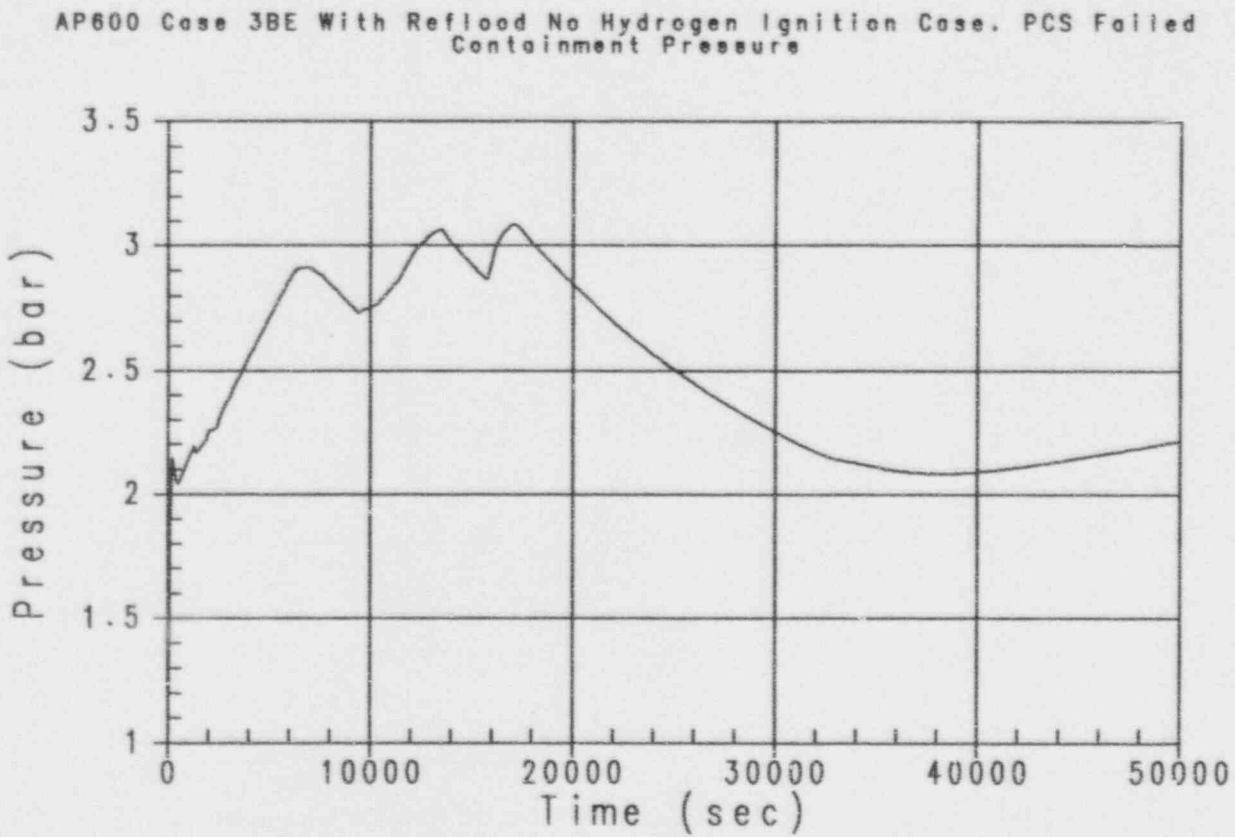


Figure 41-49



Westinghouse

ENEL
ENEL REGIONAL
FOR TECHNICAL SUPPORT

41-87

Revision: 3
February 28, 1995
u:\ap600\pwrsec41-2.wpl 1b

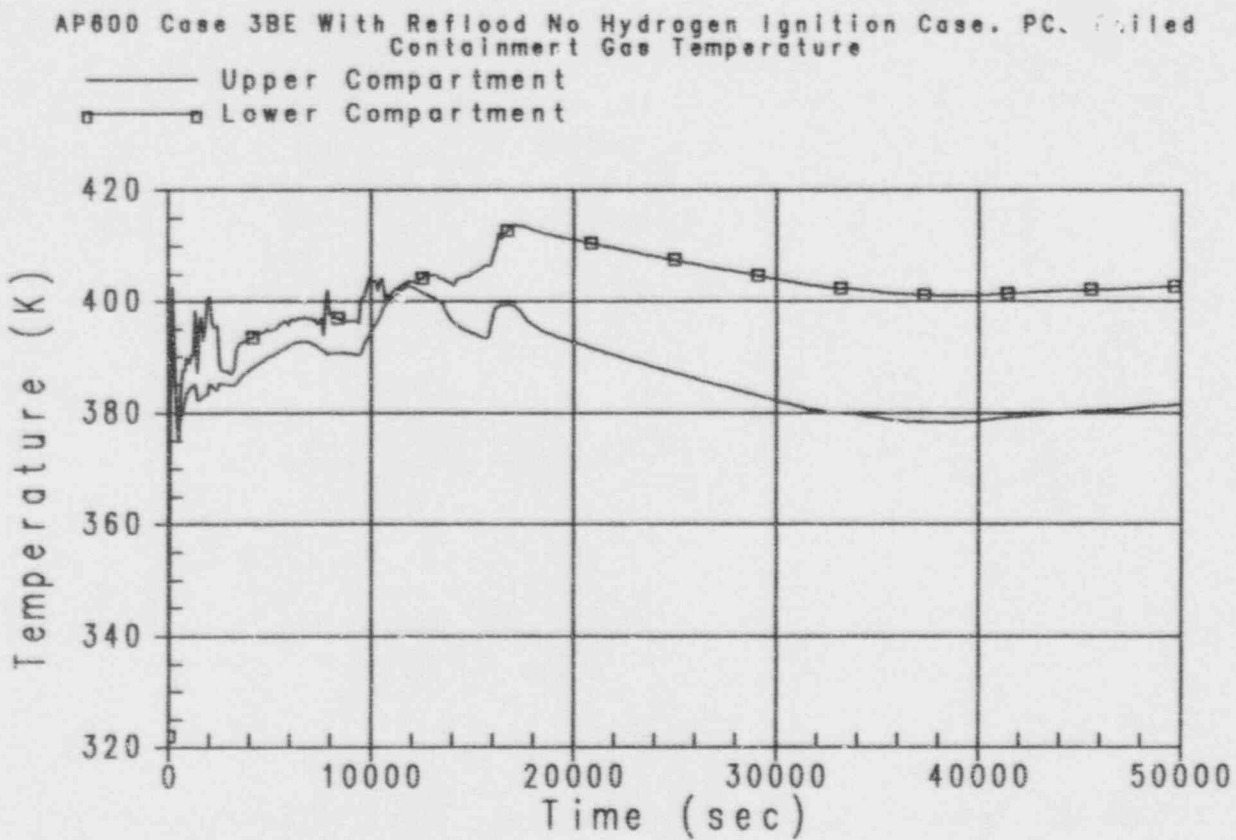


Figure 41-50

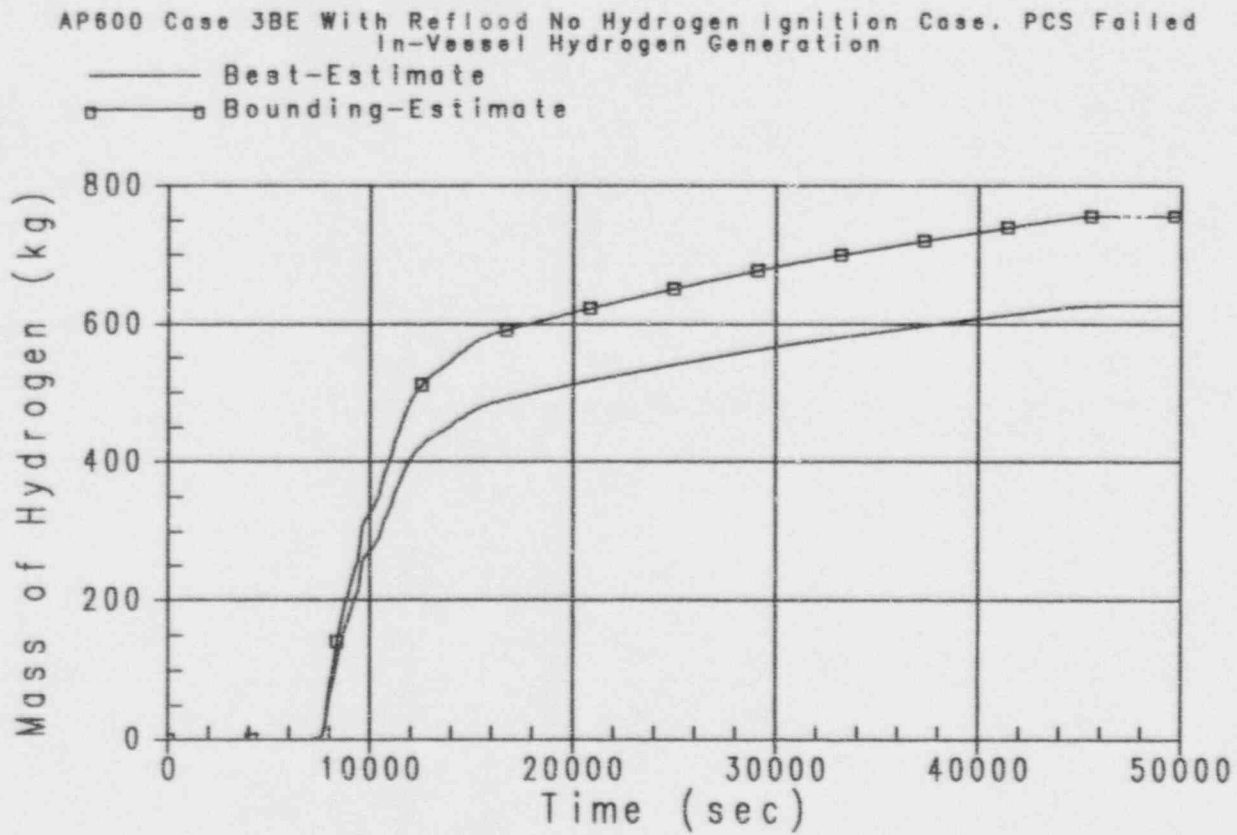


Figure 41-51



Westinghouse

ENEL
 ENEL NUCLEARE
 PIRELLA GÖTTSCHE LOWE

41-89

 Revision: 3
 February 28, 1995
 u:\ap600\prasec41-3.wpl:lb

AP600 Case 3BE With Reflood No Hydrogen Ignition Case, PCS Failed
 Best Estimate In-Vessel Hydrogen Generation
 Containment Compartment Hydrogen Mole Fractions

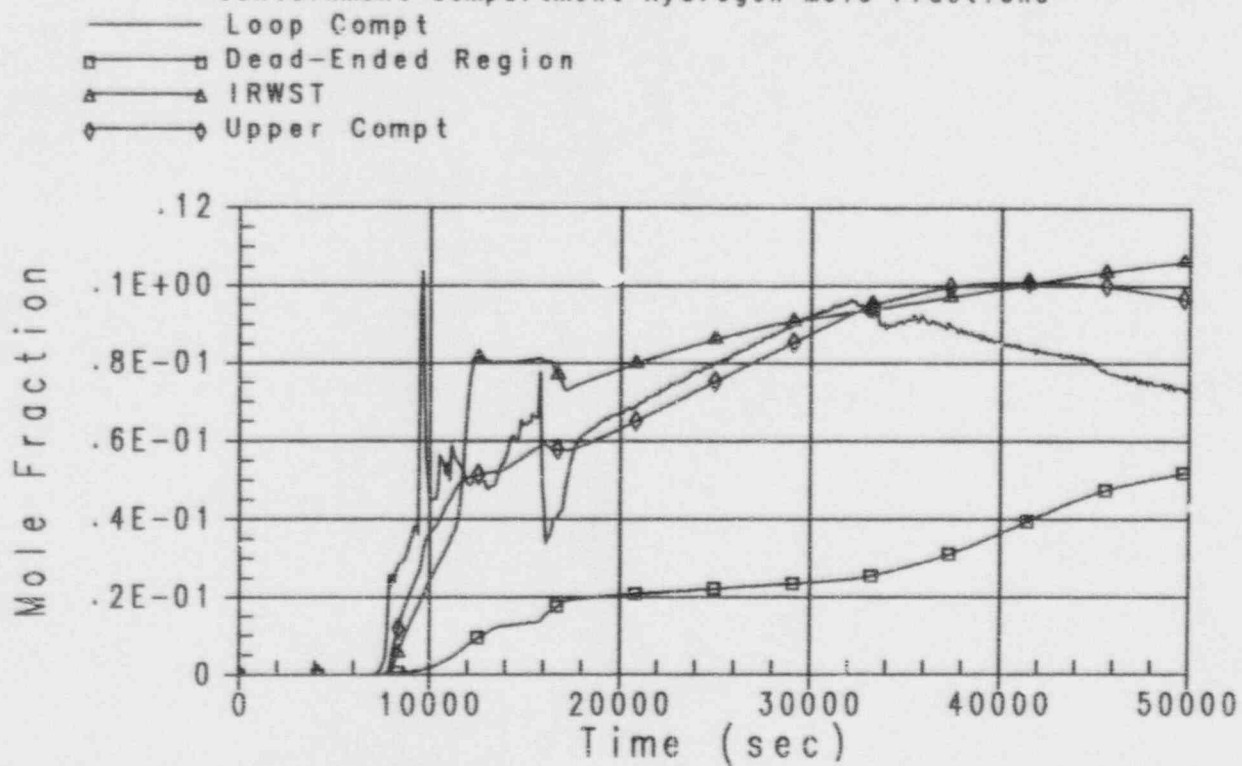


Figure 41-52

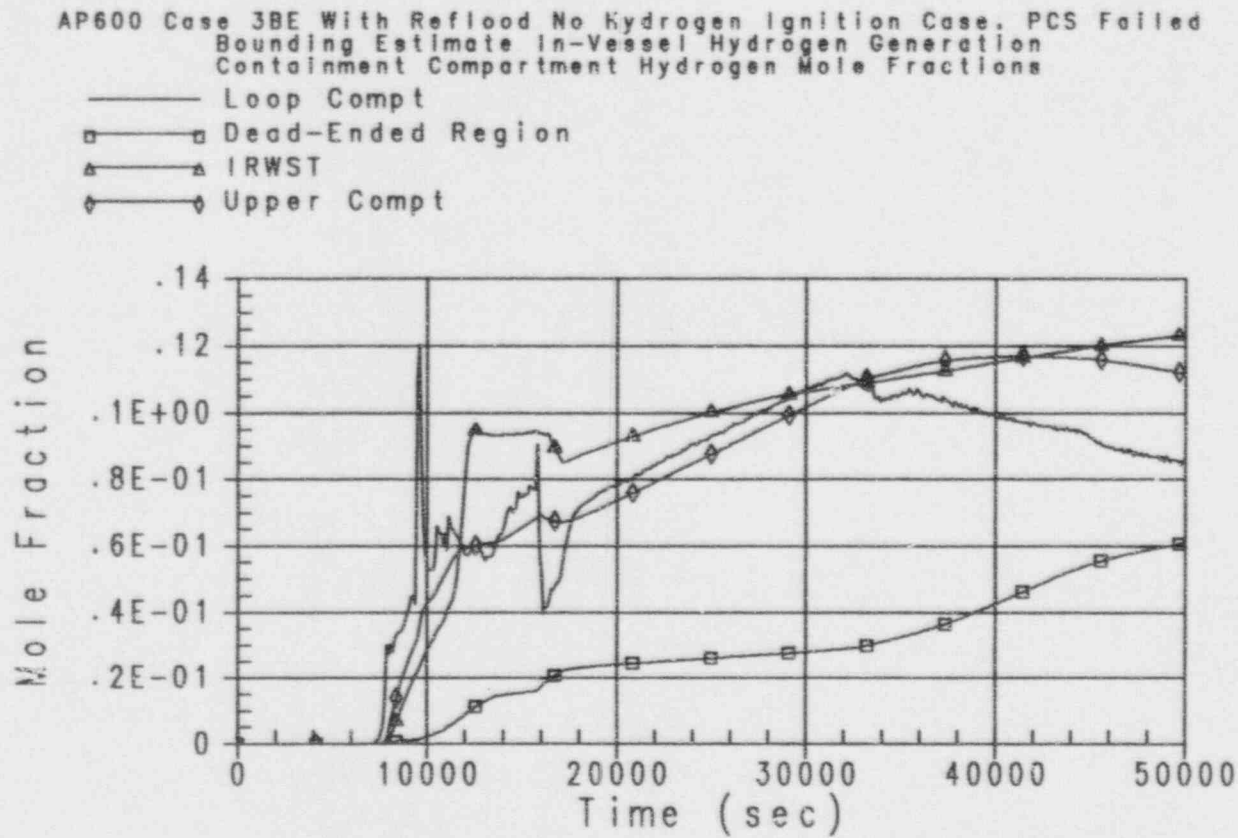


Figure 41-53



Westinghouse

ENEL
 ENEL NUCLEARE
 PER L'ENERGIA ELETTRICA

41-91

 Revision: 3
 February 28, 1995
 u:\ap600\pra\sec41-3.wpf:lb

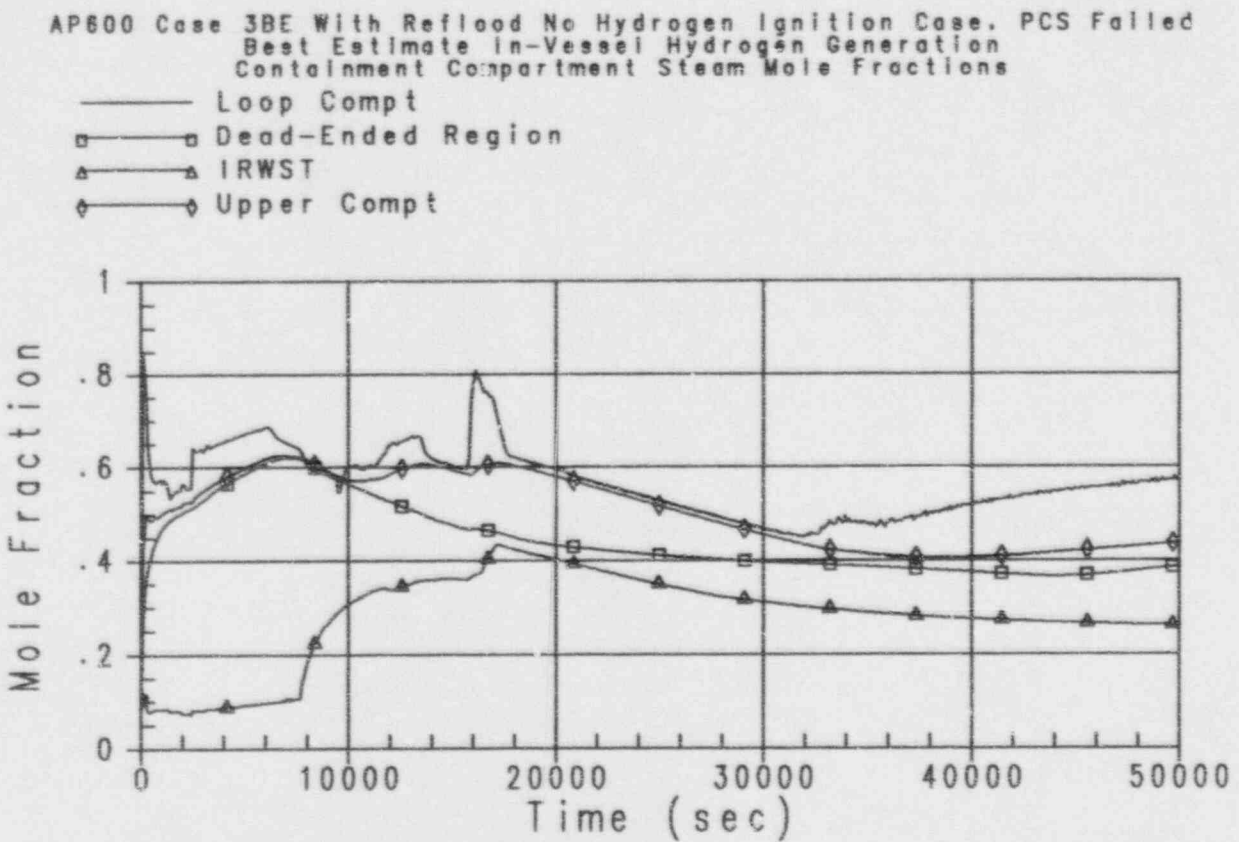


Figure 41-54

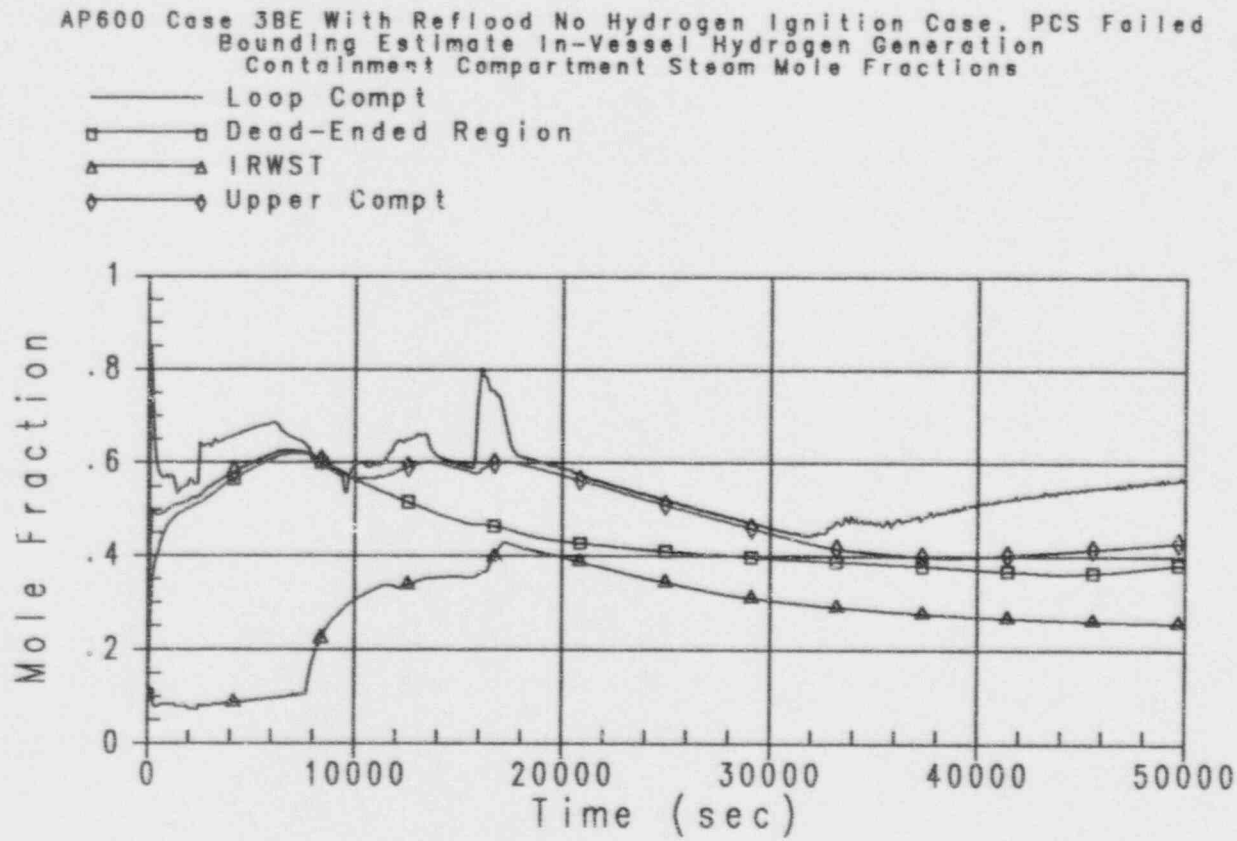


Figure 41-55



Westinghouse

ENEL
 ENVI. NUCLEON.
 PER L'ENERGIA ELETTRICA

41-93

 Revision: 3
 February 28, 1995
 u:\ap600\prafs-c41.3.wpf:1b

AP600 Case 3BE With Reflood No Hydrogen Ignition Case. PCS Failed
Best Estimate In-Vessel Hydrogen Generation
Containment Flammability Limits

— Flammability Limit for Upward Combustion
□ Flammability Limit for Downward Combustion
△ Hydrogen Concentration

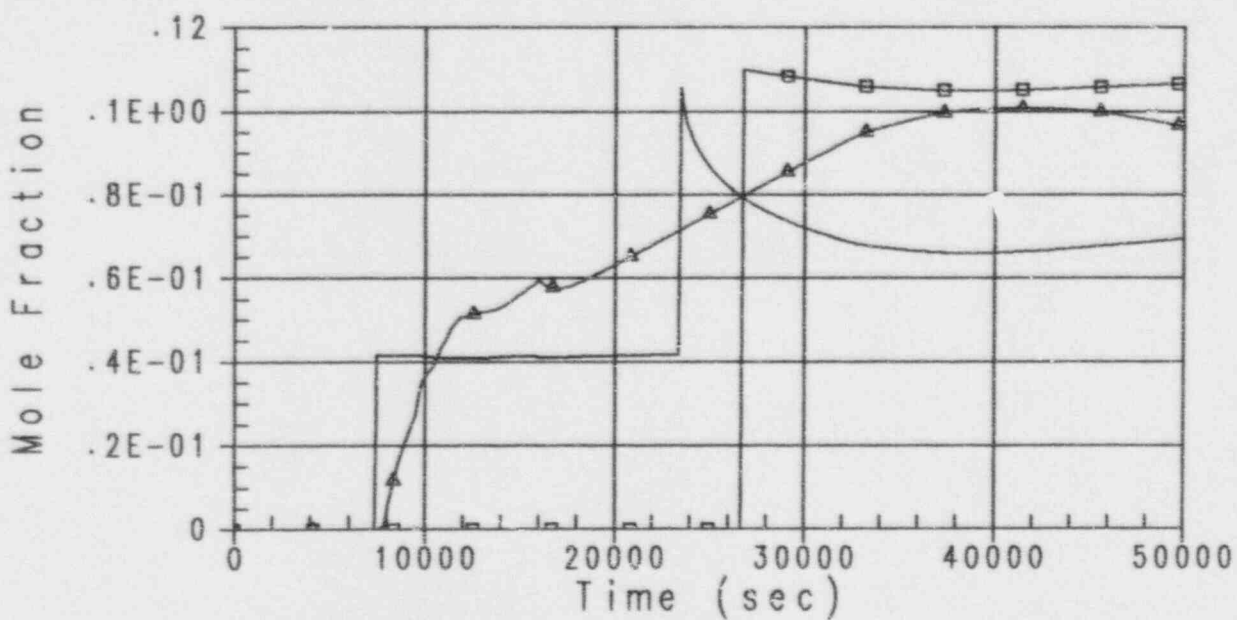


Figure 41-56

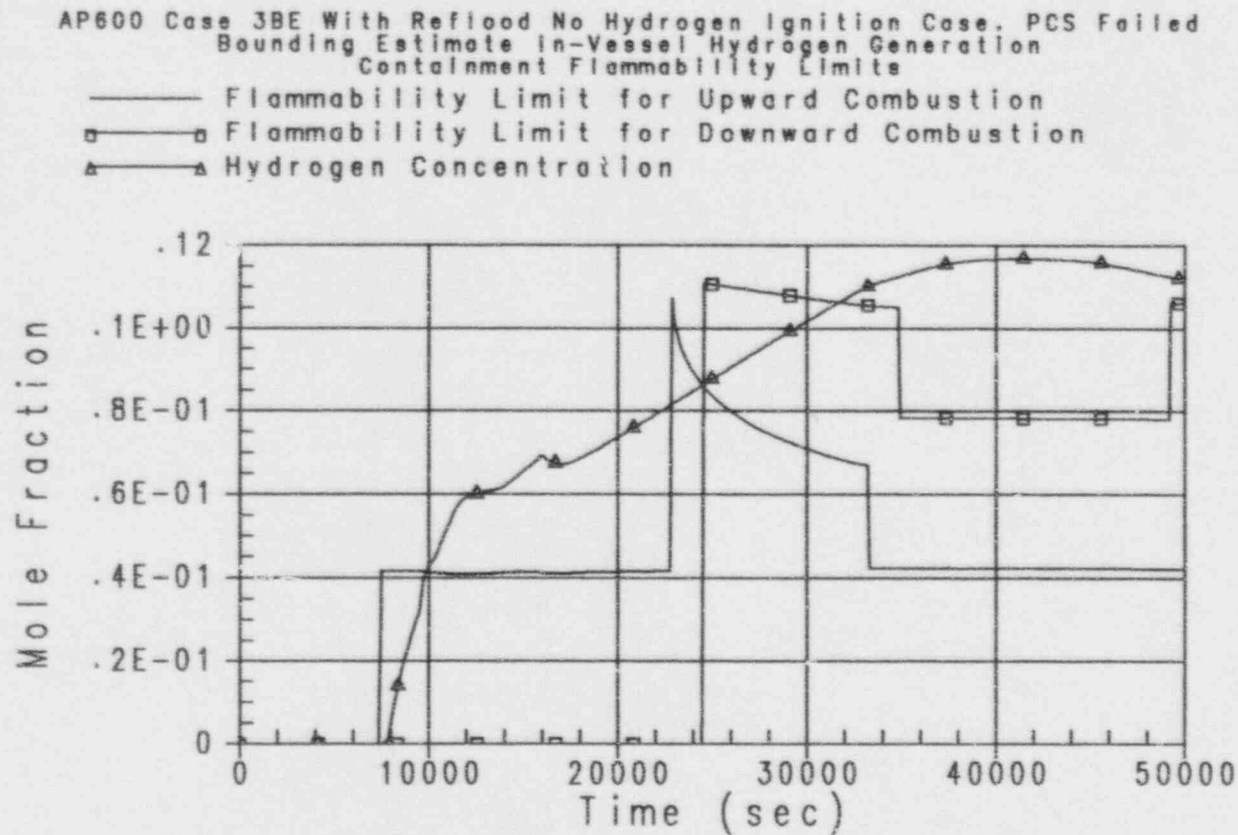


Figure 41-57



Westinghouse

ENEL
DISTRIBUTION
FOR TECHNICAL ELECTRONICS

41-95

Revision: 3
February 28, 1995
u:\ap600\praveca1-3.wpf:lb

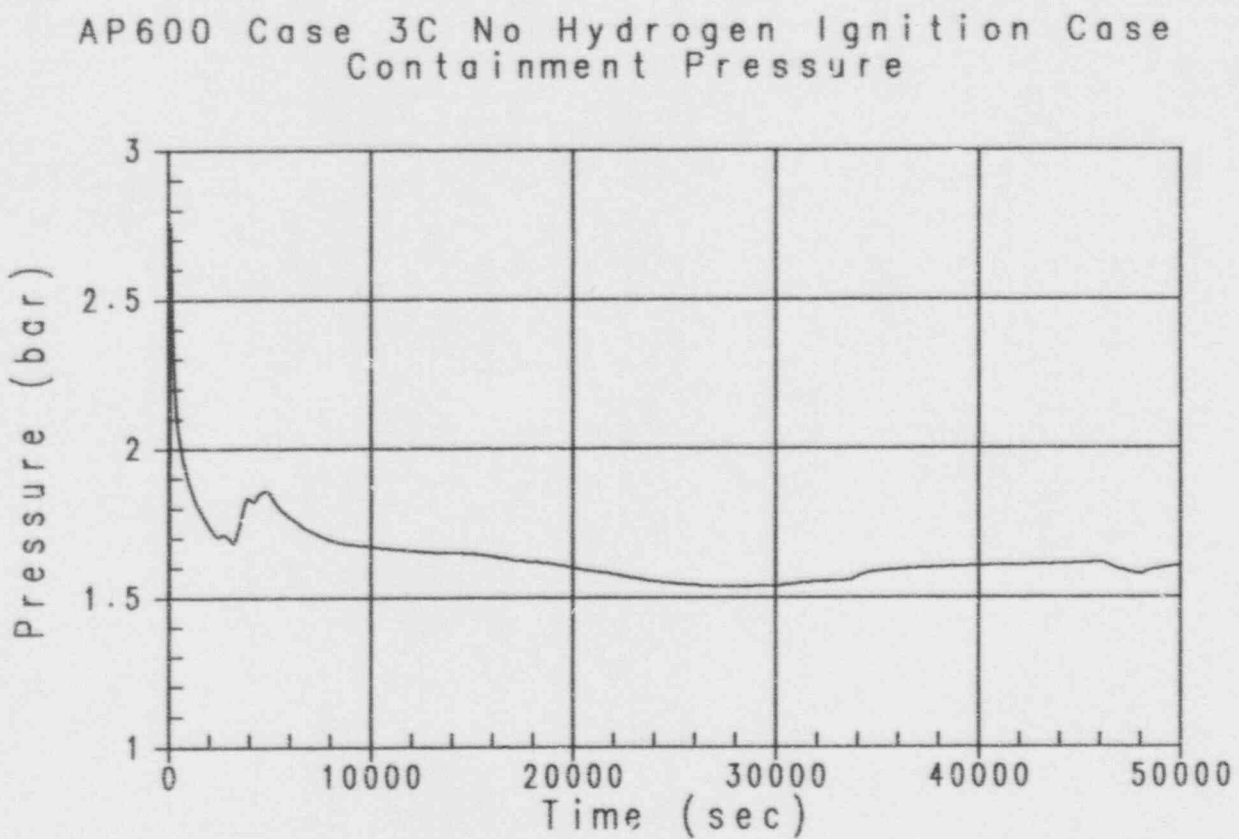


Figure 41-58

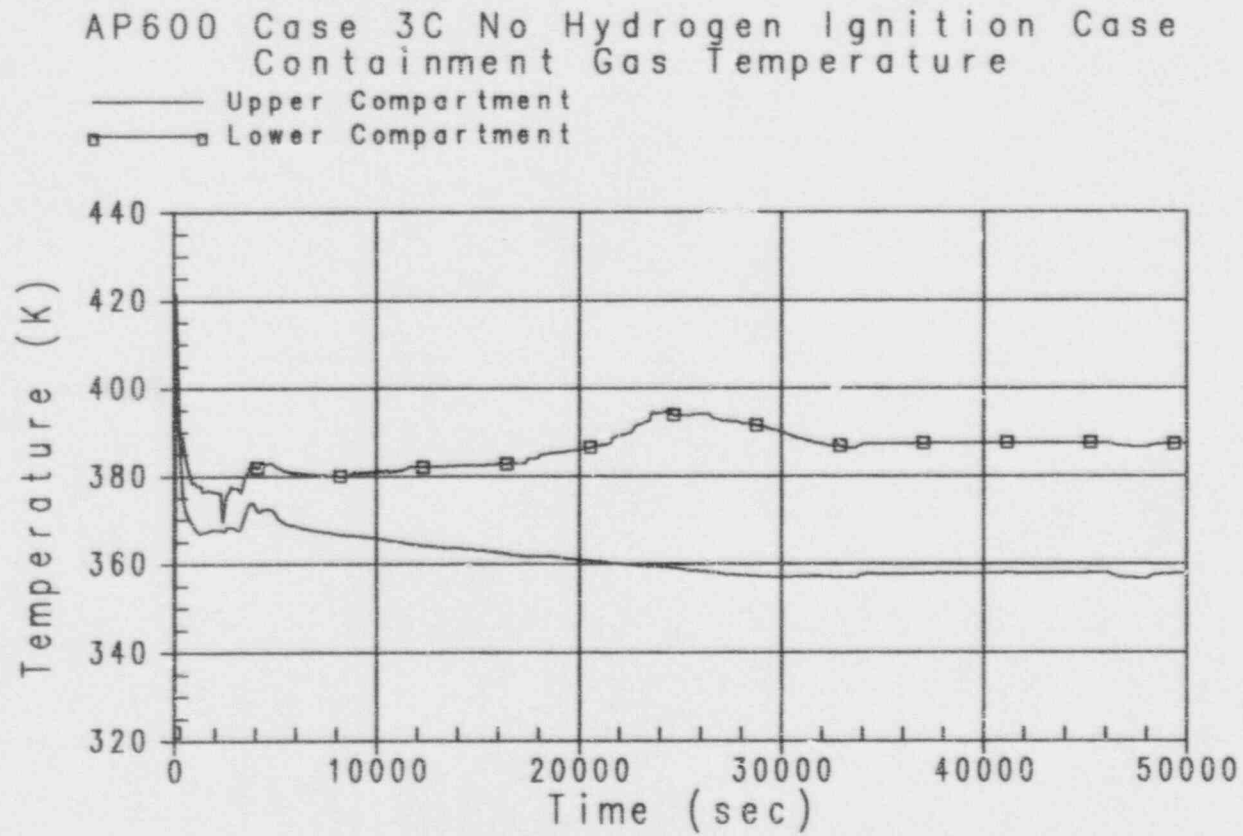


Figure 41-59



Westinghouse

ENEL
SISTEMI INTEGRATI
PER L'ENERGIA ELETTRICA

41-97

Revision: 3
February 28, 1995
u:\ap600\pralvec41-3.wp1:lb

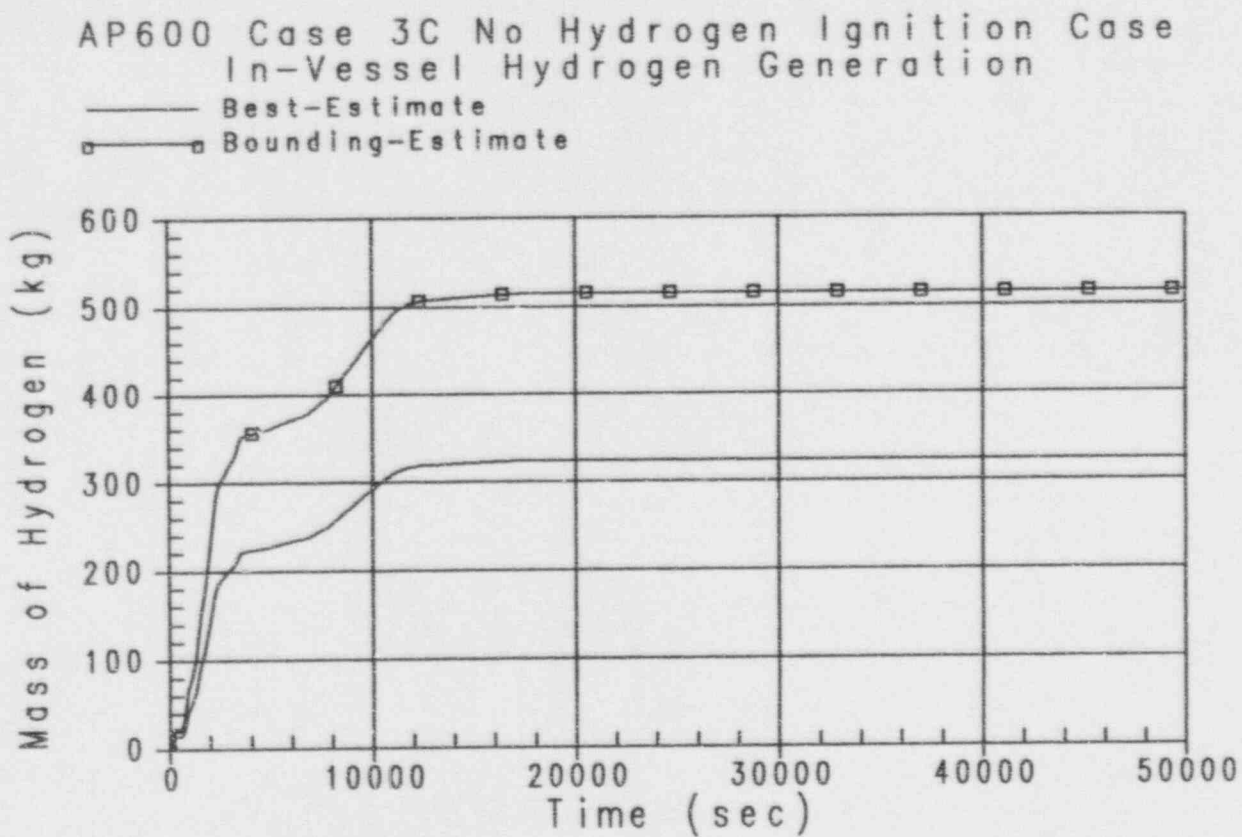


Figure 41-60

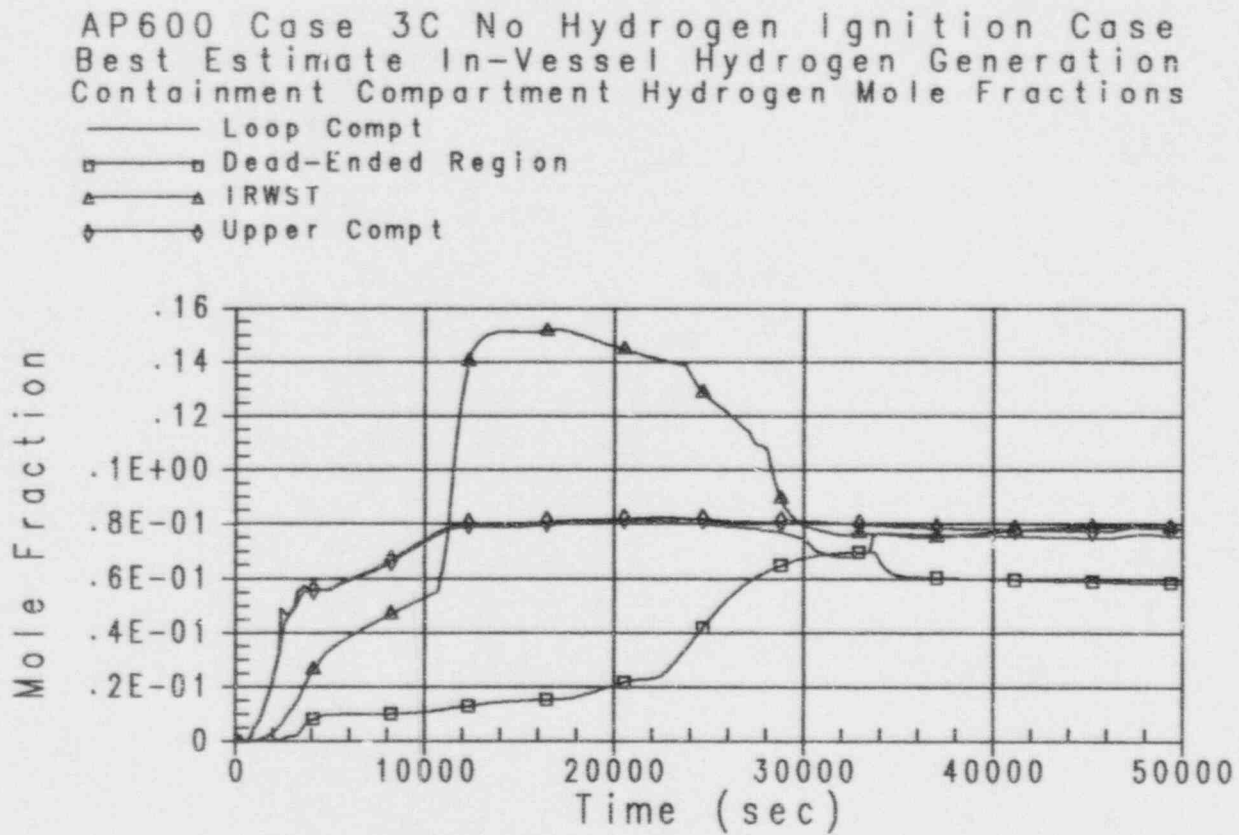


Figure 41-61



Westinghouse

ENEL
 ENVI. NUCLEARE
 PER L'ENERGIA ELETTRICA

41-99

 Revision: 3
 February 28, 1995
 u:\ap600\pna\sec41-3.wpf:1b

AP600 Case 3C No Hydrogen Ignition Case
Bounding Estimate In-Vessel Hydrogen Generation
Containment Compartment Hydrogen Mole Fractions

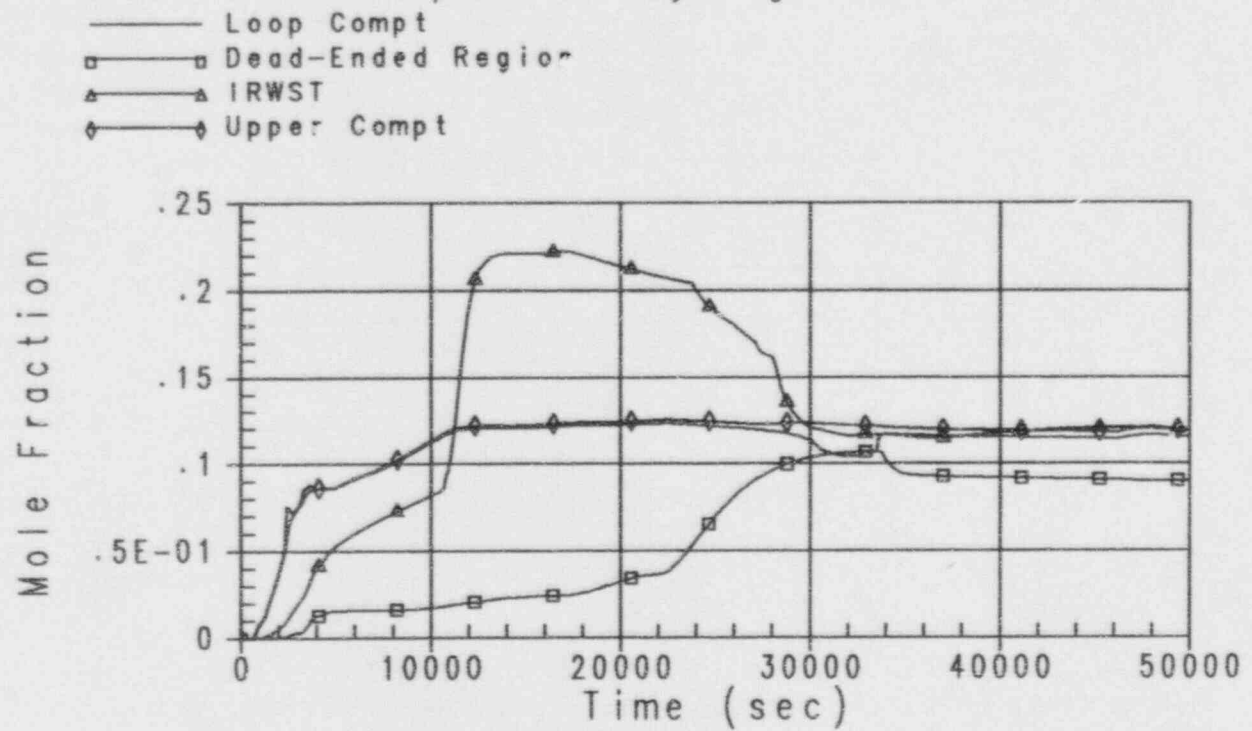


Figure 41-62

AP600 Case 3C No Hydrogen Ignition Case
 Best Estimate In-Vessel Hydrogen Generation
 Containment Compartment Steam Mole Fractions

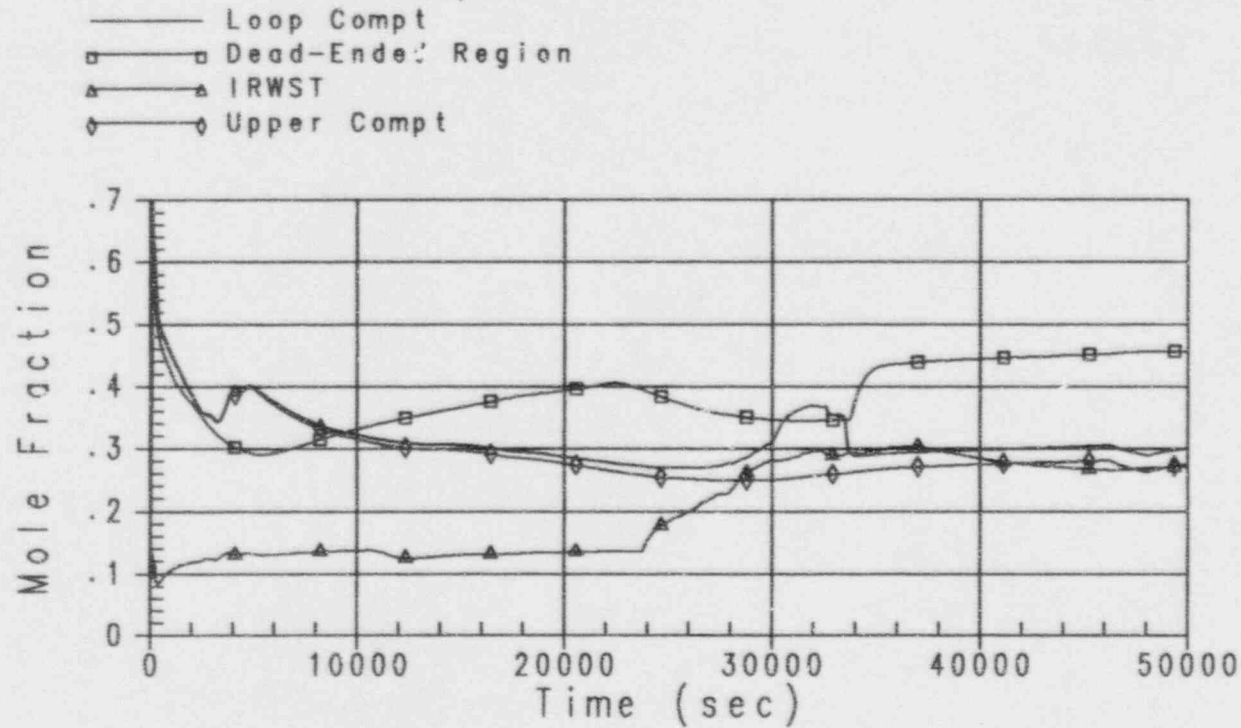


Figure 41-63



Westinghouse

ENEL
 ENVI. NAZIONALE
 PER L'ENERGIA ELETTRICA

41-101

 Revision: 3
 February 28, 1995
 u:\ap600\prv\sec41-3.wpl.tb

AP600 Case 3C No Hydrogen Ignition Case
Bounding Estimate In-Vessel Hydrogen Generation
Containment Compartment Steam Mole Fractions

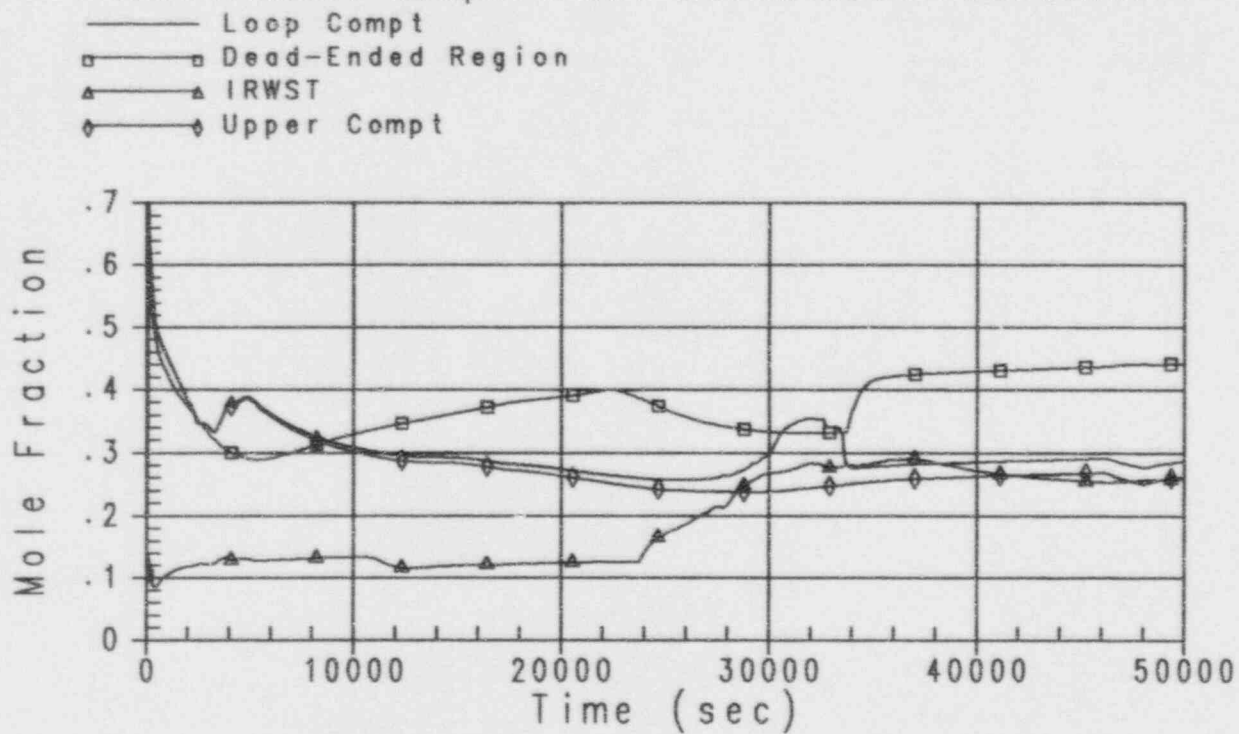


Figure 41-64



AP600 Case 3C No Hydrogen Ignition Case
 Best Estimate In-Vessel Hydrogen Generation
 Containment Flammability Limits

- Flammability Limit for Upward Combustion
- Flammability Limit for Downward Combustion
- △ Hydrogen Concentration

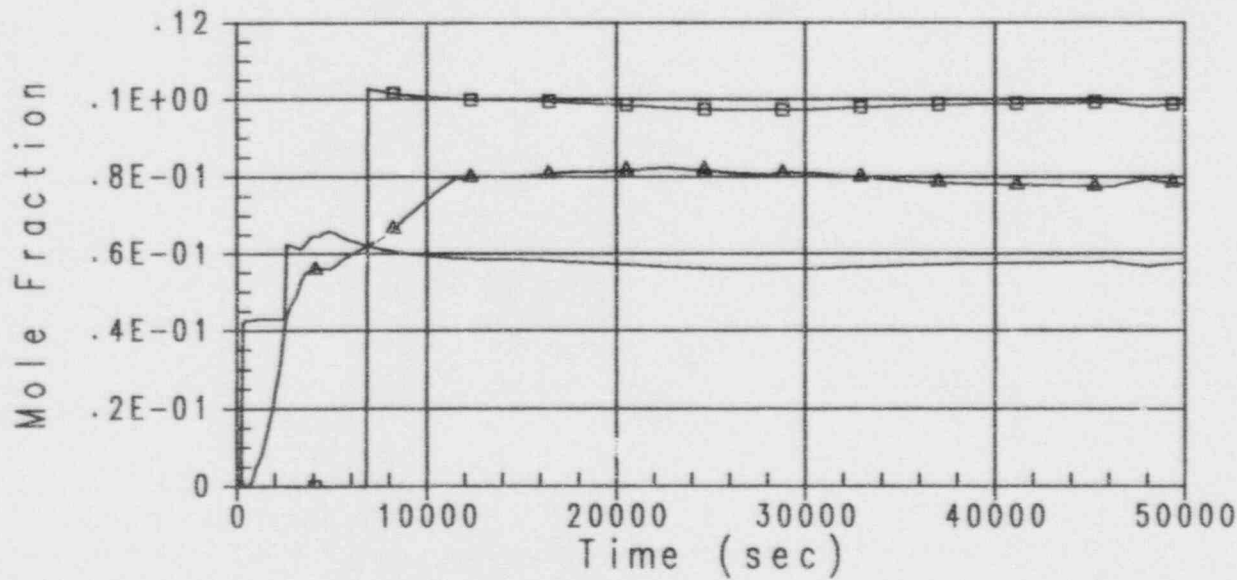


Figure 41-65



Westinghouse

ENEL
 ENR. MONITORING
 FOR LONDON ELECTRONICS

AP600 Case 3C No Hydrogen Ignition Case
 Bounding Estimate In-Vessel Hydrogen Generation
 Containment Flammability Limits

— Flammability Limit for Upward Combustion
 □ Flammability Limit for Downward Combustion
 ▲ Hydrogen Concentration

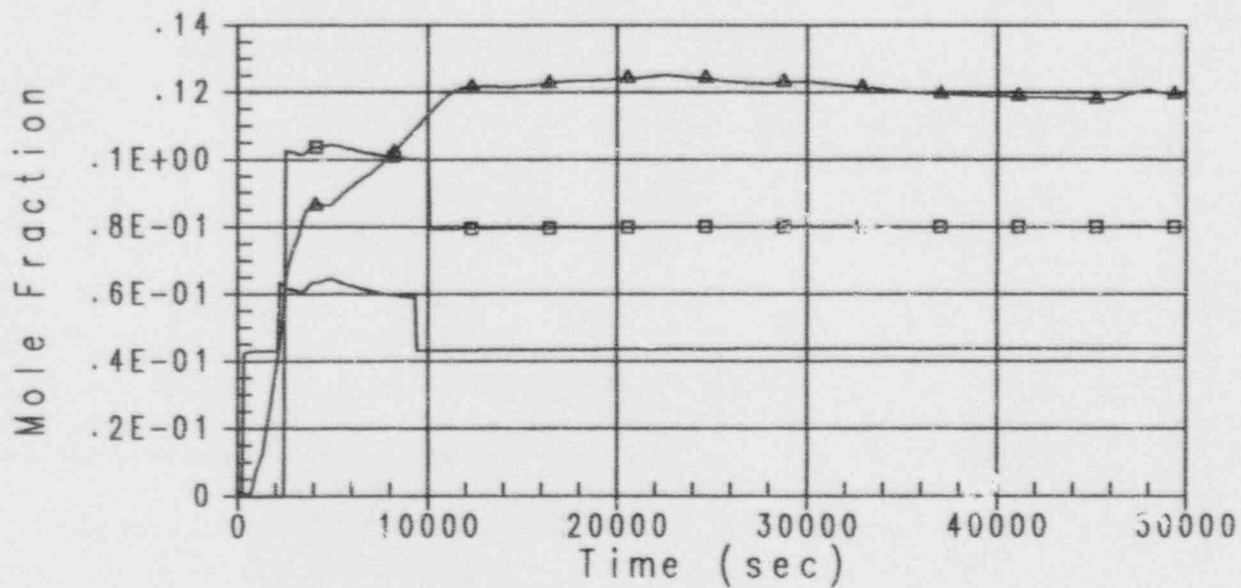


Figure 41-66

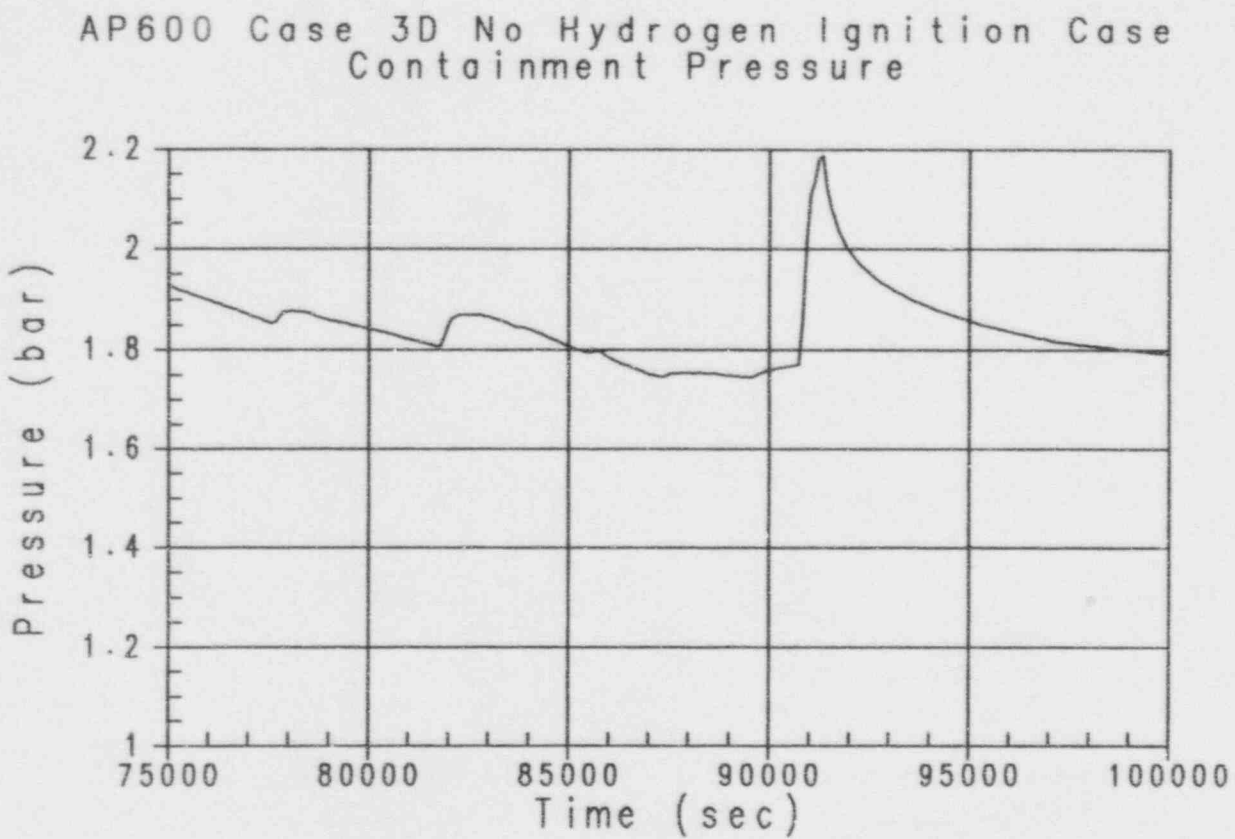
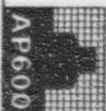


Figure 41-67



Westinghouse

ENEL
ENERGIA NUCLEARE
PER L'ENERGIA ELETTRICA

41-105

Revision: 3
February 28, 1995
u:\ap600\prts\sec41-3.wp1 1b

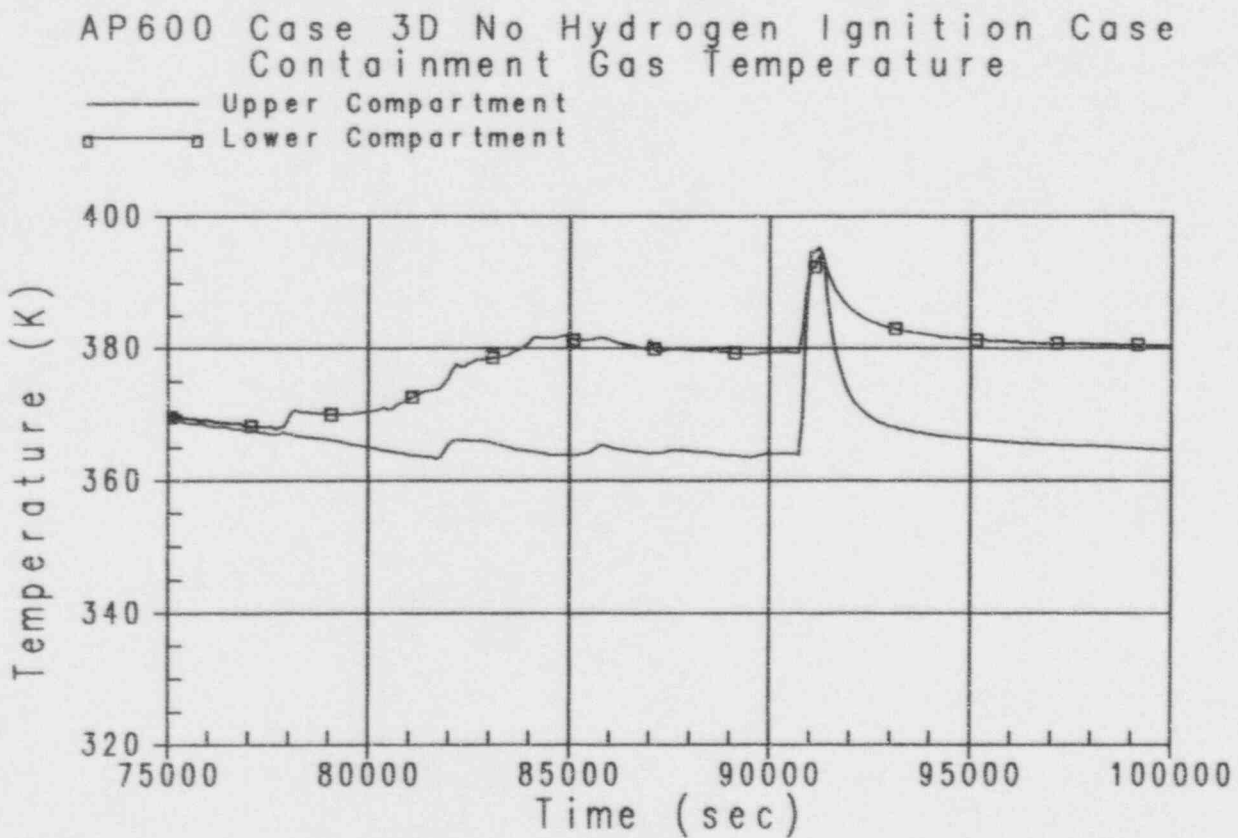


Figure 41-68

AP600 Case 3D No Hydrogen Ignition Case
In-Vessel Hydrogen Generation

— Best-Estimate
□ Bounding-Estimate

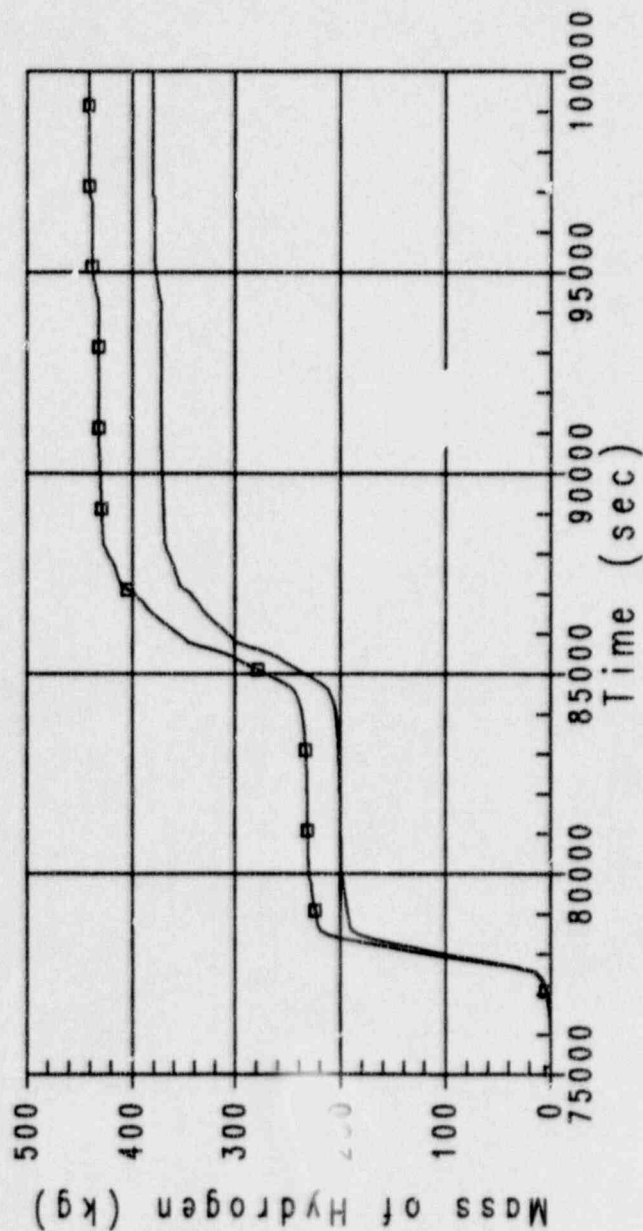


Figure 41-69

AP600 Case 3D No Hydrogen Ignition Case
Best Estimate In-Vessel Hydrogen Generation
Containment Compartment Hydrogen Mole Fractions

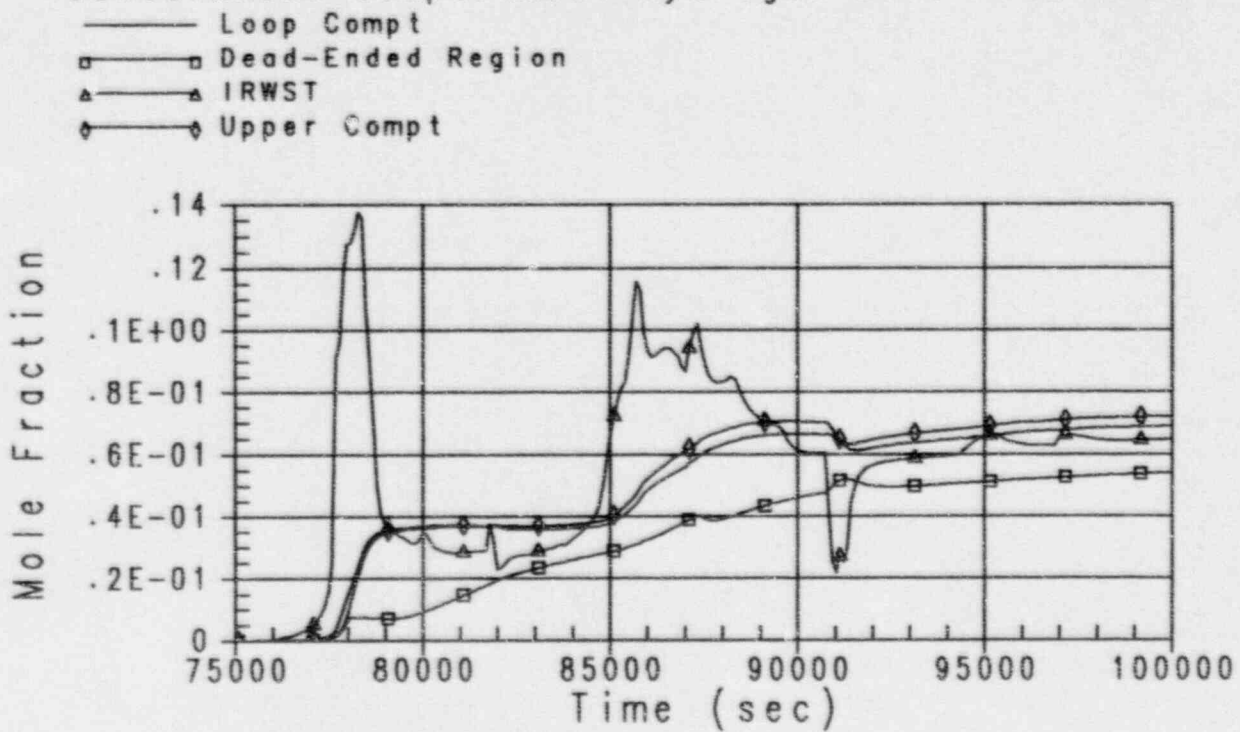


Figure 41-70

AP600 Case 3D No Hydrogen Ignition Case
 Bounding Estimate In-Vessel Hydrogen Generation
 Containment Compartment Hydrogen Mole Fractions

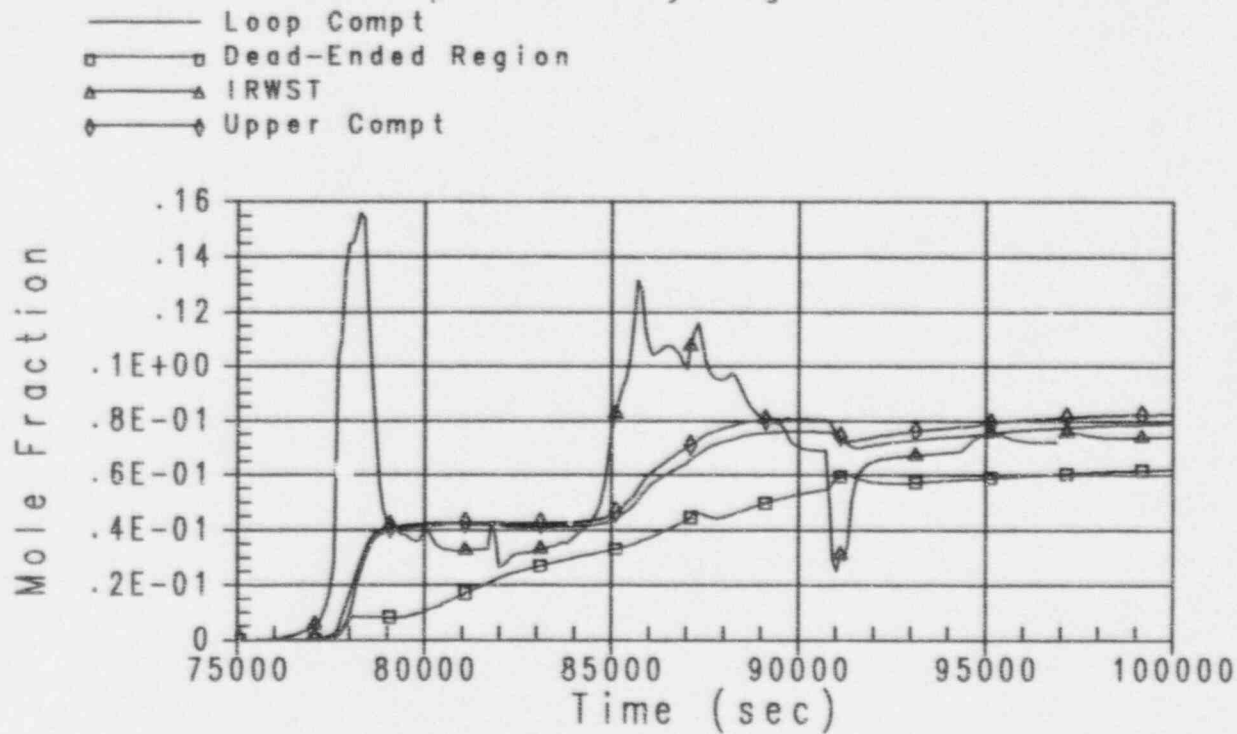


Figure 41-71



Westinghouse

ENEL
 ENERGETICAL
 PER L'ENERGIA ELETTRICA

41-109

 Revision: 3
 February 28, 1995
 u:\ap600\praisecl-3.wpf:1b

AP600 Case 3D No Hydrogen Ignition Case
Best Estimate In-Vessel Hydrogen Generation
Containment Compartment Steam Mole Fractions

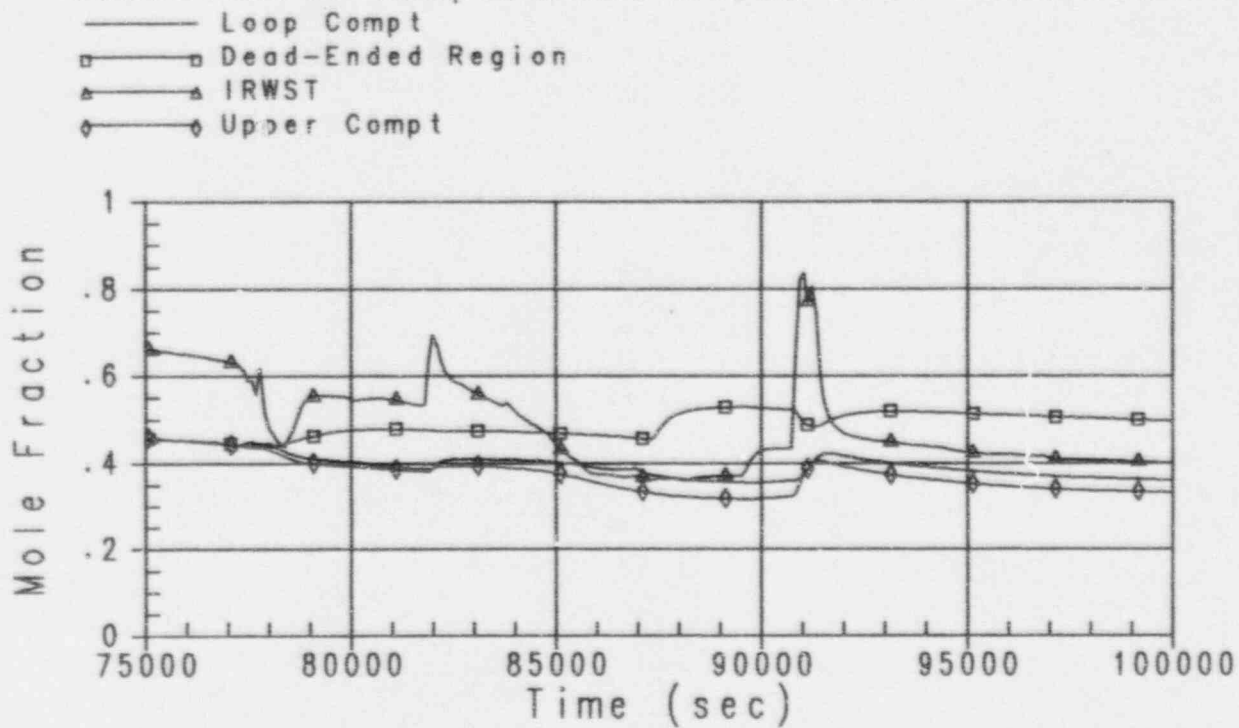


Figure 41-72

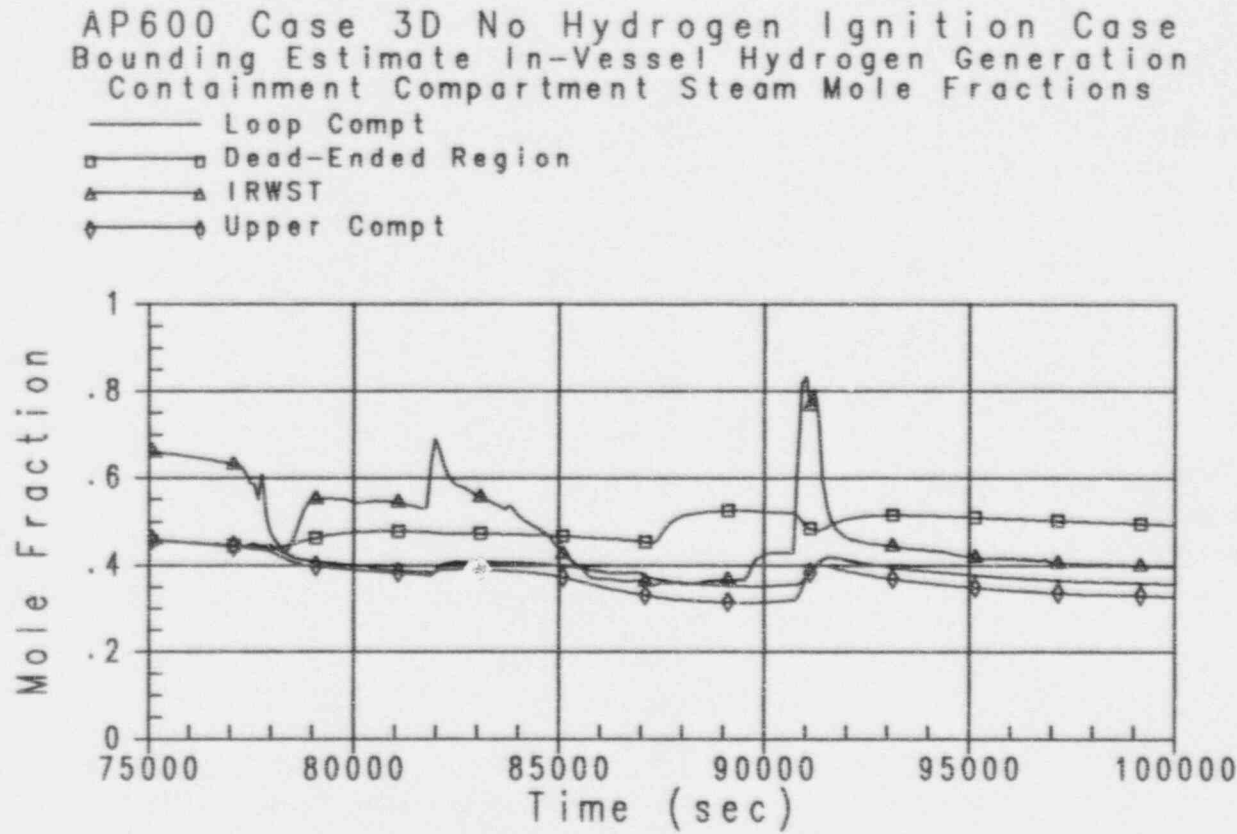


Figure 41-73



Westinghouse

ENEL
ELECTRIC
NUCLEAR
SYSTEMS
FOR
INDUSTRIAL
ELECTRICITY

41-111

Revision: 3
February 28, 1995
u:\ap600\prasec-41-3.wpf:lb

AP600 Case 3D No Hydrogen Ignition Case
Best Estimate In-Vessel Hydrogen Generation
Containment Flammability Limits

— Flammability Limit for Upward Combustion
□ Flammability Limit for Downward Combustion
▲ Hydrogen Concentration

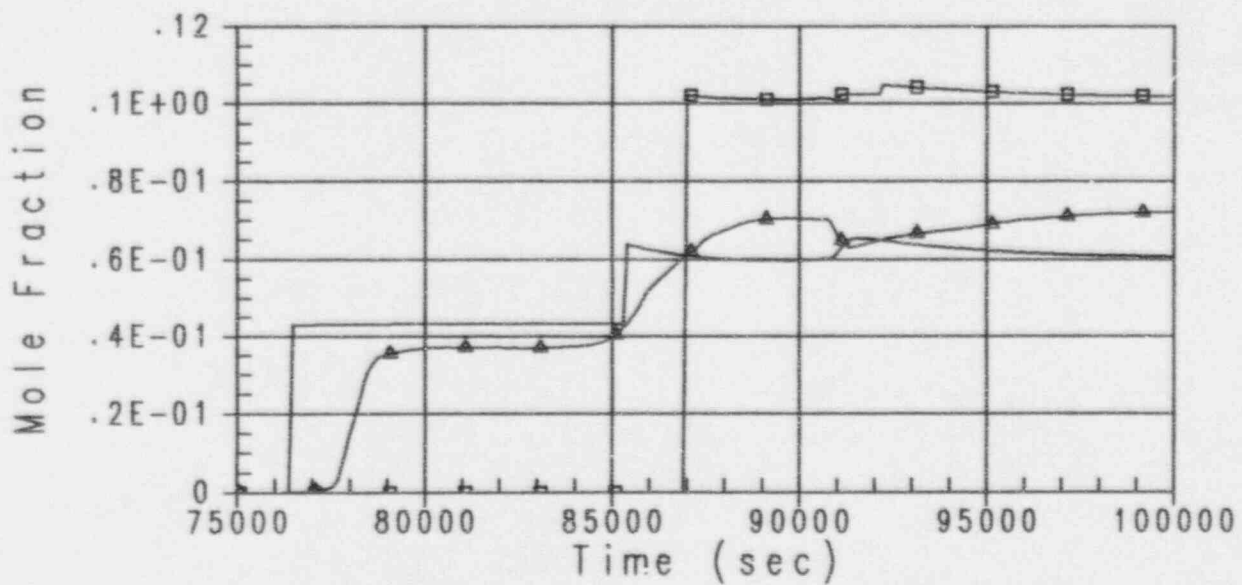


Figure 41-74

AP600 Case 3D No Hydrogen Ignition Case
 Bounding Estimate In-Vessel Hydrogen Generation
 Containment Flammability Limits

— Flammability Limit for Upward Combustion
 □ Flammability Limit for Downward Combustion
 ▲ Hydrogen Concentration

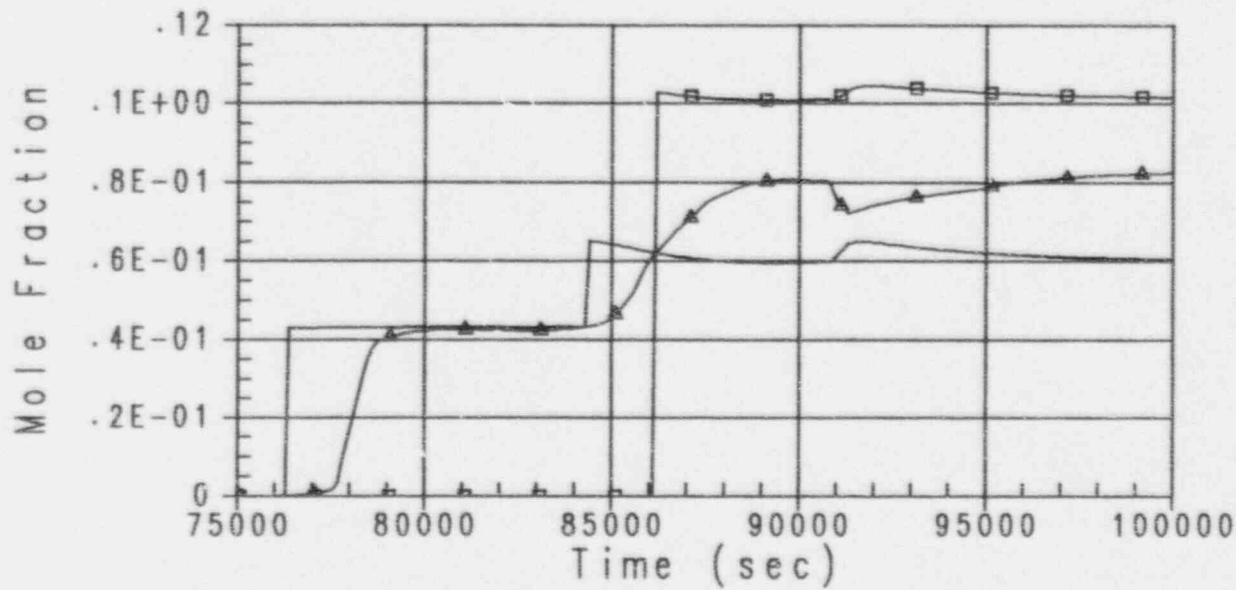


Figure 41-75

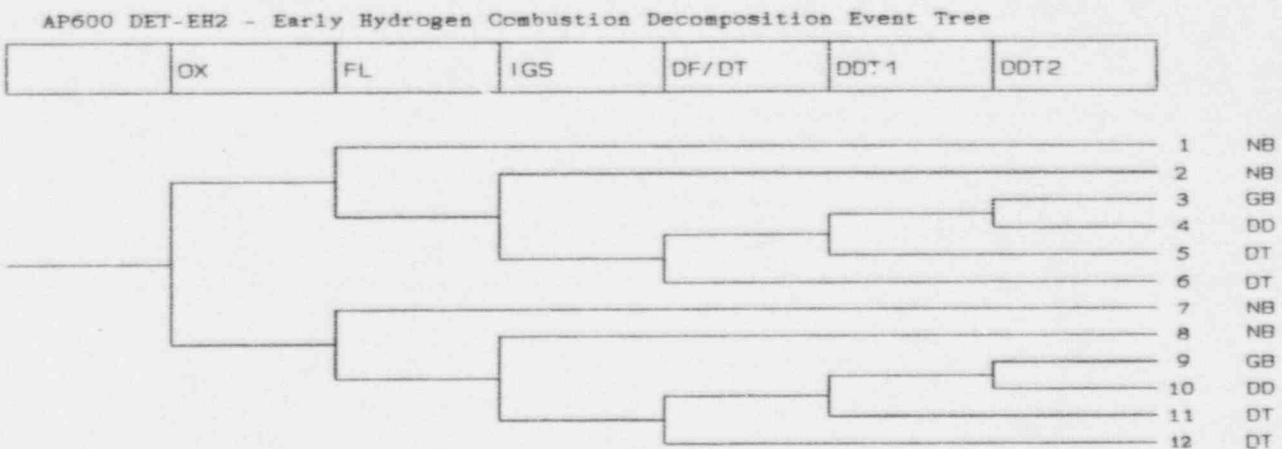


Westinghouse

 ENEL
 ENEL NUCLEARE
 PER L'ENERGIA ELETTRICA

41-113

 Revision: 3
 February 28, 1995
 u:\ap600\prasec41-3.wpf lb

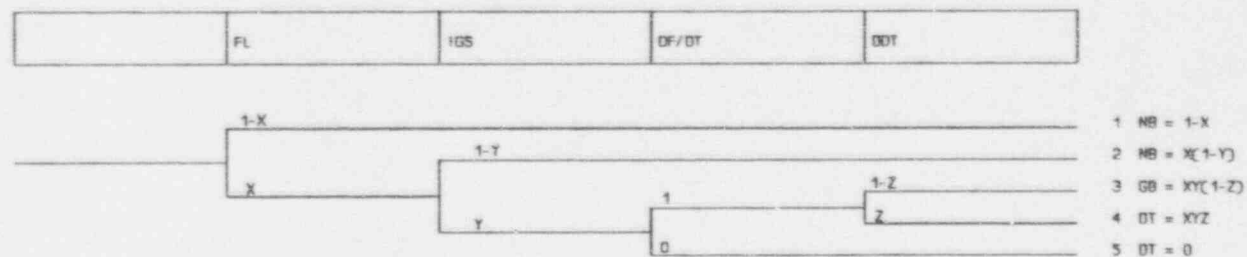


AP600 DET-EH2 - Early Hydrogen Combustion Decomposition Event Tree
List of top events

Event	Description
OX	Degree of Cladding Oxidation
FL	Exceed Hydrogen Flammability Limits
IGS	Existence of an Ignition Source
DF/DT	Detonation via Direct Energy Deposition
DDT1	Deflagration to Detonation Transition in IRWST
DDT2	Deflagration to Detonation Transition in Low Comp

Figure 41-76

AP600 DET - Intermediate and Late Hydrogen Combustion Decomposition Event Tree



AP600 DET - Intermediate and Late Hydrogen Combustion Decomposition Event Tree

List of top events

Event	Description
FL	Exceed Hydrogen Flammability Limits
IGS	Existence of an Ignition Source
DF/DT	Detonation via Direct Energy Deposition
DDT	Deflagration to Detonation Transition

Figure 41-77



Westinghouse

ENEL
ENEL NACIONAL
PER L'ENERGIA ELETTRICA

41-115

Revision: 3
 February 28, 1995
 u:\ap600\graisec41-3.wpf:1b



CHAPTER 42

CONDITIONAL CONTAINMENT FAILURE PROBABILITY DISTRIBUTION

42.1 Introduction

The probability distribution for containment failure due to internal pressurization of the containment has been developed for the AP600 containment vessel.

The AP600 containment and its structural properties are described in subsection 3.8.2 of the *AP600 Standard Safety Analysis Report (SSAR)*. Based on a detailed examination of the structural design of the AP600 containment vessel as described in subsection 3.8.2 of the SSAR, the limiting containment failure modes that have been identified include:

- General yielding of the cylindrical shell
- Buckling of the ellipsoidal head
- Buckling of the 22-ft. equipment hatch
- Buckling of the 16-ft. equipment hatch
- Yielding of the personnel airlock

Other containment failure modes are examined failure, as discussed in subsection 3.8.2 of the SSAR. Based on detailed evaluations, it was determined that other failure modes, such as general yielding of the ellipsoidal head and failure of the piping penetrations, are not considered to be independent containment failure modes. Rather, these other failure modes are bounded by more failure criteria for the limiting failure identified above.

Each of the limiting failure modes is examined to determine the best estimate of the mean failure pressure. In addition, the random and subjective uncertainties associated with each of the failure modes are identified. These failure characteristics are then used to develop a probabilistic model to predict the containment failure due to internal static pressurization. The details of the model development and the results of the analysis are presented in the following sections.

42.2 Probabilistic Model

To define the probability of a containment failure due to internal pressurization, it is necessary to select a statistical distribution with the correct properties. The engineering justification for a particular probability density function must be made based on the gathering and evaluation of relevant information that can serve to characterize the nature of the random data and physical processes that lead to the random data. The nature of the random data, and in particular any limits or bounds on the data, are as important as the predicted means and variances from statistical analysis of the data. Thus, specific limits in the data and characteristics, such as skewness, must be utilized to specify the probability density function.

Four potential probability distributions are considered: the Gaussian, the Gamma, the Gumbel, the log-normal, and the Weibull.

Based on a review of the characteristics of the four potential probability distributions, it was determined that both the Weibull and the lognormal distributions would be suitable to describe the containment failure probabilities. An additional review of the containment failure probability distributions reported in a number of the Individual Plant Examinations submitted to the Nuclear Regulatory Commission (in response to the Commission's Generic Letter 88-20) indicates that the lognormal distribution is the most commonly used distribution form for predicting containment failure from internal pressurization. Therefore, the lognormal distribution is selected to construct the conditional containment failure probability distribution.

42.3 Containment Failure Characteristics

The characteristic parameters for containment failure due to internal pressurization are derived from detailed analyses of the containment vessel, supplemented by applicable test data for certain design features of the containment, as described in subsection 3.8.2 of the SSAR. For the construction of the conditional containment failure probability distribution, the required characteristic parameters are the mean failure pressure and the statistical variance that represent the uncertainty associated with the mean value.

42.3.1 Mean Values for Containment Failure

The development of the conditional containment failure probability distribution requires the specification of the mean value for containment failure for each of the possible containment failure modes. Subsection 3.8.2 of the SSAR provides values for the ultimate containment pressure capability at 100°F and 400°F.

The information presented in subsection 3.8.2 of the SSAR is based on the most limiting failure modes with respect to internal containment pressure. The subsection also provides information that the actual containment failure would be expected to occur at an internal pressure that is about 15 percent higher than the ultimate pressure specified, based on an assumed increase in the strength of the actual materials used in construction of the containment vessel. Reference 42-1 confirms that the actual yield strength of containment construction materials can typically be expected to be 12 to 22 percent higher than the specified minimum material strength. Since the mean containment strength is used to construct a probability distribution that includes random uncertainties in material properties as well as subjective uncertainties in modelling of the containment strength, it is appropriate to use the expected, as-built containment strength (i.e., the 15 percent increase over the nominal value) for the mean value of the distribution.

The containment internal pressure value used for the mean value of the containment failure probability distribution is the expected failure pressure, evaluated at 400°F. A review of the severe accident sequences in which the containment internal pressure approaches the failure pressure of the containment (including the decomposition event trees in Section 43 of the



AP600 Level 2 PRA) leads to the conclusion that the containment shell is likely to be at the containment saturation temperature (for the internal containment pressure) for most severe accident sequences. With the passive containment cooling provided by the containment design, the highest likelihood of containment failure due to overpressurization is due to extreme cases of severe accident phenomena (e.g., hydrogen burns and noncoolable ex-vessel core debris). In the case of hydrogen burns, the highest reported containment temperature prior to the burn was on the order of 330°F. In the case of a noncoolable ex-vessel debris bed, the highest containment temperature is less than 400°F. Therefore, the use of a uniform containment shell temperature of 400°F for evaluation of the containment material properties is bounding for the prediction of the conditional containment failure probability distribution.

The values used to construct the conditional containment failure probability distribution are identified in the next section.

42.3.2 Uncertainties in Containment Failure

The uncertainties identified and examined include both random uncertainties and subjective uncertainties. The broad categories of uncertainties considered are:

Geometric Properties: This category of uncertainty is principally concerned with the variations between the as-built containment vessel and the design utilized in the analysis. Some of these variations include containment dimensions, placement of stiffeners, and thickness of the steel plates used to make up the containment vessel. Also included in this category are construction practices such as the strength of weldments, etc. It has been reported [Reference 42-1] that the overall uncertainty in the containment strength is generally insensitive to variations in geometric properties, except for buckling mode of failure.

Structural Analysis: The uncertainties in the overall containment strength can be sensitive to uncertainties in assumptions and models used in the structural analysis of the ultimate strength of the containment structure. Some of the sources of uncertainty include, but are not limited to: the definition of containment failure used in the analysis, the simplified geometric model used in the analysis, the analysis method, the analysis focus of failure locations and modes, the effect of non-uniform geometries, the effect of local temperature and the interpretation of test results to construct the analytical model. These uncertainties must be subjectively evaluated since no complete investigation of these uncertainties is available. Reference 42-1 provides several estimates of the actual-to-predicted results, which vary according to the failure mode assumed in the analysis, the person doing the evaluation, and the method of analysis. The range suggested by these values is a mean value for the actual-to-predicted results tending to unity and a standard deviation in the range between 0.08 and 0.24. Reference 42-2 suggests that a value of 0.12 be used in constructing the probability distribution for the ultimate strength of the containment.

Material Properties: Uncertainties in material properties can be important in estimating the overall containment failure uncertainty. On the surface this appears to the most easily



quantified from data on materials used in construction, particularly if field test specimens are available. However, the total uncertainties in materials should also consider, but are not limited to the estimation of statistical properties from a small sample [e.g., is the calculated mean the real mean) and assumptions on uniformity of properties. There is a wide range of application of material properties to estimate uncertainties and, except for the buckling mode of failure, most analyses neglect all uncertainties except the random, measurable variations in material properties. Reference 42-1 provides several estimates of the uncertainty in material properties that show a coefficient of variance in the range of 0.044 to 0.11 for conditions that may be applicable to the passive containment shell. Reference 42-2 recommends that a coefficient of variance between 0.06 and 0.08 be used to define the random variance in material properties for the containment shell. Finally, based on sampling of test results of material similar to that specified for the AP600 containment shell as described in subsection 3.8.2 of the SSAR, the coefficient of variance was found to be 0.048.

Gross Errors: Gross errors in construction and / or design are not quantifiable since they lead to catastrophic results that are not predictable by reliability methods.

The values used to construct the conditional containment failure probability distribution are identified in the next section.

42.4 Containment Failure Predictions

42.4.1 Containment Cylindrical Shell

The response of the cylindrical portion of the containment vessel to internal pressurization has been analyzed, and the results reported in subsection 3.8.2 of the SSAR. The best estimate of the pressure at which failure would occur is 166 psig, based on actual material properties at a uniform containment wall temperature of 100°F. This was adjusted to 138 psig to account for a 400°F upper bound wall temperature at high internal pressures, based on evaluation of the containment conditions for the range of severe accidents predicted in the PRA.

A coefficient of variance of 0.06 is used to represent the random uncertainty in material properties, consistent with References 42-1 and 42-2. For the subjective uncertainty associated with modelling of the ultimate containment failure pressure, a coefficient of variance of 0.16 is used. This value is derived from Reference 42-1 for membrane yielding failures in steel shell containment structures.

42.4.2 Ellipsoidal Upper Head

The response of the ellipsoidal upper head of the containment vessel to internal pressurization has been analyzed, and the results are reported in subsection 3.8.2 of the SSAR. Three failure modes are identified in subsection 3.8.2 of the SSAR: yielding at the crown, yielding at the knuckle region, and incipient buckling. Failures due to tensile stresses are bounded by the variations considered for yield of the cylindrical shell. Only the buckling failure mode at the

knuckle region can be considered to be an independent failure mode that must be separately considered in determining the conditional containment failure probability distribution.

The best-estimate internal pressure at which the ellipsoidal head of the containment vessel would fail due to post-yield buckling in the knuckle region is 192 psig, using minimum specified yield strength of the containment materials at 100°F. This is reduced to 163 psig at the 400°F upper bound containment wall temperature.

A coefficient of variance of 0.06 is used to represent the random uncertainty in material properties, consistent with References 42-1 and 42-2. For the subjective uncertainty associated with modelling of the ultimate containment failure pressure, a coefficient of variance of 0.14 is used. This value is consistent with References 42-1 and 42-2 for the buckling mode of containment failure.

42.4.3 Equipment Hatches

The response of the 22-ft. and 16-ft. diameter equipment hatches to internal pressurization has been analyzed, and the results are reported in subsection 3.8.2 of the SSAR. The best estimate of the pressure at which failure would occur for the 16-ft. equipment hatch is 241 psig at a uniform containment wall temperature of 100°F, based on 150 percent of the critical buckling pressure as indicated by a review of test data. The matching value for the 22-ft. hatch is 294 psig. These values are adjusted to 226 and 275 psig, respectively, to account for the 400°F upper bound containment wall temperature.

A coefficient of variance of 0.06 is used to represent the random uncertainty in material properties, consistent with References 42-1 and 42-2. For the subjective uncertainty associated with modelling of the ultimate containment failure pressure, a coefficient of variance of 0.14 is used. This value is consistent with References 42-1 and 42-2 for buckling failures.

42.4.4 Personnel Airlock

The response of the personnel airlock to internal pressurization has also been analyzed, and the results are reported in subsection 3.8.2 of the SSAR. The estimated pressure at which failure would occur is in excess of 300 psig, based on test results. Since the mean failure pressure is far above the mean failure estimates for the other containment failure modes, no further analysis of the personnel airlock is performed. Since its expected contribution to the overall containment failure probability distribution is negligible, it is not included further in the development of the conditional containment failure probability distribution.

42.5 Overall Failure Distribution

Based on the uncertainties defined above and the best-estimate containment failure pressure at the bounding severe accident temperature of 400°F, a containment failure probability distribution can be constructed. The mean value and uncertainties used to construct the lognormal distributions for each failure mode are given in Table 42-1.

The containment failure probability distribution is constructed by assuming that all of the uncertainties and all of the failure modes are independent of each other. That is, the containment failure probability distribution for a particular failure mode (e.g., cylindrical shell) is constructed by developing the failure distribution assuming only random error and then developing another distribution assuming only subjective error. The two probability distributions are then combined to define the containment failure probability distribution for that particular failure mode. This process is carried out for each failure mode and the overall containment failure probability distribution is defined by combining the failure probability distributions for each failure mode.

In all cases, a lognormal distribution is assumed. The best-estimate failure pressure is used as the mean value. The appropriate lognormal standard deviation is defined from the coefficient of variance according to:

$$COV = (\exp(\beta^2) - 1.0)^{1/2}$$

where: COV = coefficient of variation
 β = lognormal standard deviation

The failure probability distributions are combined at any given containment pressure by summing the probability of exceedance at that pressure for each distribution according to:

$$Pe_i = 1.0 - ((1.0 - Pe_1) * (1.0 - Pe_2) * \dots * (1.0 - Pe_n))$$

where: Pe_i = overall probability of exceedance at any containment pressure
 Pe_1 through Pe_n = individual probabilities of exceedance at any containment pressure

Using the parameters given in Table 42-1, the conditional containment failure probability distribution is developed using a lognormal distribution for each of the failure modes. Figure 42-1 presents a graphical representation of the conditional containment failure probability distribution for each of the failure locations as well as the overall failure distribution for the AP600 containment.



The conditional containment failure probability for each of the failure locations and the cumulative containment failure probability, over the range of 90 to 200 psig, is given in Table 42-2.

42.6 Summary and Conclusions

The cumulative containment failure probability distribution has been developed, using lognormal distribution, which is based on best-estimate predictions of containment strength and accounts for random uncertainties in material properties and subjective modelling uncertainties. Based on this model, the mean internal pressure at which the AP600 containment vessel is predicted to fail is 132 psig. This is the best-estimate or expected containment failure pressure. This value is comparable to, or slightly higher than, the expected containment failure probability for other conventional pressurized water reactor (PWR) plants using pre-stressed or post-tensioned concrete containment structures.

The 5th and 95th percentile failure probabilities are 116 psig and 146 psig, respectively.

The cutoff for consideration of containment failure due to internal pressurization during a severe accident is defined as the pressure at which the containment failure probability is less than 10^{-4} . Below this point the failure probability is so low that, when combined with the small core damage frequency numbers, the overall probability of a core damage accident resulting in containment failure is in the 10^{-10} range. This is generally considered to be a negligible calculated number. From the lognormal distribution, the containment pressure corresponding to a 10^{-4} probability of failure is 94 psig.

42.7 References

- 42-1 "Reliability of Containments Under Overpressure," L. Greimann and F. Fanous, *Pressure Vessel and Piping Technology*, 1985, pp. 835 - 856.
- 42-2 "Reliability of Steel Containment Strength," L. Greimann, et. al., NUREG/CR-2442, June 1988.



Westinghouse

ENEL
ENTE NAZIONALE
PER L'ENERGIA ELETTRICA



Table 42-1

**PARAMETERS USED IN THE CONSTRUCTION OF THE
AP600 CONTAINMENT FAILURE PROBABILITY DISTRIBUTION**

Failure Location	Failure Mode	Mean Failure Pressure ¹ (psig)	Coefficient of Variance	
			Structural	Modelling
Cylindrical Shell	Membrane Yield	138	0.06	0.10
Ellipsoidal Head	Buckling	144	0.06	0.14
22-Ft. Equipment Hatch	Buckling	275	0.06	0.14
16-Ft. Equipment Hatch	Buckling	226	0.06	0.14
Personnel Hatch	Buckling	300	0.06	0.14

¹ All mean failure pressures are those specified at 400 °F





Table 42-2

CUMULATIVE CONTAINMENT FAILURE PROBABILITY

Containment Pressure (psig)	Probability of Containment Failure				
	Cylinder	Head	22-ft. Hatch	16-ft. Hatch	Total
90	0.00	1.15E-05	0	0	1.15E-05
95	9.69E-05	6.90E-05	0	0	1.66E-04
100	6.50E-04	2.47E-04	0	0	8.97E-04
105	3.19E-03	8.62E-04	0	0	4.05E-03
110	1.22E-02	2.53E-03	0	0	1.47E-02
115	3.64E-02	6.44E-03	0	0	4.26E-02
120	9.20E-02	1.50E-02	0	0	1.06E-01
125	2.09E-01	2.91E-02	0	0	2.32E-01
130	4.02E-01	5.44E-02	0	0	4.35E-01
135	6.33E-01	9.12E-02	0	0	6.66E-01
140	8.16E-01	1.48E-01	0	3.59E-05	8.43E-01
145	9.33E-01	2.23E-01	0	1.12E-04	9.48E-01
150	9.82E-01	3.45E-01	0	3.26E-04	9.88E-01
155	9.96E-01	4.95E-01	0	8.60E-04	9.98E-01
160	9.99E-01	6.64E-01	0	2.00E-03	1.00E+00
165	1.00E+00	8.01E-01	1.06E-05	4.60E-03	1.00E+00
170	1.00E+00	9.05E-01	3.14E-05	8.99E-03	1.00E+00
175	1.00E+00	9.61E-01	8.94E-05	1.71E-02	1.00E+00
180	1.00E+00	9.88E-01	2.08E-04	2.92E-02	1.00E+00
185	1.00E+00	9.96E-01	5.00E-04	4.99E-02	1.00E+00
190	1.00E+00	9.99E-01	1.04E-03	7.76E-02	1.00E+00
195	1.00E+00	1.00E+00	2.10E-03	1.18E-01	1.00E+00
200	1.00E+00	1.00E+00	4.19E-03	1.77E-01	1.00E+00

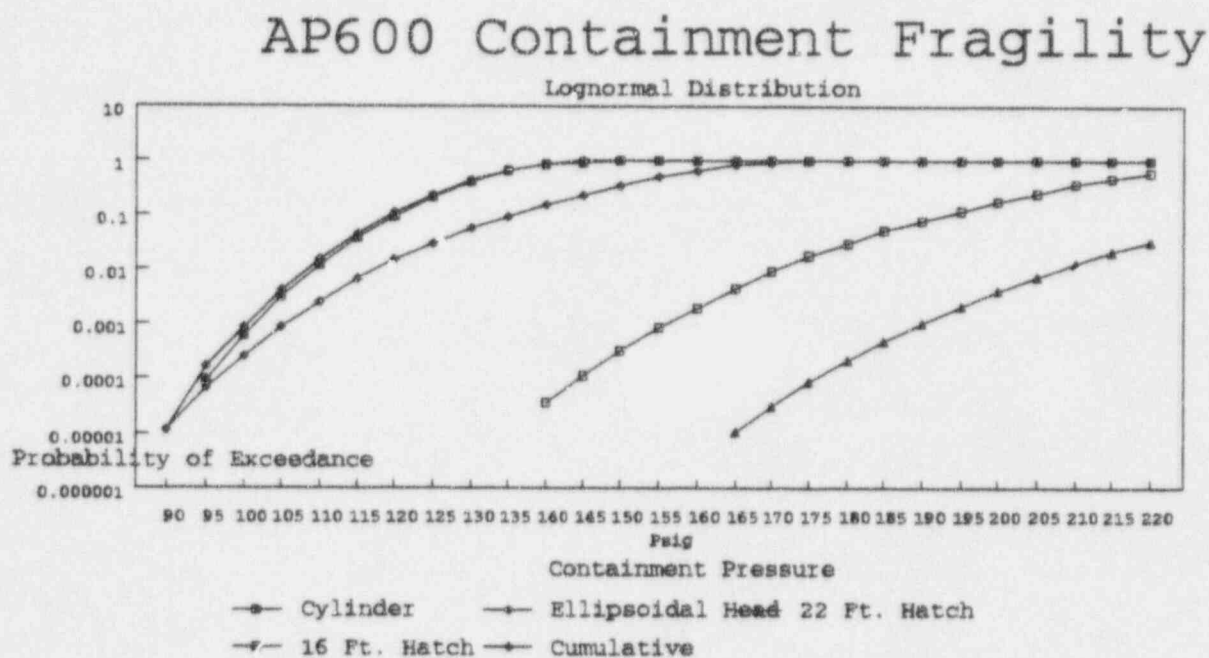


Figure 42-1

AP600 Containment Fragility



CHAPTER 43

RELEASE FREQUENCY QUANTIFICATION

43.1 Containment Event Tree Quantification

The containment event tree is quantified by linking fault trees to system nodes to define the failure probabilities at those nodes and by applying scalar probabilities obtained from the decomposition event trees to the failure probabilities for the phenomenological nodes. Table 43-1 provides a list of the nodes and the method used to quantify them. The WLINK code (Reference 43-1) was used for the fault tree linking, and the CADET code (Reference 43-2) was used for the overall containment event tree quantification.

43.1.1 Containment Event Tree Base Quantification

The split fractions (fault tree links and scalars) assigned to each node and the documentation for the assignments are provided in Table 43-2. The results and discussion of the accident class sequences from the containment event trees are presented below. The overall results are summarized in Table 43-3. The dominant sequences in each release category are presented in Tables 43-5 through 43-15.

43.1.1.1 Accident Class 1AC

Sequences initiated by a transient or a very small loss-of-coolant accident with no reactor coolant system depressurization prior to core damage are grouped into accident class 1A. Automatic depressurization system failure is often due to failure of both core makeup tanks to inject into the reactor coolant system, thus failing to generate the signals to open the depressurization valves. The containment event tree considers operator actions to depressurize the reactor coolant system following core damage. Successful depressurization allows the accumulators to inject and reflood the core and the in-containment refueling water storage tank water to inject to maintain long-term core cooling, if these systems are available. Successful depressurization cases are looped into accident class 3BRC to evaluate the long-term considerations of depressurization. Accident class 3BRC bins together sequences in which core damage occurs prior to potential gravity injection. Sequences that are not depressurized are termed 1AC sequences. Approximately 8 percent of accident class 1A goes to 1AC.

The sequences not actively depressurized are evaluated for potential thermally induced failures of the steam generator tubes and reactor coolant system piping. Sequences that have no failures of the reactor coolant system piping or steam generator tubes and fail the reactor vessel from relocation of debris to the lower head below the core debris bed level result in high-pressure melt ejection. Because of the low probability of these sequences, no analyses of the associated phenomena and their potential to challenge containment integrity were performed. Instead, high-pressure melt ejection sequences are conservatively assumed to fail containment early and produce, at a minimum, short-term core-concrete interaction. These



high-pressure melt ejection cases are binned into the CFE-C release category (0.97 percent of the 1AC sequences). Steam generator tube failure sequences are binned into the containment bypass release category BP (3.34 percent of the 1AC sequences). Given the large uncertainty in the size of a creep rupture failure, failures of the reactor coolant system piping are assumed not to be large enough to allow the in-containment refueling water storage tank water to inject and re-cover the core.

Success of containment isolation, passive containment cooling water, and igniters is evaluated for accident class 1AC. If containment isolation fails, the sequences are evaluated for possible vessel failure and fission-product release contributions due to core-concrete interactions. If the vessel does not fail, or if the debris is cooled and there is no core-concrete interaction, the sequence is binned into release category CI (32.4 percent of 1AC). If the debris is not coolable or if water cannot be recirculated to the cavity to maintain cooling, the sequence is binned into release category CI-C (0.15 percent of 1AC).

In 3.1 percent of the sequences, the hydrogen igniters are failed; in less than 0.01 percent of the sequences, passive containment cooling water fails. In 1.5 percent of the sequences, the operator action to actuate cavity flooding fails, resulting in vessel failure. If gravity injection is available, the in-containment refueling water storage tank water injects into the cavity through the reactor vessel after vessel failure and floods the cavity and lower containment. Ex-vessel debris coolability and containment water inventory for long-term debris cooling are evaluated.

The in-containment refueling water storage tank water is subcooled and, if injected after vessel failure, absorbs the decay heat of the core debris, allowing containment pressure to fall and hydrogen to become flammable during the intermediate (vessel failure to 24 hours) time frame despite the failure of the passive containment cooling water. If the debris is coolable, the water becomes saturated and the pressurization of containment inerts the containment atmosphere for late (24 to 72 hours) hydrogen combustion. The likelihood of hydrogen combustion and containment failure in the intermediate and late time frames is evaluated considering debris coolability and previous burning scenarios. If containment has not failed and the debris is coolable, the sequences are checked for possible leakage exceeding the technical specifications and resulting in a large release (release category XL, 0.5 percent of 1AC). If the debris is not coolable, the sequences are binned into the CFV release category (<0.01 percent of 1AC) to indicate possible basemat failure after 72 hours. The remaining sequences are binned into the intact containment release categories ICP (<0.01 percent of 1AC) and IC (62.6 percent of 1AC).

The frequencies of each release category for accident class 1AC, as well as the overall frequency of each release category, are presented in Table 43-3.

43.1.1.2 Accident Class 1APC

Sequences initiated by a very small loss-of-coolant accident or a small loss-of-coolant accident with successful passive residual heat removal and no reactor coolant system depressurization



prior to core damage are grouped into accident class 1AP. Automatic depressurization system failure is due mainly to common cause failure of the depressurization valves to open. The containment event tree considers operator actions to depressurize the reactor coolant system following core damage. Successful depressurization allows the in-containment refueling water storage tank water to inject to maintain long-term core cooling if the system is available. Successful depressurization cases are looped back into accident class 3BRC to evaluate the long-term considerations of depressurization. Accident class 3BRC bins together sequences in which core damage occurs prior to potential gravity injection. Sequences not depressurized are termed 1APC sequences. Approximately 17 percent of accident class 1AP goes to 1APC.

Passive residual heat removal significantly reduces the reactor coolant system pressure. The 1APC sequences do not have the potential for thermally induced failures of the steam generator tubes and reactor coolant system piping since the pressure loading on the components is small, and the heat transport from the core to the components via natural circulation is not efficient at lower pressures.

Success of containment isolation, passive containment cooling water, and igniters is evaluated for accident class 1APC. If containment isolation fails, the sequences are evaluated for possible vessel failure and fission-product release contributions due to core-concrete interactions. If the vessel does not fail, or if the debris is cooled and there is no core-concrete interaction, the sequence is binned into release category CI (1.2 percent of 1APC). If the debris is not coolable or if water cannot be recirculated to the cavity to maintain cooling, the sequence is binned into release category CI-C (0.02 percent of 1APC).

In 25 percent of the sequences, the hydrogen igniters are failed; in less than 0.01 percent of the sequences, passive containment cooling water fails. In 8.5 percent of the sequences, operator action to actuate cavity flooding fails, resulting in vessel failure. If gravity injection is available, the in-containment refueling water storage tank water injects into the cavity through the vessel after vessel failure and floods the cavity and lower containment. Debris coolability and water inventory for long-term ex-vessel debris cooling are evaluated. If the cavity flooding is successful, the vessel will most likely not fail, and the debris will be maintained in the vessel. If the vessel does fail, the failure location is expected to be above the debris pool (see Chapter 36) which would significantly limit the mass of debris that could relocate to containment. Vessel failure below the debris pool has the potential to relocate a large molten debris mass into the reactor cavity. If the vessel fails below the debris pool into a fully flooded cavity and a steam explosion occurs, then containment is assumed to fail from the inability to vent the cavity, resulting in an early containment failure with no core-concrete interaction.

The in-containment refueling water storage tank water is saturated from the operation of the passive residual heat removal and steams from the boiling due to heat transferred from the core debris or reactor vessel. The likelihood of hydrogen combustion and containment failure in the intermediate and late time frames (24 to 72 hours) is evaluated considering debris coolability and previous burning scenarios. If containment has not failed and the debris is coolable, the sequences are checked for possible leakage exceeding the technical specifications



and resulting in a large release (release category XL, 0.8 percent of 1APC). If the debris is not coolable, the sequences are binned into the CFV release category (0.02 percent of 1APC) to indicate possible basemat failure after 72 hours. The remaining sequences are binned into the intact containment release categories IC (98 percent of 1APC) and ICP (less than 0.01 percent of 1APC).

The frequencies of each release category for accident class 1APC, as well as the overall frequency of each release category, are presented in Table 43-3.

43.1.1.3 Accident Class 1D

Accident class 1D represents transients with partial reactor coolant system depressurization. It has a very low frequency of occurrence. Class 1D sequences are grouped together with class 3D, which includes loss-of-coolant accident events with partial depressurization. This combination is considered to be conservative since, in class 1D sequences, fission products are scrubbed in the in-containment refueling water storage tank prior to vessel melt-through. In class 3D, there is no fission-product scrubbing.

43.1.1.4 Accident Class 3BE

Sequences initiated by a loss-of-coolant accident with successful reactor coolant system depressurization but failure of the gravity injection prior to core damage are grouped into accident class 3BE. Failure of the gravity injection is due to common cause failures of the in-containment refueling water storage tank injection line check valves.

The 3BE sequences are fully depressurized and do not have the potential for thermally induced failures of the steam generator tubes and reactor coolant system piping since the pressure loading on the components is small, and the heat transport from the core to the components via natural circulation is not efficient at lower pressures.

Success of containment isolation, passive containment cooling water, and igniters is evaluated for accident class 3BE. If containment isolation fails, the sequences are evaluated for possible vessel failure and fission-product release contributions due to core-concrete interactions. If the vessel does not fail, or if the debris is cooled and there is no core-concrete interaction, the sequence is binned into release category CI (0.13 percent of 3BE). If the debris is not coolable or if water cannot be recirculated to the cavity to maintain cooling, the sequence is binned into release category CI-C (less than 0.01 percent of 3BE).

In 0.6 percent of the sequences, the hydrogen igniters are failed; in 0.01 percent of the sequences, passive containment cooling water fails. In 3.4 percent of the sequences, operator action to actuate cavity flooding fails, resulting in vessel failure. Gravity injection is not available, by definition of the accident class, and debris coolability and water inventory for long-term ex-vessel debris cooling are evaluated. If the cavity flooding is successful, the vessel will most likely not fail, and the debris will be maintained in the vessel. If the vessel does fail, the failure location is expected to be above the debris pool (see Chapter 36) which



would significantly limit the mass of debris that could relocate to containment. Vessel failure below the debris pool has the potential to relocate a large molten debris mass into the reactor cavity. If the vessel fails below the debris pool into a fully-flooded cavity and a steam explosion occurs, containment is conservatively assumed to fail (in absence of further analyses of the phenomena involved). No subsequent core-concrete interaction is assumed since the debris must quench to produce the steam explosion.

If the cavity is flooded, water can inject into the reactor vessel through the break, reflood the core, cool the core, and create additional hydrogen. The likelihood of hydrogen combustion and containment failure in the intermediate and late time frames (24 to 72 hours) is evaluated considering debris coolability and previous burning scenarios. If containment has not failed and the debris is coolable, the sequences are checked for possible leakage exceeding the technical specifications and resulting in a large release (release category XL, 0.8 percent of 3BE). If the debris is not coolable, the sequences are binned into the CFV release category (0.03 percent of 3BE) to indicate possible basemat failure after 72 hours. The remaining sequences are binned into the intact containment release categories IC (99 percent of 3BE) and ICP (0.01 percent of 3BE).

The frequencies of each release category for accident class 3BE, as well as the overall frequency of each release category, are presented in Table 43-3

43.1.1.5 Accident Class 3BRC

Accident class 3BR includes sequences in which the reactor coolant system is fully depressurized and the in-containment refueling water storage tank is potentially available, but the accumulators and core makeup tanks are not. Core melt occurs because the gravity injection cannot refill the vessel fast enough to prevent core damage upon the initial blowdown of the reactor coolant system. This subclass has a very low frequency of occurrence (less than 1 percent of the core damage frequency). A containment event tree is constructed mainly because of the importance of the transfers from accident classes 1A, 1AP, and 3D. Accumulators and core makeup tanks are addressed in the event tree because they are potentially available for classes 1A, 1AP, and 3D sequences, which are transferred to this accident class following successful long-term reactor depressurization. The 3BR accident class including the contributions from the 1A, 1AP, and 3D accident classes is termed 3BRC. Seventy-three percent of the frequency of accident class 3BRC comes from successfully depressurized accident class 1A sequences; 5.7 percent comes from successfully depressurized 3D sequences; and 9.6 percent of the 3BRC frequency is from successfully depressurized 1AP sequences.

The 3BRC sequences are fully depressurized and do not have the potential for thermally induced failures of the steam generator tubes and reactor coolant system piping since the pressure loading on the components is small, and the heat transport from the core to the components via natural circulation is not efficient at lower pressures.

Success of containment isolation, passive containment cooling water, and igniters is evaluated for accident class 3BRC. If containment isolation fails, the sequences are evaluated for possible vessel failure and fission-product release contributions due to core-concrete interactions. If the vessel does not fail, or if the debris is cooled and there is no core-concrete interaction, the sequence is binned into release category CI (0.6 percent of 3BRC). If the debris is not coolable or if water cannot be recirculated to the cavity to maintain cooling, the sequence is binned into release category CI-C (less than 0.01 percent of 3BRC).

In 0.5 percent of the sequences, the hydrogen igniters are failed; in 0.01 percent of the sequences, passive containment cooling water fails. The availability of cavity flooding, debris coolability, and water inventory for long-term ex-vessel debris cooling is evaluated. In almost 100 percent of the cases, the cavity flooding is successful since flooding will occur at the time of depressurization unless the gravity injection lines fail. If the cavity flooding is successful, the vessel will most likely not fail, and the debris will be maintained in the vessel. If the vessel does fail, the failure location is expected to be above the debris pool (see Chapter 36) which would significantly limit the mass of debris that could relocate to containment. Vessel failure below the debris pool has the potential to relocate a large molten debris mass into the reactor cavity. If the vessel fails below the debris pool into a fully-flooded cavity and a steam explosion occurs, then containment is conservatively assumed to fail (in absence of further analysis of the phenomena involved). No subsequent core-concrete interaction is assumed.

If the cavity is flooded, water can inject into the reactor vessel and reflood the core, cool the core, and create additional hydrogen. The likelihood of hydrogen combustion and containment failure in the intermediate and late time frames (24 to 72 hours) is evaluated considering debris coolability and previous burning scenarios. If containment has not failed and the debris is coolable, the sequences are checked for possible leakage exceeding the technical specifications and resulting in a large release (release category XL, 0.8 percent of 3BRC). If the debris is not coolable, the sequences are binned into the CFV release category (less than 0.01 percent of 3BRC) to indicate possible basemat failure after 72 hours. The remaining sequences are binned into the intact containment release categories IC (99 percent of 3BRC) and ICP (0.01 percent of 3BRC).

The frequencies of each release category for accident class 3BRC, as well as the overall frequency of each release category are presented in Table 43-3.

43.1.1.6 Accident Class 3C

Accident class 3C includes all sequences in which the core is damaged following reactor vessel rupture that occurs as an initiating event. The core melt cannot be arrested in the reactor vessel because the time required to overheat the core is less than the time needed to flood the cavity and refill the vessel through the break.

The 3C sequences are fully depressurized and do not have the potential for thermally induced failures of the steam generator tubes and reactor coolant system piping since the pressure

loading on the components is small, and the heat transport from the core to the components via natural circulation is not efficient at lower pressures.

Success of containment isolation, passive containment cooling water, and igniters is evaluated for accident class 3C. The containment isolation failure node takes into account the possibility of containment breach consequential to the initiating event (for example, due to penetration failure caused by the relative displacement of the vessel). If containment isolation fails, the sequences are evaluated for fission-product release contributions due to core-concrete interactions. If the debris is cooled and there is no core-concrete interaction, the sequence is binned into release category CI (0.2 percent of 3C). If the debris is not coolable or if water cannot be recirculated to the cavity to maintain cooling, the sequence is binned into release category CI-C (0.04 percent of 3C).

In 0.12 percent of the sequences, the hydrogen igniters are failed; in 0.01 percent of the sequences, passive containment cooling water fails. Because of the nature of the initiating event, vessel failure is ensured. The best-estimate location for the failure is considered to be a local failure at the lower head weld. Gravity injection, debris coolability, and water inventory for long-term ex-vessel debris cooling are evaluated. If the vessel fails below the debris, and the debris is ejected into a fully flooded cavity and a steam explosion occurs, then containment is assumed to fail from the inability to vent the cavity, resulting in an early containment failure with no core-concrete interaction.

If the cavity is flooded, water can inject into the reactor vessel and reflood the core, cool the core, and create additional hydrogen. The likelihood of hydrogen combustion and containment failure in the intermediate and late time frames (24 to 72 hours) is evaluated considering debris coolability and previous burning scenarios. If containment has not failed and the debris is coolable, the sequences are checked for possible leakage exceeding the technical specifications and resulting in a large release (release category XL, 0.8 percent of 3C). If the debris is not coolable, the sequences are binned into the CFV release category (0.9 percent of 3C) to indicate possible basemat failure after 72 hours. The remaining sequences are binned into the intact containment release categories IC (97 percent of 3C) and ICP (0.01 percent of 3C).

The frequencies of each release category for accident class 3C, as well as the overall frequency of each release category, are presented in Table 43-3.

43.1.1.7 Accident Class 3DC

Sequences initiated by a loss-of-coolant accident with partial reactor coolant system depressurization prior to core damage are grouped into accident class 3D. Full automatic depressurization failure is due mainly to common cause failure of stage four depressurization valves to open. The containment event tree considers operator action to depressurize the reactor coolant system following core damage. Successful depressurization allows the in-containment refueling water storage tank water to inject to possibly maintain long-term core cooling if the system is available. Successful depressurization cases are looped back into



accident class 3BRC to evaluate the long-term considerations of depressurization. Accident class 3BRC bins together sequences in which core damage occurs prior to potential gravity injection. Sequences not depressurized are termed 3DC sequences. Eighty-nine percent of accident class 3D goes to 3DC.

The 3DC sequences are depressurized and do not have the potential for thermally induced failures of the steam generator tubes and reactor coolant system piping since the pressure loading on the components is small, and the heat transport from the core to the components via natural circulation is not efficient at lower pressures.

Success of containment isolation, passive containment cooling water, and igniters is evaluated for accident class 3DC. If containment isolation fails, the sequences are evaluated for possible vessel failure and fission-product release contributions due to core-concrete interactions. If the vessel does not fail, or if the debris is cooled and there is no core-concrete interaction, the sequence is binned into release category CI (0.13 percent of 3DC). If the debris is not coolable or if water cannot be recirculated to the cavity to maintain cooling, the sequence is binned into release category CI-C (less than 0.01 percent of 3DC).

In 0.24 percent of the sequences, the hydrogen igniters are failed; in 0.01 percent of the sequences, passive containment cooling water fails. In 0.95 percent of the sequences, operator action to actuate cavity flooding fails, resulting in vessel failure. If gravity injection is available, the in-containment refueling water storage tank water injects into the cavity through the vessel after vessel failure and floods the cavity and lower containment. Debris coolability and water inventory are evaluated for long-term ex-vessel debris cooling. If the cavity flooding is successful, the vessel will most likely not fail, and the debris will be maintained in the vessel. If the vessel does fail, the failure location is expected to be above the debris pool (see Chapter 36) which would significantly limit the mass of debris that could relocate to the containment. Vessel failure below the debris pool has the potential to relocate a large molten debris mass into the reactor cavity. If the vessel fails below the debris level into a fully-flooded cavity and a steam explosion occurs, containment is conservatively assumed to fail (in absence of further analysis of the phenomena involved). No subsequent core-concrete interaction is assumed.

The in-containment refueling water storage tank water is saturated from the operation of the passive residual heat removal and steams from the boiling due to heat transferred from the core debris or reactor vessel. The likelihood of hydrogen combustion and containment failure in the intermediate and late time frames (24 to 72 hours) is evaluated considering debris coolability and previous burning scenarios. If containment has not failed and the debris is coolable, the sequences are checked for possible leakage exceeding the technical specifications and resulting in a large release (release category XL, 0.8 percent of 3DC). If the debris is not coolable, the sequences are binned into the CFV release category (0.01 percent of 3DC) to indicate possible basemat failure after 72 hours. The remaining sequences are binned into the intact containment release categories IC (99 percent of 3DC) and ICP (0.01 percent of 3DC).



The frequencies of each release category for accident class 3DC, as well as the overall frequency of each release category, are presented in Table 43-3.

43.1.1.8 Other Accident Classes

No event trees are developed for the other accident classes, given the very low frequency of occurrence (less than 0.1 percent of the overall core damage frequency). Instead, the frequencies of these accident classes are conservatively combined with the frequencies of classes leading to containment bypass (release category BP).

43.1.2 In-Vessel Retention Sensitivity Quantification

The issue of in-vessel retention of core debris is important to the AP600 severe accident response since the containment design allows the operator to flood the vessel to reduce the uncertainty contributions to containment response from ex-vessel phenomena involving the release of molten debris to containment. The conditional failure probability for in-vessel retention, given successful cavity flooding, as calculated in the IVR decomposition event tree, is low (1×10^{-4}). To determine the sensitivity of the large-release frequency to the value calculated for the failure probability of the in-vessel retention, a containment event tree quantification has been performed. It assumes that the failure probability for in-vessel retention, given a flooded reactor cavity, is increased by two orders of magnitude to 1×10^{-2} . The results of this sensitivity case are presented in Table 43-4.

The increased probability in the failure of the vessel given a flooded cavity increases the frequency of early, intermediate, and very late containment failures and the likelihood of core-concrete interaction in containment isolation failure release categories primarily in accident classes 3BE, 3BRC, and 3DC. These accident classes have a high likelihood of successful cavity flooding. However, because of the dominance of release category BP, which bypasses containment, the impact of the change to the IVR failure probability does not change the large-release frequency.

43.2 Containment Event Tree Quantification Conclusions

- The overall large-release frequency for AP600 is 1.0×10^{-8} events per reactor-year. This frequency includes containment bypass, containment isolation failure, excessive containment leakage, and containment failures. The large-release frequency is 4.1 percent of the core damage frequency.
- The frequency of containment integrity being compromised from the initiation of the accident is 9.9×10^{-9} events per reactor-year. This impaired containment frequency includes containment bypass, containment isolation failure, and excessive containment leakage. It accounts for 99 percent of the overall large-release frequency. The impaired containment frequency is 4 percent of the core damage frequency.





- The frequency of containment failure is 1.6×10^{-10} events per reactor-year. This frequency includes early, intermediate, and late containment failures. It accounts for 1.6 percent of the overall large-release frequency. The containment failure frequency is 0.06 percent of the core damage frequency.
- The frequency of containment basemat failure is 1.3×10^{-10} events per reactor-year. Basemat failure occurs more than 72 hours after the onset of core damage. The frequency accounts for 1.3 percent of the overall large release frequency. The basemat failure frequency is 0.05 percent of the core damage frequency.
- Approximately 58 percent of the initially impaired containment frequency consists of unisolated steam generator tube rupture initiating events. Approximately 1.5 percent of the initially impaired containment frequency is attributed to induced steam generator tube ruptures.
- The frequency of containment isolation failure is dominated by the accident class 1AC failures (71 percent) in which containment must often be isolated by operator action because of failures of the actuation system.
- The early containment failure contributes 1.6 percent to the large release frequency. Approximately 64 percent of the early containment failure frequency is due to early containment failures in the 3C accident class in which rupture of the reactor vessel initiates the accident. If the failure occurs below the weld at the hemispherical head, the cases are treated as vessel failures such that none of the debris is retained in the vessel. A large fraction of molten debris is released to a fully flooded reactor cavity and is assumed to generate a steam explosion. The early containment failures in accident class 3C occur based on a conservative assumption that vessel failures occurring below the core debris and releasing a large molten mass that quenches and potentially generates a steam explosion in a fully flooded reactor cavity result in failed containment.
- Approximately 0.4 percent of the early containment failure frequency is due to high-pressure melt ejection cases. Since the frequency of the high-pressure melt ejection cases is very small, no further analyses of the associated phenomena were performed. Instead, high-pressure melt ejection cases are lumped into the early containment failure release category CFE-C. The frequency of high-pressure melt ejection cases (4.4×10^{-11} events per reactor-year) is less than 0.02 percent of the core damage frequency and contributes less than 0.5 percent of the large release frequency. Given the insignificant fraction of the core damage frequency involved, no decomposition event trees were developed to demonstrate containment integrity for melt ejection phenomena despite the fact that both AP600 design features and emergency consensus on direct containment heating for existing pressurized water reactors afford considerable promise that integrity would be maintained.



- Approximately 6 percent of the AP600 severe accident sequences result in vessel failure. This includes accident class 3C which, as discussed above, is initiated by a failed vessel. If accident class 3C is eliminated from consideration of vessel failure, 2 percent of the cases result in vessel failure.
- The conditional probability of containment failure (CFE, CFE-C, CFI, CFL, and CFV), given an initially intact containment, an initially intact reactor vessel, and successful cavity flooding, is 0.65 percent. The conditional probability of containment failure, given an initially intact containment, an initially intact reactor vessel, and failure to flood the cavity, is 2.2 percent. Cavity flooding, therefore, provides a reduction in the uncertainty in containment integrity, given a severe accident.
- The following are the estimated frequencies of the containment challenges from severe accident high energy events:
 - core damage combined with failure of passive containment cooling water is 1.9×10^{-11} events per reactor-year
 - global hydrogen combustion is 8.5×10^{-10} events per reactor-year
 - unmitigated core-concrete interaction is 7.5×10^{-10} events per reactor-year
 - debris relocation to containment is 15×10^{-9} events per reactor-year
 - high-pressure melt ejection is 4.4×10^{-11} events per reactor-year
 - in-vessel fuel coolant interactions causing containment failure is approximately 0.0 events per reactor-year

43.3 References

- 43-1 *WLINK Code System User Manual for Version 3.1*, WCAP-13400 (Proprietary), June 1992.
- 43-2 *Event Tree Development and Quantification System User Manual*, WCAP-13199 (Proprietary), February 1992.



Table 43-1

**AP600 CONTAINMENT EVENT TREE NODES
QUANTIFICATION METHODS**

Node	Description	Quant Method
DP	RCS depressurization (post-core damage operator action)	FT link ⁽¹⁾
SG	Hot leg creep failure	Chapter 37
CR	SG tube creep failure	Chapter 37
IS	Containment isolation	FT link
PC	Passive containment cooling	FT link
IG	Hydrogen control system (igniters)	FT link
IR	Cavity flooding (operator action to dump in-containment refueling water storage tank)	FT link
SE	In-vessel steam explosion	Chapter 38
VF	Vessel failure	Chapter 36
HC1	Early hydrogen burn	Chapter 41
DQ	Debris quench	Chapter 40
SCC	Short term CCI	Chapter 40
CF1	Early containment failure	Chapter 41
RW	Water recirculation to cavity (long-term CCI)	FT link
HC2	Intermediate hydrogen burn	Chapter 41
CF2	Intermediate containment failure	Chapter 41
HC3	Late hydrogen burn	Chapter 41
CF3	Late containment failure	Chapter 41
CF4	Very late containment failure (from CCI)	Conditional scalar
EX	Excessive containment leakage	Conditional scalar

Note:

(1) FT link = fault tree linking



Table 43-2 (Sheet 1 of 4)

AP600 CONTAINMENT EVENT TREE NODAL SPLIT FRACTIONS

Node	Accident Class	Conditionals X. [^] = Success of Node X X.0 = Failure of Node X	Fault Tree or Fail Probability	Document
DP	1AC 1APC 3D Other		ADTLT ADTLT ADQLT n/a	Chapter 11
SG	1AC Other		3.34E-2 n/a	Chapter 37
CR	1AC Other		1.0E-2 n/a	Chapter 37
IS	1AC 1APC 3BRC 3DC 3BE 3C		CIC+PO CID+PO CIC+CNB+PO	Chapter 24
PC	All		PCT	Chapter 13
IG	All		VLH	Chapter 16
IR	1A 1AP 3BE 3D 3BR 3C		IWF IWF*IW2AB	Chapter 12
SE	All		0.0E0	Chapter 38
VF	3C Others	IR. [^] IR.0	1.0E0 1.0E-4 1.0E0	Chapter 36



Westinghouse

ENEL
 ENTE NAZIONALE
 PER L'ENERGIA ELETTRICA

Table 43-2 (Sheet 2 of 4)

AP600 CONTAINMENT EVENT TREE NODAL SPLIT FRACTIONS

Node	Accident Class	Conditionals X. [^] = Success of Node X X.0 = Failure of Node X	Fault Tree or Fail Prob	Document
HC1	1A	IG.0 and PC. [^]	5.0E-1	Chapter 41
	3BE	IG.0 and PC.0 and IR. [^]	1.25E-2	
	3BR	IG.0 and PC. [^] and IR. [^]	5.0E-1	
	3C	IG.0 and PC. [^]	1.25E-2	
	Others		0.0E0	
DQ	All		9.0E-3	Chapter 40
SCC	All		1.62E-1	Chapter 40
CF1	1A	HC1.0 and (VF. [^] or IR.0 or DQ.0)	1.0E-2	Chapter 41 Chapter 36 combined
		HC1. [^] and VF.0 and IR. [^] and DQ. [^]	1.0E-2	
		HC1.0 and VF.0 and IR. [^] and DQ. [^]	1.99E-2	
	3C	HC1.0 and (VF. [^] or IR.0 or DQ.0)	1.1E-1	Chapter 41 Chapter 36 combined
		HC1. [^] and VF.0 and IR. [^] and DQ. [^]	1.0E-2	
		HC1.0 and VF.0 and IR. [^] and DQ. [^]	1.189E-1	
	3BE 3BR	HC1.0 and (VF. [^] or IR.0 or DQ.0) and PC. [^]	2.2E-2	Chapter 41 Chapter 36
		HC1.0 and (VF. [^] or IR.0 or DQ.0) and PC.0	1.0E-2	
		HC1. [^] and VF.0 and IR. [^] and DQ. [^]	1.0E-2	
	Others	HC1.0 and VF.0 and IR. [^] and DQ. [^] and PC. [^]	3.178E-2	Chapter 36
		HC1.0 and VF.0 and IR. [^] and DQ. [^] and PC.0	1.99E-2	
		VF.0 and IR. [^] and DQ. [^]	1.0E-2	
	Default		0.0E0	
RW	1A 1AP 3D	IS. [^] and PC. [^]	IW2AB*[(CMBOTH* ACBOTH)+CM2LLT + AC2AB]	Chapter 9, 10, 12
		IS. [^] and PC.0	IW2AB*(CMBOTH+ ACBOTH)	
		IS.0	IW2AB	
	3BE 3BR 3C	IS. [^] and PC. [^]	(CMBOTH*ACBOTH) + CM2LLT+AC2AB	
		IS. [^] and PC.0	CMBOTH+ACBOTH	
		IS.0	1.0E0	



Table 43-2 (Sheet 3 of 4)

AP600 CONTAINMENT EVENT TREE NODAL SPLIT FRACTIONS

Node	Accident Class	Conditionals X.^ = Success of Node X X.0 = Failure of Node X	Fault Tree or Fail Prob	Document
HC2	1A	IG.0 and HC1.^ and (VF.^ or (DQ.^ and SCC.^ and RW.^))	4.0E-1	Chapter 41
		IG.0 and DQ.^ and RW.^ and SCC.0	3.0E-1	
	3C	IG.0 and PC.^ and HC1.^ and (VF.^ or (DQ.^ and SCC.^ and RW.^))	1.0E-2	
	3BE 3BR	IR.^ and IG.0 and PC.^ and HC1.^ and (VF.^ or (DQ.^ and SCC.^ and RW.^))	4.0E-1	
	All (except 1A)	IG.0 and PC.^ and DQ.^ and SCC.0 and RW.^	3.0E-1	
	All	IG.0 and HC1.0 and (DQ.0 or RW.0)	1.0E0	
		IG.0 and HC1.^ and (DQ.0 or RW.0)	1.0E0	
	Default		0.0E0	
CF2	1A	HC1.^ and (VF.^ or (DQ.^ and SCC.^ and RW.^)) and HC2.0	1.0E-2	Chapter 41
		DQ.^ and RW.^ and SCC.0 and HC2.0	1.0E-2	
	3C	PC.^ and HC1.^ and (VF.^ or (DQ.^ and SCC.^ and RW.^)) and HC2.0	1.0E-2	
	3BE 3BR	IR.^ and PC.^ and HC1.^ and (VF.^ or (DQ.^ and SCC.^ and RW.^)) and HC2.0	1.2E-2	
	All (except 1A)	PC.^ and DQ.^ and SCC.0 and RW.^ and HC2.0	1.0E-2	
	All	HC1.0 and (DQ.0 or RW.0) and HC2.0	1.21E-1	
		HC1.^ and (DQ.0 or RW.0) and HC2.0	8.3E-1	
	Default		0.0E0	



Westinghouse

ENEL
 ENTE NAZIONALE
 PER L'ENERGIA ELETTRICA

Table 43-2 (Sheet 4 of 4)

AP600 CONTAINMENT EVENT TREE NODAL SPLIT FRACTIONS

Node	Accident Class	Conditionals X. [^] = Success of Node X X.0 = Failure of Node X	Fault Tree or Fail Prob	Document
HC3	1A	IG.0 and PC. [^] and (HC1. [^] and HC2. [^]) and (VF. [^] or (DQ. [^] and SCC. [^] and RW. [^]))	1.0E-2	Chapter 41
	3C	IG.0 and PC. [^] and (HC1. [^] and HC2. [^]) and (VF. [^] or (DQ. [^] and SCC. [^] and RW. [^]))	2.0E-3	
	3BF 3ER	IR. [^] and IG.0 and PC. [^] and (HC1. [^] and HC2. [^]) and (VF. [^] or (DQ. [^] and SCC. [^] and RW. [^]))	1.0E-1	
	All	IG.0 and PC. [^] and HC1.0 and DQ. [^] and SCC.0 and RW. [^]	3.0E-1	
		IG.0 and (HC1. [^] and HC2. [^]) and (DQ.0 or RW.0)	1.0E0	
		IG.0 and PC. [^] and (HC1. [^] and HC2. [^]) and DQ. [^] and SCC.0 and RW. [^]	4.0E-1	
	Default		0.0E0	
CF3	1A	PC. [^] and (HC1. [^] and HC2. [^]) and (VF. [^] or (DQ. [^] and SCC. [^] and RW. [^])) and HC3.0	1.0E-1	Chapter 41
	3C	PC. [^] and (HC1. [^] and HC2. [^]) and (VF. [^] or (DQ. [^] and SCC. [^] and RW. [^])) and HC3.0	1.25E-2	
	3BE 3BR	IR. [^] and PC. [^] and (HC1. [^] and HC2. [^]) and (VF. [^] or (DQ. [^] and SCC. [^] and RW. [^])) and HC3.0	1.2E-2	
	All	PC. [^] and HC1.0 and DQ. [^] and SCC.0 and RW. [^] and HC3.0	9.33E-3	
		(HC1. [^] and HC2. [^]) and (DQ.0 or RW.0) and HC3.0	6.5E-1	
		PC. [^] and (HC1. [^] and HC2. [^]) and DQ. [^] and SCC.0 and RW. [^] and HC3.0	1.0E-2	
	Default		0.0E0	
CF4	All	DQ.0 or RW.0	1.0E0	Chapter 35
		DQ. [^] and RW. [^]	0.0E0	
EX	All		8.0E-3	Chapter 35

Table 43-3

**AP600 CONTAINMENT EVENT TREE BASE CASE QUANTIFICATION RESULTS -
RELEASE CATEGORY FREQUENCIES (PER REACTOR-YEAR)**

Base Case Release Category	1AC	1APC	3BE	3BRC	3C	3DC	6E	RC Frequency	RC Contribution
IC	2.9E-09	1.4E-09	1.2E-07	7.2E-08	9.7E-09	3.1E-08	0.0E+00	2.4E-07	9.6E-01
ICP	0.0E+00	0.0E+00	1.0E-11	5.8E-12	9.3E-13	2.2E-12	0.0E+00	1.9E-11	7.8E-05
XL	2.3E-11	1.1E-11	9.8E-10	5.8E-10	7.9E-11	2.5E-10	0.0E+00	1.9E-09	7.7E-03
BP	1.5E-10	4.9E-15	7.8E-15	8.4E-14	4.1E-15	6.4E-15	5.7E-09	5.9E-09	2.4E-02
CI	1.5E-09	1.6E-11	1.6E-10	4.1E-10	2.0E-11	4.0E-11	0.0E+00	2.1E-09	8.6E-03
CI-C	6.9E-12	2.3E-13	2.4E-12	6.6E-15	4.2E-12	0.0E+00	0.0E+00	1.4E-11	5.5E-05
CFE	7.1E-13	0.0E+00	7.3E-12	3.7E-12	8.3E-11	2.6E-14	0.0E+00	9.5E-11	3.8E-04
CFE-C	4.4E-11	0.0E+00	1.9E-14	1.2E-14	1.6E-11	5.0E-15	0.0E+00	6.0E-11	2.4E-04
CFI	3.1E-13	7.6E-13	1.6E-12	7.9E-13	9.9E-14	1.5E-14	0.0E+00	3.6E-12	1.4E-05
CFL	4.5E-14	4.3E-14	4.2E-13	1.2E-13	5.5E-15	0.0E+00	0.0E+00	6.3E-13	2.5E-06
CFV	2.2E-13	3.3E-13	3.7E-11	6.7E-14	8.9E-11	2.7E-12	0.0E+00	1.3E-10	5.2E-04
Totals	4.6E-09	1.4E-09	1.2E-07	7.2E-08	1.0E-08	3.1E-08	5.7E-09	2.5E-07	1.0E+00
Large Release Frequency								1.0E-08	4.1E-02
Initially Failed Containment								9.9E-09	4.0E-02
Induced Containment Failure								1.6E-10	6.4E-04
Basemat Penetration								1.3E-10	5.2E-04



Westinghouse

ENEL
ENVIRONMENTAL
NUCLEAR
ELECTRONICS

43-17

Revision: 3
February 28, 1995
u:\ap600\pva\sec43.wpf:1b

Table 43-4

**AP600 CONTAINMENT EVENT TREE BASE CASE QUANTIFICATION RESULTS -
RELEASE CATEGORY FREQUENCIES (PER REACTOR-YEAR)**

VF Sens. Release Category	1AC	1APC	3BE	3BRC	3C	3DC	6E	RC Frequency	RC Contribution
IC	2.9E-09	1.4E-09	1.2E-07	7.1E-08	9.7E-09	3.1E-08	0.0E+00	2.4E-07	9.6E-01
ICP	0.0E+00	0.0E+00	1.0E-11	5.8E-12	9.3E-13	2.2E-12	0.0E+00	1.9E-11	7.8E-05
XL	2.3E-11	1.1E-11	9.8E-10	5.8E-10	7.9E-11	2.5E-10	0.0E+00	1.9E-09	7.7E-03
BP	1.5E-10	3.8E-15	9.4E-15	1.2E-14	4.1E-15	6.1E-15	5.7E-09	5.9E-09	2.4E-02
CI	1.5E-09	1.6E-11	1.6E-10	4.1E-10	2.0E-11	4.0E-11	0.0E+00	2.1E-09	8.6E-03
CI-C	9.4E-12	2.5E-13	2.7E-12	7.0E-13	4.2E-12	6.8E-14	0.0E+00	1.7E-11	6.9E-05
CFE	9.4E-13	1.0E-13	1.7E-11	9.6E-12	8.3E-11	2.6E-12	0.0E+00	1.1E-10	4.5E-04
CFE-C	4.4E-13	2.0E-14	1.9E-12	1.2E-12	1.6E-11	5.0E-13	0.0E+00	2.0E-11	8.1E-05
CFI	3.2E-13	7.8E-13	1.9E-12	8.0E-13	9.9E-14	2.0E-14	0.0E+00	3.9E-12	1.6E-05
CFL	4.5E-14	4.4E-14	2.5E-13	1.2E-13	5.5E-15	0.0E+00	0.0E+00	4.6E-13	1.9E-06
CFV	4.7E-13	4.3E-13	4.7E-11	6.4E-12	8.9E-11	5.4E-12	0.0E+00	1.5E-10	6.0E-04
Totals	4.5E-09	1.4E-09	1.2E-07	7.3E-08	1.0E-08	3.1E-08	5.7E-09	2.5E-07	1.0E+00
Large Release Frequency								1.0E-08	4.1E-02
Initially Failed Containment								9.9E-09	4.0E-02
Induced Containment Failure								1.4E-10	5.5E-04
Basemat Penetration								1.5E-10	6.0E-04

Table 43-5

RELEASE CATEGORY IC DOMINANT SEQUENCES
RELEASE CATEGORY IC FREQUENCY = 2.4E-7 PER REACTOR-YEAR

Seq #	Accident Class	Frequency	RC Frequency (%)	Failed CET Nodes	Sequence Description
1	3BE	1.2E-7	49		Fully depress RCS, igniters on, cavity flooded, vessel intact
2	3BRC	7.1E-8	30		RCS depress recovery, igniters on, vessel intact
3	3DC	3.1E-8	13	DP	Partial RCS depress, igniters on, cavity flooded, vessel intact
4	3C	8.1E-9	3.4	VF	Fully depress RCS, igniters on, cavity flooded, vessel failed, debris quenched
5	3BE	3.4E-9	1.4	IR	Fully depress RCS, igniters on, cavity flooded, vessel failed, debris quenched
6	1AC	2.7E-9	1.1	DP	High press RCS, hot leg creep, igniters on, cavity flooded, vessel intact
7	3C	1.6E-9	0.7	VF, SCC	Fully depress RCS, igniters on, cavity flooded, vessel failed, short-term CCI
8	1APC	1.0E-9	0.4	DP	Partially depress RCS, igniters on, cavity flooded, vessel intact
9	3BE	6.6E-10	0.3	IR, SCC	Fully depress RCS, igniters on, cavity flooded, vessel failed, short-term CCI
10	3BE	3.2E-10	0.1	IG, HC1	Fully depress RCS, igniters failed, cavity flooded, vessel intact, early global burn

Table 43-6

RELEASE CATEGORY ICP DOMINANT SEQUENCES
RELEASE CATEGORY ICP FREQUENCY = 1.9E-11 PER REACTOR-YEAR

Seq #	Accident Class	Frequency	RC Frequency (%)	Failed CET Nodes	Sequence Description
1	3BE	1.0E-11	49	PC	Fully depress RCS, igniters on, PCS failed, cavity flooded, vessel intact
2	3BRC	5.8E-12	31	PC	RCS depress recovery, igniters on, PCS failed, cavity flooded, vessel intact
3	3DC	2.2E-12	12	DP, PC	Partially depress RCS, igniters on, PCS failed, cavity flooded, vessel intact
4	3C	7.8E-13	4.1	PC, VF	Fully depress RCS, igniters on, PCS failed, cavity flooded, vessel failed, debris quenched
5	3C	1.5E-13	0.8	PC, VF, SCC	Fully depress RCS, igniters on, PCS failed, cavity flooded, vessel failed, short-term CCI
6	3BE	1.0E-13	0.5	PC, IR	Fully depress RCS, igniters on, PCS failed, cavity flooded, vessel failed, short-term CCI

Table 43-7

RELEASE CATEGORY XL DOMINANT SEQUENCES
RELEASE CATEGORY XL FREQUENCY = 1.9E-9 PER REACTOR-YEAR

Seq #	Accident Class	Frequency	RC Frequency (%)	Failed CET Nodes	Sequence Description
1	3BE	9.4E-10	49	EX	Fully depress RCS, igniters on, cavity flooded, vessel intact, excessive leakage
2	3BRC	5.7E-10	30	EX	RCS depress recovery, igniters on, cavity flooded, vessel intact, excessive leakage
3	3DC	2.5E-10	13	DP, EX	Partially depress RCS, igniters on, cavity flooded, vessel intact, excessive leakage
4	3C	6.6E-11	3.4	VF, EX	Fully depress RCS, igniters on, cavity flooded, vessel failed, debris quench, excessive leakage
5	3BE	2.7E-11	1.4	IR, EX	Fully depress RCS, igniters on, no cavity flood, vessel failed, debris quench, excessive leakage
6	3C	1.3E-11	0.7	VF, SCC, EX	Fully depress RCS, igniters on, cavity flooded, vessel failed, short-term CCI, excessive leakage
7	1APC	8.1E-12	0.4	EX	Partially depress RCS, igniters on, cavity flooded, vessel intact, excessive leakage
8	3BE	5.3E-12	0.3	IR, SCC, EX	Fully depress RCS, igniters on, no cavity flood, vessel failed, short-term CCI, excessive leakage



Westinghouse

ENEL
 ENTE NAZIONALE
 PER L'ENERGIA ELETTRICA

Table 43-8

RELEASE CATEGORY BP DOMINANT SEQUENCES
RELEASE CATEGORY BP FREQUENCY = 5.9E-9 PER REACTOR-YEAR

Seq #	Accident Class	Frequency	RC Frequency (%)	Failed CET Nodes	Sequence Description
1	6E	5.7E-9	97		Unisolated SGTR
2	1AC	1.7E-10	3	DP, SG	High press RCS, SG tube creep failure

Table 43-9

RELEASE CATEGORY CI DOMINANT SEQUENCES
RELEASE CATEGORY CI FREQUENCY = 2.8E-9 PER REACTOR-YEAR

Seq #	Accident Class	Frequency	RC Frequency (%)	Failed CET Nodes	Sequence Description
1	1AC	1.4E-9	69	DP, IS	Containment isolation failed, high press RCS, HL creep rupture, cavity flood, vessel intact
2	3BRC	4.1E-10	20	IS	Containment isolation failed, RCS depress recovery, cavity flood, vessel intact
3	3BE	1.6E-10	7.6	IS	Containment isolation failed, fully depress RCS, cavity flood, vessel intact
4	3DC	4.0E-11	1.9	DP, IS	Containment isolation failed, partially depress RCS, cavity flood, vessel intact
5	1AC	3.4E-11	1.6	DP, IS, IR	Containment isolation failed, high press RCS, HL creep rupture, no cavity flood, vessel failed, debris quench

Table 43-10

RELEASE CATEGORY CI-C DOMINANT SEQUENCES
RELEASE CATEGORY CI-C FREQUENCY = 1.4E-11 PER REACTOR-YEAR

Seq #	Accident Class	Frequency	RC Frequency (%)	Failed CET Nodes	Sequence Description
1	1AC	6.6E-12	47	DP, IS, IR, SCC	Containment isolation failed, high press RCS, HL creep rupture, no cavity flood, vessel failed, short-term CCI
2	3C	3.9E-12	28	IS, VF, SCC	Containment isolation failed, fully depress RCS, cavity flood, vessel failed, short-term CCI
3	3BE	2.0E-12	14	IS, IR, RW	Containment isolation failed, fully depress RCS, no cavity flood, vessel failed, debris quench, long-term CCI
4	3BE	3.9E-13	2.8	IS, IR, SCC	Containment isolation failed, fully depress RCS, no cavity flood, vessel failed, short-term CCI
5	1AC	3.7E-13	2.6	DP, IS, IR, DQ	Containment isolation failed, high press RCS, HL creep rupture, no cavity flood, vessel failed, no debris quench, long-term CCI



Table 43-11

RELEASE CATEGORY CFE DOMINANT SEQUENCES
RELEASE CATEGORY CFE FREQUENCY = 9.5E-11 PER REACTOR-YEAR

Seq #	Accident Class	Frequency	RC Frequency (%)	Failed CET Nodes	Sequence Description
1	3C	8.3E-11	87	VF, CF1	Fully depress RCS, igniters on, cavity flooded, vessel failed, containment fail by ex-vessel steam explosion
2	3BE	7.2E-12	7.6	IG, HC1, CF1	Fully depress RCS, igniters failed, cavity flood, vessel intact, containment fail by early global burn
3	3BRC	3.6E-12	3.8	IG, HC1, CF1	RCS depress recovery, igniters failed, cavity flood, vessel intact, containment fail by early global burn
4	1AC	6.8E-13	0.7	DP, IG, HC1, CF1	High press RCS, HL creep rupture, igniters failed, cavity flood, vessel intact, containment fail by early global burn

Table 43-12

RELEASE CATEGORY CFE-C DOMINANT SEQUENCES
RELEASE CATEGORY CFE-C FREQUENCY = 6.0E-11 PER REACTOR-YEAR

Seq #	Accident Class	Frequency	RC Frequency (%)	Failed CET Nodes	Sequence Description
1	1AC	4.4E-11	73	DP, CR	High press RCS, containment fail by HPME
2	3C	1.6E-11	27	VF, SCC, CF1	Fully depress RCS, igniters on, flooded cavity, vessel failure, steam explosion fails containment early, short-term CCI



Table 43-13

RELEASE CATEGORY CFI DOMINANT SEQUENCES
RELEASE CATEGORY CFI FREQUENCY = 3.6E-12 PER REACTOR-YEAR

Seq #	Accident Class	Frequency	RC Frequency (%)	Failed CET Nodes	Sequence Description
1	3BE	1.6E-12	44	IG, HC2, CF2	Full depress RCS, igniters failed, cavity flood, vessel intact, containment failed by intermediate global burn
2	3BRC	7.9E-13	22	IG, HC2, CF2	RCS depress recovery, igniters failed, cavity flood, vessel intact, containment failed by intermediate global burn
3	1APC	7.1E-13	20	DP, IG, IR, DQ, HC2, CF2	Partially depress RCS, igniters failed, no cavity flood, vessel failed, no debris quench, containment fail by intermediate global burn
4	1AC	2.7E-13	7.5	DP, IG, HC2, CF2	High press RCS, HL creep rupture, igniters failed, cavity flood, vessel intact, containment fail by intermediate global burn
5	3C	9.2E-14	2.6	IG, VF, DQ, HC2, CF2	Fully depress RCS, igniters failed, cavity flood, vessel failed, no debris quench, containment fail by intermediate global burn
6	1APC	4.6E-14	1.3	DP, IG, IR, SCC, HC2, CF2	Partially depress RCS, igniters failed, no cavity flood, vessel failed, short-term CCI, containment fail by intermediate global burn



Westinghouse

ENEL
 ENTE NAZIONALE
 PER L'ENERGIA ELETTRICA

Table 43-14

RELEASE CATEGORY CFL DOMINANT SEQUENCES
RELEASE CATEGORY CFL FREQUENCY = 6.3E-13 PER REACTOR-YEAR

Seq #	Accident Class	Frequency	RC Frequency (%)	Failed CET Nodes	Sequence Description
1	3BE	2.4E-13	38	IG, HC3, CF3	Fully depress RCS, igniters failed, cavity flood, vessel intact, containment failed by late global burn
2	3BE	1.7E-13	26	IG, IR, DQ, HC3, CF3	Fully depress RCS, igniters failed, no cavity flood, vessel failed, no debris quench, containment failed by late global burn
3	3BRC	1.2E-13	19	IG, HC3, CF3	RCS depress recovery, igniters failed, cavity flood, vessel intact, cont failed by late global burn
3	1APC	4.3E-14	6.8	DP, IG, IR, SCC, HC3, CF3	Partial depress RCS, igniters failed, no cavity flood, vessel failed, short-term CCI, containment fail by late global burn



Table 43-15

RELEASE CATEGORY CFV DOMINANT SEQUENCES
RELEASE CATEGORY CFV FREQUENCY = 1.3E-10 PER REACTOR-YEAR

Seq #	Accident Class	Frequency	RC Frequency (%)	Failed CET Nodes	Sequence Description
1	3C	8.9E-11	68	VF, DQ, CF4	Fully depress RCS, igniters on, cavity flood, vessel fail, no debris quench, long-term CCI, potential basemat failure >72 hours
2	3BE	3.7E-11	28	IR, DQ, CF4	Fully depress RCS, igniters on, no cavity flood, vessel fail, no debris quench, long-term CCI, potential basemat failure >72 hours
3	3D	2.6E-12	2	DP, IR, DQ, CF4	Partial depress RCS, igniters on, no cavity flood, vessel fail, no debris quench, long-term CCI, potential basemat failure >72 hours



Westinghouse

ENEL
 ENTE NAZIONALE
 PER L'ENERGIA ELETTRICA